ADVANCES IN QUANTUM CHEMISRTY

Volume 26

John R. Sabin &
Michael C. Zerner

ADVANCES IN
QUANTUM CHEMISTRY

EDITOR-IN-CHIEF

PER-OLOV LÖWDIN

PROFESSOR EMERITUS

QUANTUM CHEMISTRY GROUP
UPPSALA UNIVERSITY
UPPSALA, SWEDEN

AND

QUANTUM THEORY PROJECT
UNIVERSITY OF FLORIDA
GAINESVILLE, FLORIDA

EDITORS

JOHN R. SABIN AND MICHAEL C. ZERNER

QUANTUM THEORY PROJECT
UNIVERSITY OF FLORIDA
GAINESVILLE, FLORIDA

VOLUME 26

ACADEMIC PRESS

San Diego New York Boston London Sydney Tokyo Toronto

This book is printed on acid-free paper. ♾

Academic Press, Inc.
A Division of Harcourt Brace & Company
525 B Street, Suite 1900, San Diego, California 92101-4495

United Kingdom Edition published by
Academic Press Limited
24-28 Oval Road, London NW1 7DX

International Standard Serial Number: 0065-3276

International Standard Book Number: 0-12-034826-8

PRINTED IN THE UNITED STATES OF AMERICA
95 96 97 98 99 00 QW 9 8 7 6 5 4 3 2 1

Contributors

Numbers in parentheses indicate the pages on which the authors' contributions begin.

H. Ågren (167), Institute of Physics and Measurement Technology, Linköping University, S-58183 Linköping, Sweden

G. Berthier (1), Institut de Biologie Physico-chimique, 75005 Paris, France

Jean-Louis Calais (35), Quantum Chemistry Group, University of Uppsala, S-751 20 Uppsala, Sweden

M. Defranceschi (1), Commissariat á l'Energie Atomique, DSM/DRECAM/ SRSIM CE Saclay, 91191 Gif sur Yvette, France.

Michaël Deleuze (35), Laboratoire de Chimie Théorique Appliquée, Facultés Universitaires Notre-Dame de la Paix, B-5000 Namur, Belgium

Joseph Delhalle (35), Laboratoire de Chimie Théorique Appliquée, Facultés Universitaires Notre-Dame de la Paix, B-5000 Namur, Belgium

Philippe C. Hiberty (99), Laboratoire de Chimie Theorique, Universite de Paris-Sud, F-91405 Orsay, France

Poul Jørgensen (167), Department of Chemistry, Aarhus University, DK-8000 Århus, Denmark

P. Lazzeretti (1), Dipartimento di Chimica, dell'Università degli Studi di Modena, 41100 Modena, Italy

Yi Luo (167), Institute of Physics and Measurement Technology, Linköping University, S-58183 Linköping, Sweden

Kurt V. Mikkelsen (167), Department of Chemistry, Aarhus University, DK-8000 Århus, Denmark

Barry T. Pickup (35), Department of Chemistry, The University, Sheffield S3 7HF, United Kingdom

Peter Raychev (239), Institute of Nuclear Research and Nuclear Energie, Bulgarian Academy of Sciences, Sofia, Bulgaria

Sason Shaik (99), Department of Organic Chemistry, and the Fritz-Haber Center of Molecular Dynamics, The Hebrew University, 91904 Jerusalem, Israel

Preface

In investigating the highly different phenomena in nature, scientists have always tried to find some fundamental principles that can explain the variety from a basic unity. Today they have shown not only that all the various kinds of matter are built up from a rather limited number of atoms but also that these atoms are composed of a few basic elements or building blocks. It seems possible to understand the innermost structure of matter and its behavior in terms of a few elementary particles: electrons, protons, neutrons, photons, etc., and their interactions. Since these particles obey not the laws of classical physics but the rules of modern quantum theory of wave mechanics established in 1925, there has developed a new field of "quantum science" which deals with the explanation of nature on this basis.

Quantum chemistry deals particularly with the electronic structure of atoms, molecules, and crystalline matter, and describes it in terms of electronic wave patterns. It uses physical and chemical insight, sophisticated mathematics, and high-speed computers to solve the wave equations and achieve its results. Its goals are great, and today the new field can boast of both its conceptual framework and its numerical accomplishments. It provides a unification of the natural sciences that was previously inconceivable, and the modern development of cellular biology shows that the life sciences are now, in turn, using the same basis. "Quantum Biology" is a new field which describes the life processes and the functioning of the cell on a molecular level and a submolecular level.

Quantum chemistry is hence a rapidly developing field which falls between the historically established areas of mathematics, physics, chemistry, and biology. As a result there is a wide diversity of backgrounds among those interested in quantum chemistry. Since the results of the research are reported in periodicals of many different types, it has become increasingly difficult for both the expert and the nonexpert to follow the rapid development in this new multidisciplinary area.

The purpose of this serial publication is to present a survey of the current development of quantum chemistry as it is seen by a number of internationally leading research workers in various countries. The authors have been invited to give their personal points of view of the subject freely and without severe space limitations. No attempts have been made to avoid overlap—on the contrary, it seems desirable to have certain important research areas reviewed from different points of view.

The response from the authors and the referees has been so encouraging that a series of new volumes is being prepared. However, in order to control production costs and speed publication time, a new format involving camera-ready manuscripts was initiated with Volume 20. A special announcement about the new format was enclosed in that volume (page xiii).

In the volumes to come, special attention will be devoted to the following subjects: the quantum theory of closed states, particularly the electronic structure of atoms, molecules, and crystals; the quantum theory of scattering states, dealing also with the theory of chemical reactions; the quantum theory of time-dependent phenomena, including the problem of electron transfer and radiation theory; molecular dynamics; statistical mechanics and general quantum statistics; condensed matter theory in general; quantum biochemistry and quantum pharmacology; the theory of numerical analysis and computational techniques.

As to the content of Volume 26, the Editors thank the authors for their contributions, which give an interesting picture of part of the current development of quantum chemistry from rather sophisticated sum rules for derivatives associated with second-order molecular properties, over size-consistency and size-intensitivity considerations of properties of polymers from the aspects of many-body quantum theory, studies of valence bond mixing and curve crossing diagrams in chemical reactivity and bonding, and treatments of response functions and their features connected with certain molecular properties to a review of modern quantum algebras and their importance for applications to nuclear and molecular spectra.

It is our hope that the collection of surveys of various parts of quantum chemistry and its advances presented here will prove to be valuable and stimulating, not only to active research workers but also to scientists in neighboring fields of physics, chemistry, and biology who are turning to the elementary particles and their behavior to explain the details and innermost structure of their experimental phenomena.

PER-OLOV LÖWDIN

ROTOTRANSLATIONAL AND VIRIAL SUM RULES FOR GEOMETRICAL DERIVATIVES OF SECOND-ORDER PROPERTIES AND NUCLEAR ELECTRIC HYPERSHIELDINGS

P. Lazzeretti,
Dipartimento di Chimica dell'Università degli Studi di Modena
Via Campi 183, 41100 Modena, Italy

M. Defranceschi,
Commissariat à l'Energie Atomique, DSM/DRECAM/SRSIM
CE Saclay, Bât. 462, 91191 Gif sur Yvette, France

G. Berthier,
Institut de Biologie Physico-chimique, 13, rue Pierre et Marie Curie;
Ecole Normale Supérieure, 24, rue Lhomond, 75005 Paris, France

Contents

ADVANCES IN QUANTUM CHEMISTRY
VOLUME 26

VIII. Conclusions

I Introduction

Quite recently a number of theoretical and experimental studies dealing with infrared spectra of molecules in the presence of external (static) electric fields have been reported [1–15]. Within these experimental conditions both frequency shifts and variations of intensity of absorption bands are observed. These changes can be accounted for in terms of electric field dependence of force constants, *i.e.*, of second derivatives with respect to nuclear coordinates (geometrical derivatives) of the energy of a molecule in the presence of electric perturbations [16],

$$W \equiv \langle \psi_a | H | \psi_a \rangle = W_0 - \mathcal{M}_\alpha^{(0)} E_\alpha - \frac{1}{2}\alpha_{\alpha\beta}E_\alpha E_\beta - \frac{1}{6}\beta_{\alpha\beta\gamma}E_\alpha E_\beta E_\gamma - \frac{1}{24}\gamma_{\alpha\beta\gamma\delta}E_\alpha E_\beta E_\gamma E_\delta + \ldots, \quad (1)$$

and in terms of derivatives of the induced electric dipole moments. The total electric dipole moment in the presence of the field is

$$\mathcal{M}_\alpha = -\frac{\partial W}{\partial E_\alpha} \equiv \langle \psi_a | \mathcal{D}_\alpha | \psi_a \rangle = \mathcal{M}_\alpha^{(0)} + \alpha_{\alpha\beta}E_\beta + \frac{1}{2}\beta_{\alpha\beta\gamma}E_\beta E_\gamma + \frac{1}{6}\gamma_{\alpha\beta\gamma\delta}E_\beta E_\gamma E_\delta + \ldots, \quad (2)$$

where all the symbols have the usual meaning [16]. In the absence of additional perturbations, within the double-harmonic approximation, the integrated absorption coefficient related to the i-th fundamental IR band is proportional to squares of derivatives, with respect to normal coordinates, of the dipole moment in the electronic ground state $\psi_a^{(0)}$ of the molecule, *i.e.*,

$$A_i^{IR} \propto \sum_\alpha \left(\frac{\partial}{\partial Q_i} \mathcal{M}_\alpha^{(0)} \right)^2 . \quad (3)$$

The derivatives with respect to Q_i can be expressed within a Cartesian reference frame via a similarity transformation, introducing atomic polar tensors (APT) [17–20]. Analytical procedures of various levels of accuracy are available for the theoretical determination of these quantities [21–26].

A connection between APT and the electric shielding tensor of nuclei has been found [27]. The latter describes the electric field induced at the nuclei of a molecule owing to linear response of the electrons to an external electric field. This result has heuristic value and provides a reinterpretation of IR

absorption: the IR radiation acting on a molecule is a dynamic electric field inducing oscillations within the electron cloud. Owing to a feedback effect, these ocillations yield an additional dynamic electric field at the nuclei, which are acted upon by an effective field (the vector sum of the external one and that arising from the perturbed electrons), *i.e.*, by a frequency-dependent Lorentz force that is responsible for changes of nuclear vibrational motion.

One can assume that the variations of intensity, observed when an electric field is switched on, could be deduced, within the framework of perturbation theory, via an equation similar to (3), by replacing $\mathcal{M}_\alpha^{(0)}$ with $\mathcal{M}_\alpha$. Accordingly, the intensity of IR bands of molecules perturbed by external electric field depends on derivatives of dipole electric polarizabilities and hyperpolarizabilities with respect to the nuclear coordinates. In other words, intensity variations of absorption of electromagnetic radiation are essentially due to non linear response of the electrons in the molecule, and, to first order in the static perturbing field E_α, can be described introducing a third-rank molecular tensor related to the geometrical derivative of the electric dipole polarizability. The same tensor can be used to rationalize also the isotropic and anisotropic contributions to Raman intensities; for instance, for the isotropic term one has [28], in the harmonic approximation,

$$A_i^{Raman} \propto \frac{1}{45} \frac{\partial}{\partial Q_i} \alpha_{\alpha\alpha} \frac{\partial}{\partial Q_i} \alpha_{\beta\beta}. \tag{4}$$

Extending the procedures of Ref. [29], this tensor can be referred to as nuclear electric (first) hypershielding [28]. It describes the electric field induced at the nuclei of the molecule by (intense) external fields.

Along the lines of the interpretation suggested above, the actual dynamic Lorentz force acting upon the nuclei of a molecule in the presence of both IR radiation and an additional (static) electric field arises from the sum of these external fields and the one generated by non-linear response of the perturbed electrons. The knowledge of the (first) hypershielding enables one to estimate this effective Lorentz force and provides a physical link to rationalize the process of IR absorption of a molecule in these experimental conditions.

As it will be clear from its analytical expression, see eq. (74), the hypershielding tensor also describes (i) the electric dipole moment induced in the electron cloud by an external electric field and by the nuclear motion, (ii) the displacement of a nucleus from its equilibrium position due to non linear response of electrons to external fields. In addition, derivatives of dipole electric polarizability are necessary to investigate the dependence of this property on molecular geometry and the contributions provided by nuclear vibration [25].

As electric first hypershieldings are related to geometrical derivatives of electric polarizability, it seems useful to define the general form of such a

derivative for an arbitrary second-order property. Other interesting examples are geometrical derivatives of mixed dipole-quadrupole polarizability, which are related to shielding of a molecule in the presence of an electric field and a field gradient. The geometrical derivatives of magnetic susceptibility are connected to electric shielding in the presence of magnetic field.

The present paper is aimed at deriving the explicit expression for the general geometric derivative of a second-order property using perturbation theory, and at analyzing some of the mathematical and physical properties of these interesting quantities. Sum rules for geometrical derivatives of polarizabilities and hyperpolarizabilities, *i.e.*, conditions for translational and rotational invariance, are discussed in Sec. III by means of force and torque theorems; in Sec. V the general case of derivatives of arbitrary second-order properties are examined. The existence of sum rules for hypershielding tensor is related to force and torque theorems in the presence of a magnetic field in Sec. VI. Constraints imposed by the virial theorem on geometrical derivatives are discussed in Sec. VII for molecules perturbed by electric and magnetic fields.

The analytical formulas for electric hypershielding obtained in the present work also provide explicit definitions for calculation *i.e.*, viable numerical recipes alternative to algorithms and techniques based on actual differentiation [21].

In analytical calculations of derivatives of molecular properties, see, for instance, Ref. [21], some of the rototranslational constraints examined in this work are automatically satisfied, as they can be directly related to actual translation and rotation of the electronic cloud. Accordingly they can be used to check a computer program for analytical molecular derivatives.

In those cases in which geometrical derivatives are evaluated via shielding and hypershielding tensors [29] directly from perturbation theory, the degree to which these sum rules are obeyed in approximate calculations, using electronic wavefunctions obtained within the algebraic approximation, gives indications on the quality of the basis set.

II Force and torque in a molecule in the presence of external fields

Let us consider a molecule with n electrons and N nuclei, whose electronic system is characterized by a closed-shell structure. Charge, mass, position with respect to the origin $\mathbf{r}_0$ of the coordinate system, canonical and angular momentum of the i-th electron are denoted by $-e, m_e, \mathbf{r}_i - \mathbf{r}_0, \mathbf{p}_i = -(i/\hbar)\nabla_i, \mathbf{l}_i(\mathbf{r}_0) = (\mathbf{r}_i - \mathbf{r}_0) \times \mathbf{p}_i, i = 1, 2 \ldots n$. Corresponding quantities for the I-th nucleus are $Z_I e, M_I, \mathbf{R}_I - \mathbf{r}_0, \mathbf{P}_I = -(i/\hbar)\nabla_I, \mathbf{L}_I(\mathbf{r}_0)$, $I = 1, 2 \ldots N$.

The operators for the centroid, total linear and angular momentum of the assembly of electrons are written

$$R_\alpha(\mathbf{r}_0) = \sum_{i=1}^{n}(r_{i\alpha} - r_{0\alpha}), \quad P_\alpha = \sum_{i=1}^{n} p_{i\alpha}, \quad L_\alpha(\mathbf{r}_0) = \sum_{i=1}^{n} l_{i\alpha}(\mathbf{r}_0). \tag{5}$$

In the presence of spatially uniform and time-independent electric and magnetic fields, E_α and B_α, the clamped-nuclei Born-Oppenheimer Hamiltonian of the molecule is, neglecting electron spin,

$$\begin{aligned} H &= H^{(0)} - \mathcal{D}_\alpha(\mathbf{r}_0)E_\alpha - m_\alpha(\mathbf{r}_0)B_\alpha - \frac{1}{2}\bar{\chi}^{\mathrm{d}}_{\alpha\beta}(\mathbf{r}_0)B_\alpha B_\beta \\ &\equiv H^{(0)} + \lambda H^\lambda + \mu H^\mu + \frac{1}{2}\mu^2 H^{\mu^2}, \end{aligned} \tag{6}$$

where the formal expansion parameters λ and μ have been introduced. The unperturbed Hamiltonian operator is

$$H^{(0)} = \sum_{i=1}^{n}\left[\frac{p_i^2}{2m_e} - \sum_{I=1}^{N}\frac{Z_I e^2}{|\mathbf{r}_i - \mathbf{R}_I|} + \frac{1}{2}\sum_{j\neq i}^{n}\frac{e^2}{|\mathbf{r}_i - \mathbf{r}_j|}\right] + \frac{1}{2}\sum_{I}^{N}\sum_{J\neq I}^{N}\frac{Z_I Z_J e^2}{|\mathbf{R}_I - \mathbf{R}_J|}, \tag{7}$$

the operators for total electric dipole of the molecule and magnetic dipole of electrons are, respectively,

$$\mathcal{D}_\alpha(\mathbf{r}_0) = \mu_\alpha(\mathbf{r}_0) + \sum_{I=1}^{N} Z_I e(R_{I\alpha} - r_{0\alpha}), \quad \mu_\alpha(\mathbf{r}_0) = -eR_\alpha(\mathbf{r}_0), \tag{8}$$

and

$$m_\alpha(\mathbf{r}_0) = -\frac{e}{2m_e c}L_\alpha(\mathbf{r}_0), \tag{9}$$

and the operator for the diamagnetic contribution to susceptibility is

$$\bar{\chi}^{\mathrm{d}}_{\alpha\beta}(\mathbf{r}_0) = -\frac{e^2}{4m_e c^2}\sum_{i=1}^{n}\left[(r_i - r_0)^2\delta_{\alpha\beta} - (r_{i\alpha} - r_{0\alpha})(r_{i\beta} - r_{0\beta})\right]. \tag{10}$$

No contribution to molecular magnetic dipole arises from the clamped nuclei, but in the description of spectral parameters of vibrational circular dichroism (VCD) it is expedient to introduce a phenomenological term accounting for the magnetic dipole moment of the nuclei [23, 30],

$$M_\alpha(\mathbf{r}_0) = \sum_{I=1}^{N}\frac{Z_I e}{2M_I c}L_{I\alpha}(\mathbf{r}_0). \tag{11}$$

The operator for the attractive Coulomb force acting upon electron i is

$$\mathbf{F}_i^I = -e\mathbf{E}_i^I, \tag{12}$$

where

$$\mathbf{E}_i^I = Z_I e \frac{\mathbf{r}_i - \mathbf{R}_I}{|\mathbf{r}_i - \mathbf{R}_I|^3} \tag{13}$$

is the electric field exerted by nucleus I, and the repulsive force due to other electrons is

$$\mathbf{F}_i^{n-i} = e^2 \sum_{j \neq i}^{n} \frac{\mathbf{r}_i - \mathbf{r}_j}{|\mathbf{r}_i - \mathbf{r}_j|^3}.$$

The Lorentz force due to the external fields is

$$\mathbf{F}_i^E + \mathbf{F}_i^B + \mathbf{F}_i^{BB} = -e\mathbf{E} - \frac{e}{m_e c}\boldsymbol{\pi}_i \times \mathbf{B}, \tag{14}$$

where

$$\boldsymbol{\pi}_i = \mathbf{p}_i + \frac{e}{c}\mathbf{A}_i, \quad \boldsymbol{\Pi} = \sum_{i=1}^{n} \boldsymbol{\pi}_i, \tag{15}$$

is the electronic mechanical momentum in the presence of the vector potential (in the Coulomb gauge)

$$\mathbf{A}_i \equiv \mathbf{A}(\mathbf{r}_i - \mathbf{r}_0) = \frac{1}{2}\mathbf{B} \times (\mathbf{r}_i - \mathbf{r}_0). \tag{16}$$

The magnetic force contains first- and second-order terms; the latter are not univocally defined, but depend on the origin,

$$\begin{aligned} F_{i\alpha}^B &= -\frac{e}{m_e c}\epsilon_{\alpha\beta\gamma} p_{i\beta} B_\gamma, \\ F_{i\alpha}^{BB} &= -\frac{e^2}{4m_e c^2} B_\beta B_\gamma \left(2r_\alpha \delta_{\beta\gamma} - r_\beta \delta_{\alpha\gamma} - r_\gamma \delta_{\alpha\beta}\right)_i. \end{aligned} \tag{17}$$

It can be observed that the operator $\boldsymbol{\pi}_i \times \mathbf{B}$ is Hermitian if the magnetic field is spatially uniform. It is Hermitian also for time-independent inhomogeneous fields [31], owing to the Maxwell equation $\nabla \times \mathbf{B} = \mathbf{0}$. Introducing a self-explanatory notation, several useful operators can be defined, *e.g.*, the operator for the total force of the nuclei on the electrons is

$$\mathbf{F}_n^N = \sum_{I=1}^{N} \sum_{i=1}^{n} \mathbf{F}_i^I, \tag{18}$$

the electric Lorentz force on all the electrons is

$$\mathbf{F}_n^E = \sum_{i=1}^{n} \mathbf{F}_i^E = -en\mathbf{E}, \tag{19}$$

etc.. Analogously the operator for the force acting on electron i in the presence of the external fields is written

$$\mathbf{F}_i = \mathbf{F}_i^N + \mathbf{F}_i^{n-i} + \mathbf{F}_i^E + \mathbf{F}_i^B + \mathbf{F}_i^{BB} \tag{20}$$

Within this notation,

$$\mathbf{E}_I^i = e\frac{\mathbf{r}_i - \mathbf{R}_I}{|\mathbf{r}_i - \mathbf{R}_I|^3} \tag{21}$$

is the operator for the electric field of electron i on nucleus I,

$$\mathbf{F}_I = \mathbf{F}_I^n + \mathbf{F}_I^{N-I} + \mathbf{F}_I^E, \tag{22}$$

is the operator for the total force on clamped nucleus I, where

$$\mathbf{F}_I^n = Z_I e\mathbf{E}_I^n, \quad \mathbf{F}_I^E = Z_I e\mathbf{E}, \tag{23}$$

and the repulsive force due to the other nuclei is

$$\mathbf{F}_I^{N-I} = Z_I e^2 \sum_{J\neq I}^{N} Z_J \frac{\mathbf{R}_I - \mathbf{R}_J}{|\mathbf{R}_I - \mathbf{R}_J|^3}.$$

The electron-electron and nucleus-nucleus forces cancelling,

$$\sum_{i=1}^{n} \mathbf{F}_i^{n-i} = \mathbf{0} = \sum_{I=1}^{N} \mathbf{F}_I^{N-I}, \tag{24}$$

the operators for the total force on the electrons and on the nuclei are rewritten

$$\mathbf{F}_n = \mathbf{F}_n^N + \mathbf{F}_n^E + \mathbf{F}_n^B + \mathbf{F}_n^{BB} = \sum_{i=1}^{n} \mathbf{F}_i, \tag{25}$$

$$\mathbf{F}_N = \mathbf{F}_N^n + \mathbf{F}_N^E = \sum_{I=1}^{N} \mathbf{F}_I. \tag{26}$$

From these definitions one finds useful equations connecting the operators for total forces acting upon nuclei and electrons,

$$\mathbf{F}_N^n = -\mathbf{F}_n^N, \tag{27}$$

$$\mathbf{F}_N = -\mathbf{F}_n + q\mathbf{E} - \frac{e}{m_e c}\boldsymbol{\Pi} \times \mathbf{B}, \tag{28}$$

where

$$q = \left(\sum_{I=1}^{N} Z_I - n\right) e \tag{29}$$

is the charge of the molecule. Denoting by

$$\mathbf{F}_n^{EXT} = \mathbf{F}_n^E + \mathbf{F}_n^B + \mathbf{F}_n^{BB}$$

the operator for the total force exerted on the electrons by the external fields, one also has

$$\mathbf{F}_n = -\mathbf{F}_N^n + \mathbf{F}_n^{EXT}. \tag{30}$$

In a similar notation, the operator for the total torque on the electrons about the origin $\mathbf{r}_0$ is

$$\mathbf{K}_n(\mathbf{r}_0) = \mathbf{K}_n^N(\mathbf{r}_0) + \mathbf{K}_n^E(\mathbf{r}_0) + \mathbf{K}_n^B(\mathbf{r}_0) + \mathcal{K}_n^B(\mathbf{r}_0) + \mathbf{K}_n^{BB}(\mathbf{r}_0), \tag{31}$$

where

$$\mathbf{K}_n^N(\mathbf{r}_0) = \sum_{i=1}^{n}(\mathbf{r}_i - \mathbf{r}_0) \times \mathbf{F}_i^N, \tag{32}$$

and

$$\mathbf{K}_n^E(\mathbf{r}_0) = \boldsymbol{\mu}(\mathbf{r}_0) \times \mathbf{E}. \tag{33}$$

The operators for the torque exerted by the magnetic field are obtained from the expressions for the magnetic Lorentz force (17) by little manipulation of the equations given in Ref. [29]. To first order in B_α, and with respect to an arbitrary origin,

$$K_{n\alpha}^B = \epsilon_{\alpha\beta\gamma} m_\beta B_\gamma, \tag{34}$$

$$\mathcal{K}_{n\alpha}^B = \frac{e}{2c} B_\beta \frac{d}{dt}\left[\sum_{i=1}^{n}\left(r^2\delta_{\alpha\beta} - r_\alpha r_\beta\right)_i\right]. \tag{35}$$

The quantum mechanical operator for the torque (about $\mathbf{r}_0$) can be obtained by replacing the total time derivative with commutators, *i.e.*,

$$K_{n\alpha}^B(\mathbf{r}_0) + \mathcal{K}_{n\alpha}^B(\mathbf{r}_0) = \epsilon_{\alpha\beta\gamma} m_\beta(\mathbf{r}_0) B_\gamma - \frac{2im_e c}{e\hbar} B_\beta \left[H^{(0)}, \bar{\chi}_{\alpha\beta}^{\mathrm{d}}(\mathbf{r}_0)\right]. \tag{36}$$

Classically the time average of a total time derivative vanishes; from the quantum mechanical point of view, the expectation values over real wavefunctions of the commutator and of the magnetic dipole operator in eq. (36) also vanish. In the presence of magnetic field, however, a contribution to the average torque is provided by operators (36), as the first-order correction to the electronic wave function is pure imaginary. Using eq. (10) and the second of eqs. (17), the contribution to the operator for electron torque about the point $\mathbf{r}_0$, to second order in the magnetic field, becomes

$$K_{n\alpha}^{BB}(\mathbf{r}_0) = \left[\epsilon_{\alpha\beta\gamma}\bar{\chi}_{\beta\delta}^{\mathrm{d}}(\mathbf{r}_0) + \epsilon_{\alpha\beta\delta}\bar{\chi}_{\gamma\beta}^{\mathrm{d}}(\mathbf{r}_0)\right] B_\gamma B_\delta, \tag{37}$$

which has a non vanishing (diamagnetic) expectation value over real reference state functions.

The operator for the torque on the clamped nuclei is

$$\begin{aligned}\mathbf{K}_N(\mathbf{r}_0) &= \sum_{I=1}^{N}(\mathbf{R}_I - \mathbf{r}_0)\times\mathbf{F}_I^n + \sum_{I=1}^{N} Z_I e(\mathbf{R}_I - \mathbf{r}_0)\times\mathbf{E} \\ &\equiv \mathbf{K}_N^n(\mathbf{r}_0) + \mathbf{K}_N^E(\mathbf{r}_0),\end{aligned} \tag{38}$$

so that

$$\mathbf{K}_N^n(\mathbf{r}_0) = -\mathbf{K}_n^N(\mathbf{r}_0), \tag{39}$$

and

$$\mathbf{K}_N(\mathbf{r}_0) = -\mathbf{K}_n(\mathbf{r}_0) + \mathcal{D}(\mathbf{r}_0)\times\mathbf{E} + \mathbf{K}_n^B(\mathbf{r}_0) + \mathcal{K}_n^B(\mathbf{r}_0) + \mathbf{K}_n^{BB}(\mathbf{r}_0). \tag{40}$$

Denoting by

$$\mathbf{K}_n^{EXT} = \mathbf{K}_n^E + \mathbf{K}_n^B + \mathcal{K}_n^B + \mathbf{K}_n^{BB}$$

the operator for the total torque exerted on the electrons by the external fields, one also has

$$\mathbf{K}_n = -\mathbf{K}_N^n + \mathbf{K}_n^{EXT}. \tag{41}$$

If the hypervirial theorems for the operators $\mathbf{R}$ and $\boldsymbol{\Pi}$, *i.e.*, the velocity and force theorems [32] for the electrons in the ψ_a state are satisfied,

$$\left\langle\psi_a\left|\frac{i}{\hbar}[H,\mathbf{R}]\right|\psi_a\right\rangle = m_e^{-1}\langle\psi_a|\boldsymbol{\Pi}|\psi_a\rangle = \mathbf{0}, \tag{42}$$

$$\left\langle\psi_a\left|\frac{i}{\hbar}[H,\boldsymbol{\Pi}]\right|\psi_a\right\rangle = \langle\psi_a|\mathbf{F}_n|\psi_a\rangle = \mathbf{0}, \tag{43}$$

then, from formula (28), the average force on the nuclei is

$$\langle\psi_a|F_{N\alpha}|\psi_a\rangle = qE_\alpha, \tag{44}$$

and, owing to eq. (30), one also has

$$\langle\psi_a|F_{N\alpha}^n|\psi_a\rangle = \left\langle\psi_a\left|F_{n\alpha}^{EXT}\right|\psi_a\right\rangle = -en\mathbf{E}, \tag{45}$$

i.e., the expectation value of the total force exerted by the electrons upon the nuclei equals the average force exerted on the electrons by the external fields. In other words, eqs. (43) and (45) state that the average force acting upon the electron cloud vanishes, as it is entirely transmitted to the nuclei.

If the hypervirial theorem for total electronic angular momentum

$$\Lambda = \sum_{i=1}^{n} \mathbf{r}_i \times \boldsymbol{\pi}_i, \tag{46}$$

i.e., the torque theorem [32] for the electrons in the ψ_a state is satisfied,

$$\left\langle \psi_a \left| \frac{i}{\hbar} [H, \Lambda] \right| \psi_a \right\rangle = \langle \psi_a | \mathbf{K}_n | \psi_a \rangle = \mathbf{0}, \tag{47}$$

then, from formula (40), the average torque on the nuclei about the point $\mathbf{r}_0$ is

$$\begin{aligned} \langle \psi_a | K_{N\alpha}(\mathbf{r}_0) | \psi_a \rangle &= \epsilon_{\alpha\beta\gamma} \langle \psi_a | \mathcal{D}_\beta(\mathbf{r}_0) | \psi_a \rangle E_\gamma + \epsilon_{\alpha\beta\gamma} \langle \psi_a | m_\beta(\mathbf{r}_0) | \psi_a \rangle B_\gamma \\ &\quad - \frac{2im_e c}{e\hbar} \left\langle \psi_a \left| \left[H^{(0)}, \bar{\chi}^{\mathrm{d}}_{\alpha\beta}(\mathbf{r}_0) \right] \right| \psi_a \right\rangle B_\beta \\ &\quad + \left[\epsilon_{\alpha\beta\gamma} \left\langle \psi_a \left| \bar{\chi}^{\mathrm{d}}_{\beta\delta}(\mathbf{r}_0) \right| \psi_a \right\rangle \right. \\ &\quad \left. + \epsilon_{\alpha\beta\delta} \left\langle \psi_a \left| \bar{\chi}^{\mathrm{d}}_{\gamma\beta}(\mathbf{r}_0) \right| \psi_a \right\rangle \right] B_\gamma B_\delta. \end{aligned} \tag{48}$$

In addition, from eq. (41), one has a result analogous to (45),

$$\langle \psi_a | K^n_{N\alpha} | \psi_a \rangle = \left\langle \psi_a \left| K^{EXT}_{n\alpha} \right| \psi_a \right\rangle, \tag{49}$$

i.e., the average torque exerted by the external fields on the electron cloud vanishes, see eq. (47), for it is fully transmitted to the nuclei.

III Rototranslational sum rules for geometrical derivatives of electric properties and the Hellmann-Feynman theorem

One can now use the fundamental equations (44) and (48) to obtain a series of constraints to all orders in the perturbing electric field. We will see that they provide conditions for translational and rotational invariance of permanent electric dipole moment, dipole polarizabilities and hyperpolarizabilities. From the Hellmann-Feynman theorem [32] one has, for the electric forces,

$$-\sum_{I=1}^{N} \nabla_I W = \left\langle -\sum_{I=1}^{N} \nabla_I H \right\rangle = \langle \mathbf{F}_N \rangle, \tag{50}$$

so that, from eqs. (1), (2) and (44), the conditions for translational invariance through fourth order in E_α are

$$\sum_{I=1}^{N} \nabla_{I\alpha} \mathcal{M}^{(0)}_\beta = q\delta_{\alpha\beta}, \tag{51}$$

$$\sum_{I=1}^{N} \nabla_{I\alpha} \alpha_{\beta\gamma} = 0, \tag{52}$$

$$\sum_{I=1}^{N} \nabla_{I\alpha} \beta_{\beta\gamma\delta} = 0, \tag{53}$$

$$\sum_{I=1}^{N} \nabla_{I\alpha} \gamma_{\beta\gamma\delta\epsilon} = 0. \tag{54}$$

These formulae are a consequence of the linear dependence on $\mathbf{E}$ of the total force (44), and are directly obtained from the definitions for the response tensors [16], explicitly showing translational invariance. The rotational constraint is less trivial. The torque due to electric forces, compare for eq. (48), is similarly obtained by the Hellmann-Feynman theorem,

$$-\sum_{I=1}^{N} \mathbf{R}_I \times \nabla_I W = \left\langle -\sum_{I=1}^{N} \mathbf{R}_I \times \nabla_I H \right\rangle = \langle \mathcal{D} \rangle \times \mathbf{E}, \tag{55}$$

and the conditions for rotational invariance are, from eqs. (1) and (2),

$$\sum_{I=1}^{N} \epsilon_{\alpha\beta\gamma} R_{I\beta} \nabla_{I\gamma} \mathcal{M}_{\delta}^{(0)} = \epsilon_{\alpha\beta\delta} \mathcal{M}_{\beta}^{(0)}, \tag{56}$$

$$\sum_{I=1}^{N} \epsilon_{\alpha\beta\gamma} R_{I\beta} \nabla_{I\gamma} \alpha_{\delta\epsilon} = \epsilon_{\alpha\beta\delta} \alpha_{\beta\epsilon} + \epsilon_{\alpha\beta\epsilon} \alpha_{\delta\beta}, \tag{57}$$

$$\sum_{I=1}^{N} \epsilon_{\alpha\beta\gamma} R_{I\beta} \nabla_{I\gamma} \beta_{\delta\epsilon\eta} = \epsilon_{\alpha\beta\delta} \beta_{\beta\epsilon\eta} + \epsilon_{\alpha\beta\epsilon} \beta_{\delta\beta\eta} + \epsilon_{\alpha\beta\eta} \beta_{\delta\epsilon\beta}, \tag{58}$$

$$\sum_{I=1}^{N} \epsilon_{\alpha\beta\gamma} R_{I\beta} \nabla_{I\gamma} \gamma_{\delta\epsilon\eta\zeta} = \epsilon_{\alpha\beta\delta} \gamma_{\beta\epsilon\eta\zeta} + \epsilon_{\alpha\beta\epsilon} \gamma_{\delta\beta\eta\zeta} + \epsilon_{\alpha\beta\eta} \gamma_{\delta\epsilon\beta\zeta} + \epsilon_{\alpha\beta\zeta} \gamma_{\delta\epsilon\eta\beta}. \tag{59}$$

Therefore there are only $3N-6$ ($3N-5$ for linear molecules) linearly independent (Cartesian) geometrical derivatives of the response tensors appearing in eqs. (1) and (2), and, more generally, of any molecular property.

IV Electric shielding and hypershielding at the nuclei

The Hellmann-Feynman theorem can also be used to outline the connections between the geometrical derivatives of permanent electric dipole moment, po-

larizabilities and hyperpolarizabilities, and electric shieldings and hypershieldings at the nuclei. The electric field induced on nucleus I can be written as a Taylor series [28,29] in the same way as (1) and (2),

$$\begin{aligned}\Delta\langle E^n_{I\alpha}\rangle &= -\gamma^I_{\alpha\beta}E_\beta + \frac{1}{2}\phi^I_{\alpha,\beta\gamma}E_\beta E_\gamma \\ &+\frac{1}{6}\eta^I_{\alpha,\beta\gamma\delta}E_\beta E_\gamma E_\delta \\ &+\frac{1}{24}\zeta^I_{\alpha,\beta\gamma\delta\epsilon}E_\beta E_\gamma E_\delta E_\epsilon + \ldots \\ &+\frac{1}{2}\rho^I_{\alpha,\beta\gamma}B_\beta B_\gamma + \ldots, \end{aligned} \tag{60}$$

so that the total field acting on the nucleus is

$$\langle E_{I\alpha}\rangle = \left\langle E^{(0)}_{I\alpha}\right\rangle + E_\alpha + \Delta\langle E^n_{I\alpha}\rangle, \tag{61}$$

where $\left\langle E^{(0)}_{I\alpha}\right\rangle$ (the electric field at nucleus I in the absence of external perturbation) vanishes for the equilibrium geometry. By applying the Hellmann-Feynman theorem one finds from eqs. (1) and (60)

$$Z_I e\left\langle E^{(0)}_{I\alpha}\right\rangle \equiv \left\langle -\nabla_{I\alpha}H^{(0)}\right\rangle, \tag{62}$$

and the equations connecting nuclear electric shielding and hypershieldings to geometrical derivatives of polarizabilities and hyperpolarizabilities are

$$\begin{aligned} Z_I e\,(\delta_{\alpha\beta} - \gamma^I_{\alpha\beta}) &\equiv \nabla_{I\alpha}\mathcal{M}^{(0)}_\beta \\ Z_I e\,\phi^I_{\alpha,\beta\gamma} &\equiv \nabla_{I\alpha}\alpha_{\beta\gamma} \\ Z_I e\,\eta^I_{\alpha,\beta\gamma\delta} &\equiv \nabla_{I\alpha}\beta_{\beta\gamma\delta} \\ Z_I e\,\zeta^I_{\alpha,\beta\gamma\delta} &\equiv \nabla_{I\alpha}\gamma_{\beta\gamma\delta\epsilon}. \end{aligned} \tag{63}$$

Explicit definitions for the various nuclear shieldings can now be obtained exploiting again the Hellmann-Feynman theorem. To this end let us use the force and torque theorems (43) and (47), and introduce the expression for the electronic wavefunction in the presence of perturbing fields,

$$\psi_a = \psi^{(0)}_a + \lambda\psi^{(1)}_a + \lambda^2\psi^{(2)}_a + \ldots. \tag{64}$$

The general Rayleigh-Schrödinger formulae for the perturbed wave functions are [33, 34]

$$\left|\psi^{(1)}_a\right\rangle = -\frac{1}{\hbar}\sum_{j\neq a}\omega^{-1}_{ja}\,|j\rangle\left\langle j\left|H^{(1)}\right|a\right\rangle, \tag{65}$$

$$\begin{aligned}\left|\psi_a^{(2)}\right\rangle &= \frac{1}{\hbar^2}\sum_{j\neq a}\sum_{k\neq a}\omega_{ja}^{-1}\omega_{ka}^{-1}\left|j\right\rangle\left\langle j\left|H^{(1)}\right|k\right\rangle\left\langle k\left|H^{(1)}\right|a\right\rangle \\ &\quad -\frac{1}{\hbar^2}\sum_{j\neq a}\omega_{ja}^{-2}\left|j\right\rangle\left\langle a\left|H^{(1)}\right|a\right\rangle\left\langle j\left|H^{(1)}\right|a\right\rangle \\ &\quad -\frac{1}{2\hbar^2}\left|a\right\rangle\sum_{j\neq a}\omega_{ja}^{-2}\left\langle a\left|H^{(1)}\right|j\right\rangle\left\langle j\left|H^{(1)}\right|a\right\rangle, \end{aligned} \tag{66}$$

denoting by

$$\left|j\right\rangle \equiv \left|\psi_a^{(0)}\right\rangle, \quad H^{(0)}\left|j\right\rangle = W_j^{(0)}\left|j\right\rangle, \quad \hbar\omega_{ja} = W_j^{(0)} - W_a^{(0)}. \tag{67}$$

To zero order in $\lambda \equiv E_\alpha$ one has the condition for translational invariance

$$\left\langle\psi_a^{(0)}\left|\mathbf{F}_n^N\right|\psi_a^{(0)}\right\rangle = \mathbf{0}, \tag{68}$$

and to first order,

$$\left(\left\langle\psi_a^{(0)}\left|\mathbf{F}_n^N\right|\psi_a^{(1)}\right\rangle + c.c.\right) + \mathbf{F}_n^E = \mathbf{0}. \tag{69}$$

The first-order perturbed function in the presence of electric field is

$$\left|\psi_a^{E_\alpha}\right\rangle = \frac{1}{\hbar}\sum_{j\neq a}\omega_{ja}^{-1}\left|j\right\rangle\left\langle j\left|\mu_\alpha\right|a\right\rangle. \tag{70}$$

Introducing the definition for the electric shielding [27] of nucleus I,

$$\gamma_{\alpha\beta}^I = \frac{1}{\hbar}\sum_{j\neq a}\frac{2}{\omega_{ja}}\Re(\left\langle a\left|E_{I\alpha}^n\right|j\right\rangle\left\langle j\left|\mu_\beta\right|a\right\rangle) \tag{71}$$

one obtains [29] from (69) the Thomas-Reiche-Kuhn sum rule in mixed length-acceleration gauge as a condition for translational invariance to first order in $\mathbf{E}$,

$$\sum_{I=1}^{N} Z_I\gamma_{\alpha\beta} = n\delta_{\alpha\beta}. \tag{72}$$

This constraint has a far-reaching nature and synthesizes several aspects [29]. Owing to eqs. (27) and (45), it also furnishes the condition for complete transmission to the nuclei of the average external force acting on the electrons. The second-order function is

$$\begin{aligned}\left|\psi_a^{E_\alpha E_\beta}\right\rangle &= \frac{1}{\hbar^2}\sum_{j\neq a}\sum_{k\neq a}\omega_{ja}^{-1}\omega_{ka}^{-1}\left|j\right\rangle\left\langle j\left|\mu_\alpha\right|k\right\rangle\left\langle k\left|\mu_\beta\right|a\right\rangle \\ &\quad -\frac{1}{\hbar^2}\sum_{j\neq a}\omega_{ja}^{-2}\left|j\right\rangle\left\langle a\left|\mu_\alpha\right|a\right\rangle\left\langle j\left|\mu_\beta\right|a\right\rangle \\ &\quad -\frac{1}{2\hbar^2}\left|a\right\rangle\sum_{j\neq a}\omega_{ja}^{-2}\left\langle a\left|\mu_\alpha\right|j\right\rangle\left\langle j\left|\mu_\beta\right|a\right\rangle, \end{aligned} \tag{73}$$

so that, by defining the hypershielding

$$\begin{aligned}\phi^I_{\alpha,\beta\gamma} &= \mathbf{S}(E^n_{I\alpha},\mu_\beta,\mu_\gamma)\frac{1}{\hbar^2}\sum_{j\neq a}\omega_{ja}^{-1}\left(\sum_{k\neq a}\langle a|E^n_{I\alpha}|j\rangle\right.\\ &\quad\times\langle j|\mu_\beta|k\rangle\langle k|\mu_\gamma|a\rangle\omega_{ka}^{-1}\\ &\quad\left.-\langle a|E^n_{I\alpha}|a\rangle\langle a|\mu_\beta|j\rangle\langle j|\mu_\gamma|a\rangle\omega_{ja}^{-1}\right),\end{aligned}\tag{74}$$

where the symbol $\mathbf{S}(...)$ implies a summation of all the terms in which the operators within brackets are permuted, the second-order condition from eq. (43) becomes, compare for eq. (52) and the second of eqs. (63),

$$\sum_{I=1}^{N} Z_I\phi^I_{\alpha,\beta\gamma} = 0.\tag{75}$$

This equation also establishes that the average force on electrons, due to the external electric fields, vanishes to second order in E_α; thus, according to theorem (45), the electrons do not transfer any force to the nuclei.

The conditions for rotational invariance from eq. (48) are, for an arbitrary origin of coordinates,

$$\sum_{I=1}^{N} Z_I e\epsilon_{\alpha\lambda\mu}R_{I\lambda}\gamma^I_{\mu\delta} = \epsilon_{\alpha\delta\beta}\langle a|\mu_\beta|a\rangle,\tag{76}$$

$$\sum_{I=1}^{N} Z_I e\epsilon_{\alpha\beta\gamma}R_{I\beta}\phi^I_{\gamma,\delta\epsilon} = \epsilon_{\alpha\beta\delta}\alpha_{\beta\epsilon} + \epsilon_{\alpha\beta\epsilon}\alpha_{\beta\delta},\tag{77}$$

and the connection with the Hellmann-Feynman geometrical derivative of electric polarizability, see also eq. (57), is obtained via the second of eqs. (63).

According to these equations, compare for theorem (49), the average torque due to the external electric fields, transferred from the electrons to the nuclei, is

$$\sum_{I=1}^{N} Z_I e\epsilon_{\alpha\beta\gamma}R_{I\beta}\gamma^I_{\gamma\delta}E_\delta,$$

and

$$\frac{1}{2}\sum_{I=1}^{N} Z_I e\epsilon_{\alpha\beta\gamma}R_{I\beta}\phi^I_{\gamma,\delta\epsilon}E_\delta E_\epsilon,$$

respectively to first and second order in E_α.

Eventually, extending the procedure of Ref. [35], one can see that the electric dipole moment induced by an external electric field and the dispacement $\mathbf{X}_I = \mathbf{R}_I - \mathbf{R}_I^{(0)}$ of nucleus I from equilibrium can be expressed via the hypershielding tensor,

$$\Delta\langle\mu_\alpha\rangle = -Z_I e\phi_{\beta,\alpha\gamma}X_{I\beta}E_\gamma.\tag{78}$$

V Generalization to geometrical derivatives of arbitrary second-order properties

The procedure based on the Hellmann-Feynman theorem could be extended to obtain sum rules for geometrical derivatives of magnetic susceptibilites. One should observe that the magnetic Lorentz forces on electrons and nuclei are not of the forms $\mathbf{F}_i = -\nabla_i H$ and $\mathbf{F}_I = -\nabla_I H$. For instance, the derivative of the Hamiltonian, compare for the the phenomenological term (11), would yield just one half of the actual magnetic force on unclamped nuclei: magnetic Lorentz forces are in fact obtained as derivatives of generalized velocity-dependent potentials [36]. On the other hand, as the operators involved are merely (26) and (38), the rototranslational sum rules could in fact be obtained via the Hellmann-Feynman theorem, using relationships similar to (50) and (55), also for magnetic properties. However, a different and more general approach, based on the definitions for geometrical derivatives of expectation values [37] and second-order properties [38], will be used in this Section. In any event we will see that the rototranslational constraints for magnetic susceptibilities are formally identical to those relative to electric polarizabilities, compare for eqs. (52) and (57).

The geometrical derivative of the expectation value over the (equilibrium) reference state, for a property Q, which does not depend on nuclear coordinates, is [37]

$$\frac{\partial}{\partial \mathbf{R}_I} \langle a | Q | a \rangle = 2\Re \left\langle \frac{\partial a}{\partial \mathbf{R}_I} | Q | a \right\rangle , \tag{79}$$

and the Hellmann-Feynman gradient of the electronic wavefunction with respect to nuclear displacements is [39]

$$|\nabla_I a\rangle = \frac{1}{\hbar} \sum_{j \neq a} |j\rangle \langle j | \mathbf{F}_I^n | a \rangle \omega_{ja}^{-1} . \tag{80}$$

From these expressions one finds the Hellmann-Feynman gradient of the expectation value

$$\nabla_{I\alpha} \langle a | Q | a \rangle = \frac{1}{\hbar} \sum_{j \neq a} 2\omega_{ja}^{-1} \Re(\langle a | F_{I\alpha}^n | j \rangle \langle j | Q | a \rangle) . \tag{81}$$

The translational and rotational sum rules for these derivatives are respectively [37]

$$\sum_{I=1}^{N} \nabla_{I\alpha} \langle a | Q | a \rangle = \frac{i}{\hbar} \langle a | [P_\alpha, Q] | a \rangle , \tag{82}$$

$$\sum_{I=1}^{N} \epsilon_{\alpha\beta\gamma} R_{I\beta} \nabla_{I\gamma} \langle a | Q | a \rangle = \frac{i}{\hbar} \langle a | [L_\alpha, Q] | a \rangle . \tag{83}$$

These formulae are easily obtained via off-diagonal hypervirial relations [37]. Accordingly, only $3N$-6 ($3N$-5 for linear molecules) gradients $\nabla_I \langle a | Q | a \rangle$ are linearly independent.

A formula similar to (79) gives the derivatives of the electronic wavefunction with respect to angular displacements of the nuclei from their equilibrium value. The interaction energy between electrons and nuclei, compare for the unperturbed electronic Hamiltonian (7),

$$V_{nN} = -\sum_{I=1}^{N} \sum_{i=1}^{n} \frac{Z_I e^2}{|\mathbf{r_i} - \mathbf{R_I}|},$$

for small angular displacements $\boldsymbol{\varphi}_I$ such that, to first order, the linear displacement of nucleus I is $\mathbf{d}_I = \boldsymbol{\varphi}_I \times \mathbf{R}_I^{(o)}$, can be written as a Taylor series

$$V_{nN} = V_{nN}^{(o)} - \sum_{I=1}^{N} \mathbf{K}_I^n \cdot \boldsymbol{\varphi}_I + \ldots , \tag{84}$$

where the torque $\mathbf{K}_I^n$ of the electrons upon nucleus I is now evaluated corresponding to the set of equilibrium positions $\{\mathbf{R}_I^{(o)}\}$ of the nuclei. An expansion similar to (84) holds for the BO electronic Hamiltonian (7) of the unperturbed molecule,

$$H^{(0)} = H_{(0)}^{(0)} + H_{(1)}^{(0)} + \ldots , \tag{85}$$

where

$$H_{(1)}^{(0)} = \sum_{I=1}^{N} \frac{\partial H^{(0)}}{\partial \boldsymbol{\varphi}_I} \cdot \boldsymbol{\varphi}_I, \quad \frac{\partial H^{(0)}}{\partial \boldsymbol{\varphi}_I} = -\mathbf{K}_I^n = \mathbf{K}_n^I. \tag{86}$$

Then, from perturbation theory, the corresponding first-order function evaluated at equilibrium is

$$\left| \frac{\partial a}{\partial \boldsymbol{\varphi}_I} \right\rangle = \frac{1}{\hbar} \sum_{j \neq a} |j\rangle \langle j | \mathbf{K}_I^n | a \rangle \omega_{ja}^{-1}, \tag{87}$$

This result is also established from the Hellmann-Feynman theorem, exploiting the canonical equation (86) and using arguments similar to those of Ref. [27]. The Hellmann-Feynman gradient of the observable Q, with respect to angular displacements of nucleus I, is therefore

$$\frac{\partial}{\partial \boldsymbol{\varphi}_I} \langle a | Q | a \rangle = \frac{1}{\hbar} \sum_{j \neq a} \frac{2}{\omega_{ja}} \Re(\langle a | \mathbf{K}_I^n | j \rangle \langle j | Q | a \rangle), \tag{88}$$

and, from the hypervirial relations [29], the relative constraint is

$$\sum_{I=1}^{N} \frac{\partial}{\partial \varphi_{I\alpha}} \langle a | Q | a \rangle = \frac{i}{\hbar} \langle a | [L_\alpha, Q] | a \rangle , \tag{89}$$

where the r.h.s. is the same as in sum rule (83).

For an arbitrary second-order electronic property,

$$(A, B)_{-1} = \frac{1}{\hbar} \sum_{j \neq a} \frac{2}{\omega_{ja}} \Re \left(\langle a | A | j \rangle \langle j | B | a \rangle \right), \tag{90}$$

where the operators A and B do not depend on nuclear coordinates, the Hellmann-Feynman derivative can be written [38]

$$\begin{aligned} \nabla_{I\alpha} (A, B)_{-1} \;=\; & \frac{2}{\hbar} \sum_{j \neq a} \omega_{ja}^{-1} \Re (\langle a' | A | j \rangle \langle j | B | a \rangle + \langle a | A | j' \rangle \langle j | B | a \rangle \\ & + \langle a | A | j \rangle \langle j' | B | a \rangle + \langle a | A | j \rangle \langle j | B | a' \rangle) \\ & + \frac{2}{\hbar^2} \sum_{j \neq a} \omega_{ja}^{-2} \Re \Big[\langle a | A | j \rangle \langle j | B | a \rangle \\ & \times \left(\left\langle a \left| H^{(0)\prime} \right| a \right\rangle - \left\langle j \left| H^{(0)\prime} \right| j \right\rangle \right) \Big]. \end{aligned} \tag{91}$$

If the Hellmann-Feynman theorem is satisfied,

$$\left\langle a \left| H^{(0)\prime} \right| a \right\rangle \equiv \nabla_I W_a^{(0)} = - \langle a | \mathbf{F}_I^n | a \rangle - \mathbf{F}_I^{N-I}, \tag{92}$$

so that the average force acting on nucleus I of an unperturbed molecule is identically vanishing for an equilibrium state, but, in general, $W_j^{(0)} \neq 0$ for $j \neq a$. At any rate, summing over I, the total force on the nuclei is zero, owing to eqs. (24) and (27), and to the force theorem (68) in the ideal case of exact eigenfunctions to a model Hamiltonian, *e.g.*, within the exact Hartree-Fock method. In order to evaluate the geometrical derivative (91) of a second-order property (90), let us slightly change the notation, rewriting the latter in the form

$$(A, B)_{-1} = -2 \sum_{j \neq 1} \Re \left(\frac{\langle 1 | A | j \rangle \langle j | B | 1 \rangle}{W_1^{(0)} - W_j^{(0)}} \right), \tag{93}$$

so that, differentiating under the conditions $\nabla_I A = \nabla_I B = 0$ gives

$$\nabla_I (A, B)_{-1} = -2 \sum_{j \neq 1} \Re \left(\frac{\langle 1' | A | j \rangle \langle j | B | 1 \rangle}{W_1^{(0)} - W_j^{(0)}} + \frac{\langle 1 | A | j \rangle \langle j | B | 1' \rangle}{W_1^{(0)} - W_j^{(0)}} \right)$$

$$-2\sum_{j\neq 1}\Re\left(\frac{\langle 1|A|j'\rangle\langle j|B|1\rangle}{W_1^{(0)}-W_j^{(0)}}+\frac{\langle 1|A|j\rangle\langle j'|B|1\rangle)}{W_1^{(0)}-W_j^{(0)}}\right)$$
$$+2\sum_{j\neq 1}\Re\left[\frac{\langle 1|A|j\rangle\langle j|B|1\rangle}{\left(W_1^{(0)}-W_j^{(0)}\right)^2}\left(\left\langle 1\left|\mathbf{F}_n^I\right|1\right\rangle-\left\langle j\left|\mathbf{F}_n^I\right|j\right\rangle\right)\right]. \tag{94}$$

Using eq. (80), the first line of (94) gives the term

$$\mathcal{A} \equiv -2\sum_{j\neq 1}\sum_{k\neq 1}\Re\left(\frac{\left\langle 1\left|\mathbf{F}_n^I\right|k\right\rangle\langle k|A|j\rangle\langle j|B|1\rangle}{\left(W_1^{(0)}-W_j^{(0)}\right)\left(W_1^{(0)}-W_k^{(0)}\right)}\right.$$
$$\left.+\frac{\langle 1|A|j\rangle\langle j|B|k\rangle\left\langle k\left|\mathbf{F}_n^I\right|j\right\rangle}{\left(W_1^{(0)}-W_j^{(0)}\right)\left(W_1^{(0)}-W_k^{(0)}\right)}\right), \tag{95}$$

and the second line can be rewritten

$$\mathcal{B} = \mathcal{C}+\mathcal{D}+\mathcal{E} \equiv -2\Re\left(\frac{\langle 1|A|2'\rangle\langle 2|B|1\rangle}{W_1^{(0)}-W_2^{(0)}}+\frac{\langle 1|A|3'\rangle\langle 3|B|1\rangle}{W_1^{(0)}-W_3^{(0)}}\right.$$
$$\left.+\frac{\langle 1|A|2\rangle\langle 2'|B|1\rangle}{W_1^{(0)}-W_2^{(0)}}+\frac{\langle 1|A|3\rangle\langle 3'|B|1\rangle}{W_1^{(0)}-W_3^{(0)}}+\ldots\right) \tag{96}$$

where, rearranging the denominators [40]

$$\frac{1}{\left(W_1^{(0)}-W_2^{(0)}\right)\left(W_2^{(0)}-W_3^{(0)}\right)}+\frac{1}{\left(W_1^{(0)}-W_3^{(0)}\right)\left(W_3^{(0)}-W_2^{(0)}\right)}$$
$$=\frac{1}{\left(W_1^{(0)}-W_2^{(0)}\right)\left(W_1^{(0)}-W_3^{(0)}\right)}, \tag{97}$$

etc., one has defined

$$\mathcal{C} \equiv 2\Re\left[\langle 1|A|1\rangle\left(\frac{\left\langle 1\left|\mathbf{F}_n^I\right|2\right\rangle\langle 2|B|1\rangle}{\left(W_1^{(0)}-W_2^{(0)}\right)^2}+\frac{\left\langle 1\left|\mathbf{F}_n^I\right|3\right\rangle\langle 3|B|1\rangle}{\left(W_1^{(0)}-W_3^{(0)}\right)^2}+\ldots\right)\right], \tag{98}$$

$$\mathcal{D} \equiv 2\Re\left[\langle 1|B|1\rangle\left(\frac{\langle 1|A|2\rangle\left\langle 2\left|\mathbf{F}_n^I\right|1\right\rangle}{\left(W_1^{(0)}-W_2^{(0)}\right)^2}+\frac{\langle 1|A|3\rangle\left\langle 3\left|\mathbf{F}_n^I\right|1\right\rangle}{\left(W_1^{(0)}-W_3^{(0)}\right)^2}+\ldots\right)\right], \tag{99}$$

$$\mathcal{E} \equiv -2\Re\left(\frac{\langle 1|A|2\rangle\left\langle 2\left|\mathbf{F}_n^I\right|3\right\rangle\langle 3|B|1\rangle}{\left(W_1^{(0)}-W_2^{(0)}\right)\left(W_1^{(0)}-W_3^{(0)}\right)}\right.$$
$$\left.+\frac{\langle 1|A|3\rangle\left\langle 3\left|\mathbf{F}_n^I\right|2\right\rangle\langle 2|B|1\rangle}{\left(W_1^{(0)}-W_2^{(0)}\right)\left(W_1^{(0)}-W_3^{(0)}\right)}\right). \tag{100}$$

The third line of (94) yields the contributions

$$\mathcal{F} \equiv 2\Re\left(\sum_{j\neq 1}\frac{\langle 1|A|j\rangle\langle j|B|1\rangle}{\left(W_1^{(0)}-W_j^{(0)}\right)^2}\left\langle 1\left|\mathbf{F}_n^I\right|1\right\rangle\right) \tag{101}$$

$$\mathcal{G} \equiv 2\Re\left(\sum_{j\neq 1}\frac{\langle 1|A|j\rangle\langle j|B|1\rangle}{\left(W_1^{(0)}-W_j^{(0)}\right)^2}\left\langle j\left|\mathbf{F}_n^I\right|j\right\rangle.\right) \tag{102}$$

We can now combine

$$\mathcal{E}+\mathcal{G}=\mathcal{H} \equiv -2\sum_{j\neq 1}\sum_{k\neq 1}\Re\left(\frac{\langle 1|A|k\rangle\left\langle k\left|\mathbf{F}_n^I\right|j\right\rangle\langle j|B|1\rangle}{\left(W_1^{(0)}-W_j^{(0)}\right)\left(W_1^{(0)}-W_k^{(0)}\right)}\right), \tag{103}$$

so that the final expression for the derivative, $\mathcal{A}+\mathcal{C}+\mathcal{D}+\mathcal{F}+\mathcal{H}$, becomes

$$\nabla_I(A,B)_{-1} = -\mathbf{S}(\mathbf{F}_I^n,A,B)\sum_{j\neq 1}\left(\sum_{k\neq 1}\frac{\langle 1|\mathbf{F}_I^n|j\rangle\langle j|A|k\rangle\langle k|B|1\rangle}{\left(W_1^{(0)}-W_j^{(0)}\right)\left(W_1^{(0)}-W_k^{(0)}\right)}\right.$$
$$\left.-\frac{\langle 1|A|j\rangle\langle j|B|1\rangle}{\left(W_1^{(0)}-W_j^{(0)}\right)^2}\langle 1|\mathbf{F}_I^n|1\rangle\right). \tag{104}$$

One eventually rewrites the final formula for the Hellmann-Feynman derivative of a second-order property [38]

$$\nabla_{I\alpha}(A,B)_{-1} = \mathbf{S}(F_{I\alpha}^n,A,B)\left[\frac{1}{\hbar^2}\sum_{j\neq a}\omega_{ja}^{-1}\right.$$
$$\times\left(\sum_{k\neq a}\omega_{ka}^{-1}\langle a|F_{I\alpha}^n|j\rangle\langle j|A|k\rangle\langle k|B|a\rangle\right.$$
$$\left.\left.-\omega_{ja}^{-1}\langle a|F_{I\alpha}^n|a\rangle\langle a|A|j\rangle\langle j|B|a\rangle\right)\right] \tag{105}$$

Incidentally, in the case of electric dipole polarizability $\alpha_{\alpha\beta} = (\mu_\alpha, \mu_\beta)_{-1}$, this equation can be used to check the second of eqs. (63), and its consistency with definition (74) for nuclear electric hypershielding obtained via the force theorem (43). For the magnetic susceptibility

$$\chi_{\alpha\beta} = \chi^{\mathrm{d}}_{\alpha\beta} + \chi^{\mathrm{p}}_{\alpha\beta}, \tag{106}$$

$$\chi_{\alpha\beta} = \langle a | \bar{\chi}_{\alpha\beta} | a \rangle , \qquad \chi^{\mathrm{p}}_{\alpha\beta} = \frac{e^2}{4m_e^2c^2} (L_\alpha, L_\beta)_{-1} , \tag{107}$$

using eqs. (81), (91) and (105), one finds the connection between geometrical derivatives and nuclear electric shielding in the presence of magnetic field appearing in eq. (60),

$$\frac{1}{Z_I e} \nabla_{I\alpha} \chi^{\mathrm{d}}_{\beta\gamma} \equiv \rho^{I\mathrm{d}}_{\alpha,\beta\gamma} = \frac{1}{\hbar} \sum_{j \neq a} 2\omega_{ja}^{-1} \Re \left(\langle a | E^n_{I\alpha} | j \rangle \left\langle j \left| \bar{\chi}^{\mathrm{d}}_{\beta\gamma} \right| a \right\rangle \right) , \tag{108}$$

$$\begin{aligned} \frac{1}{Z_I e} \nabla_{I\alpha} \chi^{\mathrm{p}}_{\beta\gamma} \equiv \rho^{I\mathrm{p}}_{\alpha,\beta\gamma} \;=\; & \mathbf{S}(E^n_{I\alpha}, m_\beta, m_\gamma) \frac{1}{\hbar^2} \sum_{j \neq a} \omega_{ja}^{-1} \left(\sum_{k \neq a} \langle a | E^n_{I\alpha} | j \rangle \right. \\ & \times \langle j | m_\beta | k \rangle \langle k | m_\gamma | a \rangle \omega_{ka}^{-1} \\ & \left. - \langle a | E^n_{I\alpha} | a \rangle \langle a | m_\beta | j \rangle \langle j | m_\gamma | a \rangle \omega_{ja}^{-1} \right). \end{aligned} \tag{109}$$

Therefore the total electric hypershielding of nucleus I in the presence of magnetic field is a sum of diamagnetic and paramagnetic contributions,

$$\rho^{I}_{\alpha,\beta\gamma} = \rho^{I\mathrm{d}}_{\alpha,\beta\gamma} + \rho^{I\mathrm{p}}_{\alpha,\beta\gamma} \equiv \frac{1}{Z_I e} \nabla_{I\alpha} \chi_{\beta\gamma}. \tag{110}$$

From the hypervirial relation [29]

$$i\omega_{ja} \langle j | \mathbf{P} | a \rangle = \left\langle j \left| \mathbf{F}^N_n \right| a \right\rangle , \tag{111}$$

and since the diagonal elements of pure imaginary Hermitian operators vanish, one has

$$\left| \sum_{I=1}^{N} \nabla_{I\alpha} a \right\rangle = -\frac{i}{\hbar} | P_\alpha a \rangle . \tag{112}$$

Accordingly, the condition for translational invariance of an arbitrary second-order property is obtained from the first two lines of (91),

$$\sum_{I=1}^{N} \nabla_{I\alpha} (A,B)_{-1} = \frac{1}{\hbar} \sum_{j \neq a} \frac{2}{\omega_{ja}} \Re \left(\left\langle a \left| \frac{i}{\hbar} [P_\alpha, A] \right| j \right\rangle \langle j | B | a \rangle + \langle a | A | j \rangle \left\langle j \left| \frac{i}{\hbar} [P_\alpha, B] \right| a \right\rangle \right). \quad (113)$$

The rotational constraint is similarly found. From the hypervirial relation [29]

$$i\omega_{ja} \langle j | \mathbf{L} | a \rangle = \left\langle j \left| \mathbf{K}_n^N \right| a \right\rangle, \quad (114)$$

one finds

$$\sum_{I=1}^{N} \epsilon_{\alpha\beta\gamma} R_{I\beta} | \nabla_{I\gamma} a \rangle = -\frac{i}{\hbar} | L_\alpha a \rangle, \quad (115)$$

and

$$\sum_{I=1}^{N} \epsilon_{\alpha\beta\gamma} R_{I\beta} \nabla_{I\gamma} (A,B)_{-1} = \frac{1}{\hbar} \sum_{j \neq a} \frac{2}{\omega_{ja}} \Re \left(\left\langle a \left| \frac{i}{\hbar} [L_\alpha, A] \right| j \right\rangle \langle j | B | a \rangle + \langle a | A | j \rangle \left\langle j \left| \frac{i}{\hbar} [L_\alpha, B] \right| a \right\rangle \right). \quad (116)$$

These rototranslational sum rules can be applied to any second-order property, for instance formulae (52) and (57) for the electric dipole polarizability $\alpha_{\alpha\beta} = (\mu_\alpha, \mu_\beta)_{-1}$ are immediately obtained from eq. (113) and (116). For the mixed dipole-quadrupole polarizability [16] $A_{\delta,\beta\gamma} = (\mu_\delta, \Theta_{\beta\gamma})_{-1}$ one finds from eq. (113)

$$\sum_{I=1}^{N} \nabla_{I\alpha} A_{\delta,\beta\gamma} = \frac{3}{2} \alpha_{\delta\gamma} \delta_{\alpha\beta} + \frac{3}{2} \alpha_{\delta\beta} \delta_{\alpha\gamma} - \alpha_{\delta\alpha} \delta_{\beta\gamma}. \quad (117)$$

This result should be matched with eq. (259) of Ref. [29], which describes the change in $A_{\delta,\beta\gamma}$ due to a *passive* coordinate transformation. The different sign appearing on the r.h.s. of eq. (117) accounts for the *active* nature of the transformation (in which the coordinate frame is left unchanged) generated by the translation operator, compare, in followings, for eq. (127). For the magnetic susceptibility, using eqs. (113) and the expression for the geometric derivative of expectation values (82), one finds

$$\sum_{I=1}^{N} \nabla_{I\delta} \chi_{\alpha\beta} = \frac{e^2}{4 m_e c^2} \left\{ m_e^{-1} \left[(P_\gamma, L_\beta)_{-1} \epsilon_{\alpha\delta\gamma} + (L_\alpha, P_\gamma)_{-1} \epsilon_{\beta\delta\gamma} \right] - 2 \langle a | R_\delta | a \rangle \delta_{\alpha\beta} + \langle a | R_\alpha | a \rangle \delta_{\beta\delta} + \langle a | R_\beta | a \rangle \delta_{\alpha\delta} \right\}. \quad (118)$$

The expression within curly brackets identically vanishes if the hypervirial theorem (42) for $\mathbf{R}$ is fulfilled, *i.e.*,

$$\langle a\,|R_\alpha|\,j\rangle = \frac{i}{m_e}\omega_{ja}^{-1}\,\langle a\,|P_\alpha|\,j\rangle\,, \tag{119}$$

so that

$$(P_\alpha, L_\beta)_{-1} = m_e\epsilon_{\alpha\beta\gamma}\,\langle a\,|R_\gamma|\,a\rangle\,, \tag{120}$$

and eq. (118) is therefore analogous to eq. (52) for electric polarizabilities.

One should observe the difference between eq. (118) and relationships which describe variations of the magnetic susceptibility arising in a gauge transformation of the vector potential (which amounts to a passive change of origin), compare for eqs. (268) and (269) of Ref. [29]. In the coordinate transformation

$$\mathbf{r}' \rightarrow \mathbf{r}'' = \mathbf{r}' + \mathbf{d}, \tag{121}$$

the diamagnetic and paramagnetic contributions to the susceptibility transform [29]

$$\begin{aligned}\chi^{\mathrm{p}}_{\alpha\beta}(\mathbf{r}'') &= \chi^{\mathrm{p}}_{\alpha\beta}(\mathbf{r}') + \frac{e^2}{4m_e^2c^2}\Big\{d_\delta\Big[\epsilon_{\alpha\gamma\delta}\Big(P_\gamma, L_\beta(\mathbf{r}')\Big)_{-1} + \epsilon_{\beta\gamma\delta}\Big(P_\gamma, L_\alpha(\mathbf{r}')\Big)_{-1}\Big] \\ &\quad + \epsilon_{\alpha\gamma\delta}\epsilon_{\beta\lambda\mu}d_\delta d_\mu\Big(P_\gamma, P_\lambda\Big)_{-1}\Big\},\end{aligned} \tag{122}$$

$$\begin{aligned}\chi^{\mathrm{d}}_{\alpha\beta}(\mathbf{r}'') &= \chi^{\mathrm{d}}_{\alpha\beta}(\mathbf{r}') + \frac{e^2}{4m_ec^2}\{2\,\langle a\,|R_\gamma(\mathbf{r}')|\,a\rangle\,d_\gamma\delta_{\alpha\beta} - \langle a\,|R_\alpha(\mathbf{r}')|\,a\rangle\,d_\beta \\ &\quad - \langle a\,|R_\beta(\mathbf{r}')|\,a\rangle\,d_\alpha - nd_\gamma d_\gamma\delta_{\alpha\beta} + nd_\alpha d_\beta\},\end{aligned} \tag{123}$$

so that, owing to the Thomas-Reiche-Kuhn sum rule in the velocity formalism,

$$(P_\alpha, P_\beta)_{-1} = m_e n\delta_{\alpha\beta}, \tag{124}$$

(exactly satisfied if the hypervirial relation (119) is fulfilled) and to constraint (120), the total susceptibility $\chi_{\alpha\beta}$ is translationally invariant. One can remark that

(i) terms quadratic in the origin translation $\mathbf{d}$, appearing in eq. (122) and (123), are not present in (118)

(ii) similar terms have opposite sign in these equations. These differences are easily understood: the active transformation (118) of the susceptibility tensor does not formally involve a corresponding transformation of the vector potential (16). One also finds, from eq. (82) and (113),

$$\sum_{I=1}^{N}\nabla_{I\alpha}\,(P_\beta, L_\gamma)_{-1} = nm_e\epsilon_{\alpha\beta\gamma} = m_e\sum_{I=1}^{N}\epsilon_{\beta\gamma\delta}\nabla_{I\alpha}\,\langle a\,|R_\delta|\,a\rangle\,. \tag{125}$$

The rotational sum rules for paramagnetic and diamagnetic contributions to magnetizability are found respectively from eq. (116) and from the expression for expectation values, see eq. (83). The equation for the total property, analogous to (57), is

$$\sum_{I=1}^{N} \epsilon_{\alpha\beta\gamma} R_{I\beta} \nabla_{I\gamma} \chi_{\delta\epsilon} = \epsilon_{\alpha\beta\delta} \chi_{\beta\epsilon} + \epsilon_{\alpha\beta\epsilon} \chi_{\delta\beta}, \tag{126}$$

and similar formulae hold separately for diamagnetic and paramagnetic contributions.

The conditions for rototranslational invariance established so far are exactly satisfied in the case of molecular electronic wavefunctions obeying the Hellmann-Feynman theorem at least locally, *i.e.* in the environment of the nuclei. Accordingly they can be used within the algebraic approximation to test the quality of a basis set and its ability to furnish, for instance, nuclear electric hypershieldings (74) and related geometrical derivatives of polarizability via eqs. (63).

It is however important to realize that essentially *the same formulae are to be exactly obeyed, irrespective of the features of the basis set, if the geometrical derivatives are calculated analytically, i.e.*, via direct differentiation of the electronic wavefunction [21]. In this case the rototranslational condition are not useful to gauge the quality of the basis set, but serve to test a computer program for analytical geometrical derivatives. To prove this statement let us introduce the operators

$$\mathcal{T}_N(\mathbf{d}) = \exp\left(\frac{i}{\hbar} \sum_{I=1}^{N} \mathbf{d} \cdot \mathbf{P}_I\right), \tag{127}$$

and

$$\mathcal{R}_N(\boldsymbol{\theta}) = \exp\left(\frac{i}{\hbar} \sum_{I=1}^{N} \boldsymbol{\theta} \cdot \mathbf{L}_I\right), \qquad \boldsymbol{\theta} = \theta \mathbf{n}_\theta, \tag{128}$$

which respectively generate a rigid translation $\mathbf{d}$ and a rigid rotation of the nuclear framework through an angle θ about the $\mathbf{n}_\theta$ axis. Incidentally we observe that the identity between the r.h.s. of eqs. (83) and (89) is due to the fact that, for small rigid displacements $\mathbf{d}$ and rotations $\boldsymbol{\varphi}$, one has to first order,

$$\mathcal{T}_N(\mathbf{d}) \equiv \mathcal{R}_N(\boldsymbol{\varphi}).$$

Operators (127) and (128) have the same effect on the electronic wavefunction as the operators

$$\mathcal{T}_n(-\mathbf{d}) = \exp\left(-\frac{i}{\hbar} \mathbf{d} \cdot \mathbf{P}\right), \tag{129}$$

and

$$\mathcal{R}_n(-\boldsymbol{\theta}) = \exp\left(-\frac{i}{\hbar}\boldsymbol{\theta}\cdot\mathbf{L}\right), \tag{130}$$

which rigidly displace and rotate the electron cloud in the opposite direction, so that,

$$\mathcal{T}_N(\mathbf{d})\,|a\rangle \equiv \mathcal{T}_n(-\mathbf{d})\,|a\rangle\,, \quad \mathcal{R}_N(\boldsymbol{\theta}) \equiv \mathcal{R}_n(-\boldsymbol{\theta}). \tag{131}$$

Owing to the equivalence (131), by applying operators (127) and (128) to an arbitrary second-order property (90), one immediately finds, to first order in $\mathbf{d}$ and $\boldsymbol{\theta}$,

$$\begin{aligned}\frac{1}{\hbar}\sum_{I=1}^{N}\mathbf{d}\cdot\mathbf{P}_I(A,B)_{-1} &= \frac{1}{\hbar}\sum_{j\neq a}\frac{2}{\omega_{ja}}\Re\left\{\left\langle a\left|\frac{i}{\hbar}[\mathbf{P},A]\right|j\right\rangle\langle j\,|B|\,a\rangle\right.\\ &\quad\left.+\langle a\,|A|\,j\rangle\left\langle j\left|\frac{i}{\hbar}[\mathbf{P},B]\right|a\right\rangle\right\}\cdot\mathbf{d}\\ &\quad+\frac{1}{\hbar^2}\sum_{j\neq a}\frac{2}{\omega_{ja}^2}\Re\left\{\langle a\,|A|\,j\rangle\langle j\,|B|\,a\rangle\right.\\ &\quad\times\left(\left\langle a\left|\frac{i}{\hbar}\left[\mathbf{P},H^{(0)}\right]\right|a\right\rangle-\langle a\,|\mathbf{F}_N^n|\,a\rangle\right.\\ &\quad\left.\left.-\left\langle j\left|\frac{i}{\hbar}\left[\mathbf{P},H^{(0)}\right]\right|j\right\rangle+\langle j\,|\mathbf{F}_N^n|\,j\rangle\right)\right\}\cdot\mathbf{d},\end{aligned} \tag{132}$$

$$\begin{aligned}\frac{1}{\hbar}\sum_{I=1}^{N}\boldsymbol{\theta}\cdot\mathbf{L}_I(A,B)_{-1} &= \frac{1}{\hbar}\sum_{j\neq a}\frac{2}{\omega_{ja}}\Re\left\{\left\langle a\left|\frac{i}{\hbar}[\mathbf{L},A]\right|j\right\rangle\langle j\,|B|\,a\rangle\right.\\ &\quad\left.+\langle a\,|A|\,j\rangle\left\langle j\left|\frac{i}{\hbar}[\mathbf{L},B]\right|a\right\rangle\right\}\cdot\boldsymbol{\theta}\\ &\quad+\frac{1}{\hbar^2}\sum_{j\neq a}\frac{2}{\omega_{ja}^2}\Re\left\{\langle a\,|A|\,j\rangle\langle j\,|B|\,a\rangle\right.\\ &\quad\times\left(\left\langle a\left|\frac{i}{\hbar}\left[\mathbf{L},H^{(0)}\right]\right|a\right\rangle-\langle a\,|\mathbf{K}_N^n|\,a\rangle\right.\\ &\quad\left.\left.-\left\langle j\left|\frac{i}{\hbar}\left[\mathbf{L},H^{(0)}\right]\right|j\right\rangle+\langle j\,|\mathbf{K}_N^n|\,j\rangle\right)\right\}\cdot\boldsymbol{\theta}.\end{aligned} \tag{133}$$

The expressions within (and) parentheses are identically vanishing for any exact or approximate wavefunctions $|a\rangle$ and $|j\rangle$, and constraints (113) and (116) are recovered: they will be satisfied as operators (127) and (128) are exactly

represented (irrespective of quality and extension of a basis set, and regardless of the approximation used to evaluate $|a\rangle$ and $|j\rangle$) when the derivatives are evaluated analytically, for the electronic wavefunction is rigidly moved as a mere geometrical entity, independently of its intrinsic accuracy.

VI Force and torque theorems in the presence of magnetic field

In the presence of magnetic field, the first-order function (65) becomes

$$\left|\psi_a^{B_\alpha}\right\rangle = \frac{1}{\hbar}\sum_{j\neq a}\omega_{ja}^{-1}\,|j\rangle\,\langle j\,|m_\alpha|\,a\rangle\,, \tag{134}$$

and the average mechanical momentum of electrons to first order in B_α is

$$\langle\Pi_\alpha\rangle^{(1)} = -\frac{e}{2c}B_\beta\left[\frac{1}{m_e}\left(P_\alpha, L_\beta\right)_{-1} - \epsilon_{\alpha\beta\gamma}\,\langle a\,|R_\gamma|\,a\rangle\right] = 0, \tag{135}$$

so that the corresponding velocity theorem (42) for the electronic wavefunction [32] can be expressed via a formula previously found [29], compare for eq. (120), identically satisfied if the wavefunction obeys the hypervirial theorem for the position operator R_α.

The average Lorentz magnetic force on the electrons vanishes, as it is well known from classical electrodynamics [34]. To second order in B_α one finds from definitions (17) an equivalent quantum mechanical condition, compare also for eq. (118),

$$\begin{aligned}\left\langle F_{n\alpha}^{B}\right\rangle^{(2)} + \left\langle F_{n\alpha}^{BB}\right\rangle^{(2)} &= \frac{e^2}{4m_e^2c^2}\Big\{2\epsilon_{\alpha\beta\gamma}\left(P_\beta, L_\delta\right)_{-1} - m_e\Big[2\,\langle a\,|R_\alpha|\,a\rangle\,\delta_{\gamma\delta} \\ &\quad - \langle a\,|R_\delta|\,a\rangle\,\delta_{\alpha\gamma} - \langle a\,|R_\gamma|\,a\rangle\,\delta_{\alpha\delta}\Big]\Big\}B_\gamma B_\delta \\ &= \sum_{I=1}^{N}\nabla_{I\alpha}\chi_{\gamma\delta}B_\gamma B_\delta = 0,\end{aligned} \tag{136}$$

which does not provide a further test on the accuracy of the electronic wavefunction, as it is also satisfied by eq. (120). In any event, even if the average Lorentz magnetic force separately goes to zero, there is a more general force theorem involving operator (18). In order to evaluate the average value of this operator to second order in B_α, one must consider the contributions arising from the perturbed functions (65) and (66), compare for Hamiltonian (6), *i.e.*, (134) and

$$\left|\psi_a^{B_\alpha B_\beta}\right\rangle = \frac{1}{\hbar^2}\sum_{j\neq a}\sum_{k\neq a}\omega_{ja}^{-1}\omega_{ka}^{-1}\,|j\rangle\,\langle j\,|m_\alpha|\,k\rangle\,\langle k\,|m_\beta|\,a\rangle$$
$$-\frac{1}{\hbar^2}\sum_{j\neq a}\omega_{ja}^{-2}\,|j\rangle\,\langle a\,|m_\alpha|\,a\rangle\,\langle j\,|m_\beta|\,a\rangle$$
$$-\frac{1}{2\hbar^2}\,|a\rangle\sum_{j\neq a}\omega_{ja}^{-2}\,\langle a\,|m_\alpha|\,j\rangle\,\langle j\,|m_\beta|\,a\rangle\,, \tag{137}$$

and

$$\left|\phi_a^{B_\alpha B_\beta}\right\rangle = \frac{1}{2\hbar}\sum_{j\neq a}\omega_{ja}^{-1}\,|j\rangle\,\left\langle j\left|\bar{\chi}^{\mathrm{d}}_{\alpha\beta}\right|a\right\rangle. \tag{138}$$

To second order in B_α, the contribution to the expectation value of operator (18) yielded by functions (134), (137) and (138) can be written in terms of nuclear electric hypershieldings, compare for eqs. (108), (109) and (110),

$$\left\langle F_{n\alpha}^N\right\rangle^{(2,p)} = -\frac{1}{2}\sum_{I=1}^{N} Z_I e\rho^{I\mathrm{p}}_{\alpha,\beta\gamma}B_\beta B_\gamma, \tag{139}$$

$$\left\langle F_{n\alpha}^N\right\rangle^{(2,d)} = -\frac{1}{2}\sum_{I=1}^{N} Z_I e\rho^{I\mathrm{d}}_{\alpha,\beta\gamma}B_\beta B_\gamma, \tag{140}$$

so that, to second order in B_α, the force theorem is formally the same as the translational sum rule for geometrical derivatives of magnetic susceptibility (118), *i.e.*, for total electric hypershielding of nucleus I in the presence of magnetic field (110),

$$\left\langle F_{n\alpha}^N\right\rangle^{(2)} = -\frac{1}{2}\sum_{I=1}^{N} Z_I e\rho^{I}_{\alpha,\beta\gamma}B_\beta B_\gamma = 0. \tag{141}$$

One should remark, however, that eq. (136) provides a constraint on the first-order function (134), whereas condition (141) furnishes a test of accuracy also for functions (137) and (138). Moreover, eqs. (136) and (141), compare for (27) and (110), state that in this case theorem (45) should read $2A = A, \rightarrow A = 0$.

The torque theorems to second order in the magnetic field are found via a similar procedure. By evaluating the average values of operators (36) and (37) via the unperturbed $\left|\psi_a^{(0)}\right\rangle$ and perturbed wavefunctions (134), (137) and (138), one finds paramagnetic and diamagnetic contributions to the Lorentz torque,

$$\left\langle K_{n\alpha}^B\right\rangle^{(2)} = \epsilon_{\alpha\beta\gamma}\chi^{\mathrm{p}}_{\beta\delta}B_\gamma B_\delta, \tag{142}$$

$$\left\langle \mathcal{K}^{B}_{n\alpha} \right\rangle^{(2)} = \epsilon_{\alpha\delta\beta}\chi^{\mathrm{d}}_{\beta\gamma}B_\gamma B_\delta, \tag{143}$$

$$\left\langle K^{BB}_{n\alpha} \right\rangle^{(2)} = \left(\epsilon_{\alpha\beta\gamma}\chi^{\mathrm{d}}_{\beta\delta} + \epsilon_{\alpha\beta\delta}\chi^{\mathrm{d}}_{\gamma\beta}\right) B_\gamma B_\delta, \tag{144}$$

so that the total diamagnetic term is

$$\left\langle \mathcal{K}^{B}_{n\alpha} \right\rangle^{(2)} + \left\langle K^{BB}_{n\alpha} \right\rangle^{(2)} = \epsilon_{\alpha\beta\gamma}\chi^{\mathrm{d}}_{\beta\delta}B_\gamma B_\delta, \tag{145}$$

and

$$\begin{aligned} \left\langle K^{N}_{n\alpha} \right\rangle^{(2,d)} &= 2\Re\left(\left\langle \psi^{(0)}_a \middle| K^{N}_{n\alpha} \middle| \phi^{B_\gamma B_\delta} \right\rangle\right) \\ &= -\frac{1}{2}\sum_{I=1}^{N} Z_I e \epsilon_{\alpha\beta\epsilon} R_{I\beta}\rho^{\mathrm{Id}}_{\epsilon,\gamma\delta}B_\gamma B_\delta, \end{aligned} \tag{146}$$

$$\begin{aligned} \left\langle K^{N}_{n\alpha} \right\rangle^{(2,p)} &= \left[2\Re\left(\left\langle \psi^{(0)}_a \middle| K^{N}_{n\alpha} \middle| \psi^{B_\gamma B_\delta} \right\rangle\right) + \left\langle \psi^{B_\gamma}_a \middle| K^{N}_{n\alpha} \middle| \psi^{B_\delta} \right\rangle\right] B_\gamma B_\delta \\ &= -\frac{1}{2}\sum_{I=1}^{N} Z_I e \epsilon_{\alpha\beta\epsilon} R_{I\beta}\rho^{\mathrm{Ip}}_{\epsilon,\gamma\delta}B_\gamma B_\delta. \end{aligned} \tag{147}$$

Thus the average Lorentz magnetic torque acting on the electrons is

$$\left\langle K^{B}_{n\alpha} \right\rangle^{(2)} + \left\langle \mathcal{K}^{B}_{n\alpha} \right\rangle^{(2)} + \left\langle K^{BB}_{n\alpha} \right\rangle^{(2)} = \epsilon_{\alpha\beta\gamma}\mathcal{M}^{(m)}_{\beta}B_\gamma, \tag{148}$$

where

$$\mathcal{M}^{(m)}_{\alpha} = \chi_{\alpha\beta}B_\beta \tag{149}$$

is the average magnetic moment induced within the electron cloud to first order in B_α. Expression (148) is formally the same as that obtained in the classical treatment [34]. The total torque on the electrons, however, vanishes, *i.e.*, by summing all the magnetic contributions according to eq. (31), one obtains the hypervirial theorem (47) for total angular momentum of electrons to second order in B_α,

$$\left\langle K_{n\alpha} \right\rangle^{(2)} = \left(\epsilon_{\alpha\beta\gamma}\chi_{\beta\delta} - \frac{1}{2}\sum_{I=1}^{N} Z_I e \epsilon_{\alpha\beta\epsilon} R_{I\beta}\rho^{I}_{\epsilon,\gamma\delta}\right) B_\gamma B_\delta = 0. \tag{150}$$

This result states the rotational sum rule for nuclear electric hypershieldings in the presence of magnetic field, equivalent to (126), compare also for eq. (110).

One can check that these results are consistent with eqs. (39), (41), and (49), in that they explicitly show how the average torqe exerted by the external magnetic field on the electrons is fully transferred to the nuclei.

VII Virial sum rules

Another set of sum rules for nuclear electric hypershieldings is yielded by the the virial thorem, *i.e.*, the hypervirial theorem [32]

$$\left\langle \psi_a \left| \frac{i}{\hbar} [H, \mathcal{V}] \right| \psi_a \right\rangle = \left\langle \psi_a \left| \sum_{i=1}^{n} \left(\frac{\partial H}{\partial \mathbf{p}_i} \cdot \mathbf{p}_i - \mathbf{r}_i \cdot \frac{\partial H}{\partial \mathbf{r}_i} \right) \right| \psi_a \right\rangle = 0, \tag{151}$$

for the virial operator

$$\mathcal{V} = \frac{1}{2} \sum_{i=1}^{n} (\mathbf{r}_i \cdot \mathbf{p}_i + \mathbf{p}_i \cdot \mathbf{r}_i) = \sum_{i=1}^{n} \mathbf{r}_i \cdot \mathbf{p}_i - \frac{3}{2} i\hbar n. \tag{152}$$

One observes that in the presence of magnetic field the virial operator formally is

$$\mathcal{V}^B = \frac{1}{2} \sum_{i=1}^{n} (\mathbf{r}_i \cdot \boldsymbol{\pi}_i + \boldsymbol{\pi}_i \cdot \mathbf{r}_i), \tag{153}$$

which becomes [32] the same as (152) within the Coulomb gauge, as $\mathbf{r} \cdot \mathbf{A} = 0$.

The operator equation for the virial relation can be found by direct evaluation of the commutator appearing in eq. (151) or by applying the Euler theorem for homogeneous functions. Accordingly, in the presence of spatially uniform, time-independent electric and magnetic fields [42,32,29,41],

$$H^{(0)} + T_n^{(0)} + \mathcal{D}_\alpha E_\alpha + \bar{\chi}^{\mathrm{d}}_{\alpha\beta} B_\alpha B_\beta = \sum_{I=1}^{N} R_{I\alpha} F_{I\alpha}, \tag{154}$$

where $F_{I\alpha}$ is given by eq. (22), and $T_n^{(0)}$ is the operator for electronic kinetic energy in the absence of perturbations. By evaluating the average values over the perturbed wavefunctions (64) in the presence of the fields,

$$\begin{aligned} \sum_{I=1}^{N} R_{I\alpha} \langle \psi_a | F_{I\alpha} | \psi_a \rangle \;=\; & \left\langle \psi_a \left| H^{(0)} \right| \psi_a \right\rangle + \left\langle \psi_a \left| T_n^{(0)} \right| \psi_a \right\rangle \\ & + \langle \psi_a | \mathcal{D}_\alpha | \psi_a \rangle E_\alpha + \left\langle \psi_a \left| \bar{\chi}^{\mathrm{d}}_{\alpha\beta} \right| \psi_a \right\rangle B_\alpha B_\beta, \end{aligned} \tag{155}$$

and, to first order in E_α one finds [43,29,41]

$$\sum_{I=1}^{N} R_{I\alpha} \nabla_{I\alpha} \mathcal{M}_\beta^{(0)} = \mathcal{M}_\beta^{(0)} + \left(T_n^{(0)}, \mu_\beta \right)_{-1}, \tag{156}$$

where

$$\left(T_n^{(0)}, \mu_\beta \right)_{-1} = \frac{1}{\hbar} \sum_{j \neq a} \frac{2}{\omega_{ja}} \Re \left(\left\langle a \left| T_n^{(0)} \right| j \right\rangle \langle j | \mu_\beta | a \rangle \right). \tag{157}$$

To second order in E_α, using the results

$$\left\langle H^{(0)}\right\rangle^{(2)} = \frac{1}{2}\alpha_{\alpha\beta}E_\alpha E_\beta, \qquad \langle F_{I\alpha}^n\rangle^{(2)} = \frac{1}{2}Z_I e\phi^I_{\alpha,\beta\gamma}E_\beta E_\gamma, \tag{158}$$

one finds

$$\sum_{I=1}^{N} R_{I\alpha}\nabla_{I\alpha}\alpha_{\beta\gamma} = 3\alpha_{\beta\gamma} + \left(T_n^{(0)}, \mu_\beta, \mu_\gamma\right)_{-2}, \tag{159}$$

where

$$\begin{aligned}\left(T_n^{(0)}, \mu_\beta, \mu_\gamma\right)_{-2} \;=\; & \mathbf{S}\left(T_n^{(0)}, \mu_\beta, \mu_\gamma\right)\left[\frac{1}{\hbar^2}\sum_{j\neq a}\omega_{ja}^{-1}\right. \\ & \times\left(\sum_{k\neq a}\omega_{ka}^{-1}\left\langle a\left|T_n^{(0)}\right|j\right\rangle\langle j\,|\mu_\beta|\,k\rangle\langle k\,|\mu_\gamma|\,a\rangle\right. \\ & \left.\left.-\omega_{ja}^{-1}\left\langle a\left|T_n^{(0)}\right|a\right\rangle\langle a\,|\mu_\beta|\,j\rangle\langle j\,|\mu_\gamma|\,a\rangle\right)\right].\end{aligned} \tag{160}$$

There is no contribution to first order in the magnetic field in the case of closed-shell electronic states, as the first-order wavefunction is purely imaginary. To second order, one has contributions to the expectation values in eq. (155) from wavefunctions (134), (137) and (138). Thus, using the results

$$\left\langle H^{(0)}\right\rangle^{(2)} = \frac{1}{2}\chi^{\mathrm{p}}_{\alpha\beta}B_\alpha B_\beta, \qquad \langle F_{I\alpha}^n\rangle^{(2)} = \frac{1}{2}Z_I e\rho^I_{\alpha,\beta\gamma}B_\beta B_\gamma, \tag{161}$$

one finds

$$\sum_{I=1}^{N} R_{I\alpha}\nabla_{I\alpha}\chi_{\beta\gamma} = \chi_{\beta\gamma} + \chi^{\mathrm{d}}_{\beta\gamma} + \left(T_n^{(0)}, \bar{\chi}^{\mathrm{d}}_{\beta\gamma}\right)_{-1} + \left(T_n^{(0)}, m_\beta, m_\gamma\right)_{-2}, \tag{162}$$

where

$$\begin{aligned}\left(T_n^{(0)}, m_\beta, m_\gamma\right)_{-2} \;=\; & \mathbf{S}\left(T_n^{(0)}, m_\beta, m_\gamma\right)\left[\frac{1}{\hbar^2}\sum_{j\neq a}\omega_{ja}^{-1}\right. \\ & \times\left(\sum_{k\neq a}\omega_{ka}^{-1}\left\langle a\left|T_n^{(0)}\right|j\right\rangle\langle j|m_\beta|k\rangle\langle k\,|m_\gamma|\,a\rangle\right. \\ & \left.\left.-\omega_{ja}^{-1}\left\langle a\left|T_n^{(0)}\right|a\right\rangle\langle a\,|m_\beta|\,j\rangle\langle j\,|m_\gamma|\,a\rangle\right)\right],\end{aligned} \tag{163}$$

$$\left(T_n^{(0)}, \bar{\chi}_{\beta\gamma}^{\mathrm{d}}\right)_{-1} = \frac{1}{\hbar} \sum_{j \neq a} \frac{2}{\omega_{ja}} \Re \left(\left\langle a \left| T_n^{(0)} \right| j \right\rangle \left\langle j \left| \bar{\chi}_{\beta\gamma}^{\mathrm{d}} \right| a \right\rangle \right). \tag{164}$$

The virial relation (162) is independent of the origin of the coordinate system for electronic functions which are exact eigenfunctions to any model Hamiltonian, *e.g.*, Hartree-Fock states. To prove this statement let us first observe that the l. h. s. of eq. (162) is origin independent, owing to translational sum rule (118); on the r. h. s. the total susceptibility is also independent, and the diamagnetic contributions transform according to eq. (123). The other tensor quantities transform

$$\left(T_n^{(0)}, \bar{\chi}_{\alpha\beta}^{\mathrm{d}}(\mathbf{r}'')\right)_{-1} = \left(T_n^{(0)}, \bar{\chi}_{\alpha\beta}^{\mathrm{d}}(\mathbf{r}')\right)_{-1} + \frac{e^2}{4m_e c^2} \Delta_{\alpha\beta}^{\mathrm{d}}, \tag{165}$$

$$\left(T_n^{(0)}, m_\beta(\mathbf{r}''), m_\gamma(\mathbf{r}'')\right)_{-2} = \left(T_n^{(0)}, m_\beta(\mathbf{r}'), m_\gamma(\mathbf{r}')\right)_{-2} + \frac{e^2}{4m_e c^2} \Delta_{\alpha\beta}^{\mathrm{p}}, \tag{166}$$

where

$$\begin{aligned} \Delta_{\alpha\beta}^{\mathrm{d}} &= 2d_\gamma \delta_{\alpha\beta} \left(T_n^{(0)}, R_\gamma(\mathbf{r}')\right)_{-1} \\ &\quad - d_\beta \left(T_n^{(0)}, R_\alpha(\mathbf{r}')\right)_{-1} - d_\alpha \left(T_n^{(0)}, R_\beta(\mathbf{r}')\right)_{-1}, \end{aligned} \tag{167}$$

$$\begin{aligned} \Delta_{\alpha\beta}^{\mathrm{p}} &= d_\delta \left[\epsilon_{\alpha\gamma\delta} \left(T_n^{(0)}, P_\gamma, L_\beta(\mathbf{r}')\right)_{-2} + \epsilon_{\beta\gamma\delta} \left(T_n^{(0)}, P_\gamma, L_\alpha(\mathbf{r}')\right)_{-2} \right] \\ &\quad + \epsilon_{\alpha\gamma\delta} \epsilon_{\beta\lambda\mu} d_\delta d_\mu \left(T_n^{(0)}, P_\gamma, P_\lambda\right)_{-2}. \end{aligned} \tag{168}$$

After some tedious algebra one finds two identities, exactly satisfied by the eigenfunctions to a model Hamiltonian,

$$\left(T_n^{(0)}, P_\alpha, P_\beta\right)_{-2} = m_e n \delta_{\alpha\beta}, \tag{169}$$

$$\left(T_n^{(0)}, P_\alpha, L_\beta\right)_{-2} = \left(P_\alpha, L_\beta\right)_{-1} + m_e \epsilon_{\alpha\beta\gamma} \left(T_n^{(0)}, R_\gamma\right)_{-1}, \tag{170}$$

so that the sum of the last three terms in the r. h. s. of expression (162) is independent of the origin if the hypervirial theorems are fulfilled. Hence the virial relation (162) to second order in the magnetic field is invariant under a coordinate transformation.

Eventually one notices that sum rules (156), (159) and (162) are immediately rewritten in terms of electric shielding and hypershielding tensors via eqs. (63) and (110). These constraints can be used to assess the degree of accuracy of electronic wavefunctions evaluated within the algebraic approximation.

VIII Conclusions

Hypervirial theorems for velocity and total angular momentum operators (*i.e.*, force and torque theorems for the electronic wavefunction of a molecule in the presence of external electric and magnetic fields) and the Hellmann-Feynman theorem yield equilibrium conditions expressible in the form of translational and rotational constraints, and lead to the definition of nuclear electric shielding and hypershielding tensors as derivatives with respect to nuclear coordinates of other properties accounting for electronic response, see Secs. II, III and IV. These quantities describe the electric field induced on the nuclei by the electrons responding to the external perturbations. For instance, the first electric hypershielding of a nucleus is a third-rank tensor that can be expressed as a geometrical derivative of electric polarizability, see Sec. IV.

The physical explanation of the connection between nuclear shielding and hypershielding, and geometrical derivatives of dipole moment and polarizabilities lies in the fact that a molecule in the presence of perturbations stretches to an equilibrium geometry different from that of the isolated system. This reaction gives rise to electric fields counteracting the external ones. IR radiation impinging on the perturbed molecular system can couple to nuclear vibration, then the effective dynamic Lorentz forces acting upon the nuclei cause transitions to different vibrational levels. Therefore nuclear first hypershieldings can be used to rationalize IR intensities of molecules pertubed by additional external fields. The same tensor is related to Raman absorption intensities.

The general equation (105) for the geometric derivative of a second-order property obtained via perturbation theory contains the transition matrix elements of a force operator. Such a formula can be used as a computational recipe for evaluating hypershieldings, that is, geometrical derivatives, avoiding explicit differentiation of the wavefunction, *etc.*. In order to obtain accurate numerical estimates within the algebraic approximation, it is expected that, suitable basis sets should be used to satisfy, at least locally, the Hellmann-Feynman theorem.

The rototranslational constraints (113) and (116), and the sum rules provided by the virial theorem (159) and (162), can give information on the overall accuracy of a calculation of nuclear hypershieldings and on the ability of a given basis set. On the other hand, the rototranslational sum rules may serve to check a computer program for derivatives of second-order properties when analytic procedures for actual differentiation of the electronic wavefunction are adopted [21], as, according to the results of Sec. V, they are identically satisfied in this case, irrespective of the quality of the basis set.

Acknowledgments

One of us (P. L.) gratefully acknowledges a fellowship of the French Ministère de la recherche et de la technologie and partial financial support to this research from the Italian Ministero dell'Università e della ricerca scientifica e tecnologica.

References

[1] Handler, P. and Aspnes, D. E. (1967). *J. Chem. Phys.* **47**, 473.

[2] Cohen De Lara, E., Kahn, R., and Seloudoux, R. (1985). *J. Chem. Phys.* **83**, 2646.

[3] Kahn, R., Cohen De Lara, E., and Möller, K. D. (1985). *J. Chem. Phys.* **83**, 2653.

[4] Duran, M., Andrés, J. L., Lledós, A., and Bertrán, J. (1989). *J. Chem. Phys.* **90**, 328.

[5] Andrés, J. L., Martí, J., Duran, M., Lledós, A., and Bertrán, J. (1991). *J. Chem. Phys.* **95**, 3521.

[6] Bauschlicher, C. Jr., (1985). *Chem. Phys. Letters* **118**, 307.

[7] Hennico, G., Delhalle, J., Raynaud, M., Raynaud, C., and Ellinger, Y. (1985). *Chem. Phys. Letters* **152**, 207.

[8] Andrés, J. L., Lledós, A., Duran, M., and Bertrán, J. (1988). *Chem. Phys. Letters* **153**, 82.

[9] Andrés, J. L., Duran, M., Lledós, A., and Bertrán, J. (1991). *Chem. Phys.* **151**, 37.

[10] Lambert, D. K. (1991). *J. Chem. Phys.* **94**, 6237.

[11] Luo, J. S., Tobin, R. G., and Lambert, D. K. (1993). *Chem. Phys. Letters* **204**, 445.

[12] Koubi, L., Blain, M., Cohen De Lara, E., and Leclercq, J. M. (1994). *Chem. Phys. Letters* **217**, 544.

[13] Bishop, D. M. (1993). *J. Chem. Phys.* **98**, 3179.

[14] Bishop, D. M., and Martí, J. (1993). *J. Chem. Phys.* **99**, 3860.

[15] Bishop, D. M. (1994). *Int. Rev. Phys. Chem.* **13**, 21.

[16] Buckingham, A. D. (1967). *Adv. Chem. Phys.* **12**, 107 Wiley, New York.

[17] Biarge, J. F., Herranz, J., and Morcillo, J. (1961). *An. R. Soc. Esp. Fis. Quim.* **A57**, 81.

[18] Morcillo, J., Zamorano, L. J., and Heredia, J. M. V. (1966). *Spectr. Acta* **22**, 1969.

[19] Person, W. B., and Newton, J. H. (1974). *J. Chem. Phys.* **61**, 1040.

[20] Newton, J. H., and Person, W. B. (1976). *J. Chem. Phys.* **64**, 3036.

[21] Amos, R. D. (1987). *Adv. Chem. Phys.* **67**, 99. Wiley, New York .

[22] Amos, R. D. (1986). *Chem. Phys. Letters* **124**, 376.

[23] Faglioni, F., Lazzeretti, P., Malagoli, M., Zanasi, R., and Prosperi, T. (1993). *J. Phys. Chem.* **97**, 2535.

[24] Jørgensen, P., and Simons, J. (1983). *J. Chem. Phys.* **79**, 334.

[25] Jørgensen, P., and Simons, J. eds., (1986). *Geometrical Derivatives of Energy Surfaces and Molecular Properties*, NATO ASI Series. Reidel, Dordrecht, and references therein.

[26] Gauss, J., and Cremer, D. (1992). *Adv. Quantum Chem.*, Vol. 23, p. 205 (P. O. Löwdin, ed.), Academic Press, New York.

[27] Lazzeretti, P., and Zanasi, R. (1984). *Chem. Phys. Letters* **112**, 103.

[28] Fowler, P. W., and Buckingham, A. D. (1985). *Chem. Phys.* **98**, 167.

[29] Lazzeretti, P. (1987). *Adv. Chem. Phys.*, Vol. 75, p. 507. Wiley, New York.

[30] Jalkanen, K. J., Stephens, P. J., Lazzeretti, P., and Zanasi, R. (1989). *J. Chem. Phys.* **90**, 3204.

[31] Young, R. H. (1969) *Mol. Phys.* **16**, 509.

[32] Epstein, S. T. (1974) "*The Variation Method in Quantum Chemistry*". Academic, New York.

[33] Hirschfelder, J. O., Byers-Brown, W., and Epstein, S. T. (1964). *Adv. Quantum Chem.*, Vol. 1, p. 267. (P. O. Löwdin, ed.), Academic Press, New York.

[34] Landau, L. D., and Lifshitz, E. M. (1979). *The Classical Theory of Fields*, 4th revised English ed., Pergamon.

[35] Lazzeretti, P., Malagoli, M., and Zanasi, R. (1991). *Chem. Phys. Letters* **179**, 297.

[36] Goldstein, H. (1980). *Classical Mechanics*, Addison-Wesley Publishing Co., Second edition.

[37] Lazzeretti, P. (1989). *Chem. Phys. Letters* **160**,49.

[38] Lazzeretti, P., and Zanasi, R. (1987). *Chem. Phys. Letters* **135**, 571.

[39] Lazzeretti, P., and Zanasi, R. (1985). *Chem. Phys. Letters* **118**, 217.

[40] Epstein, S. T. (1954). *Am. J. Phys.* **22**, 613.

[41] Lazzeretti, P., Malagoli, M., and Zanasi, R. (1991). *J. Chem. Phys.* **94**, 448.

[42] Carr, W. J. (1957). *Phys. Rev.* **106**, 414.

[43] Sambe, H. (1973). *J. Chem. Phys.* **58**, 4779.

Size-Consistency and Size-Intensivity Aspects of Many-Body Green's Function Calculations on Polymers : Characterization of the Convergence of Direct Lattice Self-energy Summations

Michaël Deleuze and Joseph Delhalle

Laboratoire de Chimie Théorique Appliquée, Facultés Universitaires Notre-Dame de la Paix, 61, rue de Bruxelles, B-5000 Namur (Belgium)

Barry T. Pickup

Department of Chemistry, The University, Sheffield S3 7HF (United-Kingdom)

Jean-Louis Calais

Quantum Chemistry Group, University of Uppsala, Box 518, S-751 20 Uppsala (Sweden)

Contents

1. Introduction

Quantum-mechanical electronic structure calculations are nowadays performed routinely on systems with periodicity in one dimension : polymers. Such calculations are of direct interest to both academic and industrial researchers [1-3], because of the invaluable tool they offer to study many physical and chemical properties [4,5] (structure, bonding, Young's modulus, electrical conductivity, optical properties, spectral features) of important materials (plastics, biopolymers, organic crystals ...), greatly needed in various advanced fields (electronics, telecommunications, engineering, biotechnology, space, ...).

Hartree-Fock (HF) equations and their solutions have played a fundamental role in the electronic theory of polymers. These equations constitute a conceptual framework providing qualitatively useful quantities such as the total ground state energy, the electron charge distribution indices, or the one-electron energy band features. The latter have enabled on many occasions a suitable analysis of the X-ray photoelectron spectra (XPS) of such systems, and their relationships with the molecular architecture [6]. As shown in recent studies conducted on polyethylene [7], polypropylene [8] and polyoxymethylene [9], band structure calculations with finite super-cell offer a particularly convenient way to investigate these relationships, since they emphasize the role played by long-range interactions in the development of configurational or conformational signatures in XPS valence bands.

Today, constant refinements of experimental techniques in the field of electron spectroscopy require the development of more accurate schemes to calculate the electronic structure of polymers, going beyond the one-particle level of description. However, because of their extraordinarily heavy computational cost and, possibly, inherent size-related difficulties, correlated band structure calculations still remain the exception [10]. The one-particle Many-Body Green's Function theory [11] (MBGF; also referred to as the one-particle propagator [12] theory), focusing on the average properties of a particle propagating in the background of an interacting many-body system, provides direct and quantitative schemes to estimate ionization and electron attachment energies [13-15]. Since the first applications [16-18] to atoms

or molecules, it has been shown to yield accurate simulations of photoionization spectra for a large variety of systems [19]. For the purpose of investigating the electronic structure of extended systems, such as polymers, the Many-Body Green's Function (MBGF) theory and the closely related Many-Body Perturbation Theory (MBPT) are of major interest, since these constitute some of the rare post-SCF many-body quantum mechanical methods which in principle provide a physically correct size-dependence of the calculated properties. Distinct types of size-dependence are reported which are often improperly mixed up in the literature.

The notion of *size-extensivity* is implicit in the original works of J. Goldstone [20] and K.A. Brueckner [21]. It is borrowed from thermodynamics and characterizes traditionally the linear size-dependence of collective properties, such as the total energy, polarizability, magnetizability ..., in the limit of an *infinite* system of finite density. On the other hand, properties implying only a restricted number of particles, such as ionization, attachment or excitation energies, transition amplitudes ..., do not depend on the size of the system in the thermodynamic limit and as such are referred to as *intensive* properties. The mathematical analysis of this type of dependence has to date only been conducted on infinite translationally invariant systems such as the nuclear matter [22], or the electron gas disposed in a uniform positive backgound [23]. For this kind of analysis, integration in $\vec{k}$ space plays an essential role.

The translational invariance of *homogeneous* systems enables major simplifications, which are not possible for real molecular or macromolecular *inhomogeneous* systems. Specifically, in the case of the electron gas model, the electroneutrality constraint at any point of the system ensures the exclusion [23] from the exact hamiltonian of some divergences induced by the long-range character of the Coulomb potential. In this particular case, the linked-cluster theorem [20-28] therefore guarantees the size-intensivity or size-extensivity of any approach based on a many-body perturbation expansion. It is clear that the thermodynamic notion of size-intensivity or size-extensivity can also be applied on real macromolecular periodic systems, such as polymers or crystals. However, nothing at first glance proves that conclusions drawn from the electron gas model can be directly transposed to such systems.

The notion of *size-consistency* has been introduced by J.A. Pople [29] to characterize the evolution of various properties calculated by means of several theoretical models incorporating electronic correlation for *molecular* systems *dissociating* into two or more distinct fragments. This notion is strictly defined in the limit of a supersystem of *non-interacting* molecules. In this limit, the physical properties obtained from a size-consistent approach must satisfy the proper *separability conditions* [30]. In particular, the total energy, as any size-extensive property, must be *additively separable* with respect to the molecular components.

Separability conditions also refer to the multiplicative separability of the wavefunction, from which all other scaling properties follow in the non-interacting limit. These can be quite complicated (consider e.g. the two particle density-matrix which contains a multiplicatively separable and additively separable part). However, multiplicative separability of the correlated wavefunction is a very strong mathematical demand and is not at all necessary for the size-consistency of most properties. For instance, MBPT does not yield a separable wavefunction, but it does yield size-consistent energy, density, polarizability, dipole moments etc., for systems consisting of non-interacting closed-shell fragments.

For finite systems, the relation between size-consistency and the linked-cluster properties of a many-body expansion is well established. This topological concept, originating from field theory, relies on a single reference state or vacuum. If the occupied and unoccupied orbitals in that reference determinant can be localized separately (*ie* if the reference determinant is multiplicatively separable), any expansion in terms of linked or connected diagrams is size-consistent.

It is commonly [31,32] assumed that size-consistency or separability conditions are equivalent to size-extensivity. In other words, a size-consistent approach could be applied in a straightforward manner to molecules of different size, including macromolecules. For closed shell systems dissociating into closed shell fragments, an RHF (Restricted Hartree-Fock) reference function is multiplicatively separable. Assuming incorrectly that a large molecule consists of a superposition of largely non interacting pair bonds [33], it is very tempting to suppose [34-36] that size-consistency (or the absence of unlinked contributions) is a sufficient condition for

size-extensivity of a correlated model based upon that reference function. The present work consists in a general analysis of these important aspects of many-body theories in the particular case of extended polymer chains, and points out some problems that need to be addressed. To our knowledge, nobody has dealt with the question discussed here or the possible computational implications for LCAO based strategies.

HF theoretical studies of polymers have proceeded by methods requiring the summation of energetic quantities over the direct lattice characterizing an ideal periodic system [37-39]. The unbounded nature of the model, which was originally overlooked, has been found to generate size-related difficulties, mathematically expressed as conditionally and/or slowly convergent series of terms involving multicenter integrals [40-52]. This has led to numerous tests [50,51,53] and analyses [48,49,54-56] on lattice sums over both Coulomb and exchange contributions, which, in the Green's function formalism, are nothing else than first-order "self-energy" terms [57]. Beyond the one-particle picture, more difficulties can be expected, because of the increasing complexity of the lattice summations needed to expand the self-energies derived at the second and higher order levels of approximation.

With the purpose of unifying notations and concepts originating from quite different fields and allowing a pictorial identification of the origin of convergence problems, we first provide a brief outline (section 2) of the diagrammatic techniques used in Many-Body Green's Function theory. Armed with the basic Crystal Orbital LCAO-SCF equations for infinite systems with periodicity in one dimension (section 3), we will then be in a position to examine (section 4) the implications of the linked-cluster theorem in the context of macromolecules. In section 5, we call attention to the singular divergent behaviour of some specific bielectron interaction elements over crystalline orbitals. The convergence properties of various self-energy simple or coupled lattice summations are characterized in the last part (section 6) of this paper.

The analysis of the convergence of the self-energy lattice sums is carried out in terms which are normally used in a SCF calculation of LCAO type. Its primary

purpose is to demonstrate the importance of carrying out lattice summations properly. We first adapt the basic Restricted Hartree-Fock-Roothaan formula to estimate the effective energy of a particle propagating in the background of an interacting system described at the first-order level with regards to the correlation potential. If we reconsider the Hartree-Fock level at this point, it is to put the many-body part in prospective, introduce it in a well-known context and point to the links between size-related difficulties at different orders of description. Very similar techniques will then be used to characterize the asymptotic convergence properties of the lattice sum expansion of the second and higher order self-energies. As we stress polymer theory aspects, this article should be considered as the counterpart of a previous contribution [58], dealing mainly with some important features of the Green's Function method when applied to oligomer systems of increasing size.

The model of a stereoregular polymer chain states the links betwen molecular and solid state quantum mechanics. One can hence expect an easy generalization of the conclusions obtained from the model of a chain with a one-dimensional periodicity to the case of a three-dimensional solid. Before entering the heart of the subject, it is useful to recall that a real polymer or solid is at the end of the day nothing else than a very large molecule. Relatedly, the periodic boundary conditions usually imposed on extended systems are simply a clever trick enabling a proper discretization of one-electron states. Any method which would not satisfy the proper size-dependence requirements both in the molecular and solid state contexts should therefore be considered with exceedingly great care.

2. Diagrammatic derivation of the Many-Body Green's Function (MBGF) and Many-Body Perturbation Theory (MBPT)

The origins of many-body perturbation theory are based [59] upon the Rayleigh-Schrödinger perturbation theory, which is well known in quantum chemistry. It is the need to remove the "unlinked clusters" and the introduction of Feynman diagrams which make the MBPT and MBGF schemes appear unfamiliar to most quantum chemists. For the purpose assigned, it is useful to recall some important results of Many-Body Green's Function and Perturbation Theories. These are most conveniently derived in a time-dependent context [60], adopting the following partitioning for the exact hamiltonian :

$$H = H_0 + V(t) \tag{1}$$

where the unpertubed hamiltonian H_0 and time-dependent perturbation V(t) are defined as :

$$H_0 = \sum_i \varepsilon_i a_i^+ a_i \tag{2}$$

$$V(t) = \frac{1}{2} \sum_{ijkl} < ij|kl > a_i^+(t) a_j^+(t) a_l(t) a_k(t)$$

$$= \frac{1}{4} \sum_{ijkl} < ij||kl > a_i^+(t) a_j^+(t) a_l(t) a_k(t) \tag{3}$$

In these equations $< ij|kl >$ and $< ij||kl >$ correspond to the standard single and antisymmetrized bielectron integrals over the spin-orbitals of an independent particle model, and ε_i are the corresponding single particle energies. Use has been made of second quantization to express H_0 and V(t) in terms of fermion construction operators, namely the creation, a_i^+, and destruction operators, a_i. In the framework of the Goldstone [20] and Hugenholtz [61] conventions, the successive contributions to summations (3) are diagrammatically represented as time-ordered uncontracted line-vertices and point-vertices, respectively, according to Figure 1.

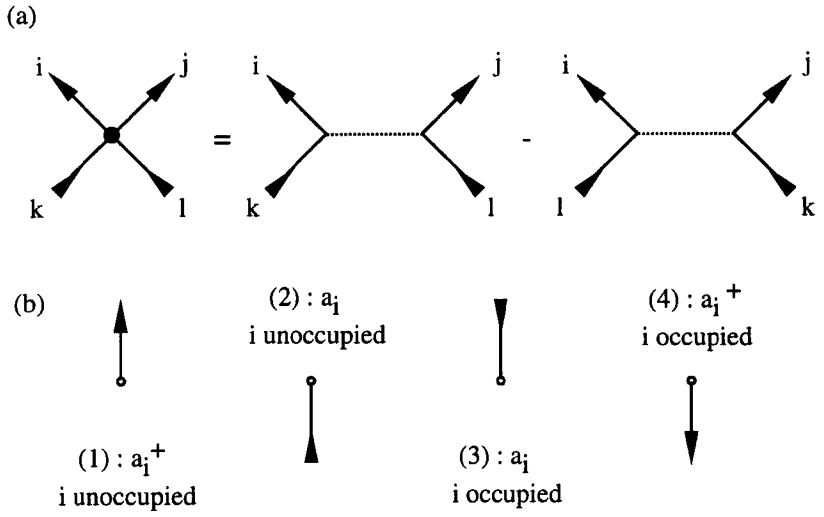

Figure 1 : (a) a point-vertex and a line-vertex ; 16 variations according to (b) : (1) creation of a particule, (2) annihilation of a particule; (3) creation of a hole; (4) annihilation of a hole.

The interaction picture (I) is adopted for the wavefunction and operators. Introducing the Wick chronological operator T_W and expanding the time-dependent Schrödinger equation, one can show that :

$$\Psi^I(t) = U(t,t_0)\Psi^I(t_0) \tag{4}$$

where the explicit and well-known form of the evolution operator is the Dyson series [62] :

$$U(t,t_0) = 1 + \sum_{n=1}^{\infty} \frac{i^{-n}}{n!} \int_{t_0}^{t} dt_n \int_{t_0}^{t} dt_{n-1} \int_{t_0}^{t} dt_{n-2} \ldots \int_{t_0}^{t} dt_1 \, T_W\left[V(t_n)V(t_{n-1})\ldots V(t_1)\right] \tag{5}$$

The effect of the perturbation is generally expressed in terms of energy and wave function differences with respect to the non-interacting ground state at the initial time $t_0 = -\infty$. The perturbation is introduced adiabatically, to find at time

$t = 0$ the exact ground state. Considering, in a particle-hole picture, $|\Psi^I(-\infty)>$ as a model vacuum, one can expand the energy shift due to the perturbation according to the Gell-Mann and Low relation [63] :

$$\Delta E = \frac{< \Psi^I(-\infty)|V(0)\,U(0,-\infty)|\Psi^I(-\infty) >}{< \Psi^I(-\infty)\,U(0,-\infty)|\Psi^I(-\infty) >} \tag{6}$$

for which a useful alternative statement is :

$$\Delta E = i\frac{\partial}{\partial t}\left[\ln R(t,-\infty)\right]_{t=0} \tag{7}$$

with $R(t,t_0)$ the so-called vacuum amplitude :

$$R(t,t_0) = < \Psi^I(-\infty)|U(t,t_0)|\Psi^I(-\infty) > \tag{8}$$

To cope efficiently with the anticommutation rules for construction operators of fermion type in the expansion of $R(t,t_0)$, one has to exploit the properties of normal products with respect to the vacuum and use the generalized Wick's theorem [64] in its time-dependent version. Each time-ordered contraction of a pair of creation and destruction operators within the vacuum defines a zeroth-order line. These lines are diagonal with respect to their indices, as a result of the anticommutation rules for fermion construction operators within a canonical basis. Depending on the time-ordering, these contraction lines can also be referred to as zeroth-order particle or hole propagators (Figure 2).

A critical step in the diagrammatic expansion [60] of the vacuum amplitude consists in partial summations [20] of the infinite series of disconnected graphs differing by the relative time-ordering of interaction elements belonging to different sub-diagrams, from which the linked-cluster theorem follows :

$$R(t,t_0) = \exp\left(\left[R(t,t_0)\right]_L\right) \tag{9}$$

with $\left[R(t,t_0)\right]_L$ the vacuum amplitude obtained as the sum of linked (or connected) contributions. To the n-th order, ΔE can hence be expressed as the summation of all the time-ordered topologically different linked diagrams (Figure 3) built up of n

interaction vertices connected by 2n contraction lines. By analogy with quantum electrodynamics and elementary particle physics from which they originate, these diagrams are often regarded as giving the fictitious time-evolution of the system in terms of creation of particles or holes under the influence of the perturbation V.

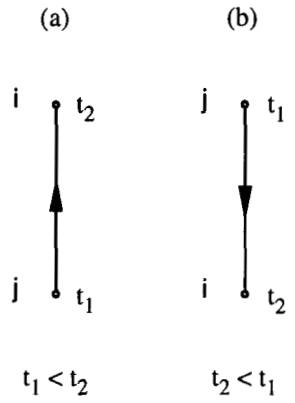

Figure 2 : representation of the zeroth-order propagators in terms of time-ordered diagonal (i=j) contraction lines. (a) particle lines : i,j virtual indices. (b) hole lines : i,j occupied indices.

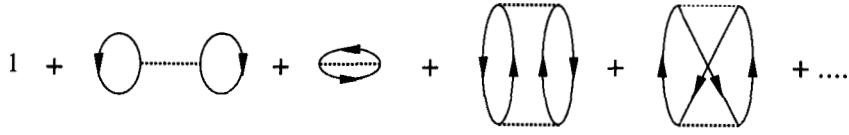

Figure 3 : diagrammatic expansion of the vacuum amplitude.

Closely related to MBPT, the exact one-particle propagator is defined in terms of the exact ground state wavefunction, as a time-ordered auto-correlation function [65] between one-electron states :

$$G_{ij}(t_2,t_1) = i^{-1} < \Psi_0^N | T_W \left[a_i(t_2) a_j^+(t_1) \right] | \Psi_0^N > \qquad (10)$$

with the fermion construction operators now expressed in the Heisenberg representation. The above contraction gives the probability amplitude [66] of propagation within a correlated background of a particle from states j to i in the retarded sector (t_1-t_2<0), or of a hole from states i to j in the advanced sector (t_1-t_2>0). As the exact hamiltonian is time-independent, **G** is time homogeneous and depends only on the difference $\tau=t_2-t_1$. Through Fourier resolution, one can derive its spectral resolution [67] in the frequency domain :

$$G_{ij}(\omega) = \lim_{\alpha\to 0^+} \sum_p \frac{<\Psi_0^N|a_i|\Psi_p^{N+1}><\Psi_p^{N+1}|a_j^+|\Psi_0^N>}{\omega-(E_p^{N+1}-E_0^N)+i\alpha} + \lim_{\alpha\to 0^+} \sum_h \frac{<\Psi_0^N|a_j^+|\Psi_h^{N-1}><\Psi_h^{N-1}|a_i|\Psi_0^N>}{\omega-(E_0^N-E_h^{N-1})-i\alpha} \qquad (11)$$

where the sums over p and h run over all the states of the (N+1)- and (N-1)-particles system. From (11) and neglecting infinitesimal convergence factors, it follows that the retarted and advanced components of $\mathbf{G}(\omega)$ have poles at the exact vertical electron-attachment and ionization energies, respectively. Making use once again of the adiabatic hypothesis in the interaction representation for switching on and off the interaction at times $t_0 = -\infty$ and $t = +\infty$, one can expand both sectors of $\mathbf{G}(\tau)$ according to [57] :

$$G_{ij}(\tau) = i^{-1}\frac{N(\tau)}{D} = i^{-1}\frac{<\Psi^I(-\infty)|T_W\,[a_i(\tau)a_j^+(0)\;U(+\infty,-\infty)]|\Psi^I(-\infty)>}{<\Psi(-\infty)|\;U(+\infty,-\infty)\;|\Psi(-\infty)>} \qquad (12)$$

where the vacuum amplitude appears in the denominator. Exploiting the Wick's theorem machinery to expand the numerator, one can factorize this into a summation over linked terms multiplied by the diagrammatic expansion of the vacuum amplitude (Figure 4). Therefore, all unlinked terms vanish (Figure 5) from the expansion of $\mathbf{G}(\tau)$. Carrying infinite summations [66] within the remaining infinite series of connected diagrams, this expansion can be achieved more efficiently using the iterative scheme of Figure 6a, whose algebraic equivalent in the frequency domain is the well-known Dyson equation :

$$\mathbf{G}(\omega) = \mathbf{G}^0(\omega) + \mathbf{G}^0(\omega)\Sigma(\omega)\mathbf{G}(\omega) \tag{13}$$

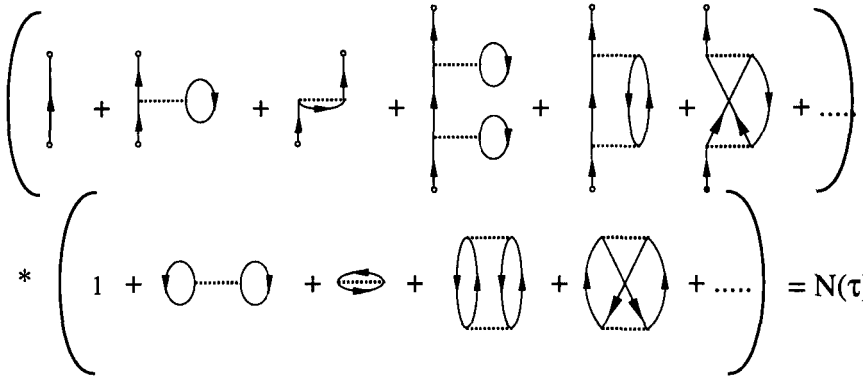

Figure 4 : Diagrammatic factorization of N(τ).

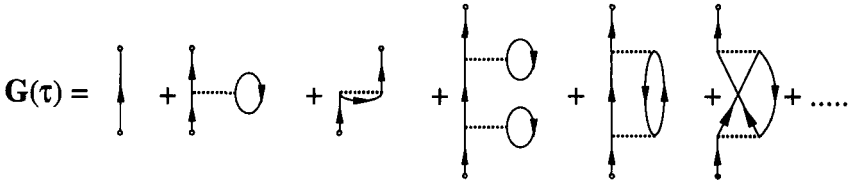

Figure 5 : Linked cluster expansion of **G**(τ).

In this renormalized form of **G**(ω), many-body effects are introduced through a non-local frequency-dependent effective potential : the so-called [60,66] irreducible self-energy Σ(ω). Figure 6a accounts for a suitable decoupling of the many-body problem, since in the time representation the probability amplitude for the overall propagation process is now described in terms of products of probability amplitudes for independent events of propagation and interaction. Through the desired order in the perturbation expansion, Σ is obtained (Figure 6b) as the sum of all the time-ordered topologically different and strongly connected diagrams (i.e. diagrams that do not fall into disconnected parts when a single contraction line is cut). An irreducible self-energy diagram of order n contains therefore n interaction vertices and (2n-1) contraction lines, as well as two hanging uncontracted lines

standing for the basis of one-particle states in which its matrix representation is cast.

The energy contribution of the successive vacuum amplitudes or self-energy graphs can be readily evaluated on the basis of well-known diagrammatic rules [13,23,32], derived by performing the time integrations in the Dyson series (equation 5) for the lowest order terms. For the forthcoming discussion, it is important to recall two specific points : (i) each line- or point-vertex results in a single or antisymmetrized bielectron integral factor in the numerator, respectively ; (ii) the contribution of a given diagram has to be summed over the particle or hole indices associated to each zeroth-order contraction line.

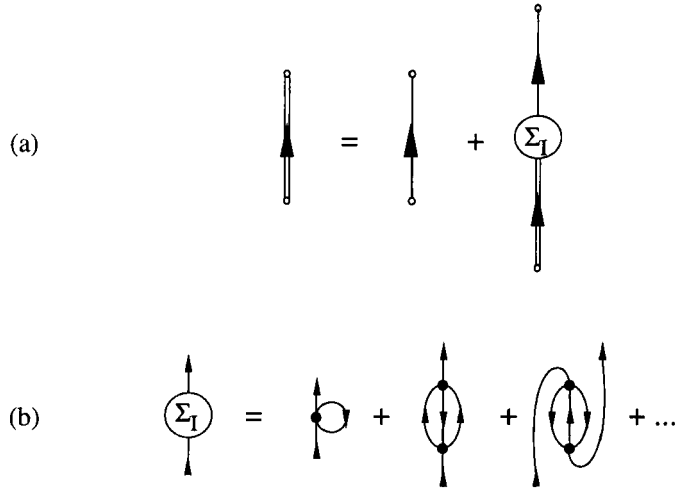

Figure 6 : (a) Diagrammatic form of the Dyson expansion and (b) expansion of the irreducible self-energy.

3. Basic CO-LCAO-SCF equations for stereoregular polymers

The periodic distribution of atoms - or groups of atoms - in the ideal model of an extended stereoregular polymer chain is conveniently expressed [38, 68-77] in terms of a one-dimensional lattice consisting of a large number ($N_0 \rightarrow \infty$) of points lined up in the direction of periodicity defined by the unit vector $\vec{e}_z$. To each lattice point corresponds a unit cell of length a_0 containing Ω_0 nuclei frozen in the Born-Oppenheimer approximation, and $2n_0$ electrons distributed along the nuclear framework. Unless mentioned, an insulating or semi-conducting closed-shell system is assumed for simplicity : therefore the process of doubly occupying the $N_0 \times n_0$ crystal orbital levels of lowest energy stops at points of no degeneracy between occupied and unoccupied levels. In the Restricted Hartree-Fock (RHF) theory, the uncorrelated polymer ground state many electron wavefunction is approximated as a single Slater determinant constructed from filled Bloch functions $\phi_n(k_n,\vec{r})\sigma(\xi)$, representing one-electron states with quasi-momenta ($k_n \vec{e}_z$) and spin-factor σ.

The usual [78] cyclic boundary constraints are assumed for the super-cell consisting of N_0 elementary units (the so-called Born - von Karman region), restricting therefore [79] the reduced wavenumbers k_n to N_0 discrete values within the first Brillouin zone [BZ], i.e. in this case the interval ($-\pi/a_0 \leq k < \pi/a_0$). Each of these values corresponds to a particular irreducible representation of the translational symmetry group, containing in principle an infinite number of Bloch functions of k_n symmetry, characterized by their band index n = 1,2,3, ...∞ . The existence of additional Euclidean symmetries, like e.g. a screw axis, a glide plane, ...etc, implies that the spatial part of the Bloch functions $\phi_n(k_n,\vec{r})$ transform according to one of the irreducible representations of a line group [80-82]. In this work, the corresponding labels are implicitly contained in the band index. To avoid unnecessary complications, no reference to the group theory will be made; only the general properties of energy bands belonging to different irreducible representations will be invoked.

The eigenfunctions $\phi_n(k_n,\vec{r})$ and eigenvalues $\varepsilon_n(k_n)$ of the Fock operator $\hat{F}(\vec{r})$ are the most convenient starting points of most projects for incorporating the electronic correlation. For closed-shell systems, the spatial part of the crystalline spin-orbital $\phi_n(k_n,\vec{r})\sigma(\xi)$ is a solution of the standard RHF equation :

$$\hat{F}(\vec{r})\phi_n(k_n,\vec{r}) = \left\{ -\frac{1}{2}\nabla^2 - \sum_{\mu}^{N_0}\sum_{\vartheta=1}^{\Omega_0} \frac{Z_\vartheta}{|\vec{r}-\vec{R}_\vartheta-\mu a_0 \vec{e}_z|} + \sum_{b=1}^{n_0}\sum_{k_b}^{BZ} \eta_b(k_b)\times\left(2\hat{J}_b(k_b,\vec{r})-\hat{K}_b(k_b,\vec{r})\right)\right\}\phi_n(k_n,\vec{r})$$
$$= \varepsilon_n(k_n)\phi_n(k_n,\vec{r}) \qquad (14)$$

where the kinetic, nuclear attraction and electron-electron repulsion parts of the Fock operator $\hat{F}(\vec{r})$ can be easily recognized. From here and henceforth, the summations over wave numbers k_i and cell indices μ are restricted to the first Brillouin zone and to the Born - von Karman region, respectively. The $\vec{R}_\vartheta$ are the position vectors associated to the nuclear charges Z_ϑ in the reference unit cell. A strict electroneutrality of the cells $2n_0 = \sum_\vartheta Z_\vartheta$ is required to ensure the stability of the chain. In the previous equation, the indices μ label the cell located at position $\mu a_0 \vec{e}_z$ with respect to the origin of the frame of coordinates. $\eta_b(k_b)$ is the standard single-particle state occupation number (1 if occupied, 0 if unoccupied), limiting the summation over the combined index (b,k_b) to occupied (hole) states only. The operators $\hat{J}_b(k_b,\vec{r})$ and $\hat{K}_b(k_b,\vec{r})$ respectively describe the classical electrostatic (Coulomb) and exchange potentials due to an average static electron distribution acting on the electron state $\phi_n(k_n,\vec{r})$.

$$\hat{J}_b(k_b,\vec{r})\phi_n(k_n,\vec{r}) = \left[\int d\vec{r}'\phi_b^*(k_b,\vec{r}')|\vec{r}-\vec{r}'|^{-1}\phi_b(k_b,\vec{r}')\right]\phi_n(k_n,\vec{r}) \qquad (15)$$

$$\hat{K}_b(k_b,\vec{r})\phi_n(k_n,\vec{r}) = \left[\int d\vec{r}'\phi_b^*(k_b,\vec{r}')|\vec{r}-\vec{r}'|^{-1}\phi_n(k_n,\vec{r}')\right]\phi_b(k_b,\vec{r}) \qquad (16)$$

Closed-form solutions to equation (14) are beyond reach, but reasonable approximations can be obtained if the electron states $\phi_n(k_n,\vec{r})$ are expressed in a LCAO expansion in terms of a basis of symmetry adapted functions : the Bloch sums $\beta_p(k_n,\vec{r})$.

$$\phi_n(k_n,\vec{r}) = \sum_{p=1}^{M_0} C_{pn}(k_n)\beta_p(k_n,\vec{r})$$

$$= \lim_{N_0\to\infty} \frac{1}{\sqrt{N_0}} \sum_{p=1}^{M_0} C_{pn}(k_n) \sum_{\mu=1}^{N_0} e^{i k_n \mu a_0} \gamma_p^{\mu}(\vec{r}) \tag{17}$$

where M_0 stands for the number of atomic functions per cell. For the atomic functions, we have adopted the compact notation :

$$\gamma_p^{\mu}(\vec{r}) = \gamma_p^0(\vec{r} - \vec{r}_p - \mu a_0 \vec{e}_z) \tag{18}$$

with $\vec{r}_p$ defining the center of γ_p.

By virtue of the translational properties inherent in equation (17), Bloch orbitals are orthonormal with respect to the quasi-momentum indices. Furthermore, the Fock equation is derived from a variation principle subject to the usual orthogonality constraints $< \phi_i(k_i) \mid \phi_j(k_j) > = \delta_{ij}\, \delta_{(k_i,k_j)}$. When expressed in terms of the primitive atomic functions γ_p, these constraints read :

$$\sum_{p=1}^{M_0}\sum_{q=1}^{M_0} C_{pi}^*(k_i) < \beta_p(k_i) | \beta_q(k_j) > C_{qj}(k_j) = \delta_{ij}\,\delta_{(k_i,k_j)} \sum_{p=1}^{M_0}\sum_{q=1}^{M_0} D_{pq,i}(k_i) S_{pq}(k_i)$$

$$= \delta_{ij}\,\delta_{(k_i,k_j)} \tag{19}$$

with $\mathbf{S}(k)$ the overlap matrix with respect to the atomic functions in the k-th irrep

$$S_{pq}(k) = \lim_{N_0\to\infty} \sum_{\mu=1}^{N_0} e^{i k \mu a_0} < \gamma_p^0 | \gamma_q^{\mu} > = \lim_{N_0\to\infty} \sum_{\mu=1}^{N_0} e^{i k \mu a_0}\, S_{pq}^{0\mu} \tag{20}$$

and $\mathbf{D}_i(k)$ the contribution of an electron in the crystal orbital $\phi_i(k)$ to the one-particle density matrix.

$$D_{pq,i}(k) = C_{pi}^*(k) C_{qi}(k) \tag{21}$$

As Bloch orbitals which belong to different irreducible representations of the translational symmetry group do not combine, the approximate solutions to

equation (14) are solutions of a generalized $M_0 \times M_0$ hermitian eigenvalue problem :

$$\sum_{q=1}^{M_0}\left[F_{pq}(k)-\varepsilon_n(k)S_{pq}(k)\right]C_{qn}(k)=0\,; \qquad \forall p,n\in\{1,M_0\}\,; \qquad \forall k\in BZ; \tag{22}$$

with the Fock matrix elements obtained as :

$$F_{pq}(k)=\lim_{N_0\to\infty}\sum_{\mu=1}^{N_0} e^{ik\mu a_0}<\gamma_p^0|\hat{F}|\gamma_q^\mu> \tag{23}$$

4. Implications of the linked cluster theorem for extended systems

In most applications, the HF eigenvalues $\phi_n(k_n,\vec{r})$ and $\varepsilon_n(k_n)$ are used to define a zeroth-order approximation $\mathbf{G^0}(\omega)$ to the exact (HF-MBGF) one-particle propagator. Suppose the equation (14) has been solved, then it is in principle easy to find the poles of the exact one-particle propagator for a one-dimensional periodic system, since they correspond to the solutions of a self-consistent eigenvalue problem of dimension $M_0 \times M_0$:

$$\det|\omega(k)-\boldsymbol{\varepsilon}(k)-\boldsymbol{\Sigma}[k,\omega(k)]|=0 \qquad \forall k\in BZ \tag{24}$$

As the propagator taken as a zeroth-order approximation in the recursive Dyson expansion is itself a renormalized form through first order in the electronic interaction, the self-energy needed to obtain $\mathbf{G}(\omega)$ by renormalization of the HF propagator has to be expanded from second-order :

$$\Sigma(k,\omega)=\Sigma^{(2)}(k,\omega)+\Sigma^{(3)}(k,\omega)+\Sigma^{(4)}(k,\omega)+... \tag{25}$$

For the sake of simplicity, we temporarily include the spin index in the band index. This will enable us to develop vacuum amplitude and self-energy diagrams in terms of antisymmetrized bielectron integrals such as $<\phi_l(k_l)\phi_m(k_m)||\phi_n(k_n)\phi_o(k_o)>$, using the conventions of Hugenholtz. These interaction elements are expanded in terms of Bloch functions and ultimately in terms of primitive atomic orbitals :

$$< \phi_l(k_l)\phi_m(k_m)| \, |\phi_n(k_n)\phi_o(k_o) > = \lim_{N_0\to\infty} (N_0)^{-2} \sum_{pqrs}^{M_0} C^*_{pl}(k_l)C_{qn}(k_n)C^*_{rm}(k_m)C_{so}(k_o) \times \sum_{\mu\mu'\mu''\mu'''}^{N_0} \left[e^{i(k_n\mu' + k_o\mu''' - k_l\mu - k_m\mu'')a_0} < \gamma_p^{\mu} \gamma_r^{\mu''} || \gamma_q^{\mu'} \gamma_s^{\mu'''} > \right] \tag{26}$$

Taking into account the lattice periodicity, we find immediately :

$$< \phi_l(k_l)\phi_m(k_m)| \, |\phi_n(k_n)\phi_o(k_o) > = \lim_{N_0\to\infty} (N_0)^{-2} \sum_{pqrs}^{M_0} C^*_{pl}(k_l)C_{qn}(k_n)C^*_{rm}(k_m)C_{so}(k_o) \times \times \sum_{\mu'\mu''\mu'''}^{N_0} \left[e^{i(k_n\mu' + k_o\mu''' - k_m\mu'')a_0} < \gamma_p^{0} \gamma_r^{\mu''} || \gamma_q^{\mu'} \gamma_s^{\mu'''} > \right] \times \sum_{\mu}^{N_0} \left[e^{i(k_n + k_o - k_l - k_m)\mu a_0} \right] \tag{27}$$

In this equation, the μ–summation strictly vanishes, unless

$$k_n + k_o = k_l + k_m + \frac{2\pi G}{a_0} \quad , \tag{28}$$

with G=0,1,2, ... N_0. As contrasted with translationally invariant systems, for which $a_0 \to 0$, the last equation shows that the conservation of momenta is not strictly satisfied in infinite periodic inhomogeneous systems. The extra term, $2\pi G/a_0$, accounts for the exchange of momentum arising from the diffraction of the electron waves on the crystal lattice. Restricting quasi-momenta to the first Brillouin zone, we obtain :

$$\sum_{\mu}^{N_0} \left[e^{i(k_n + k_o - k_l - k_m)\mu a_0} \right] = \sum_{G=1}^{N_0} \delta_{(k_n + k_o, k_l + k_m + 2\pi G/a_0)} = N_0 \, \delta_{(k_n + k_o, k_l + k_m)} \tag{29}$$

and hence :

$$< \phi_l(k_l)\phi_m(k_m)\| \|\phi_n(k_n)\phi_o(k_o) > = \lim_{N_0 \to \infty} (N_0)^{-1} \delta_{(k_n+k_o,k_l+k_m)} \tau\left(\begin{matrix} k_l & k_m \\ l & m \end{matrix} \middle| \middle| \begin{matrix} k_n & k_o \\ n & o \end{matrix}\right) \tag{30}$$

with

$$\tau\left(\begin{matrix} k_l & k_m \\ l & m \end{matrix} \middle| \middle| \begin{matrix} k_n & k_o \\ n & o \end{matrix}\right) = \sum_{pqrs}^{M_0} C^*_{pl}(k_l) C_{qn}(k_n) C^*_{rm}(k_m) C_{so}(k_o) \times \sum_{\mu\mu'\mu''}^{N_0} \left[e^{i(k_n\mu + k_o\mu'' - k_m\mu')a_0} < \gamma^0_p \gamma^{\mu'}_r \| \gamma^{\mu}_q \gamma^{\mu''}_s > \right] \tag{31}$$

a complex function, the modulus of which is independent of the number (N_0) of elementary units in the super-cell as the latter becomes infinite. From equation (30), it follows that a general interaction element displays a characteristic $(N_0)^{-1}$ size-dependence, as a final outcome of the delocalization of the canonical (supra)molecular orbitals in the thermodynamic limit ($N_0 \to \infty$). Within the first Brillouin zone, equation (30) also implies the conservation of the incident flow of quasi-momentum at any point-vertex (Figure 7).

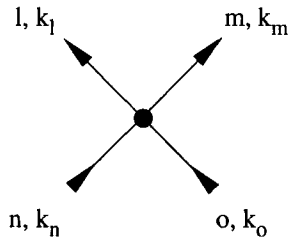

Figure 7 : the point-vertex which corresponds to integral (30).

Taking the limit $a_0 \to \infty$, all the bielectron integrals over atomic orbitals implied in equation (31) vanish through the interplay of charge distributions and overlap integrals, except those corresponding to the cell indices $\mu=\mu'=\mu''=0$. In this limit, the stereoregular chain can be regarded as dissociating into N_0 distinct molecular fragments, under the constraint of conservation of its translational symmetry. The final result of this dissociation is equivalent to an extended stereoregular chain,

consisting of N_0 artificially isolated elementary cells. In such an extreme limit, each interaction element is strictly proportional to $(N_0)^{-1}$, since :

$$\lim_{a_0 \to \infty} <\phi_l(k_l)\phi_m(k_m)||\phi_n(k_n)\phi_o(k_o)> = \lim_{N_0 \to \infty} (N_0)^{-1} \delta_{(k_n+k_o,k_l+k_m)} \tau_0 \left(\begin{matrix} k_l & k_m \\ l & m \end{matrix} \middle| \middle| \begin{matrix} k_n & k_o \\ n & o \end{matrix} \right) \tag{32}$$

where the τ function has been restricted to a four-indices summation over the M_0 atomic functions contained in the reference cell, yielding a finite result τ_0, which is independent of the size of the supersystem. Furthermore, this function does not exhibit any dependence on quasi-momenta, since in the extreme situation of a periodic system consisting of unit cells at infinitely large distance, there is no dispersion of states within an infinitely small first Brillouin zone centered around the origin of the reciprocal space. Any of these τ_0 functions can hence be regarded as one of the constants of a supersystem of non-interacting molecules, corresponding to an antisymmetrized bielectron integral over molecular orbitals localized on a given element of this supersystem.

$$\tau_0 \left(\begin{matrix} k_l & k_m \\ l & m \end{matrix} \middle| \middle| \begin{matrix} k_n & k_o \\ n & o \end{matrix} \right) = \sum_{pqrs}^{M_0} C^*_{pl}(0) C_{qn}(0) C^*_{rm}(0) C_{so}(0) < \gamma^0_p \gamma^0_r || \gamma^0_q \gamma^0_s > \tag{33}$$

The conservation of the flows of quasi-momenta plays a crucial role in the size-consistency of Many-Body theories as applied to extended systems. For periodic inhomogeneous systems, this is intimately related to translational symmetry which also allows for a k-block diagonalization of the one-particle and self-energy matrices, as a result of the conservation of the total momentum during the overall propagation process.

Taking $|\phi_c(k_c)>$ and $\omega_c(k_c)$ as the one-particle state and effective binding energy of interest, we first consider a second-order expansion of $\Sigma(k_c,\omega)$. From the conservation of the incoming flow of quasi-momentum at any vertices (Figure 8a), it follows that, for a stereoregular chain, the second-order self-energy can be obtained as :

$$\Sigma^{(2)}_{ij}(k_c,\omega)$$

$$= \lim_{N_0\to\infty} \frac{1}{2} \sum_{ars} \sum_{k_a}^{BZ} \sum_{q}^{BZ} (N_0)^{-2} \frac{\tau\left(\begin{smallmatrix} k_c & k_a \\ i & a \end{smallmatrix}\middle|\middle|\begin{smallmatrix} k_c+q & k_a-q \\ r & s \end{smallmatrix}\right)\tau\left(\begin{smallmatrix} k_c+q & k_a-q \\ r & s \end{smallmatrix}\middle|\middle|\begin{smallmatrix} k_c & k_a \\ j & a \end{smallmatrix}\right)}{\omega_c(k_c)+\varepsilon_a(k_a)-\varepsilon_r(k_c+q)-\varepsilon_s(k_a-q)}$$

$$+ \lim_{N_0\to\infty} \frac{1}{2} \sum_{abr} \sum_{k_r}^{BZ} \sum_{q}^{BZ} (N_0)^{-2} \frac{\tau\left(\begin{smallmatrix} k_c & k_r \\ i & r \end{smallmatrix}\middle|\middle|\begin{smallmatrix} k_c+q & k_r-q \\ a & b \end{smallmatrix}\right)\tau\left(\begin{smallmatrix} k_c+q & k_r-q \\ a & b \end{smallmatrix}\middle|\middle|\begin{smallmatrix} k_c & k_r \\ j & r \end{smallmatrix}\right)}{\omega_c(k_c)+\varepsilon_r(k_r)-\varepsilon_a(k_c+q)-\varepsilon_b(k_r-q)} \quad (34)$$

In the above equation, q accounts for the transfer of quasi-momentum at the interaction vertices. Since there are N_0 values of k permitted in the first Brillouin zone, the double summations over quasi-momenta result in a factor proportional to $(N_0)^2$ in the limit of an infinite system. In the limit of a non-interacting stereoregular chain $a_0 \to \infty$, this factor strictly cancels the $(N_0)^{-2}$ size-dependence arising with the two bielectron interaction elements. In this limit, the second-order self-energy contribution is independent of the size of the supersystem, and satisfies therefore the proper separability condition for an intensive property :

$$\lim_{a_0\to\infty} \Sigma^{(2)}_{ij}(k_c,\omega) = \frac{1}{2} \sum_{ars} \frac{\tau_0\left(\begin{smallmatrix} 0 & 0 \\ i & a \end{smallmatrix}\middle|\middle|\begin{smallmatrix} 0 & 0 \\ r & s \end{smallmatrix}\right)\tau_0\left(\begin{smallmatrix} 0 & 0 \\ r & s \end{smallmatrix}\middle|\middle|\begin{smallmatrix} 0 & 0 \\ j & a \end{smallmatrix}\right)}{\omega_c(0)+\varepsilon_a(0)-\varepsilon_r(0)-\varepsilon_s(0)}$$

$$+ \frac{1}{2} \sum_{abr} \frac{\tau_0\left(\begin{smallmatrix} 0 & 0 \\ i & r \end{smallmatrix}\middle|\middle|\begin{smallmatrix} 0 & 0 \\ a & b \end{smallmatrix}\right)\tau_0\left(\begin{smallmatrix} 0 & 0 \\ a & b \end{smallmatrix}\middle|\middle|\begin{smallmatrix} 0 & 0 \\ j & r \end{smallmatrix}\right)}{\omega_c(0)+\varepsilon_r(0)-\varepsilon_a(0)-\varepsilon_b(0)} \quad (35)$$

At the same order of the perturbation expansion, the vacuum amplitude diagram (Figure 8b) exhibits one more contraction line than the two self-energy diagrams of Figure 8a. Therefore, the development of the second-order correlation energy for a stereoregular chain implies one more quasi-momentum variable :

$$E^{(2)}_{corr} = \lim_{N_0\to\infty} \sum_{abrs} \sum_{k_a}^{BZ} \sum_{k_b}^{BZ} \sum_{q}^{BZ} (N_0)^{-2} \frac{\left\|\tau\left(\begin{smallmatrix} k_a & k_b \\ a & b \end{smallmatrix}\middle|\middle|\begin{smallmatrix} k_a+q & k_b-q \\ r & s \end{smallmatrix}\right)\right\|^2}{\varepsilon_a(k_a)+\varepsilon_b(k_b)-\varepsilon_r(k_a+q)-\varepsilon_s(k_b-q)} \quad (36)$$

Since in this case, a triple summation over the N_0 quasi-momenta permitted in the first Brillouin zone yields a factor $(N_0)^3$ of proportionality in the non-interacting

limit, the second order correlation energy is directly proportional to the number of isolated elements present in the supersystem, and therefore satisfies the proper separability conditions for an extensive property.

$$\lim_{a_0 \to \infty} E_{corr}^{(2)} = N_0 \times \frac{1}{4} \sum_{abrs} \frac{\left\| \tau_0 \begin{pmatrix} 0 & 0 \\ a & b \end{pmatrix} \middle| \begin{pmatrix} 0 & 0 \\ r & s \end{pmatrix} \right\|^2}{\varepsilon_a(0) + \varepsilon_b(0) - \varepsilon_r(0) - \varepsilon_s(0)} \tag{37}$$

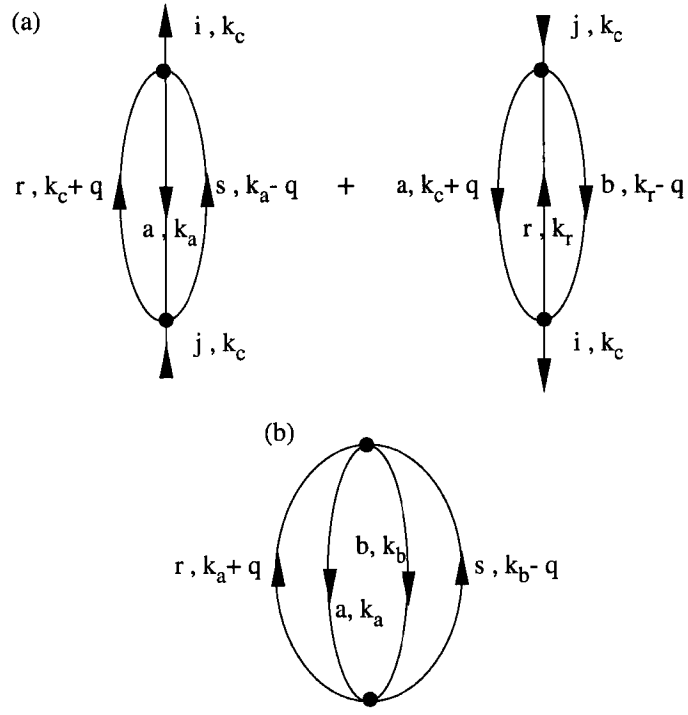

Figure 8 : Flows of quasi-momentum in second-order (a) self-energy and (b) vacuum amplitude diagrams.

Considering the topology of the diagrams representing the self-energy and the correlation energy, the above conclusions can be easily generalized to higher orders. At the n-th order, any self-energy or vacuum amplitude diagram contains n interaction vertices, each of them resulting in a factor proportional to $(N_0)^{-1}$ in the limit of a non interacting system. As any diagram of order n exhibits n-1 time intervals for independent propagation between the n interaction vertices, and since

the flow of incident quasi-momentum is conserved at any point- (or line-) vertex, it is always possible, *in a connected diagram*, to infer n-1 constraints on quasi-momenta. Therefore, there remain only (2n-1)-(n-1)=n or (2n)-(n-1)=n+1 independent quasi-momentum variables in the diagrams accounting for the n-th order contribution to the self-energy and correlation energy, respectively. Since the quasi-momentum summations run over the N_0 discrete values of k permitted in the first Brillouin zone, one readily concludes that the self-energy or correlation energy are strictly independent of or strictly proportional to the number of elements within a non-interacting supersystem, whatever the order of their expansion. In other words, the MBGF and MBPT expansions of the self-energy and of the electron correlation energy satisfy, order by order, the proper separability conditions required for the computation of intensive or extensive properties, respectively.

This is also true for more sophisticated decouplings of the many-body problem, such as various direct CI-like schemes derived within [83-85] the Equation-of-Motion [86] / algebraic superoperator [87] or Algebraic Diagrammatic Construction [88-90] approaches, since in these cases the corresponding self-energies can be expanded in terms of finite or infinite series of connected diagrams sharing some particular topological features. Well-known partial summations of self-energy terms are the (G)RPA (Generalized Random Phase Approximation) and "ladder"series displayed in Figure 9, which account for the dominant collective motions in "high density" and "low density" interacting systems, respectively [13].

The exclusion of self-energy or vacuum diagrams disconnected into m distinct sub-graphs ($m \geq 2$) is a sufficient condition for the size-consistency of any development based upon the "linked-cluster theorem". As one could find only n-m conservation contraints on the flows of quasi-momenta in such diagrams, their respective contributions should exhibit a characteristic size-dependence of $(N_0)^{m-1}$ or $(N_0)^m$ in the limit of a non-interacting supersystem of N_0 molecules.

The proper size-intensive and size-extensive behaviours of the self-energy and of the correlation energy in the non-interacting limit can alternatively be proved by making a unitary transformation to localized orbitals. This is possible because such a transformation does not affect the Hartree-Fock orbital energies (all orbitals in

one energy band are degenerate). In a localized picture, one usually infer the scaling properties of connected diagrams for two-non interacting subsystems and by induction for an infinite number of subsystems.

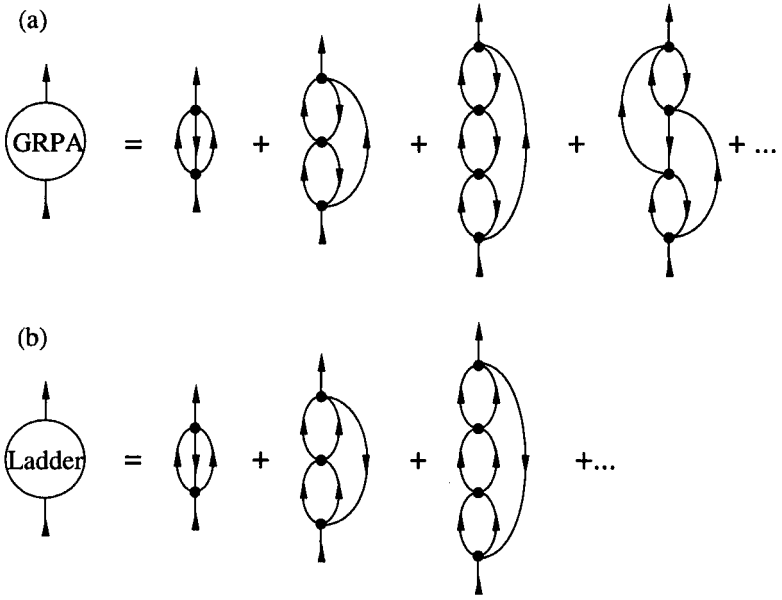

Figure 9 : (G)RPA (a) and ladder (b) expansions of the self-energy in the retarded sector of **G**.

In this section, we have stressed the essential role played by the flows of quasi-momenta in the size-consistent scaling of connected diagrams in the non-interacting limit. Since in this limit quasi-momenta reflect directly the degeneracy of one-electron states, any restriction on the summations over states for a given diagram will end in a loss of size-consistency. At this point, it is useful to consider some particular decoupling approximations, derived using the two-particle-hole Tamm-Dankoff Approximation (2ph-TDA) scheme [90] of renormalization of the self-energy kernel. This scheme, designed to deal with the leading collective effects encountered in real molecular systems with either high and low electron density regions, consists in a partial summation of the infinite series of GRPA and ladder diagrams, as well as all their possible mixings. Two subsequent approximations

are reported in the litterature. These are derived restricting the kernel to its diagonal elements :

$$\Sigma_{ij}(k_c,\omega)$$

$$= \lim_{N_0\to\infty} \frac{(N_0)^{-2}}{2} \sum_{ars} \sum_{q,k_a}^{BZ} \frac{\tau\left(\begin{matrix}k_c & k_a\\ i & a\end{matrix}\middle|\middle|\begin{matrix}k_c+q & k_a-q\\ r & s\end{matrix}\right)\tau\left(\begin{matrix}k_c+q & k_a-q\\ r & s\end{matrix}\middle|\middle|\begin{matrix}k_c & k_a\\ j & a\end{matrix}\right)}{\omega_c(k_c)+\varepsilon_a(k_a)-\varepsilon_r(k_c+q)-\varepsilon_s(k_a-q)+\Delta_{ars}(k_a,q)}$$

$$+ \lim_{N_0\to\infty} \frac{(N_0)^{-2}}{2} \sum_{abr} \sum_{q,k_r}^{BZ} \frac{\tau\left(\begin{matrix}k_c & k_r\\ i & r\end{matrix}\middle|\middle|\begin{matrix}k_c+q & k_r-q\\ a & b\end{matrix}\right)\tau\left(\begin{matrix}k_c+q & k_r-q\\ a & b\end{matrix}\middle|\middle|\begin{matrix}k_c & k_r\\ j & r\end{matrix}\right)}{\omega_c(k_c)+\varepsilon_r(k_r)-\varepsilon_a(k_c+q)-\varepsilon_b(k_r-q)-\Delta_{rab}(k_r,q)} \tag{38}$$

This expression corresponds to a second-order expansion of the self-energy, of which the energy denominators are shifted according to :

$$\Delta_{lmn}(k_l,q) = \frac{1}{N_0}\left\{\lambda\tau\left(\begin{matrix}k_l+q & k_c-q\\ m & n\end{matrix}\middle|\middle|\begin{matrix}k_l+q & k_c-q\\ m & n\end{matrix}\right) - \tau\left(\begin{matrix}k_l & k_c+q\\ l & m\end{matrix}\middle|\middle|\begin{matrix}k_l & k_c+q\\ l & m\end{matrix}\right)\right.$$
$$\left. - \tau\left(\begin{matrix}k_l & k_c+q\\ l & m\end{matrix}\middle|\middle|\begin{matrix}k_l & k_c+q\\ l & m\end{matrix}\right)\right\} \tag{39}$$

with λ=1 or λ=1/2 in the so-called [83] Shifted Born Collision (SBC) or diagonal 2ph-TDA approximations, respectively. The shifts of the 2p-1h and 2h-1p excitation energies exhibit a characteristic $(N_0)^{-1}$ size-dependence. Therefore, the SBC and diagonal 2ph-TDA renormalizations are not size-consistent, since the above self-energy terms are not independent of the size of the system in the non interacting limit $a_0 \to \infty$. Furthermore, the effect of these renormalizations tend to vanish in the thermodynamic limit $N_0 \to \infty$ (Figure 10). This loss of size-consistency beyond second-order can be attributed to the freezing of some variables accounting for the transfer of quasi-momentum in the higher order diagrams issued from the SBC or diagonal 2ph-TDA renormalizations.

The diagonal 2ph-TDA self-energy will be turned size-consistent if use is made of localized orbitals in the non-interacting limit. This observation emphasizes the point that the diagonal version of 2ph-TDA is not invariant under transformations of degenerate orbitals. More generally, it underlines how essential it is for scaling

properties that diagrams are invariant under a unitary transformations of occupied and virtual orbitals (taking into account that the inclusions of energy denominators may then require the solution of linear systems of equations).

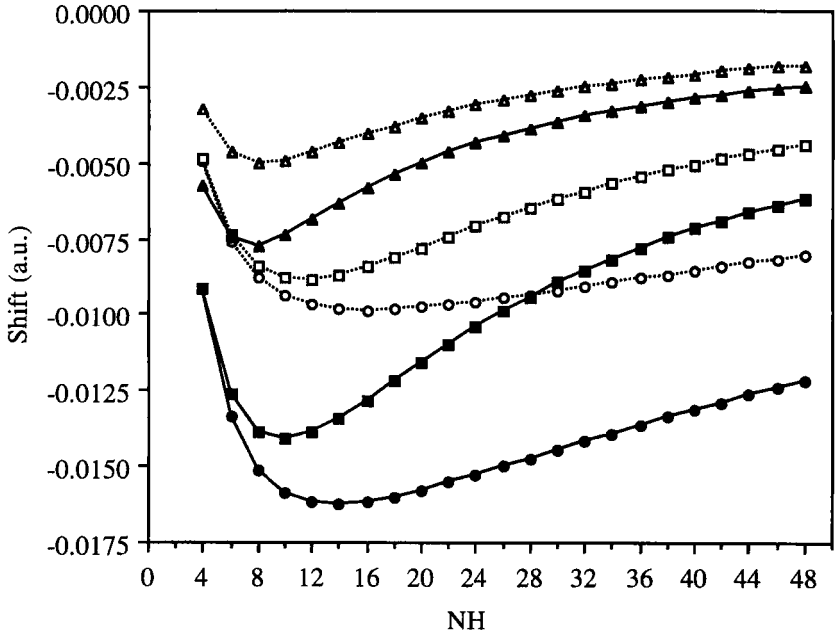

Figure 10 : Shifts arising with respect to second-order results [91a] on the first ionization energy of hydrogen chains of increasing size with the SBC or diagonal 2ph-TDA renormalizations of $\Sigma^{(2)}(\omega)$. Regular (d=1.4 hartree) and alternating (d_1=1.4 hartree; and d_2=1.8 hartree or d_2=2.8 hartree) systems have been considered. (STO-3G basis set).

Legend :

SBC(14:14) — 2ph-TDA(14:18)

2ph-TDA(14:14) — SBC(14:28)

SBC(14:18) — 2ph-TDA(14:28)

5. Singular bielectron integrals on crystalline orbitals

As stressed in the previous section, the connectivity of self-energy or vacuum amplitude diagrams is a sufficient condition to ensure their size-consistency, which appears as the final outcome of a suitable balance between the delocalization [91] and the degeneracy of one-particle canonical states in a supersystem of non-interacting molecules. However, any well-bred physicist or chemist would certainly regard a periodic chain of non-interacting monomers as a highly simplified model of a real stereoregular polymer, which does not address the long-range character of the Coulomb potential and the potentially divergent behaviour of some interaction elements. Connectivity alone does not prevent the development of full divergences when evaluating such diagrams in the limit of an infinite system. It is therefore not a sufficient condition to guarantee the thermodynamic size-extensivity or size-intensivity of a given diagram.

When dealing with real stereoregular polymers, the development of a general antisymmetrized τ function as written in equation (31) usually converges as long as the lattice summations extend to infinity, from which one may suppose that size-consistency implies automatically size-intensivity or size-extensivity. Care is however needed for the bielectron antisymmetrized integrals corresponding to point-vertices that represent interaction processes without any effective transfer of quasi-momentum between the colliding contraction lines. To highlight the size-related difficulties resulting from these integrals, it is first useful to sort out the point-vertices (Figure 11) and the associated τ functions in terms of their direct and exchange contributions :

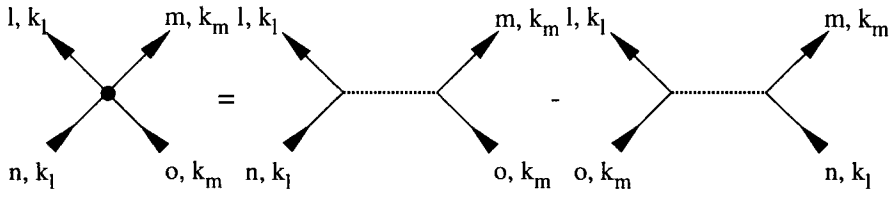

Figure 11 : point- and line-vertices corresponding to equation (40)

$$\tau\begin{pmatrix} k_l & k_m \\ l & m \end{pmatrix}\begin{pmatrix} k_l & k_m \\ n & o \end{pmatrix} = \tau\begin{pmatrix} k_l & k_m \\ l & m \end{pmatrix}\begin{pmatrix} k_l & k_m \\ n & o \end{pmatrix} - \tau\begin{pmatrix} k_l & k_m \\ l & m \end{pmatrix}\begin{pmatrix} k_m & k_l \\ o & n \end{pmatrix} \tag{40}$$

Expanding the lattice summations and taking into account once again the lattice periodicity, one can find, after a little algebra :

$$\tau\begin{pmatrix} k_l & k_m \\ l & m \end{pmatrix}\begin{pmatrix} k_l & k_m \\ n & o \end{pmatrix} = \sum_{pqrs}^{M_0} C^*_{pl}(k_l)C_{qn}(k_l)C^*_{rm}(k_m)C_{so}(k_m) \times \sum_{\mu\mu'\mu''}^{N_0}\left[e^{i(k_l\mu+k_m\mu'')a_0} < \gamma_p^0 \gamma_r^{\mu'} | \gamma_q^{\mu} \gamma_s^{\mu'+\mu''} > \right] \tag{41a}$$

$$\tau\begin{pmatrix} k_l & k_m \\ l & m \end{pmatrix}\begin{pmatrix} k_m & k_l \\ o & n \end{pmatrix} = \sum_{pqrs}^{M_0} C^*_{pl}(k_l)C_{so}(k_m)C^*_{rm}(k_m)C_{qn}(k_l) \times \sum_{\mu\mu'\mu''}^{N_0}\left[e^{i[(k_l-k_m)\mu+k_m(\mu''-\mu')]a_0} < \gamma_p^0 \gamma_r^{\mu+\mu'} | \gamma_s^{\mu''} \gamma_q^{\mu} > \right] \tag{41b}$$

To identify the convergence properties of the above lattice summations, we assume an asymptotic exponential decay with respect to μ of the atomic functions γ_p^{μ}. The integrals $< \gamma_p^0 \gamma_r^{\mu'} | \gamma_q^{\mu} \gamma_s^{\mu'+\mu''} >$ or $< \gamma_p^0 \gamma_r^{\mu+\mu'} | \gamma_s^{\mu''} \gamma_q^{\mu} >$ correspond to the electrostatic interaction between the charge distributions $\gamma_p^0\gamma_q^{\mu}$ and $\gamma_r^{\mu'}\gamma_s^{\mu'+\mu''}$, or $\gamma_p^0\gamma_s^{\mu''}$ and $\gamma_r^{\mu+\mu'}\gamma_q^{\mu}$. These observations provide a natural cut off procedure in a short-range region for series μ and μ'' in equation (41a), and for series μ' and μ'' in equation (41b), since in both cases the successive terms decay exponentially [52] as the overlap integrals ($S_{pq}^{0\mu}$ and $S_{rs}^{0\mu''}$) and ($S_{ps}^{0\mu''}$ and $S_{rq}^{0\mu'}$), respectively. The sum over μ' in the expansion of the direct term (41a), however, exhibits a logarithmically divergent character because it directly relates to Coulomb interaction terms without any μ'-dependent phase factor, which at large separations between the interacting charge distributions decay slowly as $|\mu'|^{-1}$. Similarly, for the exchange term (41b), the sum over μ may also yield a logarithmically divergent behaviour in the thermodynamic limit, when $k_l = k_m$. In both cases, divergences can be related to the lack of transfer of quasi-momentum through the corresponding line-vertices (Figure 11).

To identify the conditions ensuring the convergence of a given τ function related to such line-vertices in the thermodynamic limit, equation (41a) is rewritten as :

$$\tau\begin{pmatrix} k_l & k_m \\ l & m \end{pmatrix}\begin{pmatrix} k_l & k_m \\ n & o \end{pmatrix} = \sum_{\mu'}^{N_0}\left\{\sum_{pqrs}^{M_0} C^*_{pl}(k_l)C_{qn}(k_l)C^*_{rm}(k_m)C_{so}(k_m) \times \sum_{\mu}^{N_0} e^{ik_l\mu a_0}\sum_{\mu''}^{N_0} e^{ik_m\mu'' a_0} < \gamma_p^0 \gamma_r^{\mu'} | \gamma_q^{\mu} \gamma_s^{\mu'+\mu''} > \right\} \tag{42}$$

Since the successive terms in the μ- and μ''-series decay rapidly, it is always possible, even in the asymptotic limit $N_0 \to \infty$, to carry out the multiple summations over μ, μ', and μ'' maintaining μ' much larger than μ and μ''. Charge distributions at very large distances can hence be regarded as point charges. Considering, without any loss of generality, gaussian atomic functions of s type, the atomic bielectron integrals implied in equation (42) can be approximated to :

$$< \gamma_p^0 \gamma_r^{\mu'} | \gamma_q^{\mu} \gamma_s^{\mu'+\mu''} > = \frac{1}{a_0} \frac{S_{pq}^{0\mu} S_{rs}^{0\mu''}}{|\mu' \vec{e}_z + \vec{\Gamma}_{pq,rs}^{\mu,\mu''}|} \tag{43}$$

where $\vec{\Gamma}_{pq,rs}^{\mu,\mu''}$ is a function of the exponents, contraction coefficients, scale factors and centers of the contracted gaussian functions. As in the region under interest $|\vec{\Gamma}_{pq,rs}^{\mu,\mu''}|$ is negligible compared to $|\mu' \vec{e}_z|$, one can develop the denominator of equation (43) around $|\mu' \vec{e}_z|^{-1}$ according to the following series :

$$\frac{1}{|\mu' \vec{e}_z + \vec{\Gamma}_{pq,rs}^{\mu,\mu''}|} = \frac{1}{|\mu' \vec{e}_z|} \pm \frac{|\vec{\Gamma}_{pq,rs}^{\mu,\mu''}|}{|\mu' \vec{e}_z|^2} \mp \frac{|\vec{\Gamma}_{pq,rs}^{\mu,\mu''}|^2}{|\mu' \vec{e}_z|^3} \pm \cdots \tag{44}$$

Only the first term of equation (44) has to be considered, since summations such as $\sum_{\mu'=1}^{\infty} |\mu' \vec{e}_z|^{-x}$ always converge, provided $x > 1$. In the asymptotic region, the successive terms contributing to the μ'-summation in equation (42) behave thus like [92] :

$$\frac{1}{|\mu'\vec{e}_z|}\sum_{pqrs}^{M_0} C^*_{pl}(k_l)C_{qn}(k_l)C^*_{rm}(k_m)C_{so}(k_m)\sum_{\mu}^{N_0} e^{ik_l\mu a_0}\, S^{0\mu}_{pq}\sum_{\mu''}^{N_0} e^{ik_m\mu'' a_0}\, S^{0\mu''}_{rs}$$

$$= \frac{1}{|\mu'\vec{e}_z|}\left[\sum_{pq}^{M_0} C^*_{pl}(k_l)S_{pq}(k_l)C_{qn}(k_l)\right]\left[\sum_{rs}^{M_0} C^*_{rm}(k_m)S_{rs}(k_m)C_{so}(k_m)\right]$$

$$= \frac{\delta_{ln}\,\delta_{mo}}{|\mu'\vec{e}_z|} \qquad (45)$$

where the definition of the overlap matrix (equation 20) and the orthonormality constraint (equation 19) over crystalline spin-orbitals have been successively used. From equation (45), it follows that the orthonormality constraint ensures [93] the convergence of any bielectron integral $<\phi_l(k_l)\phi_m(k_m)|\phi_n(k_l)\phi_o(k_m)>$ related to a line-vertex without any transfer of momentum, provided there is no coincidence of the ingoing and outgoing band indices at each side of this line-vertex. In the opposite case, this integral diverges logarithmically through the interplay of the summation over μ'. From these observations, three types of antisymmetrized bielectron interaction elements without any effective transfer of quasi-momentum can be identified as diverging or potentially divergent in the thermodynamic limit :

$$<\phi_r(k_r)\phi_s(k_s)||\phi_t(k_r)\phi_u(k_s)> = <\phi_r(k_r)\phi_s(k_s)|\phi_t(k_r)\phi_u(k_s)> - <\phi_r(k_r)\phi_s(k_s)|\phi_u(k_s)\phi_t(k_r)> \qquad (46a)$$

$$<\phi_a(k_a)\phi_b(k_b)||\phi_c(k_a)\phi_d(k_b)> = <\phi_a(k_a)\phi_b(k_b)|\phi_c(k_a)\phi_d(k_b)> - <\phi_a(k_a)\phi_b(k_b)|\phi_d(k_b)\phi_c(k_a)> \qquad (46b)$$

$$<\phi_r(k_r)\phi_a(k_a)||\phi_b(k_r)\phi_s(k_a)> = <\phi_r(k_r)\phi_a(k_a)|\phi_b(k_r)\phi_s(k_a)> - <\phi_r(k_r)\phi_a(k_a)|\phi_s(k_a)\phi_b(k_r)> \qquad (46c)$$

where the sets of indices (a,b,c,d) and (r,s,t,u) denote occupied and virtual bands, respectively. The diagrams which correspond to these integrals are displayed in Figures 12 a to c ; they represent successively scattering with exchange processes of a particle against a particle (p-p), of a hole against a hole (h-h) and of a particle against a hole (p-h). In these diagrams, we have introduced wavy lines to underline singularities in k-space.

The p-p and h-h scattering terms (integrals 46 a and b) corresponding to the graphs of Figures 12a and b diverge when t=r and u=s, or a=c and b=d, respectively, through the interplay of the direct contribution. These terms can also diverge through the interplay of the exchange contribution, when r=u, s=t and $k_r=k_s$ for integral (46a), or when a=d, b=c and $k_a=k_b$ for integral (46b). On the other hand, the direct contribution to a p-h scattering term such as integral (46c) is never subject to divergence, since in a non-metallic closed-shell system, occupied bands differ necessarily from unoccupied bands, i.e. $r \neq b$ and $s \neq a$. However, these p-h scattering terms can still diverge through the interplay of their exchange contribution, when r=s, b=a, and $k_a=k_r$.

Well-known examples of such divergences are given by the first-order (HF) Coulomb and static exchange terms. From Figure 8a and equation (45), it appears that the orthonormality constraint on crystalline spin-orbitals is a sufficient condition to ensure the bounded character of the second-order self-energy. From third-order (Figure 13) and beyond, on the other hand, most diagrams are subject to a divergence, since they contain singular p-p, p-h or h-h scattering elements. More specifically, amongst the A_1 to A_6 static (frequency-independent) self-energy diagrams accounting for correlation corrections to the ground state one-electron density and hence describing the instantaneous response of a correlated many electron system to the presence of a particle or a hole, one can find such elements in diagrams A_1 and A_2. Also candidates for a divergence in the thermodynamic limit : the first graphs representative of the (G)RPA and "ladder" series, diagrams C_1, C_6, D_1 and D_6, as well as all the dynamic (frequency-dependent) diagrams resulting from a (G)RPA (Figure 9a), "ladder" (Figure 9b) and hence 2ph-TDA expansion. Finally, depending on the nature of the external band indices i and j associated to the self-energy, divergent behaviour may also be expected with the diagrams C_2 to C_5, or D_2 to D_5, which account for a first-order screening of the Coulomb forces and hence of the dynamic (on a long time scale) polarization effects within a correlated wave function, in schemes such as the extended 2ph-TDA or ADC3 levels of approximation. From third-order and beyond, all self-energy dynamic diagrams therefore contain interaction elements that may yield a divergence in the thermodynamic limit.

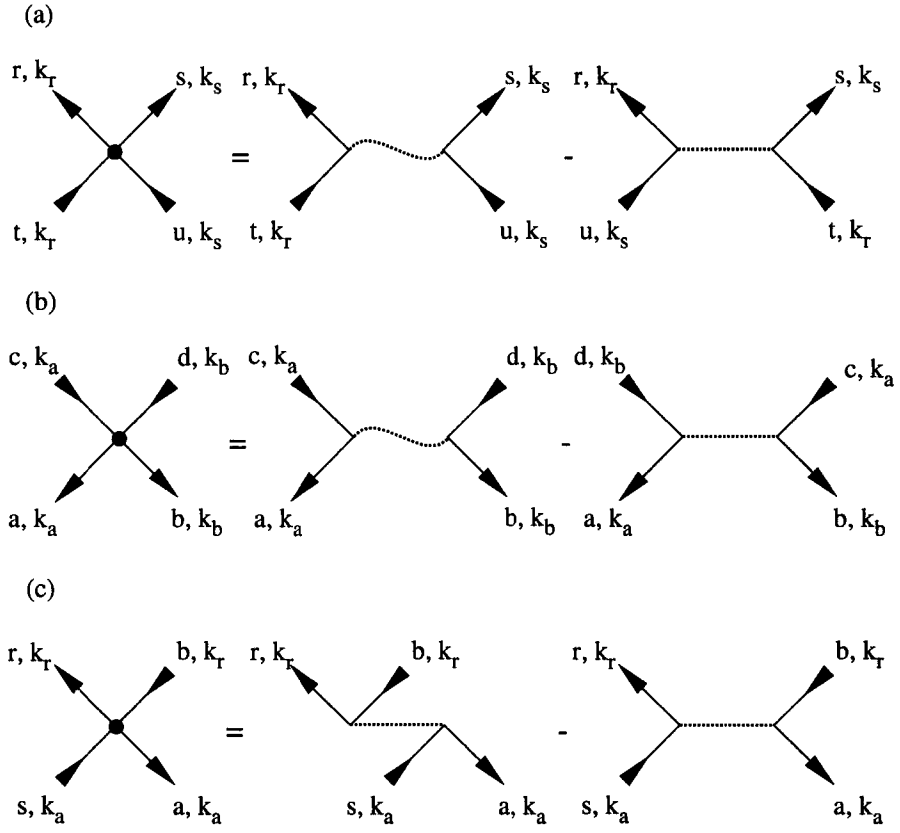

Figure 12 : scattering elements yielding logarithmic divergences after inclusion within a self-energy or vacuum amplitude diagram : (a) particle-particle; (b) hole-hole ; (c) particle-hole scattering terms. Wavy-lines underline the lack of transfer of quasi-momentum during a direct p-p or h-h process, denoting henceforth singularities in k-space. Note that all the above elements may also become singular through the interplay of their exchange contribution, when $k_r = k_s$, or $k_a = k_b$, or $k_r = k_a$, successively

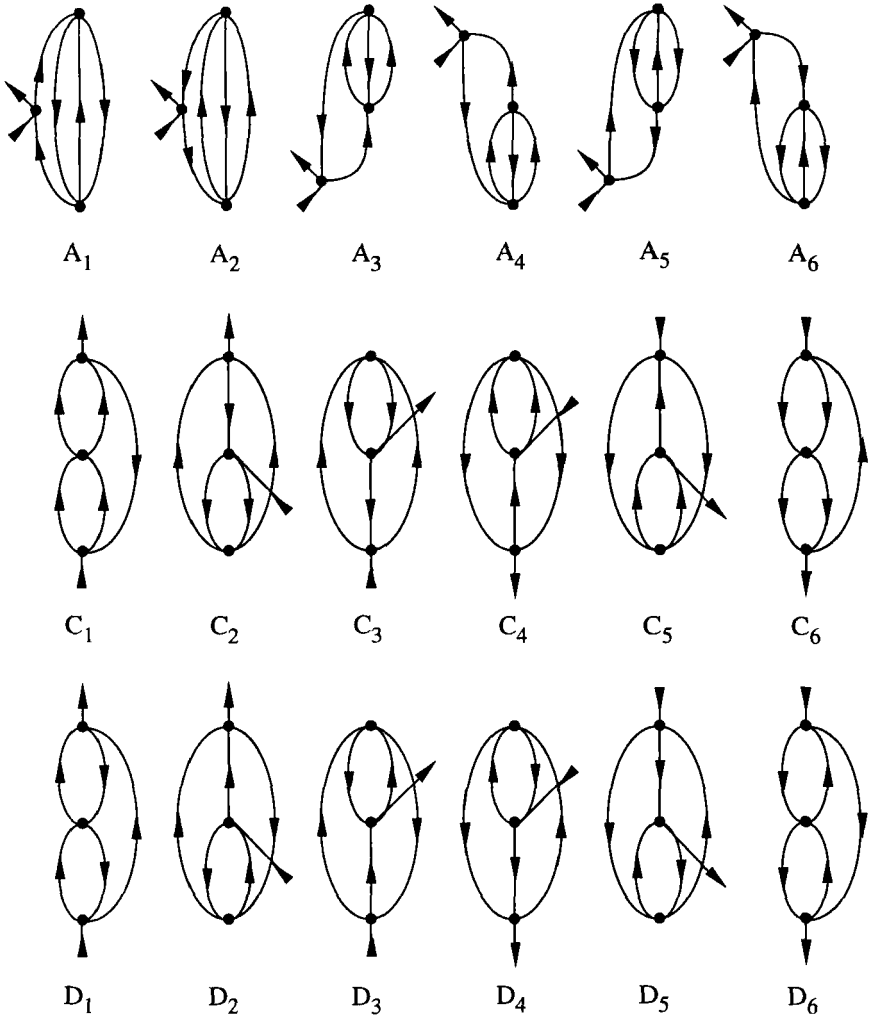

Figure 13 : the 18 Hugenholtz third-order self-energy diagrams.

6. Characterization of the convergence of self-energy lattice summations

After having identified the different singularities that may arise during the expansion of a given diagram in terms of crystalline orbitals, we now concentrate on the necessary conditions for a damping of these singularities, regardless of the orthonormality constraints (equation 45), which in most cases are not sufficient to prevent the development of complete divergences. Focusing on the convergence properties of single self-energy lattice summations and to limit the complexity of the forthcoming developments, we restrict this analysis to the first-order and second-order levels of approximation. In this section, we intentionally keep to molecular-like equations, turning to a solid-state formulation at the very end of our analysis. For the sake of understanding, we also restrict ourselves, without any loss of generality, to the quasi-particle approximation for the self-energy.

(a) Effective energy of a RHF quasi-particle.

The effective Hartree-Fock binding-energies of a particle in state $\phi_n(k_n,\vec{r})$ can be separated into two terms involving contributions of very different nature :

$$\varepsilon_c(k_c) = T_{cc}(k_c) + \Sigma^{(1)}_{cc}(k_c,+\infty) \tag{47},$$

the first term being the kinetic energy contribution :

$$T_{cc}(k_c) = \lim_{N_0\to\infty} \sum_{p=1}^{M_0}\sum_{q=1}^{M_0} D_{pq,c}(k_c) \sum_{\mu}^{N_0} e^{i k_c \mu a_0} < \gamma_p^0 | -\frac{1}{2}\nabla^2 | \gamma_p^\mu > \tag{48},$$

the second term involving all the energy contributions arising from the propagation of the particle under consideration in the static field of the fixed nuclei and of an average electron distribution. It can ultimately be partitioned into three different contributions,

$$\Sigma^{(1)}_{cc}(k_c,+\infty) = V_{cc}(k_c) + U_{cc}(k_c) + X_{cc}(k_c) \tag{49}$$

with $\mathbf{V}(k)$, $\mathbf{U}(k)$, and $\mathbf{X}(k)$ the matrix Bloch representations of the electron-nuclear attraction, the Coulomb electron-electron repulsion and the electron-electron exchange parts of the Fock operator, respectively. From equation (49), the Hartree-Fock quasi-particle [57] can be regarded as a bare particle dressed with an effective frequency-independent (static) potential $\Sigma_{cc}^{(1)}(k_c,+\infty)$ of first order in the Coulomb interactions. It is obtained as the resultant of classical electrostatic energy contributions [$V_{cc}(k_c)$ and $U_{cc}(k_c)$] together with the Fermi hole contribution [$X_{cc}(k_c)$], which reintroduces a substantial amount of the electronic correlation arising from exchange. For further discussion, it is useful to represent equation (49) by means of the Goldstone diagrams provided in Figure 14. For a closed-shell system, each of these terms can be first expanded as :

$$V_{cc}(k_c) = -\lim_{N_0\to\infty} \sum_{p=1}^{M_0}\sum_{q=1}^{M_0} D_{pq,c}(k_c) \times \sum_{\mu}^{N_0}\sum_{\mu'}^{N_0} e^{i k_c \mu a_0} < \gamma_p^0 | \sum_{\vartheta=1}^{\Omega_0} \frac{Z_\vartheta}{|\vec{r} - \vec{R}_\vartheta - \mu' a_0 \vec{e}_z|} | \gamma_q^\mu > \tag{50}$$

$$U_{cc}(k_c) = \lim_{N_0\to\infty} \frac{2}{N_0} \sum_{b=1}^{n_0} \sum_{k_b}^{BZ} \eta_b(k_b) \sum_{p=1}^{M_0}\sum_{q=1}^{M_0}\sum_{r=1}^{M_0}\sum_{s=1}^{M_0} D_{pq,c}(k_c) D_{rs,b}(k_b) \times \sum_{\mu}^{N_0}\sum_{\mu'}^{N_0}\sum_{\mu''}^{N_0} e^{i[k_c \mu + k_b(\mu''-\mu')]a_0} < \gamma_p^0 \gamma_r^{\mu'} | \gamma_q^\mu \gamma_s^{\mu''} > \tag{51}$$

and

$$X_{cc}(k_c) = \lim_{N_0\to\infty} \frac{-1}{N_0} \sum_{b=1}^{n_0} \sum_{k_b}^{BZ} \eta_b(k_b) \sum_{p=1}^{M_0}\sum_{q=1}^{M_0}\sum_{r=1}^{M_0}\sum_{s=1}^{M_0} D_{pq,c}(k_c) D_{rs,b}(k_b) \times \sum_{\mu}^{N_0}\sum_{\mu'}^{N_0}\sum_{\mu''}^{N_0} e^{i[k_c \mu + k_b(\mu''-\mu')]a_0} < \gamma_p^0 \gamma_r^{\mu'} | \gamma_s^{\mu''} \gamma_q^\mu > \tag{52}$$

where the sums over (b,k_b) are now restricted to doubly occupied levels.

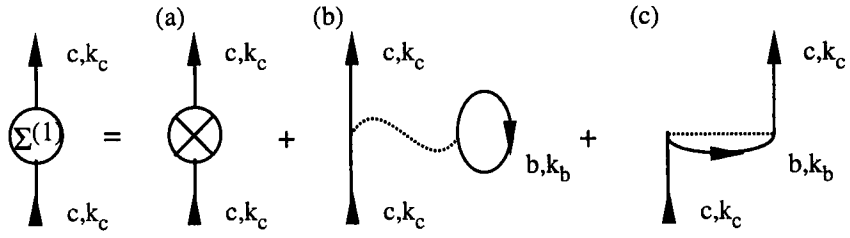

Figure 14 : The first-order self-energy terms. Wavy line vertices denote a divergent interaction. (a) electrostatic electron-nuclear attraction, (b) electrostatic electron-electron repulsion and (c) electron-electron exchange interaction.

The zeroth-order kinetic term $T_{cc}(k_c)$ does not embody any lattice-sum difficulty since the successive matrix elements involved in equation (48) decay exponentially with the distance between the atomic functions γ_p^0 and γ_q^μ. On the other hand, the terms involved in the expansion of $\Sigma_{cc}^{(1)}(k_c,+\infty)$ require more attention. The nuclear attraction matrix elements appearing in equation (50) correspond to electrostatic interactions between the electronic distribution $\gamma_p^0\gamma_q^\mu$ and the nuclear point charges which belong to the cell μ'. There is no problem with the sum over μ since the successive terms decay exponentially, as the overlap $S_{pq}^{0\mu}$. On the other hand, the electrostatic interactions decay slowly like $|\mu'|^{-1}$, i.e. the series over μ' behaves like a logarithmically divergent harmonic series.

The asymptotic properties of $U_{cc}(k_c)$ and $X_{cc}(k_c)$ are more conveniently studied after a slight rewriting :

$$U_{cc}(k_c) = \lim_{N_0\to\infty} \frac{2}{N_0} \sum_{b=1}^{n_0} \sum_{k_b}^{BZ} \eta_b(k_b) \sum_{p=1}^{M_0}\sum_{q=1}^{M_0}\sum_{r=1}^{M_0}\sum_{s=1}^{M_0} D_{pq,c}(k_c) D_{rs,b}(k_b)$$
$$\times \sum_{\mu}^{N_0}\sum_{\mu'}^{N_0}\sum_{\mu''}^{N_0} e^{i(k_c\mu + k_b\mu'')a_0} < \gamma_p^0 \gamma_r^{\mu'} | \gamma_q^\mu \gamma_s^{\mu'+\mu''} > \qquad (52)$$

$$X_{cc}(k_c) = \lim_{N_0\to\infty} \frac{-1}{N_0} \sum_{b=1}^{n_0} \sum_{k_b}^{BZ} \eta_b(k_b) \sum_{p=1}^{M_0}\sum_{q=1}^{M_0}\sum_{r=1}^{M_0}\sum_{s=1}^{M_0} D_{pq,c}(k_c) D_{rs,b}(k_b)$$
$$\times \sum_{\mu}^{N_0}\sum_{\mu'}^{N_0}\sum_{\mu''}^{N_0} e^{i[(k_c-k_b)\mu + k_b(\mu''-\mu')]a_0} < \gamma_p^0 \gamma_r^{\mu+\mu'} | \gamma_s^{\mu''} \gamma_q^{\mu} > \qquad (53)$$

Whatever the values of k_b and k_c, the sum over μ' in the expansion of the Coulomb contribution exhibits a logarithmically divergent character because it directly relates to interaction terms without any μ'-dependent phase factor, which at large separations between the interacting charge distributions decay slowly as $|\mu'|^{-1}$, like the successive terms contributing to equation (50). Similarly, for the exchange part, divergences in the μ-series at the singular point $k_b = k_c$ prevents a straightforward summation (integration) over k_b.

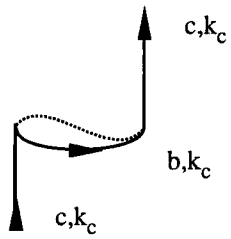

Figure 15 : singularity in the static exchange contribution to $\Sigma^{(1)}$.

For a better understanding of the mathematics beyond diagrams within the framework of extended systems, it is useful to regard the divergence of the individual electrostatic contributions $V_{cc}(k_c)$ and $U_{cc}(k_c)$ as the ultimate outcome of *resonant* interactions, which like for a resonant coupling in classical mechanics, *forbid* any transfer of momentum along the line-vertex in the corresponding graph. The diagram associated to the Coulomb term describes the interactions between the electron in state $\phi_c(k_c, \vec{r})$ under consideration and an *infinite number of static electrons*. Similarly, the diagram representing the nuclear attraction term describes interaction processes without any transfer of quasi-momentum between the electron in state $\phi_c(k_c, \vec{r})$ and an *infinite number of static nuclear charges*. Therefore, like for an ideal classical resonance, energetic divergences occur as the result of an optimal

coupling with an infinite supply of energy. On the other hand, as the exchange diagram does exhibit transfer of quasi-momentum $q = \pm(k_b - k_c)$ between the ingoing particle and hole on each side of the line vertex, no divergence is expected *except at the singular point* $k_b = k_c$ (Figure 15; q=0) in the integration interval.

When combined under the electroneutrality constraint for each unit cell, the electrostatic contributions [$V_{cc}(k_c)$ and $U_{cc}(k_c)$] can be turned into a conditionally convergent Madelung series. For this purpose, it is convenient to introduce unity from the orthonormality condition (equation 19) as :

$$\lim_{N_0\to\infty} 2\cdot \sum_{b=1}^{n_0} \sum_{k_b}^{BZ} \eta_b(k_b) \sum_{r=1}^{M_0}\sum_{s=1}^{M_0} D_{rs,b}(k_b) \sum_{\mu''}^{N_0} e^{i k_b \mu'' a_0} (2n_0)^{-1} S_{rs}^{0\mu''} = 1 \quad (54)$$

By rescaling the electron-nuclei interactions, the resultant one-particle electrostatic energy can be rewritten as :

$$V_{cc}(k_c)+U_{cc}(k_c) = \lim_{N_0\to\infty} \frac{2}{N_0} \sum_{b=1}^{n_0} \sum_{k_b}^{BZ} \eta_b(k_b) \sum_{p=1}^{M_0}\sum_{q=1}^{M_0} D_{pq,c}(k_c) \sum_{r=1}^{M_0}\sum_{s=1}^{M_0} D_{rs,b}(k_b)$$
$$\times \sum_{\mu}^{N_0}\sum_{\mu''}^{N_0} e^{i(k_c\mu + k_b\mu'')a_0}\, \theta\begin{pmatrix}\mu,\mu''\\ pq,rs\end{pmatrix} \quad (55)$$

with the troublesome μ' summation isolated in :

$$\theta\begin{pmatrix}\mu,\mu''\\ pq,rs\end{pmatrix} = \sum_{\mu'}^{N_0}\left\{ < \gamma_p^0 \gamma_r^{\mu'} | \gamma_q^{\mu} \gamma_s^{\mu'+\mu''} > - \frac{S_{rs}^{0\mu''}}{2n_0} < \gamma_p^0 | \sum_{\vartheta=1}^{\Omega_0} \frac{Z_\vartheta}{|\vec{r} - \vec{R}_\vartheta - \mu' a_0 \vec{e}_z|} | \gamma_q^{\mu} > \right\} \quad (56)$$

In the asymptotic regime, this particular summation behaves like

$$\theta\begin{pmatrix}\mu,\mu''\\ pq,rs\end{pmatrix} = \frac{1}{a_0} S_{pq}^{0\mu} S_{rs}^{0\mu''} \sum_{\mu} \left\{ \frac{1}{|\mu'\vec{e}_z + \vec{\Gamma}_{pq,rs}^{\mu,\mu''}|} - \frac{(\sum_{\vartheta=1}^{\Omega_0} Z_\vartheta)(2n_0)^{-1}}{|\mu'\vec{e}_z + \vec{\Delta}_{pq}^{\mu}|} \right\} \quad (57)$$

A satisfactory cancellation [44] of the bracketed terms is reached at medium distances (vanishing dipole) or at large distances (non-vanishing dipole) provided the electroneutrality condition is strictly satisfied.

The summation over k_b needed to calculate the exchange term is carried out via the finite Fourier Transform of $D_{rs,b}(k_b)$:

$$D^{0\mu}_{rs,b} = \lim_{N_0\to\infty} \frac{1}{N_0} \sum_{k_b}^{BZ} e^{i k_b \mu a_0} D_{rs,b}(k_b)\eta_b(k_b)$$
$$= \left(\frac{a_0}{2\pi}\right) \int_{BZ} dk_b\, e^{i k_b \mu a_0} D_{rs,b}(k_b)\eta_b(k_b) \tag{58}$$

Taking the limit $N_0 \to \infty$, this summation has been turned into an integral over a finite region, the first Brillouin Zone. Introducing the above Fourier coefficents in equation (53), $X_{cc}(k_c)$ takes the form

$$X_{cc}(k_c) = \sum_{p=1}^{M_0}\sum_{q=1}^{M_0} D_{pq,c}(k_c) \sum_{r=1}^{M_0}\sum_{s=1}^{M_0}\sum_{\mu'=1}^{\infty}\sum_{\mu''=1}^{\infty}\sum_{b=1}^{2n_0} \lambda_b\left(\begin{smallmatrix}\mu'',\mu'\\ ps,rq\end{smallmatrix}\right) \tag{59}$$

with the troublesome summation over μ isolated in :

$$\lambda_b\left(\begin{smallmatrix}\mu'',\mu'\\ ps,rq\end{smallmatrix}\right) = \sum_{\mu}^{\infty} e^{i k_c \mu a_0} D^{0(\mu''-\mu'-\mu)}_{rs,b} < \gamma^0_p \gamma^{\mu+\mu'}_r | \gamma^{\mu''}_s \gamma^{\mu}_q > \tag{60}$$

In the asymptotic region, λ_b takes the following form :

$$\lambda_b\left(\begin{smallmatrix}\mu'',\mu'\\ ps,rq\end{smallmatrix}\right) = \frac{1}{a_0} S^{0\mu''}_{ps} S^{0\mu'}_{rq} \sum_{\mu}^{\infty} \left\{ e^{i k_c \mu a_0} D^{0(\mu''-\mu'-\mu)}_{rs,b} | \mu \vec{e}_z + \vec{\Gamma}^{\mu'',\mu'}_{ps,rq} |^{-1} \right\} \tag{61}$$

Because series like

$$\sum_{\mu}^{\infty} \left\{ e^{i k_c \mu a_0} | \mu \vec{e}_z + \vec{\Gamma}^{\mu'',\mu'}_{ps,rq} |^{-1} \right\} \tag{62}$$

are poorly convergent and even divergent at $k_c=0$, the coefficients $D^{0(\mu''-\mu'-\mu)}_{rs,b}$ of the complex Fourier series representing $D_{rs,b}(k_b)$ are eventually responsible for the actual convergence of the μ-series and therefore for the boundedness of $X_{cc}(k_c)$.

The analytical properties [94-98] of the eigenvalues $\varepsilon_n(k)$ and eigenfunctions $\phi_n(k,\vec{r})$, given in Appendix 1, are first invoked to determine the asymptotic behaviour of the troublesome lattice summations implied in equation (61). The absence of degeneracy between occupied and unoccupied levels for an insulating or semi-conducting system secures the analyticity for all elements $D_{rs}(k_b)$ of the k-dependent total density matrix. Even if the band components $D_{rs,b}(k_b)$ were not analytic individually because of enforced degeneracies in a nonsymmorphic symmetry group at some points of the first Brillouin zone, this non-analytic behaviour would cancel through the b-summation over occupied bands.

Thus, the $D_{rs,b}(k_b)$ coefficients are continuous and infinitely differentiable everywhere in the first Brillouin zone. Therefore, according to one of the theorems given in Appendix 2 on the decay of Fourier coefficients [99], the series of $D^{0\ \mu}_{rs,b}$ coefficients will converge faster than any negative power of $|\mu|$, yielding a finite value for $X_{cc}(k_c)$. Furthermore, as the k-dependent density matrix is analytic everywhere in the first Brillouin zone, the $D^{0\ \mu}_{rs,b}$ coefficients will decrease exponentially with respect to μ in the asymptotic region, enabling possibly a fast convergence of expression (61).

As this exponential decay is ultimately governed by the degree of smoothness of the k-dependent density matrix, it is useful to reconsider the model of a supermolecule built of an infinite number of non-interacting monomer subunits, for which the associated band structure is absolutely flat. As in this case, there is no dispersion with respect to quasi-momenta, the Fourier series expansion of the density matrix elements,

$$D_{rs,b}(k_b) = D^{0\ 0}_{rs,b} + \sum_{\mu\neq 0} D^{0\ \mu}_{rs,b}\, e^{-i k_b \mu a_0} \quad , \tag{63}$$

reduces to $D^{0\,0}_{rs,b}$ .Therefore, the only non-vanishing contribution in the μ-summation implied in equation (60) is obtained for $\mu=\mu'+\mu''$, yielding the reduced expansion :

$$\lambda_b\left(\begin{smallmatrix}\mu'',\mu'\\ ps,rq\end{smallmatrix}\right)=\frac{1}{a_0}e^{i\,k_c(\mu''-\mu')a_0}\,D^{0\,0}_{rs,b}<\gamma^0_p\gamma^{\mu''}_r|\gamma^{\mu''}_s\gamma^{\mu''-\mu'}_q> \tag{64}$$

in which the structure of the exchange interaction still appears explicitly. The extreme situation of a periodic system containing strictly non-interacting subunits implies also the vanishing of the distributions of charges $\gamma^0_p\gamma^{\mu''}_s$ or $\gamma^{\mu+\mu'}_r\gamma^{\mu}_q$ and therefore of the overlap integrals $S^{0\mu''}_{ps}$ and $S^{0\mu'}_{rq}$ obtained from primitive atomic functions in different cells. Only the bielectron integral $<\gamma^0_p\gamma^{\mu+\mu'}_r|\gamma^{\mu''}_s\gamma^{\mu}_q>$ with $\mu'=\mu''=0$ will therefore be different from zero in equation (53), restricting all lattice summations to the cell chosen as the reference.

In the other extreme, one can consider the case of the higly interacting 'metallic' chains, characterized by the degeneracy of the highest occupied and the lowest unoccupied states. From properties enumerated in Appendix 1, a discontinuity is introduced in the graph of the function $D_{rs,b}(k_b)$, and therefore the asymptotic decay of the Fourier coefficients $D^{0\,\mu}_{rs,b}$ with respect to μ is no better than $|\mu|^{-1}$. In this particular case, for large values of μ, the terms of the μ series in equation (61) will have a characteristic $e^{i\,k_c\,\mu\,a_0}\,|\mu\,|^{-1}\,(\mu''-\mu'-\mu)^{-1}$ dependence [49-52] and many terms will be needed to stabilize the exchange summations [53].

These examples illustrate clearly the origin of size-related difficulties in band structure calculations on extended periodic systems such as polymers : the larger the interactions between monomers, the stronger the band dispersion, and the slower the decay of the Fourier coefficients $D^{0\,\mu}_{rs,b}$, in relationship to the long-range character of the Coulomb interaction. For a proper proof of the size-intensivity or size-extensivity of many-body approaches as applied to infinite systems, as well as for accurate calculations, one has to allow the interaction of any pair of electron charge distributions, even those at very large distance.

(b) Effective energy of a second-order quasi-particle

At the quasi-particle [100] level of approximation, the off-diagonal elements of the self-energy are neglected, and equation (24) is further simplified into a self-consistent one-particle equation :

$$\omega_c(k_c) = \varepsilon_c(k_c) + \Sigma_{cc}\left(k_c, \omega_c(k_c)\right) \tag{65}$$

In the framework of this approximation, the coupling between the attachment and ionization sectors of the propagator is suppressed. The ionization process is then decoupled into two independent events : the removal of an electron and the creation of a hole. Solving equation (65) allows excited 2p-1h and 2h-1p configurations to interact directly with the 1p and 1h configurations resulting from these events, hence the inclusions of dynamic correlation.

At the second-order level of expansion, the self-energy expression can be partitioned into direct polarization and polarization with exchange contributions, which enables an easier identification of the origin of the convergence difficulties in the lattice sum expansion of $\Sigma_{cc}(k_c,\omega_c)$. This partitioning is most conveniently represented (Figure 16) with the diagrams built using the conventions of Goldstone. Introducing the single-hole state occupation number $\overline{\eta}_r = 1 - \eta_r$, the 'direct polarization' (D) and 'polarization with exchange' (X) second-order self-energy terms can be expanded as :

$$\Sigma_{cc}^{(2D)}\left(k_c, \omega_c(k_c)\right) = 2 \sum_{lmn}^{M_0} \sum_{k_l}^{BZ} \sum_{q}^{BZ} \hat{P}_{lmn}(k_l, q) \frac{\left\langle \begin{matrix} k_c & k_l \\ c & l \end{matrix} \middle| \begin{matrix} k_c+q & k_l-q \\ m & n \end{matrix} \right\rangle \left\langle \begin{matrix} k_c+q & k_l-q \\ m & n \end{matrix} \middle| \begin{matrix} k_c & k_l \\ c & l \end{matrix} \right\rangle}{\omega_c(k_c) + \varepsilon_l(k_l) - \varepsilon_m(k_c+q) - \varepsilon_n(k_l-q)} \tag{66a}$$

$$\Sigma_{cc}^{(2X)}\left(k_c, \omega_c(k_c)\right) = -\sum_{lmn}^{M_0} \sum_{k_l}^{BZ} \sum_{q}^{BZ} \hat{P}_{lmn}(k_l, q) \frac{\left\langle \begin{matrix} k_c & k_l \\ c & l \end{matrix} \middle| \begin{matrix} k_c+q & k_l-q \\ m & n \end{matrix} \right\rangle \left\langle \begin{matrix} k_l-q & k_c+q \\ n & m \end{matrix} \middle| \begin{matrix} k_c & k_l \\ c & l \end{matrix} \right\rangle}{\omega_c(k_c) + \varepsilon_l(k_l) - \varepsilon_m(k_c+q) - \varepsilon_n(k_l-q)} \tag{66b}$$

where

$$\hat{P}_{lmn(k_l,q)} = \bar{\eta}_l(k_l)\eta_m(k_c+q)\eta_n(k_l-q) + \eta_l(k_l)\bar{\eta}_m(k_c+q)\bar{\eta}_n(k_l-q) \quad (67)$$

is a projector eliminating the unphysical poles of the self-energy by restricting its kernel to the two-particle-one-hole and one-particle-two-hole subspaces.

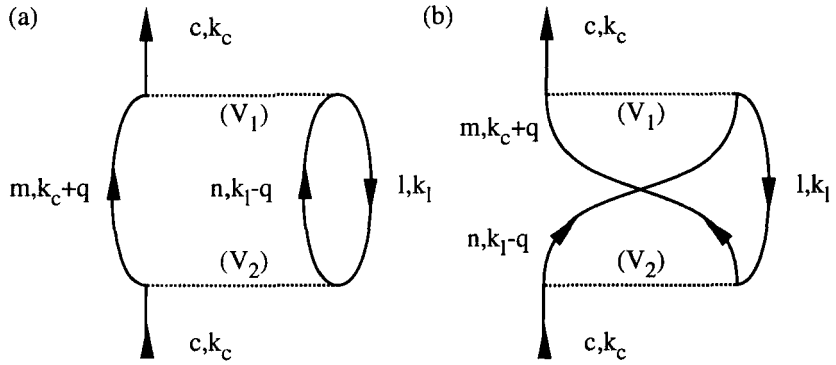

Figure 16 : Diagrammatic expansion of the second-order (particle) (a) direct (D) and (b) exchange (X) self-energy terms.

The left-hand-side two-electron interaction element is common to both the D and X self-energy expressions, as the corresponding line vertex (V_1) is common to both their diagrammatic representations. To identify the convergence difficulties arising from this particular vertex, its algebraic equivalent is most conveniently expanded in a way similar to that used previously to expand the electron-electron electrostatic contribution :

$$\left\langle \begin{matrix} k_c & k_l \\ c & l \end{matrix} \middle| \begin{matrix} k_c+q & k_l-q \\ m & n \end{matrix} \right\rangle = \lim_{N_0\to\infty} \frac{1}{N_0} \sum_{(pqrs)_l}^{M_0} C^*_{p_l c}(k_c) C_{q_l m}(k_c+q) C^*_{r_l l}(k_l) C_{s_l n}(k_l-q)$$

$$\times \sum_{\mu_l}^{N_0} \sum_{\mu_l''}^{N_0} e^{i[(k_c+q)\mu_l + (k_l-q)\mu_l'']a_0} \sum_{\mu_l'}^{N_0} e^{-iq\mu_l' a_0} < \gamma^0_{p_l} \gamma^{\mu_l'}_{r_l} | \gamma^{\mu_l}_{q_l} \gamma^{\mu_l'+\mu_l''}_{s_l} > \quad (68)$$

On the other hand, compared to the D-self-energy diagram, the line vertex (V_2) exhibits an exchanged ordering of the ingoing lines in the X-diagram. If the corresponding bielectron matrix element, appearing as the right-hand-side numerator factor of the D self-energy expression, is expanded as a complex conjugate of expression (68),

$$\left\langle \begin{matrix} k_c+q & k_1-q \\ m & n \end{matrix} \middle| \begin{matrix} k_c & k_1 \\ c & 1 \end{matrix} \right\rangle = \lim_{N_0\to\infty} \frac{1}{N_0} \sum_{(pqrs)_2}^{M_0} C_{p_2 c}(k_c) C^*_{q_2 m}(k_c+q) C_{r_2 l}(k_1) C^*_{s_2 n}(k_1-q)$$

$$\times \sum_{\mu_2}^{N_0} \sum_{\mu_2"}^{N_0} e^{-i[(k_c+q)\mu_2+(k_1-q)\mu_2"]a_0} \sum_{\mu_2'}^{N_0} e^{iq\mu_2' a_0} < \gamma^{\mu_2}_{q_2} \gamma^{\mu_2'+\mu_2"}_{s_2} | \gamma^0_{p_2} \gamma^{\mu_2'}_{r_2} > \tag{69}$$

the algebraic counterpart of the line vertex (V_2) in the X-diagram will be more conveniently expanded in a way similar to that used previously for the first-order exchange energy contribution :

$$\left\langle \begin{matrix} k_1-q & k_c+q \\ n & m \end{matrix} \middle| \begin{matrix} k_c & k_1 \\ c & 1 \end{matrix} \right\rangle = \lim_{N_0\to\infty} \frac{1}{N_0} \sum_{(pqrs)_2}^{M_0} C_{p_2 c}(k_c) C^*_{q_2 m}(k_c+q) C_{r_2 l}(k_1) C^*_{s_2 n}(k_1-q)$$

$$\times \sum_{\mu_2'}^{N_0} \sum_{\mu_2"}^{N_0} e^{-i[(k_1-q)\mu_2"-k_1\,\mu_2']a_0} \sum_{\mu_2}^{N_0} e^{i(k_1-k_c-q)\mu_2 a_0} < \gamma^{\mu_2"}_{s_2} \gamma^{\mu_2}_{q_2} | \gamma^0_{p_2} \gamma^{\mu_2+\mu_2'}_{r_2} > \tag{70}$$

In general, there is no particular problem with the sums over the μ_1 and μ_1" or μ_2 and μ_2" cell indices in expressions (68) or (69) since in each case the successive terms decay exponentially. Similarly, the summations over the μ_2' and μ_2" cell indices in expression (70) will not yield any size-related difficulties.

As previously mentioned, convergence problems can be expected from those scattering terms without any effective transfer of quasi-momentum between the interacting particles. More precisely, if no transfer of quasi-momentum (q=0) occurs at the (V_1) line vertex, divergent behaviour can be expected from both the μ_1', or μ_2' summations in expressions (68) and (69), since the successive terms will decay slowly as $|\mu_1'|^{-1}$ and $|\mu_2'|^{-1}$ without any μ_1' or μ_2' phase-dependent factor, respectively. Similarly, if the ingoing particle and / or holes at the (V_1) line

vertex exchange their quasi-momenta ($q=k_l-k_c$), the summations over μ_2 in expression (70) will also exhibit a logarithmically divergent behaviour.

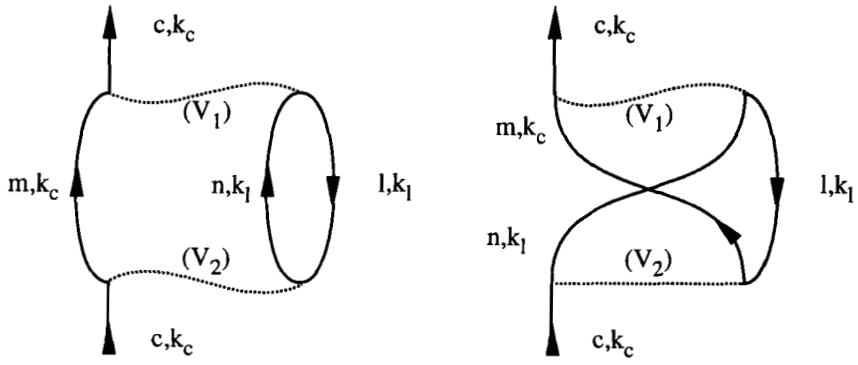

Figure 17. ($q=0$)

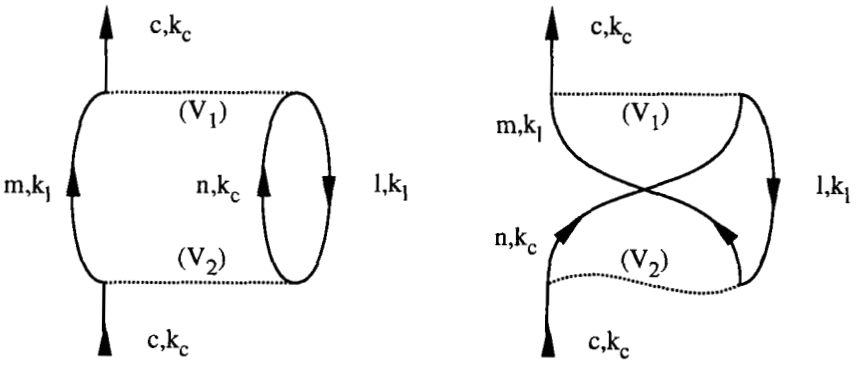

Figure 18. ($q=k_l-k_c$)

Figures 17 and 18 : a particular subset of the self-energy diagrams at the singular line $q=0$ and $q=k_l-k_c$ in twe two-dimensional space (k_l,q) of integration over the quasi-momentum variables implied in the expansion of the second-order contributions to quasi-particle energies.

Therefore, the D-term will exhibit, in the two-dimensional quasi-momentum space defined by the variables q and k_l, a double possibility of divergence at the singular line q=0 (Figure 17), preventing straightforward integrations over quasi-momenta indices. Similar difficulties can be expected for the X-term, because the line vertices (V_1) and (V_2) exhibit a simple possibility of divergence at two different singular lines (Figures 17 and 18), respectively q=0 and $q=k_l-k_c$, in the same integration subspace.

To perform the integration over q, the expansion of the second-order self-energy terms is carried out in several steps :

$$\Sigma_{cc}^{(2D)}(k_c,\omega) = \lim_{N_0\to\infty} 2 \sum_{lmn}^{M_0} \sum_{p_1}^{M_0} \sum_{p_2}^{M_0} D_{p_1 p_2,c}(k_c) \times \sum_{(qrs)_1}^{M_0} \sum_{(qrs)_2}^{M_0} \sum_{\mu_1\mu_1"}^{N_0} \sum_{\mu_2\mu_2"}^{N_0} \Lambda_{lmn}^{(D)}\left(\begin{pmatrix}\mu\mu"\\pqrs\end{pmatrix}_1;\begin{pmatrix}\mu\mu"\\pqrs\end{pmatrix}_2\right) \tag{71a}$$

$$\Sigma_{cc}^{(2X)}(k_c,\omega) = \lim_{N_0\to\infty} -\sum_{lmn}^{M_0} \sum_{p_1}^{M_0} \sum_{p_2}^{M_0} D_{p_1 p_2,c}(k_c) \times \sum_{(qrs)_1}^{M_0} \sum_{(qrs)_2}^{M_0} \sum_{\mu_1\mu_1"}^{N_0} \sum_{\mu_2'\mu_2"}^{N_0} \Lambda_{lmn}^{(X)}\left(\begin{pmatrix}\mu\mu"\\pqrs\end{pmatrix}_1;\begin{pmatrix}\mu'\mu"\\psrq\end{pmatrix}_2\right) \tag{71b}$$

The troublesome summations are isolated in

$$\Lambda_{lmn}^{(D)}\left(\begin{pmatrix}\mu\mu"\\pqrs\end{pmatrix}_1;\begin{pmatrix}\mu\mu"\\pqrs\end{pmatrix}_2\right) = \left(\frac{a_0}{2\pi}\right)^2 \int_{BZ} dk_1 \int_{BZ} dq\, \hat{P}_{lmn}(k_1,q) \times \Theta_{lmn}^{(D)}\left(k_1,q;\begin{pmatrix}\mu\mu"\\pqrs\end{pmatrix}_1;\begin{pmatrix}\mu\mu"\\pqrs\end{pmatrix}_2\right) \delta_{lmn}^{-1}(k_1,q) \sum_{\mu_1'\mu_2'}^{N_0} \sum^{N_0} e^{-iq(\mu_1'-\mu_2')a_0} \times < \gamma_{p_1}^0 \gamma_{r_1}^{\mu_1'} | \gamma_{q_1}^{\mu_1} \gamma_{s_1}^{\mu_1'+\mu_1"} > < \gamma_{q_2}^{\mu_2} \gamma_{s_2}^{\mu_2'+\mu_2"} | \gamma_{p_2}^0 \gamma_{r_2}^{\mu_2'} > \tag{72a}$$

$$\Lambda^{(X)}_{lmn}\left(\begin{pmatrix}\mu\mu''\\ pqrs\end{pmatrix}_1;\begin{pmatrix}\mu'\mu''\\ psrq\end{pmatrix}_2\right)$$
$$=\left(\frac{a_0}{2\pi}\right)^2 \int_{BZ} dk_1 \int_{BZ} dq\, \hat{P}_{lmn}(k_1,q)\Theta^{(X)}_{lmn}\left(k_1,q;\begin{pmatrix}\mu\mu''\\ pqrs\end{pmatrix}_1;\begin{pmatrix}\mu'\mu''\\ psrq\end{pmatrix}_2\right)$$
$$\times\delta^{-1}_{lmn}(k_1,q)\sum_{\mu_1'}^{N_0} e^{-iq\mu_1' a_0} < \gamma^0_{p_1}\gamma^{\mu_1'}_{r_1}|\gamma^{\mu_1}_{q_1}\gamma^{\mu_1'+\mu_1''}_{s_1} >$$
$$\times\sum_{\mu_2}^{N_0} e^{i[k_1-k_c-q]\mu_2 a_0} < \gamma^{\mu_2''}_{s_2}\gamma^{\mu_2}_{q_2}|\gamma^0_{p_2}\gamma^{\mu_2+\mu_2'}_{r_2} > \tag{72b}$$

with the following definitions :

$$\Theta^{(D)}_{lmn}\left(k_1,q;\begin{pmatrix}\mu\mu''\\ pqrs\end{pmatrix}_1;\begin{pmatrix}\mu\mu''\\ pqrs\end{pmatrix}_2\right)$$
$$= e^{i[(k_c+q)(\mu_1-\mu_2)+(k_1-q)(\mu_1''-\mu_2'')]a_0}$$
$$\times D_{q_2q_1,m}(k_c+q)D_{r_1r_2,l}(k_1)D_{s_2s_1,n}(k_1-q) \tag{73a}$$

$$\Theta^{(X)}_{lmn}\left(k_1,q;\begin{pmatrix}\mu\mu''\\ pqrs\end{pmatrix}_1;\begin{pmatrix}\mu'\mu''\\ psrq\end{pmatrix}_2\right)$$
$$= e^{i[(k_c+q)\mu_1-k_1\mu_2'+(k_1-q)(\mu_1''-\mu_2'')]a_0}$$
$$\times D_{q_2q_1,m}(k_c+q)D_{r_1r_2,l}(k_1)D_{s_2s_1,n}(k_1-q) \tag{73b}$$

$$\delta_{lmn}(k_1,q)=\omega_c(k_c)+\varepsilon_l(k_1)-\varepsilon_m(k_c+q)-\varepsilon_n(k_1-q) \tag{74}$$

The assumption of an insulating or semi-conducting system, preventing the closure of the fundamental gap, ensures the boundedness of the inverse of any excitation energies defined in equation (74) and prevents any ambiguity on the projectors $P_{lmn}(k_1,q)$. From the properties enumerated in Appendix 1, the absence of degeneracy also secures the analyticity of the density matrix elements contained in equations (72) everywhere in the first Brillouin zone. As products of analytic functions are themselves analytic [101], the convergence of the coefficients of the Fourier series underlying the integration over the quasi-momentum variables q and k_1 in equations (71) of the combined $\Theta\delta^{-1}$ function over the lattice cells (μ_1' and μ_2') or (μ_1' and μ_2) indices will be of exponential type (Appendix 2). As for the

first-order exchange term, this ensures boundedness of the Λ functions (equation 72) and would hence guarantee (equation 71) the size-intensivity of the second-order self-energy terms, even if those were to be calculated without exploiting the orthonormality of HF crystalline orbitals.

Compared to the first-order static exchange contribution, however, the analysis of the asymptotic decay of these coefficients should be complicated by the coupling of the lattice summations corresponding to each of the interaction vertices V_1 and V_2 through density matrix elements and phase factors (equations 72 and 73).

Ignoring for simplicity the integration over the particle or hole quasi-momentum index k_l, the Λ functions take the following asymptotic form :

$$\Lambda^{(D)}_{lmn}\left(\begin{pmatrix}\mu\mu''\\pqrs\end{pmatrix}_1;\begin{pmatrix}\mu\mu''\\pqrs\end{pmatrix}_2\right) \propto S^{0\ \mu_1}_{p_1q_1} S^{0\ \mu_1''}_{r_1s_1} S^{0\ \mu_2}_{p_2q_2} S^{0\ \mu_2''}_{r_2s_2}$$
$$\times \sum_{\mu_1'}^{N_0}\sum_{\mu_2'}^{N_0}\left\{ e^{-\alpha|\mu_1'-\mu_2'|}\cdot\frac{1}{|\mu_1'\vec{e}_z+\vec{\Gamma}\left(\begin{smallmatrix}\mu,\mu''\\pq,rs\end{smallmatrix}\right)_1|}\cdot\frac{1}{|\mu_2'\vec{e}_z+\vec{\Gamma}\left(\begin{smallmatrix}\mu,\mu''\\pq,rs\end{smallmatrix}\right)_2|}\right\} \tag{75a}$$

$$\Lambda^{(X)}_{lmn}\left(\begin{pmatrix}\mu\mu''\\pqrs\end{pmatrix}_1;\begin{pmatrix}\mu'\mu''\\psrq\end{pmatrix}_2\right) \propto S^{0\ \mu_1}_{p_1q_1} S^{0\ \mu_1''}_{r_1s_1} S^{0\ \mu_2''}_{p_2s_2} S^{0\ \mu_2'}_{r_2q_2}$$
$$\times \sum_{\mu_1'}^{N_0}\sum_{\mu_2}^{N_0}\left\{ e^{-\alpha|\mu_1'+\mu_2|}\cdot\frac{1}{|\mu_1'\vec{e}_z+\vec{\Gamma}\left(\begin{smallmatrix}\mu,\mu''\\pq,rs\end{smallmatrix}\right)_1|}\cdot\frac{1}{|\mu_2\vec{e}_z+\vec{\Gamma}\left(\begin{smallmatrix}\mu'',\mu'\\ps,rq\end{smallmatrix}\right)_2|}\right\} \tag{75b}$$

The coupling of the interaction lines (V_1) and (V_2) should ultimately yield exacerbated convergence problems in comparison to those encountered with the first-order static exchange term $X_{cc}(k_c)$. This coupling is transposed to the Fourier coefficients which ensure boundedness of the Λ functions. It necessarily prevents the exponential convergence of one of the two troublesome lattice summations in equations (75), as shown after an ultimate manipulation over cell indices :

$$\Lambda^{(D)}_{lmn}\left(\begin{pmatrix}\mu\mu''\\ pqrs\end{pmatrix}_1;\begin{pmatrix}\mu\mu''\\ pqrs\end{pmatrix}_2\right) \propto S^{0\ \mu_1}_{p_1q_1}\, S^{0\ \mu_1''}_{r_1s_1}\, S^{0\ \mu_2}_{p_2q_2}\, S^{0\ \mu_2''}_{r_2s_2}$$

$$\times \sum_{\mu_1'}^{N_0}\sum_{\mu_2'}^{N_0}\left\{ e^{-\alpha|\mu_1'|}\cdot\frac{1}{|(\mu_1'+\mu_2')\vec{e}_z+\vec{\Gamma}\left(\begin{smallmatrix}\mu,\mu''\\ pq,rs\end{smallmatrix}\right)_1|}\cdot\frac{1}{|\mu_2'\vec{e}_z+\vec{\Gamma}\left(\begin{smallmatrix}\mu,\mu''\\ pq,rs\end{smallmatrix}\right)_2|}\right\} \tag{76a}$$

$$\Lambda^{(X)}_{lmn}\left(\begin{pmatrix}\mu\mu''\\ pqrs\end{pmatrix}_1;\begin{pmatrix}\mu'\mu''\\ psrq\end{pmatrix}_2\right) \propto S^{0\ \mu_1}_{p_1q_1}\, S^{0\ \mu_1''}_{r_1s_1}\, S^{0\ \mu_2''}_{p_2s_2}\, S^{0\ \mu_2'}_{r_2q_2}$$

$$\times \sum_{\mu_1'}^{N_0}\sum_{\mu_2}^{N_0}\left\{ e^{-\alpha|\mu_1'|}\cdot\frac{1}{|(\mu_1'-\mu_2)\vec{e}_z+\vec{\Gamma}\left(\begin{smallmatrix}\mu,\mu''\\ pq,rs\end{smallmatrix}\right)_1|}\cdot\frac{1}{|\mu_2\vec{e}_z+\vec{\Gamma}\left(\begin{smallmatrix}\mu'',\mu'\\ ps,rq\end{smallmatrix}\right)_2|}\right\} \tag{76b}$$

The exponential convergence for the summation over μ_2' in equation (76a) and μ_2 in equation (76b) is lost at the expense of the summation over μ_1'. Basically, the successive terms will decay slowly like $|\mu_2'|^{-2}$ or $|\mu_2|^{-2}$, respectively. These summations remain bounded, but a much larger number of terms will be needed to stabilize their contributions to the second-order dynamic self-energy at a level of accuracy equivalent to the one requested for the first-order static exchange self-energy. Actually, whatever the nature of the polymer chain, the decay of the successive terms in these summations is reminiscent of the decay of the successive terms implied in equation (61) to calculate the exchange term $X_{cc}(k_c)$ in a metallic case.

7. Conclusions

Any many-body perturbation expansion of quantities such as the self-energy or the correlation energy can be expressed in terms of *connected* diagrams, corresponding to *size-consistent* contributions, i.e. to contributions that satisfy the *separability conditions* required in the limit of a *non-interacting* supersystem of molecules or molecular fragments. In this limit, size-consistency is the final outcome of a suitable balance between the *delocalization* and the *degeneracy* of

one-particle canonical states. This can be related to the possibility to transform to a localized picture. Any restriction on the degrees of freedom in a given diagram results in a loss of this property, as illustrated with the SBC or diagonal 2ph-TDA renormalizations whose effect tends to vanish in the limit of an infinite system.

However, in contradiction to an improper extrapolation of conclusions drawn in the early seventies for the model of the electron gas disposed in a uniform background, the connectivity of self-energy or vacuum amplitude diagrams is not a sufficient condition to ensure their proper *size-intensive* or *size-extensive* scaling in the *thermodynamic limit* of an infinite system with finite density of charges. When tackling properly with the long-range character of the Coulomb potential within *extended periodic inhomogeneous* systems such as polymers, it is not possible to exploit the *cell electroneutrality* to prevent divergences beyond the first-order Hartree-Fock level of description. At the second-order level of description, such divergences can be easily avoided by exploiting the *orthonormality* of the HF crystalline orbitals. From third-order and beyond, however, most diagrams contain some interaction elements which logarithmically diverge with the size of the system, in spite of the cell electroneutrality and of the orthogonality constraints. Clearly, a direct expansion of third and higher-order diagrams would lead to a rapidly increasing number of lattice sums and integrations over quasi-momenta, yielding multiple singularities and therefore exacerbated size-related difficulties.

Diagrammatic techniques help to identify the origin of the size-related difficulties in correlated band structure calculations. A given diagrammatic contribution to the self-energy, obtained for frozen quasi-momenta, will be *singular* if that diagram contains one or several particle-particle, particle-hole or hole-hole antisymmetrized scattering elements without any effective transfer of quasi-momentum between the colliding lines. This is a necessary and sufficient condition for a logarithmic singularity. In spite of this, the presence of such elements does not necessarily imply a complete divergence when integrating in k-space. A diagram will be overall logarithmically divergent only if at least one of its singular vertices necessarily forbids any transfer of quasi-momentum, as for instance the first-order electrostatic self-energy graphs.

When combined under the electroneutrality constraint, the individually diverging nuclear attraction and Coulomb electron-electron contributions yield a finite electrostatic contribution to the energy of a (R)HF quasi-particle. All the corresponding diagrams reflect processes of interactions without any transfer of momentum, of which the accumulating energy contributions would lead to an infinite result if not properly combined. For a better understanding of the mathematics beyond diagrams, such divergences can be regarded as resulting from unphysical "perfect" *resonant* interactions : "unphysical" because they yield a divergence ; "perfect" because (1) an infinite supply of energy is present, and (2) any variation in quasi-momentum is necessarily impossible because of the static nature of the electron-electron Coulomb repulsion contributions. Therefore, an infinite amount of energy can be transferred from the Fermi sea to the particle under consideration.

Proper integration over quasi-momenta is needed when dealing with the first order static correlation arising from exchange and with the higher-order dynamic correlation. The corresponding self-energy diagrams exhibit some simple or multiple singularities that one can associate with a pointwize lack of transfer of quasi-momentum at the level of some vertices. The integration over quasi-momenta damps these singularities. The processes described by these diagrams should be qualified as physical "imperfect" resonant interactions : (1) "physical" because they lead to a finite contribution and (2) "imperfect" because a particle can be scattered at the interaction with variation in its quasi-momentum, the successive scatterings leading to the *dispersion* of the energy dynamically transferred from the correlated sea to the particle under consideration. Within the framework of this analogy, it is very tempting to compare dynamic self-energy (or vacuum amplitude) diagrams to hydraulic systems and quasi-momenta to viscous fluids, in which some frictional forces accounting for energy dispersion also prevent "perfect" but unphysical resonant situations. These dispersion effects ensure the correct size-intensive scaling of the dynamic self-energy in the thermodynamic limit. A corollary of this result is the size-extensivity of the correlation energy obtained using any approach based on the linked cluster theorem.

On the other hand, although they are size-consistent in the non-interacting limit, some static self-energy diagrams such as the A_1 and A_2 third-order graphs (Figure 13) tend to individually diverge through the interplay of their direct contribution in the thermodynamic limit, since no dispersion effect prevents the development of a full resonance at the level of at least one of their line-vertices (Figure 19). At the third-order level, it is interesting to note that the divergent diagrams A_1 and A_2 belong to a pair of *antigraphs* [13], which reduces to the combination of approximately opposite contributions ($A_{1cc} \approx -A_{2cc}$) in the framework of the quasi-particle approximation. This property is however insufficient to ensure a strict compensation of individually divergent behaviours in the thermodynamic limit.

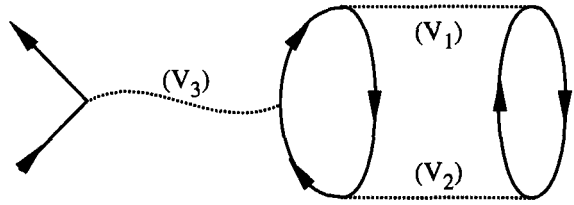

Figure 19 : The direct third-order static contribution to the self-energy arising from diagram A_1. From the conservation of the flows of quasi-momenta, it follows that the interaction element V_3 is singular at any-point of the tridimensional domain of integration in k-space related to this diagram. Therefore, A_1 diverges in the thermodynamic limit.

At this point, it is useful to recall that the static self-energy diagrams account for correlation corrections to the Hartree-Fock ground state electron density. In a scheme dealing properly with the electroneutrality constraint for each unit cell, this contribution would ideally take part in a suitable balance of divergences together with the HF electron density and the nuclear point charges. Such diagrams would be excluded from a many-body expansion of the self-energy based on a modified Coulomb-Balance Hamiltoninan, as the one introduced by Fetter and Walecka to tackle the electron gas. In polymer calculations based on HF eigenvalues and eigenvectors, the size-related difficulties resulting from these particular diagrams

should be alternatively circumvented by a suitable renormalization of the static part of the self-energy .

There is an obvious relationship between the diverging behaviour arising from the absence of transfer of quasi-momentum and the slow decay of the Coulomb interaction over the successive points of the direct lattice : even at large distances, charge distributions can provide very small but additively non-negligible contributions to electrostatic, exchange or correlation energies. Therefore, even if a localized molecular orbital basis is used (like Wannier functions), care is needed for the truncation of any lattice summations. This is particularly true with the static self-energy components, but also with the dynamic self-energy contributions, which should imply some lattice summations of quadratic convergence because of the coupling between the successive vertices, whatever the nature of the polymer.

From this contribution, the concept of exchange and correlation appears to have a special meaning for extended systems, where they play a qualitatively different role than for finite systems. By means of the tools developed here, which can be easily transposed to other situations (See Appendix 3), we get a new perspective for dealing with many-body effects in polymers and solids.

Appendix 1 : Properies of $\varepsilon_n(k)$ and $\phi_n(k,r)$

As the Hartree-Fock one-particle potential is continuous in the elementary cells except possibly at a finite number of points where it can become negatively infinite, it can be shown [94-98] that :

(a) the energy bands $\varepsilon_n(k)$ are bounded and continuous functions of k over the first Brillouin zone. The same property applies to the one-particle state $\phi_n(k_n,\vec{r})$, except at a point of degeneracy between bands where they become discontinuous.

(b) Single-particle states $\phi_n(k_n,\vec{r})$ corresponding to nondegenerate bands are analytic everywhere in the first Brillouin zone. This result applies within the respective invariant subspaces associated to each irreducible representation of the

line group, and accordingly an accidental degeneracy resulting from band crossing does not affect the analytic properties of the crossing bands and states.

(c) From equation (14), properties (a) and (b) apply also to the LCAO expansion coefficients of the crystal orbital $\phi_n(k_n,\vec{r})$.

Appendix 2 : Properties of Fourier coefficients

Let f(k) a function of bounded variation in the Brillouin zone be represented by a complex Fourier series

$$f(k) = \sum_{\mu} C_{\mu} e^{i k \mu a_0} \quad ; \quad |k| \leq \frac{\pi}{a_0} \quad , \tag{77}$$

where the Fourier coeffiecients C_μ are obtained as

$$C_{\mu} = \int_{BZ} dk\, f(k) e^{i \mu k a_0} \quad . \tag{78}$$

It can be shown [99] that :

(a) if f(k) is piecewise continuous, then

$$|C_{\mu}| = \mathcal{V}[f(k)] \cdot |\mu|^{-1} \quad , \tag{79}$$

where $\mathcal{V}[f(k)]$ is the total variation of f(k) over BZ. No improvement to the above estimate can be made if f(k) is entirely continuous.

(b) If f(k) has derivatives up to the order (m-1) inclusive ($m \geq 2$) and the derivative at the (m-1)th-order is absolutely continuous, then

$$|C_{\mu}| = O\left[|\mu|^{-m}\right] \quad , \tag{80}$$

Therefore, an important corollary to this result is that the Fourier coefficients C_μ decrease asymptotically with increasing μ faster than any power of $|\mu|$ if f(k) is infinitely differentiable (and thus integrable since the integration interval is finite).

(c) if f(k) is analytic, then the Fourier coefficients decrease exponentially with their index for all indices higher than a certain limiting and positive index m, i.e.,

$$|C_\mu| \leq A e^{-\alpha|\mu|} \quad ; \quad \alpha > 0. \tag{81}$$

As α is related to Max[$f^{(m)}(k)$], the rate of decay for the Fourier coefficients C_μ is ultimately related to the "degree of smoothness" of the function.

Appendix 3 : Size-consistency and size-extensivity of the RPA expansion of the electric polarizability

Computation of linear responses such as the electric polarizability are also of major interest in polymer quantum chemistry. However, because of the unbounded character of the dipole moment operator [102], the evaluation beyond the S.O.S. level of approximation of the static longitudinal polarizabilities for infinite periodic systems can only be carried out using various decoupling schemes based on the polarization propagator. Polarizabilities can be for instance calculated at a level equivalent to a CPHF [103-106] (Coupled Hartree-Fock) development taking the Random Phase Approximation (RPA) to expand the polarization propagator [107-110]. For a closed-shell stereoregular polymer, the static longitudinal polarizability can be obtained as [111,112] :

$$\alpha_{zz}(\mathrm{RPA}) = 2\begin{bmatrix}\Omega^* & \Omega\end{bmatrix}\begin{bmatrix}\mathbf{A} & \mathbf{B} \\ \mathbf{B}^* & \mathbf{A}^*\end{bmatrix}^{-1}\begin{bmatrix}\Omega \\ \Omega^*\end{bmatrix} \tag{82}$$

together with the following definitions :

$$A_{ra,sb}(k,k') = \left(\varepsilon_r(k) - \varepsilon_a(k)\right)\delta_{rs}\,\delta_{ab}\,\delta_{(k,k')} + 2\langle\phi_r(k)\phi_b(k')|\phi_a(k)\phi_s(k')\rangle - \langle\phi_r(k)\phi_b(k')|\phi_s(k')\phi_a(k)\rangle \tag{83a}$$

$$B_{ra,sb}(k,k') = \langle\phi_a(k)\phi_b(k')|\phi_s(k')\phi_r(k)\rangle - 2\langle\phi_a(k)\phi_b(k')|\phi_r(k)\phi_s(k')\rangle \tag{83b}$$

In the above equation, the dipole transition strengths $\Omega_{ra}(k)$ are defined in terms of the periodic component $u_i(k)$ of the crystalline spin-orbitals $[\phi_i(k) = e^{ikz}\, u_i(k)]$:

$$\Omega_{ra}(k) = < u_r(k) | \frac{\partial}{\partial k} u_a(k) > \tag{84}$$

This coupling term describes a vertical excitation process of an electron from an occupied to a virtual band. By construction, it becomes independent of the number of cells (N_0) present in the Born - von Karman super-cell, in the limit of this number becoming infinite.

In equation (82), the matrices **A** and $\mathbf{A}^*$ account for the expansion of the linear p-h (particule-hole) and h-p (hole-particle) responses in the retarded and advanced sector of the polarization propagator, respectively, according to the Goldstone diagrams of Figure 21. In the same equation, the matrices **B** and $\mathbf{B}^*$ account to first order for the successive couplings between these two sectors (Figure 20).

In the limit of a stereoregular chain dissociating into N_0 isolated monomers, the Ω vertices are strictly independent of the size of the system. When exploiting the conservation of the flows of momenta inside the diagrams displayed in Figures 20 and 21, it is easy to show that each term contributing to the RPA polarizablity satisfies the proper separability conditions for an extensive property : at the n-th order, each of the diagrams under consideration contains n line-vertices together with n+1 independent variables of quasi-momentum.

When considering a real polymer, none of the diagrams issued from a direct development of the p-h and h-p linear responses or from the coupling between these responses contains singular line-vertices diverging logarithmically with N_0. This is not the case with the diagrams originating from the exchange part of the interaction displayed in Figure 21, since these imply particle-hole or hole-particle scattering processes. By using a suitable integration procedure [113], it should be possible to damp these singularities, ensuring therefore the thermodynamic extensivity of the RPA polarizability.

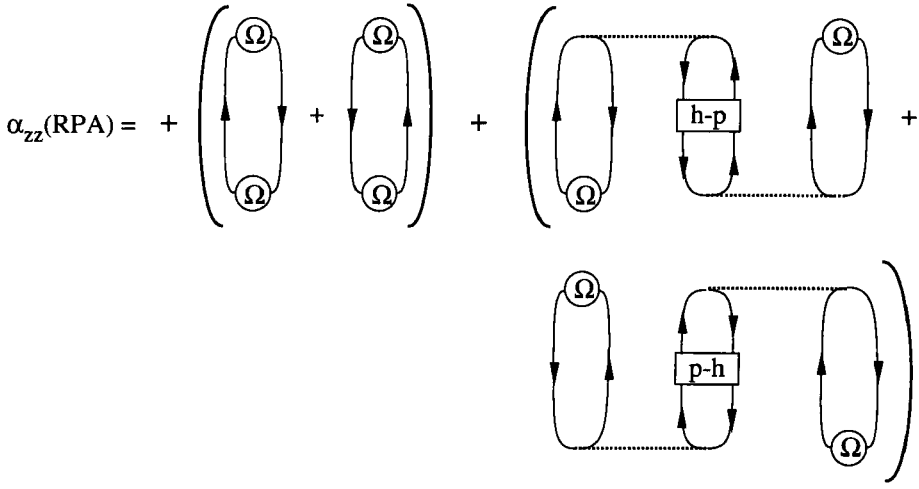

Figure 20 : Diagrammatic representation of equation (82).

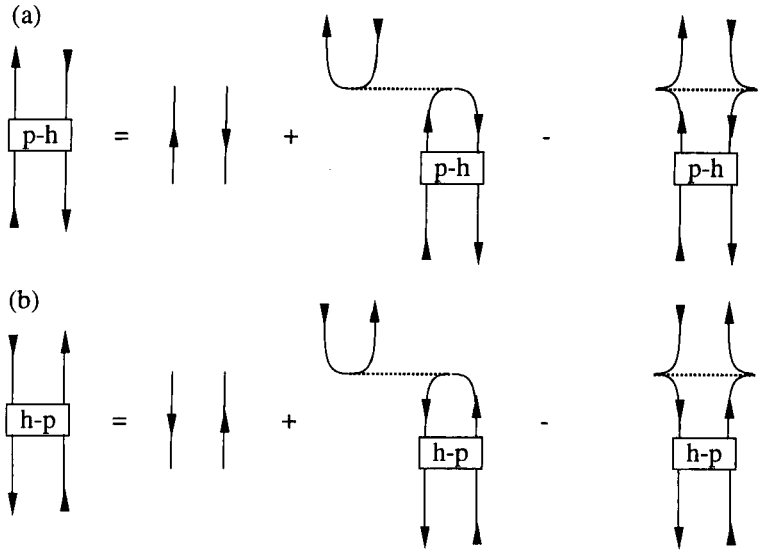

Figure 21 : RPA expansion of the p-h and h-p linear responses .

Acknowledgments

M. Deleuze is grateful to the FNRS (Belgian National Fund for Scientific Research) for his research assistant position. The authors thank Professor J.-M. André for its interest in this work. M.D. and J.D. are especially grateful to Dr. J. Fripiat (F.U.N.D.P. - Namur) for useful discussions in the field of quantum theories for polymers. M.D. would like to thank also Dr. M. Nooijen for enlightening comments about the concepts of size-consistency and size-extensivity. J.L.C. and B.T.P. would like to express their warm gratitude to the Laboratoire de Chimie Théorique Appliquée of the Facultés Universitaires Notre-Dame de la Paix in Namur, where they had the pleasure to work as guests scientists so many times. The authors acknowledge the support of this project within the framework of the 1990-1994 scientific agreements between the British Council (UK) and the CGRI-Communauté Française de Belgique/FNRS (Belgium).

References

1 : J.M. André, in *Advances in Quantum Chemistry* , P.O. Löwdin, Ed. (Academic, New-York, 1980, Vol 12, pp. 65-102).

2 : M. Kertesz, in *Advances in Quantum Chemistry* , P.O. Löwdin, Ed. (Academic, New-York, 1980, Vol 15, pp. 161-214).

3 : *Electronic Properties of Polymers,* J. Mort and G. Pfister Eds. (Wiley, New-York, 1982).

4 : *Quantum Theory of Polymers as Solids*, by J. Ladik (Plenum Press, New-York, 1988).

5 : *Quantum Chemistry Aided Design of Organic Polymers*, by J.M. André, J. Delhalle, and J.L. Brédas (World Scientific Publishing, London, 1991).

6 : J. Delhalle and M. Deleuze, J. Mol. Struct (Theochem), **261**, 187 (1992).

7 : M. Deleuze, J.-P. Denis, J. Delhalle, B.T. Pickup, J. Phys. Chem., **97**, 5115 (1993).

8 : I. Flamant, D.H. Mosley, M. Deleuze, J.M. André, J. Delhalle, Int. J. Quantum Chem., **S28**, xxx (1994 ; in press).

9 : M. Deleuze, D.H. Mosley, J. Delhalle, J.M. André, Physica Scripta (in Press)

10 : (a) S. Suhai, Int. J. Quantum. Chem., **23**, 1239 (1983). (b) S. Suhai, Phys. Rev., **27**, 3506 (1983). (c) C.M. Liegener, J. Phys.C, **18**, 6011 (1985). (d) C.M. Liegener, J. Ladik, Phys. Rev. B, **35**, 6403 (1987). (e) C.M. Liegener, J. Chem. Phys., **88**, 6999 (1988). (f) C.M. Liegener, Chem.Phys.Letters, **167**, 555 (1990). (g) P. Otto, A. Sutjanto, J. Mol.Struct (Theochem), **231**, 277 (1991). (h) C.-M. Liegener, Phys. Rev. B, **47**, 1607 (1993).

11 : A.J. Layser, Phys. Rev., **129**, 897 (1963).

12 : J. Linderberg and Y. Öhrn, *Propagators in Quantum Chemistry* (Academic, London, 1973).

13 : L.S. Cederbaum, W. Domcke, Adv. Chem. Phys., **36,** 205 (1977).

14 : L.S. Cederbaum, G. Hohlneicher, W. Von Niessen, Mol. Phys., **26**, 1405 (1973).

15 : R. Mc Weeny, B.T. Pickup, Rep. Progr. Phys., **43**, 1065 (1980).

16 : F. Ecker, G. Hohlneicher, Theor. Chim. Acta, **25**, 289 (1972).

17 : L.S. Cederbaum, G. Hohlneicher, W. Von Niessen, Mol. Phys., **26**, 1405 (1973).

18 : B.T. Pickup, O. Goscinski, **26**, 1013 (1973).

19 : W. von Niessen, J. Schirmer, L.S. Cederbaum, Comput. Phys. Rep, **1**, 57 (1984) and references therein.

20 J. Goldstone, Proc. Roy. Soc. London, **239**, 267 (1957).

21 : (a) K.A. Brueckner, Phys. Rev., **97**, 1353 (1955). (b) K.A.Brueckner, Phys. Rev., **100**, 36 (1955).

22 : (a) K.A.Brueckner, J.L. Gommel, Phys. Rev.,**109**, 1023 (1958). (b) K.A. Brueckner, K.S. Jr Masterson, **128**, 2267 (1962). (c) B.H.Brandow, Rev. Mod. Phys., **39**, 771 (1967).

23 : A.L. Fetter, J.D. Walecka, *Quantum Theory of Many-Particle Systems*, Mc Graw Hill, New-York (1971).

24 : I. Lindgren, J. Phys. B: Atom. Mol. Phys., **7**, 2441 (1974).

25 : R. Manne, Int. J. Quantum Chem., **S11**, 175 (1977).

26 : J. Paldus et J. Čisek, Adv. Quantum Chem., **9**, 105 (1975).

27 : V. Kvasnička, Adv. Chem. Phys., **36**, 345 (1977).

28 : J. Paldus, *Coupled Cluster theory*, in *Methods in computational molecular physics*, S.E. Wilson and G.H.F. Diercksen (Eds.), (Plenum, New-York, 1992) p99.

29 : J.A. Pople, J.S. Binkley and R. Seeger, Int. J. Quantum Chem., **10**, 1 (1976).

30 : W. Kutzelnigg, J. Chem Phys., **77**, 3081 (1982).

31 : R.J. Bartlett, I. Shavitt, G.D. Purvis, J. Chem. Phys., **71**, 281 (1979).

32 : A. Szabo and N.S. Ostlund, *Modern quantum chemistry* (Macmillan, New-York, 1982).

33 : R.J. Bartlett, Ann. Rev. Phys. Chem., **32**, 359 (1981).

34 : R.J. Bartlett, G.D. Purvis, Int. J. Quantum Chem., **14**, 561 (1978).

35 : R.J. Bartlett, G.D. Purvis, Physica Scripta, **21**, 255 (1980).

36 : R.J. Bartlett, G.D. Purvis, Ann. NY Acad. Sci, **367**, 62 (1981).

37 : T.E. Peacock and R. Mc Weeny, Proc. Roy. Soc. London, **74**, 385 (1959).

38 : G. Del Re, J. Ladik, and G. Biczo, Phys. Rev., **155**, 385 (1967).

39 : J. Cizek, G. Biczo, and J. Ladik , Theor. Chim. Acta, **8**, 175 (1967).

40 : F.E. Harris, in *Theoretical Chemistry Advances and Perspectives* , edited by D. Henderson and H. Eyring (Academic, New-York, 1957), Vol 1, pp 147-218 .

41 : F. O'Shea and D.P. Santry, Chem. Phys. Lett., **25**, 164 (1974).

42 : I.I. Ukrainski, Theor. Chim. Acta, **38**, 139 (1975).

43 : M. Kertesz, Acta Phys. Acad. Sci. Hung., **41**, 107 (1976).

44: J. Delhalle, J.M. André, Ch. Demanet, and J.L. Brédas, Chem. Phys. Lett., **77**, 143 (1978).

45 : L. Piela and J. Delhalle, Int. J. Quantum Chem., **13**, 605 (1978).

46 : J. Delhalle, L. Piela, J.L. Brédas and J.M. André, Phys. Rev. B, **22**, 6254 (1980).

47 : S. Suhai, J. Chem. Phys., **13**, 3843 (1980).

48 : L. Piela, J.M. André, J.G. Fripiat, and J. Delhalle, Chem. Phys. Lett., **77**, 143 (1981).

49 : H. Monkhorst, and M. Kertesz, Phys. Rev. B, **24**, 3025 (1981).

50 : P.R. Surjan, M. Kertesz, A. Karpfen, and J. Koller, Phys. Rev. B, **27**, 7583 (1983).

51 : R. Dovesi, Int. J. Quantum Chem., **26**, 197 (1984).

52 : J. Delhalle and J.L. Calais, J. Chem. Phys., **85**, 5286 (1986).

53 : J.G. Fripiat, J. Delhalle, J.M. André, J.L. Calais, Int. J. Quantum Chem., **S24**, 593 (1990).

54 : J. Delhalle, Int. J. Quantum Chem., **26**, 717 (1984).

55 : J. Delhalle and F.E. Harris, Phys. Rev. B, **31**, 6755 (1985).

56 : J. Delhalle, and J.L. Calais, Phys. Rev. B, **35**, 9460 (1987).

57 : A.D. Mattuck, *A Guide to Feynman Diagrams in the Many-Body Problem*, Mc Graw Hill, New-York (1967).

58 : M. Deleuze, J. Delhalle, B.T. Pickup and J.L. Calais, Phys. Rev. B, **46**, 15668 (1992).

59 : K.F. Freed, Ann. Rev. Phys. Chem., **32**, 359 (1981).

60 : N.H. March, W.H. Young and S.Sampatar, *The many-body problem in quantum mechanics* (Cambride University Press, Cambridge, 1967).

61 : (a) N.M. Hugenholtz, Physica, **23**, 481 (1957). (b) L. Van Hove, N.M. Hugenholtz and L. Howland, *Quantum theory of many-particle systems* (Benjamin, New-York, 1961).

62 : (a) F.J. Dyson, Phys. Rev., **75**, 486 (1949). (b) F.J. Dyson, Phys. Rev., **75**, 1736 (1949).

63 : M. Gell-Mann et F. Low, Phys. Rev., **84**, 350 (1951).

64 : G.C. Wick, Phys. Rev., **80**, 268 (1950).

65 : D.N. Zubarev, Sov. Phys. Uspehki, **3**, 320 (1960).

66 : G. Csanak, H.S. Taylor et R. Yaris, Adv. At. Mol. Phys., **7**, 287 (1971).

67 : H. Lehman, Nuovo Cimento, **11**, 342 (1954).

68 : S. Yomosa, J.Phys. Soc. Jpn, **19**, 1718 (1964).

69 : J.M. André, L. Gouverneur and G. Leroy, Int. J. Quantum Chem., **1**, 427 (1967).

70 : J.M. André, L. Gouverneur and G. Leroy, Int. J. Quantum Chem., **1**, 451 (1967).

71 : J.M. André and G. Leroy, Theor. Chim. Acta, **9**, 123 (1967).

72 : J. Ladik, Adv. Quantum Chem., **7**, 397 (1973).

73 : J.M. André and J. Ladik (Eds.), *Electronic structure of polymers and molecular crystals*, (Plenum, New-York, 1975).

74 : J.M. André, J. Delhalle and J. Ladik (Eds.), *Quantum theory of polymers* (Reidel, New-York, 1978).

75 : J. Ladik, Adv. Quantum Chem., **12**, 65 (1980).

76 : M. Kertesz, Adv. Quantum Chem., **15**, 161 (1982).

77 : J. Ladik and J.M. André (Eds.), *Quantum chemistry of polymers : solid state aspects* (Reidel, Dordrecht, 1984).

78 : M. Born and T. Karman, Phys. Z., **13**, 297 (1912).

79 : R.H. Bube, *Electronic properties of crystalline solids - an introduction to fundamentals* (Academic Press, New-York, 1974), chapter V.

80 : M. Vujicic, I. Bozovic, and F. Herbut, J. Phys. A, **10**, 1271 (1977).

81 : M. Vujicic, I. Bozovic, and F. Herbut, J. Phys. A, **11**, 2133 (1978).

82 : I. Bozovic, and M. Vujicic, J. Phys. A, **14**, 777 (1981).

83 : Y. Öhrn and G. Born, Adv. Quantum Chem., **13**, 1 (1981).

84 : M.F. Herman, K.F. Freed and D.L. Yeager, Adv. Chem. Phys., **48**, 1 (1981).

85 : (a) J. Baker et B.T. Pickup, Mol. Phys., **49**, 651 (1983). (b) J. Baker, Chem. Phys., **79**, 117 (1983). (c) J. Baker, Chem. Phys., **79**, 2693 (1984).

86 : D.J. Rowe, Rev. Mod. Phys., **40**, 153 (1968).

87 : O. Goscinski and B. Lukman, Chem. Phys. Lett., **7**, 573 (1970).

88 : J. Schirmer, Phys. Rev. A, **26**, 2395 (1982).

89 : J. Schirmer, L.S. Cederbaum and O. Walter, Phys. Rev. A, **28**, 1237 (1983).

90 : O. Walter and J. Schirmer, J. Phys. B, **14**, 3805 (1981).

91 : (a) M. Deleuze, J. Delhalle and J.M. André, Int. J. Quantum Chem., **41**, 243 (1992). (b) M. Deleuze, J. Delhalle, and B.T. Pickup, Theor. Chim.

Acta, **82**, 309 (1992).(c) M. Deleuze, J. Delhalle, and B.T. Pickup, J. Electron. Spect. Rel. Phenom, **60**, 37 (1992).

92 : B. Champagne, D.H. Mosley and J.-M. André, Chem. Phys. Lett., **210**, 232 (1993).

93 : P. Daling, P. Unger, P. Fulde and W. van Haeringen, Phys. Rev. B, **43**, 1851 (1991).

94 : W. Kohn, Phys. Rev. **115**, 1460 (1959).

95 : D.S. Bulyanitsa and Yu E. Svetlow, Sov. Phys. -Solid State, **4**, 981 (1962).

96 : J. Des Cloizeaux, Phys. Rev., **129**, 554 (1963); **135**, A685, A698 (1964).

97 : G. Eilenberger, preprint 105, Quantum Chem. Group, Uppsala (1963).

98 : B. Lix, Phys. Status Solidi B, **44**, 411 (1971).

99 : N.K. Bary, *Treatise on Trigonometric Series* (Pergamon, Oxford, 1964).

100 : S.T. Pantelides, D.J. Mickish, A.B. Kunz, Phys. Rev. B, **10**, 2602 (1974).

101 : H.A. Priestley, *Introduction to Complex Analysis* (Revised Edition), Oxford University Press, Oxford (1990).

102 : J. Callaway, *Energy band theory* (Academic, New-York, 1964).

103 : J.A. Pople, R. Krishnan, H.B. Schlegel et J.S. Binkley, Int. J. Quantum Chem., **S13**, 225 (1979).

104 : C.E. Dykstra et P.G. Jasien, Chem. Phys. Lett., **109**, 388 (1984).

105 : C.E. Hurst et M. Dupuis, IBM Tech. Rep. KGN 160 (1987).

106 : S.P. Karna et M. Dupuis, J. Comp. Chem., **12**, 487 (1991).

107 : P. Jørgensen, Ann. Rev. Phys. Chem., **26**, 359 (1975).

108 : J. Oddershede, Adv. Quantum Chem., **11**, 257 (1978).

109 : J. Oddershede in *Methods in computational molecular physics*, G.H.F. Diercksen et S. Wilson (Reidel, New-York, 1983) p249.

110 : J. Oddershede, *Response and propagator methods*, in *Methods in computational molecular physics*, G.H.F. Diercksen and S. Wilson (Plenum Press, New-York, 1992) p303.

111 : B. Champagne, J.G. Fripiat and J.M. André, J. Chem. Phys., **36**, 8330 (1992).

112 : B. Champagne, D.H. Mosley, J.G. Fripiat and J.M. André, Int. J. Quantum Chem., **46**, 1 (1993).

113 : M. Deleuze, B.T. Pickup (to be published).

VALENCE BOND MIXING AND CURVE CROSSING DIAGRAMS IN CHEMICAL REACTIVITY AND BONDING

by Sason Shaik[a] and Philippe C. Hiberty[b]

(a) Department of Organic Chemistry and the Fritz-Haber Center of Molecular Dynamics, The Hebrew University, 91904, Jerusalem.

(b) Laboratoire de Chimie Theorique, Bat 490, Universite de Paris-Sud, 91405 Orsay Cedex, France

List of Contents

ADVANCES IN QUANTUM CHEMISTRY
VOLUME 26

1. INTRODUCTION

Effective paradigms are needed to guide the generation and solution of chemical problems and to pattern the mass of existing data. This manuscript is about reactivity paradigms; the Valence Bond (VB) mixing diagrams [1-19], which have been developed to answer a fundamental question of chemical reactivity [1]: "What is the origins of the barrier in a chemical reaction, and what is the mechanism of transition state formation?" If a mechanism of barrier formation exists, one can then analyze the structure and energy of the transition state [18], and predict relationships which may exist between the transition state and properties of its precursor and successor reactants and products.

New paradigms are needed when existing ones cease to be effective tools for creating order and making new predictions. Consider for example the following 10 questions which often present themselves separately or together from the experimental reactivity data:

(a) What is the origin of the barrier in reactions that are not forbidden by the orbital symmetry principles [1, 3, 4]?
(b) What is the origin of rate-equilibrium relationships, and why do they occasionally breakdown [6-9]?
(c) What are the factors which govern the variation of intrinsic barriers [6]?
(d) What is the origin of reactivity crossovers and zigzags [9]?
(e) What is the origin of reaction intermediates [2, 3, 7-9]?
(f) Why some forbidden reactions possess very low barriers [3,10, 17] while some allowed ones have very high barriers [3]?
(g) Why isoelectronic species (e.g., like X_n, X being a monovalent atom) display stability patterns which range from unstable transition states all the way to stable clusters [3, 10, 16]?
(h) Why do reaction barriers generally decrease as we move down a column of the periodic table [3, 7, 10, 16, 17]?
(i) Why some classical polar reactions exhibit the same reactivity patterns as electron transfer reactions [1, 2, 6, 7, 13, 17, 18]?
(j) What is the relationship between the group of concepts which derive from classical physical organic chemistry (e.g., the Bell-Evans-Polanyi principle, etc.), and the group which derive from quantum chemistry (e.g., orbital symmetry, frontier orbital effects, etc.) [7, 9]?

Application of the VB mixing diagrams leads to a unified mechanism of barrier formation for all reactions which involve bond exchange (and/or formal redox). As such, the VB mixing model answers the above questions in a unified manner, and creates thereby a bridge between the disciplines of quantum chemistry and physical organic chemistry [6-9]. Following these 10 guiding questions, the present manuscript reviews the applications of the VB mixing paradigms by the authors and their coworkers to a variety of chemical problems [1-19].

The manuscript is composed of two main parts which provide an overview and current know-how on the qualitative applications and quantitative implementations of the VB mixing ideas. The first part (**Section 2**) presents an effective VB approach based on a review [4] and lecture-notes [19] by the authors. This section is designed in order to introduce a VB language which is lucid and easy to use, on the one hand, but contains the essence of a complex treatment, on the other hand. The utility of this effective VB approach is demonstrated by application to two problems in chemical bonding. The second part (**Section 3**) describes the key elements of the VB mixing diagrams and their principles of applications to chemical problems. Most of the applications are within the domain of chemical reactivity, but also discussed are some problems of bonding and structure, e.g., clustering and hypercoordination, which can be couched as chemical transformations bearing similarity to a chemical reaction [3]. This section is designed to provide the tools and modes of thinking on chemical problems, and therefore detailed treatments of specific reactions are avoided. Such specific treatments have been achieved, and can be found in the previous reviews [3, 6, 9, 10, 11] and in the original literature cited therein.

While the present contribution has been restricted, for the sake of economy, to summarize our own work, this limitation does not mean to disregard other contributions to the understanding of chemical reactivity and to the application of VB ideas in this area. Indeed, the activity in this area has been traditionally appealing and there is a sense of a Renaissance in VB theory and its applications. Much of this work will not be reviewed, but will be mentioned whenever appropriate in relation with our own approach.

2. THE VALENCE BOND LANGUAGE: AN EFFECTIVE VB APPROACH

A chemical reaction consists of the breaking and making of interactions between centers, be they atoms or complex fragments. Therefore, to construct a

curve crossing diagram, it is essential to know the qualitative VB description of all types of interactions between two centers, and this is the major aim of this section. This is achieved by means of an effective VB theory which is lucid enough to serve as a qualitative approach, but at the same time contains essential features of the complex VB treatment [20]. The effective VB approach has been reviewed [4, 19], and what follows here is a brief summary of the key points.

2.1. Overlaps and Hamiltonian Matrix Elements in Valence Bond Theory.

Due to the non-orthogonality of the orbitals used in VB theory, the enumeration and calculation of the hamiltonian matrix elements and of the overlap between determinants is more complicated than in MO-CI theory. This is the famous "n! problem" which precludes the use of the simple Slater rules. Consider, for example, a four-electron determinant composed of two doubly occupied atomic orbitals a and b, and let us calculate the overlap of this determinant with itself, expressed in equation (2.1). The spin-orbitals with spin down are indicated by a bar over the letter. Otherwise the spin-orbital is with spin-up.

$$\Delta = \langle |a\bar{a}\,b\bar{b}| \,|a\bar{a}\,b\bar{b}| \rangle \qquad (2.1)$$

The procedure consists of expanding the determinant into its 24 (n! = 24) permutations of spin-orbital products, and then computing the overlaps between these 576 products. Fortunately, the estimation of similar overlap terms can be avoided, by using the projection operator property of the antisymmetrizer of a Slater determinant. Then, only one of the determinants has to be expanded, while the other one is reduced to a single unique permutation, specified later. Further simplification can be achieved by eliminating the unnecessary permutations which give zero matrix elements, and retaining only those permutations which operate on spin-orbitals with identical spins and which thereby lead to non vanishing matrix elements [4]. For the example at hand, Δ will be accordingly the sum of the four terms in equation (2.2).

$$\begin{aligned}\Delta = &\langle a_{(1)}\,\bar{a}_{(2)}\,b_{(3)}\,\bar{b}_{(4)} \,|\, a_{(1)}\,\bar{a}_{(2)}\,b_{(3)}\,\bar{b}_{(4)} \rangle \\ &- \langle a_{(1)}\,\bar{a}_{(2)}\,b_{(3)}\,\bar{b}_{(4)} \,|\, b_{(1)}\,\bar{a}_{(2)}\,a_{(3)}\,\bar{b}_{(4)} \rangle \\ &- \langle a_{(1)}\,\bar{a}_{(2)}\,b_{(3)}\,\bar{b}_{(4)} \,|\, a_{(1)}\,\bar{b}_{(2)}\,b_{(3)}\,\bar{a}_{(4)} \rangle\end{aligned}$$

$$+ < a_{(1)}\,\bar{a}_{(2)}\,b_{(3)}\,\bar{b}_{(4)} \mid b_{(1)}\,\bar{b}_{(2)}\,a_{(3)}\,\bar{a}_{(4)} > \qquad (2.2)$$

The first term here is obtained by bringing the orbitals of both determinants into maximum correspondence, and is called the leading term [4]. This initial rearrangement of the orbitals in the determinant determines also the unique permutation to be used for the leading term. The other terms are obtained, using the above rule, by permuting orbitals in the righthand side of the leading term. Each such permutations is given a sign which corresponds to the parity of the permutation (pairwise single permutations are always odd, while doubles are even, and so on). The resulting expression for the determinant's overlap is obtained then as a sum of the contributing terms, and is given in equation (2.3) where S is the overlap between orbitals a and b in the determinant in equation (2.1).

$$\Delta = 1 - S^2 - S^2 + S^4 = (1 - S^2)^2\,;\; S = < a \mid b > \qquad (2.3)$$

The calculation of the hamiltonian matrix elements follow the same principles, and once again the resulting expressions involve a leading term and secondary terms of lesser importance. For qualitative applications, the reasonings are often restricted to the leading terms, as it has been shown that neglecting the secondary terms in both the hamiltonian matrix elements and in the overlaps between determinants leads to cancellation of errors [4, 19]. We shall eventually use these approximate matrix elements in our qualitative analyses. However, for the moment we would like to discuss some simple problems where the n! problem is either a minor one or can be avoided by comparison between VB and MO expressions.

2.2. The Two-Center/Two-Electron Bond in the Framework of an Exact Spin Free Hamiltonian.

2.2.1 General formulation. Historically, the first VB description of a two-electron bond between two centers A and B, bearing the atomic orbitals a and b, was the Heitler-London wavefunction Ψ_{HL}:

$$\Psi_{HL} = N_{HL}\,(|a\,\bar{b}| + |b\,\bar{a}|)\,;\; N_{HL} = 1/[2(1+S^2)]^{1/2} \qquad (2.4)$$

The Heitler-London description [21] is purely covalent, and symbolized by the notation (A·—·B) in **1**, which means that the atoms exchange their electrons but always remain neutral. It is important to note that the Heitler-London wavefunction

dissociates correctly to the radicals A• and •B and occasionally accounts for a large part of the bonding energy , e.g., in the H_2 molecule.

1 **2**

A more accurate description of a two-electron bond requires the zwitterionic structures ($A:^- B^+$) and ($A^+ :B^-$), as in equations (2.5)-(2.5b):

$$\Psi_L = (A—B) = c_1\,(A^{\cdot}—^{\cdot}B) + c_2\,(A:^- B^+) + c_3\,(A^+ :B^-) \qquad (2.5)$$

$$(A:^- B^+) = |a\,\bar{a}| \qquad (2.5a)$$

$$(A^+ :B^-) = |b\,\bar{b}| \qquad (2.5b)$$

This wave function (Ψ_L) , that will be referred to as a "Lewis bond" is shown in **2** in the cartoon form used throughout the text. The Lewis bond is the most general expression of two-electron bonding [22] and, depending on the magnitude of the variationally optimized coefficients c_1-c_3, can describe any type of bond ranging from purely covalent to purely ionic. In this framework, a homopolar bond (A and B being the same atoms or having comparable electronegativities) is of course mainly covalent, but the zwitterionic components are far from being negligible, with a weight of typically 10% each, at equilibrium distance. These weights diminish as the A---B distance increases, and at infinity the wave function becomes a pure HL structure corresponding to two noninteracting radicals with total spin of singlet [22b-d].

In contrast to the VB wavefunction in equation (2.5) which behaves properly upon dissociation, the Hartree-Fock MO description yields a wavefunction that, once decomposed into its VB components, gives precisely, and irrespective of the A---B distance, 50% ionic structures and 50% covalent structures. The correct covalent/ionic ratio can be recovered by means of configuration interaction (CI). In a minimal basis set, the 3X3 MO-CI description of the two-electron bond and the 3X3 VB description, in equation (2.5) are strictly equivalent, although differently represented, and correspond to the "exact" wavefunction in this basis set. However, in extended basis sets the requisite CI correction to the MO wave function becomes extensive and tedious, while the VB picture still retains its essential compact description in equation (2.5). As has been shown recently for a few bonds, notably

F-F, the compact VB description yields quite accurate dissociation energy curves, provided the orbitals of each VB structure are independently optimized and allowed to be different from one structure to the other [23].

2.2.2. The HL bond and the triplet state of H_2. In a minimal basis set, the HL bond and the triplet state (with $M_S = 0$) of H_2 share the same two determinants, $|a\bar{b}|$ and $|b\bar{a}|$, and can therefore be treated simultaneously. Since each of these determinants involves only one spin-orbital of a given spin, no permutations are needed for the calculation of integrals. These diagonal and off-diagonal terms are expressed in equations (2.6) - (2.9).

$$< |a\bar{b}| \, |\mathbf{H}| \, |a\bar{b}| > = h_{aa} + h_{bb} + J_{ab} = \boldsymbol{Q} \tag{2.6}$$

$$< |a\bar{b}| \, | \, |a\bar{b}| > = 1 \tag{2.7}$$

$$< |a\bar{b}| \, |\mathbf{H}| \, |b\bar{a}| > = 2h_{ab}S + K_{ab} = \boldsymbol{K} \tag{2.8}$$

$$< |a\bar{b}| \, | \, |b\bar{a}| > = S^2 \, ; \, S = < a \, | \, b > \tag{2.9}$$

Here, **H** is the usual spin free hamiltonian, h is the core monoelectronic integral and J and K are coulombic and exchange integrals. The diagonal and off-diagonal hamiltonian matrix elements are traditionally noted as $\boldsymbol{Q}$ and $\boldsymbol{K}$, respectively [20a].

Combining the expressions of the singlet HL wavefunction (eq. (2.4)) and that of the triplet state Ψ_T in equation (2.10),

$$\Psi_T = N_T \, (|a\bar{b}| - |b\bar{a}|) \, ; \; N_T = 1/[2(1-S^2)]^{1/2} \tag{2.10}$$

leads to the following energies of these spin states in equations (2.11) and (2.12), where V_{NN} is nuclear repulsion expressed in equation (2.13) in terms of the interatomic distance, R.

$$E_S = E(\Psi_{HL}) = (\boldsymbol{Q} + \boldsymbol{K})/(1 + S^2) + V_{NN} \tag{2.11}$$

$$E_T = E(\Psi_T) = (\boldsymbol{Q} - \boldsymbol{K})/(1-S^2) + V_{NN} \tag{2.12}$$

$$V_{NN} = 1/R \tag{2.13}$$

The singlet and triplet state energies are seen to depend on the same Q and K, and on the nuclear repulsion. It is interesting to note that the quantity (Q + 1/R), known as the quasiclassical energy, is nearly constant at all distances not shorter than the equilibrium bond length [24]. Thus the bonding energy, as well as the repulsive energy of the triplet, derive from the K term, that itself is a negative quantity. This property will be used below to derive simple approximate expressions for the triplet and HL singlet interaction energies.

2.3. An Effective Hamiltonian for VB Problems.

For qualitative applications it is desirable to describe all elementary interactions (1-4 electrons) by means of expressions based on the same unique parameter, and it is therefore necessary to get rid of the bielectronic part of the hamiltonian. This can be achieved by using an effective polyelectronic hamiltonian $\mathbf{H}_{\text{eff}}$ [4, 19, 25], defined as a sum of monoelectronic hamiltonians, in complete analogy with qualitative MO theory:

$$\mathbf{H}_{\text{eff}} = \mathbf{h}(1) + \mathbf{h}(2) + \ldots + \mathbf{h}(n) \tag{2.14}$$

Here n is the number of electron and $\mathbf{h}(i)$ is an effective monoelectronic hamiltonian which applies to electron i; $\mathbf{h}(i)$ is of course different from the core monoelectronic part of the exact hamiltonian in equations (2.6) or (2.8).

2.3.1 The two-electron interaction. Using the effective hamiltonian for the H_2 problem, the terms Q and K will now be expressed as functions of the effective monoelectronic terms which follow in equations (2.15) and (2.16).

$$Q = h_{aa} + h_{bb} \tag{2.15}$$

$$K = 2h_{ab}S \tag{2.16}$$

Since the quasiclassical energy (Q + 1/R) is nearly constant [24] at all distances and equal to the energy of the separated fragments, one can define the stabilization energy ΔE_S of the covalent HL singlet as:

$$\Delta E_S(A^{\cdot}\!\!-\!\!-^{\cdot}B) = E_S - (Q + 1/R) \tag{2.17}$$

$$\Delta E_S(A^{\cdot}\!\!-\!\!-^{\cdot}B) = (K - QS^2)/(1 + S^2) \tag{2.18}$$

$$\Delta E_S(A^{\cdot}\!\!-\!\!-^{\cdot}B) = 2\beta S/(1 + S^2) \tag{2.19}$$

Similarly, one gets the following expression for ΔE_T, the repulsion energy of the triplet state:

$$\Delta E_T(A^{\cdot}\ {}^{\cdot}B) = -2\beta S/(1-S^2) \tag{2.20}$$

where β is the reduced resonance integral [24] defined in equation (2.21) in the same form used in qualitative MO theory.

$$\beta = h_{ab} - 0.5(h_{aa} + h_{bb})S; \quad \beta < 0 \tag{2.21}$$

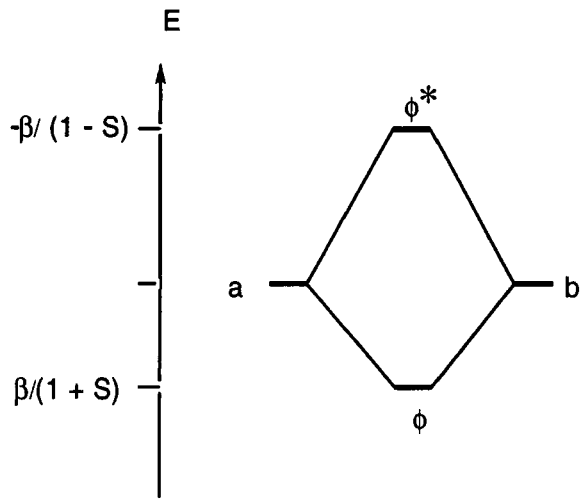

Fig. 1. MO interaction diagram for two identical AO's. Shown are the bonding and anti bonding MO's (ϕ and ϕ^*).

2.3.2 Comparison with qualitative MO theory. In qualitative MO theory (using again an effective hamiltonian), bringing together two degenerate atomic orbitals leads to the formation of two MOs, as shown in Fig. 1. The bonding MO is stabilized by the quantity $\beta/(1+S)$ relative to the non-bonding level, while the antibonding MO is destabilized by $-\beta/(1-S)$. The total energies of the singlet

and triplet states arising from the occupation of these MOs, in Fig. 1, are simply the sums of the corresponding MO energies. The resulting interaction energies for the ground state singlet, $\Delta E_S^{(MO)}$, and for the triplet state, $\Delta E_T^{(MO)}$ become then the following:

$$\Delta E_S^{(MO)} = 2\beta/(1+S) \tag{2.22}$$

$$\Delta E_T^{(MO)} = -2\beta S/(1-S^2) \tag{2.23}$$

It is apparent that the qualitative VB and MO theories give rise to different expressions for the singlet state interaction energy (equations (2.19) vs (2.22)). This is not at all surprising, since the singlet MO wavefunction is half-ionic and half-covalent, while the HL VB wavefunction is purely covalent. In contrast with the singlet state situation, the MO and VB expressions for the triplet state's interaction energy are identical (equations (2.20) vs (2.23)). This is a natural consequence of the equivalence between the MO and VB triplet wavefunctions.

To appreciate the identity of the triplet VB and MO expressions, consider one of the three possible triplet MO wavefunctions which is composed of two determinants each involving the two singly occupied MOs ϕ and ϕ^* in Fig. 1. This MO wave function in equation (2.24) can be expanded into its VB constituents and shown to be identical with the triplet VB wavefunction. Dropping the normalization constants, this identity is expressed in equation (2.24):

$$\Psi_T^{(MO)} = |(a+b)\ (\bar{a}\bar{b})| - |(a-b)\ (\bar{a}+\bar{b})| \propto |a\bar{b}| - |b\bar{a}| = \Psi_T^{(VB)} \tag{2.24}$$

Since identity of the wavefunctions requires identity of the corresponding energies, we may take advantage of the triplet state example to generalize [19]:

Statement 2.1: Whenever the VB and MO wavefunctions of an electronic state are equivalent, the VB energy can be estimated by using qualitative MO theory.

This generalization is exploited below, in order to bypass the n! problem.

2.3.3 The four-electron interaction. Before doing any calculation, let us compare the MO and VB descriptions for this interaction which brings two orbitals and four electrons into play. In this case, both the bonding and antibonding MOs (see Fig. 1) will be doubly occupied. It is apparent that the corresponding MO

determinant, once decomposed as in (2.25), is equivalent to the VB wavefunction composed of a single determinant having two doubly occupied AO's.

$$|(a+b)\,(\bar{a}+\bar{b})\,(a-b)\,(\bar{a}-\bar{b})| \quad \propto \quad |a\,\bar{a}\,b\,\bar{b}| \tag{2.25}$$

Since the wavefunctions are identical, then in line with *Statement 2.1*, the VB interaction energy can be easily determined from the MO expression by summing up the energies of the occupied spinorbitals in the MO wavefunction. This is shown in equation (2.26).

$$\Delta E(A\!:\!B) = 2\beta/(1+S) - 2\beta/(1-S) = -4\beta S/(1-S^2) \tag{2.26}$$

The 4-e interaction is of course purely repulsive, as is the triplet 2-e interaction, the former repulsion being twice as large as the latter. More generally, the VB theory states [4]:

Statement 2.2: The electronic repulsion in an interacting system is equal to the quantity $-2n\beta S/(1-S^2)$, *n being the number of electron pairs with identical spins.*

This electronic repulsion is a result of the Pauli exclusion principle, and is referred to as an exchange repulsion. The analogy with MO theory further shows that the exchange repulsion of VB theory is nothing else but the overlap repulsion in MO theory.

2.3.4 The three-electron interaction. Consider VB structures with three electrons on two centers, (A: •B) and (A• :B) . The interaction energy of each one of these structures by itself is repulsive and following *Statement 2.2* will be given by the exchange or overlap repulsion term in equation (2.27):

$$\Delta E((A\!:\!\bullet B) \text{ and } (A\bullet\!:\!B)) = -2\beta S/(1-S^2) \tag{2.27}$$

It is seen that the 3-electron repulsion has the same expression as the triplet repulsion.

Consider now the three-electron bond A:B, which is a resonance hybrid between the two limiting VB structures, (A: •B) and (A• :B), that differ from each other by an electron transfer.

$$\Psi(A\!:\!B) = c_1(A\!:\!\bullet B) \longleftrightarrow c_2(A\bullet\!:\!B) \tag{2.28}$$

In order to determine the total interaction energy for this bond, we should evaluate the matrix element between the two VB structures and combine the result with the intrinsic repulsive energy of the 3-electron structures. This lengthy procedure can be by-passed by reference to the MO picture of the three-electron bond. For homonuclear cases where A = B (or A and B of equal electronegativities) the coefficients of the two configurations are equal and the MO-VB equivalence becomes apparent. Thus, expanding the three-electron MO ground state into its VB components leads to the identity in equation (2.29), leaving out normalization constants.

$$|(a+b)\,(\bar{a}+\bar{b})\,(a-b)| \;\propto\; |a\,\bar{a}\,b| - |b\,\bar{b}\,a| \tag{2.29}$$

Once again, therefore, the VB interaction energy (relative to the separated fragments) can be calculated from MO theory as a sum of the corresponding orbital energies (Fig. 1):

$$\Delta E(A\therefore B) = 2\beta/(1+S) - \beta/(1-S) = \beta(1-3S)/(1-S^2) \tag{2.30}$$

The three-electron bonding interaction is therefore attractive when the overlap between the interacting orbitals is smaller than 1/3, and repulsive for larger overlaps. This dependence on the overlap arises from the interplay between the 3-electron repulsion, which for each VB structure varies as $-2\beta S/(1-S^2)$, and the attractive VB mixing element that varies as β itself [4].

2.3.5 The one-electron interaction. One-electron bonds are described, in VB theory, as a charge-shift resonance between two VB structures:

$$\Psi(A^{\bullet}B) = c_1(A^{\bullet}\ B) \longleftrightarrow c_2(A\ ^{\bullet}B) \tag{2.31}$$

Once again, since the MO and VB wavefunctions are the same, the interaction energy of the one-electron bond (relative to the fragments at infinity) becomes simply:

$$\Delta E(A^{\bullet}B) = \beta/(1+S) \tag{2.32}$$

2.4. Test Applications of the Effective VB Theory.

Having established expressions for all elementary 2-center interaction energies (1-e through 4-e) as functions of a single parameter β, we can now apply the formulae in order to check the validity of qualitative VB predictions. This is done for two intriguing bonding problems.

2.4.1 One-electron vs two-electron bonds. The qualitative MO picture (Fig. 1) leads to the natural prediction that one-electron bonds are always weaker than their corresponding two-electron bonds, since only one electron is stabilized in the first case vs two in the second. There are however some intriguing experimental facts which defy this very intuitive prediction. For example, while in the di-hydrogen case the two-electron bond is shorter and stronger than the corresponding one-electron bond, this does not hold true for the di-lithium case. Here the one-electron bond of Li_2^+ is both longer and *stronger* than the corresponding two-electron bond of Li_2; the corresponding bond energies being 30 and 24 kcal/mol [26].

This counterintuitive finding arises naturally by use of the above VB theory. Thus, from the expressions for the interaction energies of the two- and one-electron bonds in equations (2.19) and (2.32), it is possible to derive the ratio of these bonding energies in terms of the atomic overlap only, in equation (2.33).

$$[\Delta E_S(A\cdot\!\!-\!\!\cdot B)\,/\Delta E(A^{\bullet}B)] = 2S\,(1+S\,)/(1+S^{\,2}) \qquad (2.33)$$

It is seen that the ratio of the two bond energies can be larger or smaller than unity, depending on the size of the overlap. When the overlap is larger than a critical value of 0.414, like in the H_2/H_2^+ case, the two-electron bond will be the stronger of the two types, but for weak binders like lithium the diatomic overlap is small enough to reverse this order. This is the reason why the longer Li_2^+ bond is also stronger than the shorter Li_2 bond [19, 24].

2.4.2 Perfect pairing vs diradical bonding in the dioxygen molecule. O_2 is a particularly interesting example, because it is one of the very few molecules, made of main-elements, which prefers a diradical bonding even though it has a perfect pairing alternative available to it. Qualitative MO theory predicts, in a straightforward manner, that this diradical option is the preferred bonding mode in the ground state. However, it is often claimed that one failing of VB theory is its inability to predict this diradical bonding in a simple and lucid way.

We would like to show how the above qualitative VB theory leads to the right prediction [27] in a straightforward manner.

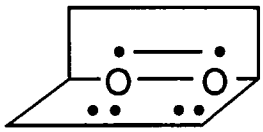

3

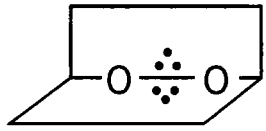

4

O_2 possesses six π electrons which can be arranged in two distinct bonding situations shown in **3** and **4**, where the two planes signify the π planes and the line connecting the O atoms corresponds to the σ bond (σ lone-pairs are omitted). Structure **3** is a perfect pairing configuration, in which the oxygen atoms maintain a double bond between them, and the remaining 4π-electrons reside in the perpendicular plane to the π bond. Structure **4** is the diradical bonding alternative, where the six π electrons are distributed in the two π-planes and form two mutually perpendicular three-electron π-bonds. We are not concerned right now with spin states [28], but we would like to establish the intrinsic energy factors of the two electronic distribution schemes in **3** and **4**; namely perfect-pairing vs diradical bonding.

Since the σ bond appears in both structures, we may disregard this bond and estimate only the difference in π electronic contribution to bonding. Using the effective VB expression for the two-electron bond (2.19), the four-electron expression (2.26), and the three-electron bonding expression (2.30), the energies; E(**3**) and E(**4**) of **3** and **4**, as well as their energy difference follow easily in equations (2.34) - (2.36).

$$E(\mathbf{3}) = 2\beta S/(1+S^2) - 4\beta S/(1-S^2) \tag{2.34}$$

$$E(\mathbf{4}) = 2\beta(1 - 3S)/(1-S^2) \tag{2.35}$$

$$E(\mathbf{3}) - E(\mathbf{4}) = -2\beta(1-S)^2/(1-S^4) > 0 \tag{2.36}$$

It is seen that the energy of the perfect pairing state, E(**3**), depends on the balance between the π-bond and the 4-electron π–repulsion in the perpendicular plane. On the other hand, the energy of the diradical alternative, E(**4**), is a sum of the two three-electron π–bonds and will be stabilizing, as long as the p_π-p_π overlap does not exceed the critical value of 1/3 which is certainly true for the O--O case

(S_π= 0.1454 , using Slater orbitals). Equation (2.36) refers to the energy difference between the two bonding options, and shows decisively that, since the reduced resonance integral is negative, the energy of the diradical bonding is lower than that of the perfect pairing state for any value of atomic overlap [19]. Therefore, the ground state of O_2 is predicted to be of diradical nature, in agreement with experiment.

Of course, our effective VB theory has chosen to disregard the bielectronic terms in an explicit manner, and therefore the theory in its present formulation will not tell us what is the lowest spin state in the O_2 diradical. This however is a simple matter, because further consideration can be made by calling Hund's rule which is precisely what qualitative MO theory has to do in order to predict the triplet nature of the O_2 ground state. Thus, among the two diradical states of the general type **4**, the triplet $^3\Sigma g^-$ is lower than the $^1\Sigma g^+$ singlet state alternative. The remaining excited states can be constructed from symmetry-adapted combinations of **3** and **3'** (the latter is analogous to structure **3** with inverted electron distribution in the two planes), by inclusion of electron repulsion terms. This is however, really out of context in the present paper and the reader is referred to the explanations in footnote [28].

What is of more interest to us here is to establish an ability to predict such diradical bonding in other cases. It is apparent from the above analysis, that a major factor of the relatively high energy of the perfect pairing situation, **3**, is the 4-electron overlap repulsion. On the other hand, the resonating perpendicular three-electron bonds in **4** allow to get rid of the overlap repulsion and to replace it by net bonding. We may therefore say that O_2 *adapts the diradical bonding option to avoid the overlap repulsion in the perfect pairing alternative.*

The application of this simple principle enables to think about ground state bonding in more complex situations than O_2, e.g., in the positive metal oxide ion FeO^+. In this case, the frontier MO ordering does not allow a simple prediction of the identity of the ground state. Using however the qualitative VB guideline shows that the perfect-pairing bonding between $O(^3P; s^2p^4)$ and $Fe^+(^6D; s^1d^6)$ encounters overlap repulsion of the $d\pi$-$p\pi$ type, and consequently FeO^+ should prefer the diradical bonding option, in the high spin $^6\Sigma^+$ state [29], over the lower spin states which maintain perfect-pairing. Indeed, sophisticated calculations show that FeO^+ assumes a $^6\Sigma^+$ ground state, with a bonding block consisting of a σ bond and two mutually perpendicular three-electron π bonds [29, 30]. Furthermore, other metal oxides, NiO^+ and CoO^+, appear to follow this prediction and to prefer in their ground states diradical bonding over perfect pairing [31].

2.5. Guidelines for the Application of Qualitative VB Theory for Polyatomic Species.

The above examples show that an effective VB theory which is based on a single effective parameter, the reduced resonance integral, is capable of making some nice predictions about chemical bonding. The reduced resonance integral itself is proportional to the corresponding overlap integral. Thus, our effective VB approach is in fact an overlap based theory, which considers explicitly the overlap consequences of spin-pairing and of Pauli's exclusion principle. These elements are quite general and can be applied to polyatomic species as well. We shall now outline the use of these concepts in general situations.

2.5.1. Bond-pairs. The VB notion of spin-pairing is not restricted to atomic orbitals. The HL wave function in equation (2.4) is a general expression for a bond-pair. The bond-pair consists of two electrons which reside in two orbitals, *of general form and nature*, and which at the same time are spin-paired into a singlet state. Thus, a general expression for a bond pair is equation (2.37), where the parenthetical term refers to all other orbitals which form a core of doubly occupied orbitals for the bond pair.

$$\Psi(\text{bond-pair}) = N\,[\,|\,(\text{core})\,a\,\bar{b}\,| + |\,(\text{core})\,b\,\bar{a}\,|\,] \qquad (2.37)$$

The orbitals, a and b, which appear in the expression may be pure atomic orbitals or hybrids, in which case the wave function would describe the diatomic HL structure with pure AO's. In the more complex case, these orbitals may be delocalized AO's, for example the Coulson-Fischer [32] atomic orbitals emerging from GVB [33] and SCVB [34] computations. For these situations equation (2.37) would represent a Lewis-type structure [35] where the ionic structures are taken into account through the delocalization tails of the AO's. In the most general situation, the orbitals in equation (2.4) may be delocalized group orbitals, and the bond-pair would represent then a bond between two delocalized orbitals of molecular fragments. In this latter situation, one introduces orbital-symmetry considerations into the effective VB scheme [4]. The general cartoon which will be used for describing a bond-pair, between two fragments A and B of general and unspecified complexity, is the same one as used to describe the HL structure in **1**, above, with a line connecting the two electrons to indicate their spin-pairing into a bond-pair.

All bond-pairs possess common expression for the bond-pairing energy component [4] of the total energy. This is expressed in equations (2.38) where now the term βS refers to the product of the resonance and overlap integrals defined over the bond-pair orbitals of general form and nature.

$$\Delta E(\text{bond-pairing}) = 4N^2\beta S \sim 2\beta S \qquad (2.38)$$

Thus, for example, the bond-pair orbitals may correspond to the coupling of a radical with an anion radical that is described by a three-electron bond. In this case the bond-pairing energy terms β and S will correspond to the reduced resonance and overlap integrals between the orbital of the radical and the anti-bonding orbital of the anion-radical.

2.5.2. Overlap repulsions. In many electron situations, there will be bond-pairs as well as repulsive situations between electrons which possess identical spins. These identical spin pairs are contributed by three situations which were discussed above: (i) triplet situations of two electrons, (ii) three electron situations, and (iii) 4-electrons in closed shell situations. The total effective VB energy is a sum of all the terms [4] which correspond to bond-pairing and overlap repulsion.

Disregarding the effects of the normalization constant, the overlap repulsion component of the energy can be expressed most simply as in equation (2.39).

$$\Delta E(\text{overlap repulsion}) \sim \Sigma_{\text{pairs}}(-2\beta S) \qquad (2.39)$$

Here too the β and S are defined over the orbitals which possess electrons with identical spins; and the summation is over the total number of such pairwise interactions between the electrons, as follows from *Statement 2.2* .

2.5.3. Mixing rules for VB structures. From the discussion of the diatomic interactions, it is apparent that there exist two types of matrix elements which correspond to two different resonating situations. The first resonating situation was encountered above in the odd electron situations, where the VB state was made from a resonance hybrid of structures that differ by a charge-shift e.g., in equations (2.28) and (2.31). This resonance typifies all situations of mixed-valency (where the average number of electrons per orbital is noninteger), and plays a key role in electron transfer, electron hopping and electron transport processes [4, 36].

The second situation appeared in the HL structure and related bond-pair situations, in equations (2.4) and (2.37). In these cases too there is a resonance of

two structures, but now these structures are VB determinants which differ by a spin-flip over two orbitals. This resonance typifies all iso-valent situations which possess one electron per orbital, and is responsible for the bond-pairing stablization [4]. In the most general situation, this type of resonance will be encountered between VB determinants which differ in two spin-orbitals (e.g., $|a\bar{a}|$ and $|b\bar{b}|$, and so on).

These are the largest and most important matrix elements in our effective VB approach. We may therefore state the following VB mixing rules which would be used for qualitative purposes [4]:

Mixing rule 1: Structures which differ by one spin-orbital (i.e., generated by means of a single electron shift or transfer; a $\longrightarrow$b) are connected by a matrix element which is proportional to the reduced resonance integral, βab, of the orbitals which are different in the two structures.

Mixing rule 2: Structures which differ by two spin orbitals ((a,a') $\longrightarrow$(b,b')) are connected by a matrix element which is proportional to the product of the resonance and overlap integrals of the corresponding orbitals ($Sab\beta a'b' + Sa'b'\beta ab$)).

The only caveat that should be kept in mind is that there will be cases where the two types of matrix elements will occur in the same VB mixing situation, and one may be advised occasionally to use all the permutations in order to retrieve all the important terms. The fuller details are discussed in references 4 and 36.

3. VB DIAGRAMS FOR CHEMICAL REACTIONS: AUFBAU PRINCIPLES

The foregoing sections lay the foundation for a qualitative application of effective VB theory to chemical reactivity. In so doing, the approximations and limitations which have been stated in the preceding sections should be always kept in mind. Alongside the qualitative applications we shall review also some quantitative VB applications which use mostly multistructure VB computations [14, 15, 37-46]. The goal here is to outline general features and know-how of the model.

3.1. VB Configuration Sets for Chemical Reactions

3.1.1. Effective VB configurations. The main advantage of representing chemical reactions in terms of VB configurations is the potential insight which can be gained from such representations. To maximize the insight, the VB window is generally restricted to the "active bonds" and the "active orbitals"; those which are involved in the bonds which are being broken and made during the reaction. All other bonds and electron pairs, are not treated explicitly in a VB sense and are termed collectively "inactive bonds" [14, 15, 37-45]. The inactive bonds and electron pairs form an effective core which influences the energies of the VB configurations, as well as the shape and size of their active orbitals. As such, the VB structures used to describe a chemical reaction are "effective VB configurations [4, 9] which account for the effect of the inactive bonds in an implicit manner. This division has implications both on the computational procedures [42] as well as on the qualitative application [9 (especially p 284)] of the VB paradigms.

Consider as an example, the process in equation (3.1) which is formally a 4-electron/3-center group transfer process embracing S_N2 reactions (e.g., A = CH_3), proton transfers (A = H), and so on [1-6].

$$X_l{:}^- + A{-}X_r \rightarrow X_l{-}A + {:}X_r^- \; ; \; l,r = \text{left, right} \qquad (3.1)$$

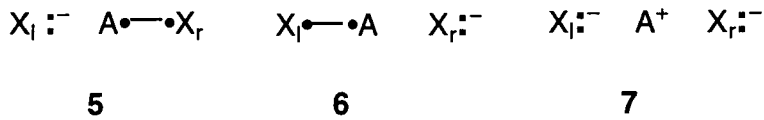

5 **6** **7**

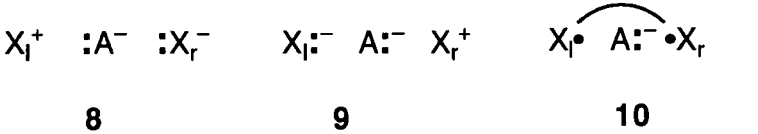

8 **9** **10**

Drawings **5**-**10** show the six effective configurations which are necessary to describe the process in equation (3.1). These effective configurations are generated by distributing the four electrons in the active orbitals in all possible ways. In any one of the configurations, the electronic distribution on the fragments takes effective account of the influence exerted by the inactive orbitals, e.g., stabilization (or

destablization) of the positive charge on A^+ in **7** by different substituents on A, and so on [9].

Drawings **5** and **6** represent the HL structures for the active bonds of reactants and products. Drawings **7-9** are the ionic structures which contribute to the electron pair bonding in reactants and products. Structure **10** is the long bond structure [47] that couples the odd electrons on the X groups into a singlet pair. Note that **10** does not contribute to the bonding of either the reactants or the products, but may become important at other points along the reaction coordinate. This is what we call a "foreign configurations" [4] which is absent in reactants and products, but is present in all other critical species along the reaction coordinate.

The selection of the effective set of VB configurations for other reactions follow the preceding example. Thus, once the active bonds and orbitals are defined, the corresponding electrons are distributed in the active orbitals in all possible ways which span the VB configuration set for the reaction. For reactions which can be described by reorganization of electron-pair bonding schemes, the effective VB set will always include two HL forms which describe the active bonds of reactants and products, and all possible ionic configurations which mix into the HL forms to account for the electron-pair bonding. In addition, there will be some "foreign configurations", to complement the description of points other than reactants and products along the reaction coordinate. For reactions which involve reorganization of electron-pair bonding schemes, the foreign configurations will generally correspond to odd-electron bonding situations, as for example in structure **10** which involves 3-electron situations between A and X.

There exist reactions where the reactants and products possess different bonding types, as for example in the nucleophilic cleavage process in equation (3.2):

$$Nu:^- + (R\cdot X)^+ \rightarrow Nu{-}R + \cdot X \qquad (3.2)$$

Here, the reactants possess a one-electron bond while the products possess electron-pair bonds only. In such a reaction, the effective configuration set will involve the corresponding one-electron VB structures $R\cdot\ X^+$ and $R^+\cdot X$, which are needed in order to account for the one-electron bond in the reactant, and the HL and its associated ionic configurations that describe the electron-pair bonding in the Nu—R product. To these structures we add a foreign configuration which in this case is the HL structure $Nu\cdot\ (R\cdot\!\!-\!\!-\cdot X)$ [48]. In general, for reactions which involve reorganization of odd- with even-electron bonding schemes the foreign configurations correspond to electron-pair bonding situations.

3.1.2. Neglect of high energy effective VB configurations in qualitative applications. The qualitative application of the model requires the maximum permitted economy. For example, in the 4 electron/3 center group transfer the ionic configurations **8** and **9** place a positive charge on the X group and the charge distribution is unfavorable (relative to **7**). Since in most of the actual chemical processes X is more electronegative than A, these two configurations are going to be very high in energy and will be often ignored in our qualitative thinking. A case where these configurations cannot be ignored is when both X and A fragments are identical. In this case, symmetry requires to include these configurations in the description of the electron-pair bonds of reactants and products (e.g., the example of H^- + H-H in reference 4). Thus, some rather simple considerations will allow us to eliminate from the set of effective configurations those which do not add essential qualitative or chemical features.

3.1.3. Participation of "inactive bonds". Ocassionally the inclusion of "inactive bonds" in the VB set is either necessary or worthwhile, either because they do participate in the electronic reorganization, or because their inclusion may lead to some new insight [3, 43, 44. 49].

The trivial case of inactive bond participation involves electronic delocalization by substituents on the reaction centers. For example, the heterolysis of benzyl halide can still be described by just a pair of configurations, $R^{\bullet}\!-\!-^{\bullet}X$ and $R^+ :X^-$ [2, 8, 50], which take into account the electronic delocalization effect due to the phenyl substituent in the fragments R^+ and $R^{\bullet}$. Each such effective configuration will be made of a linear combination of VB structures which possess the same charge distribution and spin-pairing mode defined by the types $R^{\bullet}\!-\!-^{\bullet}X$ and $R^+ :X^-$. The so formed collective VB configurations include the effect of intra-fragment electronic delocalization [9 (p 284)], for example, the effective $R^+ :X^-$ structure will be composed of a linear combination of structures which delocalize the positive charge over all the possible positions defined by the structure of R^+.

Other cases involve inactive bond participation due to symmetry. For example, in the S_N2 reaction the molecule may contain a few identical X groups, e.g., CH_2Cl_2. In this case, symmetry dictates to utilize, especially for the reactant's excited state, equivalent VB configurations which represent the two identical linkages [6, 51].

A third situation of the involvement of inactive bonds is the incursion of intermediate states along the reaction coordinate. Nucleophilic substitution on olefins [49] in equation (3.3) is an example where inactive bonds participate in the electronic reorganization.

$$Y:^- + R_2C{=}CHX \rightarrow R_2CH{=}CHY + :X^- \qquad (3.3)$$

Here the net transformation does not involve the π-bond of the olefin, but the actual process does proceed generally through an initial attack on the π-bond. In this case, the VB configuration set will have to include the π-type configurations.

The effects of the inactive bond participation can be handled quantitatively and qualitatively in a systematic manner [3, 6, 9, 42, 45]. The role of inactive bonds will be illustrated later in the discussion, by use of specific examples. For the moment we proceed with the construction of curve crossing diagrams made from the effective VB configuration set of the active bonds.

3.2. Explicit Curve Crossing VB Diagrams

A "curve crossing VB diagram" is obtained when the effective VB structures of a chemical reaction are traced *individually* along a reaction coordinate or, in the general case, along a deformation coordinate. As such *the curve crossing VB diagram is a general fingerprint of chemical reactivity and forms the basis for understanding the origins of barriers in chemical reactions.*

Let us consider for example, the effective configurations for the 4-electron/ 3-center group transfer reaction, eq. (3.1), and let us neglect right at the outset the high energy ionic structures **8** and **9** [45]. Figure 2 is a typical [4] curve crossing diagram which shows the behavior of the VB structures **5-7** and **10** along the reaction coordinate that stretches between *R* (reactants) and *P* (products) extremes and passes through the midpoint, *M*, where the distances $d(X_l \cdots A)$ and $d(A \cdots X_r)$ are equal. The most stable configuration at any one of the extremes of the reaction coordinate is one of the HL structures **5** and **6**. Above the HL configurations there lie the ionic and long-bond structures **7** and **10**.

The behavior of the configurations can be rationalized by simple considerations of electrostatic and bonding interactions. Let us start with the ionic and long bond structures. The ionic structure **7** possesses favorable electrostatic interactions of A^+ with the X^- groups, and the interactions are symmetric for the two X groups. Since the reaction coordinate involves shortening of one A-X linkage and lengthening of the other, the two interactions roughly cancel out and the curve varies in a horizontal manner along the reaction coordinate. This curve may have a minimum or a maximum at the midpoint of the reaction coordinate [3, 14, 44, 45], but roughly speaking the global variation is horizontal. The same considerations

apply to the long bond structure, **10**, which possesses symmetric interactions of the two X· groups with A:⁻.

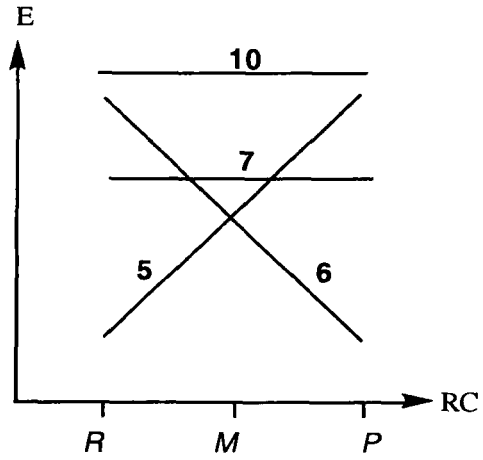

Fig. 2. Explicit curve crossing VB diagram for the process in equation (3.1) using the effective VB configurations **5-7** and **10**.

The most important feature of the diagram in Fig. 2 is the behavior of the two HL configurations (**5** and **6**) which interchange along the reaction coordinate. The reason for this curve crossing is, that along the reaction coordinate, in each HL curve a bonding interaction is replaced by a repulsive three electron interaction, and consequently the HL structures rise sharply from being a ground configuration in one reaction coordinate extreme to being an excited configuration in the other reaction coordinate extreme. This crossing of the HL structures reflects the interchange of the electron pair bonds which occurs during the chemical reaction in equation (3.1). The same pattern will be observed for any reaction that involves reorganization of bonding schemes based on electron-pair bonding. In all these cases, the HL configurations will interchange along the reaction coordinate, while the ionic and foreign structures will vary roughly in a horizontal manner along the reaction coordinate.

3.3. Compact Lewis- and State Correlation-Diagrams (SCD's)

The HL curves in Fig. 2 are seen to be anchored in two pairs of ground and excited configurations and to form thereby a spine for the curve crossing diagram. If

we use this spine as a basis and dress it with all other configurations we shall generate more compact representations of the curve crossing VB diagram. To achieve that we must first establish the mixing patterns of the ionic and long bond configurations with the spine configurations and this can be done on two different levels of complexity which are finalized in Figs. 3a and 3b.

3.3.1.Compact diagrams made from the Lewis curves. Figure 3a uses the spine-curves and the ionic structure **7**, while leaving out for the moment the long bond structure **10**. The ionic structure differs from each one of the HL structures by a single electron shift from A to the X group that is bonded to A by a HL bond. The ensuing VB mixings, according to *Mixing rule 1*, are proportional to the overlaps between the active orbitals of A and X groups across the linkage that is spin-paired in the HL structure. Consequently, **7** mixes into the two spine-curves, at all points except for the extreme excited point of each curve [3, 6, 9].

Following the VB mixing considerations it is possible to analyze the nature of the VB diagram in Fig. 3a. Thus, mixing of **7** into the HL spine-curve **5** generates a new curve having a mixed covalent-ionic character. This new curve is referred to as a Lewis curve because its ground state is the Lewis structure of the reactants, X_l :$^-$ / (A—X_r). Similarly, mixing of **7** into the HL spine-curve **6** generates the second Lewis curve whose ground state is the Lewis structure of the products, (X_l —A) / :X_r^-. Thus, by dressing the HL spine-curves (Fig. 2) with the ionic structure we generate a more compact curve crossing VB diagram, in Fig. 3a, made from the Lewis curves of reactants and products.

We could have in fact started from Lewis structures and followed their own evolution along the reaction coordinate. This is actually what was done in the pioneering studies of Evans and Polanyi in their search for ways to locate transition states [52]. In so doing we would have obtained directly Fig. 3a without having to go through the mixing procedure. Thus, it is seen that each Lewis structure is destabilized as we move from one extreme of the reaction coordinate to the other, because the Lewis A-X bond is broken and is replaced by three-electron exchange repulsion across the other linkage between A and X. As such, the pair of Lewis structures at the reaction coordinate extremes are mutually related as ground and excited configurations. This interchange of the Lewis structures is simply a mirror of the electronic and structural reorganization symbolized in equation (3.1). The crossing of the Lewis curves can be generalized for all reactions which involve reorganization of electron-pair bonding schemes.

3.3.2. Compact diagrams anchored in spectroscopic states: State correlation diagrams (SCD's). Inspection of Fig. 3a shows that, in each extreme of the reaction coordinate, the excited configuration is generated from the ground state below it by a single electron transfer from the $X:^-$ to the X which is bonded to A. Thus, the diagram in Fig. 3a describes two curves which are anchored in two ground states, of reactants and products and in their corresponding *charge transfer configurations*. These *charge transfer configurations are still not states*, and their conversion to states is achieved by bringing structure **10** into the mixing procedure (within our minimal set this is sufficient).

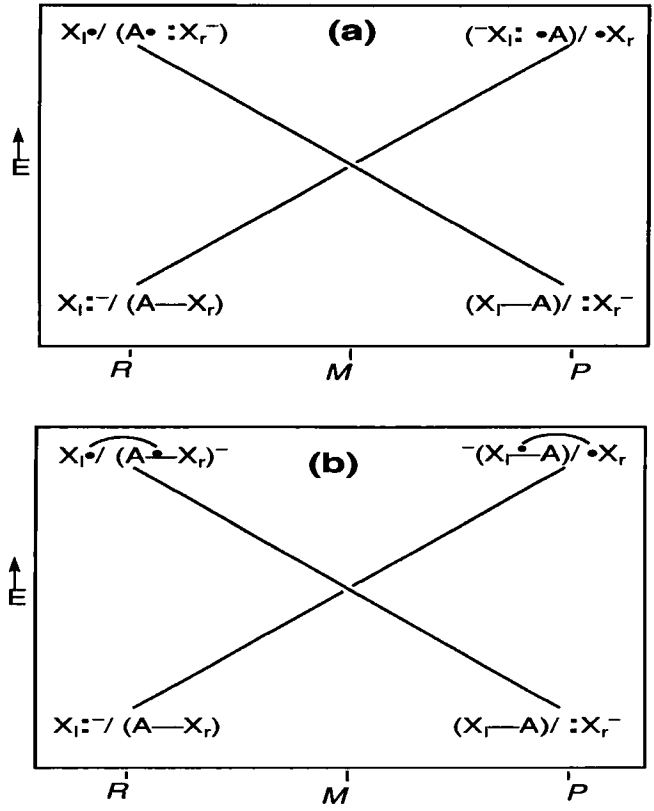

Fig. 3. (a) A Lewis curve crossing diagram for the process in equation (3.1). (b) State anchored curves after mixing of the long bond structure (**10**).

Following *Mixing rule 1*, structure **10** can mix into the two the excited anchor points of the Lewis curves, but not into the ground states of the curves. When this mixing takes place, the three electron ($A^{\bullet}\ :X^{-}$) moieties become three electron bonds by acquiring some ($A:^{-}\ ^{\bullet}X$) character. Consequently, the excited configurations become simply valence charge transfer states which are shown in Fig. 3b, and the resulting curve crossing VB diagram is anchored now in well defined spectroscopic states of reactants and products.

The relationship of Figs. 3a and 3b shows that the state-anchored curves are descendent from the reactant and product Lewis curves by dressing the latter with the foreign VB configuration, which contributes to the description of the excited state. Thus, Fig. 3a which is based on the Lewis curves should be considered as an approximation for the state-anchored curves in Fig. 3b [53].

3.3.3. VBCM and SCD models: Localized and delocalized VB versions. It is instructive to compare at this point the VB diagrams in Figs. 2 and 3b. Figure 2 involves pure VB configurations, and therefore each curve refers to a particular electronic distribution in the active orbitals, as specified in the VB configuration set **5-7** and **10**. By mixing these VB curves we would eventually get the final states along the reaction coordinate. We often refer to these many curve diagrams and to their final product of VB mixing as the VB configuration mixing (VBCM) model [2, 5, 6, 8, 54].

Figure 3b on the other hand involves only two curves made from the same VB configuration set **5-7** and **10**. Now each curve is a mixture of *a subset of configurations which define a particular bonding situation*, itself specified by a particular Lewis structure. Since the two curves in Fig. 3b are anchored in spectroscopic states of reactants and products we refer to these diagrams and to their final product of mixing as state correlation diagram (SCD's) [1, 3, 6, 9]. It is apparent therefore that the two models, VBCM and SCD are mutually related as localized and delocalized VB approaches.

A similar kind of relationship exists in qualitative MO theory. Thus, one can start at the AO level and construct the MO's from linear combinations of pure localized AO's. Alternatively, one can start with fragment orbitals and make from them linear combinations to construct the MO's. As long as one reaches the same end point the two procedures are equivalent, but generally they differ considerably in the type of insight they provide into a given problem. The same analogy holds for the relationship between the SCD and VBCM models; they are equivalent but designed to provide different insights into reactivity. Application of the VBCM leads

to information about the electronic structure of the transition state and to its charge distributions [55]. On the other hand, application of the SCD model provides information about the geometric features of the transition state and the origins and height of the barrier [6, 9]. These are complementary aspects of reactivity and we shall therefore make use of the two models in the discussion of reactivity patterns.

3.4. SCD's for Chemical Reactions

The construction of the SCD in Fig. 3b from the VB configuration set in **5-10** outlines the general aufbau procedure. One has to identify first the spine-curves and then to dress them with the other configurations. In reactions which involve reorganization of electron-pair bonding schemes the spine-curves are formed by the HL structures of reactants and products. There are however reactions, like the nucleophilic cleavage of one-electron bonds in equation (3.2), where different bond-types rearrange during the reaction. In such cases, the spine-curves will correspond to the bond-types which interchange, e.g., for equation (2.3) they involve a HL curve and a one-electron bond curve. Nevertheless, the principles are the same once the spine-curves are definitive [48]. In order to restrict the scope of this review we shall not be concerned with reactions which involve odd-electron bonded species. Therefore, each time we refer to spine-curves these would be the HL curves of the reaction.

3.4.1. A General procedure for qualitative construction of SCD's. It is possible to analyze many reaction-types and go through the entire aufbau procedure of the SCD, as demonstrated above. This however turns out to be unecessary since the excited states of the SCD are nothing else but the HL configurations themselves dressed with secondary VB structures. We might say therefore that the ground states of the SCD dissolve into *specific excited states* that are made up from the HL structures of reactants and products. As such, the excited states of the SCD are image forms of the ground states at the bottom end of the SCD curves. These image states can be identified by inspection of the HL configurations for any given reaction.

Figure 4a shows the general form of an SCD for a process R $\rightarrow$ P which involves reorganization of electron-pair bonding schemes. The SCD curves are anchored in two ground states and two excited states. The excited states are the image states, also called the "prepared excited states" to qualify their relationship to the ground states. For example, Ψ_{RP}^* is the vertical excited state that possesses the

electron pairing scheme of the product. As such, Ψ_{RP}^* is the "prepared product state" at the geometry of the reactant. Likewise Ψ_{PR}^* is the "prepared reactant state" at the geometry of the product.

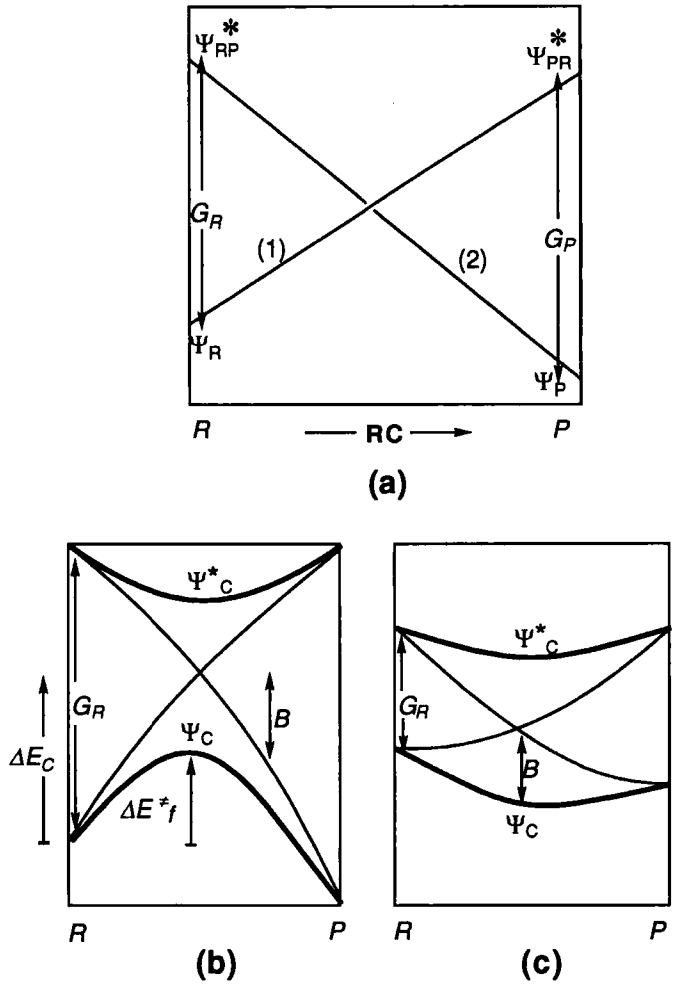

Fig. 4. (a) A general SCD anchored at ground states and "prepared excited states" of reactants and products. (b) and (c) are corresponding avoided crossing diagrams for a case with large excitation gaps (b), and for a case a case with very small excitation gaps (c). The adiabatic profiles after avoided crossing are drawn in thicker lines.

Using the terms "prepared excited states" is reminiscent of the way VB looks at bonding between atoms which possess paired electrons, e.g., formation of CH_4 from $C(s^2p^2)$ and four hydrogen atoms. Thus, to create the requisite number of bonds with the hydrogen atoms the C atom participates in bonding in "a prepared state" that possesses four unpaired electrons (s^1p^3). Similarly, the SCD in Fig. 4a tells us that since the reactant (Ψ_R) possesses electrons which are paired up in the active bonds, the only way to transform to products (Ψ_P) is by bringing in the prepared excited state (Ψ_{RP}^*) that possesses the required number of odd electrons needed to reorganize the active bonds from the bonding situation of the reactants to the bonding situation of the product.

3.4.2. The anchor states of the SCD: Their relation to the HL structures. The intimate link between the excited and ground states of the diagram enables to specify the prepared excited states by simply considering *the excitations which are required in order to produce the requisite electronic reorganization which typifies the reaction* [3, 9]. The following statements summarize the nature of the excitations required to generate the "prepared excited state" in the generalized SCD of Fig. 4a.

Statement 3.1: The prepared excited states of the SCD can be deduced from the HL structures of reactants and products, by considering changes in electron count of each reaction center.

Statement 3.2: For reactions which involve no formal redox of reaction centers, the "prepared excited states" involve only singlet →triplet excitations, one for each bond which has to be broken in the transformation. The odd electrons are coupled into bond-pairs to fit the number of bonds which are formed at the bottom end of the correlation line. These reactions will be termed henceforth, "iso-valent reactions", to emphasize the absence of formal redox of the reaction centers.

Statement 3.3: For reactions which involve a formal redox of reaction centers in addition to bond exchanges, the "prepared excited states" involve one charge transfer excitation for each pair of centers which undergo formal redox. The rest of the excitations will be of the singlet→triplet variety. The odd electrons are coupled into bond-pairs to fit the number of bonds which are formed at the bottom end of the correlation line. These reactions will be termed henceforth "mixed-valent reactions", to emphasize the formal requirement for redox.

To demonstrate the use of these statements, consider the S_N2 reaction. Following *Statement 3.1*, we have to inspect the corresponding HL structures expressed in equation (3.4):

$$Y:^- + R\bullet\!\!-\!\!-\bullet X \rightarrow Y\bullet\!\!-\!\!-\bullet R + X:^- \qquad (3.4)$$

It is seen that $Y:^-$ loses one electron to $X\bullet$, while in the reverse process it is $X:^-$ that loses one electron to $Y\bullet$. The reaction involves therefore a formal redox of two reaction centers (Y, X). Following *Statement 3.3*, we utilize vertical charge transfer excitations; from $Y:^-$ to R—X in the reactant extreme and from $X:^-$ to R—Y in the product extreme. These charge transfer excitations are in fact precisely the states that we generated in Fig. 3b above for the prototypical 4-electron/3-center group transfer reaction in equation (3.1) by means of a detailed VB mixing. Indeed, vertical charge transfer states will be the prepared excited states for all the mixed-valent processes which involve the combinations of electrophile and nucleophile or donor and acceptor, e.g., electron transfer reactions, anion-cation recombinations (and its reverse process, the S_N1 reaction), proton transfers, hydride transfers [56], and so on. The corresponding excitation gaps for these mixed-valent processes (the G_R and G_P in Fig. 4a) will accordingly be vertical charge transfer excitations, and this is irrespective of the mechanistic details of the reaction between the donor and the acceptor [2, 11, 13].

Consider another transformation which is shown in equation (3.5) using the corresponding HL structures of reactants and products.

$$Y\bullet + R\bullet\!\!-\!\!-\bullet X \rightarrow Y\bullet\!\!-\!\!-\bullet R + \bullet X \qquad (3.5)$$

Since there is no formal redox in this case, then following *Statement 3.2* the prepared excited state is obtained by triplet unpairing of the R—X bond and recoupling the electrons of the triplet $R\bullet\uparrow\uparrow\bullet X$ to the odd electron of $Y\bullet$ to generate a bond-pair [41, 57, 58]. The same considerations apply for the reverse process, and the corresponding prepared excited state involves a triplet RY coupled to $X\bullet$ to form a bond-pair. Radical additions to double bonds and radical abstractions are analogous iso-valent reactions which involve triplet excitations in the prepared excited states of the corresponding SCD's [59, 60].

Cycloaddition reactions are generally iso-valent reactions. An archetypal forbidden reaction is the 2+2 cycloaddition, which is shown in **11** using the HL structures of reactants and products. It is seen that the electronic reorganization does not involve formal redox, and therefore the prepared excited states will involve

triplet unpairing of the two π-bonds which are broken during the reaction. The resulting four unpaired electrons are coupled across the intermolecular linkages to a spin singlet [1, 9, 61].

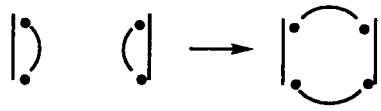

11

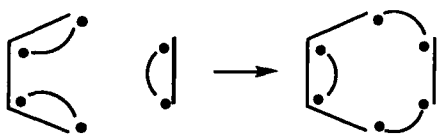

12

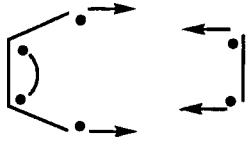

13

In complete analogy with the 2+2 reaction, the prepared excited state of a 2+2+2 cycloaddition of three olefins involves triplet unpairing of the three π-bonds [3, 62]. It is apparent therefore that the more bonds participate in the reaction, the greater will be the number of triplet excitations needed to generate the prepared excited state. The same conclusions apply of course to the exchange of σ-bonds (e.g., the $H_2 + D_2$ exchange and so on), and in general *the number of triplet excitations in the prepared excited states equals the number of bonds which participate in the exchange.* This would of course create very high barriers in multi-bond exchange reactions [3, 62].

The Diels-Alder reaction [61b,c, h; 62] is an analogous case with a special twist caused by the intramolecular linkage of the π-bonds in the butadiene reactant. The HL structures of reactants and products are shown in **12**. The reaction requires accordingly, the triplet excitation of all the π-bonds and their recoupling across the C-C linkages to be formed at the product. However, due to the intramolecular linkage in the diene, the net effect of its excitation and the recoupling of the four spins is a mono-excitation of the singlet-triplet type, shown in **13**. The result of the intramolecular linkage is seen therefore to decrease considerably the excitation gap for the prepared excited state, and this is a general principle in reactivity related to the "intramolecular catalysis effect" [62].

In summary: all reactions which involve bond *exchange* with or without formal redox can be represented by SCD's. Many reactions will involve prepared excited states of a mixed charge transfer and triplet characters. The elimination

reaction which proceeds by the E2 mechanism is an example of such a reaction [63], and the Michael addition is another such example. *All these cases can be deduced by adhering to Statement 3.1*; writing down the HL configurations and simply counting electrons on the reaction centers to deduce the formal redox pairs.

3.4.3. Avoided crossing diagrams made from SCD's. The final reaction profile is obtained by the avoided crossing of the SCD curves of Fig. 4a above. Figures 4b and 4c which are drawn alongside Fig. 4a show how the avoided crossing generates a pair of bonding and antibonding states. The bonding state is stabilized relative to the crossing point by the amount B, called the avoided crossing interaction or the quantum mechanical resonance energy of the transition state [3, 4, 36].

The two avoided crossing diagrams illustrate also how an extreme variation of the excitation gap may create a progression from unstable resonating transition states to stable resonating intermediates. Thus, a large excitation gap is predicted to generate unstable clusters which are transition states for the transformation, while very small gaps can result in stable resonating clusters. This qualitative prediction has been recently supported using multistruture VB computations of the avoided crossing diagram for the two extreme species, H_3 and Li_3 (the singlet-triplet excitation gap for H-H is 256 kcal/mol while for Li-Li it is only 33 kcal/mol). The quantitative calculations show that the seemingly counterintuitive prediction of stable intermediate states arising from avoided crossing is well founded [3, 41].

3.4.4. Ab initio calculations of SCD's. SCD's and their avoided crossing versions can be computed by means of ab initio computations. Two major approaches have been used so far in the literature.

The first approach is a direct application of VB theory using multistructure VB calculations [14, 15, 37, 38], VBSCF calculations [64], or an increased valence VB approach [53, 58]. Using VB theory one generates the individual curves by a variational calculation within the subset of configurations which define a bonding situation. A bonding situation is defined as a specific HL configuration and all the secondary ionic and foreign structures which can mix with this HL structure. After generating the two curves, they are allowed to mix and avoid the crossing in a separate calculation. In a minimal AO basis set the avoided crossing bonding state and the corresponding adiabatic state are identical. However, in extended basis sets the avoided crossing state, generated from the variational curves, is somewhat higher in energy than the full adiabatic state which is obtained by a variational procedure in the entire set of VB configurations [14, 15]. Further CI restores

identity of the avoided crossing state to its full adiabatic situation. Within the context of the original model [9 (p 205)] this CI is a second order mixing of additional excited states into the primary SCD curves, and amounts therefore to their effective mixing.

A technical complication with the variational procedure has been pointed out recently for the F^-/CH_3F S_N2 reaction [45]. In this case the ionic structure ($F^- CH_3^+ F^-$) is the lowest configuration and lies well below the HL structures in a considerable section of the reaction coordinate. Consequently, beyond the crossing point of the SCD, the variational curves artificially terminate at the pure ionic structure. The intended correlation to the charge transfer states has to be achieved by different means. Despite these occasional difficulties, the procedure is still a powerful means to provide variational values for all the curve crossing and avoided crossing quantities that are important for discussing reactivity [42, 45].

The second approach involves diabatization of MO-CI (or CASSCF) calculations and/or projection of the wave functions unto two bonding situations which define the intersecting curves [61a-e, 65]. The major inconvenience of these approaches is that the avoided crossing and curve crossing parameters depend on the way one defines the VB structures. The structures may lose sometimes their original chemical nature [66], and the avoided crossing interactions obtained by diabatization are often very large in comparison with the variational quantities [42]. Our own experience with diabatization of the adiabatic multistructure VB states into two localized bonding situations shows that, relative to the variational calculation, the diabatized crossing point is higher and the avoided crossing interaction becomes accordingly larger [15].

Irrespective of technical details and intricacies of the various methods, the VB outlook shows that *an avoided crossing is a unified mechanism for barrier formation in chemical reactions.* Thus, unlike MO theory that provides a mechanism for barrier formation only in forbidden reactions where orbital symmetry conservation can be invoked, the VB approach handles all barrier problems in a single unified manner via the avoided crossing mechanism of the SCD curves.

3.5. Reactivity Factors in the SCD Model: Origins of Reactivity Patterns.

Let us focus now on chemical reactions which possess barriers and transition states, and let us develop the necessary insight to predict and understand reactivity patterns. The barrier factors are the excitation gaps, the curvature of the curves, the

reaction thermodynamics (driving force) and the avoided crossing interaction, all of which may be discussed by reference to Figs. 4a and 4b (above), and to Figs. 5a and 5b (see later).

For any given direction of the process R $\rightarrow$ P, the $\Delta E^{\ddagger}$ may be written as a balance between the height of the crossing point (relative to reactants or products) and the avoided crossing interaction [3, 4, 6]. Using Fig. 4b, the barrier in the forward direction $\Delta E_f^{\ddagger}$ is given as shown in equation (3.6). where ΔE_C is the height of the crossing point relative to reactants.

$$\Delta E_f^{\ddagger} = \Delta E_C - B \tag{3.6}$$

Furthermore, the height of the crossing point can most simply be related to the excitation gap, G_R , as a fraction (f) of it, that is,

$$\Delta E_C = fG_R \tag{3.7}$$

The expression for the barrier becomes then equation (3.8).

$$\Delta E_f^{\ddagger} = fG_R - B \tag{3.8}$$

This is the general form of the barrier and of the mechanism of barrier formation. Thus, *the barrier originates because two states that are initially separated by an excitation gap need to achieve resonance at the crossing point in order to enable the passage from reactants to products.*

The equation may be further articulated, by use of the classical approach of linear free energy relationships. Suppose that in a reaction series there exists a linear relationship between the barriers and the excitation gaps. Of course, if one can isolate such genuine reaction families [4, 36] then the slopes and intercepts of such linear plots will possess a clear theoretical significance that draws from equation (3.8) and the activation mechanism represented in Fig. 4. Otherwise such plots simply tell us that the dominant variation of the reaction series is the excitation gap, while the slope and intercept have no physical meaning. Clearly, a more common case in a reaction series is a lack of any correlation of the barriers with the excitation gaps. In such cases, it is useful to inquire whether the reactivity patterns are determined by the dominant variations of the f and B quantities in equation (3.8). The following sections characterize the different reactivity patterns which are predicted from equation (3.8).

3.5.1. The excitation energy gap and "excitation energy gap patterns" of reactivity. The fundamental and foremost important factor is the excitation gap which originates the barrier. All the other reactivity factors scale the barrier which is *gauged* by the excitation gap. The excitation gap can be deduced by following the excitations needed to generate the prepared excited states in *Statements 3.1* and *3.2*. In addition, it is important to link these excitations to fundamental properties which are shared by all molecules; ionization potentials, electron affinities, bond energies, and so on [6, 9]. This will be done, in part, by considerations of the effective VB approach.

For example, in identity S_N2 reactions of CH_3X derivatives the vertical charge transfer energy gap (in the gas phase reaction) can actually be approximated by the C-X bond energy. Strictly speaking the charge transfer gap at infinite separation of the reactants (or products) is given by the difference between the vertical ionization potential (I^*) of the $X:^-$ anion and the vertical electron affinity (A^*) of the molecule, as shown in equation (3.9a) below.

$$G\,(X:^-/CH_3X) = I^*\,(X:^-) - A^*\,(CH_3X) \tag{3.9a}$$

$$G\,(X:^-/CH_3X) \approx 2D(C\text{-}X) \tag{3.9b}$$

Consideration of the archetypal Lewis-curves diagram in Fig. 3a and equations (2.38) and (2.39) for bond-pairing and exchange-repulsion energies, allow to approximate this expression for the gas phase reaction. It is seen, that each Lewis curve involves breaking of a Lewis bond and creating of a three-electron repulsion on the other linkage. Since the VB expressions for the three-electron overlap repulsion and for the two-electron bond energy are the same (to within overlap terms in the normalization constants), then the entire energy destabilization of the Lewis structure in going from the ground state to the prepared excited state, is roughly twice the C-X bond energy, as expressed above in equation (3.9b). Of course, some modification of the expression for the full SCD curves is expected, but the proportionality between the excitation gap and the bond energy will survive [7, 11]. In solution, the bond energy terms will be joined by solvation and solvent reorganization terms [6, 9, 67]. Thus, basically the bond strength of the active bonds as well as solvation and solvent reorganization terms determine the size of the excitation gap for 3-electron/4-center reactions.

For more complex reactions between electrophiles and nucleophiles, we can still show relations of the gaps to the bond strengths of the bonds being broken and made. However, a much simpler procedure would be to consider the excitation gap

from an encounter complex and to express the gap simply as the vertical charge transfer transition, which is a measurable quantity for many nucleophile/ electrophile (Nu/El) pairs [68]. Accordingly, for all polar and electron transfer reactions of Nu/El pairs the gap is given by equation (3.10).

$$G\,(\mathrm{Nu/El}) \;=\; \Delta E_{CT} \tag{3.10}$$

Iso-valent reactions require singlet–triplet excitation gaps which according to the effective VB approach can be set proportional to the bond energies of the bonds that are broken during the reaction. For example, for the iso-valent identity process $X^{\bullet} + A{-}X \rightarrow A{-}X + {}^{\bullet}X$, the excitation gap is the singlet-triplet excitation of the A-X bond as given by equation (3.11a) [57]. In turn, the singlet-triplet excitation is proportional to the bond strength of the A-X bond, as expressed in equation (3.11b).

$$G\,(X^{\bullet}/A{-}X) = \Delta E_{ST}\,(A{-}X) \tag{3.11a}$$

$$G\,(X^{\bullet}/A{-}X) \approx \mathrm{kD}(A{-}X);\quad 1<k<2.5 \tag{3.11b}$$

In many cases, the proportionality constant, k in equation (3.11b), is approximately 2, as suggested by application of the effective VB approach. More precisely though, k is itself proportional to the bond energy, so that as the bond gets stronger k increases in the direction of the higher limit [3, 41, 69]. We may therefore state, quite definitively that strong bonds possess large singlet-triplet gaps, and the opposite is true for weak bonds. In iso-valent reactions which involve breaking of π-bonds, it is just as simple to use directly the singlet-triplet transitions which are available experimentally and which can be computed quite readily [62].

In many reaction series, the excitation energy gap varies in a dominant fashion with no adverse effect of the other quantities. The reaction series will form then an "excitation gap pattern"; namely, there will exist a correlation between the barrier and the corresponding excitation gap.

The "excitation gap pattern" in mixed-valent reactions. Series of this kind are abundant in the seminal works of Kochi and Fukuzumi on charge transfer activation [68] where the following general correlation is observed between free energy barriers and charge transfer excitation energies for classical polar reactions, such as bromination of olefins and arenes, and so on.

$$\Delta G^{\ddagger} = a(h\nu_{CT}) + b\,;\ a, b = \textit{linear correlation constants} \qquad (3.12)$$

Excitation gap patterns in classical polar processes have been observed by us in S_N2 reactivity [6, 9, 11], in nucleophilic vinylic attacks [49], in electrophile-nucleophile reactivities [70, 71]. In all of these cases, the barriers were found to vary in proportion to the vertical charge transfer energy (or its components), as generally outlined by equation (3.12).

Correlations like equation (3.12), of barriers with charge transfer energies, have the same format as the barrier expression in equation (3.8), and may be interpreted therefore within the mechanism of activation which is enfolded in equation (3.8). Thus, the correlation reflects that the transition state of the polar reaction is achieved by the avoided crossing of the ground state and the charge transfer state, which are initially separated by the charge transfer excitation gap, $h\nu_{CT}$. Such correlation may not be taken, however, as evidence for *an actual electron transfer mechanism.* This correlation is simply reflecting the charge transfer nature of the prepared excited states, which are common for mixed-valent reactions of both polar and electron transfer characters. It is precisely to avoid this confusion that we have named the polar reactions "single electron shift mechanisms", to distinguish them from "single electron transfer mechanisms" which proceed via the intermediary of electron transferred radical species [2].

The "excitation gap pattern" in iso-valent reactions. A recent treatment [72] of hydrogen abstraction reactions, shows that the barriers for the identity reactions in equation (3.13)

$$R\bullet + H{-}R \longrightarrow R{-}H + \bullet R \qquad (3.13)$$

vary in proportion to the strength of the C-H bond which is broken and remade in the reaction; the stronger the bond the larger the barrier. It is seen [72] that this correlation follows the excitation singlet-triplet gap which varies as the bond energy, as indicated in equation (3.11).

A fascinating trend which follows the excitation gap pattern has been demonstrated for the isoelectronic series of the types X_n (n = 3, 4, 6), where X is a monovalent atom [10, 41]. Neither the isoelectronic analogy nor qualitative MO arguments can account in a satisfactory manner for the stability trends in these series. For example, the identity transformation of triatomics made of monovalent atoms in equation (3.14),

$$X^{\bullet} + X{-}X \rightarrow X{-}X + {\bullet}X \qquad (3.14)$$

exhibits the entire progression; from X_3 transition states (e.g., H_3, F_3, and so on) to stable intermediate states (e.g., Li_3). This behavior correlates with the variation of the excitation gap given by the singlet–triplet excitation of the diatomic molecule. As this gap decreases, the energy of the X_3 species gradually decreases until it becomes a stable cluster in metallic cases like alkali trimers, Cu_3, and Ag_3, as predicted by Fig. 4c [10].

Excitation gap patterns in allowed cycloadditions: Excitation gap patterns were observed also for allowed cycloadditions and their bond exchange analogs [10, 62]. An interesting comparison is the Diels-Alder (D-A) reaction which was found by computational means to possess a much smaller barrier than the cycloaddition of three ethylenes, despite the opposite effect in the corresponding reaction exothermicities. The electronic advantage in the relative barrier heights was found to be approximately 26 kcal/mol. The effect was shown to be exerted through a stabilization of the prepared excited state for the D-A reaction by the intramolecular effect on the spin coupling in the triplet state of the butadiene, as discussed above in **13**. The reduction of the excitation energy gap for the D-A reaction amounts to 124 kcal/mol and leads therefore to a reduction of the barrier by ~26 kcal/mol.

Another example is the trimerization of acetylene to benzene which possesses a very large barrier (~ 62 kcal/mol at the MP3/6-31G*//HF/6-31G* level [73]), despite the fact that the reaction is symmetry allowed, and can potentially proceed with an enormous thermodynamic advantage of $\Delta H \approx -140$ kca/mol. The origins of the very large barrier is again the excitation gap which is ca. 375 kcal/mol, and is so large because it is composed of threefold singlet-triplet excitation of the acetylene reactants. It is seen that the major factor which sizes the barrier is the excitation gap *and an allowed reaction can therefore possess very large barriers if its excitation gap is large*. Multibond reactions are generally unfavorable due to very large excitation gaps.

Excitation gap patterns in forbidden cycloaddition. 2 + 2 cycloadditions of olefins or carbonyls have normally high barriers, while silaethylenes and disilenes dimerize instantaneously [74]. Thus, despite of the fact that all of these reactions are formally forbidden they exhibit very different reactivity features. Recent computational studies [75] show that all of these reactions proceed via diradicals [75b]. However, the computed barriers to diradical formation are much smaller for the sila-analogs of ethylene, so small (< 10 kcal/mol) that they call

attention. The excitation gaps for 2+2 cycloadditions are the sums of the singlet-triplet excitations of the molecules. Thus, the dimerization of formaldehyde has the largest excitation gap (~ 240 kcal/mole) and the largest calculated barrier (65 and 73 kcal/mol, respectively for the head to head and head to tail dimerizations [75b]). Ethylene has a somewhat smaller gap (~ 200 kcal /mole) and a smaller barrier (51-53 kcal/mole [75b]), while silaethylene with the much smaller excitation gap (~120 kcal/mole) has indeed a tiny dimerization barrier (5.3 kcal/mole for the head to tail process [75b]). One might expect that the disilene with the smallest gap (~ 88 kcal/mole) should possess even smaller barriers. This trend for forbidden cycloadditions demonstrates the impact of the excitation gap on reactivity. Thus, *forbidden reactions can possess very small barriers if their excitation gaps are small.* This statement is correct irrespective of the mechanism of the forbidden reaction.

Summary of excitation gap patterns. According to the SCD model, the origins of the barrier in mixed-valent and iso-valent reactions originates in the avoided crossing of two states which are separated initially by excitation gaps of the charge transfer and singlet-triplet varieties. The foregoing examples indicate that oftentimes *the excitation gap factor would be the organizing quantity for the global behavior in an isoelectronic series.* Broadly speaking as we go down the columns of the main elements in periodic table, all excitations become smaller and we expect therefore that all barriers should accordingly decrease. Similarly, as we move to the left of the periodic table, to the region of the metallic elements, the bond energy decreases, the ionization energies decrease and therefore all the excitations become smaller and all barriers are expected accordingly to decrease.

Within these broad generalizations there are great many variations in the barrier heights and there exist secondary correlations which are caused by variations in the other reactivity factors in equation (3.8). These variations are discussed below.

3.5.2. The *f* factor and its reactivity manifestations According to equation (3.7) f is given by, the following expression:

$$f = \Delta E_C / G_R \tag{3.15}$$

Thus, f *sizes the barrier for a given excitation gap* and is a measure of how much of the excitation gap enters under the crossing point [3, 4, 6, 7, 9]. According to Figs. 5a and 5b the quantity f depends on the curvature of the curves as well as on the thermodynamic driving force of the reaction.

As shown in Fig. 5a, for a constant value of the excitation gap, the height of the crossing point is determined by the curvature of the curves [3, 4, 6, 7, 9]. Thus, *concave* curves give rise to small f values, while *convex* curves give rise to large f values. Before we discuss the chemical factors which control the curvature of the curves, it is worthwhile to provide the reader with some orders of magnitude of the f factor for elementary curves generated from the effective HL and Lewis structures of the chemical reaction. Based on the computational experience with crossing of VB structures [14, 15], the dependence of f on the curve type can be summarized in equations (3.16) - (3.20).

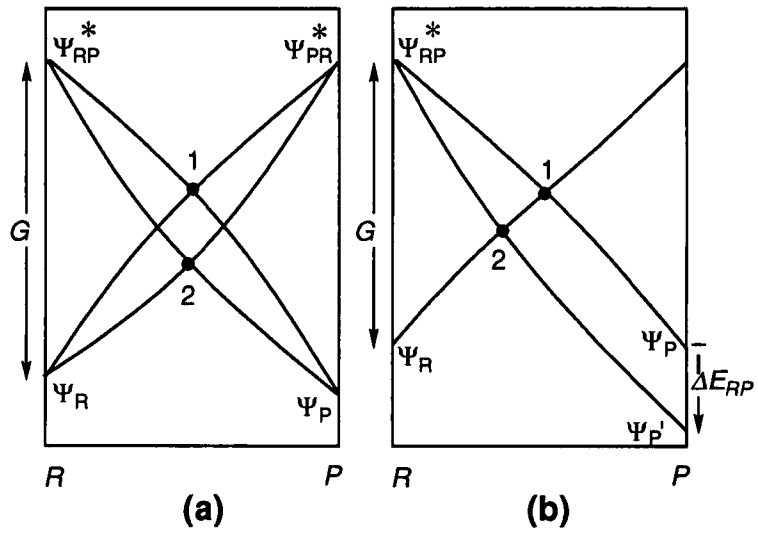

Fig. 5. The quantity f. Effects of (a) the curvature, and (b) the reaction exothermicity. Crossing points (1) possess larger f values than crossing points (2).

Thus, according to equation (3.16), the f factor for HL curve-crossing is generally larger than the corresponding f factor for Lewis curve-crossing. Since the only difference between HL and Lewis curves comes from the inclusion of the ionic structures of the corresponding bond, it follows therefore, that inclusion of bond ionicity makes the curves more concave than the pure HL curves.

$$f_{HL} > f_L \tag{3.16}$$

Equations (3.17) and (3.18) summarize the computed [14, 15, 64] average values of the f quantities.

$$f_{HL}\ (\text{average}) = 0.37 \tag{3.17}$$

$$f_{L}(\text{average}) = 0.29 \tag{3.18}$$

The above f values fall within the limits of simple mathematical curves; $f = 0.25$ for two intersecting parabolas and $f = 0.5$ for two intersecting straight lines. Thus, the Lewis and HL VB curves are slightly less concave than parabolae and slightly more concave relative to straight lines.

Equation (3.19) refers to the relationship between the f values for the total SCD curves and for the Lewis-only curves. Thus, the inclusion of foreign configurations and electronic delocalization effects generates SCD curves which are more convex (larger f) than pure Lewis curves. Generally, the deviation of f_{SCD} from f_L is not large and the f_L values are good approximations for the total values.

$$f_{SCD} \geq f_{L} \tag{3.19}$$

Equation (3.20) shows the range of f_{SCD} values which have been computed by the Orsay group [14, 15].

$$f_{SCD} = 0.13\text{-}0.42 \tag{3.20}$$

It is seen that these values deviate significantly from the average values summarized above for Lewis curves. The significant deviations were observed, in fact, in three situations:

The first situation deals with reactions of very weak binders, like the combination of Li with Li_2 which results in a stable Li_3 cluster. In this case, all the f values are well below the average ($f_{HL} = 0.24$; $f_L = 0.12$, $f_{SCD} = 0.13$ [15]).

The second deviant situation is observed in 4-electron/3-center reactions which are endowed with high bond ionicities. A typical case is the S_N2 reaction of F^- with CH_3F, which possesses extremely small f_L and f_{SCD} values (0.12, 0.15), eventhough the corresponding HL curves have a normal f value (0.31) which falls well within the above average values in equation (3.18) [14].

The third situation corresponds to the reaction of H^- with CH_4, and is responsible for the uppermost f value in equation (3.20). Thus, in this reaction the f value deviates significantly relative to the Lewis value, and increases from 0.25 (for

the Lewis curves) to 0.42 (for the SCD curves) due to the delocalization of the electrons in the prepared excited state.

It is important to analyze the origins of these deviations and establish some chemical intuition about the main effect on the curvature factor. These are discussed below.

The exchange repulsion effect on f_{SCD}. The exchange repulsion is one of the factors which determine the ascent of the curves from the ground states toward the crossing point. The bond-pair coupling, on the other hand, determines the descent of the prepared excited states toward the crossing point. The ratio of these effects will determine therefore the global curvature of the curves. For a given atom, this ratio is expressed in equation (3.21), in terms of the singlet–triplet excitation and the bond energy of the diatomic molecule [3, 17, 41, 69]. The dependence of f, on the identity of the atoms which participate in the reaction, is related to this ratio and can be predicted from equation (3.22) using appropriate empirical data (use D corrected for the internal fragment excitations).

$$\mathbf{a} = (\Delta E_{ST} - D)/D \tag{3.21}$$

$$f \propto \mathbf{a} \tag{3.22}$$

Thus, for atoms which form strong bonds, the singlet-triplet excitation is $\geq$ 2D, and therefore for these atoms the ratio **a** is ≥ 1, and the corresponding f is large. On the other hand, for atoms which are very weak binders, the singlet triplet excitation is <2D and the ratio **a** is therefore small, and along with it there results a small f. This is in fact the result of recent VB computations of the SCD's [41] for the exchange reaction of a monovalent atom with the diatomic molecule, $X^{\bullet} + X\text{-}X$, where the computed f values are 0.37 for X = H, and only 0.13 for X = Li. It may be expected therefore that *small f values will be associated with atoms at the bottom of the periodic table and at the metallic blocks.* No doubt, an important factor, in the decrease of barriers down the periodic table, is the reduction in the curvature factors which cause the establishment of very low crossing point.

Bond ionicity effects on f. The discussion of f values for HL and Lewis curves highlights that the inclusion of bond ionicity decreases the f value. The inclusion of bond ionicity in electron-pair bonding simply strengthens the bond coupling interactions and weakens the exchange repulsion along the reaction coordinate. Consequently, the descent of the prepared excited states toward the

crossing point becomes steeper and the ascent of the ground states become shallower. The curves become thereby more concave with a smaller f value and a concomitant lowering of the crossing point.

Equations (3.17) and (3.18) define the normal range of the variations caused by bond ionicity. However, when bond ionicity becomes a dominant feature of the SCD curves, a dramatic lowering of f will be expected. This has been observed for cases where bond ionicity effects are very strong, e.g., in 4-electron/3-center reactions involving A-F bonds, e.g., F^-/HF, F^-/CH_3F and F^-/SiH_3F [14]. In these cases, the initial bond ionicity is already high and the triple ion structure, $F^- A^+ F^-$ (of the type **7**) becomes very stable and dominates the SCD curves in a large section of the reaction coordinate [45]. An example is the F^-/CH_3F where the f_{HL} value is 0.31 while the f_{SCD} value after inclusion of bond ionicity effect is halved to 0.15 [14].

Delocalization effects on f. The factor that is responsible for the large f_{SCD} for the H^-/CH_4 reactions has been predicted early on [76]. Thus, it was argued that when the bond-pair electrons become delocalized away from the active orbitals, the bond-pair coupling in the prepared excited states is inhibited, along the reaction coordinate, and the resulting f will be large.

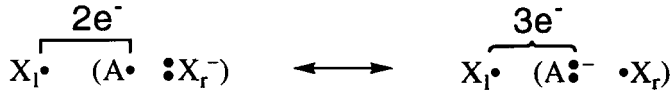

14

To illustrate the effect of delocalization on the descent of the prepared excited states, consider the already familiar prepared excited state of the ionic exchange process which is described by the SCD in Fig. 3b above and shown here in **14**. It is seen that the odd electron is delocalized in the $(A\overset{\bullet}{-}X)^-$ species over its two centers, and therefore the bond coupling interaction of A with $X_l^\bullet$ in one of the VB structures is counteracted by a repulsive three-electron interaction in the second VB structure. Thus, the effect of delocalization in the prepared excited states is to place on the two union centers more than two electrons and to reduce thereby the two-electron stabilization by overlaying it with exchange repulsion [3]. Clearly then, when the prepared excited states are delocalized, they are not well prepared for bonding, and as a result these excited states will descend in a shallow manner leading to a high crossing point for a given constant gap, that is, a large f factor in equation (3.15).

Delocalization effects can involve also the inactive bonds. This will be encountered when there exist identical active bonds which can participate in the reaction, as in the S_N2 reactions of X^- with CH_2X_2. Thus, in the prepared excited state $X^{\bullet}/CH_2X_2^{-\bullet}$, the odd electron in the anion-radical state $CH_2X_2^{-\bullet}$ is delocalized over the two identical C-X linkages. Consequently, the bond coupling interaction will be reduced and the prepared excited state will descend in a shallow manner leading to a large f quantity. As the number of identical C-X linkages increases, the delocalization of the bond-pair electrons also increases and the f quantity will further increase. This is precisely why the f quantity of the H^-/CH_4 S_N2 reaction [14, 42] jumps from 0.25 for a Lewis curve-crossing, where the anion radical states are localized in a single C-H bond, to 0.42 in the full SCD curve-crossing where the anion-radical $CH_4^{-\bullet}$ involves delocalization of the odd electron into the four C-H linkages.

Delocalization effects have been identified also in isovalent reactions. For example, in the radical addition to substituted olefins the prepared excited state involves the $^3\pi\pi^*$ state of the olefin coupled to the radical to a total doublet spin. The corresponding strength of bond coupling to the radical will depend on the spin density distribution on the triplet olefin. The attack on the olefin site that possesses the higher spin density will involve the stronger bond coupling and will therefore lead to the lower crossing point; namely a smaller f value.

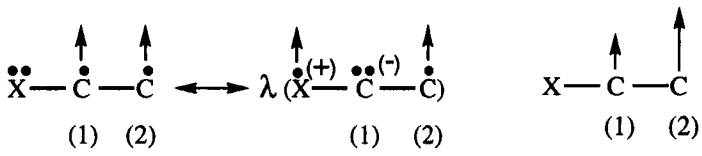

15 **16**

The spin density in the triplet state of a substituted olefin can de predicted by considering the VB structures which contribute to the triplet state. Thus, consider in **15** the $^3\pi\pi^*$ state of an olefin substituted by X which possesses a lone pair (e.g., X = F, Cl, OR, etc.) or by an X which can donate an electron pair in conjugation (e.g., CH_3, etc.). The principal VB form (left) in **15** is purely covalent and the secondary form (right, $\lambda < 1$) is zwitterionic. The net result of the VB mixing is to take up spin density from C_1 and to increase thereby the C_2 spin density [59]. This spin density distribution pattern, of the $^3\pi\pi^*$ state, is summarized in **16** where the sizes of the arrows indicate relative spin densities.

The qualitative conclusion summarized in **16** has been tested [59] for a variety of olefins by computing the triplet spin density and the results verify the

qualitative picture that *the more substituted carbon is the spin poor site in the triplet* $^3\pi\pi^*$ state. Thus the attack on the more substituted site which is spin poor will cause a shallow descent of the excited state and a large f value. On the other hand, an attack on the less substituted site which is spin rich site will result in a small f.

The rate-equilibrium effects: The"Bell-Evans-Polanyi (BEP) principle". Figure 5b above illustrates that a lowering of the crossing point will be caused by increasing the exothermicity of the reaction, which in terms of equation (3.15) is effectively a lowering of the f factor. It is seen that, in the absence of an adverse variation of the other reactivity factors, making the reaction more exothermic will lower also its barrier. This is the well known Bell-Evans-Polanyi (BEP) principle which forms one of the foundations of classical physical organic chemistry; the rate equilibrium relationship. But, in the background of the preceding factors, it becomes apparent why the BEP principle is nor a global reactivity rule and neither the most fundamental one. Rate equilibrium effects will be manifested when the primary factors (above) do not vary adversely. The principle will break down otherwise. The breakdown of rate-equilibrium relationships as a result of the dominant variations of the gap, delocalization, and bond ionicity factors has been analyzed in details before [2, 3, 6-9].

Summary of reactivity patterns related to the factors of f. The f variable in equation (3.7) sizes the height of the crossing point for a given excitation gap in the SCD. Roughly speaking, the f factor of the SCD is related to the classical structure-reactivity parameters (e.g., Hammett's ρ and Bronsted coefficients) which measure the sensitivity of the barrier in a reaction family to a change of substituents. A typical ballpark figure for the f quantity in *organic reactions* is in the range of 0.2-0.3. Special dominant effects -- e.g., delocalization of the prepared excited states, strong bond ionicities, extreme changes in the ratio of exchange repulsion to bond coupling, and the reaction exothermicity -- which are discussed above will cause deviations from these average values either upward or downward. While this creates some complexity in application of the quantity to reactivity, we hope that the above detailed discussion will assist to predict these effects by judicious applications of the VB mixing principles. It is clear from equations (3.7) and (3.8) that whenever the variations of the excitation gaps cease to be dominant, it is the f quantity which will form the basis for the reactivity patterns. In such reactivity patterns, *the height of the barrier will increase as the f quantity itself increases.*

Reactivity patterns of the f factor have been observed amply in S_N2 reactivity [6, 9, 11]. For example, the increase of f by delocalization of the prepared excited

states is the root cause for the α halo-effect observed in the S_N2 reactions of e.g., Cl^- with CH_3Cl, CH_2Cl_2, $CHCl_3$, and CCl_4 [51]. In these cases, the excitation gaps do not vary in a dominant manner, and the observed barriers are found to increase in the order of increasing f, that is, $Cl^-/CH_3Cl < Cl^-/CH_2Cl_2 < Cl^-/CHCl_3 < Cl^-/CCl_4$. A few other interesting predictions in S_N2 reactivity, including reactivity crossovers and reactivity-selectivity zigzags have been made by relying on the interplay between the f and the excitation gap quantities [9, 51]. Similarly, the regioselectivity of radical attack on substituted olefins is a manifestation of the f factor. Thus, radical attacks generally occur on the site of the higher spin density in the triplet olefin [59] in accord with the smaller f quantity for the attack on this site (see **16**).

A possible manifestation of bond ionicity effect in S_N2 reactivity, is the very facile reactions of CH_3OCH_2Cl [77] molecules in solution, as opposed to its normal reactivity in the gas phase [78]. Thus, the donor substituent on the carbon reaction center stabilizes the $Nu^- R^+ Cl^-$ VB structure but, in the gas phase this effect is not sufficient to reduce the f quantity much below the average values. In solution, the solvent further stabilizes this VB structure which now becomes dominant along the reaction coordinate. Consequently, the effective f value in solution is reduced dramatically and the barrier is thereby lowered. Indirect evidence allows us, in fact, to ascertain that the f value for these S_N2 reactions is extremely small. Thus, whenever f is small the sensitivity of the rate constants to substituent changes will also be small [9], and a reaction with a small f value will generally possess small structure-reactivity coefficients, e.g. Bronsted coefficients like β_{Nuc} and α. Indeed, the Bronsted coefficients for the reactions of nucleophiles with CH_3OCH_2Cl are generally extremely small and correspond to a high contribution of the $Nu^- R^+ Cl^-$ VB structure [9, 45].

3.5.3. The avoided crossing interaction, *B*, and its manifestations in reactivity. The avoided crossing interaction B in Fig. 4b is the stabilization of the bonding state, the transition state, relative to the crossing point of the SCD. We accordingly refer to B also as the QMRE (quantum mechanical resonance energy) of the transition state. In the absence of adverse variations in the other factors, the relative reactivity will be determined by the variations in the resonance energy of the transition state. Like in the preceding reactivity factors, here too we start with a discussion of the main effects on the B quantity.

Modeling of the *B* quantity. Direct application of VB theory to some elementary 3-center reactions shows that the QMRE is proportional to the strength of the various bonds or to their singlet-triplet excitations at the geometry of the transition state [36]. A striking illustration of the bond strength effect on *B* is provided by our recent ab initio VB computations of this quantity for X_3 species. Thus, *B* (H_3) is 43 kcal/mol, while *B* (Li_3) is 6 kcal/mol [41]. Similarly, recent VBSCF calculations [64] of FHF yield a value of ~43 kcal/mol for *B* (FHF), in line with the strong H-F bond.

It is noted that drastic variations of the bond strength (e.g., from H-H and H-F to Li-Li) are needed to observe considerable changes in *B*. This is because the crossing in the SCD is achieved at the expense of distortions. Molecules with strong bonds possess larger excitation gaps in the SCD and require, therefore, more bond stretching to achieve the crossing [3, 4, 6, 9, 11]. This causes some levelling off of the bond strengths of the avoided crossing state, and one may therefore expect that in reaction series where the initial bond strengths exhibit modest variations, the *B* itself will vary modestly. This is indeed our experience at the time of the writing of this review.

A complementary insight is gained by relating the QMRE to the energy gap between the pair of adiabatic states which result from the avoided crossing, and are denoted as Ψ_C and $\Psi_C{}^*$ in Fig. 4b [3, 4, 36]. Judging by our applications to elementary three center processes, this gap can be approximated generally by the corresponding gap between the HOMO and LUMO of the transition state itself, as shown in equation (3.23), where S_{12} refers to the overlap of the two VB bonding schemes at the crossing point of the general curve crossing diagram in Fig. 4a.

$$B = [(1 - S_{12})/2]\Delta E\,(\Psi_C, \Psi_C{}^*) \sim [(1-S_{12})/2]\Delta E\,(\mathrm{HOMO,LUMO}) \qquad (3.23)$$

Thus, equation (3.23) establishes a link between the resonance energy of the transition state and a physical observable of the transition state; the electronic transition from the transition state to its companion anti bonding state.

Our recent experience shows that the marriage of VB and MO insights in equation (3.23) can be quite useful. Thus, the VB insight regarding the dependence of *B* on the singlet-triplet excitation of the bonds in the transition states, is used to parametrize the Extended Huckel (EH) scheme. The most straightforward parametrization involves fitting of the HOMO-LUMO gaps of two-electron bonds to their empirical (or computed) singlet-triplet excitations. This parametrization employs a single constraint [18]; that the resulting self energy of the atomic orbitals (the H_{ii} parameters of the EH method) must conserve the order of the

electronegativity of the atoms. Using this parametrized EH scheme, one calculates the HOMO-LUMO gap of the transition state or of any delocalized species for that matter, and by use of equation (3.23) one then obtains the corresponding B quantity. The so calculated B values fit quite well to the VB values which are computed ab initio using the *variational curves and variational adiabatic states* [18, 36].

An important conclusion deduced from the ab initio VB calculations is that the B values obtained from Lewis-only curves are very good approximations to the values which are obtained from the full SCD curves [14, 15, 45, 64]. This conclusion is important, because it allows to conceptualize B in simple terms of the overlap of bond wavefunctions, and of the geometric dependence of the HOMO-LUMO gaps of the transition state. Our most recent studies of B are summarized below in the light of equation (3.23).

The effect of the HOMO - LUMO gap of the transition state on its B value. Two important factors determine the HOMO-LUMO gap of a given transition state or a delocalized state. The first factor is the bond strength, while the second factor is the geometry of the state. The effect of intrinsic bond strength is discussed above with reference to the B values of H_3 vs Li_3, and needs no rehearsal. The strength of the transition state bonds depends also on the extent of bond stretching that a given bond is required to undergo in order to achieve the resonance at the crossing point of the SCD. Broadly speaking, the extent of bond stretching depends on both the excitation gap and the f factor of the SCD. Large excitation gaps and f factors require more bond stretching to achieve the transition state. Thus, the transition state geometry and bond strengths are intimately linked and it is important therefore to ascertain the effects of different geometric factors on the HOMO-LUMO gap and B value of the transition state.

An extensive study of three-center reactions with three and four electrons, of the general types (XAX) and $(XAX)^-$ reveal the following trends of the HOMO-LUMO gaps [18, 36]:

(i) Starting from symmetric (XAX) and $(XAX)^-$ structures and elongating of one or both of the A-X bonds causes a decrease of B, owing to a decrease of the HOMO-LUMO gap. Thus, *loose transition states and outer-sphere (one long A-X distance) transition states possess small B values.*

(ii) An asymmetric distortion of the two A-X bonds, by $\pm\Delta r$, leaves B constant because the HOMO-LUMO gap is unaffected by this geometric distortion. Therefore, *a series of transition states which are related to a symmetric structure by*

an asymmetric distortion will share a common B value, a constant of the series. A transition state series of this kind may occur in a reaction family such as the Hammett families.

(iii) Bending of the XAX angle away from linearity narrows down the HOMO-LUMO gap and causes a concomitant decrease of *B*. Thus, in cases like X_3 and X_3^- an equilateral triangular geometry leads to a zero *B* value. Clearly, the vanishing avoided crossing corresponds to the well known state degeneracies of these equilateral triangles [4].

The effect of transition state ionicity on *B* values for mixed-valent reactions. Our most significant experience comes from modeling of *B* values of S_N2 reactions and a few analogous 4-electron/3-center reactions of the general type $X^- + AX$ [18, 36]. For these cases, the Lewis curves are generated from the mixing of the ionic VB structure $X^- A^+ X^-$ into each of the two intersecting HL curves. Now as the ionic structure is a VB determinant shared by both Lewis structures, it is obvious that the overlap S_{12} between the Lewis curves increases as the ionic form gets more important. Furthermore, the charge Q_A on the central group is also linked to the weight of the ionic form in the ground state of the transition state. It follows that the overlap of the Lewis structures should increase with the ionicity of the transition state.

It is apparent from equation (3.23) that an increase of the overlap will reduce the value of *B*. We may therefore expect, that as the ionicity of the transition state increases the resonance energy will decrease. This is a logical result, because at the limit of full ionicity the two curves are both the same and identical to the ionic structure, and their resonance interaction is, by definition, zero.

This dependence of *B* on ionicity means that largest *B* value is expected for zero ionicity, namely for the pure HL curves. These are precisely the results of ab initio VB computations [14, 15] and of the *B* modeling in terms of equation (3.23). We may therefore express the resonance energy of the transition state in terms of its ionicity, approximately as follows in equation (3.24).

$$B \approx B_{HL}(1\text{-}Q); \quad Q = Q_A \tag{3.24}$$

Thus, for a charge of +1/2 at the central group of $(XAX)^-$ the *B* value is approximately halved relative to the B_{HL}, while for a charge of unity the resonance energy vanishes. The B_{HL} itself varies in correlation with the strength of the A-X bond in the transition state.

The dependence of B on the charge of the central group leads to some interesting consequences. One of these consequences has been observed in a recent study of S_N2 reactions of CH_3X derivatives [18]. The B values for the identity reactions and their nonidentity combinations -- for different X groups, H, F, Cl, Br, I-- were found to obey equation (3.25), which clearly shows a small sensitivity of B to the nature of X (X, Y, if $X \neq Y$). Thus, even though B still depends on the C-X and C-Y bond strengths, the B values cluster closely around the average.

$$B\,(YCH_3X)^- = \quad 20.0 \pm 2.7 \text{ kcal/mol} \tag{3.25}$$

This remarkably narrow range of the B values results from a special combination of the bond strength and ionicity factors which counteract each other. Consider for example, the $(XCH_3X)^-$ series of the halides. The C-X bond strength varies in the following order of X: F > Cl > Br > I. However, the charge at the CH_3 group varies also in the same order. These two effects mutually compensate one another according to equation (3.24), and the resulting B values are therefore quite close (albeit the trend, $B_F > B_{Cl} > B_{Br} > B_I$ is still maintained). This is a major factor why the B quantity in S_N2 reactions behaves as a passive variable. This passivity is the root cause why our past assumption of a constant B value of 14 kcal/mol [6, 9, 11] did not appear to affect the utility of the model to pattern the data of S_N2 barriers derived from ab initio or from experimental gas phase studies [6]. In fact, the generally successful predictions of the barrier heights have always strengthened the feeling that the assumption of a quasi-constant B value is probably not a bad one.

Our modeling of B for S_N2 reactions leads to a tantalizing relationship of the quantities for identity and nonidentity reactions. Thus, given the following transition states, $(XRX)^-$ the $(YRY)^-$ the $(YRX)^-$, the corresponding B quantities obey the average relationship in equation (3.26).

$$B_{YX} \approx 0.5\,(B_{XX} + B_{YY}) \tag{3.26}$$

This relationship is observed for the corresponding HL as well as the full B values. While we do not as yet fully understand the origins of this relationship, it is very clear that if it is of a general scope then it may have some important implications on transition state properties in reaction series.

The effect of transition state ionicity on B values for iso-valent reactions. Ab initio VB computations of B values for a few 3-electron/3-center

reactions [15] show opposite trends in comparison with the corresponding mixed-valent reactions. Thus, in $(XAX)^{\bullet}$ transition states and delocalized clusters, the B_{HL} values are smaller than the corresponding B values calculated from the Lewis curves or from the full SCD curves. The reason for this pattern can be understood by invoking once again the overlap term in equation (3.23). The situation is now reversed relative to mixed-valent reactions: the HL wavefunctions for the reactants ($X^{\bullet}$ / AX) and products (XA / $^{\bullet}X$) now share a common VB determinant [4], unlike the two ionic configurations which are distinct and different for each curve (e.g., $X^{\bullet}$ A^{+} $:X^{-}$ mixes only into the HL structure of the reactants, while $X:^{-}$ A^{+} $^{\bullet}X$ mixes only with the HL structure of the products). Consequently, the HL structures overlap strongly with each other while the ionic structures do not, and mixing of the latter structures to the HL combination tends to *decrease* the overlap between the intersecting diabatic states, leading to an increase of the B value following equation (3.23).

***B* in "forbidden" and "allowed" reactions, and the connection to transition state aromaticity.** Computations of B values for X_6 and X_4 species show that $B(X_6)$ is more than twofold larger than the $B(X_4)$ values [79]. The first part of equation (3.23) which relates B to the energy gap between the avoided crossing states, is always valid. Now however, the approximation in terms of the HOMO-LUMO gap in the same equation does not hold for the X_4 squares because the HOMO and LUMO are strictly degenerate, eventhough the ΔE (Ψ_C ,Ψ_C^*) itself is finite due to electron-electron repulsion terms. On the other hand, for the X_6 hexagons the HOMO-LUMO gap is large. Thus, the ΔE (Ψ_C ,Ψ_C^*) gap for the X_6 species will be significantly larger than the gap for the X_4 species. This is generally the case, whenever we compare aromatic vs antiaromatic transition states. In some antiaromatic transition states, the gap ΔE (Ψ_C ,Ψ_C^*) is itself zero, e.g., in equilateral triangular X_3^-. We may therefore use equation (3.23) to generalize the following relationship for formally allowed and forbidden transition states [3, 4, 61h]:

$$B \text{ (allowed)} > B \text{ (forbidden)} \tag{3.27}$$

This relationship projects the connection between the avoided crossing diagrams and the orbital symmetry and frontier orbital theoretics ideas [80]. Thus, symmetry rules refer only to the avoided crossing interaction, but not to other factors of the SCD. This is the reason why there exist formally allowed reactions with large barriers and formally forbidden ones with very small barriers. It is

important to understand therefore that the only topological difference between allowed and forbidden reactions is strictly concerned with the choice of degree of concert of all the bonds in the transition state. Thus, formally forbidden reactions may always prefer stepwise pathways, not because the concerted ones have very high barriers in an absolute sense, but because the reduction of the degree of concert in the transition state (e.g., in a stepwise mechanism) results in a larger avoided crossing interaction. On the other hand, an allowed reaction will possess the largest B value in a concerted transition state. This difference however does not mean that the barrier for the forbidden reaction should be high and that for the allowed reaction should be low.

3.5.4. Reactivity patterns: An overview of the SCD model. The above discussion was based on equation (3.8) in which the f parameter incorporates a few factors. Equation (3.28) is an explicit expression which shows the dependence of the barrier on all the reactivity factors in the SCD in Fig. 4; the two different diagram gaps, two independent f factors and a non zero reaction driving force (ΔE_{RP}).

$$\Delta E^{\ddagger} = \\ = [(f_R + f_P)G_R + (1 - f_R + f_P)\Delta E_{RP}]\{(G_P + \Delta E_{RP})/(G_R + G_P)\} - B \qquad (3.28)$$

The f quantities are individual curvature factors of the curves which emanate from reactants and products, as specified by the subscript [6]. These curvature factors take account of all the effects discussed above in section **3.5.2**, with the exception of the reaction thermodynamic driving force that appears explicitly in equation (3.28).

Equation (3.8) is, in fact, an effective representation of equation (3.28), and the f quantity in equation (3.8) is an effective parameter which takes into account all the curvatures effects which size down the height of the crossing point relative to the excitation gap at the reactant's onset. For example, in a case where the diagram gaps are equal and the reaction energy is zero, the effective f in equation (3.8) will simply be the algebraic average of the two curvature factors in equation (3.28).

An expression for the intrinsic barrier derived from equation (3.28) is shown in equation (3.29) and seen to depend on the excitation gaps, curvature factors and avoided crossing interaction.

$$\Delta E_0^{\ddagger} = [(f_R + f_P)G_R G_P / [G_R + G_P] - B \qquad (3.29)$$

Thus, equation (3.28) allows to determine intrinsic barriers of a chemical reaction, even in those cases where there exist no identity reactions for application of the Marcus averaging procedure to obtain intrinsic barriers [6].

Equation (3.28) is therefore a master equation that provides a unified outlook of reactivity as an intricate interplay of the excitation gaps, the curvature factors, the reaction thermodynamics and the resonance energy of the transition state. This is an important feature since occasionally all or many of the reactivity factors vary simultaneously in a reactions series and the reactivity patterns, which are discussed above individually, will consequently blend. Thus, the master equation on the one hand unifies the global reactivity features, and on the other hand it allows to resolve the individual patterns within the collage of data. An explicit application of equation (3.28) is a challenging task which has been achieved in a few cases.

The most extensive application of equations (3.28) and (3.29) was devoted to S_N2 reactivity in the gas phase and in solution phase [6, 9, 11]. The vertical excitation gaps were estimated using a combination of a thermochemical scheme and an empirical VB calculations of electron affinities. As already mentioned, the resonance energy of the transition state was assumed to be a quasi-constant quantity for all the reactions of CH_3X derivatives. Based on our modeling results for B in equation (3.25), this assumption appears quite reasonable. The curvature quantities, f, were quantified from the delocalization indexes of the bond-pairs (see e.g., **14**) in the charge transfer states. Using this scheme, *all reactivity patterns in S_N2 reactivity (including barriers, intrinsic barriers and transition state geometries) have been shown to result from the interplay between the excitation gaps, the delocalization properties of the charge transfer states and the reaction thermodynamics.*

Within this collage of S_N2 patterns it was further possible to define reaction families in which a single factor dominates the reactivity pattern. Consider for example, the identity barriers X^-/CH_3X. Here the vertical electron transfer energy gap increases in proportion to the C-X bond energy (equation (3.9)), and the f factor *decreases* as the electron affinity, $A_X^{\bullet}$, of the X group *increases* [6, 11]. Using these thermochemical quantities, it is straightforward to organize the reactions in terms of the X groups. Thus, when X is varied down the column of the periodic table, the C-X bond strength decreases while the X electron affinity remains approximately constant. Similarly, when X is varied from left to right along a row of the periodic table, the X electron affinity increases considerably, while the C-X bond strength varies moderately. These simple thermochemical patterns provide a convenient means to predict the reactivity order. Thus, *as X is varied down a column or from left to right in a row of the periodic table, both the identity barrier as*

well as the percentage of C-X bond stretching in the transition state will decrease [6]. Most of the trends that are known about the identity S_N2 reactions are in harmony with these predictions (an exception is X = F vs X = Cl with approximately equal barriers). All other applications and predictions in this reactivity area can be found in the original literature, reviews and a monograph [3, 6, 9, 11].

Another complete study has been carried out on the transformation, $X^{\bullet} + X{-}X \longrightarrow [X_3^{\bullet}] \longrightarrow X{-}X + {\bullet}X$ [3, 10, 15, 41]. Based on the discussion of the SCD quantities, it is apparent that when the atom X becomes a weaker binder all the reactivity factors; the excitation gap, the curvature quantity f and the avoided crossing interaction, all become simultaneously smaller. This has a double impact on the height of the crossing point fG, which thereby decreases more rapidly than the resonance energy B, as the bonding strength of X is reduced. Consequently, the $[X_3^{\bullet}]$ isoelectronic series exhibits all the range from unstable transition states to stable clusters. This global behavior can be *predicted by consideration of a single quantity, the singlet–triplet excitation gap*, because all other factors follow the behavior of the gap.

Reactivity zigzags may be manifested whenever there is a clash between reactivity factors, i.e., when two factors vary in an opposite manner in a reaction series. This effect has been discussed amply in S_N2 reactivity where a π-acceptor substituent on the central carbon was shown to lead to a clash between the gap and curvature factors [9, 51, 81]. An interesting manifestation of the clash between reactivity factors is the regioselectivity zigzags observed in the addition of radicals to substituted olefins [59]. As discussed already, the "normal" regioselectivity of radical attack occurs on the *less substituted* olefinic site which possesses the highest spin density in the triplet prepared state of the olefin. However, in the reactions of $F_2C{=}CHF$ with radicals like CH_3, the thermodynamic preference for attack on the more substituted site becomes very large and an "inverted regioselectivity" is observed, in favor of the more substituted site. As the radical is changed from CH_3 to H and then to CF_3, the thermodynamic advantage for the attack on the more substituted site is weakened and the normal regioselectivity of radical attack on the less substituted site is restored.

3.6. VBCM Diagrams for Chemical Reactions

Many chemical transformations are mediated by an intermediate which separates its precursor and successor reactants and products. In all of these cases, it

is both necessary and also illuminating to use a VBCM diagram which involves more than just two curves [2, 3, 8].

3.6.1. VBCM diagrams involving active bonds only: Intermediate states due to covalent-ionic avoided crossings. When only active bonds are used in the VB representation it is always possible to generate an SCD. However, sometimes the SCD will conceal important information which can be revealed by looking at the VB configurations individually. For example, the SCD for the process, $F^- + HF \rightarrow FH + F^-$, has been computed [14] and showed that the stable $(FHF)^-$ intermediate for the transformation originates because the ascent of the curves from the ground states to the crossing point is so shallow that the resulting f factor of the SCD is negative. This unusual f value is of course a result of a dominant bond ionicity caused by the triple ionic stucture $F^- H^+ F^-$.

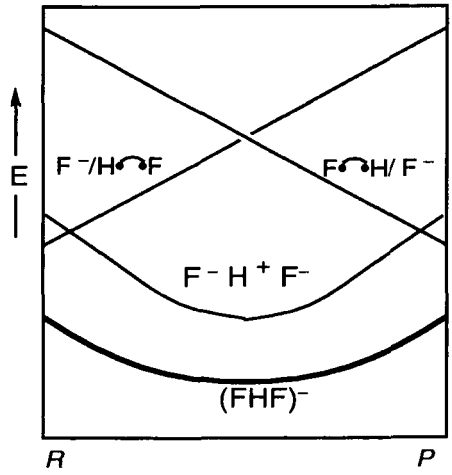

Fig. 6. Covalent-ionic curve crossing for the process $F^- + HF \rightarrow FH + F^-$.

Indeed, an alternative illuminating representation is the corresponding VBCM diagram in Fig. 6. The diagram shows quite vividly, that the stability of the $(FHF)^-$ intermediate is due to a covalent-ionic avoided crossing of the HL and triple-ion structures. It is seen that at the middle of the diagram the triple-ion structure is much more stable than the HL structures. This excess stability of the ionic structure at the clustered geometry arises mainly due to the small "size" of H^+ which permits very short $H^+ F^-$ distances and very large electrostatic stabilization. This short H--F distance at the symmetric structure is also the root cause for the very large resonance

stabilization of the triple-ion structure due to its VB mixing with the HL configurations. This large resonance stabilization (>90 kcal/mol) is also the root cause why the final adiabatic state retains the memory of the VB crossing and give rise to an intermediate $(FHF)^-$ state.

The tremendous impact of the ionic structure can be appreciated by looking at the corresponding iso-valent transformation with one electron less, $F^\bullet + HF \rightarrow FH + {}^\bullet F$. Here the triple-ionic structure simply disappears and is replaced by mono-ionic structures (e.g., $F^\bullet \; H^+ \; :F^-$) which are much less stabilized. Consequently, the covalent-ionic crossing vanishes and the $(FHF)^\bullet$ cluster that results from the avoided crossing is a high energy transition state. In fact, for the same reason, many $(XHX)^-$ clusters are either stable or only slightly distorted, while their iso-valent analogs $(XHX)^\bullet$ are unstable transition states.

A related type of covalent-ionic curve crossing occurs in the S_N1 and E1 mechanisms. In these cases, though, the positive ion R^+ is an encumbered carbenium ion, much larger than the H^+, and does not allow a compact ion-paired structure with significant electrostatic stabilization. Here, the solvent has to be involved and to stabilize the ion-paired structure below the crossing point of the two covalent forms. A similar description applies to the $E1_{CB}$ mechanism [3, 8, 63] with the exception that here the ionic form is $H^+ \; :R^-$.

3.6.2. VBCM diagrams involving inactive bonds: Intermediate States due to avoided crossing with foreign states. Occasionally, one of the excited states which does not involve the active bonds is stabilized and descends low enough to cross the two principal curves of the SCD, significantly below their own crossing point. This new structure defines an intermediate species which mediates the stepwise transformation from *R* to *P*. A general curve crossing diagram of this type is shown in Fig. 7. Here, unlike the covalent-ionic curve crossing, all the curves are anchored in states of the reactants and products.

An example for such a stepwise mechanism is the nucleophilic substitution (eq. (3.3)) on a vinylic system, $Y:^- + RR'C{=}CR''X \rightarrow RR'C{=}CR''Y + X:^-$). Here the direct substitution involves principal curves anchored at the σ-charge transfer states in analogy with the curves in the SCD of the S_N2 reaction. The intermediate curve is anchored at the π-charge transfer state [49], and it is this state that gives rise to the intermediary of carbanions in the substitution process. Of course, when the σ– and π– charge transfer states are close to each other, the reaction will proceed in a synchronous manner [49].

The $S_{RN}1$ mechanism in the dark [82] is of a similar origins. Initially, an avoided crossing of the reactant state ($ArX / Y:^-$) and the π-charge transfer state

takes place. The avoided crossing occurs along a trajectory which is devoid of bond-pair coupling, and results therefore in a radical plus radical anion species ($Y^{\bullet}$ and $ArX^{-\bullet}$). Following that, the avoided crossing of the π- and σ-charge transfer states leads to the decomposition of the radical anion intermediate to a radical $Ar^{\bullet}$ and an anion $X:^{-}$. Thus, the overall process, $ArX + Y:^{-} \rightarrow Y^{\bullet} + Ar^{\bullet} + X:^{-}$, is described by a diagram that involves the avoided crossing of the reactant state and the π- and σ-charge transfer states. The photo-stimulated mechanisms [82] starts with the photo-generated radical anion species ($ArX^{-\bullet}$) and proceeds by decomposition to a radical $Ar^{\bullet}$ and an anion $X:^{-}$ as described above. The chain mechanism, in each case, is established by trapping of the $Ar^{\bullet}$ radical by $Y:^{-}$. This process involves avoided crossing of the σ- and π-charge transfer states and regenerates the radical anion intermediate necessary to propagate the chain.

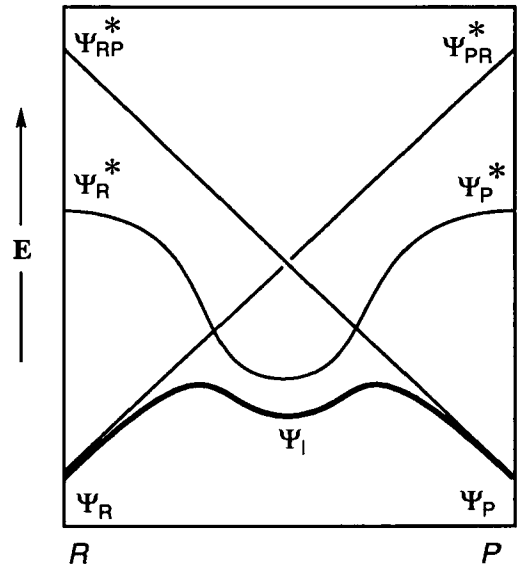

Fig. 7. A curve crossing diagram with three curves anchored at states of reactants and products. Avoided crossing is shown by the thick line.

3.6.3. Stepwise mechanisms of organic reaction. Figures 6 and 7 appear to be common to many stepwise mechanisms of organic reactions. In fact, *all stepwise classical mechanisms in physical organic chemistry obey this general scheme* [2, 3, 6, 8, 9, 54]. Certain stepwise mechanisms derive from the covalent-ionic curve crossing, while others involve foreign state crossing. Of course the

realization of these stepwise mechanisms depends on the availability of low lying ionic configurations or foreign states. Thus, whenever the concerted single step mechanism requires too high a barrier, the process will occur by a stepwise pathway. This pathway involves VB mixing of low lying ionic configuration or foreign states which cross the principal curves and mediate the process with a lower barrier than the concerted pathway.

3.6.4. Hypercoordination: A VBCM modeling. An insight into the origins of hypercoordination may be gained by viewing the problem as a chemical reaction with an intermediate state being the hypecoordinated state [83]. Thus, we trace the VB configurations that describe the transformation of the two normal-coordinated structures along a reaction coordinate that passes through the hypercoordinated geometry. Recent studies, along these lines, indicate that the major mechanism of hypercoordination involves a horizontal crossing, of the principal structures, by a third structure as in Figs. 6 and 7 above. The intermediate structures identified by us [14, 83] are either ionic VB structures or foreign states with bonding characteristics devoid of d orbitals.

An archetype of the covalent-ionic curve crossing is the formally "10 electron anions" of pentacoordinated Si . Thus, for example the stability of $(FSiH_3F)^-$ was found to originate in the crossing of the triple ion structure $F:^- SiH_3^+ :F^-$ below the HL structures as in Fig. 6. The covalent-ionic mixing stabilization calculated with a pseudo potential basis set [14] is very large, ca 65 kcal/mol, and typical for charge shift bonding [35, 40]. It is reasonable to expect that the triple ionic structure $X:^- SiX_3^+ :X^-$ will be stabilized for other cases and give rise thereby to pentacoordinated SiX_5^- by avoided crossing of the covalent-ionic type in Fig. 6. Thus, the ionic-covalent avoided crossing is likely to be a general model for pentacoordinated Si by electronegtative groups. The generality of this model may go well beyond pentacoordination of Si, and may well be a general model for formally "10-electron systems".

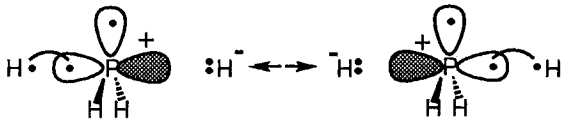

17

An archetypal example for hypercoordination induced by a foreign state, in line of Fig. 7, is the formally "nine electron" PH_4 radical [83]. In this case, the

intermediate foreign state derives from the $n\sigma^*$ excited state at the extremes of the reaction coordinate. At the hypercoordinated geometry, this state corresponds primarily to the resonating structure shown in **17**. It is seen that by allowing one of the phosphorous lone pair electrons to delocalize into the active P-H bonds, structure **17** acquires covalent bonding across one P-H linkage and electrostatic stabilization across the other P-H linkage. These features stabilize **17** at the hypercoordinated geometry and give rise thereby to the finite stability of the hypercoordinated radical PH_4. Other radicals which are formally "nine electron" species follow the same description and have been discussed and reviewed before [83, 84].

The above archetypal examples illustrate the general insight that VBCM can provide into the problem of hypercoordination [85]. More studies will be needed though to explore the full potential of the ideas into a consistent scheme like the reactivity overview discussed above in section **3.5.4.**

4. CLOSING REMARKS

We have stated at the outset the role of paradigms in chemistry, and made a case for the need of new effective paradigms by posing 10 questions about barriers, reactivity patterns and bonding. To answer these questions, we have presented the Valence Bond (VB) crossing and mixing diagrams [1-19] and tried to demonstrate how a jigsaw of chemical problems can be collated in terms of just two archetypal diagrams shown in Fig. 4 and 7. Having done so, we may conclude that Valence Bond (VB) crossing and mixing diagrams possess the potential to serve as a unified basis for conceptualization of chemical phenomena which involve species connected via deformation coordinates, and related by electronic and bond reorganizations.

Acknowledgements: The research at the Hebrew University is being supported in part by the Basic Research Foundation (BRF) administered by the Israel Academy of Sciences and Humanities. The Laboratoire de Chimie Theorique is associated with the CNRS, UA 506. We indebted to our many coworkers; R. Bar, A. Bartuv, E. Buncel, E. Canadell, J. K. Cho, D. Cohen, D. Danovich, Y. Apeloig, A. Demoliens, J. P. Dinnocenzo, E. Duzy, L. Eberson, O. Eisenstein, A. Ioffe, J. M. Lefour, P. Maitre, G. Ohanessian, A. Pross, A. C. Reddy, H. B. Schlegel, G. Sini, I. H. Um, F. Volatron, D. Weinberg and S. Wolfe. Special thanks are due to the authors of TURTLE (ref. 46e) for making their program

available to us. Figs. 3-7 and drawings **5-10**, and **14** are adapted from ref. 3 with permission of Springer-Verlag.

REFERENCES AND NOTES

1. S. S. Shaik, J. Am. Chem. Soc. **103**, 3692 (1981).
2. A. Pross and S. S. Shaik, Acc. Chem. Res. **16**, 363 (1983).
3. S. S. Shaik and P. C. Hiberty, in: "Theoretical Models for Chemical Bonding", Z. B. Maksic, Ed., Springer Verlag, Heidelberg, 1991, Vol. **4**.
4. S. S. Shaik, in: "New Concepts for Understanding Organic Reactions", J. Bertran and G. I. Csizmadia, Eds., ASI NATO Series, C267, Kluwer, Dordrecht, 1989, pp 165-218 .
5. T. H. Lowry and K. S. Richardson, "Mechanism and Theory in Organic Chemistry", Harper and Row, New York, 1987, pages 604-608; 359-360.
6. S. S. Shaik, H. B. Schlegel and S. Wolfe, "Theoretical Aspects of Physical Organic Chemistry. The S_N2 Mechanism", Wiley, New York, 1992.
7. S. S. Shaik, Pure Appl. Chem. **63**, 195 (1991) .
8. A. Pross, Adv. Phys. Org. Chem. **21**, 99 (1985) .
9. S. S. Shaik, Prog. Phys. Org. Chem. **15**, 197 (1985) .
10. S. S. Shaik, P. C. Hiberty, G. Ohanessian and J. M. Lefour, J. Phys. Chem. **92**, 5086 (1988) .
11. S. S. Shaik, Acta Chem. Scand. **44**, 205 (1990).
12. S. Shaik, in: "Molecules in Natural Science and Medicine. An Encomium for Linus Pauling", Z. B. Maksic and M. -E. Maksic, Eds., Ellis Horwood, London, 1991, Ch. 12.
13. A. Pross, Acc. Chem. Res. **18**, 212 (1985).
14. G. Sini, Ph.D. Thesis, Universite de Paris-Sud, Orsay, France, 1991.
15. P. Maitre, Ph.D. Thesis, Universite de Paris-Sud, Orsay, France, 1991.
16. P. C. Hiberty, G. Ohanessian, S. S. Shaik and J. P. Flament, Pure Appl. Chem. **65**, 35 (1993) .
17. S. Shaik, J. Mol. Liq., **61**, 49 (1994).
18. S. Shaik and A. C. Reddy, J. Chem. Soc. Faraday Trans. **90**, 1631 (1994).
19. P.C. Hiberty, Lecture Notes for the Summer School:*Université d'été de Physico-chimie théorique*, Lalonde-les-Maures, France, 1993.

20. See e.g., (a) R. McWeeny, "Methods of Molecular Quantum Mechanics", Academic Press, New York, 1992, Ch. 7. (b) L. Pauling and E. Bright Wilson, Jr., "Introduction to Quantum Mechanics", McGraw-Hill, N,Y. 1935. (c) For the treatment of matrix elements for non-orthogonal orbitals, see: P. -O. Lowdin, Phys. Rev. **97**, 1474 (1955). See also pp 46-66 in ref. 20 (a).
21. W. Heitler and F. London, Z. Physik. **44**, 455 (1927).
22. (a) G. N. Lewis, J. Am. Chem. Soc. **38**, 762 (1916). (b) L. Pauling, "The Nature of the Chemical Bond", Cornell University Press, Ithaca, 1960. (c). C. A. Coulson, "Valence", Oxford University Press, London, 1961, pp 113. (d) J. C. Slater, Phys. Rev. **38**, 1190 (1931).
23. P.C. Hiberty, J. P. Flament and E. Noizet, Chem. Phys. Lett. **189**, 259 (1992).
24. W. Kutzelnigg, in: "Theoretical Models for Chemical Bonding", Z. B. Maksic, Ed., Springer Verlag, Heidelberg, 1991, Vol. **2**.
25. For effective hamiltonian VB treatments, see: (a) J.P. Malrieu and D. Maynau, J. Am. Chem. Soc. **104**, 3021 (1982); **104**, 3029. (b) M.A. Fox and F.A. Matsen, J. Chem. Educ. **62**, 477 (1985). (c) J.P. Malrieu, D. Maynau and J.P. Daudey, Phys. Rev. **B30**, 1817 (1984). (d) See discussions, in: N. D. Epiotis, Lecture Notes Chem. **29**, 1-305 (1982). (e) Z.G. Soos, *Isr. J. Chem.* **23**, 37 (1983).
26. R.A. Bernheim, L.P. Gold, T. Tipton, J. Chem. Phys. **78**, 363 (1983). (b) K.K Verma, M.E. Koch, and W.C. Stwalley. J. Chem. Phys. **78**, 3614 (1983) ; M. M. Hessel and C. R. J. Vidal, J. Chem. Phys. **70**, 4439 (1979). (c) M. N. Glukhovtsev and P. v. R. Schleyer, Isr. J. Chem. **33**, 455 (1993).
27. (a) W.H. Goddard, III, T.H. Dunning, Jr, W.J. Hunt and P.J. Hay, Acc. Chem. Res. **6**, 368 (1973). (b) R. McWeeny, J. Mol. Struct. (THEOCHEM), **229**, 29 (1991). (c) R. D. Harcourt, J. Phys. Chem. **96**, 7616 (1992).
28. The diradical structure **4** has singlet as well as triplet states. Invoking Hund's rule (i.e., inclusion of the K_{ab} term in the matrix element between the two determinants, eq. (2.8)) leads to a triplet ground state, $^3\Sigma_g^-$. There exist two perfect-pairing structures, of the type **3**, which interchange the plans of the π-bond and the four π-electrons.These two structures form two linear combinations $\mathbf{3} \pm \mathbf{3'}$, which differ in their electron-electron repulsion. Upon inclusion of bi-electronic terms, it can be shown that the lowest energy perfect-pairing state is the negative combinations (**3 - 3'**). This combination

(**3** - **3'**) and the singlet diradical state (type **4** with singlet overall spin) constitute the two components of the $^1\Delta_g$. The $^1\Sigma_g^+$ state is the highest excited state and correspond to the positive linear combination (**3** + **3'**). This state ordering can be easily predicted from VB theory by inclusion of bielectronic terms in the effective energy expressions.

29. E.A. Carter and W. A. Goddard, III. J. Phys. Chem. **92**, 2109 (1988).
30. A. Fiedler, J. Hrusak, W. Koch and H. Schwarz, Chem. Phys. Lett. **211**, 242 (1993).
31. A. Fiedler, D. Schroder, S. Shaik and H. Schwarz, J. Am. Chem. Soc. **116**, xxx (1994).
32. C. A. Coulson and I. Fischer, Philos. Mag. **49**, 255 (1949) .
33. F. B. Bobrowicz and W. A. Goddard, III, in: "Methods of Electronic Structure Theory", H. F. Schaefer Ed., Plenum Press, New York, 1977, pp. 79-127.
34. D. L. Cooper, J. Gerratt and M. Raimondi, Adv. Chem. Phys. **69**, 319 (1987) .
35. P. C. Hiberty and D. L. Cooper, J. Mol. Structure (THEOCHEM), **169**, 437 (1988).
36. S. S. Shaik, E. Duzy and A. Bartuv, J. Phys. Chem. **94**, 6574 (1990).
37. P.C. Hiberty and J. M. Lefour, J. Chim. Phys. **84**, 607 (1987).
38. (a) A multistructure VB program by, J.P. Flament (DCMR, Ecole Polytechnique, 91128 Palaiseau Cedex, France) (b) P. Maitre, J.M. Lefour, G. Ohanessian and P. C. Hiberty, J. Phys. Chem. **94**, 4082 (1990).
39. G. Sini, P. Maitre, P. C. Hiberty and S. S. Shaik, J. Mol. Structure (THEOCHEM). **229**, 163 (1991).
40. S. Shaik, P. Maitre, G. Sini and P.C. Hiberty, J. Am. Chem. Soc. **114**, 7861 (1992).
41. P. Maitre, P.C. Hiberty, G. Ohanessian and S. S. Shaik, J. Phys. Chem. **94**, 4089 (1990).
42. G. Sini, S. S. Shaik, J.M. Lefour, G. Ohanessian and P.C. Hiberty, J. Phys. Chem. **93**, 5661 (1989).
43. G. Sini, P.C. Hiberty and S. S. Shaik, J. Chem. Soc. Chem. Commun. 772 (1989).
44. G. Sini, G. Ohanessian, P.C. Hiberty, and S. S. Shaik, J. Am. Chem. Soc. **112**, 1407 (1990).
45. G. Sini, S. Shaik and P. C. Hiberty, J. Chem. Soc. Perkin Trans. 2., 1019 (1992).

46. For related multistructure VB methods, see:(a) R.N. Yardley, and G.G. Balint-Kurti, Mol. Phys. **31**, 921 (1976).(b) J. H. van Lenthe and G. G. Balint-Kurti, Chem. Phys. Lett. **76**, 138 (1980). (c) J. H. van Lenthe and G. G. Balint-Kurti, J. Chem. Phys. **78**, 5699 (1983). (d) K. Verbeek, Ph. D. Dissertation, University of Utrecht, Utrecht, The Netherlands. (e) TURTLE package of multistructure VB calculations, by: J. Verbeek, J. H. van Lenthe, J. H. Landenberg, and C. Byrman.
47. R.D. Harcourt, Lecture Notes Chem. **30**, 1-260 (1982).
48. S. Shaik, A. C. Reddy, D. Danovich, A. Ioffe, and J. P. Dinnocenzo, J. Am. Chem. Soc., submitted for publication.
49. D. Cohen, R. Bar and S.S. Shaik, J. Am. Chem. Soc. **108**, 231 (1986).
50. (a) H. J. Kim and J. T. Hynes, J. Am. Chem. Soc. **114**, 10508, 10528 (1992). (b) A. Warshel, Acc. Chem. Res. **14**, 284 (1981). (c) R. A. Ogg, Jr. and M. Polanyi, Trans. Faraday Soc. **31**, 604 (1935).
51. S. S. Shaik J. Am. Chem. Soc. **105**, 4359 (1983).
52. (a) M.G. Evans and M. Polanyi, Trans. Faraday Soc. **34**, 11 (1938); M.G. Evans and M. Polanyi, Trans. Faraday Soc. **31**, 1401 (1935). (b) M.G. Evans and E. Warhurst, Trans. Faraday Soc. **34**, 614 (1938).
53. An alternative way of generating the SCD is by use of increased valence structures, see: R. D. Harcourt, New J. Chem. **16**, 667 (1992).
54. A. Pross, "Physical and Theoretical Principles of Organic Chemistry", Wiley, in press.
55. S. Shaik, A. Ioffe, A. C. Reddy and A. Pross, J. Am. Chem. Soc. **116**, 262 (1994).
56. Y. Apeloig, O. M.-A. Aharoni, D. Danovich, A. Ioffe, and S. Shaik, Isr. J. Chem. **33**, 387 (1993).
57. Using strictly the HL wavefunctions of reactants and products, the vertical gap becomes 3/4(ΔE_{ST}). However, allowance for a more general coupling of the three-spin system leads to the gap used here. See discussions in reference 41 (above) and in: S.S. Shaik, P.C. Hiberty, J.M.Lefour and G. Ohanessian, J. Am. Chem. Soc. **109**, 363 (1987).
58. R. D. Harcourt and R. Ng, J. Phys. Chem. **97**, 12210 (1993).
59. S. S. Shaik and E. Canadell, J. Am. Chem. Soc. **112**, 1446 (1990).
60. M. W. Wong, A. Pross and L. Radom, Isr. J. Chem. **33**, 415 (1993).
61. (a) F. Bernardi, A. Bottoni, M. J. Field, M. F. Guest, I. H. Hillier, M. A. Robb, and A. Venturini, J. Am. Chem. Soc. **110**, 3050 (1988) (b) M.A. Robb and F. Bernardi, in: "New Concepts for Understanding Organic Reactions", J. Bertran and G. I. Csizmadia, Eds., ASI NATO Series, C267,

Kluwer, Dordrecht, 1989, pp 101-146. (c) F. Bernardi, M. Ollivucci, and M.A. Robb, in: "New Concepts for Understanding Organic Reactions", J. Bertran and G. I. Csizmadia, Eds., ASI NATO Series, C267, Kluwer, Dordrecht, 1989, pp 147-164. (d) F. Bernardi, M. Olivucci and M.A. Robb, Research on Chemical Intermediates, **12**, 217 (1989). (e) F. Bernardi, M. Olivucci, J. J. W. McDouall and M. A. Robb, J. Chem. Phys. **89**, 6365 (1988). (f) W. T. A. M. Van Der Lugt and L. J. Osterhoff, J. Am. Chem. Soc. **91**, 6042 (1969). (g) J. Michl, Topics Curr. Chem.**46**, 1 (1974). (h) D. M. Silver and M. Karplus, J. Am. Chem. Soc. **97**, 2645 (1975).

62. A. Ioffe and S. Shaik, J. Chem. Soc. Perkin Trans. 2., 2101 (1992).
63. A. Pross and S. S. Shaik, J. Am. Chem. Soc. **104**, 187 (1982).
64. P. R. Benneyworth, G. G. Balint-Kurti, M. J. Davies, and I. H. Williams, J. Phys. Chem. **96**, 4346 (1992).
65. O. K. Kabbaj, M. B. Lepetit, J. P. Malrieu, G. Sini and P. C. Hiberty, J. Am. Chem. Soc. **113**, 5619 (1991). (b) O. K. Kabbaj, F. Volatron and J. P. Malrieu, Chem. Phys. Lett. **147**, 353 (1988).
66. G. Ohanessian and P. C. Hiberty, Chem. Phys. Lett. **137**, 437 (1987).
67. S. S. Shaik, J. Am. Chem. Soc. **106**, 1227 (1984).
68. (a) J. K. Kochi, Angew. Chem. Int. Ed. Engl. **27**, 1227 (1988). (b) K. Fukuzumi and J. K. Kochi, J. Am. Chem. Soc. **104**, 7599 (1922).
69. J. P. Malrieu, New J. Chem. **10**, 61 (1986) .
70. S. S. Shaik, J. Org. Chem. **52**, 1563 (1987).
71. E. Buncel, S. S. Shaik, I.H. Um and S. Wolfe, J. Am. Chem. Soc. **110**, 1275 (1988).
72. A. Pross, H. Yamataka, and S. Nagase, J. Phys. Org. Chem. **4**, 135 (1991).
73. R. D. Bach, J. W. Wolber, and H. B. Schlegel, J. Am. Chem. Soc. **107**, 2837 (1985).
74. (a) R. West, Angew Chem. Int. Ed. Engl, **26**, 1201 (1987). (b) Y. Apeloig, in: "The Chemistry of Organic Silicon Compounds", S. Patai and Z. Rappoport, Eds., Wiley, Chichester, 1989, Ch. 2. (c) D. B.-Zhitovskii, V. Braude, A. Stanger, M. Kapon, and Y. Apeloig, Organometallics, **11**, 2326 (1992).
75. (a) F. Bernardi, A. Bottoni, M. Ollivucci, M. A. Robb, and A. Venturini, J. Am. Chem. Soc. **115**, 3322 (1993). (b) F. Bernardi, A. Bottoni, M. Ollivucci, A. Venturini, and M. A. Robb, J. Chem. Soc. Faraday Trans. **90**, 1617 (1994). (c) E. T. Seidl, R. G. Grev, and H. F. Schaefer III, J. Am. Chem. Soc. **114**, 3643 (1992).

76. (a) S. S. Shaik, New J. Chem. **6**, 159 (1982). (b) S. S. Shaik and A. Pross, J. Am. Chem. Soc. **104**, 2708 (1982).
77. (a) C. -A. Craze, A.J. Kirby and R. Osborne, J. Chem. Soc. Perkin 2, 357 (1978). (b) B. L. Knier and W. P. Jencks, J.Am.Chem. Soc. **102**, 6789 (1980).
78. S. Wolfe, D. J. Mitchell, and H. B. Schlegel, Can. J. Chem. **60**, 1291 (1982).
79. G. Ohanessian, P.C. Hiberty, J.-M. Lefour, J.-P. Flament, and S. S. Shaik, Inorg. Chem. **27**, 2219 (1988).
80. (a) R. B. Woodward and R. Hoffmann, The Conservation of Orbital Symmetry, Academic Press, New York, 1970. (b) Fukui, K. "Theory of Orientation and Stereoselection", Wiley-Interscience, New York, 1976.
81. S. S. Shaik, New J. Chem. **7**, 201 (1983).
82. (a) N. Kornblum, Angew. Chem. Int. Ed. Engl. **14**, 734 (1975). (b) G. A. Russell, Chem. Soc. Spec. Publ. **24**, 271 (1970). (c) J. F. Bunnett, Acc. Chem. Res. **11**, 413 (1978).
83. A. Demoliens, O.Eisenstein, P.C. Hiberty, J.M. Lefour, G. Ohanessian, S. S. Shaik and F. Volatron, J. Am. Chem. Soc. **111**, 5623 (1989).
84. F. Volatron, J. Mol. Struct (THEOCHEM.) **186**, 167 (1989).
85. For extensive treatments of hypercoordination, see: (a) ; N. D. Epiotis, Lecture Notes Chem. **34**, 1-585 (1983), Ch. 9. (b) A. E. Reed and P. v. R. Schleyer, J. Am. Chem. Soc. **112**, 1434 (1990).

RESPONSE THEORY AND CALCULATIONS OF MOLECULAR HYPERPOLARIZABILITIES

Yi Luo and Hans Ågren

Institute of Physics and Measurement Technology
Linköping University
S-58183, Linköping, Sweden

Poul Jørgensen and Kurt V. Mikkelsen

Department of Chemistry
Aarhus University
DK-8000 Århus, Denmark

ADVANCES IN QUANTUM CHEMISTRY
VOLUME 26

Contents

1 Introduction

Molecular compounds with specific non-linear electric and magnetic properties hold great promises in optical and electronic technology[1, 2, 3, 4, 5, 6, 7, 8, 9]. Such compounds can conceivably be used as conductors (conducting polymers) and switches (charge transfer compounds) in various electronic components. The design of UV-lasers, ultra-compact discs, magneto-optic storage devices, opto-electronic switches and display technologies are few of many examples relevant to this area. The understanding of the microscopic origin of strong non-linearity of electric and magnetic properties has benefited much from theoretical investigations which within recent years have lead to a large number of contributions in the field. This research has also been challenged by the experimental progress in determining non-linear molecular spectra and properties.

The continuous development of basic theory is a prerequisite for future computational applications in the area of non-linear phenomena. One of the major goals is to develop and use computational methods to give a mechanistic insight into the origin of the non-linear properties and to make structure-to-property interpretations, and, in the end, predictions. The goal is thus to predict specific properties and functions of *e.g.* bridges and substituent groups, and to make it possible to *screen* candidate compounds, thereby avoiding time-consuming and expensive laboratory tests. This attempts to relate the appearance of strong non-linearity with both electronic and geometric structures of the molecules and to design devices that are optically active or conducting leading to future components in photonics. Another major goal for the theoretical development has been to calibrate different quantum methods and to accurately reproduce experimental data. This goal also involves a determination on the origin of the non-linear property in terms of quantum mechanical concepts, such as electronic structures, parametrizations of the wave function, role of molecular vibrations and influence of time-dependent external electric fields, etc. These two main goals have followed a theoretical development that traditionally has progressed along two lines, the first uses semi-empirical methods that can address larger systems at a coarse level of accuracy, the other uses *ab initio* methods and can give ever higher accuracy for smaller sized systems. As described in the present text, response theory has the potential of uniting these two major goals from the outset of a common theoretical framework.

The semi-empirical methods developed and employed by numerous groups (see the excellent review[9] by D. R. Kanis, M. A. Ratner and T. J. Marks and references therein) have clearly shown how quantum chemical approaches can give guidelines to the design of materials having interesting nonlinear optical effects. The objectives of these groups are along the lines of interpreting and predicting hyperpolarizabilities and not along the lines of performing very accurate and parameter-free calculations. The present review concerns primarily the developments related to ab-initio response methods; for a more general overview we refer to the special issue of Chemical Reviews, 1994, on optical nonlinearities in chemistry.

Response theory methods for calculations of general molecular properties have during the last few years been drastically improved. One such branch of development is defined by calculations that obtain linear and quadratic response properties with the random phase approximation (RPA, time-dependent Hartree-Fock (TDHF)) [10, 11, 12, 13] and with the multi-configuration response methods[14, 15, 16]. These methods are based on non-correlated, self-consistent field- (SCF), and correlated, multi-configuration self-consistent

field (MCSCF) reference wave functions, respectively. From the early applications of multi-configuration linear response (MCLR, multi-configuration TDHF (MCTDHF)) devoted to dipole spectra of singlet excitation energies and transition moments, these methods have now diversified to applications on a whole range of different properties; time-independent properties evaluated at zero frequency of the external electromagnetic field have thus been extended with their dynamic, frequency dependent analogues; a number of magnetic properties have been added to the electric field generated properties; likewise have calculations of linear response functions been generalized to non-linear response functions. The vacuum or gas-phase response method has also been extended to solvated molecules by establishing the self-consistent reaction field (SCRF [17]) and the multi-configuration self-consistent reaction field (MCSCRF [18]) response methods for solving the response equations for a solvated molecule[19]. In the present work we review the development and application of response theory with respect to a particular molecular property, namely the hyperpolarizability, and demonstrate the potential of this development with some illustrative examples.

The hyperpolarizability plays a key role in understanding the non-linear optical response of molecules, and much attention in recent quantum chemical studies has therefore been laid on this quantity. Materials with strong second and third harmonic generations, SHG and THG, can be used for doubling and tripling of laser frequencies introducing laser technology into the blue and near-UV wavelength regions. Other examples are given by the electro-optical Kerr effects, which describe the action of an external field on the polarization directions of light. Both the SHG and the Kerr capabilities, which exhibit great potential use in optical data storing, are directly connected to the molecular hyperpolarizability tensors. A third example is given by strong charge transfer complexes with potential use in optical switching. The hyperpolarizability tensor components determine 1-,2- or 3-dimensional charge transfer capabilities, for which strong in-plane orthogonal excitations and "phase-matching" are suitable properties for non-linear materials.

Many of the calculations have focussed on accurate predictions of hyperpolarizabilities of small molecules, and have proceeded along several lines. The bulk of *ab initio* calculations for frequency dependent polarizabilities and hyperpolarizabilities have utilized one-determinant self-consistent field wave functions [20, 21, 22, 23]. The wave functions utilized in correlated treatments of frequency dependency have been both of perturbational Møller-Plesset[24, 25, 26, 27], coupled cluster[28, 29, 30, 31, 32, 33] and multi-configurational self-consistent field types[15, 23, 34]. The latter, given in an analytical implementation, is the topic on which we focus.

It has become clear that the accuracy of *ab initio* calculations of molecular hyperpolarizabilities critically depends on elements of several categories, to mention: basis sets, electron correlation, frequency dependencies and vibrational corrections. Furthermore, since most measurements are carried out in solution, an appropriate consideration of the influence of the medium becomes relevant for comparisons with experiment in such cases. Basis sets evidently need the flexibility to describe any polarization of the electronic cloud correctly and therefore to describe the more diffuse regions properly. Electron correlation has been found to be quite significant for many molecules. In extreme cases correlation increases the first hyperpolarizability β by as much as 70% (NH_3[35]).

One of the most important factors is the frequency dependency of the hyperpolarizabilities. The experimental data always refer to dynamical processes and relate therefore to

frequency dependent molecular properties. The extrapolation to zero frequency often introduces problems for the comparison between theory and experiment; an example of this is the second hyperpolarizability of the N_2 molecule, where the extrapolated experimental frequency dependent hyperpolarizabilities have lead to an inaccurate static value[36]. That particular case stresses the importance of carrying out calculations right at the frequencies where experiments are performed.

Occasionally, the comparison of theory and experiment is performed by adding the frequency dispersion of the hyperpolarizability calculated by a self-consistent field (SCF) method to the correlated static results [29]. This approach assumes that the frequency dispersion in the two cases is the same. It might be true for small frequencies which are far from resonance, but it is not the case when the frequencies of the exciting electromagnetic field are close to transitions (resonances) within the molecule. For example at the frequency of the commonly employed ruby laser the SCF dispersion is almost identical to the correlated dispersion for molecules like HF and H_2O, because the frequency is rather far from the first resonance, while for the isoelectronic NH_3 species[35] the SCF results can not give an accurate description of the frequency dispersion, since the laser frequency is close to resonances within NH_3. Therefore, it is important to describe the frequency dispersion features at a correlated level in order to predict the hyperpolarizabilities at frequencies at which experimental data are not available. It is clear that the independent particle self-consistent field results may not be of sufficient accuracy for this purpose.

The importance of vibrational corrections for hyperpolarizabilities is now widely recognized, see e.g. the recent review by Bishop[37] focusing on diatomic molecules. Vibrational averaging of hyperpolarizabilities has also been considered for molecules like the neon iso-electronic hydrides and performed at a correlated level of electronic structure calculations[35, 38, 39]. These corrections may increase the electronic first hyperpolarizabilities by as much as 10%.

It has become clear that any calculation that aims at describing the experimental results within the precision of the error bars must account for all requirements discussed above. The multi-configuration self-consistent (MCSCF) response method offers an approach to such calculations. In this approach the response of an MCSCF wave function to a periodic homogeneous time-dependent field is determined. The MCSCF linear response (MCLR) function determines the frequency-dependent polarizabilities and was first derived by Yeager and Jørgensen [40] and Dalgaard [41]. In 1985, Olsen and Jørgensen derived expressions for the linear, quadratic and cubic response functions using a general formulation[23]. Modern implementations of MCLR and MCQR (multi-configuration quadratic response) have been described in the articles by Jørgensen et al.[14], respectively, and by Hettema et al.[15]. More recently, such implementations have also been performed for triplet operators[16]. Calculations using this methodology have made it possible to interpret non-linear properties of small systems, and have in some cases even advanced the experimental predictions for such species.

As noted in the beginning of this section, due to the large non-linear optical response exhibited by, e.g., conjugated organic molecules, extensions to larger molecules are desirable. The hyperpolarizability of larger molecular systems has mostly been investigated by semiempirical methods[9]. A comparison of the semiempirical and *ab initio* results indicates that significant differences can be found and that these differences may increase by systematic improvements of the *ab initio* calculations. A recent development towards

larger molecules has recently taken place within the realm of the response theory calculations considered here; the double-direct computational scheme for the Random Phase Approximation (RPA) described in ref. [42] has enabled the use of larger basis sets and calculation of hyperpolarizabilities of much larger molecules than would otherwise be possible. However, because of the comparably small amount of applications of this method yet available, we present only a few examples here and postpone the review of response theory on very large systems to a later date, and focus on available results for small and intermediate sized molecules.

Before going into response theory, we discuss in the following section some aspects concerning the definitions of the hyperpolarizability and conventions used when relating the microscopic quantity to the corresponding experimentally determined macroscopic quantity. These aspects as well as the so-called local field factors, discussed in the same section, have unfortunately been the source for much confusion previously. The theory section outlines the basics of the response method for a multi-configuration wave function and discusses the differences between this approach and other methods for obtaining hyperpolarizabilities. After the theory section we describe applications of response theory for different types of molecules, representing small molecules, charge-transfer compounds and oligomeric chains. In the former case we describe general trends in results obtained for the neon iso-electronic series including neon itself; Ne, HF, H_2O, NH_3 and CH_4. We also compare with important results obtained by other correlating methods. The neon isoelectronic series provides a good platform for a collected display of the importance of basis sets, electron correlation, frequency dependency, vibrational contributions and solvent effects, each of these factors are separately discussed in subsections. We then turn to the N_2 and O_2 molecules, as representing molecules with special correlation effects, being triply bonded and open-shell, respectively. For hyperpolarizabilities of intermediate size molecules we have chosen to review calculations on para-nitroaniline and diamino-nitroaniline, representing one-, respectively, two-dimensional charge-transfer compounds. In this section we also focus on the role of a solvent when determining hyperpolarizabilities, and on the use of simplifying few-state models. In the last section we review results of hyperpolarizability calculations of polyenes and polyynes, representing oligomers.

2 The mechanism of hyperpolarizabilities

I Definitions

The response of a molecular system in a state $| 0 \rangle$ to an external field can be described in terms of the Hamiltonian operator

$$\hat{H} = \hat{H}_0 + \hat{W} + \hat{V}(t) \tag{1}$$

where $\hat{H}_0$ is the Hamiltonian of an isolated molecule, and $\hat{W}$ is the interaction operator describing the interaction between the molecule and the surrounding medium. This interaction is important for example to describe a solvated molecule. The interaction operator describing the interaction between the molecule and the external field can in the frequency domain be expressed as

$$V(t) = \int_{-\infty}^{+\infty} d\omega V^{\omega} \exp(-i\omega t) \tag{2}$$

In the gas phase, the contribution from W is negligible and the Hamiltonian operator can be written as

$$\hat{H} = \hat{H}_0 + \hat{V}(t) \tag{3}$$

We assume that the eigenvalues and -functions of H_0 are known for the reference state,

$$H_0|0\rangle = E_0|0\rangle \tag{4}$$

and for the complementary set of eigenstates

$$H_0|n\rangle = E_n|n\rangle \tag{5}$$

where the set $\{|n\rangle\}$ is orthogonal to $|0\rangle$. We use time-dependent perturbation theory to determine the time evolution of $|0\rangle$. Following Ref.[23] , we write the time-dependent state $|\tilde{0}\rangle$ as

$$|\tilde{0}\rangle = \exp(i\ S(t))|0\rangle \tag{6}$$

where $S(t)$ is given by

$$S(t) = \sum_n [S_n|n\rangle\langle 0| + S_n^*|0\rangle\langle n|]. \tag{7}$$

Essential in the theory is that we require that Ehrenfest's theorem to hold for the time-dependent state $|\tilde{0}\rangle$ for the excitation-deexcitation operators Λ, which are elements of the set $\{|n\rangle\langle 0|; |0\rangle\langle n|\}$.

$$\langle\tilde{0}|\Lambda|\dot{\tilde{0}}\rangle + \langle\dot{\tilde{0}}|\Lambda|\tilde{0}\rangle = -i\langle\tilde{0}|[\Lambda, H_0 + V(t)]|\tilde{0}\rangle. \tag{8}$$

Expanding $S(t)$ in a power series in $\hat{V}(t)$

$$S(t) = S(t)^{(1)} + S(t)^{(2)} + \ldots \tag{9}$$

and expanding the exponential generates a power series expansion of the wave function. The perturbed functions $|0^{(n)}\rangle$ are determined by requiring Ehrenfest's theorem to hold in all powers of the perturbation.

The response functions are defined by considering the expansion coefficients of the expectation value of an operator A.

$$\begin{aligned} A_{av}(t) =& < \tilde{0} \mid A \mid \tilde{0} > = < 0|A|0 > + \int_{-\infty}^{+\infty} d\omega_1 << A; V^{\omega_1} >>_{\omega_1} \exp(-i\omega_1 t) \\ &+ \frac{1}{2}\int_{-\infty}^{+\infty} d\omega_1 \int_{-\infty}^{+\infty} d\omega_2 << A; V^{\omega_1}, V^{\omega_2} >>_{\omega_1+i\epsilon,\omega_2} \exp((-i\omega_1 - i\omega_2)t) + \ldots\ldots \end{aligned} \tag{10}$$

Expressed as a sum over the intermediate state $|m>$, the linear response function is given by

$$\langle\langle A; V^{\omega_1}\rangle\rangle_{\omega_1} = \sum_{m>0}\left\{\frac{\langle 0|A|m\rangle\langle m|V^{\omega_1}|0\rangle}{\omega_1 - \omega_{m0}} - \frac{\langle 0|V^{\omega_1}|m\rangle\langle m|A|0\rangle}{\omega_1 + \omega_{m0}}\right\}. \tag{11}$$

where $\omega_{m0} = E_m - E_0$ is the energy difference between the excited state $|m>$ and ground state $|0>$ and ω_1 the frequency of electric field.

The quadratic response function can be written as

$$\langle\langle A; V^{\omega_1}, V^{\omega_2}\rangle\rangle_{\omega_1,\omega_2} = \sum_{m,n>0}\Big\{\frac{\langle 0|A|m\rangle\,[\langle m|V^{\omega_1}|n\rangle - \delta_{mn}\langle 0|V^{\omega_1}|0\rangle]\,\langle n|V^{\omega_2}|0\rangle}{(\omega_1+\omega_2-\omega_{m0})(\omega_2-\omega_{n0})}$$
$$+\frac{\langle 0|V^{\omega_2}|n\rangle\,[\langle n|V^{\omega_1}m\rangle - \delta_{mn}\langle 0|V^{\omega_1}|0\rangle]\,\langle m|A|0\rangle}{(\omega_1+\omega_2+\omega_{m0})(\omega_2+\omega_{n0})}$$
$$-\frac{\langle 0|V^{\omega_1}|m\rangle\,[\langle m|A|n\rangle - \delta_{mn}\langle 0|A|0\rangle]\,\langle n|V^{\omega_2}|0\rangle}{(\omega_1+\omega_{m0})(\omega_2-\omega_{n0})}$$
$$+\frac{\langle 0|A|m\rangle\,[\langle m|V^{\omega_2}|n\rangle - \delta_{mn}\langle 0|V^{\omega_2}|0\rangle]\,\langle n|V^{\omega_1}|0\rangle}{(\omega_1+\omega_2-\omega_{m0})(\omega_1-\omega_{n0})}$$
$$+\frac{\langle 0|V^{\omega_1}|n\rangle\,[\langle n|V^{\omega_2}|m\rangle - \delta_{mn}\langle 0|V^{\omega_2}|0\rangle]\,\langle m|A|0\rangle}{(\omega_1+\omega_2+\omega_{m0})(\omega_1+\omega_{n0})}$$
$$-\frac{\langle 0|V^{\omega_2}|m\rangle\,[\langle m|A|n\rangle - \delta_{mn}\langle 0|A|0\rangle]\,\langle n|V^{\omega_1}|0\rangle}{(\omega_2+\omega_{m0})(\omega_1-\omega_{n0})}\Big\}. \qquad (12)$$

where ω_1 and ω_2 are the frequencies of electric field. The expression for the cubic response function can be found in Ref.[23].

The explicit form of the interaction operator depends on the field that interacts with the molecule. For a homogeneous periodic electric field of frequency ω, the field can be represented as

$$\mathbf{F(t)} = \frac{1}{2}\mathbf{F^0}[exp(-i\omega t) + exp(i\omega t)] = \mathbf{F^0}cos\omega t \qquad (13)$$

where $\mathbf{F^0}$ is the electric field strength. The interaction operator then becomes

$$V^t = -(\mu\mathbf{F^0})cos\omega t \qquad (14)$$

where $\mu = (\mu^x, \mu^y, \mu^z)$ represents the electric dipole moment operator of the molecular system. The operator V^ω then becomes

$$V^\omega = -\frac{1}{2}(\mu\mathbf{F^0})[\delta(\omega-\omega_0) + \delta(\omega+\omega_0)] \qquad (15)$$

For A being the dipole operator, $A_{av}(t)$ becomes the total dipole moment induced by the field $\mathbf{F(t)}$, μ_i^{ind}, which may be expressed in a series,

$$\mu_i^{ind} = \mu_i^T + \alpha_{ij}^T(-\omega;\omega)F_j^\omega + \frac{1}{2}\beta_{ijk}^T(-2\omega;\omega,\omega)F_j^\omega F_k^\omega$$
$$+\frac{1}{6}\gamma_{ijkl}^T(-3\omega;\omega,\omega,\omega)F_j^\omega F_k^\omega F_l^\omega + ... \qquad (16)$$

The Einstein summation convention is here used. The expansion coefficients μ_i^T, α_{ij}^T, β_{ijk}^T and γ_{ijkl}^T define the properties of the molecular system corresponding to the dipole moment, frequency dependent polarizability, first hyperpolarizability and second hyperpolarizability, respectively. The subscripts i, j, k and l correspond to the molecular axes x, y and z. F_i^ω is the component of the interacting field $\mathbf{F(t)}$ at the frequency, ω.

The polarizability and hyperpolarizabilities can be expressed in terms of response functions as

$$\alpha_{ij}^T(-\omega_\sigma;\omega_1) = -\langle\langle\mu_i;\ \mu_j\rangle\rangle_{\omega_1};\ \ \omega_\sigma = \omega_1$$

$$\beta^T_{ijk}(-\omega_\sigma;\omega_1,\omega_2) = -\langle\langle \mu_i;\mu_j,\mu_k\rangle\rangle_{\omega_1,\omega_2};\ \ \omega_\sigma = \omega_1+\omega_2$$
$$\gamma^T_{ijkl}(-\omega_\sigma;\omega_1,\omega_2,\omega_3) = -\langle\langle \mu_i;\mu_j,\mu_k,\mu_l\rangle\rangle_{\omega_1,\omega_2,\omega_3};\ \ \omega_\sigma = \omega_1+\omega_2+\omega_3; \qquad (17)$$

The polarizability and hyperpolarizabilities contain a summation over a complete set of exact states. In most calculations the explicit reference to the excited states is removed and the summation over the excited states is rewritten such that the summation is carried out indirectly through solving sets of linear equations. We return to this point when we describe calculations of polarizabilities and hyperpolarizabilities for SCF and MCSCF wave functions.

In some cases, the electric-field-dependent dipole moment is written as a perturbation series expansion,

$$\mu_i^{ind} = \mu_i + \alpha^B_{ij}F^{\omega_0}_j + \beta^B_{ijk}F^{\omega}_j F^{\omega_0}_k + \gamma^B_{ijkl}F^{\omega_0}_j F^{\omega_0}_k F^{\omega_0}_l + ... \qquad (18)$$

The difference between eqs.16 and 18 is evident. The electric-field-induced dipole moment is independent of convention and the following relations, $\alpha^T_{ij} = \alpha^B_{ij}$, $\beta^T_{ijk} = 2\beta^B_{ijk}$ and $\gamma^T_{ijkl} = 6\gamma^B_{ijkl}$ therefore hold between properties obtained using the different conventions.

Molecular properties of solutes have mainly been measured in two-component solutions. Singer and Garito have proposed an infinite dilution extrapolation procedure for determining the solute molecular polarizability and hyperpolarizabilities [43]. In these solutions, a single solute molecule is completely surrounded by the solvent molecules. The molecular properties are in such a system defined by the system Hamiltonian, $\hat{H}_0 + \hat{W}$. When the external field is applied, the solvent molecules induce a field, which is characterized as a screened field (the combined internal and external field) that the solute molecules experiences. The effects of the solvent are two fold (i) screening of the externally applied field and; (ii) being part of the unperturbed molecular Hamiltonian and therefore included in the response equations. The screening of the external field is usually incorporated into the experimentally observed molecular properties through local field factors as we will discuss in more detail in the next section. Point (ii) is addressed in the section on solvent induced hyperpolarizabilities, section 4

II Local field corrections

The experimental measurements describe the response of the investigated system to the external electric field. The measured total polarization $\bar{P}_i$ (i=x,y,z) of the investigated system can be expressed as a power series in the external field strength $\bar{\mathbf{E}}(\omega)$. When a Taylor series is applied, it becomes

$$\bar{P}_i = \chi^{(1)}_{ij}\bar{E}_j{}^{\omega} + \frac{1}{2}\chi^{(2)}_{ijk}\bar{E}_j{}^{\omega}\bar{E}_k{}^{\omega} + \frac{1}{6}\chi^{(3)}_{ijkl}\bar{E}_j{}^{\omega}\bar{E}_k{}^{\omega}\bar{E}_l{}^{\omega} + ... \qquad (19)$$

where $\chi^{(i)}$ is the susceptibility tensor of rank $(i+1)$. The susceptibility tensor is connected with the molecular microscopic polarizabilities. For an SHG measurement, one has

$$\bar{P}_i(2\omega) = \frac{1}{2}\chi^{(2)}_{ijk}(-2\omega;\omega,\omega)\bar{E}_j{}^{\omega}\bar{E}_k{}^{\omega} \qquad (20)$$

In order to determine the value of $\chi^{(2)}_{ijk}$, the total polarization $\bar{P}_i$ and the strength of the external field must be measured.

In general, the investigated system is assumed to consist of polarizable entities. The external electric field induces a total polarization per unit volume. The total polarization per unit volume is expressed as a sum of effective entity dipoles induced by the electric field acting at the position of the entities. However, the entities of the assembly interact with each other, the field acting on each entity is not rigorously the external field. When an external field is applied on the system, each entity induces a field. The field felt by one entity is termed the local field (the combination of the external field and the sum of the induced fields from the other entities). Therefore, the relation between the macroscopic polarizabilities (usually called susceptibilities) and microscopic polarizabilities can be written as [44, 45]

$$\chi^{(1)}(-\omega;\omega) = N f^{(1)}(-\omega;\omega)\bar{\alpha}(-\omega;\omega) \tag{21}$$

$$\chi^{(2)}(-\omega_m-\omega_n;\omega_m,\omega_n) = N f^{(2)}(-\omega_m-\omega_n;\omega_m,\omega_n) \tag{22}$$

$$\times\bar{\beta}(-\omega_m-\omega_n;\omega_m,\omega_n) \tag{23}$$

$$\chi^{(3)}(-\omega_m-\omega_n-\omega_l;\omega_m,\omega_n,\omega_l) = N f^{(3)}(-\omega_m-\omega_n-\omega_l;\omega_m,\omega_n,\omega_l) \tag{24}$$

$$\times\bar{\gamma}(-\omega_m-\omega_n-\omega_l;\omega_m,\omega_n,\omega_l) \tag{25}$$

In the above equations, N is the number density, $f^{(n)}$ represents a local field factor that accounts for the effect of the induced field, and $\bar{\alpha}$, $\bar{\beta}$ and $\bar{\gamma}$ are the orientationally averaged microscopic molecular properties determined in the experiments.

Comparison between experimental measurements and theoretical calculations requires that special care must be exercised. For the gas phase, the local field factors are approximately equal to one. The experimentally determined microscopic molecular properties can therefore be directly compared to the results from the theoretical calculations in gas phase. For the liquid phase, the experimentally determined microscopic molecular properties should be compared to the results from the theoretical calculation in liquid phase. They can not be compared with the results in gas phase as is done in many studies. The local field effects do not take account of the effects of the intermolecular interactions that arise when a molecule is solvated. The interaction between a molecule and a solvent determines the difference between molecular properties in the gas and liquid phases, and must be included in the quantum description of molecular properties. The solvent effects are addressed in section 4 below.

The determination of the local field factors has been much discussed in the literature. Using the Lorentz model one obtains

$$f^{(1)}(-\omega;\omega) = f^{\omega} f^{\omega} \tag{26}$$

$$f^{(2)}(-\omega_m-\omega_n;\omega_m,\omega_n) = f^{\omega_m+\omega_n} f^{\omega_m} f^{\omega_n} \tag{27}$$

$$f^{(3)}(-\omega_m-\omega_n-\omega_l;\omega_m,\omega_n,\omega_l) = f^{\omega_m+\omega_n+\omega_l} f^{\omega_m} f^{\omega_n} f^{\omega_l} \tag{28}$$

where

$$f^{\omega} = \frac{1}{3}(n_{\omega}^2+2) \tag{29}$$

where n_ω is the index of refraction at the frequency ω of the externally applied field. These are called the Lorentz local field factors. In the static limit the Onsager expression is often used to describe the local field factor

$$f^{0} = \frac{\epsilon(n^2+2)}{(n^2+2\epsilon)} \tag{30}$$

where ϵ is the dielectric constant.

III Conventions

Many different conventions have been used to tabulate experimental hyperpolarizabilities. The major bulk of the most reliable experimental data are from electrical-field-induced second harmonic generation (ESHG) measurements, where the field-induced dipole moment is determined at the second harmonic frequency 2ω produced by fields at frequency ω and zero. Using a Taylor series expansion (convention T), the field-induced dipole moment becomes

$$\mu_i^{ind}(2\omega) = \frac{1}{4}\beta_{ijk}^T(-2\omega;\omega,\omega)F_j^\omega F_k^\omega + \frac{1}{4}\gamma_{ijkl}^T(-2\omega;\omega,\omega,0)F_j^\omega F_k^\omega F_l^0 + ... \qquad (31)$$

The measured effective polarization $\bar{P}_i^{2\omega}$ containing the contributions from the first and second hyperpolarizabilities is

$$\begin{aligned}\bar{P}_i^{2\omega} &= \frac{1}{4}Nf^{(3)}(-2\omega;\omega,\omega,0)(\bar{\gamma}^T(-2\omega;\omega,\omega,0) + \frac{\mu_0\beta_{||}^T(-2\omega;\omega,\omega)}{3kT})(F_i^\omega)^2F_i^0 \\ &= \frac{1}{4}Nf^{(3)}(-2\omega;\omega,\omega,0)(\bar{\gamma}^T(-2\omega;\omega,\omega,0) + \frac{\mu_0\beta_z^T(-2\omega;\omega,\omega)}{5kT})(F_i^\omega)^2F_i^0 \qquad (32)\end{aligned}$$

where the thermal average over the orientations of a dipolar molecule in a static electric field[37] has been performed. The component $\beta_{||}^T$ denotes the vector component of the third order tensor β_{ijk}^T in the direction of the dipole moment, $\beta_{||}^T = \frac{1}{5}\sum_j(\beta_{zjj}^T + \beta_{jjz}^T + \beta_{jzj}^T)$, $(j = x,y,z)$, and β_z^T is the z component of the vector quantity frequently used by experimentalists, $\beta_{||}^T = \frac{3}{5}\beta_z^T$. $\bar{\gamma}^T$ is the scalar component of the fourth order tensor γ_{ijkl}, $\bar{\gamma}^T = \frac{1}{15}\sum_{jk}(\gamma_{jjkk}^T + \gamma_{jkkj}^T + \gamma_{jkjk}^T)$, $(j,k = x,y,z)$. The local field factor is defined in eq. (28) and $f^{(3)}(-2\omega;\omega,\omega,0) = f^{2\omega}(f^\omega)^2f^0$

When a perturbation series (convention B) is applied, the field-induced dipole moment becomes

$$\mu_i^{ind}(2\omega) = \frac{1}{2}\beta_{ijk}^B(-2\omega;\omega,\omega)F_j^\omega F_k^\omega + \frac{3}{2}\gamma_{ijkl}^B(-2\omega;\omega,\omega,0)F_j^\omega F_k^\omega F_l^0 + ... \qquad (33)$$

and

$$\bar{P}_i^{2\omega} = \frac{3}{2}Nf^{(3)}(-2\omega;\omega,\omega,0)(\bar{\gamma}^B(-2\omega;\omega,\omega,0) + \frac{\mu_0\beta_z^B(-2\omega;\omega,\omega)}{15kT})(F_i^\omega)^2F_i^0 \qquad (34)$$

In some cases, the electric-field-dependent dipole moment is written as a simple series expansion (convention X) where the coefficients in convention T have been removed, i.e.

$$\mu_i^{ind}(2\omega) = \beta_{ijk}^X(-2\omega;\omega,\omega)F_j^\omega F_k^\omega + \gamma_{ijkl}^X(-2\omega;\omega,\omega,0)F_j^\omega F_k^\omega F_l^0 + ... \qquad (35)$$

thus

$$\bar{P}_i^{2\omega} = Nf^{(3)}(-2\omega;\omega,\omega,0)(\bar{\gamma}^X(-2\omega;\omega,\omega,0) + \frac{\mu_0\beta_z^X(-2\omega;\omega,\omega)}{5kT})(F_i^\omega)^2F_i^0 \qquad (36)$$

In ref. [46] another convention (convention C) has been used, for example in measurements of the hyperpolarizabilities of para-nitroaniline (PNA) in solutions[47, 48]. The measured effective polarization $\bar{P}_i^{2\omega}$ is in this convention given by

$$\bar{P}_i^{2\omega} = \frac{3}{2}Nf^{(3)}(-2\omega;\omega,\omega,0)(\bar{\gamma}^C(-2\omega;\omega,\omega,0) + \frac{\mu_0\beta_z^C(-2\omega;\omega,\omega)}{5kT})(F_i^\omega)^2F_i^0 \qquad (37)$$

The relations connecting the different conventions for the hyperpolarizabilities in ESHG experiments can be summarized as

$$\beta^T = 2\beta^B = 4\beta^X = 6\beta^C \tag{38}$$

and

$$\gamma^T = 6\gamma^B = 4\gamma^X = 6\gamma^C \tag{39}$$

It is essential to recognize which convention is used for the hyperpolarizabilities when comparing theoretical calculations and experimental results.

3 Response functions in the MCSCF approximation

Response functions describe how an observable represented by an hermitian operator respond to a time-dependent field. The response can be linear in the field in which case we have the linear response function, the quadratic response gives the quadratic response function etc. If the operator is the electric dipole operator and the time-dependent field is a periodic electric field then the linear response function is the frequency dependent polarizability, the quadratic response function the frequency dependent first hyperpolarizability etc. The residues of the response functions determine transition matrix elements, in the above case the residue of the linear response function determines the one-photon transition moments and one of the residues of the quadratic response function determine the two-photon transition moments.

The response function formalism we use dates back to Zubarev[49]. SCF linear and quadratic response functions were derived in the sixties and seventies[50]. An elegant derivation of the SCF quadratic response function was presented by Dalgaard in 1982[51]. The MCSCF linear response function was first derived in the late seventies[40, 41]. A general formulation of the MCSCF linear, quadratic, and cubic response functions were given in 1985 by Olsen and Jørgensen[23]. The derivation we present use a similar outline. The MCSCF linear response function has also been given by Funchs et al.[52] and Kotuku et al.[34] have rederived the linear, quadratic and cubic response functions. Response functions have also been derived for other wave functions: Linear response functions have been obtained using second order perturbation theory in the so-called second order polarization propagator approach[53]. A formulation of time-dependent perturbation theory which only allows the determination of the frequency dependent polarizability and first hyperpolarizability has been derived in the context of second order many-body perturbation theory(MP2)[26, 24, 25, 27]. A disadvantage of the latter approach is that the pole structure is determined by the SCF response equations and therefore uncorrelated (RPA poles). Linear response functions have also been derived for a Coupled Cluster wave function by Monkhorst[28] and Dalgaard and Monkhorst[30]. A general formulation of Coupled Cluster response function theory including a derivation of the linear and quadratic response functions has been given by Koch and Jørgensen[31].

The second order many-body perturbation theory approach (MP2) differs substantially from the other approaches. It is a two step approach where the time development of an uncorrelated SCF wave function is used to evaluate frequency dependent correlated MP2 molecular properties. The pole structure of the frequency dependent molecular properties therefore occurs at the uncorrelated poles of the SCF wave function. Transition matrix

elements, such as one- and two-photon transition moments, can not be obtained in this approach. In all other approaches the time development is determined for the correlated wave function and the pole structure is therefore also determined by the correlated wave function and therefore correlated. Residues at the poles therefore gives correlated transition matrix elements.

In this section, we discuss the evaluation of the linear and quadratic response functions for an MCSCF wave function. In the first subsection we discuss the parametrization of the time evolution of the MCSCF state and determine the equations of time evolution through second order in the interaction operator. In the second subsection we derive the linear and quadratic response functions for an MCSCF state. Subsection three describes the formulas resulting from the linear transformations that are necessary for evaluating the linear and quadratic response functions. In the last subsection we describe the intricacies connected to programming the resulting expressions.

I Parametrization of the time development of an MCSCF state

We assume that the unperturbed wave function is an MCSCF state

$$|0\rangle = \sum_g C_{g0}|\phi_g\rangle \tag{40}$$

where $|\phi_g\rangle$ is a set of configuration state functions (CSF's). Variations in the orbital space is described in terms of the orbital excitation and deexcitation operators

$$\begin{aligned} q_\nu^\dagger &= \sum_\sigma a_k^\dagger a_l = E_{kl}; \\ q_\nu &= \sum_\sigma a_l^\dagger a_k = E_{lk} \end{aligned} \tag{41}$$

with $k > l$ and the variations in the configuration space are described in terms of state transfer operators

$$\begin{aligned} R_n^\dagger &= |n\rangle\langle 0|; \\ R_n &= |0\rangle\langle n| \end{aligned} \tag{42}$$

where $|n>$ denotes an orthogonal basis for the orthogonal complement. The symbols $q^\dagger$ and $R^\dagger$ without subscripts denote vectors consisting of $q_\nu^\dagger$ and $R_n^\dagger$, respectively. We include only the non-redundant orbital operators[54, 55].

We require that $|0\rangle$ satisfy the generalized Brillouin condition

$$\begin{pmatrix} \langle 0|[q^\dagger, H_0]|0\rangle \\ \langle 0|[R^\dagger, H_0]|0\rangle \end{pmatrix} = \begin{pmatrix} 0 \\ 0 \end{pmatrix} \tag{43}$$

that is, we assume that $|0\rangle$ is optimized with respect to variations in the orbital and configuration space.

The time development of $|0\rangle$ is parametrized as

$$|\bar{0}\rangle = \exp[i\kappa(t)]\exp[iS(t)]|0\rangle \tag{44}$$

where $\exp[i\kappa(t)]$ describes variations in the orbital space

$$\kappa(t) = \kappa_\nu q_\nu^\dagger + \kappa_\nu^* q_\nu, \tag{45}$$

and $\exp[iS(t)]$ describes variations in the configuration space

$$S(t) = S_n R_n^\dagger + S_n^* R_n, \tag{46}$$

The parameters κ and S in these equations depend on time.

The operators are collected in a row vector

$$T = (t^\dagger, t) = (q^\dagger, R^\dagger, q, R) \tag{47}$$

and the amplitudes in a column vector

$$\beta = \begin{pmatrix} \gamma \\ \gamma^* \end{pmatrix} = \begin{pmatrix} \kappa \\ S \\ \kappa^* \\ S^* \end{pmatrix} \tag{48}$$

It is often convenient to describe the time development in a more general basis

$$O = (t^\dagger, t)\mathbf{X} \tag{49}$$

where the transformation matrix

$$\mathbf{X} = \begin{pmatrix} {}^1X & {}^2X^* \\ {}^2X & {}^1X^* \end{pmatrix} \tag{50}$$

is chosen to conserve the adjoint structure of the basis. In this basis the rotation parameters become

$$\alpha = \mathbf{X}^{-1} \begin{pmatrix} \gamma \\ \gamma^* \end{pmatrix} \tag{51}$$

and the adjoint nature of γ is thus conserved in α. We use O_j for a general rotation operator; O_{c_j} for the configuration part $\{R, R^\dagger\}$ of O_j and O_{o_j} for the orbital rotation part $\{q, q^\dagger\}$ of O_j. We use the notation of ref. [23] (Eq. 5.19) where the orbital and state rotation operators are written as

$$\begin{aligned} \kappa(t) &= \textstyle\sum_{j=-d}^{d} \alpha_j O_{o_j} \\ S(t) &= \textstyle\sum_{j=-d}^{d} \alpha_j O_{c_j} \end{aligned} \tag{52}$$

where the dimension d is the total dimension of the space of configuration and orbital rotation operators. We further define a superoperator $\hat{O}$, by

$$\hat{O}A = [O, A] \tag{53}$$

The time development is determined by imposing Ehrenfest's theorem on the set of rotation operators in the time-transformed orbital basis (see Eq. (5.20) in ref. [23])

$$\tilde{T}^{+} = \begin{pmatrix} \tilde{q}^{\dagger} \\ \tilde{R}^{\dagger} \\ \tilde{q} \\ \tilde{R} \end{pmatrix} \tag{54}$$

The evaluation of Ehrenfest's theorem for this set of operators with respect to the time-dependent MCSCF wave function (18) is straightforward but tedious and is described in detail in Eq's 5.20 - 5.50 in ref. [23]. The resulting series of coupled equations reads (Eq. (5.49) in ref. [23])

$$\sum_{n=1}^{\infty}(i)^n S^{[n+1]}_{jl_1l_2\ldots l_n}\dot{\alpha}_{l_1}\prod_{\mu=2}^{n}\alpha_{l_\mu} = -\sum_{n=0}^{\infty}(i)^{n+1}E^{[n+1]}_{jl_1l_2\ldots l_n}\prod_{\mu=1}^{n}\alpha_{l_\mu}$$

$$-\sum_{n=0}^{\infty}(i)^{n+1}\int_{-\infty}^{+\infty}d\omega_1(\exp[-i(\omega_1+i\epsilon)]t)V^{\omega_1}_{jl_1l_2\ldots l_n}\prod_{\mu=1}^{n}\alpha_{l_\mu} \tag{55}$$

where α refers to a combined set of orbital and configuration parameters. The expressions for all the quantities involved are explicitly given below.

$$E^{[n+1]}_{jl_1\ldots l_n} = \sum_{k=0}^{n}\frac{(-)^n}{(k!(n-k)!)}\Big\{\langle 0|\left[O^{\dagger}_{c_j},\prod_{\mu=1}^{k}\hat{O}_{c_{l_\mu}}\left(\prod_{\mu=k+1}^{n}\hat{O}_{o_{l_\mu}}H_0\right)\right]|0\rangle$$
$$+\langle 0|\prod_{\mu=1}^{k}\hat{O}_{c_{l_\mu}}\left[O^{\dagger}_{o_j},\left(\prod_{\mu=k+1}^{n}\hat{O}_{o_{l_\mu}}H_0\right)\right]|0\rangle\Big\}; \tag{56}$$

$$S^{[n+1]}_{jl_1\ldots l_n} = \sum_{k=0}^{n-1}\frac{1}{k!(n-k)!}\Big\{(-)^k\langle 0|\prod_{\mu=2}^{k+1}\hat{O}_{c_{l_\mu}}\left[O^{\dagger}_{o_j},\left(\prod_{\mu=k+2}^{n}\hat{O}_{c_{l_\mu}}O_{c_{l_1}}\right)\right]|0\rangle$$
$$+(-)^{(n-1)}\langle 0|\prod_{\mu=2}^{k+1}\hat{O}_{c_{l_\mu}}\left[O^{\dagger}_{o_j},\left(\prod_{\mu=k+2}^{n}\hat{O}_{o_{l_\mu}}O_{o_{l_1}}\right)\right]|0\rangle$$
$$+(-)^{(n-1)}\langle 0|\left[O^{\dagger}_{c_j},\prod_{\mu=2}^{k+1}\hat{O}_{c_{l_\mu}}\left(\prod_{\mu=k+2}^{n}\hat{O}_{o_{l_\mu}}O_{o_{l_1}}\right)\right]|0\rangle\Big\}$$
$$+\frac{(-)^{(n-1)}}{n!}\langle 0|\left[O^{\dagger}_{c_j},\prod_{\mu=2}^{n}\hat{O}_{c_{l_\mu}}O_{c_{l_1}}\right]|0\rangle; \tag{57}$$

$$V^{\omega_1[n+1]}_{jl_1\ldots l_n} =$$
$$\sum_{k=0}^{n}\frac{(-)^n}{(k!(n-k)!)}\Big\{\langle 0|\left[O^{\dagger}_{c_j},\prod_{\mu=1}^{k}\hat{O}_{c_{l_\mu}}\left(\prod_{\mu=k+1}^{n}\hat{O}_{o_{l_\mu}}V^{\omega_1}\right)\right]|0\rangle +$$
$$\langle 0|\prod_{\mu=1}^{k}\hat{O}_{c_{l_\mu}}\left[O^{\dagger}_{o_j},\left(\prod_{\mu=k+1}^{n}\hat{O}_{o_{l_\mu}}V^{\omega_1}\right)\right]|0\rangle\Big\}. \tag{58}$$

In terms of these quantities, the first order equation becomes

$$iS^{[2]}_{jl}\dot{\alpha}^{(1)}_{l} - E^{[2]}_{jl}\alpha^{(1)}_{l} = -iV^{t[1]}_{j} \tag{59}$$

and the second order equation reads

$$iS^{[2]}_{jl}\dot{\alpha}^{(2)}_l - E^{[2]}_{jl}\alpha^{(2)}_l = iS^{[3]}_{jlm}\dot{\alpha}^{(1)}_l\alpha^{(1)}_m + iE^{[3]}_{jlm}\alpha^{(1)}_l\alpha^{(1)}_m + V^{t[2]}_{jl}\alpha^{(1)}_l. \tag{60}$$

where the relation between $V^{\omega_1[n+1]}_{jl_1\ldots l_n}$ and $V^{t[n+1]}_{jl_1\ldots l_n}$ is given in ref. [23](Eq.s (5.47) and (5.48)).

II Response functions in the MCSCF approximation

We now give the expressions for the linear and quadratic response functions in the MCSCF approximation. The expectation value of an operator A is, in the MCSCF approximation, written as $\langle\bar{0}|A|\bar{0}\rangle$, which, by defining $A^{[n]}_{l_1\ldots l_n}$ as

$$A^{[n]}_{l_1\ldots l_n} = \sum_{k=0}^{n}\frac{(-)^n}{k!(n-k)!}\langle 0|\prod_{\mu=1}^{k}\hat{O}_{c_{l_\mu}}\left(\prod_{\mu=k+1}^{n}\hat{O}_{o_{l_\mu}}A\right)|0\rangle \tag{61}$$

can be written as

$$\langle\bar{0}|A|\bar{0}\rangle = \sum_{n=0}^{\infty}(i)^n A^{[n]}_{l_1,\ldots,l_n}\prod_{\mu=1}^{n}\alpha_{l_\mu} \tag{62}$$

(see Eq. (5.86) in [23]). In ref. [23] it is described how the first and second order equations in Eq. (59) and (60) can be solved. We denote the Fourier transforms of the solution vectors $\alpha^{(1)}(t)$ and $\alpha^{(2)}(t)$ by $f^{(1)}(\omega_1)$ and $f^{(2)}(\omega_1,\omega_2)$, respectively. The first and second order equations can be expressed in the basis where $E^{[2]}_{jl}$ and $S^{[2]}_{jl}$ are simultaneously diagonal

$$E^{[2]}X_j = \omega_{j0}S^{[2]}X_j \tag{63}$$

We find

$$f^{(1)}_j(\omega_1) = \frac{V^{\omega_1[1]}_j}{\omega_1 - \mathrm{sgn}(j)\omega_j + i\epsilon} \tag{64}$$

and

$$f^{(2)}_j(\omega_1,\omega_2) =$$
$$\left\{\tfrac{1}{2}\left\{\mathrm{sgn}(lm)\left[E^{[3]}_{jlm} + E^{[3]}_{jml} - S^{[3]}_{jlm}(\omega_1+i\epsilon) - S^{[3]}_{jml}(\omega_2+i\epsilon)\right]\times f^{(1)}_l(\omega_1)f^{(1)}_m(\omega_2)\right\}\right.$$
$$\left.+\tfrac{1}{2}\left\{\mathrm{sgn}(l)\left[V^{\omega_1[2]}_{jl}f^{(1)}_l(\omega_2) + V^{\omega_2[2]}_{jl}f^{(1)}_l(\omega_1)\right]\right\}\right\}\times$$
$$\left\{\frac{1}{\omega_1+\omega_2-\mathrm{sgn}(j)\omega_j+2i\epsilon}\right\} \tag{65}$$

in terms of which the response functions in the MCSCF approximation can be defined [23] (Einsteins summation convention is here assumed). We have here symmetrized the expression for $f^{(2)}_j(\omega_1,\omega_2)$ in ω_1 and ω_2.

The linear response function is seen to be

$$\langle\langle A;V^{\omega}\rangle\rangle_{\omega} = \mathrm{sgn}(j)f^{(1)}_j(\omega_1)A^{[1]}_j \tag{66}$$

and the quadratic response function

$$\langle\langle A; V^{\omega_1}, V^{\omega_2}\rangle\rangle_{\omega_1,\omega_2} = P(1,2)\left\{\mathrm{sgn}(jk)A^{[2]}_{jk}f^{(1)}_j(\omega_1)f^{(1)}_k(\omega_2) + \mathrm{sgn}(j)A^{[1]}_j f^{(2)}_j(\omega_1,\omega_2)\right\} \tag{67}$$

Using the notation B for V^{ω_1} and introducing expression 64 for $f^{(1)}(\omega_1)$, we may write the linear response formulation

$$\langle\langle A; B\rangle\rangle_{\omega_1} = sgn(j)\frac{A^{[1]}_j B^{[1]}_j}{\omega_1 - sgn(j)\omega_j + i\epsilon)} \tag{68}$$

Similarly, using B for V^{ω_1} and C for V^{ω_2}, and introducing the explicit expressions for $f^{(1)}(\omega_1)$ and $f^{(2)}(\omega_1,\omega_2)$ we may write the quadratic response function

$$\begin{aligned}
\langle\langle A; B, C\rangle\rangle_{\omega_1,\omega_2} &= \mathrm{sgn}(jk)\frac{B^{[1]}_j\left(A^{[2]}_{jk} + A^{[2]}_{kj}\right)C^{[1]}_k}{(\omega_1 - \mathrm{sgn}(j)\omega_j + i\epsilon)(\omega_2 - \mathrm{sgn}(k)\omega_k + i\epsilon)} \\
+\mathrm{sgn}(jlm)\times &\frac{A^{[1]}_j\left(E^{[3]}_{jlm} + E^{[3]}_{jml} - S^{[3]}_{jlm}(\omega_1 + i\epsilon) - S^{[3]}_{jml}(\omega_2 + i\epsilon)\right)B^{[1]}_l C^{[1]}_m}{(\omega_1 + \omega_2 - \mathrm{sgn}(j)\omega_j + 2i\epsilon)(\omega_1 - \mathrm{sgn}(l)\omega_l + i\epsilon)(\omega_2 - \mathrm{sgn}(m)\omega_m + i\epsilon)} \\
&+\mathrm{sgn}(jl)\frac{A^{[1]}_j C^{[2]}_{jl} B^{[1]}_l}{(\omega_1 + \omega_2 - \mathrm{sgn}(j)\omega_j + 2i\epsilon)(\omega_1 - \mathrm{sgn}(l)\omega_l + i\epsilon)} \\
&+\mathrm{sgn}(jl)\frac{A^{[1]}_j B^{[2]}_{jl} C^{[1]}_l}{(\omega_1 + \omega_2 - \mathrm{sgn}(j)\omega_j + 2i\epsilon)(\omega_2 - \mathrm{sgn}(l)\omega_l + i\epsilon)}
\end{aligned} \tag{69}$$

We can identify the second order moment by taking the residue of the quadratic response function at $\omega_2 \to \omega_f$ and by comparing to the residue of the response function for an exact state

$$\begin{aligned}
&-\left\{\frac{\langle 0|A|j\rangle(\langle j|B - \langle 0|B|0\rangle)|f\rangle}{\omega_j - \omega_f + \omega_1} + \frac{\langle 0|B|j\rangle(\langle j|A - \langle 0|A|0\rangle)|f\rangle}{\omega_j - \omega_1}\right\} \\
+ &\frac{\mathrm{sgn}(j)B^{[1]}_j\left(A^{[2]}_{jf} + A^{[2]}_{fj}\right)}{(-\omega_1 - \mathrm{sgn}(j)\omega_j)} + \mathrm{sgn}(jl)\frac{A^{[1]}_j\left(E^{[3]}_{jlf} + E^{[3]}_{jfl} + \omega_1 S^{[3]}_{jlf} - \omega_f S^{[3]}_{jfl}\right)B^{[1]}_l}{(\omega_f - \omega_1 - \mathrm{sgn}(j)\omega_j)(-\omega_1 - \mathrm{sgn}(l)\omega_l)} \\
&+\mathrm{sgn}(j)\frac{A^{[1]}_j B^{[2]}_{jf}}{(\omega_f - \omega_1 - \mathrm{sgn}(j)\omega_j)}
\end{aligned} \tag{70}$$

and the transition moment between excited states by taking the residue of the quadratic response function at $\omega_1 \to -\omega_g$ and $\omega_2 \to \omega_f$, and then comparing to the exact state

$$\langle g|A - \langle 0|A|0\rangle|f\rangle =$$

$$-(A^{[2]}_{-gf} + A^{[2]}_{f-g}) - \frac{\mathrm{sgn}(j)A^{[1]}_j\left(E^{[3]}_{j-gf} + E^{[3]}_{jf-g} + \omega_g S^{[3]}_{j-gf} - \omega_f S^{[3]}_{jf-g}\right)}{(\omega_f - \omega_g - \mathrm{sgn}(j)\omega_j)} \tag{71}$$

The calculation of the quadratic response function and its residues may be performed in a similar manner, since they contain the same matrices.

In order to evaluate the quadratic response function and its residues it is convenient to work in the basis represented by the elementary operators. Rewriting the above equations is done by using (ref. [23]; Eq. 6.6)

$$\frac{-f_j g_j}{\omega_j - \mathrm{sgn}(j)C} = -{}^e\mathbf{f}({}^eE^{[2]} - X\,{}^eS^{[2]})^{-1}\,{}^e\mathbf{g} \tag{72}$$

where X is a constant. The linear response function may be expressed in terms of the solution of one linear response equation

$$N^b(\omega_1) = \left[\left({}^eE^{[2]} - \omega_1\,{}^eS^{[2]}\right)^{-1}\right]{}^eB^{[1]} \tag{73}$$

Inserting this equation into Eq. 68 gives the linear response function

$$\langle\langle A_j; B_j\rangle\rangle_{\omega_1} = {}^eA_j^{[1]}N_j(\omega_1) \tag{74}$$

The quadratic response function may be expressed in terms of the solution vectors of three linear response equations

$$\begin{aligned} N^a(\omega_1+\omega_2) &= \left[\left({}^eE^{[2]} - (\omega_1+\omega_2)\,{}^eS^{[2]}\right)^{-1}{}^eA^{[1]}\right]^\dagger \\ N^b(\omega_1) &= \left({}^eE^{[2]} - \omega_1\,{}^eS^{[2]}\right)^{-1}{}^eB^{[1]} \\ N^c(\omega_2) &= \left({}^eE^{[2]} - \omega_2\,{}^eS^{[2]}\right)^{-1}{}^eC^{[1]} \end{aligned} \tag{75}$$

Inserting these solution vectors into Eq. 69 gives for the hyperpolarizability

$$\begin{aligned} \langle\langle A; B, C\rangle\rangle_{\omega_1,\omega_2} &= N_j^a(\omega_1+\omega_2)\,{}^eB_{jl}^{[2]}N_l^c(\omega_2) \\ &+N_j^a(\omega_1+\omega_2)\,{}^eC_{jl}^{[2]}N_l^b(\omega_1) + N_j^b(\omega_1)\left({}^eA_{jk}^{[2]} + {}^eA_{kj}^{[2]}\right)N_k^c(\omega_2) \\ &-N_j^a(\omega_1+\omega_2)\left({}^eE_{jlm}^{[3]} + {}^eE_{jml}^{[3]} - \omega_1\,{}^eS_{jlm}^{[3]} - \omega_2\,{}^eS_{jml}^{[3]}\right)\times N_l^b(\omega_1)N_m^c(\omega_2). \end{aligned} \tag{76}$$

The second order transition moment between the reference state $|0\rangle$ and the final state $|f\rangle$ may be expressed in terms of the two solution vectors $N_j^a(\omega_f-\omega_1)$ and $N_m^b(-\omega_1)$ and the eigenvector X_{lf}

$$\begin{aligned} &-\left\{\frac{\langle 0|A|j\rangle\langle j|(B-\langle 0|B|0\rangle)|f\rangle}{(\omega_j-\omega_f+\omega_1)} + \frac{\langle 0|B|j\rangle\langle j|(A-\langle 0|A|0\rangle)|f\rangle}{(\omega_j-\omega_1)}\right\} = \\ &-N_j^a(\omega_f-\omega_1)\,{}^eB_{jl}^{[2]}X_{lf} - N_j^b(-\omega_1)\left({}^eA_{jl}^{[2]} + {}^eA_{lj}^{[2]}\right)X_{lf} \\ &+N_j^a(\omega_f-\omega_1)\times \\ &\left({}^eE_{jml}^{[3]} + {}^eE_{jlm}^{[3]} - \omega_1\,{}^eS_{jml}^{[3]} - \omega_f\,{}^eS_{jlm}^{[3]}\right)N_m^b(-\omega_1)X_{lf}. \end{aligned} \tag{77}$$

The transition matrix element between excited states $\langle g|$ and $|f\rangle$ may be expressed in terms of the solution vector $N_j^a(\omega_f - \omega_g)$ and the eigensolutions X_{lf} and X_{m-g}

$$\langle g|A|f\rangle - \delta_{gf}\langle 0|A|0\rangle = -\left({}^eA_{jl}^{[2]} + {}^eA_{lj}^{[2]}\right) X_{j-g}X_{lf}$$

$$+N_j^a(\omega_f - \omega_g)\left({}^eE_{jml}^{[3]} + {}^eE_{jlm}^{[3]} + \omega_g\,{}^eS_{jml}^{[3]} - \omega_f\,{}^eS_{jlm}^{[3]}\right) X_{lf}X_{m-g}. \tag{78}$$

The evaluation of the linear response function requires one first order linear response equation to be solved. The evaluation of the quadratic response function requires three first order linear response equations to be solved in accordance with the common $2n + 1$ rule in perturbation theory. To evaluate the residue in Eq. (77) we require two linear response equations to be solved and one eigensolution to be determined. The transition moment between excited states, given in Eq. (78) requires one linear response equation to be solved and the determination of two eigensolutions. The evaluation of both the quadratic response function and its residues requires linear transformations of $E^{[3]}$ and $S^{[3]}$ with two solution vectors and $A^{[2]}$ and $V^{[2]}$ with one solution vector.

III Evaluation of the linear transformations

The evaluation of the linear and quadratic response functions requires that a set of linear response equations are solved. To calculate properties for a state different from the reference state, the eigenvectors and eigenvalues for the response eigenvalue equation Eq. (63) must be determined for the state. Due to the fact that the dimension of each of the matrices $E^{[2]}$ and $S^{[2]}$ may be very large, iterative techniques must be used to solve these equations. In [56] we have described how both the linear response equations and the linear response eigenvalue equations can be solved efficiently using iterative techniques. Very essential for obtaining an efficient algorithm is to use the paired structure of the $E^{[2]}$ and $S^{[2]}$ matrices. We refer to [56] for details. Iterative techniques require linear transformations of $E^{[2]}$ and $S^{[2]}$ on trial vectors N. The same linear transformations are needed for solving the linear response equations and the linear response eigenvalue equation. Here we give explicit expressions for these linear transformations as well as the linear transformations that are needed for evaluating the quadratic response function. These include the multiplication of $E_{jkl}^{[3]}$ on ${}^1N_k$ and ${}^2N_l$; $S_{jlm}^{[3]}$ on ${}^1N_l$ and ${}^2N_m$; $A_{jl}^{[2]}$ on N_l and $V_{jl}^{[2]}$ on N_l. A trial vector has the general structure

$${}^iN = \begin{pmatrix} {}^i\kappa \\ {}^iS \\ {}^i\kappa' \\ {}^iS' \end{pmatrix}, i = 1, 2. \tag{79}$$

Before we give the linear transformations we introduce some definitions of quantities that enter in the linear transformations. These include the transformed Hamiltonian

$$H_0(\kappa) = [(\kappa_l q_l^\dagger + \kappa_l' q_l), H_0], \tag{80}$$

the doubly transformed Hamiltonian

$$H_0({}^1\kappa, {}^2\kappa) = [({}^1\kappa_k q_k^\dagger + {}^1\kappa_k' q_k), [({}^2\kappa_k q_k^\dagger + {}^2\kappa_k' q_k), H_0]], \tag{81}$$

and the transformed states

$$|0^R\rangle = -S_k R_k^\dagger |0\rangle; \quad \langle 0^L| = \langle 0|(S_k' R_k) \tag{82}$$

The linear transformation of $E^{[2]}$ on a trial vector can now be written as

$$\begin{aligned} {}^e E^{[2]}_{jlk} N_k \quad &= -\begin{pmatrix} \langle 0^L|[q_j, H_0]|0\rangle + \langle 0|[q_j, H_0]|0^R\rangle \\ \langle j|H_0|0\rangle \\ \langle 0^L|[q_j^\dagger, H_0]|0\rangle + \langle 0|[q_j^\dagger, H_0]|0^R\rangle \\ -\langle 0^L|H_0|j\rangle \end{pmatrix} \\ &\quad -\begin{pmatrix} \langle 0|[q_j, H_0(\kappa)]|0\rangle \\ \langle j|H_0(\kappa)|0\rangle \\ \langle 0|[q_j^\dagger, H_0(\kappa)]|0\rangle \\ -\langle 0|H_0(\kappa)|j\rangle \end{pmatrix} - \langle 0|H_0|0\rangle \begin{pmatrix} 0 \\ S_j \\ 0 \\ S_j' \end{pmatrix} \end{aligned} \tag{83}$$

We will in the next subsection see that the transformed Hamiltonian has the form of a normal Hamiltonian, but with one-index transformed integrals. These one-index transformed integrals have only permutational symmetry between the two electrons. The linear transformation of $S^{[2]}$ on trial vector becomes

$$\begin{aligned} \sum_k S^{(2)0}_{jk} N_k \qquad &= -\begin{pmatrix} \langle 0|[q_j, \hat{\kappa}]|0\rangle \\ \langle j|\hat{\kappa}|0\rangle \\ \langle 0|[q_j^\dagger, \hat{\kappa}]|0\rangle \\ -\langle 0|\hat{\kappa}|j\rangle \end{pmatrix} \\ &\quad + \begin{pmatrix} \langle 0|q_j|0^R\rangle - \langle 0^L|q_j|0\rangle \\ S_j \\ \langle 0|q_j^\dagger]|0^R\rangle - \langle 0^L|q_j^\dagger|0\rangle \\ -S_j{}' \end{pmatrix} \end{aligned} \tag{84}$$

For the symmetrized version of $E^{[3]}$ the linear transformations on two vectors becomes

$$\begin{aligned} (E^{[3]}_{jkl} + E^{[3]}_{jlk})\, {}^1N_k\, {}^2N_l = \quad & \tfrac{1}{2}\begin{pmatrix} \langle 0|[q_j, H_0({}^1\kappa, {}^2\kappa)]|0\rangle \\ \langle j|H_0({}^1\kappa, {}^2\kappa)|0\rangle \\ \langle 0|[q_j^\dagger, H_0({}^1\kappa, {}^2\kappa)]|0\rangle \\ -\langle 0|H_0({}^1\kappa, {}^2\kappa)|j\rangle \end{pmatrix} + \tfrac{1}{2}\begin{pmatrix} \langle 0|[q_j, H_0({}^2\kappa, {}^1\kappa)]|0\rangle \\ \langle j|H_0({}^2\kappa, {}^1\kappa)|0\rangle \\ \langle 0|[q_j^\dagger, H_0({}^2\kappa, {}^1\kappa)]|0\rangle \\ -\langle 0|H_0({}^2\kappa, {}^1\kappa)|j\rangle \end{pmatrix} \\ & + \begin{pmatrix} \langle 0^{2L}|[q_j, H_0({}^1\kappa)]|0\rangle + \langle 0|[q_j, H_0({}^1\kappa)]|0^{2R}\rangle \\ \langle j|H_0({}^1\kappa)|0^{2R}\rangle \\ \langle 0^{2L}|[q_j^\dagger, H_0({}^1\kappa)]|0\rangle + \langle 0|[q_j^\dagger, H_0({}^1\kappa)]|0^{2R}\rangle \\ -\langle 0^{2L}|H_0({}^1\kappa)|j\rangle \end{pmatrix} \\ & + \begin{pmatrix} \langle 0^{1L}|[q_j, H_0({}^2\kappa)]|0\rangle + \langle 0|[q_j, H_0({}^2\kappa)]|0^{1R}\rangle \\ \langle j|H_0({}^2\kappa)|0^{1R}\rangle \\ \langle 0^{1L}|[q_j^\dagger, H_0({}^2\kappa)]|0\rangle + \langle 0|[q_j^\dagger, H_0({}^2\kappa)]|0^{1R}\rangle \\ -\langle 0^{1L}|H_0({}^2\kappa)|j\rangle \end{pmatrix} \\ & + \begin{pmatrix} \langle 0^{1L}|[q_j, H_0]|0^{2R}\rangle + \langle 0^{2L}|[q_j, H_0]|0^{1R}\rangle \\ 0 \\ \langle 0^{1L}|[q_j^\dagger, H_0]|0^{2R}\rangle + \langle 0^{2L}|[q_j^\dagger, H_0]|0^{1R}\rangle \\ 0 \end{pmatrix} \end{aligned} \tag{85}$$

This expression has been given in a somewhat modified form in ref. [23]. It may be evaluated using a generalization of the techniques for evaluating an MCSCF gradient, which will be described in the next subsection.

$S^{[3]}_{jlm}\ {}^1N_l\ {}^2N_m$ can be seen to give

$$
\begin{aligned}
S^{[3]}_{jlm}\quad {}^1N_l\ {}^2N_m = -\tfrac{1}{2}&\begin{pmatrix}
\langle 0|[q_j,[({}^2\kappa_m q_m^\dagger + {}^2\kappa'_m q_m),({}^1\kappa_l q_l^\dagger + {}^1\kappa'_l q_l)]]|0\rangle \\
\langle j|[[({}^2\kappa_m q_m^\dagger + {}^2\kappa'_m q_m),({}^1\kappa_l q_l^\dagger + {}^1\kappa'_l q_l)]|0\rangle \\
\langle 0|[q_j^\dagger,[({}^2\kappa_m q_m^\dagger + {}^2\kappa'_m q_m),({}^1\kappa_l q_l^\dagger + {}^1\kappa'_l q_l)]]|0\rangle \\
-\langle 0|[[({}^2\kappa_m q_m^\dagger + {}^2\kappa'_m q_m),({}^1\kappa_l q_l^\dagger + {}^1\kappa'_l q_l)]|j\rangle
\end{pmatrix} \\
-&\begin{pmatrix}
\langle 0^{2L}|[q_j,({}^1\kappa_l q_l^\dagger + {}^1\kappa'_l q_l)]|0\rangle + \langle 0|[q_j,({}^1\kappa_l q_l^\dagger + {}^1\kappa'_l q_l)]|0^{2R}\rangle \\
\langle j|({}^1\kappa_l q_l^\dagger + {}^1\kappa'_l q_l)|0^{2R}\rangle \\
\langle 0^{2L}|[q_j^\dagger,({}^1\kappa_l q_l^\dagger + {}^1\kappa'_l q_l)]|0\rangle + \langle 0|[q_j^\dagger,({}^1\kappa_l q_l^\dagger + {}^1\kappa'_l q_l)]|0^{2R}\rangle \\
-\langle 0^{2L}|({}^1\kappa_l q_l^\dagger + {}^1\kappa'_l q_l)|j\rangle
\end{pmatrix} \\
+&\begin{pmatrix}
\langle 0^{2L}|q_j|0^{1R}\rangle + \langle 0^{1L}|q_j|0^{2R}\rangle \\
0 \\
\langle 0^{2L}|q_j^\dagger|0^{1R}\rangle + \langle 0^{1L}|q_j^\dagger|0^{2R}\rangle \\
0
\end{pmatrix} \\
-&\begin{pmatrix}
0 \\
{}^2S_j\langle 0|({}^1\kappa_l q_l^\dagger + {}^1\kappa'_l q_l)|0\rangle \\
0 \\
{}^2S'_j\langle 0|({}^1\kappa_l q_l^\dagger + {}^1\kappa'_l q_l)|0\rangle
\end{pmatrix} \\
+&({}^1S_l\,{}^2S'_l + {}^1S'_l\,{}^2S_l)\begin{pmatrix}
\langle 0|q_j|0\rangle \\
0 \\
\langle 0|q_j^\dagger|0\rangle \\
0
\end{pmatrix}
\end{aligned}
\tag{86}
$$

We note that Eq. (86) is not symmetric in vector ${}^1N$ and vector ${}^2N$.

The linear transformation of $V^{[2]}_{jl}$ on one vector becomes

$$
\begin{aligned}
V^{[2]}_{jl}N_l \qquad = &-\begin{pmatrix}
\langle 0|[q_j,V^\omega(\kappa)]|0\rangle \\
\langle j|V^\omega(\kappa)|0\rangle \\
\langle 0|[q_j^\dagger,V^\omega(\kappa)]|0\rangle \\
-\langle 0|V^\omega(\kappa)|j\rangle
\end{pmatrix} \\
-&\begin{pmatrix}
\langle 0^L|[q_j,V^\omega]|0\rangle + \langle 0|[q_j,V^\omega]|0^R\rangle \\
\langle j|V^\omega|0^R\rangle \\
\langle 0^L|[q_j^\dagger,V^\omega]|0\rangle + \langle 0|[q_j^\dagger,V^\omega]|0^R\rangle \\
-\langle 0^L|V^\omega|j\rangle
\end{pmatrix} \\
-&\langle 0|V^\omega|0\rangle\begin{pmatrix}
0 \\
S_j \\
0 \\
S'_j
\end{pmatrix}
\end{aligned}
\tag{87}
$$

In the same way, using the expression for $A^{[2]}_{jk}$, we find, using the previous definitions

$$\begin{aligned} A^{[2]}_{jk}N_k &= \begin{pmatrix} \frac{1}{2}\langle 0|[q_j^\dagger, A(\kappa)]|0\rangle \\ -\langle 0|A(\kappa)|j\rangle \\ \frac{1}{2}\langle 0|[q_j, A(\kappa)]|0\rangle \\ \langle j|A(\kappa)|0\rangle \end{pmatrix} \\ &+\tfrac{1}{2}\begin{pmatrix} 0 \\ -\langle 0^L|A|j\rangle \\ 0 \\ \langle j|A|0^R\rangle \end{pmatrix} \\ &+\tfrac{1}{2}\langle 0|A|0\rangle \begin{pmatrix} 0 \\ S'_j \\ 0 \\ S_j \end{pmatrix} \end{aligned} \tag{88}$$

IV Computational implementation

In this subsection, we discuss the implementation of the expressions above, especially the ones related to $E^{[2]}$ multiplied on one vector and $E^{[3]}$ multiplied on two vectors. The orbital part related to the linear transformation is formally equivalent to evaluating a gradient of an orbital excitation operator, but now with transformed Hamiltonians and states. We use the technology of linear transformations discussed earlier. We start with the form of the Hamiltonian in second quantization

$$H_0 = \sum_{pq} h^1_{pq} E_{pq} + \sum_{pqrs} h^2_{pqrs} e_{pqrs} \tag{89}$$

where we have used the definitions

$$E_{pq} = \sum_\sigma a^\dagger_{p\sigma} a_{q\sigma} \tag{90}$$

and

$$e_{pqrs} = E_{pq}E_{rs} - \delta_{qr}E_{ps}. \tag{91}$$

If we now consider the Hamiltonian $H_0(\kappa)$, we get

$$H_0(\kappa) = \sum_{i,j}[\kappa_{ij}a^\dagger_i a_j, H_0] = \sum_{pq}\tilde{h}^1_{pq}E_{pq} + \sum_{pqrs}\tilde{h}^2_{pqrs}e_{pqrs} \tag{92}$$

where the one-index transformed integrals $\tilde{h}^1_{pq}$ and $\tilde{h}^2_{pqrs}$ are defined as

$$\begin{aligned} \tilde{h}^1_{pq} &= \sum_i (\kappa_{pi}h^1_{iq} - \kappa_{iq}h^1_{pi}) \\ \tilde{h}^2_{pqrs} &= \sum_i (\kappa_{pi}h^2_{iqrs} + \kappa_{ri}h^2_{pqis} - \kappa_{is}h^2_{pqri} - \kappa_{iq}h^2_{pirs}) \end{aligned} \tag{93}$$

In the same way, we can define the doubly one-index transformed integrals, by operating again with an orbital operator on $H_0(\kappa)$,

$$H_0({}^1\kappa, {}^2\kappa) = \sum_{ij}[{}^1\kappa_{ij}E_{ij}, H_0({}^2\kappa)] = \sum_{pq}\tilde{\tilde{h}}^1_{pq}E_{pq} + \sum_{pqrs}\tilde{\tilde{h}}^2_{pqrs}e_{pqrs} \tag{94}$$

where the doubly one-index transformed integrals can be determined using Eqs. (93). The one-index transformed and double one-index transformed integrals possess only the symmetry reflecting the interchange of particle 1 and particle 2, all other permutation symmetry is lost.

We consider now a generalized Hamiltonian K

$$K = \sum_{pq} k^1_{pq} E_{pq} + \sum_{pqrs} k^2_{pqrs} e_{pqrs} \tag{95}$$

where the integrals k^1_{pq} and k^2_{pqrs} for example can be the transformed integrals defined above.

We will determine the elements of a gradient with the operator K. Inspection of the previous formulas leads us to consider, for the orbital part of the linear transformations

$$F_{mn} = \langle L|[E_{nm}, K]|R\rangle \tag{96}$$

where $\langle L|$ and $|R\rangle$ are either the reference state wave function or one of the transformed states defined above. We denote inactive orbitals by i, j, k, l, active orbitals by t, u, v, w, x, y and secondary orbitals by a, b, c, d. General indices of the orbitals are m, n, p, q, r, s. Following a standard procedure, we define generalized one- and two-particle density matrices

$$\begin{aligned} D_{pq} &= \langle L|E_{pq}|R\rangle, \\ d_{pqrs} &= \langle L|e_{pqrs}|R\rangle, \end{aligned} \tag{97}$$

We assume that the density matrices are real. From Eq. 96 we find

$$F_{mn} = f^1_{nm} - f^2_{mn} \tag{98}$$

with f^1_{nm} and f^2_{mn} defined as

$$\begin{aligned} f^1_{nm} &= \textstyle\sum_\sigma \langle L|a^\dagger_{n\sigma}[a_{m\sigma}, K]|R\rangle \\ f^2_{mn} &= \textstyle\sum_\sigma \langle L|[K, a^\dagger_{n\sigma}]a_{m\sigma}|R\rangle \end{aligned} \tag{99}$$

Evaluating the commutators gives straightforward expressions in terms of density matrices

$$\begin{aligned} f^1_{nm} &= \textstyle\sum_p k^1_{mp} D_{np} + \sum_{pqr} k^2_{mpqr} d_{npqr} \\ f^2_{mn} &= \textstyle\sum_p k^1_{pn} D_{mp} + \sum_{pqr} k^2_{pqrn} d_{mrqp} \end{aligned} \tag{100}$$

The possible states $\langle L|$ and $|R\rangle$ differ only in the occupation of the active orbitals. This has the consequence that the density matrix elements which contain inactive or secondary orbital indices simplify as

$$\begin{aligned} D_{ip} &= D_{pi} = 2\delta_{ip} \\ D_{ap} &= D_{pa} = 0 \end{aligned} \tag{101}$$

and

$$\begin{aligned} d_{ipqr} &= d_{qrip} = 2\delta_{ip} D_{qr} - \delta_{ri} D_{qp} \\ d_{apqr} &= d_{qrap} = 0 \end{aligned} \tag{102}$$

Introducing generalizations [14] of the inactive Fock matrix F^I,

$$F^I_{pq} = k^1_{pq} + \sum_j [2k^2_{pqjj} - k^2_{pjjq}], \tag{103}$$

the active Fock matrix

$$F^A_{pq} = \sum_{xy} [2k^2_{pqxy} - k^2_{pyxq}] D_{xy}, \tag{104}$$

and the Q matrices

$$\begin{aligned} Q^A_{pq} &= \textstyle\sum_{xvw} k^2_{xvwp} d_{xvwq} \\ Q^B_{pq} &= \textstyle\sum_{xvw} k^2_{pwxv} d_{qwxv}. \end{aligned} \tag{105}$$

we may express all elements of the gradient in terms of these Fock matrices as

$$\begin{aligned} F_{ai} &= 2F^I_{ai} \langle\, L \mid R \,\rangle + 2F^A_{ai} \\ F_{ia} &= -2F^I_{ia} \langle\, L \mid R \,\rangle - 2F^A_{ia} \\ F_{ti} &= 2F^I_{ti} \langle\, L \mid R \,\rangle + 2F^A_{ti} - \textstyle\sum_x F^I_{xi} D_{xt} - Q^A_{it} \\ F_{it} &= -2F^I_{it} \langle\, L \mid R \,\rangle - 2F^A_{it} + \textstyle\sum_x F^I_{ix} D_{tx} + Q^B_{it} \\ F_{ta} &= \textstyle\sum_x F^I_{xa} D_{xt} - Q^A_{at} \\ F_{at} &= \textstyle\sum_x F^I_{ax} D_{tx} + Q^B_{at} \\ F_{ut} &= +\textstyle\sum_x F^I_{ux} D_{tx} + Q^B_{ut} - \sum_x F^I_{xt} D_{xu} - Q^A_{tu} \end{aligned} \tag{106}$$

The configuration terms of the transformations in the previous subsection are evaluated using the CI technology described in[57]. We may work out individual terms of $\langle L|K|R\rangle$ as

$$\langle L|K|R\rangle = \sum_i [F^I_{ii} + k^1_{ii}] + \sum_{xy} F^I_{xy} D_{xy} + \tfrac{1}{2} \sum_{xyuv} k^2_{xyuv} d_{xyuv} \tag{107}$$

The second and third terms may be calculated with direct CI technology [58]. The one-electron integrals (the inactive Fock matrix elements) may not be symmetric and the two-electron integrals may only have permutation symmetry between particle 1 and particle 2.

We have implemented the above formulas in the following manner. First, the linear response solution vectors and the eigensolutions determining the linear and quadratic response property are evaluated using the linear response program described earlier[14]. Subsequently, using the solution vectors, the gradients given in Eq:s (85) - (88) are calculated and combined with the solution vectors. This gives all separate contributions to the required linear and quadratic response property. The integral transformations of Eq:s (92) - (94) are performed on the fly when evaluating the matrices F^I, F^A and Q^A and Q^B matrices. Our program has the requirement that the computer memory must be large enough to keep $4\frac{1}{2}$ vectors in core and a set of two-electron integrals on disk.

4 Solvent induced hyperpolarizabilities

As exemplified by the present review, theory has advanced to the point where computed results successfully can reproduce many gas phase experiments. However, the great bulk of

measurements are carried out for condensed phase samples, either in solvated, crystalized or polymerized forms. The solvated molecule, the solute, is affected by the environment, the solvent, and its molecular properties changed compared to vacuum. The solvent interaction can be of both long- and short-range nature and the solvent induced changes can change the vacuum property even in a qualitative way. The need for developing methods and computational schemes for describing the condensed phase effects on molecular properties is thus obvious.

Theoretical investigations of solvent effects on properties of solvated compounds started out by consideration of solvation energies[59, 60, 61, 62] and have developed into an increasingly important research area within theoretical chemistry[63, 64, 65, 66, 67, 68, 69, 70, 71] [72, 73, 74, 75, 76, 77, 78, 79]. Many-electron descriptions of the solvated molecule and the solvent induced effects on the molecular properties have evolved around three model types; (i) supermolecular models; (ii) continuum models, and; (iii) semi-continuum models. In the first class an electronic structure method is applied on a molecule solvated by a cluster of solvent molecules; the SCF method is the most used electronic structure method. Problems associated with supermolecular models are basis set superposition errors, the neglect of long-range effects, the choice of cluster structure and difficulties in identifying if effects originate from the solvent cluster or from the solute. The latter reflects the problems of calculating hyperpolarizabilities of a solute in a supermolecular system; the hyperpolarizability is obtained for the total supermolecular system and not just for the solute. The continuum models are based on the notion that the solvated molecule induces polarization charges in an outer medium which give rise to an extra potential at the position of the solvated molecule. The response field or reaction field from the induced polarization charges thus interacts with the molecular system giving rise to a solvent effect. The continuum models are generalizations of Kirkwood's original model[60] with point charges enclosed by a spherical cavity and embedded in a structureless polarizable medium described by the macroscopic bulk dielectric constant. Generalizations include a multipole expansion of the molecular charge distribution within the cavity from which the reaction field is generated[67, 78, 79, 73, 17, 18] and a self-consistent quantum mechanical treatment of the reaction field interaction with the cavity molecules, the self-consistent reaction field model, SCRF, or the multi-configuration self-consistent reaction field model, MCSCRF. These models do not take the short-range interactions between solvent molecules and solute into account. The semi-continuum models are appropriate for taking account of local and specific solvent effects around the solute[80, 81, 82, 83]. They combine the two other approaches by surrounding the solute with a cluster of solvent molecules and embedding this supermolecule in a dielectric medium. This approach is advantageous from the point of view that it describes long range polarization effects and can describe short range effects (charge transfer and exchange) by accounting for the electronic structure of the first solvation shell quantum mechanically.

Few researchers have addressed the problem of solving time-dependent quantum mechanical equations for a molecular system coupled to a solvent [17, 84, 85, 80, 19, 86]. In the present section we outline the recently established response method for solving the time-dependent response equations when the solvated molecule is perturbed by an external perturbation, such as an electromagnetic field.

The physical model presented here starts out by embedding the solute molecule (contained in a spherical cavity) in a dielectric medium. The charge distribution of the solute molecule induces polarization moments in the dielectric medium. The polarization of the dielectric

medium is described by the polarization vector relation

$$\mathbf{P}^{tot} = \mathbf{P}^{in} + \mathbf{P}^{op} \tag{108}$$

$\mathbf{P}^{tot}$ is the total polarization vector which is the sum of the inertial polarization vector, $\mathbf{P}^{in}$ and the optical polarization vector $\mathbf{P}^{op}$. The polarization corresponding to the optical polarization vector stems from the response of the electronic degrees of freedom of the solvent or polymer and it is assumed that the optical polarization vector responds instantaneously to changes in the solute charge distribution within the cavity.

The polarization of the medium corresponding to the inertial polarization vector is related to the vibrational and molecular motion of the condensed phase. Sudden changes in the charge distribution of the solute within the cavity change the inertial polarization of the dielectric medium. These changes do not occur instantaneously but with a relaxation time constant that is characteristic of the solvent. The total and optical polarization vectors of the dielectric medium are related to the static dielectric constant (ϵ_{st}) and optical dielectric constants (ϵ_{op}), respectively. According to eq.(108) the inertial polarization vector is obtained as the difference between the total and the optical polarization vectors.

The perturbation (the electric field in the case of hyperpolarizabilities) that is applied to the solvated/embedded molecule is either time-independent or time-dependent. In general the latter is of frequencies that are much larger than the frequencies associated with the molecular vibrations. The electronic response of the solute molecule is assumed to be slower than the optical polarization and faster than the relaxation time of the inertial polarization. Therefore the optical polarization vector is always in equilibrium with the charge distribution of the solute.

Application of a high-frequency perturbation on the solvated molecule leads to a non-equilibrium solvent state which is represented by an optical polarization vector in equilibrium with the charge distribution of the solute adjusted to the perturbation and an inertial polarization given by the charge distribution of the solute before the perturbation has been turned on. In this case the inertial polarization is not in equilibrium with the actual solute charge distribution but it is related to the charge distribution of the solute before application of the perturbation. One obtains the following expression for the dielectric polarization energy [19, 84]

$$E_{sol} = \sum_{lm} R_{lm}(\rho, \epsilon_{op}) < T_{lm}(\rho) > + R_{lm}(\rho', \epsilon_{st}, \epsilon_{op})(2 < T_{lm}(\rho) > - < T_{lm}(\rho') >) \tag{109}$$

where ρ is the total charge distribution of the solute (electronic and nuclear) after the application of the perturbation and ρ' is the total charge distribution of the solute before the perturbation was turned on. The solute charge distribution is given by the expectation values of the charge moment operators T_{lm} and the response of the dielectric medium is given by the expectation values of the solvent polarization operators R_{lm}. The latter ones are related to the charge distributions of the solute and for a solute contained within a spherical cavity are given by the following relations

$$R_{lm}(\rho, \epsilon_{op}) = g_l(\epsilon_{op}) < T_{lm}(\rho) > \tag{110}$$

and

$$R_{lm}(\rho', \epsilon_{st}, \epsilon_{op}) = g_l(\epsilon_{st}, \epsilon_{op}) < T_{lm}(\rho') > \tag{111}$$

where the factors $g_l(\epsilon_{op})$ and $g_l(\epsilon_{st}, \epsilon_{op})$ are given by

$$g_l(\epsilon) = \frac{1}{2} a^{-(2l+1)} \frac{(l+1)(\epsilon - 1)}{l + \epsilon(l+1)} \tag{112}$$

and

$$g_l(\epsilon_{st}, \epsilon_{op}) = g_l(\epsilon_{st}) - g_l(\epsilon_{op}) \tag{113}$$

a is the radius of the spherical cavity.

The charge distribution of the solute has here been expanded in a multipole expansion. The charge moments are given by the $< T_{lm}(\rho) >$ elements and are expressed as expectation values of the nuclear and electronic solvent operators as

$$< T_{lm} >= T^n_{lm} - < T^e_{lm} > \tag{114}$$

$$T^n_{lm} = \sum_g Z_g t^{lm}(R_g) \tag{115}$$

$$T^e_{lm} = t^{lm}(r) = \sum_{pq} t^{lm}_{pq} E_{pq} \tag{116}$$

where Z_g and R_g are the nuclear charge and position vector of the nucleus g, respectively. The subscripts p and q represent the orbitals ϕ_p and ϕ_q and the operator E_{pq} is given by

$$E_{pq} = \sum_\sigma a^+_{p\sigma} a_{q\sigma} \tag{117}$$

where we sum over the spin quantum number σ and the operators, $a^+_{p\sigma}$ and $a_{p\sigma}$ are the usual creation and annihilation operators for an electron in spin-orbital $\phi_{p\sigma}$. The following notation is used

$$< T^e_{lm} >= \frac{< O|T^e_{lm}|O >}{< O|O >} = \sum_{pq} D_{pq} t^{lm}_{pq} \tag{118}$$

where $|O\rangle$ is the reference electronic wave function for the system under consideration,

$$t^{lm}_{pq} =< \phi_p|t^{lm}|\phi_q > \tag{119}$$

and D_{pq} is the one-electron density matrix.

The functions $t^{lm}(Rg)$ and t^{lm}_{pq} are defined through the conventional spherical harmonics, S^μ_l, where μ is a positive integer [17, 18]

$$\begin{aligned} t^{l0} &= S^0_l \\ t^{l\mu} &= (2)^{-(1/2)}(S^\mu_l + S^{-\mu}_l) \\ t^{l-\mu} &= (2i)^{-(1/2)}(S^\mu_l - S^{-\mu}_l) \end{aligned} \tag{120}$$

As an initial investigation we have considered a model where the two charge distributions ρ' and ρ are the same and in which the dielectric medium is represented by a single dielectric constant.

The electronic wave function of the solute is given by a (multi-configuration) self-consistent reaction field wave function $|0>$ corresponding to the ground state or an excited state of the solute molecule. It is obtained by applying the variation principle to the total energy, the sum of the standard electronic energy for isolated molecules in vacuum and the interaction energy E_{sol}[18].

We will consider the mathematical implication of introducing the solvent-solute interaction term into the Ehrenfest equation of motion of an operator B

$$\frac{d < B >}{dt} = < \frac{\partial B}{\partial t} > -i < [B, H] > \tag{121}$$

where

$$H = H_o + W_{sol} + V_{pert}(t) \tag{122}$$

The expectation values are determined from the time-dependent wave function $|O^t>$ at time t as.

$$< \ldots\ldots\ldots >=<^t O|\ldots\ldots\ldots|O^t> . \tag{123}$$

Following ref. [18] we assume that our system is described by a multi-configuration self-consistent reaction field (MCSCRF) wave function. Thereby we have a wave function fully optimized with respect to all orbital and configurational parameters and which satisfies the generalized Brillouin theorem

$$\begin{pmatrix} < O|[q^+, H_o + W_{sol}]|O > \\ < O|[R^+, H_o + W_{sol}]|O > \end{pmatrix} = \begin{pmatrix} 0 \\ 0 \end{pmatrix} \tag{124}$$

The wave function of the MCSCRF state is given as

$$|O>= \sum_g C_g |\Phi_g\rangle \tag{125}$$

where $|\Phi_g>$ is a set of configuration state functions (CSF). Each CSF is a linear combination of Slater determinants

$$|\Phi_f>= \prod_r a_r^+ |\text{vac}> \tag{126}$$

where we make use of the standard ordered product of spin orbitals. We have used that

$$q_{pq}^+ = a_p^+ a_q, \; p > q \tag{127}$$

$$R_n^+ =| \; n \; \rangle\langle \; O \; | \tag{128}$$

where $|n>$ denotes the orthogonal complement space to $|\; O \;\rangle$ spanned by Φ_g .

The new term in the Hamiltonian in eq. (122) is the solvent-solute interaction part , W_{sol}, given by

$$\begin{aligned} W_{sol} = 2 \sum_{lm,pq,p'q'} g_l(\epsilon) t_{pq}^{lm} E_{pq} |O\rangle\langle O| t_{p'q'}^{lm} E_{p'q'} \\ -2 \sum_{lm,pq} g_l(\epsilon) T_{lm}^n t_{pq}^{lm} E_{pq} + \sum_{lm} g_l(\epsilon) T_{lm}^n T_{lm}^n \end{aligned} \tag{129}$$

The expectation value of this effective Hamiltonian with respect to a state $|O>$ is

$$\begin{aligned} < O|W_{sol}|O >= \sum_{lm} g_l(\epsilon)(T_{lm}^n)^2 + < O|T_g|O > \\ = \sum_{lm} g_l(\epsilon)((T_{lm}^n)^2 - 2 < T_{lm}(\rho) >< O|T_{lm}^e|O >) \\ = \sum_{lm} g_l(\epsilon)(< T_{lm}(\rho) >^2 + < O|T_{lm}^e|O >^2) \\ = E_{sol} + \sum_{lm} g_l(\epsilon) < O|T_{lm}^e|O >^2 \end{aligned} \tag{130}$$

where E_{sol} is the equilibrium interaction energy given by

$$E_{sol} = \sum_{lm} R_{lm}(\rho, \epsilon) < T_{lm}(\rho) > \tag{131}$$

It is clear that the expectation value of W_{sol} is not the contribution to the total energy due to the presence of the solvent, but it is the one corresponding to the effective solvent Hamiltonian satisfying the generalized Brillouin condition.

The Hamiltonian H_o for the many-electronic system in vacuum and the perturbation interaction operator representing the applied field are given as in eq.(3).

The molecular system evolves when the field is applied and the time evolution may be parametrized as[23]

$$|O^t >= exp(ik(t))exp(iS(t))|O > \tag{132}$$

where $exp(ik(t))$ describes a unitary transformation in orbital space

$$\begin{aligned} k &= \sum_{rs}(k_{rs}(t)a_r a_s + k'_{rs}(t)a_s a_r) \\ &= \sum_{k}(k_k(t)q_k^+ + k'_k(t)q_k) \end{aligned} \tag{133}$$

$$\tag{134}$$

and where $exp(iS(t))$ describes a unitary transformation in configuration space

$$S(t) = \sum_{n}(S_n(t)R_n^+ + S_n^*(t)R_n) \tag{135}$$

The evolution of the molecular system is described by the following operators:

$$T = q_i^+, R_i^+, q_i, R_i \tag{136}$$

These operators are collected in a row vector and a general vector in this basis is written as a column vector

$$N = \begin{pmatrix} k_j \\ S_j \\ k'_j \\ S'_j \end{pmatrix} \tag{137}$$

Thus N_j may refer to an orbital rotation parameter or a configuration parameter. The time evolution of $|O^t >$ is determined with the requirement that Ehrenfest's theorem is satisfied through each order in the interaction operator.

Next we will consider the modifications arising from the solvent-solute interaction terms in the linear transformation with the $E^{[2]}$-matrix. It is clearly seen that the linear response function for an MCSCRF state has the same structure as the vacuum linear response function. The only difference being that some terms are added to the Hessian type matrix $E^{[2]}$ in the reaction field model. This matrix enters the linear response calculations either through the solution of sets of linear response equations or through the linear response eigenvalue equations. In either case these equations are solved by using iterative techniques where only linear transformations of $E^{[2]}$ on a trial vector N are carried out[23, 14, 87, 88]

$$d = E^{[2]}N \tag{138}$$

To express the solvent contribution to the linear transformation[88] on a trial vector of the form of eq.(137) we introduce the following states

$$|O^R >= -S_n R_n^+ |O >= -S_n |n > \tag{139}$$

and

$$<^L O| =< O|(S'_n R_n^+) = S'_n < n| \tag{140}$$

and the one-index transformed solvent integrals

$$\sum_{pq} [k(t), t_{pq}^{lm} E_{pq}] = \sum_{pq} Q_{pq}^{lm} E_{pq} \tag{141}$$

where

$$Q_{pq}^{lm} = \sum_s [k_{ps} t_{sp}^{lm} - t_{ps}^{lm} k_{sp}] \tag{142}$$

We further define the effective one-electron operators

$$T_g = -2 \sum_{lm,pq} g_l(\epsilon) < T_{lm} > t_{pq}^{lm} E_{pq} \tag{143}$$

$$T_{yo} = -2 \sum_{lm,pq} g_l(\epsilon) < T_{lm} > Q_{pq}^{lm} E_{pq} \tag{144}$$

$$T_{xo} = 2 \sum_{lm,pq} g_l(\epsilon) < Q_{lm} > t_{pq}^{lm} E_{pq} \tag{145}$$

$$T_{xc} = 2 \sum_{lm,pq,p'q'} g_l(\epsilon) t_{p'q'}^{lm} t_{pq}^{lm} (< O^L|E_{pq}|O > + < O|E_{pq}|O^R >) E_{p'q'} \tag{146}$$

The elements of the linear transformation with the $E^{[2]}$-matrix due to the solute-solvent interactions thus become

for q_j

$$\begin{aligned} E^{[2]}(q_j) = &-< O^L|[q_j, T_g]|O > + < O|[q_j, T_g]|O^R > \\ &- < O|[q_j, T_{yo}]|O > - < O|[q_j, T_{xo}]|O > - < O|[q_j, T_{xc}]|O > \end{aligned} \tag{147}$$

for q_j^+

$$\begin{aligned} E^{[2]}(q_j^+) = &-< O^L|[q_j^+, T_g]|O > + < O|[q_j^+, T_g]|O^R > \\ &- < O|[q_j^+, T_{yo}]|O > - < O|[q_j^+, T_{xo}]|O > - < O|[q_j^+, T_{xc}]|O > \end{aligned} \tag{148}$$

for R_j

$$\begin{aligned} E^{[2]}(R_j) = &-< j|T_g|O^R > + < O|T_g|O > S_j \\ &- < j|T_{yo}|O > - < j|T_{xo}|O > - < j|T_{xc}|O > . \end{aligned} \tag{149}$$

and for R_j^+

$$\begin{aligned} E^{[2]}(R_j^+) = &-< O^L|T_g|j > - < O|T_g|O > S'_j \\ &+ < O|T_{yo}|j > + < O|T_{xo}|j > - < O|T_{xc}|j > \end{aligned} \tag{150}$$

The latter four equations form together with the definitions of the effective one-electron operators the mathematical results of the introduction of solute-solvent interactions into the response formalism. The implementation of this method as presented in Ref. [88] thus enables MCSRCF linear response calculations of properties of a molecular system surrounded by a dielectric medium.

The advantage of this procedure compared to more conventional approaches is; (i) the more appropriate representation of the charge distribution of the solute; (ii) the scheme for obtaining excitation energies, transition moments, polarizabilities, hyperpolarizabilities etc. in one set of reaction field response calculations; (iii) the incorporation of the total Hamiltonian into the response equations. The first point relates to the fact that the Onsager reaction field model applied by [89] assumes that the dipole moment of the solute is sufficient for describing the charge distribution of the solute. This assumption works well for solutes without charge monopoles and higher charge moments than the dipole moment, but is in general a rather crude approximation for the charge distribution of the solute and is therefore quite restricted for the description of the solute-solvent interaction. The inappropriate representation of the charge distribution of the solute may to some extent be compensated for by applying non-spherical cavity shapes, as seen in [90]. The strength of the response theory is clearly seen in the second point, namely the possibility of obtaining many molecular properties in one single response calculation, such as excitation energies, transition moments, frequency dependent and independent polarizabilities and hyperpolarizabilities. The last point of incorporating the total Hamiltonian, molecular Hamiltonian and solvent interactions, into the response equations opens the possibility for new methods and calculations of time-dependent molecular properties of solvated compounds.

5 Hyperpolarizabilities of small molecules

I Neon

Neon has during recent years been studied quite extensively with respect to its hyperpolarizability. Considering this fact and the simple structure of the neon atom it is ironic to learn that results obtained in various theoretical as well as experimental investigations have been quite disparate. Even the sign of the hyperpolarizability dispersion has been disagreed upon. The confusion has very recently been resolved primarily because of response theory calculations[91, 92] of the kind presented in this review article. Because of this fact and because of that neon presents an obvious first test case for quantum methods, we briefly recapitulate below the story of the determination of the neon hyperpolarizability and its dispersion.

The discussion about whether the dispersion of the hyperpolarizability is anomalous or not started with Shelton's[93, 94] observation of a negative dispersion in ESHG experiments. The dispersion of the hyperpolarizability can be expanded in a power series in $\omega_L^2 = \omega_\sigma^2 + \omega_1^2 + \omega_2^2 + \omega_3^2$ [95, 96]

$$\gamma_{zzzz}(-\omega_\sigma;\omega_1,\omega_2,\omega_3) = \gamma_{zzzz}(0;0,0,0)(1 + A\omega_L^2 + B\omega_L^4) \tag{151}$$

where we put $\omega_1 = 0, \omega_2 = \omega_3 = \omega$, and $\omega_\sigma = 2\omega$ to describe ESHG. For neon, Shelton[94] determined $\gamma_{zzzz}(0;0,0,0) = 119.2$ au, A=-9.267 au and B=160.10 au. How-

Table 1: The hyperpolarizability $\gamma_{zzzz}(-2\omega;0,\omega,\omega)$ of neon in au.

Frequency	HF[a)]	CAS[a)] 3-shell	Experiment[b)]
0.000000	68.75	94.64	119(±3)
0.034544	69.99	96.40	111.1
0.042823	70.52	97.37	109.9
0.065625	73.02	101.25	
0.076641	74.68	103.84	102.7
0.088559	76.84	107.23	109.3
0.093215	77.80	108.75	114.5

a) Ref. [91]. b) Table III in ref. [94].

ever, Bishop[97], who identified the negative contributions and estimated them from the experimental sum rules, concluded that theory could not be able to reproduce the size of the anomalous dispersion. The negative dispersion observed by Shelton [93, 94] were not found in Hartree-Fock calculations. Shelton therefore suggested that the negative dispersion could be caused by correlation[93].

The negative dispersion was further challenged by Jensen et al.[91], who carried out MC-SCF response function calculations and obtained a perfectly normal dispersion. In their calculations the basis set of Maroulis and Thakkar[98] with all the Cartesian d and f components was used and they showed that this basis set could properly describe the hyperpolarizability. In Table 1, the hyperpolarizabilities are given for the frequencies used in the experiments by Shelton[93, 94] at the SCF level and with a CASSCF space consisting of 2s, 2p, 3s, 3p and 3d orbitals (the three-shell CAS level). As seen in the Table the dispersion is not anomalous, which casts doubts on the existence of a negative dispersion caused by correlation as suggested by Shelton[93]. The expansion coefficients in Eq. 151 are A=2.311 au, B=4.043 au for the SCF and A=2.551 au, B=5.897 au for the CASSCF calculations. The positive dispersion is thus found to be even larger in the correlated calculation than in the SCF calculation.

In a repeated experiment Shelton[99] concluded that the dispersion is not anomalous and similar to the one predicted by Jensen et al., thereby settling the arguments. Using large restricted active space (RAS) wave functions containing single double and single double triple quadruple excitations, the static second hyperpolarizability of neon has been recalculated by Christiansen and Jørgensen[92] giving an estimation of 106 ± 5 au in agreement with the recent experimental result of 108 ± 2 au by Shelton[99]. Other large-scale calculations of the static second hyperpolarizability have been reported by Chong and Langhoff[100] and by Rice et al.[22] giving $\gamma = 110.0$ au and $\gamma = 109.8$ au, respectively, in both cases using CCSD(T) calculations.

II The Neon isoelectronic series

The first row hydrides isoelectronic with neon probably constitutes the most well studied series of molecules with respect to hyperpolarizabilities, experimentally as well as theo-

retically. Being systems of only 10 electrons they lend themselves as good test cases for different aspects of the applied quantum methods.

In their pioneering investigations on the role of electron correlation for hyperpolarizabilities using fourth-order many-body perturbation theory (MP4), Bartlett and Purvis [101, 102] found that electron correlation affected the static first hyperpolarizabilities β of the HF and H_2O molecules as much as 28% - 50%. This indicated that noncorrelated predictions of hyperpolarizabilities would be unlikely to provide reliable agreement with experiment. A direct comparison with experimental data was not possible because of the lack of information on frequency dependence and vibrational corrections. Later, Sekino and Bartlett[103, 10] carried out calculations for vibrational and dispersion corrections to β of HF (these effects were estimated separately). The dispersion was performed within the time-dependent Hartree-Fock (TDHF) approximation. The various contributions to β were firstly analyzed in detail by Jaszunski et al.[104] using MCSCF response theory calculations. Using MP4, the static hyperpolarizabilities of H_2O were also reported by Maroulis[105]. For HF the role of basis sets and electron correlation has thus been been thoroughly studied. The sole comprehensive study on the first hyperpolarizability β of H_2O was carried out by Luo et al.[38] using MCSCF response theory calculations. Basis sets, electron correlation, frequency dependence and vibrational averaging were discussed in detail on the basis of an excellent agreement with experimental data. The hyperpolarizabilities of NH_3 have been investigated by Maroulis[106], who discussed the importance of basis sets and correlation with the MP4 method, and by Rice et al.[107], who analyzed the correlation and frequency dependence at the MP2 level. Recently, Spirko et al.[35] carried out a detailed investigation on the first hyperpolarizability of NH_3 with respect to correlation, frequency dependency and vibrational averaging. Sekino and Bartlett[29] have very recently performed a systematic study of the hyperpolarizabilities of several small molecules in which the HF, H_2O and NH_3 molecules also were included, accounting for the correlation and dispersion effects. The correlation effect on the static hyperpolarizabilities was calculated at the CCSD and CCSD(T) levels, while dispersion effects were estimated with the TDHF method.

In the remainder of this section we will compare the first hyperpolarizabilities obtained by the multi-configuration quadratic response theory method (MCQR) of the ten electron neon series with respect to basis sets, electron correlation, frequency dependency and vibrational corrections. Comparison with experimental results as well as with other theoretical results will be discussed. In this section we focus on the first hyperpolarizability β, and because this quantity is zero for CH_4 due to the cancellation between the individual components caused by the high symmetry, this species is not considered.

II-A Basis sets

Large basis sets are prerequisites to obtain hyperpolarizabilities of an accuracy within a few percent. One motivation for using large basis sets is evidently to insure that the calculated correlation effect is not just a compensation for a basis set deficiency. Hyperpolarizabilities are quite sensitive to the tail regions of the electron distribution, and the employed basis sets must be able to describe this region adequately. It is also very important that the chosen basis sets will give uniformly accurate results from one molecule to the next. We have found two types of gaussian basis sets to be particularly useful as starting points for accurate calculations of molecular hyperpolarizabilities. One is the correlation consistent,

Table 2: The SCF static dipole polarizabilities and the first hyperpolarizabilities of the neon iso-electrons molecules in au.

		α_{zz}	α_{xx}	α_{yy}	α	β_{zzz}	β_{zxx}	β_{zyy}	$\beta_{\|\|}$
HF									
	Response[a]	5.749	4.470	4.470	4.896	−8.508	−0.434	−0.434	−5.621
	CL[b]	5.7314	4.4485	4.4485	4.8761	−8.381	−0.434	−0.434	5.549
	AB[c]	5.75	–	–	–	−8.5	–	–	–
H_2O									
	Response[d]	8.52	7.91	9.20	8.54	−8.03	−1.69	−9.39	−11.47
	PB[e]	8.47	7.95	9.18	8.53	−5.2	−0.5	−9.6	−9.18
	Ma[f]	8.514	7.892	9.169	8.525	−8.11	−1.46	−9.53	−11.46
NH_3									
	Response[g]	–	–	–	–	−11.28	−7.41	−7.41	−15.66
	SB[h]	–	–	–	–	−11.1	−7.0	−7.0	−15.1

a) Ref. [104]. b) Ref. [100]. c) Ref. [111]. d) Ref. [38] for basis set P3. e) Ref. [102]. f) Ref. [105] for basis set W2. g) Ref. [35]. h) Ref. [29].

atomic natural orbital (ANO)(generally contracted), basis sets of Widmark et al.[108], the other is the polarizability consistent (POL) basis sets of Sadlej[109]. The latter one is of modest size but has still almost the same ability as the larger ANO basis sets in reproducing the molecular dipole polarizabilities. These two types of basis sets have also been appreciated in other types of hyperpolarizability calculations, see e.g. recent account of coupled cluster calculations by Sekino and Bartlett[29]. These authors also suggest a particular procedure to add lone-pair type functions to improve the description of polar molecules, as an alternative to addition of many high-angular momentum functions on the heavy atom. Very accurate hyperpolarizabilities require a further extension of the ANO and POL types of basis sets by addition of more diffuse functions, suggestingly in the form of geometric progressions. A special scheme for adding diffuse functions to ANO basis sets for H, O and F atoms has been suggested in ref. [100] and for POL type of basis sets in ref. [29].

In the MCQR studies of the neon iso-electronic series of molecules both ANO and POL types of basis sets have been employed[35, 38, 104]. In the calculations of the HF molecule[104], an F(8s6p4d3f)/ H(5s3p2d) basis has been used, which was obtained from an F(4s3p2d1f)/ H(3s2p1d) ANO basis of Widmark et al.[108] by adding the diffusion functions specified by Chong and Langhoff[100]. This basis set yields accurate SCF results for the static properties of interest. As shown in Table 2, the calculated parallel component of the polarizability is very close to the values obtained in a numerical Hartree-Fock calculation[110, 111] where basis set errors are eliminated.

Several basis sets have been used in the calculations of the H_2O molecule[38]. It is found that a modest basis set O(8s5p3d1f)/H(4s2p1d) (basis set P3 in ref. [38]) used by Diercksen et al[112] is sufficient for describing the molecular properties. The Hartree-Fock total energies for this basis set is -76.06279 au, in close agreement with the Hartree-Fock limit; -76.068 au. In Table 2, the SCF results for the static polarizability and hyperpolarizability are shown together with previous results.

The SCF results for the static properties of NH_3 can also be found in Table 2. An

N(8s5p3d1f)/H(4s2p1d) basis set has been employed in the calculations[35], which is a combination of the ANO and PLO basis sets. For the N atom, it contained the N(13s8p) primitive set contracted to (8s6p) using the ANO basis of Widmark et al.[108]. The four d functions were obtained in a geometric progression, with a factor of $\frac{1}{3}$, starting from the polarizing d function of Sadlej[109]. The most diffuse f function in the ANO set was used. The basis set for the H atom is the same as the one used in the calculations of H_2O[38].

II-B Electron correlation

As for other molecular properties there exist two mainstreams of methods that account for the correlation contribution to the hyperpolarizability; non-variational and variational methods. Perturbation and coupled cluster response function methods are representatives of the former and the MCSCF response function approach is a representative of the latter. The two types of approaches are complementary in a number of respects. A conventional division of the non-variational and the variational approaches with respect to the correlation contributions in the reference wave function is that the former account for the dynamic (non-valence-, non-structured-) part of the correlation and the latter for the static (valence-, structured-) part. Improvements in the two types of wave functions would then progressively take into account the other part. For instance in the variational approach, the complete active space (CAS) method gives good wave functions for simulation of the valence correlation, and an expansion of the active orbital space matched with restrictions in the electronic excitations (restricted active space (RAS) approach) will account for an increasing part of the dynamic correlation. Vice versa, perturbation or cluster- expanded single-determinantal wave function improves on the static correlation by adding determinants to the reference wave function. A disadvantage of perturbation theory approaches based on extensions of Møller-Plesset perturbation theory is that the poles in these approaches are not correlated (RPA poles) even though correlation are introduced into the description. The dispersion of the polarizability and hyperpolarizabilities is therefore basically non-correlated in these approaches. In all other correlated response function methods correlation of the pole structure and of the response functions are an integrated part in the definition of the response functions. The dispersion is therefore described at a correlated level.

The MCSCF approach has general validity even when the one-particle Hartree-Fock description of the wave function is poor, such as for excited states or at transition states away from equilibrium, or for open-shell species. Molecular oxygen, described in section III-B, is a good example; the (restricted) Hartree-Fock wave function of this molecule even gives the wrong sign for the hyperpolarizability. On the other hand, when the one-determinantal Hartree-Fock description is good, such as often is the case at equilibrium geometries of closed shell species, the perturbational and coupled cluster approaches have a comparative advantage in that the dynamic part of the correlation is easily accounted for. For comparison of different perturbation approaches to molecular hyperpolarizabilities; Møller-Plesset perturbation theory (MP2, MP4)-, and coupled cluster (CCSD, CCSD(T))- approaches, we refer to the work of Sekino and Bartlett [29].

The neon iso-electronic hydride series, discussed in the present subsection, is an example where the perturbational approach *a priori* can be expected to give more accurate hyperpolarizabilities. Correlated calculations of hyperpolarizabilities for the HF, H_2O and NH_3 molecules by the MCQR method have nevertheless indicated that comparatively small

Table 3: The definition of the complete active space with eight active electrons used in the calculations for the hyperpolarizabilities of neon iso-electrons molecules.

Molecule	Symmetry	CAS-A	CAS-B
HF	$C_{\infty v}$	$2-5\sigma, 1-2\pi$	$2-6\sigma, 1-3\pi, 1\delta$
H_2O	C_{2v}	$2-5a_1, 1-2b_1, 1-2b_2$	$2-7a_1, 1-3b_1, 1-3b_2, 1a_2$
NH_3	C_{3v}	$2-3a_1, 1-2a_2, 1-2e$	$2-3a_1, 1-3a_2, 1-3e$

Table 4: The static first hyperpolarizabilities of the neon iso-electrons molecules at CAS-A and CAS-B levels in au.

	HF[a]		H_2O[b]		NH_3[c]	
	CAS-A	CAS-B	CAS-A	CAS-B	CAS-A	CAS-B
β_{zzz}	−8.722	−8.850	−12.10	−12.37	−33.69	−32.22
β_{zxx}	−1.045	−1.102	−5.11	−5.07	−5.63	−7.03
β_{zyy}	−1.045	−1.102	−8.93	−9.00	−5.63	−7.03
$\beta_{\|\|}$	−6.487	−6.632	−15.68	−15.86	−26.97	−27.77

a) Ref. [104]. b) Ref. [38] for basis set P3. c) Ref. [35].

variational (active space) wave functions reproduce results of CCSD quality[29] quite well. Two types of active spaces both with eight active electrons have been chosen for all ten-electrons molecules, denoted as CAS-A and CAS-B in Tables 3 and 4, and were selected from the size of the occupation numbers of the second-order Møller-Plesset (MP2) natural orbitals. The first of these two active spaces (CAS-A) contains one active correlating orbital for each occupied valence orbital. Within the C_{2v} point group CAS-A and CAS-B comprise the $4a_1$,$2b_1$,$2b_2$,$0a_2$ and $6a_1$,$3b_1$,$3b_2$,$1a_2$ orbital spaces, respectively. The transformations of these active spaces in the point groups of the other hydrides is listed in Table 3, the heavy atom 1s orbital is non-correlated in all cases. The MCSCF calculations of individual components of the static first hyperpolarizability of the neon iso-electronic hydrides are reported in Table 4.

Compared with the SCF results, the CAS-A calculations change the β value by 15%, 33% and 72% for HF, H_2O and NH_3, respectively. The values of the hyperpolarizabilities increase slightly in the calculations with the active space CAS-B. It thus seems that a small active space recovers the major part of electron correlation for the hyperpolarizabilities for these hydrides. The correlation effects do not influence the individual components in a similar manner. For the NH_3 molecule electron correlation increases the value of β_{zzz} by as much as a factor 3, whereas the value of the β_{zxx} component decreases.

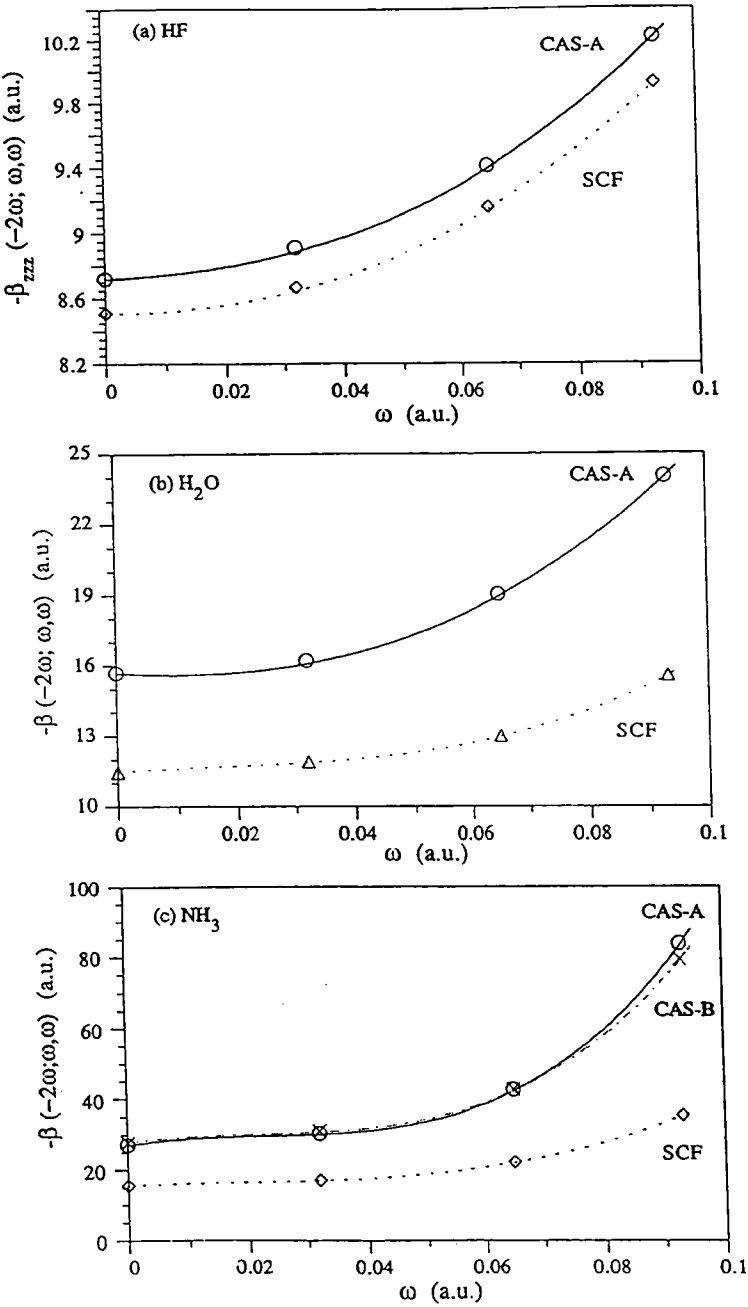

Figure 1: The first hyperpolarizability dispersion curves for the neon isoelectronic series of molecules obtained from RPA and MCQR calculations. a) HF, b) H_2O, NH_3.

II-C Frequency dependence

The experimental data always refer to dynamic processes and relate to frequency-dependent molecular properties at the frequency where experiment is carried out. The extrapolation to zero frequency often introduces problems in the comparison of theory and experiment and it is therefore preferable to carry out calculations of frequency-dependent molecular properties. The ability to do so is one of the nice features that can be obtained using the theory of response functions, recapitulated in section 3. The importance of frequency dependence for hyperpolarizabilities is adequately shown by the dispersion percentages. For instance, at ω=0.0656 au, corresponding to the ruby laser wavelength, the values of β have increased relatively to the static values by 10%, 21% and 58% at CAS-A level for HF, H_2O and NH_3, respectively. The dispersion is reasonably well described at the SCF level for the HF molecule[104]. For the H_2O[38] and NH_3[35] molecules, the difference between the SCF and the correlated calculations becomes evident, especially at larger frequencies. The dispersion curves for $\beta(-2\omega;\omega,\omega)$ of H_2O and NH_3, at both the SCF and CAS-A levels, are shown in Figure 1; including hyperpolarizabilities calculated at two other laser frequencies corresponding to the wavelengths 1319 nm and 488.8 nm.

NH_3 is the member in the hydride series with the largest frequency dependency for the first hyperpolarizability. The difference between the SCF and the correlated calculations is also the largest for this molecule. The dispersion percentages at ω=0.0656 au are 42% and 58% for SCF and CAS-A. It thus shows that the comparison with experimental data performed by adding the dispersion of an SCF calculation to the correlated static results is not reliable. The correlated dispersion of NH_3 has also been reported from MP2 calculations[22]. The MP2 dispersion was quite close to the SCF dispersion at ω=0.0656 au, which is due to the incorrect location of the molecular resonance by MP2. Kleinman symmetry should not be assumed in accurate calculations at relatively large frequencies, as at ω=0.0656 au, where most of the experimental data are obtained. For instance, both for SCF and CAS-A wave functions the frequency dependency of the β_{zxx} component differs significantly from the β_{xxx} component[38, 35].

II-D Vibrational effects

Vibrational averaging of electronic hyperpolarizabilities for the HF, H_2O and NH_3 molecules have been accounted for by MCSCF/MCQR calculations at the correlated CAS-A level, see refs. [113, 38, 35]. Werner and Rosmus[113] performed the vibrational averaging of the hyperpolarizability for HF using two types of potential functions, CAS-A and SCEP/CEPA potential functions. The results for hyperpolarizability averages in the $v = 0$ state differed only by about 1% between the choice of potential functions, and increased the electronic hyperpolarizability by about 9%.

H_2O illustrates the procedure to obtain effective state-dependent polarizabilities and hyperpolarizabilities for the small hydrides. In ref. [38] these were evaluated as the following matrix elements

$$< \alpha >=< v_1, v_2, v_3|\alpha(S_1, S_2, S_3)|v_1, v_2, v_3 > \quad (152)$$

$$< \beta >=< v_1, v_2, v_3|\beta(S_1, v_2, S_3)|v_1, v_2, v_3 > \quad (153)$$

where S_i (i=1,2,3) are the vibrational symmetry coordinates, and $|v_1, v_2, v_3 >$ are eigen-

Table 5: Effective static and first hyperpolarizabilities of H_2O in au[a].

State			$\beta_{\|\|}(-2\omega;\omega,\omega)$	
v_1	v_2	v_3	ω=0	ω=0.0656
0	0	0	−17.06	−20.85
0	1	0	−17.25	−21.13
0	2	0	−17.46	−21.43
1	0	0	−17.98	−22.22
0	0	1	−18.07	−22.22

a) Ref. [38].

functions of an approximate vibrational Hamiltonian[114]

$$H = \frac{1}{2}\sum_{ij} G_{ij}P_iP_j + V(S_1, S_2, S_3) \tag{154}$$

P_k are the momenta conjugate to the S_k for the pure vibrational part of the total Hamiltonian, G_{ij} are the elements of Wilson's G matrix at equilibrium, and V is the potential energy function. The function V has been assumed to have the same form as the functions α and β, which are expanded as a power series in the vibrational symmetry coordinates, its coefficients have been derived from Jensen's potential energy function[115]. The vibrational eigenfunctions were obtained variationally by diagonalizing the Hamiltonian as a matrix over basis functions expressed as products of the eigenfunctions of the corresponding uncoupled Schrödinger equations.

A similar procedure has been made for the vibrational averaging of NH_3[35]. To accomplish this, the data were evaluated over a wide range of values for the inversion coordinate. The dependence of the data on the remaining coordinates is much weaker, hence, it was probed for small vibrational displacements only. The effective state-dependent inversional hyperpolarizabilities have been evaluated as the following matrix elements

$$< \beta(v_6, v_6') = < v_1 = 0, v_6|\beta(S_1, S_6)|v_1 = 0, v_6' > \tag{155}$$

where S_1 is the symmetric stretching coordinate, S_6 the inversion symmetric coordinate.

The vibrationally averaged results of the first hyperpolarizabilities of H_2O and NH_3 at the static limit and at frequency ω=0.0656 au for the ground state and several excited states, are listed in Tables 5 and 6. For the polyatomic members of the series, such calculations require quite large sets of densely chosen points containing results from the hyperpolarizability calculations (e.g. 27 points and 39 points were evaluated for H_2O and NH_3 in refs. [38] and [35], respectively). The dependence of β on the vibrational state is small for the H_2O molecule, but very large for NH_3, which can be referred to the rather unusual features of the NH_3 hypersurface. The vibrationally averaged value of β increased the pure electronic part of β by about 9%, 10% and 6% for HF, H_2O and NH_3, respectively. Such significant contributions can evidently not be neglected in accurate predictions of β.

The vibrational contribution to hyperpolarizabilities has been studied for HF, H_2O and NH_3 molecules by Bishop et al.[39, 116]. These authors found that in general for the static case the vibrational hyperpolarizabilities are large and of the same order of magnitude

Table 6: Effective hyperpolarizabilities $< \beta(v_6, v_6') >$ of ammonia (atomic units)[a].

		$\beta_{\|\|}(-2\omega;\omega,\omega)$	
v_6	v_6'	$\omega = 0$	$\omega = 0.0656$
0^+	0^-	$-28.2(-26.5)$	$-45.1(-42.0)^b$
0^+	1^-	$-2.2(-0.5)$	$-1.7(1.0)$
0^+	2^-	$0.4(1.3)$	$0.6(1.8)$
0^-	1^+	$-2.4(-0.8)$	$-2.2(0.4)$
0^-	2^+	$0.6(1.5)$	$1.3(2.6)$
1^+	1^-	$-26.2(-23.6)$	$-42.4(-38.1)$
1^+	2^-	$-3.6(-1.1)$	$-4.2(-0.5)$
1^-	2^+	$-8.0(-5.7)$	$-11.7(-8.1)$
2^+	2^-	$-22.2(-19.0)$	$-36.2(-32.0)$

a) Ref. [35], values given in parenthesis correspond to purely inversional hyperpolarizability functions.

as the electronic hyperpolarizabilities. However, the vibrational hyperpolarizabilities for dynamic SHG β values are always very small due to the much slower response time for the vibrational motion to a high frequency electromagnetic field.

II-E Solvent effects

We illustrate solvent effects on hyperpolarizabilities through a sequence of calculations on H_2O solvated in different solvents. We use the multi-configurational self-consistent reaction field response model[19] which recently has been used to describe the first set of calculations of frequency dependent- and independent polarizabilities of solvated molecules. For the purpose of obtaining frequency dependent and -independent hyperpolarizabilities we have performed finite field (the E-field is place along the z-axes) reaction field response calculations of the polarizabilities. We have utilized the basis used in ref. [19] and CAS-A as the active space. The solvents are represented by their dielectric constants; either the static (ϵ_{st}) dielectric constant or the optical (ϵ_{op}) dielectric constant. The hyperpolarizability of H_2O is obtained for the following solvents: 1,4 dioxane (ϵ_{op}=2.023); benzene (ϵ_{op}=2.023); ethylacetate (ϵ_{st}=6.02); hexanol (ϵ_{st}=13.3); acetone (ϵ_{st}=20.7); methanol (ϵ_{st}=32.63) and water (ϵ_{st}=78.54). In Figure 2 we give the hyperpolarizability of solvated water relative to the vacuum value as a function of dielectric constants and of applied frequencies. Several different frequencies were computed, results for the frequencies 0.0 au and $9.32*10^{-2}$ au are shown in Fig. 2. For all frequencies the hyperpolarizability β_{zxx} of H_2O becomes more negative with increasing dielectric constant, the hyperpolarizability for the lowest frequency changes the most. From Figure 2 we notice that β_{zyy} gets substantially more negative than β_{zxx} when changing the solvent. At the same time it is the hyperpolarizability for the highest frequency that changes the most. The values of β_{zzz} start out being more negative than the values in vacuum while for dielectric constants larger than 30 the values of β_{zzz} for all four freqeuncies become less negative than β_{zzz} for vacuum. The variation of the vector β_z as a function of the dielectric constant is also shown in Figure 2.

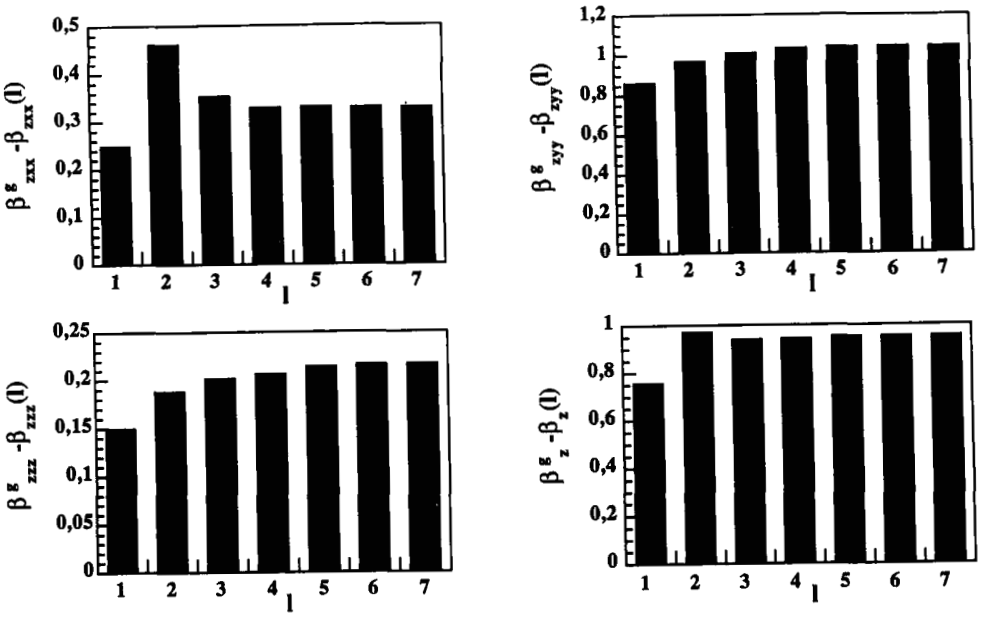

Figure 2: Difference of solvent and gas phase values for the hyperpolarizability components $\delta\beta_{zii}=\beta_{zii}^{sol}-\beta_{zii}^{gas}$, i=x,y,z, and for the averaged hyperpolarizability β_z of the water molecule as a function of the dielectric constant. ω_1 and ω_2 denote frequencies 0.0 au and 0.0932 au, respectively.

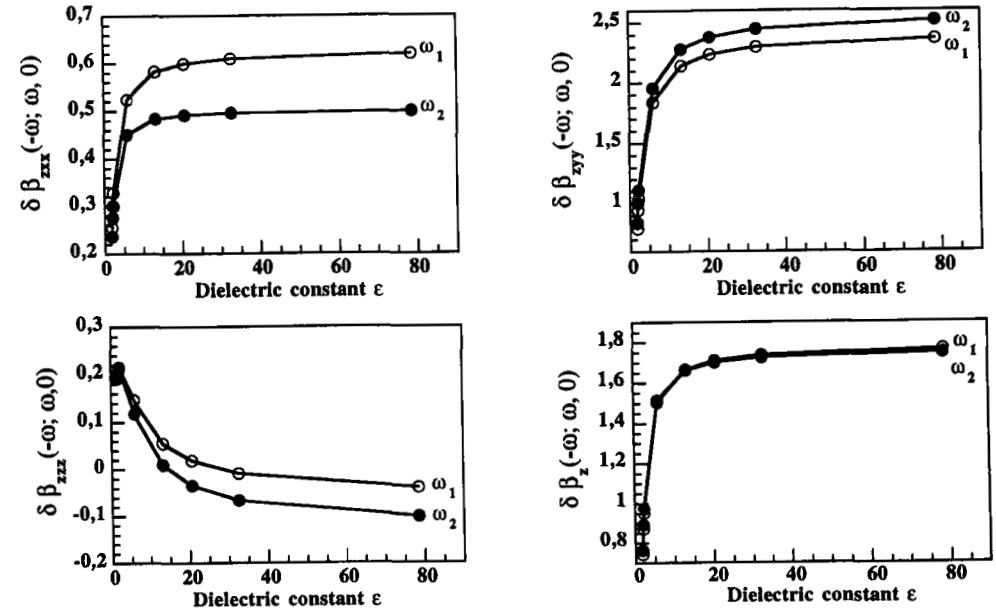

Figure 3: Cumulative multipolar contributions to the solvent induced static hyperpolarizability components β_{zxx}, β_{zyy}, β_{zzz} and the averaged static hyperpolarizability β_z of the water molecule in dioxane solution (ε=2.21)

We have utilized Kleinman symmetry when evaluating

$$\beta_z = \frac{1}{5}\sum_j [\beta_{zjj} + \beta_{jjz} + \beta_{jzj}] \tag{156}$$

where $j = x, y, z$ and we obtain

$$\beta_z = \frac{3}{5}[\beta_{zxx} + \beta_{zyy} + \beta_{zzz}] \tag{157}$$

Increasing the dielectric constant of the dielectric media makes the vector β_z more negative compared to the one for H_2O in vacuum. The solvent induced changes in the hyperpolarizabilities vary strongly from component to component. It is not straightforward to rationalize how the components of the hyperpolarizability tensor will change relative to one another.

With the self-consistent reaction field method described in section 4, the solute charge field and the solvent reaction field can be expanded in arbitrary high multipoles. This makes it possible to check the validity of truncated solvent interactions models, such as the commonly maintained dipolar interaction model. Figure 3 shows the cumulative multipolar contributions to the solvent induced static hyperpolarizability components β_{xxz}, β_{yyz}, β_{zzz} and the averaged static hyperpolarizability β_z of the water molecule in dioxane solution (ϵ=2.21). As seen in this figure the dipolar term indeed gives the largest fraction, but still lacks roughly 20 % of the full interaction. The quadropolar term picks up most of the remaining part. The convergence feature is different for the various components, for example for the β_{xxz} component the quadropolar term gives almost the same contribution as the dipolar term, and the octopolar term gives a significant negative contribution.

Effects of the first solvation shell have been investigated by calculating frequency dependent hyperpolarizabilities for four different cases: (i) H_2O + solvation shell (ii) solvation shell (iii) H_2O + solvation shell + dielectric medium (iv) solvation shell + dielectric medium. The solvation shell contains four water molecules forming, with the center water molecule, the pentamer structure. The computational task of H_2O is at a level where investigations by a semi-continuum approach can be done. This allows for scrutinizing the effects of hydrogen bonding on hyperpolarizabilities.

For each of the previously mentioned cases we obtained the hyperpolarizabilities for four different frequencies (same as above). The hyperpolarizabilities of the center water molecule was calculated by the difference between the hyperpolarizabilities case(i)-case(ii) (supermolecular model) and the difference case(iii)-case(iv) (semicontinuum model). The hyperpolarizability of the centrally placed water molecule in the supermolecular model including the first solvation shell but excluding the dielectric medium differs quite significantly from the values obtained from continuum model. In general a large increase in the components β_{iiz}; $i = x, y, z$ is observed, compared to the values in vacuum and even a change of sign[117]. Including both the first solvation shell and a dielectric medium resembling water (semi-continuum model) leads to a further increase; the hyperpolarizability becomes more positive, with a magnitude larger than that for a single water molecule[117]. It is thus clear that the different media: pure dielectric, pure cluster, and cluster+dielectric, here represented by the continuum, supermolecular and semi-continuum models, respectively, have significant, but varying, impacts on the hyperpolarizability.

Table 7: The best prediction of MCQR for the ES HG $\beta(-2\omega;\omega,\omega)$ at $\omega = 0.0656$ for the neon iso-electrons molecules in au.

	Ne	HF	H_2O	NH_3	CH_4
$\beta_{\|\|}^{calcu.}$	0	$-7.8^{a)}$	$-20.85^{b)}$	$-45.1^{c)}$	0
$\beta_{\|\|}^{exp.}$	0	$-10.9 \pm 0.95^{d)}$	$-21.76 \pm 0.92^{e)}$	$-48.4 \pm 1.2^{e)}$	0

a) Ref. [104]. b) Ref. [38]. c) Ref. [35]. e) Ref. [118]. b) Ref. [119].

II-F Comparison with experimental data

The predictions by MCQR theory for the first hyperpolarizability ESHG values at frequency 0.0656 au for the HF, H_2O and NH_3 molecules are shown in Table 7 along with the corresponding experimental data. The β value of H_2O is in excellent agreement with the experimental value, within the error bars of the experiment. For NH_3, the calculated value is in good agreement (7%) with the experimental data. For HF, however, a 28% difference appears between experiment and the MCQR calculation. Such a discrepancy has also been found by other high-level correlated calculations. Sekino and Bartlett[29] have reported a detailed discussion concerning this particular molecule. It was pointed out that it is unlikely that such a discrepancy can be resolved without reconsideration of experimental measurements.

It has been found that the sign of the hyperpolarizability of solvated water changed compared to gas phase and the numerical value increased by a factor of 1.5[120, 119]. Such a substantial effect of the solvent on the hyperpolarizabilities of the water molecule has been well described by the calculations involving the semi-continuum and supermolecular models[117].

III Diatomic Molecules

Molecular nitrogen and molecular oxygen serve as good examples for small species with strong and unusual electron correlation, N_2 because of its triple bond and O_2 because of its open shell. Their obvious role in atmospheric chemistry has made an accurate determination of their properties including hyperpolarizability an important goal for quantum chemistry. These molecules are also special from the point of view that they contain inversion centers, implying that the first hyperpolarizability β vanishes.

III-A Molecular Nitrogen

Most studies of the hyperpolarizability γ of N_2 have been carried out at the static limit[121, 122, 123, 124, 29]. The frequency-dependent γ has been reported using generalized time-dependent Hartree-Fock (TDHF) theory[124, 29]. The comparison with the experimental data has been performed by adding the dispersion of an SCF calculation to the correlated static results. Such an approach is not always reliable, as we have seen from the calculations of NH_3 discussed in the previous section. Furthermore, as highlighted by the

Table 8: **The SCF static dipole polarizabilities and the second hyperpolarizabilities of N_2 in au.**

	A1[a)]	A2[a)]	A3[a)]	A4[a)]	SB[b)]	JF[c)]	MT[d)]	LA[e)]	JJHO[f)]
α_{zz}	15.025	15.023	15.024	15.019		14.944	14.960	14.868	15.03
α_{xx}	9.807	9.832	9.828	9.827		9.648	9.788	10.098	9.82
α	11.546	11.562	11.560	11.558		11.413	11.512	11.753	11.56
γ_{zzzz}	782	791	795	802	791	775	808		
γ_{xxxx}	506	606	669	594	664	662	563		
γ_{xxxx}	245	251	250	252	268	240	254		
γ	622	682	716	679	727	700	665		

a) Ref. [36]. b) Ref. [124]. c) Ref. [121]. d) Ref. [123]. e) Ref. [125]. f) Ref. [126].

N_2 example the fitting procedures used in the experiments could not give an accurate description for the dispersion of γ at the lower frequency region. This stresses once more that it is important to carry out calculations at the frequencies where experiments are carried out.

Calculations of the frequency-dependent γ both at the SCF and MCSCF levels were carried out in ref .[36]. On the basis of a very good agreement with experimental data several conclusions concerning the large second hyperpolarizability value for this molecule could be drawn. In the response theory calculations of ref. [36] the basis set investigations have been performed using four basis sets, denoted A1 - A4. The first of these (A1) is the same as the one used for the calculations of NH_3, the others are obtained by addition of f and g functions to the basis set A1 (for details we refer to ref. [36]). The static polarizabilities and hyperpolarizabilities at the SCF level obtained for these basis sets are shown in Table 8 together with other theoretical results. The dipole polarizabilities are very stable for all basis sets and all α_{zz} components are in perfect agreement with the seminumerical partial wave value of ref. [122]. The addition of diffuse f functions has a comparatively large effect on γ, especially the xxxx component, while the g functions play a minor role.

The correlated calculations have been performed with a CAS MCSCF reference state containing ten active electrons. The core $1\sigma_g$ and $1\sigma_u$ orbitals were inactive and the active space consisted of the 2-$5\sigma_g$, 2-$3\sigma_u$, $1\pi_g$ and $1\pi_u$ orbitals. The active space has thus the similar structure as the CAS-A space used for the neon isoelectronic series, i.e. contains one correlating orbital for each occupied valence orbital. Electron correlation increases the value of γ by 24% for basis set A3, however, the correlation contribution to γ_{zzzz} is 46%. The static γ value is 885 au. All components of the frequency-dependent hyperpolarizabilities γ at different optical frequencies calculated at CAS MCSCF level with basis set A3 are listed in Table 9. The difference between the γ_{zzxx} and γ_{zxxz} components becomes appreciable as ω increases. It confirms that Kleinman symmetry can only be applied at frequencies far below the resonance.

Mizrahi and Shelton[127] have performed ESHG measurements for the ratios of γ for N_2 and He for wavelength ranging from 457.9 to 700.0 nm. They used *ab initio* results of Sitz and Yaris[128] for γ of He to get γ for N_2. In order to compare directly with their experimental data, the calculated ratios of γ for N_2 and He have been shown in Table 10

Table 9: The hyperpolarizability $\gamma(-2\omega;0,\omega,\omega)$ of N_2 in au, from ref. [36].

Frequency	γ_{zzzz}	γ_{zzxx}	γ_{xxzz}	γ_{xxxx}	γ_{xxzz}	γ_{xzxz}	γ
0.00000	1162	310	310	758	310	310	885
0.06563	1353	364	356	874	362	362	1026
0.07200	1398	377	367	901	374	373	1059
0.07723	1439	389	376	925	385	384	1089
0.09337	1601	436	414	1022	429	426	1208

Table 10: Comparison of theoretical and experimenta l frequency-dependent values of the $\gamma_{N_2}(-2\omega;0,\omega,\omega)$ / $\gamma_{He}(-2\omega;0,\omega,\omega)$ ratio.

Frequency	Calculation[a)]	Experiment[b)]
0.06563	22.48	23.17(14)
0.07200	22.93	23.72(10)
0.07723	23.33	24.25(9)
0.09337	24.92	25.86(13)

a) Ref. [36]. b) Ref. [127]. The uncertainty of the last digits is indicated in parentheses.

where the most accurate γ values of He reported by Bishop and Pipin[129] have been used. Our calculated hyperpolarizability ratios are in excellent agreement with the corresponding experimental results and are for all frequencies within 3% of the experimental data.

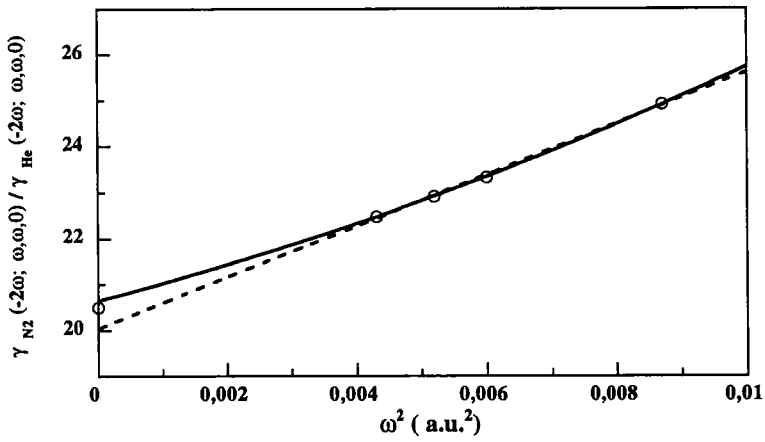

Figure 4: The ratio of hyperpolarizabilities between N_2 and He as a function of squared frequency. Circles denote calculated points. Dotted and solid lines denote fitting functions F1 and F2, respectively, defined in the text

For frequencies well below an electronic resonance the $\frac{\gamma_{N_2}(\omega)}{\gamma_{N_2}(\omega)}$ ratio may be expanded in even powers of ω. Mizrahi and Shelton[127] indicated that term in ω^4 and higher were unimportant for fitting their experimental data. Using γ values of He of Sitz and Yaris[128], they obtained the static γ value of N_2 to be 865 $\pm$ 5 au. Maroulis and Thakkar[123] rescaled the experimental results using a more accurate value for He[130] and obtained the static γ value of N_2 to be 850 $\pm$ 5 au. Their estimations are, however, too small compared with the value of 885 au calculated in ref.[36]. As shown in the latter work the fitting functions must be very flexible in order to accurately predict the static value or the values at low frequencies. The ω^4 term is necessary for describing the dispersion especially for the low frequency range. Results from fitting functions of the form $F_1(\omega) = A_1(1 + B_1\omega^2)$, used in ref. [127], and $F_2(\omega) = A_2(1 + B_2\omega^2 + C_2\omega^4)$ are plotted in Figure 4. It is clear that in the frequency range where experimental data were obtained, the two functions give almost identical dispersions. However, for the lower frequency range larger differences appear. The most accurate hyperpolarizability γ of He in ref. [129] can be used to determine γ of N_2. The static value of γ_{N_2} obtained from the function $F_2(\omega)$ is 889 au and the value from function $F_1(\omega)$ is 864 au. The value obtained from function $F_2(\omega)$ thus compares favorably with the static value of 885 au calculated from the response function method[36], while the value obtained from function $F_1(\omega)$ is too small.

The vibrational averaging for the dipole polarizability and hyperpolarizability in the $v = 0$ state is carried out for frequencies 0.0 and 0.072 au. Calculations were performed over several internuclear distances using calculated CAS MCSCF potential functions. The so obtained averaged dipole polarizabilities α are 11.67 au and 11.83 au for frequencies 0.0 and 0.072 au, respectively, which are in excellent agreement with the experimental values of 11.74 $\pm$0.06 au[131] and 11.92 au[132]. The values for vibrationally averaged hyperpolarizabilities have increased by about 1% from the results at the equilibrium bond length. The values are 894 and 1070 au for frequencies 0.0 and 0.072 au, respectively. However, it can be seen that the vibrational averaging effect is quite small. Shelton[133] predicted the vibrational contribution to be very small for ESHG at 633 nm.

III-B Molecular Oxygen

Because of its open-shell nature, the location of the lowest excited states, and the unusual type of electron correlation, with competing valence and dynamic contributions, the hyperpolarizability of O_2 has presented a notoriously difficult test case. For the systems described in the preceding paragraphs it was found that even though electron correlation is important for the description of the hyperpolarizability, it can often be recovered by fairly modest efforts in terms of the size of the correlating (self-consistent field) wave functions. Small active orbital spaces in which a correlating orbital is added for each occupied valence orbital have thus given hyperpolarizabilities in excellent agreement with the experiment. This holds also for N_2 as shown above, but definitely not for O_2; open-shell Hartree-Fock gives a hyperpolarizability of O_2 that not only differs in magnitude from that experimentally determined and but that even has a wrong sign. This extremely poor Hartree-Fock description introduces problems for the perturbationally oriented approaches in addressing the hyperpolarizability of O_2. MCSCF based response theory approaches reviewed in this work conceivably presents a better strategy, because the important valence-type correlation can easily be incorporated in the reference wave functions and the dynamic correlation can be successively added by increasing the correlating orbital space. We therefore briefly

Table 11: The static polarizability and hyperpolarizability of O_2.

	BAS[a,b]	α_{xx}	α_{zz}	α	γ_{zzzz}	γ_{zzxx}	γ_{xxxx}	γ
RHF								
	$cct-ds-p3$	7.5050	20.788		−3620.5	582.19	429.92	
	POL	7.4756	20.718		−3548.5	558.78	393.02	
	$POL-p1-f$	7.4873	20.780		−3643.2	584.22	424.92	
CAS-2p								
	$cct-ds-p3$	7.339	14.432	9.703	717.39	266.08	384.29	561.30
	POL	7.311	14.372	9.665	704.11	254.78	356.29	534.67
	$POL-p1-f1$	7.320	14.396	9.679	712.44	266.01	380.67	558.32
RAS								
	POL	7.832	14.978	10.214	720.80	340.45	483.63	674.46

a) see the explanation in ref. [134]
b) the number of contracted basis functions are 158, 90 and 138, respectively.

recapitulate some results for the difficult second hyperpolarizability of molecular oxygen obtained in the recent work of Luo et al[134].

Results for the hyperpolarizability of O_2 using different basis sets and correlation spaces are shown in Table 11 (the full Tables of results are given in ref. [134]). The basis sets are the correlation consistent ANO (cct) and polarizability consistent POL basis sets optimized for the oxygen atom. Decontractions and additions of diffuse functions have been performed. Three types of wave functions for the reference ground state of $^3\Sigma_g^-$ molecular oxygen was employed in ref. [134]. The first is the open-shell Hartree-Fock wave function, the second is a complete active space wave function containing all 2p orbitals with 8 active electrons (2p-CAS). The third is a restricted active space (RAS) wave function comprising the full n=1,2,3 main shells of orbitals, with the 2p space being complete. The RAS calculation thus includes part of the dynamic correlation not considered by the 2p-CAS type wave function.

The basis set dependence is quite evident. Decontraction is not so important, while addition of diffuse s, p, d and f functions significantly changes both the polarizability and hyperpolarizability, especially for the components perpendicular to the molecular axis. As for N_2[36] f functions are important to obtain an accurate γ_{xxxx} component of the hyperpolarizability while g functions are not. The dominant effect of the f functions is due to the fact that the ϕ orbitals can be reached in two successive dipole allowed transitions where π orbitals are occupied in the reference state. Results from the largest basis sets shown in Table 11 (cct-p3 and POL-p2) seem to have reached the Hartree-Fock limit values.

There is a very significant contribution to the hyperpolarizability from electron correlation, it even changes the sign of the γ_{zzzz} component of the hyperpolarizability. Although this component presents the major error for RHF, it changes only slightly going from CAS-2p to RAS calculations. By contrast, the results from the RAS calculations for the γ_{zzxx} and γ_{xxxx} components are increased by about 35% compared with the CAS-2p calculations. Thus while the γ_{zzzz} component is fairly well converged at the CAS level the γ_{xxxx} (or the γ_{xxzz}) component is not, the CAS calculations reproduces about 50 % of the averaged hyperpolarizability, γ_z, and the RAS calculations about 80 %. It is interesting to note that

the polarizability of O_2 is in very good agreement with the experimental measurement already at the CAS level, and reproduces the experimentally determined polarizability $\alpha = 10.66$ [135] and $\alpha = 10.59$ [136] by a few %, (α=10.22 versus α=10.66[137]).

As for the hydrides described above, an experimental comparison should be verified by estimating contributions to the hyperpolarizability γ by frequency dispersion and vibrational averaging. The dispersion depends strongly on correlation, and is different for the different components, limiting the validity of Kleinman symmetry at higher frequencies. As for N_2 discussed in the previous subsection vibrational averaging or vibrational contributions can add at most a few % and the lacking 20 % can not be referred to these effects. Rather the correlation contribution to the γ_{xxxx} component is the most relevant cause. Rationalizations of results for the polarizability and the hyperpolarizability can be made by computing the one- and two-photon spectra, for molecular oxygen it turns out that both quantities depend critically on the description of the Schumann-Runge band, which corresponds to a state with a very steep potential at the ground state equilibrium. It is therefore interesting to note that while the 2p-CAS wave function describes the polarizability well it is quite poor for the hyperpolarizability. For molecular oxygen there is a delicate balance between intra-valence and dynamic correlation. Evidently a prohibitly large space is required to obtain a converged value for the γ_{xxxx} component. The rather particular structure of the low-lying excited states, in particular triplet states, for molecular oxygen may also have a bearing on the hyperpolarizability problem, for instance the $<^1 \Sigma_g^- \mid H_{so} \mid^3 \Pi_g >$ spin-orbit coupling might contribute to the orthogonal γ_{xxxx} component of the $^1\Sigma_g^-$ hyperpolarizability.

6 Hyperpolarizabilities of charge transfer organic molecules

Organic materials with large non-linear optical susceptibilities are considered to be strong potential candidates in current optical technology and constitute viable alternatives to the inorganic materials for applications in optoelectronics[44, 5]. Of particular interest is the possibility for strong Kerr effects and capacity for frequency multiplying in organic molecular crystals. Intracavity frequency doubling has indeed been reported in several organic crystals recently, see e.g. ref. [138]. The large size of the hyperpolarizabilities β in many of these compounds is often associated with intramolecular charge transfers (CT), resulting from the electron donor and acceptor groups communicating through a π-conjugated molecular framework[44, 5]. Benzene substituted by one or several donor and acceptor groups constitute both simple and illustrative model molecules for optical active materials, and have furthermore been well investigated experimentally. The para-disubstituted compounds are one-dimensional charge transfer compounds, while the multiply substituted analogues simulate molecules with non-linear optical activity due to two- and three-dimensional charge transfer capabilities. These molecules have also become popular test cases for model analysis as well as by recent more refined quantum calculations, as described below.

Some of the simpler disubstituted benzenes possess particularly strong donor-acceptor character due to the strong localization of the HOMO and LUMO orbitals and, consequently, due to a small HOMO-LUMO gap[139]. In the ultraviolet spectra of these compounds strong bands appear which cannot be interpreted as local excitations within ring, donor, acceptor groups but which have purely charge transfer (CT) character[140, 141].

For these compounds the CT excitation is essentially a HOMO-LUMO transition of low energy between the donor and the acceptor groups, since the HOMO is located to the donor and the LUMO to the acceptor. The simple additivity model for the hyperpolarizability based on the molecular constituents fails because of the extra charge transfer transition present for each particular donor-acceptor complex. The low energy and strong oscillator strengths of the charge-transfer transitions lead to very large polarizabilities (α) and hyperpolarizabilities (β and γ) and thus to a large non-linear optical response. Because of the dominance of one single transition (di-substituted benzenes) or few transitions (poly-substituted benzenes) involving well-defined energy levels, the polarizability character of such compounds have been the object for several simplifying models, so-called few-state models. Below we go through response theory calculations of one-dimensional, di-substituted, compounds represented by para-nitroaniline, and two-dimensional, poly-substituted, compounds, represented by diamino-nitrobenzene.

I Hyperpolarizabilities of para-nitroaniline

Among the disubstituted benzenes, para-nitroaniline is an extreme case, but also the most well-documented case for both theory and experiment. It has constituted a test case for models that aim at predicting hyperpolarizabilities of larger charge-transfer compounds. From this point of view it is noteworthy that considerable differences prevail between results obtained between experiment and theory, but also mutually between different experimental measurements and mutually between the different, semi-empirical, calculations, see the compilation of data in the work of Karna et al.[11]. Considerable fluctuations in the measured ESHG values, with deviations up to 50 % have been reported for identical solutions and identical frequencies. To some extent this refers to confusion in the proper definition of the experimental hyperpolarizabilities as discussed in section 2. Most of the calculations are referred to the hyperpolarizability of PNA in gas phase, while the experimental data have been extracted from the measurements in solvent using local field factors. As discussed in the section 2, such experimental data can not be compared directly with the calculations carried out for the gas phase. Stähelin et al.[48] have measured the first hyperpolarizabilities of PNA in a variety of solvents and determined that, despite accounting for the differing local field factors, the hyperpolarizability values span a range of a factor of 2. The solvent effect has thus to be addressed explicitly. Using MCSCF linear and quadratic response theory, systematical *ab initio* calculations of the polarizabilities and hyperpolarizabilities of PNA in gas and solvent phases were carried out in refs.[42, 142, 86]. We review here some essentials of these calculations.

I-A Gas phase

The sizes of para-nitroaniline and other substituted benzenes are on the limit for conventional *ab initio* calculations. The applications on PNA have therefore partly been based on techniques for direct atomic orbital solutions of the SCF and the RPA equations[42] Thus static and dynamic hyperpolarizabilities of PNA were obtained in ref.[42], using the direct SCF and direct quadratic response theory with a number of basis sets containing up to 300 contracted gaussian functions. The quality of these basis sets were systematically improved, being of "standard" (DZ) "extended" (TZ), "polarizing" (DZP and TZP) and "diffuse" (TZPD) character. The static hyperpolarizabilities as well as the dynamic hyper-

Table 12: Frequency dependent of the polarizabilities and first hyperpolarizabilities of para-nitroaniline for different basis sets (α in 10^{-24}esu, γ in 10^{-30}esu), from Ref. [42, 143].

	basis set	α_{xx}	α_{yy}	α_{zz}	α_z	β_{zxx}	β_{zyy}	β_{zzz}	β_z^a
$\omega = 0$									
	DZ	13.15	4.85	17.83	11.94	−1.05	−0.06	5.75	4.65
	TZ	13.71	6.70	19.00	13.14	−1.02	−0.18	6.33	5.12
	DZP	14.32	7.22	20.15	13.90	−0.90	−0.11	5.10	4.09
	TZP	13.93	7.37	19.71	13.67	−0.90	−0.19	5.37	4.28
	$TZPD$	14.39	7.83	20.55	14.26	−0.89	−0.16	5.03	3.98
$\omega = 0.065eV$									
	DZ	13.20	4.87	17.96	12.01	−1.11	−0.06	6.24	5.08
	TZ	13.76	6.72	19.14	13.21	−1.09	−0.19	6.88	5.62
	DZP	14.37	7.23	20.29	13.96	−0.96	−0.12	5.58	4.50
	TZP	13.98	7.39	19.85	13.74	−0.96	−0.19	5.84	4.71
	$TZPD$	14.44	7.84	20.71	14.33	−0.95	−0.17	5.49	4.39

a) $\beta_z = \beta_z(-2\omega;\omega,\omega)$

polarizabilities $\beta_{ijk}(-2\omega;\omega,\omega)$ and $\beta_{ijk}(0;\omega,-\omega)$ at ω=0.650 eV were computed. Average dynamic hyperpolarizabilities $\beta_z = \frac{1}{3}\sum_j(\beta_{zjj}+\beta_{jzj}+\beta_{zzj})$ were also given assuming the so-called Kleinman symmetry. This symmetry was found to be a good approximation for all basis sets at this frequency. This is a general observation for response calculations carried out at frequencies well below the first resonance frequency of the molecular compound (see, however, results for two-dimensional CT species discussed below). The order of the dynamic polarizabilities are found to be $\beta_z(-2\omega;\omega,\omega) > \beta_z(0;\omega,-\omega) > \beta_z(-\omega;0,\omega)$, all three quantities being larger than the static polarizability.

From the results of ref. [42], recapitulated in Table 12, it was found that the basis set dependency of the static and dynamic hyperpolarizabilities tend to follow each other, and that even the moderate DZP calculation gives values close to the large basis set limit (TZPD). Further enlargement of the basis set beyond TZPD did not expand the variational space, but rather introduced linear dependencies which were tested for and removed. For the first polarizability the basis set convergence seems to be even faster, see Table 12. The best estimated dynamic hyperpolarizability $\beta_z(-2\omega;\omega,\omega)$ at ω=0.650 eV is 4.39 (10^{-30} esu) with the TZPD basis and is considered to be close to the Hartree-Fock limit but it is still far from the corresponding experimental result of 28.8±1.5 (10^{-30} esu) for PNA in solution. This discrepancy is due to electron correlation and, in particular, solvent effects. In order to investigate the first of these two possible sources of error, MCSCF quadratic response theory calculations were carried out, see ref.[142]. The charge transfer (CT) resulting from the electron donor and acceptor groups communicating through a π-conjugated molecular framework[44, 5] and it is therefore natural to first check the role of π electron correlation by means of complete active spaces correlating all π-electrons. The DZP basis set was used in these calculations, which give almost the same quality as the TZPD basis set at the RPA level, see Table 12. It is found that such electron correlation indeed gives significant contributions to the frequency-independent first hyperpolarizability of PNA as well as to its dispersion. It changes the RPA results by about 32% at the static limit and by 44%

Table 13: The hyperpolarizability dispersion of PNA (10^{-30} esu).

Freq.	Level	β_{zzz}	β_{zxx}	β_{zyy}	β_z	Experiment[a]
ω=0						
	RPA	5.10	−0.90	−0.11	4.09	
	MCQR	5.93	0.13	−0.13	5.93	
ω=0.65 eV						
	RPA	5.58	−0.96	−0.12	4.50	
	MCQR	6.50	0.15	−0.13	6.52	28.8 ± 1.5
ω=1.17 eV						
	RPA	6.94	−1.13	−0.13	5.68	
	MCQR	8.12	0.23	−0.15	8.20	50.7 ± 1.2
ω=1.364 eV						
	RPA	7.88	−1.24	−0.14	6.50	
	MCQR	9.24	0.29	−0.15	9.38	75 ± 3
ω=1.494 eV						
	RPA	8.74	−1.35	−0.15	7.24	
	MCQR	10.25	0.34	−0.16	10.43	120 ± 9

a) Experimental values from ref.[47] multiplied by a factor of three according to the convention given in ref.[46]. b) Conversion factors for β from au to SI and esu units: 1 au = 3.206361 x 10^{-53} C^3 m^2 J^{-2} = 8.639418 x 10^{-33} esu

at the larger frequency of ω=1.494 eV. Table 13 shows the SCF and CAS MCSCF results of $\beta(-2\omega;\omega,\omega)$ at different frequencies obtained with the DZP basis set. However, as expected, a large deviation still remains between MCQR vacuum and experimental solvent results, especially for the dispersion of β. Perturbation schemes (MP2)[46], giving an even larger correlation correction, have lead to the same conclusion, namely that the solvent effects are crucial for the hyperpolarizabilities measured in solutions. Calculations of the solvent effects will be discussed in some detail in the next subsection.

I-B Solvent phase

Using the reaction field linear response theory, the solvent induced polarizabilities and hyperpolarizabilities of PNA in different solvents were carried out at the SCF and MCSCF levels in ref.[86]. The solvent effects on the CT state and the quantities entering the two-state model were also addressed. The intensive charge transfer (CT) excitation involving the amino HOMO ($4b_1$) and nitro LUMO ($5b_1$) orbitals is known to be the main contributor to the low-lying absorption spectrum of PNA, and as for other substituted benzenes (see above), the description of non-linear optical processes is to a large degree linked to the description of this transition. A large solvatochromatic shift for PNA in solvents of different polarities have been observed experimentally, implying a general lowering of the CT transition. Because of the dominance of this longitudal CT transition, the hyperpolarizability of PNA, like for many other one-dimensional para-substituted benzenes, can be simulated considering mainly the CT state in addition to the ground state.

Table 14 recapitulates calculated results of the excitation energies of the CT state for PNA in different solvents with SCF and CAS MCSCF electronic wave functions using the

Table 14: Calculated solvation energy shifts (in cm^{-1}) for the CT state for PNA in different dielectric environments. The cavity radius is 9.82 au.

Solvents	Diel.	SCF		MCSCF		Experimental[a]	
	const.	E	shift	E	shift	E	shift
gas	1	40664		41802		35090	
1,4 dioxane	2.21	39470	0	40301	0	28239	0
benzene	2.28	39430	−40				
ethylacetate	6.02	38397	−1073	38938	−1363	27916	−323
hexanol	13.3	37937	−1533				
acetone	20.7	37784	−1686	38156	−2145	27190	−1049
methanol	32.63	37695	−1775	38022	−2279	27029	−1210
DMF[b]	36.71	37679	−1791	37996	−2305	26141	−2098
water	78.54	37590	−1880				

a) Ref. [48]. Gas phase value from ref. [144]. b) DMF = dimethylformamide

solvent linear response method described in section 4. It should be noted that the CT excitation energy in vacuum using the π-CAS wave function is higher than that of RPA (5.18 versus 5.04 eV given in ref. [142]), indicating that π electron correlation is more important in the ground than in the excited state (this can be derived from the biradical nature of the NO_2 group in the ground state). This is one of several anomalous properties associated with molecules like PNA with extreme donor-acceptor character. The predicted shifts, relating to PNA in dioxane, are quite significant. As seen in Table 14 the MCSCF calculations predict larger shifts than those obtained from SCF. The SCF results happen to be closer to the experimental results for PNA in acetone and methanol, while for DMF solution the MCSCF results are closer to the experimental data. We consider the close agreement to be somewhat coincidental, since any experimental comparison must be qualified by the set of parameters used in the reaction field model and by the presence of competing solvent effects, e.g. hydrogen bonding, not accounted for by a reaction field model. Utilizing the total polarization vector and thereby the static dielectric constant leads to an overestimation of the solvent response for the electronic excited state, as mentioned in the previous section and to a too large solvent shift. This is clearly seen in Table 14.

It can be expected that in addition to shifts of the CT excitation energy, the solvent effects on the transition moment and on the dipole moments of ground and CT states are also significant[142]. Table 15 shows the calculated values of the transition moment between the ground and CT states, μ_{eg}, the ground state dipole moment, μ_g, and dipole moment difference between ground and CT states, $\Delta\mu$, for PNA in different solvents at the SCF and MCSCF levels. All these quantities are calculated directly from the response solvent model. The dipole transition moment μ_{eg} is calculated from the residue of the linear response function and the difference in dipole moments $\Delta\mu$ (which is a residue of the quadratic response function) was obtained from a finite field calculation of the CT excitation energy. At the SCF level, the solvent dependent μ_{eg}, μ and $\Delta\mu$ increase by 13 - 30%, 9 - 22% and 18 - 48%, respectively, compared with the gas phase result. At the MCSCF level a similar smooth dependence of these quantities with respect to the solvent polarity can be found. The correlation effect shows quite a large contribution for the dipole moment; the ground state dipole moment is decreased by roughly 25%,

Table 15: The ground state dipole moment, μ_g, transition moment between the ground and CT states, μ_{eg}, and the change of dipole moments between ground and the CT states $\delta\mu$ for PNA in different dielectric environments.(D) The cavity radius is 9.82 au.

Diel.	SCF			MCSCF		
const.	μ_g	$\Delta\mu$	μ_{eg}	μ_g	$\Delta\mu$	μ_{eg}
1	8.02	4.07	4.68	6.36	7.40	4.80
2.21	8.72	4.82	5.29	6.93	8.64	5.24
2.28	8.74	4.85	5.31			
6.02	9.31	5.50	5.74	7.35	9.63	5.64
13.3	9.57	5.79	5.95			
20.7	9.65	5.88	6.00	7.61	10.23	5.85
32.63	9.71	5.95	6.05	7.65	10.34	5.90
36.71	9.72	5.96	6.06	7.66	10.35	5.91
78.54	9.77	6.02	6.10			

while the CT dipole moment is increased by roughly the same amount. The correlation contribution to the transition moment is smaller, giving a decrease of only a few per cent. The correlated result for the dipole moment in the gas phase, $6.36D$, agrees well with the experimental value of $6.3D$[145] where the SCF value is 8.02 D. The dipole moments of ground and CT states have been determined by Wortmann et al[146] for PNA in dioxane in an electrooptical absorption measurement (EOAM) to $6.02D$ and $15.33D$, respectively, in good agreement with the MCSCF correlated values of $6.93D$ and $15.57D$, the SCF values are $8.72D$ and $13.54D$. This indicates that the used complete active space wave function represents the solvent induced dipole moments of PNA quite well.

The SCF and MCSCF values of frequency dependent polarizabilities $\alpha(-\omega;\omega)$ and hyperpolarizabilities $\beta(-\omega;\omega,0)$ of PNA in the different solvent environments are shown in Tables 16 and 17. At the SCF level, the static polarizability shows an increase of 7- 18 %. A more pronounced solvent effect is found for the first hyperpolarizabilities which increase in the range 45-150% for the dielectric constants covered. A similar feature has also been found by Willetts and Rice[89] in their study of solvent effects on hyperpolarizabilities of acetonitrile. The solvent affects the various hyperpolarizability components differently; the effect is almost completely concentrated in the zzz component of β, while the other two components hardly change. This is consistent with the dominance of the dipole contribution to the total multipolar solvent effect, see below. At finite frequency, but far from the first resonance, here ω=1.17 eV, these patterns are largely preserved.

The frequency dependent polarizabilities $\alpha(-\omega;\omega)$ of PNA in various solvents at both SCF and MCSCF levels are recapitulated in Table 16 and 17. The first hyperpolarizabilities referring to the Kerr effect, $\beta(-\omega;\omega,0)$, and obtained from finite-field calculations are also given. The electron correlation effect is thus very important for the hyperpolarizability; it increases the hyperpolarizabilities for all solvents, but less so for the polarizability, as shown in Table 17. The dispersion effect at ω =1.17 eV (used in most experiments), is small, which reflects the fact that this frequency is far from the first resonance.

The reaction field model employs a cavity to separate the solute and the dielectric systems. The dependence on cavity radius is generally large for shifts of excitation energies[147] and molecular properties[89] for small species. The dependence on cavity radius is evident

Table 16: The SCF frequency dependent polarizabilities $\alpha(-\omega;\omega)$ (10^{-24} esu) and hyperpolarizabilities $\beta(-\omega;\omega,0)$ (10^{-30} esu) for PNA in different dielectric environments. The cavity radius is 9.82 au.

	α_{xx}	α_{yy}	α_{zz}	α	β_{zxx}	β_{zyy}	β_{zzz}	β_z
$\omega = 0$								
1	14.32	7.22	20.15	13.90	−0.90	−0.11	5.10	4.09
2.21	15.02	7.42	22.20	14.88	−1.10	−0.13	7.18	5.95
2.28	15.04	7.43	22.28	14.92	−1.11	−0.13	7.27	6.03
6.02	15.57	7.59	24.09	15.75	−1.30	−0.14	9.52	8.08
13.3	15.78	7.65	24.93	16.12	−1.39	−0.15	10.68	9.15
20.7	15.85	7.67	25.20	16.24	−1.42	−0.15	11.09	9.52
32.63	15.90	7.68	25.39	16.33	−1.44	−0.15	11.38	9.79
36.71	15.91	7.68	25.43	16.34	−1.44	−0.15	11.44	9.84
78.54	15.95	7.70	25.60	16.42	−1.46	−0.16	11.69	10.07
$\omega = 1.17eV$								
1	14.48	7.25	20.62	14.12	−0.93	−0.12	5.63	4.58
2.21	15.19	7.46	22.79	15.15	−1.14	−0.13	7.97	6.70
2.28	15.22	7.46	22.88	15.19	−1.15	−0.13	8.07	6.79
6.02	15.75	7.62	24.82	16.06	−1.34	−0.15	10.64	9.15
13.3	15.97	7.68	25.71	16.45	−1.44	−0.15	11.99	10.40
20.7	16.04	7.70	26.01	16.59	−1.47	−0.16	12.46	10.83
32.63	16.09	7.71	26.22	16.67	−1.49	−0.16	12.79	11.14
36.71	16.10	7.72	26.26	16.69	−1.49	−0.16	12.86	11.21
78.54	16.14	7.73	26.44	16.77	−1.51	−0.16	13.15	11.48

Table 17: The MCSCF frequency dependent polarizabilities $\alpha(-\omega;\omega)$ (10^{-24} esu) and hyperpolarizabilities $\beta(-\omega;\omega,0)$ (10^{-30} esu) for PNA in different dielectric environments. The cavity radius is 9.82 au.

	α_{xx}	α_{yy}	α_{zz}	α	β_{zxx}	β_{zyy}	β_{zzz}	β_z
$\omega = 0$								
1	15.12	7.20	19.00	13.78	0.13	−0.13	5.93	5.93
2.21	16.00	7.41	20.88	14.77	0.26	−0.13	8.88	9.01
6.02	16.72	7.58	22.64	15.65	0.13	−0.18	11.76	11.71
20.7	17.10	7.62	23.68	16.15	0.11	−0.19	13.79	13.71
32.63	17.17	7.68	23.86	16.24	0.10	−0.20	14.22	14.12
36.71	17.18	7.69	23.90	16.26	0.10	−0.20	14.26	14.16
$\omega = 1.17eV$								
1	15.39	7.23	19.41	14.01	0.16	−0.13	6.57	6.60
2.21	16.31	7.45	21.41	15.08	0.28	−0.13	9.82	9.96
6.02	17.06	7.62	23.29	15.99	0.14	−0.19	13.11	13.06
20.7	17.46	7.70	24.41	17.12	0.16	−0.20	15.57	15.53
32.63	17.53	7.72	24.60	16.62	0.16	−0.20	16.04	15.99
36.71	17.54	7.72	24.64	16.63	0.16	−0.20	16.14	16.09

also for the hyperpolarizability of PNA, but much less significant than that for smaller molecules (like acetonitrile[89]). Another critical factor is the form of the cavity; the spherical cavities are conceivably better for the two- or three-dimensional CT complexes than for the one-dimensional (see below). Another important aspect to be monitored is the convergence of the multipolar expansion of the charge field of the solvent molecule and thus the solvent polarization and reaction field energies. The dipole contribution often only gives a fraction of the total solvent effect and more systematic studies of reaction field models show that properties (like solvatochromatic shifts) only have a fraction recovered by the dipole interaction, and that higher multipolar contributions are important, see e.g. ref. [147]. The reaction field contribution, i.e. the difference between the self-consistent energy and the polarization energy (evaluated with the vacuum electronic wave function), can even be equally important as the polarization energy itself. Because of the close link between the hyperpolarizability and the shift in excitation spectra, these findings indicate that shifts of β in general should be accounted for, with a full expansion of the molecular charge field and with a self-consistent handling of the reaction field interaction. This was shown in section II-E for the solvent induced hyperpolarizability of water, see also Fig. 3. Para-substituted benzenes with donor and acceptor groups can due to their geometrical form and charge distribution still be well described by the dipolar interaction, actually, in ref. [86] it was shown that the difference between dipole approximation and multipole expansion is only 10% for the hyperpolarizability β. The dipolar approximation is thus still warranted for molecules with ultra-strong longitudal charge transfer excitations like PNA.

I-C Application of the two-state model

It is well known that the first hyperpolarizabilities β of strong, one-dimensional, charge transfer systems like PNA are well described by the so-called two-state model. Two- or few-state models connects the linear optical properties of the molecule with its hyperpolarizability, and constitutes, perhaps, the most cherished tool for analyzing qualitative, mechanistic, and sometimes quantitative, trends in hyperpolarizabilities for different compounds. It can be seen as a truncation of the sum-over-state perturbation expression for the hyperpolarizability as implemented by the quadratic response function of eq. 12. For general molecules, for example the neon iso-electronic hydrides treated in section 5, the convergence of the terms in the perturbation expression is slow. In such cases the direct solution for the sum-over-states value obtained by response theory is particularly benefitial. It gives the exact *size consistent* hyperpolarizability for the particular set of parameters optimized for the reference wave function. As explained in section 3, because the sum-over-state value is obtained by solving equations rather than by explicit summations, large dimension of the parameter space of the wave functions can be employed. Slow convergence in the sum over state expression prevails when the dipolar spectrum is sparse without low-lying intense transitions; in the opposite case the number of levels in the few-state approximation should correspond to the number of strong dipolar states. For strong one-dimensional charge transfer compounds it is sufficient to consider only one state in addition to the ground state. The truncated sum-over state values for β can be obtained either by computing the ingoing quantities as expectation and transition expectation values (dipole moments of ground and excited states) or from the linear and quadratic response functions (transition energies and transition dipole moments); the transition moments between the ground and excited states are obtained from the linear

response function and the transition moments between the excited states are given by the double residues of the quadratic response functions.

We consider here the two-state model applied to one-dimensional change-transfer (CT) compounds, in which β is determined only by considering the ground and a first-excited state possessing (CT) character. Generally, we have

$$\beta_{tsm}(-\omega_1 - \omega_2; \omega_1, \omega_2) = \beta_0 D(\omega_1, \omega_2) \tag{158}$$

$$\beta_0 = 3\mu_{eg}^2(\mu_e - \mu_g)/\omega_{eg}^2 \tag{159}$$

and

$$D(\omega_1, \omega_2) = \frac{1 - \omega_1\omega_2/\omega_{eg}^2}{(1 - \omega_1^2/\omega_{eg}^2)(1 - \omega_2^2/\omega_{eg}^2)(1 - (\omega_1 + \omega_2)^2/\omega_{eq}^2)} \tag{160}$$

where β_{tsm} is the hyperpolarizability given by the two-state model in a perturbation series definition (the so-called B convention[46]). β_0 represents here the static hyperpolarizability, μ_g and μ_e the dipol moments of ground and CT levels, μ_{eg} the transition dipole moment between the two states, and ω_{eg} the excitation energy of the CT state. $D(\omega)$ represents the dispersion effect, it is a function of frequencies of the external field. For the Kerr effect it reads

$$D(\omega, 0) = \frac{1}{(1 - \omega^2/\omega_{eg}^2)^2} \tag{161}$$

for the SHG case it becomes

$$D(\omega, \omega) = \frac{1}{(1 - \omega^2/\omega_{eq}^2)(1 - 4\omega^2/\omega_{eq}^2)} \tag{162}$$

The first use of the two-state model is to analyze the sign of β which largely is dictated by $(\mu_e - \mu_g)$. In general the excited state dipole moment is larger, indicating positive sign, but the reverse holds in several cases, and in the extreme case the ground and excited state dipole moments have different signs as encountered in some organometallic CT compounds[9]. Another use of the two-state model is to predict the relationship between measured values of the absorption maximum (λ_{max}) and the hyperpolarizability β (sometimes a linear correlation between these values have been used to verify the two-state model). The underlying assumption is then that the excitation energy variation between different compounds, e.g. different substituents in donor-acceptor compounds or different solutions, is the major factor that dictates the variation of β. A practical problem of such correlations is the restriction to compounds which absorb in the visible wavelength region. In general, however, the application of the two-state model to the solvent dependence of the hyperpolarizability requires consideration of solvent induced changes of the transition moment and the dipole moment difference, in addition to the excitation energy, for the CT state. The solvent dependence of these quantities are given in Tables 14 and 15. The static and Kerr hyperpolarizabilities β derived from the two-state model are displayed in Fig. 5 together with the experimental hyperpolarizabilities (results of solvent response calculations are given in Tables 16 and 17). The two-state model works quite well for both static and Kerr hyperpolarizabilities at the SCF level. The discrepancy is in the range of 11%-20% for PNA in solutions. A larger discrepancy has been found at the MCSCF level, around 25%-34%. The dispersion as derived by Kerr results at frequency $\omega = 1.17eV$ is reproduced well by the two-state model both at the SCF and MCSCF levels. For instance, the dispersion of the Kerr effect for PNA in acetone is 13% in both the two-state model and the exact calculation, and at both the SCF and MCSCF levels.

As we can see from Figure 5, the static hyperpolarizabilities obtained from the two-state model at the correlated level are larger than those from the direct calculations. Such differences represent the collected contributions from other states. Since other states either are quite far from the CT state or have small oscillator strengths, (for the low applied field frequencies) the contributions from these other states to the dispersion are expected to be minor. Furthermore, since the dispersion of the hyperpolarizability $\beta(-2\omega;\omega,0)$ can be described very well by the two-state model it is reasonable to assume

$$\beta_{est.}(-2\omega;\omega,\omega) = \beta_{tsm}(-2\omega;\omega,\omega) + \beta_{oth}(0;0,0) \tag{163}$$

where $\beta_{oth}(0;0,0)$ is the contribution from other states to the hyperpolarizability.

We have shown in the previous section that our correlated calculations can provide accurate results for the dipole moments of the ground and CT states. The critical quantity in the two-state model calculations is the excitation energy. Both in gas and solution phases the excitation energy is overestimated. When the two-state model is used this leads to an underestimation of the hyperpolarizabilities. If we had used an electronic structure model

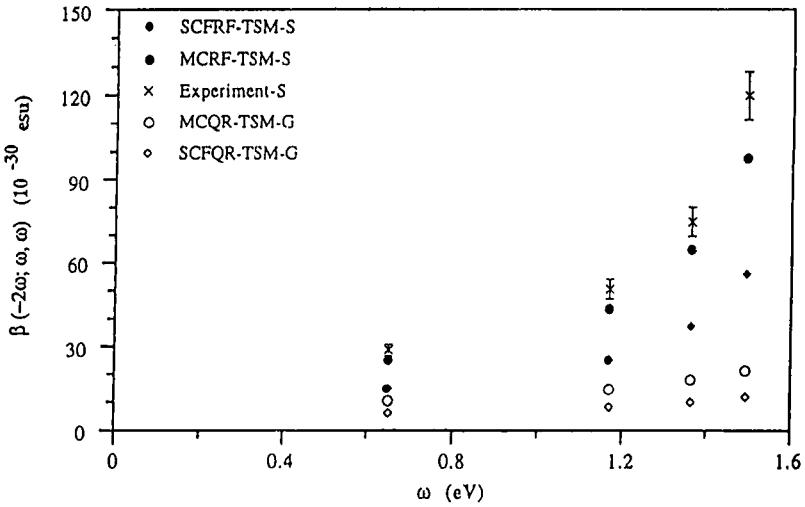

Figure 5: Comparison of hyperpolarizability dispersion for gas phase PNA and for PNA in 1,4-dioxane solution obtained from experiment and from the two-state model as applied to SCF and MCSCF reaction field calculations. G and S denote gas and solvent phase experimental excitation energies, respectively. Details are given in the text.

Table 18: The best estimated ESHG hyperpolarizability $\beta(2\omega;\omega,\omega)$ of PNA in different solvents. The B convention has been used. The cavity radius is 9.82 au.

	Best Est.		Expt.[a]	
	β_z $(10^{-30}esu)$	$\mu\beta_z$ $(10^{-30}esuD)$	β_z $(10^{-30}esu)$	$\mu\beta_z$ $(10^{-30}esuD)$
$\omega = 1.17eV$				
1	14.46	92		
2.21	43.95	305	48.9	342
6.02	58.43	430	67.8	456
20.7	74.77	569	77.7	567
32.63	78.48	600	96.0	585
36.71	91.23	699	90.0	657

a) Ref.[48]

that considered explicitly the dynamical part of the correlation the obtained excitation energy would be improved significantly whereas the dipole moment and transition moments would hardly be expected to change. Improved values for $\beta_{tsm}(-2\omega;\omega,\omega)$ would therefore be obtained by introducing experimental excitation energies into the two-state formula. The hyperpolarizabilities we report in Table 18 are obtained with such experimental excitation energies[48]. As seen from Table 18, the largest deviation between experimental and calculated β_z values is about 25 % (for PNA in methanol solution). It should be noted that in order to obtain values of β from the ESHG experiments, the dipole moment must also be measured. The accuracy of the experimental estimated hyperpolarizabilities depends also on the accuracy of the measurements of dipole moments and therefore it is more relevant (and reliable) to compare the values of $\mu \times \beta$. It can be seen from Table 18 that the present results for $\mu \times \beta$ are in very good agreement with the corresponding experimental values. The dispersion of the hyperpolarizability for PNA in 1.4-dioxane solution has been reported by Teng and Garito[47] and are displayed in Figure 5. As illustrated in Figure 5, our calculated results for PNA in 1.4-dioxane solution at the MCSCF level can describe the dispersion effect very well. The dispersion of the hyperpolarizability for PNA in gas phase at SCF and MCSCF levels are also shown in Figure 5 for the two-state model with experimental excitation energies. The importance of correlation is clearly seen. The steep nature of the measured hyperpolarizability dispersion is due to strong solvent effects.

II Hyperpolarizabilities of 3,5-dinitroaniline

Two- or three-dimensional charge transfer compounds are interesting because of their role as model compounds for non-linear optical active materials. From a material science point of view, one-dimensional charge transfer organic molecules, like PNA, suffer several drawbacks. They have a large permanent dipole moment in the ground state, and on crystallization the dipoles tend to be aligned oppositely, leading to bulk material without the first non-linear susceptibility. The so-called "phase-matching" requirement can not be realized either, since the wave vectors $\mathbf{k}_\omega$ and $\mathbf{k}_{2\omega}$ are parallel. Furthermore, the frequency doubled photons get closer in resonance with the charge transfer state, leading to the so-called efficiency-transparency problem. For the two- or three- dimensional charge transfer

Table 19: The dipole moments μ (D), static polarizabilities α (10^{-24} esu) and hyperpolarizabilities β (10^{-30} esu) for 3,5-DNA in gas phase at SCF, CAS44 and CAS64 level.

	μ	α_{xx}	α_{yy}	α_{zz}	α	β_{zxx}	β_{zyy}	β_{zzz}	β_z
SCF									
DZ	7.61	18.39	6.27	19.12	14.59	1.04	−0.10	0.23	1.18
DZp	7.38	20.19	7.30	19.58	15.69	1.32	−0.02	0.37	1.67
DZP	7.28	20.27	8.08	20.03	16.12	1.12	−0.07	0.34	1.39
CAS44									
DZ	5.91	17.42	6.41	19.22	14.35	−1.86	−0.10	3.90	1.93
DZp	5.91	19.69	7.29	20.56	15.85	−2.36	−0.02	4.89	2.52
CAS64									
DZ	5.75	17.50	6.31	19.13	14.31	−1.39	−0.09	4.47	2.99
DZp	5.76	19.62	7.25	20.47	15.78	−1.88	−0.02	5.34	3.45

compounds, these problems can be eliminated. For instance, the most extreme of these compounds, the so-called octopolar compounds, e.g. 1,3,5,-triamino-2,4,6-trinitrobenzene (TATB), which has a C_3 symmetry axis and no dipole moment but, nevertheless, a larger hyperpolarizability than PNA[148, 149, 146]. These compounds require (at least) three levels in a few-state model as $\delta\mu$ in the two-state model in Eq. 159 is zero, and evidently more than the first (Onsager) dipolar term to account for the reaction field contribution to the solvent induced hyperpolarizability. The occurrence of another charge transfer transition perpendicular to the molecular axis perturbs also the Kleinman symmetry of this system[146]. Furthermore, as predicted in semiempirical work of Joffre et al[149], the role of correlation is crucial for these compounds[149].

In order to explore some of the multi-dimensional charge transfer features for the hyperpolarizability in the response theory framework, calculations were recently carried out for the 3,5-dinitroaniline compound in gas and solvent phases. As found for the PNA molecule, the results from DZP basis have almost reached the Hartree-Fock limit. Due to the size of 3,5-dinitroaniline (3,5-DNA) molecule, it is still necessary to examine the ability of smaller basis sets in order to investigate correlation and solvent effects. DZ and DZp basis sets were constructed for this purpose by fully or partly removing the polarization functions in the DZP basis set. Table 19 recapitulates some of the RPA results of dipole moments, static polarizabilities and first hyperpolarizabilities with these three basis sets; for the larger basis set direct-atomic-orbital quadratic response calculations[42] were required. Although the basis set dependence is evident, it is found that the smaller basis set (DZ) reproduces the values of the DZp basis set for dipole moment μ, polarizability α and hyperpolarizability β to 95%, 90% and 85% , respectively.

3,5-DNA contains 16 π-electrons and requires therefore restricted excitation schemes if all $\pi-$orbitals are included in a correlating active space, or alternatively restricted sets of π orbitals if a complete active space scheme is employed. A natural orbitals analysis of perturbational calculations serves as a good guide to restrict either the orbital space or the electron excitations also for compounds of the size of 3,5-DNA. In ref. [150] the correlation effect on β was studied using two complete active space wave functions containing $4b_1$,$4a_2$ and $6b_1$,$4a_2$ active orbitals with 8 and 10 electrons, respectively. Calculations of dipole

Table 20: The excitation energies (eV) and osc illator strengths of A_1 and B_2 states for 3,5-DNA in gas phase with DZ basis set at SCF, CAS44 and CAS64 levels.

	SCF		CAS44		CAS64	
	E(eV)	Osci.	E(eV)	Osci.	E(eV)	Osci.
$2A_1$	5.16	0.0098	4.85	0.1543	4.76	0.1484
$3A_1$	5.90	0.0706	5.97	0.0000	5.99	0.0001
$4A_1$	6.55	0.5355	6.14	0.0010	6.14	0.0122
$5A_1$	7.30	0.5125	6.98	0.8203	6.85	0.6931
$6A_1$	9.28	0.0004	7.61	0.0400	7.00	0.0605
$1B_2$	4.43	0.1252	4.82	0.0640	4.27	0.0252
$2B_2$	5.95	0.0821	5.47	0.0986	4.74	0.0903
$3B_2$	6.84	0.5849	6.68	0.5731	6.60	0.5602
$4B_2$	8.39	0.0510	7.70	0.0189	6.98	0.0164
$5B_2$	8.57	0.0014	7.87	0.0235	7.62	0.0016

moments, polarizabilities and hyperpolarizabilities (carried out with DZ and DZp basis sets) indicated that the basis set dependence is almost the same as that for the RPA calculations. The correlation effect was found relatively small for the dipole moment and polarizability, however, very strong for the hyperpolarizability β. The correlated calculation of the β_{zzz} component is almost 20 times larger than the SCF result. The correlation even changes the sign of the β_{zxx} component, but hardly changes the β_{zyy} component. Both these components are important for the two-dimensional charge transfer character of this molecule. The average hyperpolarizability β_z increases by 160% and 250% for CAS44 and CAS64 calculations, respectively (the DZ basis set). These correlation effects are thus much stronger than observed from calculations of PNA, and indicates, in line width semi-empirical CI results on TATB and other octopolar compounds considered by Joffre et al[149], that the prediction of β in many-dimensional charge transfer organic molecules requires a correlated level of theory.

The hyperpolarizability of the PNA molecule is dominated by the β_{zzz} component and could therefore be described by the two-state model where only the ground and the charge transfer states are considered. As argued above such a two-state model will no longer be applicable for the two-dimensional charge transfer molecule, and one can expect that there should be at least two CT states distributed into different symmetries. The excitation energies and oscillator strengths for excited states of the 3,5-DNA molecule was carried out in ref. [150] using the linear response theory at SCF and two CAS MCSCF levels with the DZ basis set. Since the β_{zzz} and β_{zxx} components are connected with the A_1 and B_2 states, results shown in Table 20 are restricted to the five lowest excited states having the symmetries A_1 and B_2, respectively. As for the total hyperpolarizability, correlation effects have strong influence on the excitation energies and the oscillator strengths, in particular for the latter. From the SCF results, one can see that there are two A_1 ($4A_1$, $5A_1$) and one B_2 ($3B_2$) states with relatively strong oscillator strengths. However, at the correlation level, only one A_1 ($5A_1$) and one B_2 ($3B_2$) states have been found to dominate the absorption spectra of 3,5-DNA. Although the oscillator strength of the first excited A_1 state is smaller than that of the $5A_1$ state, it might give relatively large contributions to the hyperpolarizability due to its low excitation energy. In contrast to TATB, we find that

Table 21: The dipole moments μ (D), static p olarizabilities α (10^{-24} esu) and hyperpolarizabilities β (10^{-30} esu) for 3,5-DNA in different dielectric environments at SCF and CAS44 levels with DZ basis set. The cavity radius is 9.82 au.

	μ	α_{xx}	α_{yy}	α_{zz}	α	β_{zxx}	β_{zyy}	β_{zzz}	β_z
SCF									
1	7.61	18.39	6.27	19.12	14.59	1.04	−0.10	0.23	1.18
2.21	8.15	19.80	6.40	20.56	15.59	1.38	−0.10	0.44	1.71
6.02	8.61	21.00	6.50	21.78	16.43	1.71	−0.10	0.67	2.28
20.7	8.86	21.67	6.55	22.45	16.89	1.92	−0.10	0.82	2.63
32.63	8.90	21.78	6.56	22.56	16.97	1.96	−0.10	0.84	2.70
78.54	8.94	21.90	6.56	22.68	17.05	2.00	−0.10	0.87	2.76
CAS44									
1	5.91	17.42	6.41	19.22	14.35	−1.86	−0.10	3.90	1.93
2.21	6.32	18.71	6.55	20.86	15.37	−2.46	−0.10	5.26	2.70
6.02	6.68	19.83	6.66	22.30	16.26	−3.17	−0.11	6.77	3.50
20.7	6.85	20.45	6.71	23.11	16.76	−3.58	−0.11	7.70	4.01
32.63	6.88	20.56	6.72	23.24	16.67	−3.70	−0.11	7.91	4.10
78.54	6.92	20.67	6.73	23.39	16.93	−3.77	−0.11	8.10	4.22

a few-level (here three-level) model is too restricted to be of real value. In the TATB case, there are three doubly degenerate excited states which are responsible for the octopolar β and which cancels each others dipole components[149, 9]. In 3,5-DNA there is no such canceling, which might be a reason for that the few-level models (four, respectively three levels) are of different quality in the two cases.

The SCF and MCSCF values of dipole moment, static polarizabilities $\alpha(0,0)$ and hyperpolarizabilities $\beta(0;0,0)$ of 3,5-DNA in the different solvent environments are shown in Table 21 (DZ basis set). At the SCF level the dipole moment and static polarizability show an increase of 7-18%. The solvent effect on the first hyperpolarizability has been found to be much stronger, and increases the hyperpolarizability in the range 45-135% for the dielectric constants covered. This solvent dependence is quite similar to that of PNA. Due to the two-dimensional charge transfer character of 3,5-DNA, the solvent effect is mostly focussed on the zzz and zxx components of β, while the zyy component hardly changes. The correlation plays the same role as that in the gas phase. It decreases the values of μ and α, but increases the value of β drastically. The solvent dependence is found to be the same as that at the SCF level. The correlated result for the dipole moment in dioxane, 6.32D, is close to the experimental value of 5.76 D[146] while the SCF value is 8.15D. The frequency dependent polarizabilities $\alpha(-\omega;\omega)$ and first hyperpolarizabilities $\beta(-\omega;\omega,0)$, referring to the Kerr effect, for 3,5-DNA in various solvents are reported in Table 21. As seen in the table the dispersion at ω =1.17 eV is quite small.

7 Hyperpolarizabilities of polyenes and polyynes

Short polyenes and polyynes are frequently used as test compounds for a variety of methods addressing properties of oligomers. The theoretical efforts focus now on non-linear

properties of these systems because of the well-known fact that conjugated polymers show conducting properties and large, ultrafast, non-linear optical responses. Studies of hyperpolarizabilities of oligomer sequences explore the length dependence and the convergence of this property to its polymer value. Out of several *ab initio* methods the random phase approximation seems to have the greatest potential for large scale (large molecule) applications on linear and non-linear properties, since it is amendable for so-called direct atomic orbital techniques[143, 42]. The hyperpolarizabilities of short polyenes have been intensively studied recently including the effects of electron correlation. Those investigations fall into two categories. One, using *ab initio* methods, attempts to accurately reproduce experimental hyperpolarizabilities[151, 152, 153]. The other category of investigations attempts to find the underlying mechanism behind optical non-linearity[154, 155, 156] in conjugated polymers and has involved primarily semi-empirical methods. Using *ab initio* coupled Hartree-Fock theory (equivalent to the RPA), Karna et al computed the frequency-dependent hyperpolarizabilities of the short polyenes and obtained good agreement with available experimental gas phase results[151], see also recent results by Luo et al[157] for the prolonged series[157]. The basis set dependence has been discussed by Hurst et al[152], who concluded that the basis set and dispersion effects play the dominant role in determining the hyperpolarizabilities of polyenes. The correlation effect is, however, apparently small[151, 158, 157].

One has attempted to find simple relations between the static polarizabilities and the hyperpolarizabilities for the oligomeric chains, and also the exponential factor (η) entering power law expressions that connect the hyperpolarizability of n units with that of one unit. The "correlation length" for the polymer where the hyperpolarizability values flatten out is also of particular interest. Semi-empirical theory and experimental investigations are in acceptable agreement concerning the exponential factor for β; ($1.5 < \eta_{calc} < 2.0$; $1.9 < \eta_{exp} < 3.2$), although theory predicts consistently a somewhat lower power law exponent than that determined from experiment[9]. From arguments given in section 4 it is plausible that a large part of the discrepancy origin in environmental (solvent) effects. Investigations of these features within the scope of response theory were recently carried out by means of calculations for the static and dynamic hyperpolarizabilities of polyynes, $C_{2n}H_2$, by Jaszunski et al.[159], and polyenes, $C_{2n}H_{2n+2}$, by Luo et al.[157]. In polyynes and polyenes, like in other polymeric compounds, the longitudinal component of the hyperpolarizability, γ_{xxxx}, is the most important component for a description of the hyperpolarizability, in the case of polyynes the ratio of the longitudinal component to the next largest component increases with the chain length from about 10 : 1 for C_6H_2 to 30 : 1 for C_8H_2. Due to the presence of the inversion center the first hyperpolarizability, β^0, is zero (the superscript indicates the finite-field strength); the second hyperpolarizability $\gamma(-\omega_1 - \omega_2; \omega_1, \omega_2, 0)$ is obtained from the first hyperpolarizability by numerical differentiation, which for any set of frequencies gives

$$\gamma(-\omega_1 - \omega_2; \omega_1, \omega_2, 0) = \beta^F(-\omega_1 - \omega_2; \omega_1, \omega_2)/F \tag{164}$$

As shown in ref.[159] the Hartree-Fock limit can be reached for γ with basis sets containing s, p, d, and f functions on the carbons and s, p and d functions on the hydrogens. In the previous studies[151, 152] it was found that a 4-31G* basis set provided good descriptions for the hyperpolarizabilities of polyenes.

Using a logarithmic fit to the SCF results, it was found for $C_{2n}H_2$ that $\alpha(C_{2n}H_2) = \alpha(C_2H_2)n^{1.41}$ and $\gamma(C_{2n}H_2) = \gamma(C_2H_2)n^{2.98}$ (for n=1-6)[159]. The exponents are not affected significantly by correlation. Similarly, for $C_{2n}H_{2n+2}$, $\alpha(C_{2n}H_{2n+2}) = \alpha(C_2H_4)n^{1.26}$

Table 22: Frequency dependent polarizabilities and hyperpolarizabilities for $C_{2n}H_2$ (n=1-6) molecules (α in a.u., γ in 10^3 a.u.), from Ref. [159].

		$\alpha(0;0)$	A	$\gamma_{xxxx}(0;0,0,0)$	A
SCF	C_2H_2	31.39	5.15	3.163	10.5
	C_4H_2	86.53	8.70	21.89	13.6
	C_6H_2	143.16	10.08	62.75	14.0
	C_8H_2	217.89	11.38	175.7	14.7
	$C_{10}H_2$	306.48	13.16	377.3	15.4
	$C_{12}H_2$	398.71	14.42	631.2	15.5
MCSCF	C_2H_2	30.01	4.88	3.189	9.47
	C_4H_2	75.13	7.18	19.18	11.40
	C_6H_2	120.58	8.17	56.29	11.99
	C_8H_2	173.59	8.83	150.0	12.62

and and $\gamma(C_{2n}H_{2n+2}) = \gamma(C_2H_4)n^{3.51}$ (for n=1-6)[157]. It can be seen that the hyperpolarizabilities of polyenes show a stronger length dependence than those of polyynes.

The frequency-dependent hyperpolarizabilities were calculated for a description of the ESHG experiment, $\gamma^{ESHG} = \gamma(-2\omega;\omega,\omega,0)$, and the DC Kerr effect, $\gamma^{Kerr} = \gamma(\omega;\omega,0,0)$. It was found that the calculated results could well be approximated using the formula [160, 161]

$$\gamma(\omega_1;\omega_2,\omega_3,\omega_4) = \gamma(0;0,0,0)(1 + A\omega_L^2 + B\omega_L^4 + ...) \tag{165}$$

where $\omega_L^2 = \omega_1^2 + \omega_2^2 + \omega_3^2 + \omega_4^2$ and the expansion coefficients A and B are independent of the optical property. The dispersion in the region of interest is well described by the ω^2 term. The expansion in Eq.(165) applied to ESHG and to Kerr yields similar values for A. The SCF ratio $A(ESHG)/A(Kerr)$ is 0.95, 0.90, 0.90, 0.87 and 0.84 for n=1-5 of the polyynes, and 1.02, 1.04, 1.06, 1.08 and 1.08 for n=1-5 of the polyenes. Tables 22 and 23 give the static hyperpolarizabilities and the coefficient A for the all molecules studied in Ref. [159], and some of the molecules studied in Ref. [157]. The coefficient A is fitted from ESHG results. The frequency dependence of the hyperpolarizabilities for the polyene molecules is much stronger when the length of the molecule is increased. It reflects the factor that the "band gap" in polyenes gets narrower as the chain gets longer. A similar relation as in the static case can be found for the dynamic hyperpolarizability

$$\gamma^{ESHG}(C_{2n}H_2) = \gamma^{ESHG}(C_2H_2)n^X \tag{166}$$

where the optimal value of X increases slightly (5-10%) with ω. This occurs since the dispersion, the A coefficient, becomes larger with n.

The geometry dependence of the hyperpolarizability is a difficult factor that remains to be studied systematically. On the other hand, for polyynes like for polyenes the effect of electron correlation turns out to be rather insignificant for various properties. Even though this partly must be ascribed cancellation effects (of valence versus dynamic correlation), it motivates further applications of direct-atomic-orbital RPA (DDRPA) techniques on larger members of the oligomer sequences for calculations of properties like hyperpolarizabilities. Such calculations are now in operation in our laboratory, using DDRPA on polyenes up to

Table 23: Frequency dependent polarizabilities and hyperpolarizabilities for $C_{2n}H_{2n+2}$ (n=1-6) molecules (α in a.u., γ in 10^4 a.u.), from Ref. [157].

		$\alpha(0;0)$	A	$\gamma_{xxxx}(0;0,0,0)$	A
SCF	C_2H_4	24.68	6.38	0.36	12.13
	C_4H_6	53.38	9.51	2.59	24.78
	C_6H_8	90.13	14.18	11.70	28.68
	C_8H_{10}	139.75	21.92	41.64	39.59
	$C_{10}H_{12}$	179.08	22.97	85.75	47.57
	$C_{12}H_{14}$	231.33	27.32	176.44	56.94

30 carbon atoms[157]. Already obtained results at the RPA level for the smaller members is indeed encouraging for both the polarizability and the hyperpolarizability[157].

Because of the close connection between polarizabilities and hyperpolarizabilities with one- and two-photon spectra, the latter have also been extensively studied theoretically and experimentally. For polyenes, the two-photon absorption of even states is of particular interest, since it is the key point for understanding optical non-linearity[158]. The excited states of polyenes are divided into two categories according to the selection rules imposed by symmetry. The first kind of states are one-photon allowed only, while the second kind is only reached by two-photon transitions[162, 158]. Several semi-empirical calculations are available[154, 155], but with rather disparate conclusions with respect to the allocation of the two-photon maximum and validity of few-state models for the hyperpolarizability. For instance, Soos et al.[163, 154] found a strong two-photon absorption (TPA) around 1.5 E_g, (E_g refers to the "band gap" excitation energy of the 1^1B_u state) of the polyenes and proposed a three-state model for the hyperpolarizability. This was supported by Heflin[164], while Dixit et al.[155, 156] found a strong TPA to be close to E_g, and argued that a four-state model would be required to determine the hyperpolarizability. These different conclusions have led to different explanations for the mechanism of the optical non-linearity for the polyenes.

In ref. [158] systematic *ab initio* calculations of one- and two-photon absorption (TPA) moments of polyenes were obtained by response theory and the results were used, in addition to assigning the TPA spectra, to explore the validity of few-state models for the hyperpolarizability. It was demonstrated that accurate results for the one-photon excitation spectra of these short polyenes can be obtained already at the lowest level of response theory, namely the random phase approximation (RPA). Excellent agreement was obtained with data from one-photon spectra, with errors of only one or two tenths of an eV. The polarizabilities generated by RPA are within a few % of the vapour phase values at the corresponding frequencies, and hyperpolarizabilities have reached high accuracy as well[151, 157]. The two-photon absorption maxima was found at 1.5-1.7 E_g for the short polyenes (up to trans-octatetraene). The first one-photon forbidden ^1A_g state was found to have a very small two-photon amplitude, and is therefore not likely to contribute to the non-linear properties, although it might intrude the one-photon band-gap for the somewhat larger polyenes.

The *ab initio* RPA calculations by Luo et al[158] were recently used to reexamine the

Table 24: The transition moments between 1^1B_u and the even states for butadine, hexatriene and octatetraene molecule (in atomic units). From ref. [158][a].

Basis	Even state	Butadine M_x	Butadine M_y	Hexatriene M_x	Hexatriene M_y	Octatetraene M_x	Octatetraene M_y
ANO[b]							
	1^1A_g	2.254	−0.672	3.182	−0.735	3.995	−0.740
	2^1A_g	1.304	−0.882	0.815	−0.109	−0.841	0.122
	3^1A_g	1.092	0.455	1.032	−0.291	−0.162	−0.214
	4^1A_g	0.218	−0.028	0.437	0.339	1.231	−0.010
	5^1A_g	0.444	0.227	−0.231	0.229	0.429	−0.063
	6^1A_g	0.170	−0.405	2.766	−0.083	0.065	−0.343
	7^1A_g	1.578	0.023	0.217	0.003	3.186	−0.056
	8^1A_g	−0.044	−0.109	−0.042	−0.131	0.228	−0.043
	9^1A_g	0.177	0.096	0.246	−0.016	−0.093	0.005
431-G*							
	1^1A_g	2.338	−0.731	3.240	−0.766	4.117	−0.823
	2^1A_g	1.073	−0.558	1.159	−0.309	0.703	−0.140
	3^1A_g	0.570	−1.066	0.201	−0.149	−0.584	0.052
	4^1A_g	1.691	−0.172	2.616	−0.197	3.670	−0.147
	5^1A_g	0.456	0.684	1.341	0.235	0.257	−0.058
	6^1A_g	0.182	0.107	0.260	−0.686	3.539	−0.315
	7^1A_g	0.642	0.057	0.245	−0.094	−0.642	−0.037
	8^1A_g	0.022	−0.257	0.045	−0.020	1.645	0.139
	9^1A_g	0.348	0.063	−0.658	0.115	0.119	0.009

a) Coordinates have been rotated from the ones presented in Ref.[158] (but are identical to those used in ref.[157]). b) Generally contracted ANO basis set used, see Ref. [158].

mechanism of optical non-linearity. The hyperpolarizability of polyenes is dominated by the component along the chain, the xxxx component, which is controlled by the transition route

$$1^1A_g \rightarrow a^1B_u \rightarrow b^1A_g \rightarrow c^1B_u \rightarrow 1^1A_g$$

where a, b and c denote state numbers. The first odd state, 1^1B_u, presents the major feature of the one-photon absorption spectrum of polyenes. In the three-state approximation, only the 1^1A_g, 1^1B_u and m^1A_g states are considered[154]. The m^1A_g state, with the strongest TPA intensity, is found at 1.7 E_g. For the four-state approximation, an additional odd state (n^1B_u) is included[156], the strongest TPA (m^1A_g) state has been claimed to be very close to the 1^1B_u state.

From the sum-over-states expression of the cubic response function (see ref. [23]), the following expressions for the static hyperpolarizability can be derived. The four-state model:

$$\gamma_4 = \frac{4}{\omega_{mA1A}}\left(\frac{M_{1A1B}M_{mA1B}}{\omega_{1A1B}} + \frac{M_{1AnB}M_{mAnB}}{\omega_{1AnB}}\right)^2 - \frac{4M_{1A1B}^2}{\omega_{1A1B}^2}\left(\frac{M_{1A1B}^2}{\omega_{1A1B}} + \frac{M_{1AnB}^2}{\omega_{1AnB}}\right) \quad (167)$$

The three-state model:

$$\gamma_3 = \frac{4M_{1A1B}^2}{\omega_{1A1B}^2}\left[\frac{M_{mA1B}^2}{\omega_{mA1B}} - \frac{M_{1A1B}^2}{\omega_{1A1B}}\right] \quad (168)$$

M_{ij} and ω_{ij} represent the transition moment and the energy difference between states i and j, respectively. The expression for the three-state model is straightforward to analyze. When the transition moment between the odd ($1B_u$) state and the excited even state (mA_g) is larger than that between the ground state and the odd ($1B_u$) state, the hyperpolarizability is positive, otherwise it is negative. For polyenes the xxxx component of the hyperpolarizability has large positive values, and in order for the three-state approximation to be valid it is required that the magnitude of M^2_{mA1B} should be much larger than that of M^2_{1A1B}. Such a requirement should also be sufficient for the four-state model, since the transition moment between the ground state and the nB_u state is always very small. Beside the even two-photon states, the 1^1B_u state has a key role for the non-linearity, and to examine the validity of the few-state models, the transition moments between this state and the even states must be obtained. This was accomplished for the butadiene, hexatriene and octatetraene molecules in ref. [158] by exploiting the double residues of the quadratic response functions (see theory section 3). The results, recapitulated in Table 24, show relatively strong transition moments for the even states around $1.4E_g$ and $1.6E_g$, and these even states also show strong two-photon transition intensities in this region. However, none of the transition moments between the even states to the 1^1B_u state is larger than the transition moment between the ground state and the 1^1B_u state. This severely limits the validity of the three-state approximation for the short polyenes. A similar analysis of the four-state model shows that this approximation is also quite limited. By taking full account of all possible transitions, a large positive value for the xxxx component of the hyperpolarizability was obtained, as shown in Table 23. Thus, although there is an even state which dominates the TPA spectrum, RPA calculations tell that there are several other transitions that contribute significantly to the hyperpolarizability. This contrasts the findings for the charge-transfer compounds analyzed in section I for which even a two-state model is quite good, and indicates that the validity of these models cannot be taken for granted but must rather be evaluated from case to case.

8 Summary

Ab initio calculations of hyperpolarizabilities have turned into an important research area of quantum chemistry. In the present article we have reviewed recent progress in this area with emphasis on the development of multi-configurational (MCSCF) theory. Hyperpolarizabilities can be expressed in terms of response functions which represent an elegant and efficient way of rationalizing the results of time-dependent perturbation theory. The residues of the response functions determine e.g. the one- and two-photon transition matrix elements. We have described an analytic implementation of the linear and quadratic response functions for an MCSCF state. The implementation is direct in the sense that response matrices are never set up explicitly, only linear transformations of the response matrices on trial vectors and iterative techniques are used to solve the response matrix equations. One of the benefits of these techniques is that large, many-dimensional-, and therefore accurate reference wave functions can be employed; calculations with configuration spaces containing several million determinants can thus routinely be carried out.

The potential of response theory and its range of applications on molecular hyperpolarizabilities is illustrated by a selection of studies covering different types of molecular species, and highlighting different mechanisms underlying the hyperpolarizability. We have reviewed response calculations of molecular hyperpolarizabilities of molecules in the

gas and solution phases exploring the effects of vibrational averaging, frequency dependence, solvent dependence, electron correlation and choice of one-particle basis sets. The applications include various molecules of small, intermediate and extended size. The neon isoelectronic sequence: Ne, HF, H_2O, NH_3 was chosen to demonstrate the various physical effects and computational aspects of molecular hyperpolarizabilities. Molecular oxygen and nitrogen were chosen to represent small molecules with special correlation effects.

The single molecule calculations presented here describe gas phase experiments. With properly chosen configuration spaces MCSCF hyperpolarizability calculations can for smaller molecules be pushed towards experimental accuracy. In some cases calculations have challenged experimental results, in the case of neon the calculations showed that the dispersion was not anomalous and for hydrogen fluoride the calculations suggested that a reinvestigation of the experiment would be appropriate. Correlation is in general very important to obtain accurate results. Comparison of SCF and MCSCF results shows that changes of 50 per cent are not unusual. In many cases the dispersion is well described at the SCF level but in some cases, e.g. for NH_3, it is important also to describe the dispersion at a correlated level, even at the infrared frequencies that are used in ESHG experiments. The effect of vibrational averaging can vary in magnitude and may be as large as 10 per cent.

For the larger molecules it is evidently more difficult to obtain results of experimental accuracy, however, it is still important to push for methods that both can give high accuracy for small species and that can give trends and the possibility to provide a mechanistic insight and structure-to-property interpretations of larger species. By implementing a reaction field response function model for solvent contributions to the hyperpolarizability and by developing direct atomic-orbital techniques for SCF based calculations on isolated but extended systems, we have indicated that a common response theory formalism can unit these two goals. We have carried out hyperpolarizability calculations on the charge transfer complexes para-nitro aniline and 3,5-dinitroaniline, for gas and solvent phases. Solvent effects are found particularly significant for these types of systems, both concerning the hyperpolarizability and the hyperpolarizability dispersion. Solvent effects are important to estimate for most systems simply because the great bulk of measurements are carried out in solutions. We have also performed calculations of hyperpolarizabilities for oligomers as represented by small members of the polyyne and polyene series. For these molecules SCF and MCSCF hyperpolarizabilities are very similar. This is important since it will soon be possible to push the range of applications of quadratic response theory to very large systems containing several hundred atoms using the double-direct computational scheme. This will allow a reliable extrapolation to the infinite chain behaviour, and the prediction of non-linear and other related properties of polymers, such as correlation lengths, solitons and conductivity.

Acknowledgements

We thank Trygve Helgaker, Hans Jørgen Aa. Jensen, Jeppe Olsen, Hinne Hettema, Vladimir Spirko, Michal Jaszunski, Olav Vahtras and Henrik Koch for a rewarding collaboration in various projects involving molecular hyperpolarizabilities. This work was supported by CRAY Research Inc.

References

[1] N. Bloembergen. In *Nonlinear Optics.* Benjamin, Reading, 1965.

[2] R.L. Swafford and A.C. Uricht. *Annu. Rev. Phys. Chem.*, 29:421, 1978.

[3] In H. Walther, editor, *Laser Spectroscopy of Atoms and Molecules.* Springer, Berlin, 1976.

[4] In D. P. Craig and T. Thirunachandran, editors, *Molecular Quantum Electrodynamics.* Academic, New York, 1984.

[5] In D. S. Chemla and J. Zyss, editors, *Nonlinear optical properties of organic molecules and crystals.* Academic, New York, 1987.

[6] In J.O. Hirschfelder, R. E. Wyatt, and R. D. Coalson, editors, *Molecules, Lasers and Methods,* volume 73, 1989.

[7] In T. Kobayashi, editor, *Nonlinear Optical Properties of Organics and Semiconductors, Tokyo, Japan.* Springer, Berlin, 1989.

[8] In M. A. Ratner, editor, *Molecular Nonlinear Optics, Special issue,* volume 43, 1992.

[9] D.R. Kanis, M.A. Ratner, and T.J. Marks. *Chem. Rev.*, 94:195, 1994.

[10] H. Sekino and R. J. Bartlett. *J. Chem. Phys.*, 85:976, 1986.

[11] S.P. Karna, P.N. Prasad, and M. Dupuis. *J. Chem. Phys.*, 94:1171, 1991.

[12] J. E. Rice, R. D. Amos, S. M. Colwell, N. C. Handy, and J. Sanz. *J. Chem. Phys.*, 93:8828, 1990.

[13] H.J.Aa. Jensen, H. Koch, P. Jørgensen, and J. Olsen. *Chem. Phys.*, 119:297, 1988.

[14] P. Jørgensen, H. J. Aa. Jensen, and J. Olsen. *J. Chem. Phys.*, 89:3654, 1988.

[15] H. Hettema, H.J.Aa. Jensen, P. Jørgensen, and J. Olsen. *J. Chem. Phys.*, 97:1174, 1992.

[16] O. Vahtras, H. Ågren, P. Jørgensen, H.J.Aa. Jensen, T. Helgaker, and J. Olsen. *J. Chem. Phys.*, 97:9178, 1992.

[17] K.V. Mikkelsen, E. Dalgaard, and P. Swanstrøm. *J. Phys. Chem.*, 79:587, 1987.

[18] K.V. Mikkelsen, H. Ågren, H.J.Aa. Jensen, and T. Helgaker. *J. Chem. Phys.*, 89:3086, 1988.

[19] K.V. Mikkelsen, P. Jørgensen, and H. J. Aa. Jensen, 1994.

[20] S. P. Sarna and M. Dupuis. *Chem. Phys. Lett.*, 171:201, 1990.

[21] H. Sekino and R. J. Bartlett. *J. Chem. Phys.*, 94:3665, 1991.

[22] J. E. Rice, G. E. Scuseria, T. J. Lee, P. R. Taylor, and J. Almlöf. *Chem. Phys. Lett.*, 191:23, 1992.

[23] J. Olsen and P. Jørgensen. *J. Chem. Phys.*, 82:3235, 1985.

[24] J. E. Rice and N. Handy. *J. Chem. Phys.*, 94:4959, 1991.

[25] J. E. Rice and N. Handy. *Int. J. Quant. Chem.*, 43:91, 1992.

[26] P. E. S. Wormer and W. Rijks. *Phys. Rev. A*, 75:2928, 1986.

[27] F. Aiga, K. Sasagane, and R. Itoh. *J. Chem. Phys.*, 99:3779, 1993.

[28] H.J. Monkhorst. *Int. J. Quant. Chem.*, 11:421, 1977.

[29] H. Sekino and R. J. Bartlett. *J. Chem. Phys.*, 98:3022, 1993.

[30] E. Dalgaard and H.J. Monkhorst. *Phys. Rev. A*, 28:1217, 1983.

[31] H. Koch and P. Jørgensen. *J. Chem. Phys.*, 93:3333, 1990.

[32] R. Kobayashi, H. K. Koch, and P. Jørgensen. *Chem. Phys. Lett.*, 00:0000, 1994.

[33] C. R. Moylan M. Stähelin, D. M. Burland, A. Willetts, J. E. Rice, E. A. Donley, and D. P. Shelton. *J. Chem. Phys.*, 98:5595, 1993.

[34] S. Kotoku, F. Aiga, and R. Itoh. *J. Chem. Phys.*, 99:3738, 1993.

[35] V. Spirko, Y. Luo, H. Ågren, and P. Jørgensen. *J. Chem. Phys.*, 99:9815, 1993.

[36] Y. Luo, O. Vahtras, H. Ågren, and P. Jørgensen. *Chem. Phys. Lett.*, 205:555, 1993.

[37] D. M. Bishop. *Rev. Mod. Phys.*, 62:343, 1990.

[38] Y. Luo, H. Ågren, O. Vahtras, P. Jørgensen, V. Spirko, and H. Hettema. *J. Chem. Phys.*, 98:7159, 1993.

[39] D. M. Bishop, B. Kirtman, H. A. Kurtz, and J. E. Rice. *J. Chem. Phys.*, 98:8024, 1993.

[40] D.L. Yeager and P. Jørgensen. *Chem. Phys. Lett.*, 65:77, 1979.

[41] E. Dalgaard. *J. Chem. Phys.*, 72:816, 1980.

[42] H. Ågren, H. Koch, O. Vahtras, P. Jørgensen, and T. Helgaker. *J. Chem. Phys.*, 98:6417, 1993.

[43] K. D. Singer and A. F. Garito. *J. Chem. Phys.*, 75:3572, 1981.

[44] P. N. Prasad and D. J. Williams. In *Introduction to nonlinear optical effects in organic molecules and polymers.* Wiley, New York, 1991.

[45] R. W. Boyd. In *Nonlinear optics.* Academic Press, New York, 1992.

[46] A. Willets, J.E. Rice, D.M. Burland, and D.P. Shelton. *J. Chem. Phys.*, 97:7590, 1992.

[47] C.C. Teng and A.F. Garito. *Phys. Rev. B*, 28:6766, 1983.

[48] M. Stähelin, D.M. Burland, and J.E. Rice. *Chem. Phys. Lett.*, 191:245, 1992.

[49] In D. N. Zubarev, editor, *Nonlinear Statistical Thermodynamics.* Plenum, New York, 1974.

[50] In *The Quantum Mechanics of Many-Body Systems.* Academic Press, 1961.

[51] E. Dalgaard. *Phys. Rev. A*, 26:42, 1982.

[52] C. Funchs, V. Bonacic-Koutecky, and J. Koutecky. *J. Chem. Phys.*, 98:3121, 1993.

[53] E.S. Nielsen, P. Jøergensen, and J. Oddershede. *J. Chem. Phys.*, 73:6238, 1980.

[54] E. Dalgaard and P. Jørgensen. *J. Chem. Phys.*, 69:3833, 1978.

[55] M. R. Hoffmann, D. J. Fox, J. F. Gaw, Y. Osamura, Y. Yamaguchi, R. S. Grev, G. Fitzgerald, H. F. Schaefer, P. J. Knowles, and N.C. Handy. *J. Chem. Phys.*, 80:2660, 1984.

[56] J. Olsen, H. J. Aa. Jensen, and P. Jørgensen. *J. Comput. Phys.*, 74:265, 1988.

[57] J. Olsen, B. O. Roos, P. Jørgensen, and H. J. Aa. Jensen. *J. Chem. Phys.*, 89:2185, 1988.

[58] B. O. Roos. *Chem. Phys. Lett.*, 15:153, 1972.

[59] M. Born. *Z. Phys.*, 1:45, 1920.

[60] J.G. Kirkwood. *J. Chem. Phys.*, 2:351, 1934.

[61] J.G. Kirkwood and F. Westheimer. *J. Chem. Phys.*, 6:506, 1936.

[62] L. Onsager. *J. Am. Chem. Soc.*, 58:1486, 1936.

[63] J. Hylton, R.E. Christoffersen, and G.G. Hall. *Chem. Phys. Lett.*, 24:501, 1974.

[64] D.L. Beveridge and G.W. Schnuell. *J. Phys. Chem.*, 79:2562, 1975.

[65] M. D. Newton. *J. Phys. Chem.*, 79:2795, 1975.

[66] J.O. Noell and K. Morokuma. *Chem. Phys. Lett.*, 36:465, 1975.

[67] J.L. Rivail and D. Rinaldi. *Chem. Phys.*, 18:233, 1976.

[68] A. Warshel. *Chem. Phys. Lett.*, 55:454, 1978.

[69] D. Rinaldi. *Comput. Chem.*, 6:155, 1982.

[70] E. S. Marcus, B. Terryn, and J. L Rivail. *J. Phys. Chem.*, 87:4695, 1985.

[71] R. Contreras and A. Aizman. *Int. J. Quant. Chem.*, 27:193, 1985.

[72] Y. Inone H. Hoshi, M. Sakurai and R. Chujo. *J. Chem. Phys.*, 87:1107, 1987.

[73] G. Karlström. *J. Phys. Chem.*, 93:4952, 1989.

[74] C.J.F. Böttcher. *Theory of Electric Polarization.* Elsevier, 1952.

[75] C.P. Smyth. *Dielectric Behaveiour and Structure.* McGraw-Hill, 1955.

[76] H. Fröhlich. *Theory of Dielectrics.* University Press, Oxford, 1958.

[77] R. Pethig. *Dielectric and Electronic Properties of Biological Materials.* Wiley, 1979.

[78] O. Tapia. In H. Ratajczak and W.J. Orville-Thomas, editors, *Molecular Interactions.* Wiley, New York, 1980.

[79] O. Tapia. In R. Daudel, A. Pullman, L. Salem, and A. Veillard, editors, *Quantum Theory of Chemical Reactions*, volume 3. Wiley, Dordrecht, 1980.

[80] K.V. Mikkelsen and M. Ratner. *J. Chem. Phys.*, 90:4237, 1989.

[81] K.V. Mikkelsen and M. Ratner. *J. Phys. Chem.*, 93:1759, 1989.

[82] C. Medina-Llanos, H. Ågren, K. Mikkelsen, and H.J.Aa. Jensen. *J. Chem. Phys.*, 90:6422, 1989.

[83] H. Ågren, C. Medina-Llanos, K. Mikkelsen, and H.J.Aa. Jensen. *Chem. Phys. Lett.*, 153:322, 1989.

[84] K.V. Mikkelsen. *Z. Phys. Chem.*, 170:129, 1991.

[85] K.V. Mikkelsen and M. Ratner. *Int. J. Quant. Chem.*, 21:341, 1987.

[86] K. V. Mikkelsen, Y. Luo, H. Ågren, and P. Jørgensen. *J. Chem. Phys.*, 100:8240, 1994.

[87] J. Olsen, H. J. Aa. Jensen, and P. Jørgensen. *J. Comp. Chem.*, 74:265, 1988.

[88] K. V. Mikkelsen, P. Jørgensen, and H.J.Aa. Jensen. *J. Chem. Phys.*, 00:000, 1994.

[89] A. Willetts and J. E. Rice. *J. Chem. Phys.*, 99:426, 1993.

[90] D. Rinaldi. *Z. Phys. Chem.*, 00:000, 1994.

[91] H.J.Aa. Jensen, P. Jørgensen, H. Hettema, and J. Olsen. *Chem. Phys. Lett.*, 187:387, 1992.

[92] O. Christiansen and P. Jørgensen. *Chem. Phys. Lett.*, 207:367, 1993.

[93] D. P. Shelton. *Phys. Rev. Lett.*, 62:2660, 1989.

[94] D. P. Shelton. *Phys. Rev.*, 42:2578, 1990.

[95] V. Mizrahi and D. P. Shelton. *Phys. Rev. A*, 31:3145, 1985.

[96] D.M. Bishop. *J. Chem. Phys.*, 90:3192, 1989.

[97] D.M. Bishop. *Phys. Rev. Lett.*, 65:1688, 1990.

[98] G. Maroulis and A. J. Thakkar. *Chem. Phys. Lett.*, 156:87, 1989.

[99] D. P. Shelton. *Chem. Phys. Lett.*, 195:591, 1992.

[100] D. P. Chong and S. R. Langhoff. *J. Chem. Phys.*, 93:570, 1990.

[101] R. J. Bartlett and G. D. Purvis III. *Phys. Rev. A*, 20:1313, 1979.

[102] G. D. Purvis III and R. J. Bartlett. *Phys. Rev. A*, 23:1594, 1981.

[103] H. Sekino and R. J. Bartlett. *J. Chem. Phys.*, 84:2726, 1986.

[104] M. Jaszunski, P. Jørgensen, and H. J. Aa. Jensen. *Chem. Phys. Lett.*, 191:293, 1992.

[105] G. Maroulis. *J. Chem. Phys.*, 94:1182, 1991.

[106] G. Maroulis. *Chem. Phys. Lett.*, 195:85, 1992.

[107] J. E. Rice and N. C. Handy. *Int. J. Quant. Chem.*, 43:91, 1992.

[108] P.-O. Widmark, P.Å. Malmquist, and B.O. Roos. *Theor. Chim. Acta*, 77:291, 1990.

[109] A. J. Sadlej. *Coll. Czech. Chem. Commun.*, 53:1995, 1988.

[110] L. Adamowicz and R. J. Bartlett. *J. Chem. Phys.*, 84:4988, 1986.

[111] L. Adamowicz and R. J. Bartlett. *J. Chem. Phys.*, 86:7250, 1987.

[112] G. H. F. Diercksen, V. Kellö, and A. J. Sadlej. *J. Chem. Phys.*, 79:2918, 1983.

[113] H. J. Werner and P. Rosmus. *J. Chem. Phys.*, 73:2319, 1980.

[114] V. Spirko, N. M. Daadoch, H. J. Aa. Jensen, P. Jørgensen, and T. Helgaker. *Chem. Phys. Lett.*, 185:265, 1991.

[115] P. Jensen. *J. Mol. Spectrosc.*, 133:438, 1989.

[116] D.M. Bishop and B. Kirtman. *J. Chem. Phys.*, 95:2646, 1991.

[117] K. V. Mikkelsen, Y. Luo, H. Ågren, and P. Jørgensen. *J. Chem. Phys.* in press .

[118] J. W. Dudley and J. F. Ward. *J. Chem. Phys.*, 82:4673, 1985.

[119] J. F. Ward and C. K. Miller. *Phys. Rev. A*, 19:826, 1979.

[120] B.F. Levine and C.G. Bethea. *J. Chem. Phys.*, 65:2429, 1976.

[121] C. J. Jameson and P. W. Fowler. *J. Chem. Phys.*, 85:3432, 1986.

[122] G. Maroulis and D. M. Bishop. *Mol. Phys.*, 58:273, 1986.

[123] G. Maroulis and A. J. Thakkar. *J. Chem. Phys.*, 88:7623, 1988.

[124] H. Sekino and R. J. Bartlett. *J. Chem. Phys.*, 94:3665, 1991.

[125] S. R. Langhoff, C. W. Bauschlicher Jr., and D. P. Chong. *J. Chem. Phys.*, 78:5287, 1983.

[126] H. J. Aa. Jensen, P. Jørgensen, T. Helgaker, and J. Olsen. *Chem. Phys. Lett.*, 162:355, 1989.

[127] V. Mizrahi and D. P. Shelton. *Phys. Rev. Lett.*, 55:696, 1985.

[128] P. Sitz and R. Yaris. *Chem. Phys.*, 49:3546, 1968.

[129] D. M. Bishop and J. Pipin. *J. Chem. Phys.*, 91:3549, 1989.

[130] D. M. Bishop and B. Lam. *Phys. Rev. A*, 37:464, 1988.

[131] G. R. Alms, A. W. Burham, and W. H. Flygare. *J. Chem. Phys.*, 63:3321, 1975.

[132] In E. W. Washbrum, editor, *International critical tables*, volume 7. McGraw-Hill, New York, 1930.

[133] D. P. Shelton. *Mol. Phys.*, 60:65, 1987.

[134] Y. Luo, H. Ågren, and P. Jørgensen. *THEOCHEM*, in press.

[135] A.C. Newell and R.C. Baird. *J. Appl. Phys.*, 36:3751, 1965.

[136] G.D. Zeiss and W.J. Meath. *Mol. Phys.*, 33:1155, 1977.

[137] H. Hettema, P.E.S. Wormer, P. Jørgensen, H.J.Aa. Jensen, and T.U. Helgaker. *J. Chem. Phys.*, 100:1297, 1994.

[138] S. Ducharme, W. P. Risk, W. E. Moerber, V. Y. Lee, R. J. Tweig, and G. C. Bjorklund. *Appl. Phys. Lett*, 57:537, 1990.

[139] H. Ågren, B. O. Roos, P. S. Bagus, U. Gelius, P. Å Malmquist, R. Maripuu, and K. Siegbahn. *J. Chem. Phys.*, 77:3893, 1982.

[140] S. Nakagura. *Pure Appl. Chem.*, 7:79, 1963.

[141] H.C. Longuet-Higgins and J.N. Murrell. *Proc. Phys. Soc. London Sect. A*, 68:601, 1955.

[142] Y. Luo, H. Ågren, O. Vahtras, and P. Jørgensen. *Chem. Phys. Lett.*, 207:190, 1993.

[143] H. Koch, H. Ågren, P. Jørgensen, T. Helgaker, and H.J.Aa. Jensen. *Chem. Phys.*, 172:13, 1993.

[144] F. Bertinelli, P. Palmieri, A. Brillante, and C. Taliani. *Chem. Phys.*, 25:333, 1977.

[145] A. L. McClellan. Tables of Experimental Dipole moments; Rahara: EL Cerrito, CA, 1974.

[146] R. Wortmann, P. Krämer, C. Glania, S. Lebus, and N. Detzer. *Chem. Phys.*, 173:99, 1993.

[147] H. Ågren, S. Knuts, K. V. Mikkelsen, and H. J. Aa. Jensen. *Chem. Phys.*, 159:211, 1992.

[148] J.L. Bredas, F. Meyers, B.M. Pierce, and J. Zyss. *J. Am. Chem. Soc.*, 114:4928, 1992.

[149] M. Joffre, D. Yaron, R.J. Silbey, and J. Zyss. *J. Chem. Phys.*, 97:5607, 1992.

[150] Y. Luo, H. Ågren, K. V. Mikkelsen, and P. Jørgensen. To be published.

[151] S. P. Karna, G. B. Talapatra, W. M. K. P. Wijekoon, and P. N. Prasad. *Phys. Rev. A*, 45:2763, 1992.

[152] G. J. B. Hurst, M. Dupuis, and E. Clementi. *J. Chem. Phys.*, 89:385, 1988.

[153] P. Chopra, L. Carlacci, H. F. King, and P. N. Prasad. *J. Phys. Chem.*, 93:7120, 1989.

[154] P. C. M. McWilliams, G. W. Hayden, and Z. G. Soos. *Phys. Rev. B*, 43:9777, 1991.

[155] S. N. Dixit, D. Guo, and S. Mazumdar. *Phys. Rev. B*, 43:6781, 1991.

[156] Y. Kawabe, F. Jarka, N. Peyghambarian, D. Guo, S. Mazumdar, S. N. Dixit, and F. Kajzar. *Phys. Rev. B*, 44:6530, 1991.

[157] Y. Luo, H. Ågren, H. Koch, P. Jørgensen, and T. Helgaker. *Phys. Rev. B*, in press.

[158] Y. Luo, H. Ågren, and S. Stafstrøm. *J. Phys. Chem.*, 98:7782, 1994.

[159] M. Jaszunski, P. Jørgensen, H. Koch, H. Ågren, and T. Helgaker. *J. Chem. Phys.*, 98:7229, 1993.

[160] D. P. Shelton. *J. Chem. Phys.*, 84:404, 1986.

[161] D. M. Bishop and J. Pipin. *Int. J. Quant. Chem.*, 43:83, 1992.

[162] V. Galasso. *J. Chem. Phys.*, 89:4529, 1988.

[163] Z. G. Soos and S. Ramasesha. *J. Chem. Phys.*, 90:1067, 1989.

[164] J. R. Heflin, K. Y. Wong, O. Zamani-Khamiri, and A. F. Garito. *Phys. Rev. B*, 38:1537, 1988.

QUANTUM GROUPS: Application to Nuclear and Molecular Spectroscopy

Peter Raychev
Institute of Nuclear Research and Nuclear Energie
Bulgarian Academy of Sciences
SOFIA, BULGARIA

ADVANCES IN QUANTUM CHEMISTRY
VOLUME 26

1. Introduction

Quantum groups and quantum algebras are powerful and beautiful mathematical structures that appear in the Quantum Inverse Scattering Method (QISM), a method for constructing integrable quantum systems. This method was developed by Fadeev, Sklyanin and Takhtajan [1-3] in order to formulate a quantum theory of solitons. The quantum algebras appear also in some exactly solvable statistical mechanical models, in the study of the solution of the Yang – Baxter equation [4-7] and in a series of papers [8-9] motivated by other reasons.

Recently quantum groups and quantum algebras have been attracting much attention in physics, and in quantum chemistry as well. This is due to the fact that the properties of quantum algebras and of Lie – algebras are very similar in their representation theory and their numerous physical applications. For example in nuclear physics the quantum algebra $SU_q(2)$ has been successfully used for the description of rotational bands in the deformed and superdeformed nuclei [13-22]. The quantum symmetries have also been successfully used for the description of the rotational [23-24], vibrational [25-27] and rotational - vibrational spectra [28-29] of diatomic molecules. Recently an attempt has been made to apply the quantum group for the description of the hydrogen atom and the structure of atoms in general [30 -34]. Quantum groups turn out to be also successful in description of some simple nuclear models [35-40] and in some other phenomenological approaches [41] in nuclear physics. They find application in many other fields of physics, for example

in conformal field theory [10], in the description of spin chains [11-12] and in other problems. For example it was shown [119] that the backbanding phenomena, known for more than 20 years in nuclear spectroscopy, is present in molecules as well. These phenomena also can be described in terms of quantum algebras.

Drinfeld [42] and Jimbo [43] were the first to find out that both quantum groups and quantum algebras have the structure of Hopf algebras [44]. Hopf algebras constitute a very abstract field of modern mathematics (see for example [45-51]) and this creates a lot of difficulties for everyone who is interested not so much in abstract mathematics, but in the applications of these new symmetries in the description of physical systems.

The aim of this paper is to acquaint the reader who is not an expert in abstract mathematics with quantum groups and their applications in the description of physical systems. Fortunately there is an easy way to do this, using the quantum – algebraic analogue of the harmonic oscillator which was proposed independently by Biedenharn [52] and Macfarlane [53]. In this approach the analogues of the creation and annihilation operators of oscillator quanta (called q-deformed boson creation and annihilation operators) are introduced. They satisfy the commutation relations which "slightly differ" from the commutation relations for the standard boson creation and annihilation operators for the harmonic oscillator , but from a mathematical point of view this difference is very essential. Unlike the standard boson operators whose commutation relations close a Lie – algebra, the commutation relations of the q-deformed boson operators form a Hopf algebra. However one can deduce the basic properties of the q-deformed boson operators making use only of their commutation relations and utilizing the fact that they form a Hopf algebra only by implication [54-60].

As a next step one can construct more sophisticated (quantum) algebras, in terms of these q-deformed boson operators, using again only their commutation relations. The most important fact is however that one can use these q-deformed boson operators to construct the operators of the observables of the physical system, by analogy with the constructions employing the "standard" boson operators. These observables will also be "q-deformed" and will belong to some Hopf algebra. In this way the quantum algebras can

be adapted for the description of the physical systems. This approach is much more appealing to the physical intuition and in such a way we can bridge the gap between the abstract mathematics connected with the Hopf algebras and its physical applications.

It should be noted that, as far as the "standard" quantum mechanic is essentially based on the commutation relation of the "standard" boson operators, the change of these commutation relations gives rise to new (q-deformed) quantum mechanics which describes the deviation of the quantum systems from the classical symmetries given by the usual Lie groups and Lie algebras. The question is whether this "q-deformed" quantum mechanics describe reality or it is just a mathematical game. We shall try to answer this question too, considering the application of this q-deformed quantum mechanics in the description of the properties of some real physical systems.

Our approach in this paper will be based on the q-deformed boson operators introduced by Biedenharn. However in Sec. 2 we shall begin with some simple examples of a quantum group and a quantum algebra as they appear for the first time in physics. This will allow us to enlighten some important features of these mathematical structures avoiding the abstract mathematical considerations.

In Sec. 3 we shall consider the q-deformed boson operators first introduced by Biedenharn and Macfarline and discuss their properties in more detail. We shall consider also the representation of the algebra of these operators and shall give for them expressions (known as q-deformed functionals) in terms of standard boson operators.

In Sec. 4 we will consider the q-deformation of the standard algebra of angular momentum $SU(2)$. This deformation of $SU(2)$ (known as the q-deformed $SU_q(2)$- algebra) finds numerous applications in many fields of physics and we shall consider the representations of this algebra in more detail. On the other hand it is well known that $SU(2)$ - algebra is closely related to the algebra of the standard boson creation and annihilation operators. We shall see that these relations survive in the q-deformed case too and this will not only enlighten the "origin" of the q-deformed boson operators but will show us how in principle one can build, in terms of them, the operators of the more sophisticated algebra of the observables.

As is well known, the algebra of the angular momentum and the related concept of the tensor operators play a very important role in the application of the algebraic methods. It turns out that the algebra of the standard angular momentum is very similar to the q-deformed $SU_q(2)$ - algebra. The Sec. 5 will be devoted to the generalization of the concepts of the tensor operators, the Clebsch – Gordan coefficients and the theorem of Wigner – Eckart in the q-deformed case.

In the last section (Sec. 6) we shall concentrate our attention on certain applications of the quantum groups in the description of some real physical systems. Between the numerous physical applications we shall choose only these which are of interest for molecular physics, namely the description of the rotational and vibrational spectra of diatomic molecules. For the sake of completeness however we shall consider the rotational spectra of the deformed nuclei too, which show great similarity to those of diatomic molecules. This similarity obviously is due to the fact that the internal structure of these objects has some common features, namely they are both deformable and their moment of inertia depends on the angular momentum (or, what is the same, on the energy) of the states. As a result, the rotational spectra of the diatomic molecules and of the deformed nuclei do not obey the law $J(J+1)$, but are "squeezed", i.e the distances between the levels are smaller than the ones predicted by the above mentioned law. It turns out also that the vibrational motion in the diatomic molecules, predicted by the q-groups, irrespective of the fact that it is described by a simple Hamiltonian (which does not take into account the interaction between the q-bosons) shows significant anharmonicity. This can be accounted also by the deformability of the molecule which is described in a simple way by the q-deformed boson operators.

The comparison with the experimental data suggests that the q-defor - med algebras describe certain small deviations from the standard symmetries (ruled by the Lie algebras) and that they are appropriate for the description of the objects which are space-extended and deformable. It is remarkable that in the limit in which the parameter q determining the deformation of the q-algebra (or its deviation from the standard Lie algebra) tends to one, the q-deformed (quantum) algebra turns into a "standard" Lie algebra and

the q-deformed quantum mechanics built in terms of the q-deformed boson operator, turns into a standard quantum mechanics. It means that in this limit, in agreement with the correspondence principle, the deformability of the molecular or nuclear structures is neglected and they are considered as rigid and point-like objects.

2. Example of a Quantum Group and a Quantum Algebra

The Hopf algebras (i.e the quantum groups and quantum algebras) are really abstract mathematical tools. However one can more easily understand what a quantum group and a quantum algebra are if simple examples of these mathematical structures are considered.

It should be noted from the very beginning that quantum groups are not groups in the ordinary sense of this word and quantum algebras are not the Lie algebras which are widely used in quantum mechanics. However both the quantum groups and the quantum algebras have the remarkable property that their structure depends on a real or complex parameter q and in the limit case when $q \to 1$ the quantum groups turn into ordinary groups and the quantum algebras turn into ordinary Lie algebras. For this reason we can consider the quantum groups and the quantum algebras as some sort of a "deformation" of the ordinary groups and Lie algebras and call them simply q-deformed groups and q-deformed algebras.

Before going into a more detailed discussion of the q-deformed groups and algebras it will be useful to consider two examples of quantum groups and quantum algebras [7].

Example 1: *q-deformation of the group* $SL(2,C)$ $\quad (SL_q(2,C))$. Let us consider the algebra $\mathcal{A}_q$ generated by the elements a, b, c and d which satisfy the relations

$$\begin{aligned} ab - qba = 0 \qquad & bd - qdb = 0 \\ ac - qca = 0 \qquad & cd - qdc = 0 \\ bc = cb \qquad & ad - da = (q - q^{-1})bc \end{aligned} \tag{1.1}$$

where q is a real or complex number. We can also form the matrix

$$T = \begin{pmatrix} a & b \\ c & a \end{pmatrix}$$

Let us note that the elements (a, b, c, d) of this matrix do not commute and their realization in ordinary numbers is not possible. In this sense the matrix T is also not an ordinary matrix and we shall call it a "quasi-matrix". However in the case when $q \to 1$ these elements commute and the matrix T turns to the ordinary matrix which belongs to $GL(2, C)$-group or to $SL(2, C)$-group, provided that $detT = 1$.

Further let us consider two commuting copies of elements (a', b', c', d') and (a'', b'', c'', d'') belonging to the same algebra $\mathcal{A}_q$ and let us form the matrices

$$T' = \begin{pmatrix} a' & b' \\ c' & d' \end{pmatrix} \qquad \text{and} \qquad T'' = \begin{pmatrix} a'' & b'' \\ c'' & d'' \end{pmatrix}$$

The very important property of the algebra $\mathcal{A}_q$ is that the elements (a, b, c, d) of the product matrix

$$T = T'.T'' = \begin{pmatrix} a & b \\ c & d \end{pmatrix}$$

obtained by the usual rules for matrix multiplication also satisfy (1.1), i.e belong to $\mathcal{A}_q$.

In this sense the set of matrices T has one of the properties of the groups, namely, that if the matrix elements of two matrices T' and T'' belong to the set $\mathcal{A}_q$, then the matrix elements of their product matrix have the same property (i.e the matrix multiplication preserves the properties of the matrix elements)

The set of matrices T would form a group if and only if for every T there exists an inverse matrix T^{-1} such that $T.T^{-1} = T^{-1}.T = I$, where I is the unit matrix. However it can be easily seen that the matrix T^{-1} obtained from T by the standard formula for the inverse matrix does not have this property. For this reason the set of matrices T do not form a group in the ordinary sense of this word. On the other hand one can check out that to any matrix T one can put in correspondence the matrix

$$S(T) = \begin{pmatrix} d & -q^{-1}b \\ -qc & a \end{pmatrix}$$

with the property

$$S(T).T = T.S(T) = I.det_q T$$

Here

$$det_q T = ad - qbc$$

is the so called q-determinant ("quantum determinant") which commutes with all elements of the algebra $\mathcal{A}_q$. If we do not take into account the quantum determinant we can consider $S(T)$ as an analogue of the inverse matrix[1] T^{-1}, whose existence is the necessary condition for considering the set of matrices T as a group.

We see that the set of quasi-matrices T, whose elements have the property (1.1), is not exactly a matrix group but "something like a group". (Woronowich labelled it as "compact matrix pseudo-group"). However in the limit $q \to 1$ this set of matrices turns into a $SL(2,C)$- group and we can call this set for arbitrary values of q ($q \neq 1$) the *q-deformation* of $SL(2,C)$ or "quantum qroup"[2] $SL(2,C)$. We shall denote this q-deformed group by $SL_q(2,C)$.

This example gives an idea of what a quantum group is. Now let us give an example of a quantum algebra.

Example 2: *q-deformation of $SU(2)$-Lie algebra (quantum algebra $SU_q(2)$).* As is well known, the Lie - algebra of the group $SU(2)$ (the group of angular momentum in quantum mechanics) consists of three elements L_+, L_- and L_0 which satisfy the commutation relations

[1]We shall call the quasi-matrix $S(T)$ "antipode" of T in order to distinguish it from T^{-1}.

[2]The word "quantum" is used to remind us of the origin of this mathematical object – the Quantum Inverse Scattering Method (QISM). There is one more reason for this choice, but it will be discussed in Example 2.

$$\begin{aligned}[L_{\pm}, L_0] &= \pm L_0 \\ [L_+, L_-] &= 2L_0\end{aligned} \tag{1.2}$$

and the unitary condition

$$(L_+)^{\dagger} = L_- \tag{1.3}$$

(If the unitary condition (1.3) is not imposed, (1.2) is the Lie-algebra of $SL(2, C)$ – the group of all 2×2- matrices with unit determinant.)

Studying the solution of Yang-Baxter equation mechanics, Kulish and Reshetichin [4] introduced the algebra

$$\begin{aligned}[J_{\pm}, J_0] &= \pm J_0 \\ [J_+, J_0] &= \frac{\sinh(2hJ_0)}{\sinh(h)}\end{aligned} \tag{1.4}$$

This algebra essentially differs from (1.2), but it has the remarkable property that when $h \to 0$ it goes into $SU(2)$-algebra (1.2). As a matter of fact

$$\lim_{h \to 0} \frac{\sinh(2hJ_0)}{\sinh(h)} = 2J_0$$

and the second equation of (1.4) goes into the second equation of (1.2). We can consider (1.4) as some "deformation" of the $SU(2)$ and call this algebra the "quantum" algebra $SU(2)$. We can also call it a q-deformed $SU(2)$ and denote it by $SU_q(2)$.

One can consider the $SU(2)$-algebra as a "classical" (or exact) symmetry algebra, and the deviation of this classical symmetry is described by the quantum algebra $SU_q(2)$. This deviation, as we shall see later on, includes effects of anisotropies, deformability of the quantum systems etc. When $h \to 0$ the quantum symmetry turns into the classical one. We can see here certain analogy with the transition from quantum to classical mechanics in the case when the Planck constant can be neglected ($\hbar \to 0$). This explains the origin of the word "quantum algebra" used for the labeling of certain new symmetries which differ from the "classical" (or standard) symmetries.

Remark:1. The names quantum group and quantum algebra are to some extent misleading. The Lie-groups and the Lie-algebras which describe some exact symmetries of the physical systems lie at the basis of quantum mechanics. The deviation of these exact symmetries described by what is known as "quantum group" and "quantum algebras" should describe some deviations of the standard quantum mechanics. For this reason we prefer to denote these mathematical structures as "q-deformed" groups and algebras.

It is important to note that the q-deformed algebra $SU_q(2)$ *is not a Lie-algebra* at all. As a matter of fact, by definition, an arbitrary Lie- algebra is a set of elements (generators) $I_1, I_2, \ldots I_f$ which is closed under the commutation

$$[I_i, I_s] = \sum_k C_{is}^k I_k$$

i.e. the commutator of any pair of generators is a *linear combination* of the same set of generators. This is certainly the case with the $SU(2)$- algebra (1.2), but in the case of $SU_q(2)$ the commutator of J_+ and J_- is a *function* of J_0 which can be expanded in infinite series in powers of J_0. We have

$$[J_+, J_-] = \frac{1}{\sinh(h)} \left(\frac{2hJ_0}{1!} + \frac{(2hJ_0)^3}{3!} + \frac{(2hJ_0)^5}{5!} + \ldots \right)$$

This means that the commutator of J_+ and J_- belongs to the universal enveloping algebra[3] of $SL(2, C)$ (no unitarity condition is imposed). For this reason for this algebra we sometimes employ the alternative designation *"quantized universal enveloping algebra"* (QUE - algebra) and the notation $U_q(sl(2))$ is used instead of $SL_q(2)$.

Remark 2. The set of the matrices T of Example 1 depends on the parameter q and goes into a $SL(2, C)$ – group in the case when the parameter $q \to 1$, while the $SU_q(2)$ – algebra (which depends on the parameter h) goes

[3]We recall that the universal enveloping algebra $U(A)$ of a given Lie algebra A with generators $I_1, I_2, \ldots, I_f$ consists of all monomials of these generators. For example, the universal enveloping algebra of $SL(2, C)$ consists of all monomials of the type $J_-^n J_0^m J_+^p$, $(n, l, p = 0, 1, 2, \ldots)$.

to $SU(2)$, in the case when $h \to 0$. However one can achieve a unified parameterization replacing $h = \ln q$ or $(q = e^h)$. Obviously in the case when $q \to 1$ we have $h \to 0$. Replacing $h = \ln q$ in the second equation (2.4) we obtain

$$[J_+, J_-] = \frac{q^{2J_0} - q^{-2J_0}}{q - q^{-1}} \tag{2.5}$$

The r.h.s of (2.5) goes into $2J_0$ when $q \to 1$,i.e $\lim_{q\to 1} SU_q(2) = SU(2)$.

Remark 3. The algebra (2.4) introduced by Kulish and Reshetikhin may appear in different forms [53]. For example Sklyanin introduced a quadratic algebra with elements $S_0, S_3, S_\pm$, which algebra can be written in the form

$$\begin{aligned} [S_0, S_3] &= 0 & [S_0, S_\pm] &= \tanh^2(h/2)(S_\pm S_3 + S_3 S_\pm) \\ [S_+, S_-] &= 4S_0 S_3 & [S_3, S_\pm] &= \pm (S_\pm S_0 + S_0 S_\pm) \end{aligned} \tag{2.6}$$

This algebra also contains the parameter h (or $q = e^h$) and, by analogy with (2.4), can be considered as a kind of a deformed or a quantum algebra. One can write

$$S_\pm = \pm(S_1 \pm iS_2), \quad \mathbf{S}^2 = S_1^2 + S_2^2 + S_3^2$$

and check that

$$K_0 = S_0^2 + \mathbf{S}^2, \qquad K_1 = \mathbf{S}^2 + \tanh^2(h/2) S_3^2$$

are the Casimir operators (i.e they commute with all elements of this algebra). However K_0 and K_1 are not independent since it can be shown that

$$K_0 - K_1 = S_0^2 - S_3^2 \tanh^2(h/2) = 4 \sinh^2(h/2)$$

Further we can introduce the new operators $J_0, J_\pm$

$$\begin{aligned} S_0 &= \sinh(h/2) \cosh(hJ_0) \\ S_3 &= \cosh(h/2) \sinh(hJ_0) \\ J_\pm &= S_\pm / 2 \sinh(h) \end{aligned}$$

This allows to show that $J_0, J_\pm$ so defined, satisfy (2.4) i.e. form the $SU_q(2)$ – algebra. This example shows that quantum algebras that look quite different at a first sight may have the same mathematical structure.

Remark 4. We referred to the set of "quasi – matrices" T of Example 1 as a guantum *group* $SL_q(2)$ and the three-elements-algebra of Example 2 as a quantum *algebra* $SU_q(2)$ (or $SL_q(2)$). We shall see however that the difference between the quantum group and the quantum algebra is not essential. First we must note that due to the fact that $SU_q(2)$ is not a Lie algebra at all, the exponention of its generators ,i.e the elements of the form

$$e^{\alpha J_+} e^{\beta J_0} e^{\gamma J_-}$$

does not form a (quantum) group in the general case. This means that the link of QUE – algebras to q-groups differs from the standard connection between Lie groups and Lie algebras. However, one can construct the QUE – algebra generators out of the q-group elements and vice versa [61]. As a matter of fact using the elements a, b, c, d satisfying (2.1), one can construct the following formal functionals

$$J_+ = \frac{2i}{q-q^{-1}} a\sqrt{1+\frac{1}{qbc}} \quad J_0 = \frac{\ln\sqrt{bc}}{\ln q} \quad J_- = \frac{2i}{q-q^{-1}}\sqrt{1+\frac{1}{qbc}}\, d \qquad (2.7)$$

One can check that these functionals satisfy the commutation relations

$$[J_0, J_\pm] = \pm J_\pm$$

$$[J_+, J_-] = -\frac{1}{(q-1/q)^2}\left((1+q/bc)ad - (1+1/qbc)da\right) = [2J_0]$$

which coincide with commutation relations (2.4) for $SU_q(2)$. In this way (2.7) represents the $SU_q(2)$– generators in terms of elements of the algebra $\mathcal{A}_q$ given by (2.1) and vice versa one can easily show that the elements of $\mathcal{A}_q$ can be expressed in terms of generators of $SU_q(2)$ (or $U_q(sl(2))$

$$a = -i(q-1/q)J_+\sqrt{\frac{2}{1+q^{-2J_0-1}}}, \qquad d = -i(q-1/q)\sqrt{\frac{2}{1+q^{-2J_0-1}}}J_-,$$

$$bc = q^{2J_0} \tag{2.8}$$

This example shows that the quantum group of Example 1 and the quantum algebra of Example 2 have a common mathematical structure. The reason for this is that they both are Hopf algebras.

For the reader who would like to go more deeply into the mathematical details we shall give a more rigorious definition of Hopf algebras in Appendix A. The knowlege of these definitions however is not necessary for understanding the problems which will be discussed below. Therefore it is sufficient to employ a modification (or a q-deformation) of the well known algebra of Heisenberg – Weyl which lies in the basis of the standard quantum mechanics and which will be discussed in the next section.

3. q- Deformed Harmonic Oscillator and q-Deformed Boson Operators

3. 1. Quantum mechanics and the Heisenberg – Weyl algebra

Let us consider the classical mechanical system whose Hamiltonian $H(p_\mu, q_\mu)$ is constructed in terms of the canonical coordinates q_μ and their canonical conjugate momenta p_μ. The transition to the quantum description or *quantization* of this system is carried out by replacing q_μ and p_μ by the operators Q_μ and P_μ satisfying what is known as the *canonical commutation relation*

$$[Q_\mu, P_\nu] = i\hbar\delta_{\mu\nu} I, \tag{3.1}$$

where I is the identity operator. The set of the elements Q_μ, P_ν and $\hbar I$ close an algebra known as the *Heisenberg algebra* $\mathcal{H}$.

It is also convenient to represent the algebra $\mathcal{H}$ in terms of the elements

$$b_\mu^\dagger = \sqrt{\frac{1}{2\hbar}}(Q_\mu - iP_\mu), \qquad b_\mu = \sqrt{\frac{1}{2\hbar}}(Q_\mu + iP_\mu). \tag{3.2}$$

These operators satisfy the commutation relations

$$[I, b_\mu^\dagger] = [I, b_\mu] = 0,$$

$$[b_\mu, b_\nu^\dagger] = \delta_{\mu\nu} I.$$

For the sake of simplicity we shall consider the one-dimensional case, in which the three operators $b^\dagger$, b and I satisfy

$$[I, b^\dagger] = [I, b] = 0,$$

$$[b, b^\dagger] = I. \tag{3.3a}$$

The operators $b^\dagger$ and b are referred to as boson creation and annihilation operators. Important is also the role of the operator $B = b^\dagger b$, called the operator of the number of bosons, which satisfies the relations

$$[B, b^\dagger] = b^\dagger, \qquad [B, b] = -b. \tag{3.3b}$$

The four element algebra consisting of $b, b^\dagger, B$ *and* I *which satisfy the commutation relations (3.3) will be referred to as Heisenberg – Weyl algebra* $\mathcal{H}_4$.[4]

It is clear that quantum mechanics is based essentially on the Heisenberg – Weyl algebra. If one changes (or "deforms") the underlying algebra, replacing, for example, the commutation relations (3.3) between $b, b^\dagger$ and B by some others commutation relations, the quantum mechanics based on this new algebra will have a different form. As a matter of fact, using (3.2) one can express Q_μ and P_μ in terms of the "deformed" $b^\dagger$ and b. The replacement of q_μ and p_μ in the classical Hamiltonian and in the other classical observables by the "deformed" analogues of Q_μ and P_μ will generate the observables whose properties will differ from the properties of the corresponding observables in "standard" quantum mechanics.

[4]It should be noted that the set of the three elements b, $b^\dagger$, I themselves close an algebra, too. The number operator B, which is a product of b and $b^\dagger$, belongs to the universal enveloping algebra of this three-element algebra.

In this connection the following questions arise:

1.Is it possible to transform the Heisenberg algebra $\mathcal{H}_4$ into a q-deformed $\mathcal{H}_4^q$ algebra approximately in the same way (see Example 2 of Sec. 2) as the $SU(2)$ algebra is deformed to the $SU_q(2)$?

2. If the answer to the first question is in the affirmative and if it is possible to formulate a new quantum mechanics based on $\mathcal{H}_4^q$ it is reasonable to ask in what way this new quantum mechanics is connected with reality. Will the new quantum mechanics based on the algebra $\mathcal{H}_4^q$ describe some real physical systems or will it remain only an exercise in pure mathematics?

In this paper we shall try to give an answer to these questions.

We shall start the discussion of these problems by mentioning that the deformation of $\mathcal{H}_4$ implies that, for example, the commutator of b and $b^\dagger$ must be a function of the elements of the universal enveloping algebra (in this case a function of $B = b^\dagger b$). This function must depend on some parameter q, i.e. must be of the form $f_q(B)$ and must have the property $\lim_{q\to 1} f_q(B) = I$. In this sense, in the limit $q \to 1$ the q-deformed algebra $\mathcal{H}_4^q$ will tend to the Heisenberg – Weyl algebra $\mathcal{H}_4$ and the "q-deformed" quantum mechanics based on $\mathcal{H}_4^q$ will tend to the "standard" quantum mechanics. We shall consider the gradual transition from the "q-deformed" to the "standard" quantum mechanics as a specific manifestation of the correspondence principle, which establishes the relationship between the "old" theory and the "new" theory (describing the deviations from the old one).

Let us now discuss the q-deformed Heisenberg- Weyl agebra.

3. 2. q-Deformed Boson Operators

The q-commutators. In order to define the q-deformed Heisenberg – Weyl algebra we shall introduce a new operation called a q-commutator of the operators A and B. By definition the q-commutator of A and B is given by the expression:

$$[A, B]_q = AB - qBA. \tag{3.4}$$

Obviously the q-commutator has the following property

$$[A,B]_q = -q[B,A]_{q^{-1}}. \tag{3.5}$$

As is well known, when one uses ordinary commutators (as is the case of Lie algebras) any three operators A, B and C satisfy the identity

$$[A,[B,C]] + [B,[C,A]] + [C,[A,B]] = 0$$

which ie reffered to as Jacobi identity. In the case of the q-commutators, however, this identity is not valid. Quesne [62] has shown that in the case of the q-commutators *the generalized form of the q-deformed Jacobi identity* holds, namely

$$q^{b/2}[A,[B,C]_{q^a}]_{q^{c-b}} + q^{c/2}[B,[C,A]_{q^b}]_{q^{a-c}} + q^{a/2}[C,[A,B]_{q^c}]_{q^{b-a}} = 0 \tag{3.6a}$$

where a, b and c are real numbers. Chachian et al [63] give another two-parametric form of the q-Jacobi identity, namely

$$[A,[B,C]_{q_1}]_{q_2} + q_2[B,[C,A]_{q_1}]_{q_2^{-1}} + [C,[A,B]]_{q_1 q_2} = 0,. \tag{3.6b}$$

which, however, can be considered as a special case of (3.6a)

The relations (3.6) show that even when the set of operators $A, B, C, \ldots$ etc., are closed under q-commutation and form in such a sense an algebra, this algebra is not a Lie algebra.

The q-deformed Heisenberg-Weyl algebra. Now we can give the following

DEFINITION. *The algebra of the three elements N, a and $a^\dagger$, which satisfy the commutation relations*

$$[N,a^\dagger] = a^\dagger, \qquad [N,a] = -a, \tag{3.7a}$$

$$[a,a^\dagger]_q = aa^\dagger - qa^\dagger a = q^{-N}, \tag{3.7b}$$

and the conditions of hermitian conjugation

$$(a^\dagger)^\dagger = a, \qquad N^\dagger = N, \tag{3.7c}$$

will be referred to as a q-deformed Heisenberg algebra $\mathcal{H}_4^q$, *while* $a^\dagger$ *(a) will be referred to as a q-deformed boson creation (annihilation) operator.*[5]

It is useful to note that N *is not* $a^\dagger a$.

Remark: The definition of the q-deformed Heisenberg–Weyl algebra in the form (3.7) was given by Biedenharn [52] following some geometrical constructions of Manin [51]. This definition has an unusual form and needs, of course, some motivation. We shall discuss this question later on (see Sec. 4.3). Here we shall mention only that the standard Heisenberg – Weyl algebra can be considered as a contracted form of the $SU(2)$ algebra (i.e. it can be obtained from the $SU(2)$-algebra through some standard operations). By analogy, the q-deformed Heisenberg – Weyl algebra can be obtained in the same way as a contracted form of the q-deformed $SU_q(2)$ algebra which was shortly discussed in Example 2 of Sec. 2 and which will be considered in more detail in Sec. 4.3.

Properties of q-deformed boson operators.. From the definition equations (3.7) we can deduce the following properties of the q-deformed boson operators

Proposition 1. The elements of $\mathcal{H}_4^q$ *satisfy the relations*

$$a^\dagger f(N) = f(N-1)a^\dagger \qquad af(N) = f(N+1)a. \tag{3.8}$$

and

$$[N, a^\dagger a] = [N, aa^\dagger] = 0, \tag{3.9a}$$

or in general

$$[aa^\dagger, f(N)] = [a^\dagger a, f(N)] = 0. \tag{3.9b}$$

where $f(N)$ *is an arbitrary function of* N.

[5]We shall preserve the notations $b^\dagger$, b and $B = b^\dagger b$ for the standard (undeformed) boson operators.

PROOF: Eq (3a) can be rewritten in the form $a^\dagger N = Na^\dagger - a^\dagger = (N-1)a^\dagger$. Then obviously $a^\dagger N^2 = (N-1)a^\dagger N = (N-1)^2 a^\dagger$, and by induction we obtain

$$a^\dagger N^s = (N-1)^s a^\dagger.$$

For an arbitrary function $f(N) = \sum c_s N^s$ we have

$$a^\dagger f(N) = \sum c_s a^\dagger N^s = \sum c_s (N-1)^s a^\dagger = f(N-1)a^\dagger.$$

The second equation (3.8) can be proved in the same way. Combining these two equations we obtain (3.9). Q.E.D.

Proposition 2. The parameter q is either a real or a pure phase (i.e. it is of the form $q = e^{-i\tau}$, where τ is real).

PROOF: As a matter of fact, the hermitian conjugate of eq.(3.7b) is

$$aa^\dagger - q^* a^\dagger a = (q^*)^{-N}$$

The conjugate equation will coincide with (3.7b) if and only if $q^* = q$ or $q^* = q^{-1}$. Q.E.D.

Proposition 3. The products of the operators a and $a^\dagger$ are equal to

$$a^\dagger a = [N], \qquad aa^\dagger = [N+1] \tag{3.10}$$

Here we use the notation

$$[x] = \frac{q^x - q^{-x}}{q - q^{-1}} \tag{3.11}$$

where x may be a number or an operator as well. Often the expressions of the type (3.11) are referred to as q-numbers.

PROOF: From eq.(3.7b) one can subtract the same equation in which q is replaced by q^{-1} to obtain, as a result,

$$(q - q^{-1})a^{\dagger}a = q^N - q^{-N}$$

or

$$a^{\dagger}a = \frac{q^N - q^{-N}}{(q - q^{-1})}$$

Q.E.D.

Obviously the q-numbers can be represented in the form

$$[x] = \frac{sh(\tau x)}{sh(\tau)} \qquad \text{if } q = e^{\tau}, \tag{3.12a}$$

and

$$[x] = \frac{sin(\tau x)}{sin(\tau)} \qquad \text{if } q = e^{i\tau}. \tag{3.12b}$$

In the limit $q \to 1$ the q-numbers (or operators) tend to the ordinary numbers (operators), i.e.

$$\lim_{q \to 1}[x] = \lim_{\tau \to 0} \frac{sin(\tau x)}{sin(\tau)} \to x$$

In such a way in the limit $q \to 1$ (or $\tau \to 0$) we obtain

$$a^{\dagger}a = [N]_{q \to 1} = N \qquad aa^{\dagger} = [N+1]_{q \to 1} = N + 1$$

and as a result we have

$$aa^{\dagger} - a^{\dagger}a = I$$

i.e. *in the limit $q \to 1$ the q-deformed boson operators coincide with the ordinary boson operators and the q-deformed Heisenberg algebra H^q coincides with the standard Heisenberg algebra*, which is in agreement with the correspondence principle, according to which the "new" theory must contain the "old" one as a limiting case.

Equivalent definitions of $\mathcal{H}^q$. The quantum algebra $\mathcal{H}_4^q$ may be defined in terms of other set of operators which differ from (3.7). These definitions are equivalent to (3.7) but in some cases they have some advantages from

a practical point of view and here we shall introduce some of them. Such equivalent definitions of $\mathcal{H}_4^q$ are:

1. The q-deformed Heisenberg – Weyl algebra can be defined in terms of operators

$$a, \qquad a^\dagger, \qquad K^+ = q^{N/2}, \qquad K^- = q^{-N/2}. \tag{3.13}$$

These operators satisfy the commutation relations

$$K^+K^- = K^-K^+ = 1, \qquad aK^\pm = q^{\pm 1}K^\pm a \tag{3.14ab}$$

and in addition

$$[a, a^\dagger]_q = \frac{q^N - q^{-N}}{q - q^{-1}} = \frac{(K^+)^2 - (K^-)^2}{q - q^{-1}} \tag{3.14b}$$

Obviously in this case the q-commutator of a and $a^\dagger$ also belongs to the universal enveloping algebra but instead of in infinite series of N it is expressed in finite degrees of K^+ and K^- only. This formulation is mathematically perfect, but has no clear physical meaning.

2. It can be also defined in terms of the operators

$$\alpha = q^{-N/2}a, \qquad \alpha^\dagger = a^\dagger q^{-N/2}, \qquad \text{and} \qquad N \tag{3.15}$$

These operators satisfy the following commutation relations

$$[N, \alpha^\dagger] = \alpha^\dagger, \qquad [N, \alpha] = -\alpha$$
$$[\alpha, \alpha^\dagger] = q^{-2N} \tag{3.16}$$

In this way the use of the q-commutator is avoided. However it can be easily shown that the bilinear products of α and $\alpha^\dagger$ equal to

$$\alpha^\dagger\alpha = [N]q^{-N+1}, \qquad \alpha\alpha^\dagger = [N+1]q^{-N} \tag{3.16}$$

The equivalence of the above definitions with (3.7) can be easily checked.

"Coordinate representation" of the q-deformed boson operators. As is well known, the "standad" boson operator can be represented in a "coordinate" form if we consider the creation operator $b^\dagger$ as an operator of multiplication by the complex variable z acting on a suitble chosen function $f(z)$ and the annihilation operator b as an operator of differentiation, i.e. $b = \frac{\partial}{\partial z}$. We have $[\frac{\partial}{\partial z}, z]f(z) = f(z)$, hence $[b, b^\dagger] = 1$ as can be expected.[6] .

In the q-deformed case we can also consider the creation operator $a^\dagger$ as effecting multiplication by the complex variable z, but here the annihilation operator a is replaced by a finite difference operator D_z^q defined by

$$D_z^q f(z) = \frac{f(qz) - f(q^{-1}z)}{(q - q^{-1})z} \tag{3.17}$$

for a suitable function $f(z)$. Evidently, when $q \to 1$ we can replace q by $1+\epsilon$, (or q^{-1} by $1-\epsilon$) and it is easily seen that

$$\lim_{q\to 1} D_f^q(z) = \frac{\partial f(z)}{\partial z}$$

We can also define the number of boson operator

$$Nf(z) = z\frac{\partial f(z)}{\partial z} \tag{3.18}$$

One can check that under these definitions the commutation relations (3.7) are satisfied and that

$$a^\dagger a = zD_z^q = [N] \qquad a^\dagger a = D_z^q z = [N+1]$$

which is in agreement with (3.10).

A useful property of the finite difference operator D_z^q is

$$D_z^q z^n = [n]z^{n-1} \tag{3.19}$$

One can also define the q-exponential function $exp_q(x)$ by

$$exp_q(z) = \sum_q \frac{z^n}{[n]!} \tag{3.20}$$

---

[6]This representation of b and $b^\dagger$ is known as Fock representation of the creation and annihilation operators

which is a q- analogue of the exponential function. Although this definition is not unique, from (3.17) and (3.19) it follows that

$$D_z^q exp_q(Az) = Aexp_q(Az) \tag{3.21}$$

where A is a constant, or an operator independent of z. In the same way one can define the q-analogue of the hypergeometric functions and develop a new branch of the analysis known as a q-analysis. It should be noted however that the operator D_z^q and the q-extension of the classical function were not introduced for q-qroups but can be dated back to Heine in the middle of the last century (See Andrews [64] and Exton [65]). It is really surprising that these two quite independent branches of mathematics meet together in the cosideration of the physical problem connected with the deformation of the commutation relation of quantum mechanics. The introduction of the D- derivative opens the door for the formulation of the equations of the q-deformed quantum mechanics as equations in finite differences. Here however we shall not qo into this problem.

3. 3. Representations of the Heisenberg – Weyl Algebra and Related Questions

Eigenvectors of N. Matrix elements of a and $a^\dagger$. Here we shall introduce a system of basic vectors which are eigenvectors of N, and calculate the matrix elements of $a^\dagger$ and a between these vectors. Let us *suppose* that $|\alpha\rangle_q$ is an eigenvector of N, i.e. that

$$N|\alpha\rangle_q = \alpha|\alpha\rangle_q \quad .$$

Using (3.7) we obtain

$$\begin{aligned} Na^\dagger|\alpha\rangle_q &= (\alpha+1)a^\dagger|\alpha\rangle_q \\ Na|\alpha\rangle_q &= (\alpha-1)a|\alpha\rangle_q \quad . \end{aligned}$$

This means that $a^\dagger|\alpha\rangle_q$ and $a|\alpha\rangle_q$ are also eigenvectors of N belonging to the eigenvalues $\alpha \pm 1$, i.e.

$$a^\dagger|\alpha\rangle_q \sim |\alpha+1\rangle_q \quad ,$$

$$a|\alpha\rangle_q \sim |\alpha - 1\rangle_q \quad .$$

The operator $a^\dagger$ raises the eigenvalue of N and is referred to as a raising operator, while the operator a lowers the eigenvalues of N and is referred to as a lowering operator. Applying k-times a to $|\alpha\rangle_q$ we shall obtain the eigenvector of N belonging to the eigenvalue $\alpha - k$. Obviously, if there are no additional restrictions on the eigenvalues of N, the number $\alpha - k, k = 1, 2, \ldots$ may become negative and we can obtain an infinite number of states with negative eigenvalues of N. In order to obtain the representation of $\mathcal{H}_4^q$ bounded below we postulate that there exists a vector $|0\rangle_q$ (q-deformed vacuum state) with the properties

$$a|0\rangle_q = 0, \qquad N|0\rangle_q = 0 \quad . \tag{3.22}$$

The next step is to introduce, by analogy with the undeformed case, the states

$$|n\rangle_q = A_n(a^\dagger)^n|0\rangle_q$$

where A_n is a normalization factor. Obviously

$$N|n\rangle_q = n|n\rangle_q \quad ,$$

i.e. the eigenvalues of N are integers and we can interpret N as the operator of the number of the q-deformed bosons. The state $|0\rangle_q$ corresponds to the eigenvalue of N equal to zero and can be interpreted as a state without bosons (i.e. as a vacuum state). The raising operator $a^\dagger$ increases the number of the bosons in the state $|n\rangle_q$ by one unit and can be interpreted as a boson creation operator. By analogy the lowering operator lowers the number of the bosons by one unit and can be interpreted as a boson annihilation operator.

In order to calculate the normalization factor A_n we shall take into account that

$$\begin{aligned} A_n^{-2} &= \langle n|n\rangle_q = \langle 0|a^n(a^\dagger)^n|0\rangle_q = \langle 0|a^{n-1}aa^\dagger(a^\dagger)^{n-1}|0\rangle_q \\ &= \langle n-1|[N+1]|n-1\rangle_q = [n]\langle n-1|n-1\rangle_q \end{aligned}$$

Repeating this process we find

$$A_n^{-2} = [n]\langle n-1|n-1\rangle_q = \ldots = [n]!\langle 0|0\rangle_q$$

where

$$[n]! = [n].[n-1]\ldots[1] \tag{3.23}$$

is the q-analogue of the factorial which is related to the q-analogue of the gamma function. This function has the propery

$$\Gamma_q(z+1) = [z]\Gamma_q(z), \ldots, \quad \Gamma_q(0) = 1 \quad .$$

Provided that $\langle 0|\ 0\rangle_q = 1$ we can construct the normalized eigenstates of N

$$|n\rangle_q = \frac{(a^\dagger)^n}{\sqrt{[n]!}}|0\rangle_q \tag{3.24}$$

and it can be easily checked that

$$\begin{aligned} N|n\rangle_q &= n|n\rangle_q \\ a^\dagger|n\rangle_q &= \sqrt{[n+1]}|n+1\rangle_q \\ a|n\rangle_q &= \sqrt{[n]}|n-1\rangle_q \quad . \end{aligned} \tag{3.25}$$

Obviously the matrix elements of a and $a^\dagger$ are

$$\langle n+1|a^\dagger|n\rangle_q = \sqrt{[n+1]} \qquad \langle n-1|a|n\rangle_q = \sqrt{[n]} \tag{3.26}$$

and (in the general case) these operators can be represented as infinite- dimensional matrices

$$\|a^\dagger\| = \begin{pmatrix} 0 & \sqrt{[1]} & 0 & \ldots & 0 & \ldots \\ 0 & 0 & \sqrt{[2]} & \ldots & 0 & \ldots \\ 0 & 0 & 0 & \ldots & 0 & \ldots \\ \ldots & \ldots & \ldots & \ldots & \ldots & \ldots \\ \ldots & \ldots & \ldots & \ldots & \sqrt{[n]} & \ldots \\ \ldots & \ldots & \ldots & \ldots & \ldots & \ldots \end{pmatrix} \tag{3.27a}$$

and

$$\|a\| = \begin{pmatrix} 0 & 0 & 0 & \ldots & \ldots \\ \sqrt{[1]} & 0 & 0 & \ldots & \ldots \\ 0 & \sqrt{[2]} & 0 & \ldots & \ldots \\ 0 & 0 & \sqrt{[3]} & \ldots & \ldots \\ \ldots & \ldots & \ldots & \ldots & \ldots \end{pmatrix} \tag{3.27b}$$

Case when q is a root of unity. The expression (3.24) for the eigenstates $|n\rangle_q$ of N is meaningful for every value of n only if q is a positive number. We have

$$|n\rangle_q = \frac{(a^\dagger)^n}{\sqrt{[n]!}}|0\rangle_q \tag{3.24}$$

If q is of the form $q = e^{i\tau}$ (τ - real) there exist critical values of n, denoted here by n_c, for which the denominator in (3.24) "blossoms out" and the expression (3.24) loses its meaning. As a matter of fact the q-number is given by

$$[n] = \frac{q^n - q^{-n}}{q - q^{-1}} = \frac{\sin \tau n}{\sin \tau}$$

Obviously for every given $\tau \ll 1$ there exists an integer n_c, such that

$$n_c \tau \approx k\frac{\pi}{2} \qquad \text{where} \quad k \quad \text{is integer.} \tag{3.28a}$$

Thus $[n_c]! \approx 0$,i.e. $\frac{1}{\sqrt{[n_c]!}} \to \infty$. On the other hand if n is not restricted by additional conditions there must exist values of n such that

$$\pi > n\tau > 2\pi \qquad \text{and hence} \quad [n] < 0 \quad . \tag{3.28b}$$

For such negative values of n the denominator in (3.24) also loses its meaning.

Unfortunately, when one tries to apply the q-deformed algebras for the description of the real physical system, it turns out that one can achieve a good agreement with the experimental data if q is chosen in the form $e^{i\tau}$. Thus we must face the problem of the "unwanted states" (whose denominators become meaningless). Of course, we can allow ourselves the light-mindedness to deal with small values of n (which are sufficient to explain the experimental data) and pay no attention to what will happen when n becomes big enough. Another way to avoid these difficulties is to "cut-off" the basis artificially. It is, however, evident that both these "approaches" are unsatisfactory from a mathematical point of view.

There is however a situation when the basis (3.24) is cut -off automatically. This is the *case when q is a root of unity.* We must mention from the very beginning that the case when q is a root of unity, as a matter of fact, represents a whole domain in the realm of the q- algebras and many

papers [67-70] are devoted to it. However we shall not discuss this probem from a mathematical point of view and will consider it only for "practical" purposes.

Let us suppose that Φ is an integer such that

$$q^{\Phi+1} = 1 \tag{3.29}$$

which means that $e^{i\tau(\Phi+1)} = e^{2\pi i}$. Thus we obtain

$$\tau = \frac{2\pi}{\Phi+1} \tag{3.30}$$

and for q-numbers we have

$$[n] = \left(\sin\frac{2\pi}{\Phi+1}\right)^{-1} \cdot \sin\frac{2\pi n}{\Phi+1}$$
$$n = 1, 2, \ldots, \Phi \tag{3.31}$$

For values $n > \Phi$, the result is

$$[\Phi+1] = 0, \quad [\Phi+2] = [1], \quad [\Phi+3] = [2], \qquad \text{etc.} \tag{3.32}$$

For this reason the matrices (3.24) decompose in an infinite set of finite-dimensional matrices

$$\|a^\dagger\| = \begin{pmatrix} 0 & \sqrt{[1]} & 0 & \ldots & 0 & 0 \\ 0 & 0 & \sqrt{[2]} & \ldots & 0 & 0 \\ 0 & 0 & 0 & \ldots & \ldots & \ldots \\ \ldots & \ldots & \ldots & \ldots & \ldots & \ldots \\ \ldots & \ldots & \ldots & \ldots & 0 & \sqrt{[\Phi]} \\ 0 & 0 & 0 & \ldots & 0 & 0 \end{pmatrix} \tag{3.33a}$$

$$\|a\| = \begin{pmatrix} 0 & 0 & 0 & \ldots & 0 & 0 \\ \sqrt{[1]} & 0 & 0 & \ldots & 0 & 0 \\ 0 & \sqrt{[2]} & 0 & \ldots & 0 & 0 \\ 0 & 0 & \sqrt{[3]} & \ldots & 0 & 0 \\ \ldots & \ldots & \ldots & \ldots & \ldots & \ldots \\ 0 & 0 & 0 & \ldots & \sqrt{[\Phi]} & 0 \end{pmatrix} \tag{3.33b}$$

These matrices are *nilpotent*, that is, they have the propery that

$$\|a\|^{\Phi+1} = 0, \qquad \|a^\dagger\|^{\Phi+1} = 0 \quad . \tag{3.34}$$

Thus for $n = \Phi + 1$ not only the denominator but also the numerator in (3.24) equals to zero and the basis is truncated at this value of n. This of course is valid not only for the matrix representation of a and $a^\dagger$ but for any other representation as well.

We can consider the fact that $(a^\dagger)^n \neq 0$ for $n = 0, 1, \ldots, \Phi$ but $(a^\dagger)^{\Phi+1} = 0$ as a *generalization of the Pauli principle for the q deformed bosons: one can put Φ particles in one and the same state but in this state there is no place for the $(\Phi + 1)$-th particle.*

The q-deformed one-dimensional harmonic oscillator. At this point it will be instructive to consider in more detail how the replacement of the Heisenberg – Weyl algebra $\mathcal{H}_4$ with its q-deformed version $\mathcal{H}_4^q$ affects the description of the physical system, that is, to study what kind of new physical effects appear when the operators of the coordinates Q and the momenta P of the system are replaced with the corresponding q-deformed quantities. For this purpose we must consider some simple quantum mechanical systems in order to compare the energy spectra, the matrix elements of the operators etc., in the "standard" and in the q-deformed case. The simplest physical system is of course the one - dimensional harmonic oscillator, which we shall consider first.

We shall define, by analogy with the standard quantum mechanics, the q-position (Q_q) and the q-momentum of the particle by the expressions

$$Q_q = \sqrt{\frac{\hbar}{2m\omega}}(a^\dagger + a), \qquad P_q = i\sqrt{\frac{\hbar}{2m\omega}}(a^\dagger - a) \tag{3.35}$$

Using this expressions we define, again by analogy, the q-analogue of the Hamiltonian of the harmonic oscillator as

$$H^q = \frac{1}{2m}P_q^2 + \frac{m\omega^2}{2}Q_q^2 \tag{3.36}$$

Substituting (3.35) in (3.36) we obtain

$$H^q = \frac{\hbar\omega}{2}(a^\dagger a + aa^\dagger) = \frac{\hbar\omega}{2}([N+1] + [N])$$

Obviously the states

$$|v\rangle = \frac{1}{\sqrt{[v]!}}(a^\dagger)^v|0\rangle_q$$

are the eigenstates of H^q and the corresponding eigenvalues are

$$E_v^q = \frac{\hbar\omega}{2}([v+1]+[v]) = \begin{cases} \dfrac{\hbar\omega}{2}\dfrac{\sinh(\tau(v+1/2))}{\sinh(\tau)} & \text{if} \quad e^\tau \\ \dfrac{\hbar\omega}{2}\dfrac{\sin(\tau(v+1/2))}{\sin(\tau)} & \text{if} \quad e^{i\tau} \end{cases} \tag{3.37}$$

In both cases we have

$$\lim_{\tau\to 0} E_v^q = \frac{\hbar\omega}{2}(v+1/2)$$

i.e. in the limit $\tau \to 0$ the energy of the q-deformed harmonic oscillator coincides with the energy of the standard harmonic oscillator.

From eq (3.37) one can see that in the case $\tau \neq 0$ the energy levels of the harmonic oscillator are no more equidistant and that the behavior of the energy spectra is completely different in the cases $q = e^\tau$ and $q = e^{i\tau}$ respectively. In the case $q = e^\tau$ (i.e. when q is real) the distances between levels increase with the value of v, i.e. the spectrum is "extended". On the contrary, when $q = e^{i\tau}$ the distances between the levels decrease with the increase of v, i.e. the spectrum is "squeezed". What is more, in the last case, due to the fact that the dependence of the energy of the vibrational quantum number v is of the form $\sin\tau(v+1/2)$, there exists a critical value of v, namely v_{max}, such that for the values $v \geq v_{max}$ the values of the energy levels begin to decrease, which is of course unacceptable from the point of view of physics. For this reason we must postulate that the spectrum contains only a limited number of levels and terminates at v_{max}. Obviously, v_{max} is determined from the condition

$$\tau(v_{max}+1/2) \leq \frac{\pi}{2} \leq \tau(v_{max}+3/2) \tag{3.38}$$

The expression (3.37), in the case when $q = e^{i\tau}$, represents many characteristic features of the anharmonic oscillator. As is well known, the energy

levels of the anharmonic oscillator are not equidistant but their separation decreases when the value of v increases. The energy values of the anharmonic oscillator are given by [96]

$$E_v = \hbar\omega(v+\frac{1}{2}) - \hbar x_e\omega(v+\frac{1}{2})^2 + \hbar y_e\omega(v+\frac{1}{2})^3 - \dots \tag{3.39}$$

where $x_e\omega << \omega, y_e\omega << x_e\omega$, etc. It should be mentioned also that v can take only a limited number of values (i.e. $v \leq v_{max}$) due to the finite depth of the potential wall.

For example, when the potential curve of the anharmonic oscillator can be approximated by the Morse potential

$$\begin{aligned} V &= D(e^{-2\alpha x} - 2e^{-\alpha x}) \\ &\approx -D + \frac{1}{2}M\omega^2 x^2 - D\alpha^3 x^3 \qquad \text{(for small } x\text{)} , \end{aligned}$$

the eigenvalues of the Schroedinger equation are

$$E_v^M = -D + \hbar\omega(v+\frac{1}{2}) - \frac{\hbar\omega}{\xi}(v+\frac{1}{2})^2 \tag{3.40}$$

where $\xi = 2\sqrt{2MD}/\alpha\hbar$ is the anharmonicity parameter and the values of v are limited by the condition

$$v < \frac{1}{2}(\xi - 1)$$

On the other hand, (3.37) gives the following expansion for the energy values of the q-deformed harmonic oscillator

$$\frac{E^q}{\hbar\omega} = \frac{\tau}{2\sin\tau/2}\left[(v+\frac{1}{2}) - \frac{\tau^2}{6}(v+\frac{1}{2})^3 + \dots\right] \tag{3.41}$$

and the values of v are limited by (3.37). The comparison of these expressions with (3.39) and (3.40) shows that there is a great similarity between the spectrum of the q-deformed harmonic oscillator and those of the anharmonic oscillator describing the vibrational spectra of the diatomic molecules. At the same time, one can see that this coincidence is only a qualitative one. This is due to the fact that the expression (3.41) contains only the odd powers of

$(v + 1/2)$, while the expression (3.39) contains the odd and the even powers of this quantity as well.

It is not surprising that the q-deformed harmonic oscillator describes the vibrational molecular spectra only qualitatively because this system is obviously too simple to describe reality. It might seem bewildering that such a simple system (with a very simple Hamiltonian) is able to describe the anharmonicity in the vibrational spectra at all. The latter, however, shows that this anharmonicity is itself incorporated in the q-deformed boson operators.

The replacement of the coordinate Q and momentum P by their q-deformed versions Q_q and P_q leads to a "deformation" of the commutation relation between the q-position and q-momentum, which gives rise to the modification of the uncertainty principle. One can easily check that

$$[Q_q, P_q] = i\frac{\cos\frac{\tau}{2}(N + \frac{1}{2})}{\cos\frac{\tau}{2}}$$

So we obtain that in the oscillator basis

$$\Delta Q_q \Delta P_q \approx \frac{\cos\frac{\tau}{2}(v + \frac{1}{2})}{\cos\frac{\tau}{2}} \tag{3.42}$$

This means that we have a "normal" uncertainty only in the ground state of the q-deformed oscillator. With the increase of v the uncertainty decreases and in the highest state (the state with maximum value of v) we have $\Delta Q_q \Delta P_q \approx 0$, which is closed to classical limit.

The q-deformed functionals. In this section we shall show that the q-deformed boson operators can be expressed in terms of the standard boson creation and annihilation operators. For this purpose let us denote, as usual, by b and $b^\dagger$, the ordinary boson operators which satisfy the standard commutation relations

$$[b, b^\dagger] = 1 \qquad ,$$

and let

$$B = b^\dagger b$$

be the standard number of boson operator. We shall try to represent the q-deformed boson operators in the form

$$a = b\varphi(B) \qquad a^\dagger = \varphi(B)b^\dagger \tag{3.43}$$

where $\varphi(B) = \varphi(b^\dagger b)$ is a function which must be determined from the condition that a and $a^\dagger$ must satisfy the commutation relations (3.7). The formal functions $\varphi(B)$ are often referred to as *q-deformed functionals* [61].

To determine the q-deformed functionals we first form the bilinear product $aa^\dagger = b|\varphi(B)|^2 b^\dagger$ and, taking into account (3.8) and also that $bb^\dagger = b^\dagger b + 1 = B + 1$, we obtain

$$aa^\dagger = F(B+1)(B+1) \qquad where \qquad F(B) = |\varphi(B)|^2 \tag{3.44a}$$

In the same way we have

$$a^\dagger a = F(B)B \tag{3.44b}$$

Inserting (3.44a) and (3.44b) in (3.7b) we obtain

$$F(B+1)(B+1) - qF(B)B = q^{-N} \tag{3.45}$$

For the function $\varphi(B)$ this equation can be solved in regards to $F(B)$ if we accept that

$$N = B \qquad \text{i.e.} \qquad N = b^\dagger b \tag{3.46}$$

The solution of eq (3.45) is

$$F(B) = \frac{[B]}{B} \qquad or \qquad \varphi(B) = \sqrt{\frac{[B]}{B}}$$

Note. The solution of eq. (3.45) can be found as follows: First we rewrite (3.45) in the form

$$F(x+1)(x+1) - qF(x)x = q^{-N}$$

and putting $x = 0, 1, 2, \ldots, n$ we obtain the system of equations in finite differences

$$\begin{aligned} F(1) &= 1 \\ 2F(2) - qF(1) &= q^{-1} \\ 3F(3) - 2qF(2) &= q^{-2} \\ &\cdots \\ nF(2) - (n-1)qF(n-1) &= q^{-n+1} \end{aligned}$$

Now we add the first two equations and obtain

$$2F(2) = q + q^{-1} = \frac{q^2 - q^{-2}}{q - q^{-1}} = [2]$$

i.e. $F(2) = [2]/2$. Then we add the second and third equations and obtain

$$3F(3) = q[2] + q^{-2} = q\frac{q^2 - q^{-2}}{q - q^{-1}} + q^{-2} = \frac{q^3 - q^{-3}}{q - q^{-1}} = [3]$$

Thus by induction we have

$$F(n) = \frac{[n]}{n} \qquad \Longrightarrow \varphi(n) = \sqrt{\frac{[n]}{n}} \qquad Q.E.D.$$

Thus we come to the conclusion that *the operators*

$$N = b^\dagger b \equiv B$$

$$a = b\sqrt{\frac{[B]}{B}} \qquad a^\dagger = \sqrt{\frac{[B]}{B}}b^\dagger \tag{3.47}$$

satisfy the commutation relations (3.7) for the q-deformed Heisenberg- Weyl algebra $\mathcal{H}_4^q$.

Remark: The realization of the q-deformed boson operators in the form of q-deformed functionals can be considered as a *mapping* of a and $a^\dagger$ onto the Hilbert space of the "standard" boson creation and annihilation operators.

First we shall note that in the case when the q-deformed boson operators are represented in the form of the q-deformed functionals (3.47), the q-deformed vacuum $|0\rangle_q$ coincides with the "standard" vacuum state $|0\rangle$. As a matter of fact we have

$$a|0\rangle_q = 0 \quad \longmapsto \quad b\sqrt{\frac{[B]}{B}}|0\rangle_q = 0$$

Using the formulae $bf(B) = f(B+1)b$, which is analogous to (3.8), we can come to the conclusion that

$$a|0\rangle_q = 0 \quad \longmapsto \quad B|0\rangle_q = b|0\rangle_q = 0$$

which means that *in this realization* $|0\rangle_q$ and $|0\rangle$ coincide.

Further we can represent the state with n q-deformed bosons in the form

$$|n\rangle_q = \frac{\left(a^\dagger\right)^n}{\sqrt{[n]!}}|0\rangle_q = \frac{1}{\sqrt{[n]!}}\sqrt{\frac{[B]}{B}}b^\dagger\sqrt{\frac{[B]}{B}}b^\dagger\ldots\sqrt{\frac{[B]}{B}}b^\dagger|0\rangle$$

Now, taking into account that $b^\dagger f(b) = f(B-1)b^\dagger$, all operatotrs $b^\dagger$ can be "shifted" to the right and we obtain

$$|n\rangle_q = \frac{1}{\sqrt{[n]!}}\sqrt{\frac{[B]!}{B!}}\left(b^\dagger\right)^n|0\rangle = \frac{1}{\sqrt{n!}}\left(b^\dagger\right)^n|0\rangle = |n\rangle$$

In this way using the q-deformed functionals we actually perform the mappings

$$|0\rangle_q \longmapsto |0\rangle \quad |n\rangle_q \longmapsto |n\rangle \quad a \longmapsto b\sqrt{\frac{[B]}{B}} \quad a^\dagger \longmapsto \sqrt{\frac{[B]}{B}}b^\dagger$$

which means that we can perform the calculations with the "images" given above instead of with the q-deformed operators and states.

From (3.47) we can also obtain the expressions for a and $a^\dagger$ in the form of infinite series of b and $b^\dagger$

$$\begin{aligned} a &= b(c_0 + c_1 b^\dagger b + c_2 b^\dagger b^\dagger bb + \ldots) \\ a^\dagger &= (c_0 + c_1 b^\dagger b + c_2 b^\dagger b^\dagger bb + \ldots)b^\dagger \end{aligned} \tag{3.48}$$

where the coefficients c_i can be obtained by expanding $\sqrt{\frac{[B]}{B}}$ in series of B and rearranging $b^\dagger$ and b in the expansion terms. The expression (3.48) may be considered as a *boson expansion* of a and $a^\dagger$. The physical interpretation of (3.35) is that, despite the fact that the q-deformed operators $a^\dagger$ and a describe "free particles" (i.e. particles outside a potential field), these operators "accumulate" certain correlations which describe some implicit interactions between the ordinary particles. We can also say that some anharmonicities are "built in" from the very beginning in the q-deformed Heisenberg – Weyl algebra. The price we pay is the necessity to work with the complicated commutation relations; what we gain is that we can describe

the complicated systems using simple Hamiltonians expressed in terms of the q-deformed boson operators.

4. The q-deformed $SU_q(2)$ algebra and its representations.

4.1 The q-deformed $SU_q(2)$ algebra

Commutatation relations of $SU_q(2)$. The q-deformed $SU_q(2)$- algebra was shortly discussed in example 2 of Sec. 2. Let us recall that this algebra consists of three generators J_+^q, J_-^q and J_0^q which satisfy the commutation relations [7]

$$\begin{aligned} [J_\pm^q, J_0^q] &= \pm J_\pm^q \\ [J_+^q, J_-^q] &= \frac{q^{2J_0^q} - q^{-2J_0^q}}{q - q^{-1}} \\ &\equiv [2J_0^q] \end{aligned} \tag{4.1a}$$

and the unitarity conditions

$$(J_+)^\dagger = J_-, \qquad (J_0)^\dagger = J_0 \quad . \tag{4.1b}$$

As usual here we use the notation

$$[A] = \frac{q^A - q^{-A}}{q - q^{-1}} \tag{4.2}$$

[7] Roughly speaking the set of operators J_m^q,$(m = 0, \pm)$, form an algebra because this set is closed under the commutations of its elements (i.e. the commutator of any two operators is expressed in terms of the other operators). It should be noted however that the commutator of J_+^q and J_-^q is a *nonlinear function* of J_0^q and for this reason $SU_q(2)$ *is not a Lie algebra* at all (See the text after Remark 1 in Sec. 2). This function depends on the parameter q and, as we shall see later on, goes into $2J_0$ when $q \to 1$. Therefore, in this limit the algebra (4.1) goes into the $SU(2)$-algebra. For this reason we can consider (4.1) as a "deviation" from the $SU(2)$ algebra (or as its "deformation").

where A may be an ordinary number or an operator as well. It should be noted that in the expresion (4.2) the parameter q is an arbitrary but *fixed* number. In this sense different values of q correspond to q-algebras with different q-deformations. In order to distinguish these algebras we have supplied the operators J_m^q, $(m = 0, \pm)$, with the index q. This index will be omitted when this does not lead to misunderstanding.

In the same way as in Sec. 3.2 it can be shown that the parameter q can be either a real number represented as $q = e^{\tau}$ or it can be a pure phase represented as $q = e^{i\tau}$ (τ is a real number). The expresions for the q-numbers [A] in these cases are given by (3.12) i.e.

$$[A] = \frac{sh(\tau A)}{sh(\tau)} \qquad \text{if } q = e^{\tau},$$

and

$$[A] = \frac{sin(\tau A)}{sin(\tau)} \qquad \text{if } q = e^{i\tau}.$$

In the limit $q \to 1$ or, which is the same, in the limit $\tau \to 0$, we have

$$\lim_{q \to 1} [A] = A. \tag{4.3}$$

In order to consider the $(q \to 1)$-limit of (4.1) we denote

$$\lim_{q \to 1} J_m^q = L_m. \tag{4.4}$$

Thus in the limit $q \to 1$, from (4.1), we obtain

$$\begin{aligned} [L_0, l_{\pm}] &= \pm L_{\pm} \\ [L_+, L_-] &= 2L_0 \end{aligned} \tag{4.5a}$$

and the unitarity conditions

$$(L_+)^{\dagger} = L_-, \qquad (L_0)^{\dagger} = L_0 \quad . \tag{4.5b}$$

One can easily recognize in (4.5) the "standard" $SU(2)$ Lie algebra (the algebra of the angular momentum). In spite of the fact that (4.5) is a Lie algebra and (4.1) is not, there is an obvious similarity between these two algebras.

We can summarize the basic characteristic feature of the q-deformed algebra $SU_q(2)$ in the following way

a) The fundamental commutation relations are changed or as we usualy say - "deformed". That is known as a *kinematical symmetry breaking.*

b) The result of "addition of q-angular momenta" depends on the *order of the addition.* For exapmple if we add the spin to the orbital momentum we shall obtain a result which is different from the result which we would obtain if we add the orbital momenta to the spin.

This property determines a very important charcteristic difference between the quantum and the standard $SU(2)$-algebras and can be put in the basis of the experiments which would decide to which extent the q-deformed $SU_q(2)$-algebra governs the atomic proceses.

Quite often in the literature one comes across the conclusion that one of the properties of $SU_q(2)$ is that the inherent symmetry of the group manifold is broken. This seems to be evident, because from the $SU_q(2)$-commutation relations, for example, one can see that the z-direction of the three dimentional space is singled out.

This however is not correct. Duiring the preparation of this paper we received a very interesting comment on this point from L. C. Biedenharn [120] and we can not resist the temptaiton to cite his comments here:

" The algebra of the three $SU_q(2)$ generators *does* look as if the generator $J_3(q)$ plays a distinguished rôle, but this is not correct. The error comes from the fundamental fact in *Lie groups* that the generators are a basis for the adjoint irrep. *This is not true for quantum groups.* The algebra of a quantum group involves generators belonging to the universal enveloping algebra (of the undeformed group) and are denumerably infinite in number.

By contrast, there exists an irrep of the quantum group (for generic q) having the same dimensionality as the adjoint irrep of the undeformed group. One can identify the basis of this irrep with the algebraic generator basis of the quantum group. (This sounds very learned and difficult, but it is really very simple. Take $SU_q(2)$. Then J_+^q, J_-^q, J_3^q are three algebraic generators

such that in the commutation relations $J_+^q, J_-^q, J_3^q, (J_3^q)^3, (J_3^q)^5 \cdots$ occur. But in the 3-dimensional q-group irrep all three basis elements (J_x^q, J_y^q, J_z^q) are *equivalent* (stated physically this means that the three states in the q-group irrep [2 0] are *degenerate*). We can therefore choose any one of these to be "J_3^q" and construct all the generators of the q-group.

Hence, at a deeper level, one sees that if $SU_q(2)$ really applied to physical three-space, all directions would still be equivalent."

The Casimir operator of $SU_q(2)$. The similarity between $SU(2)$ and $SU_q(2)$ algebras becomes more evident if one considers the expressions of the Casimir operators for these algebras. As is well known, the Casimir operator of the $SU(2)$ Lie algebra, which will be denoted by $C_2(SU(2))$, is a bilinear combination of its generators which by definition commute with all generators of the algebra. The Casimir operator $C_2(SU(2))$ coincides with the square of the "length of angular momentum" i.e.

$$\begin{aligned} C_2(SU(2)) \equiv \mathbf{L}^2 &= \frac{1}{2}(L_+L_- + L_-L_+) + L_0^2 \\ &= L_-L_+ + L_0(L_0+1) \end{aligned} \tag{4.6}$$

(The expression in the second row is obtained after the commutation of L_- and L_+ in the first term of the first row).

The Casimir operator $C_2^q(SU_q(2))$ for the q-deformed $SU_q(2)$-algebra is also defined by the condition that all the generators J_m^q must commute with it. One can show that this operator has the form

$$C_2^q(SU_q(2)) = J_-J_+ + [J_0][J_0+1], \tag{4.7}$$

i.e. it can formally be obtained from (4.6) by the replacement

$$L_-L_+ \longmapsto J_-J_+ \quad \text{and} \quad L_0(L_0+1) \longmapsto [J_0][J_0+1]$$

Remark 1: *Proof of the formula* (4.7) . Due to the fact that the commutation relations of L_0 with $L_\pm$ coincide with the commutation relations of J_0 with $J_\pm$ one can suggest that the first terms of (4.6) and (4.7) coincide and the Casimir operator C_2^q of $SU_q(2)$, in analogy to (4.6), has the form

$$C_2^q = J_- J_+ + F(J_0) \tag{4.8}$$

where $F(J_0)$ is still an unknown function of J_0. Obviously (4.8) commutes with J_0 and, to determine $F(J_0)$, we must calculate the commutator of C_2^q with J_+ and J_-. The commutator with J_+ gives

$$\begin{aligned}[J_+, C_2^q] &= [J_+, J_-]J_+ + [J_+, F(J_0)] \\ &= [2J_0] + J_+ F(J_0) - F(J_0)J_+\end{aligned}$$

Now we shall take into account that [8]

$$J_+ F(J_0) = F(J_0 - 1)J_+$$

and obtain that

$$[J_+, C_2^q] = 0 \longmapsto [2J_0] + F(J_0 - 1) - F(J_0) = 0$$

This is an equation in finite differences for $F(J_0)$ and it can be solved by the following prescription: Let us make the replacemant $J_0 \longmapsto x, x = 1, 2, \ldots n$,

[8] This identity can be obtained as follows: From (4.6) we have that $J_+ J_0 = J_0 J_+ - J_0 = (J_0 - 1)J_+$. Thus we obtain

$$J_+ J_0^n = (J_0 - 1)J_+ J_0^{n-1} = \ldots = (J_0 - 1)^n J_+.$$

Then for every function $F(J_0)$ which can be expressed in series $F = \sum a_k J_0^k$ we have

$$J_+ F(J_0) = \sum a_k J_+ J_0^k = \sum a_k (J_0 - 1)^k J_+ = F(J_0 - 1)J_+$$

which results in the followimg system of equations

$$\begin{aligned} F(1) - F(0) &= [2.1] \\ F(2) - F(1) &= [2.2] \\ &\cdots\cdots \\ F(n) - F(n-1) &= [2.n] \quad . \end{aligned} \tag{4.9}$$

Adding these equations we obtain

$$F(n) - F(0) = \sum_{k=1}^{n} [2.k] \quad .$$

Now we can take into account that C_2^q is determined only up to the additive constant (since every constant commutes with all J_m) and therefore we can put $F(0) = 0$. The sum in the r.h.s. of the above equation can be written in the form

$$\sum_{k=1}^{n} [2.k] = \frac{1}{q - q^{-1}} \left(\sum_{k=1}^{n} q^{2k} - \sum_{k=1}^{n} q^{-2k} \right)$$

The summation in the above equation can be easily done using the formula for a geometric progression which results in

$$F(n) = [n][n+1]$$

and after replacement $x \longmapsto J_0$ we obtain formula (4.7).

This result was obtained taking the commutator of J_+ with C_2^q. One can easily check, however, that expression (4.7) commutes also with J_-, i.e. (4.7) commutes with all the generators of $SU_q(2)$. Q.E.D.

The Casimir operator $C_2^q(SU_q(2)$ plays an important role in the representation theory of $SU_q(2)$ which is due to the fact that its eigenvalues, in full analogy with the Casimir operator of the "standard" $SU(2)$ algebra, determine the representations of $SU_q(2)$.

4.2 Representations of q-deformed $SU_q(2)$ algebra

Representations of $SU(2)$ Lie algebra. The similarity of $SU(2)$ and $SU_q(2)$ algebras leads to the close similarity of their representation theory. Let us first recall some well known facts from the representation theory of the $SU(2)$- algebra.

Remark 1: We shall shortly recall *what is a representation of an algebra.* Let us suppose that each generator J_m of the algebra $\mathcal{A}$ is related to an $(n \times n)$ - dimensional matrix $\tilde{L}_m$ (we say that there exists a mapping $J_m \longmapsto \tilde{L}_m$). Let us also assume that the matrices $\tilde{L}_m$ satisfy the same commutation relations as the generators J_m of the algebra. In this case the mapping $J_m \longmapsto \tilde{L}_m$ is said to be a representation $\mathcal{D}^n$ of the algebra $\mathcal{A}$.

The matrices $\tilde{J}_m$ act in the n-dimensional vector space V_n, which is referred to as a representation space. The dimension n of a representation space is referred to as a dimension of the representation $\mathcal{D}^n$ and the basic vectors of this space are referred to as basic vectors of the representation.

The representation is said to be *unitary* if the matrices of the representation $\tilde{J}_m$ are unitary. The representation $\mathcal{D}^n$ is said to be *irreducible* if the representation space cannot be decomposed into parts each of which transforms into itself under the action of *all* of the matrices of representation.

The unitary irreducible representations (UIR) $\mathcal{D}^j$ of the $SU(2)$ - algebra are determined by the integer or half-integer number $j = 0, 1/2, 1, 3/2, \ldots$ The dimension of these representations is

$$dim\mathcal{D}^j = 2j + 1.$$

The basis vectors $|jm\rangle$ of UIR $\mathcal{D}^j$ of $SU(2)$ are common eigenvectors of the Casimir operator $C_2(SU(2)) \equiv \mathbf{L}^2$ and the operator L_3 (the projection of $\mathbf{L}$ on the z-axes), and satisfy the equations

$$\begin{aligned} \mathbf{L}^2|jm\rangle &= j(j+1)|jm\rangle \qquad j = 0, 1/2, 1.3/2, \ldots, \\ L_3|jm\rangle &= m|jm\rangle \qquad\quad m = j, j-1, \ldots, -j. \end{aligned} \tag{4.10}$$

The operators L_+ and L_- are referred to as raising and lowering operators, respectively, because they raise and lower the eigenvalue of L_3 by one unit.

The action of these operators on the basic vectors $|jm\rangle$ is given by

$$L_+|jm\rangle = \sqrt{(j-m)(j+m+1)}|jm+1\rangle$$
$$L_-|jm\rangle = \sqrt{(j+m)(j-m+1)}|jm-1\rangle \tag{4.11}$$

Obviously the basic vectors of UIR 's of $SU(2)$ can be found by the simultaneous solution of the equations (4.10). There is however another way to find these vectors which is fully equivalent to the solution of (4.10) and is widely used. Each UIR $\mathcal{D}^j$ of $SU(2)$ is determined also by the highest vector of the representation, i.e. by the vector with a maximal projection of L_3. This vector will be denoted by $|jj\rangle$ and satisfies the equations

$$L_3|jj\rangle = j|jj\rangle$$
$$L_+|jj\rangle = 0. \tag{4.12}$$

The vectors with an arbitrary value of m (i.e. the vectors $|jm\rangle$) can be obtained from $|jj\rangle$ by the successive application of L_- which lowers step by step the value of L_3. We have

$$|jm\rangle = N_m(L_-)^{j-m}|jj\rangle$$

where N_m is a normalization constant.

We shall see that these properties of the UIR of $SU(2)$ have an immediate generalization for the representations of the q-deformed $SU_q(2)$.

Representations of $SU_q(2)$. As has already been mentioned, the similarity of the "standard" and q-deformed $SU(2)$ algebras leads to a similarity in their representation theory. Jimbo has shown [43] that the unitary irreducible representations $\mathcal{D}^j$ of $SU_q()2)$ are determined, by analogy with the representations of $SU(2)$, by an integer or half-integer number $j = 0, 1/2, 1, 3/2, \ldots$. The representation $\mathcal{D}^j$ is determined by its highest weight vector which satisfies the equations

$$J_0|jj\rangle_q = j|jj\rangle_q$$
$$J_+|jj\rangle_q = 0 \tag{4.13}$$

All vectors of the representation space can be obtained from the highest weight vector $|jj\rangle_q$ by the successive application of the lowering operator as follow

$$|jk\rangle_q = N_k(J_-)^k|jj\rangle_q, \qquad k = j - m \quad . \tag{4.14}$$

The constant N_k can be calculated from the normalization condition

$$1 = \langle jm|jm\rangle_q = N_k^2\langle jj|(J_+)^k(J_-)^k|jj\rangle_q \tag{4.15}$$

To proceed with the calculations, one needs the following formula, which was proved by Rosso [71] by induction,

$$J_+(J_-)^k = (J_-)^k J_+ + [k](J_-)^{k-1}[2J_0 - k + 1]. \tag{4.16}$$

Here we shall give another proof of this formula in order to demonstrate some useful technique in the use of q-numbers.

Remark 2:*Proof of formula* 4.16. We start with the well known formula valid for the commutator of any product of operators

$$[A, B_1B_2 \dots B_k] = \sum_{i=1}^{k} B_1 \dots B_{i-1}[A, B_i]B_{i+1} \dots B_k$$

(This formula can be easily proved by induction). Applying this formula to the commutator of J_+ and J_-^k, we obtain

$$\begin{aligned}[J_+, (J_-)^k] &= \sum_{i=1}^{k}(J_-)^{i-1}[J_+, J_-](J_-)^{k-i} \\ &= \sum_{i=1}^{k}(J_-)^{i-1}[2J_0](J_-)^{k-i}\end{aligned}$$

Now we can carry all J_- on the left side of $[J_0]$ using the formula

$$F(J_0)J_- = J_-F(J_0 - 1)$$

which can be proved as in the footnote in Sec. 4.1 .Thus we have

$$[2J_0]J_-^s = J_-[2J_0 - 2]J_-^{s-1} = \dots = J_-^s[2J_0 - 2s]$$

and finally, we obtain

$$[J_+,(J_-)^k] = (J_-)^{k-1}\sum_{i=1}^{k}[2J_0 - 2k + 2i]. \tag{4.17}$$

To take the sum in the r.h.s of the above equation we shall replace $2J_0 - 2k$ with $2a$ and write down

$$\sum_{i=1}^{k}[2a + 2i] = \frac{1}{q - q^{-1}}\left(\sum_{i=1}^{k} q^{2a+2i} - \sum_{i=1}^{k} q^{-2a-2i}\right)$$

One can sum this expression making use of the formula for the geometric progression which results in

$$\sum_{i=1}^{k}[2a + 2i] = [k][2a + k + 1]. \tag{4.18}$$

Replacing again $2a$ by $2J_0 - 2k$ in (4.17) we obtain (4.16). Q.E.D.

Using (4.16) one can easily obtain

$$\begin{aligned}\langle jj|(J_+)^k(J_-)^k|jj\rangle_q &= [k][2j - k - 1]\langle jj|(J_+)^{k-1}(J_-)^{k-1}|jj\rangle_q = \dots \\ &= [k]![2j - k + 1][2j - k + 2]\dots[2j]\langle jj|jj\rangle_q \\ &= \frac{[k]![2j]!}{[2j - k]!}\langle jj|jj\rangle_q\end{aligned}$$

Now, taking into account that $k = j - m$ and (4.15), we have

$$|jm\rangle_q = \sqrt{\frac{[j + m]!}{[2j]![j - m]!}}\ (J_-)^{j-m}|jj\rangle_q. \tag{4.19}$$

From the expression for the normalization constant in (4.19) we can find the minimal and the maximal values of m (i.e. m_{min} and m_{max} respectively). For this purpose we should take into account that by definition $[0]! = 1$ and that $[-n]! = \infty$ for every real positive value of n. This means that for $m > j$ and for $m < -j$ the normalization constant in (4.19) vanishes or loses

its meaning. [9] We conclude that $m_{max} = j$ (as it should be by definition) and $m_{min} = -j$. Thus we have

$$m_{max} - m_{min} = 2j$$

However we can step down from m_{max} to m_{min} stepwise changing m by one unit and the difference $m_{max} - m_{min}$ must be an integer, i.e.

$$2j = \quad \text{integer}$$

If this integer is even, i.e $2j = 2k$, j must be an integer and if this integer is odd, i.e. $2j = 2k + 1$, j must be half integer. Thus we come to the conclusion that the possible values of the number j which determine the representation $\mathcal{D}^j$ of $SU_q(2)$ are

$$j = 0, 1/2, 1, 3/2, \ldots$$

and the possible values of m which ennumerate the eigenvectors in the representation $\mathcal{D}^j$ are

$$m = j, j-1, \ldots, -j$$

which illustrate the similarity of the representation theory of the "standard" Lie algebra $SU(2)$ and the q-deformed $SU_q(2)$.

It can be easily shown that one can obtain the vector with an arbitrary value of m if one starts from the vector with the minimal value of m (i.e. from the lowest weight vector $|j-j\rangle_q$) and apply to it an appropriate power of the raising operator J_+. We have

$$|jm\rangle_q = \sqrt{\frac{[j-m]!}{[2j]![j+m]!}} \quad (J_+)^{j-m}|j-j\rangle_q \tag{4.20}$$

$$= \sqrt{\frac{[j+m]!}{[2j]![j-m]!}} \quad (J_-)^{j-m}|jj\rangle_q$$

[9] We must note that we should be very careful with these considerations when $q = exp(i\tau)$ because in this case for some critical values of $2j$, $j+m$ and $j-m$ the factors in (4.19) may be approximately zero . Even more dangerous is the case when q is a root of unity. In the last case we may have $[\alpha] = 0$ also when $\alpha \neq 0$ (See Sec. 3.3 and the formulae (3.25) - (3.28).) However here we shall not go into these details.

In analody with (4.11) using the expession (4.19) for the normalization constant we can also obtain the action of the raising and lowering operators on the basic vectors

$$J_{\pm}|jm\rangle_q = \sqrt{[j \pm m][j \mp m + 1]}|jm \pm 1\rangle_q$$
$$J_0|jm\rangle_q = m|jm\rangle_q \tag{4.21}$$

At the end we must note that Smirnov et al [82] give a generalization of (4.16) in the form[10]

$$(J_+)^s(J_-)^p = \sum_{k=0}^{msx(s,p)} \frac{[s]![p]!}{[k]![s-k]![p-k]!}(J_-)^{p-k}(J_+)^{s-k}\frac{[2J_0 - p + s]!}{[2J_0 - p + s - k]!} \tag{4.22}$$

This formula, which can be proved by induction, is useful when one considers more complicated commutation relations which are needed, for example, for the calculation of the Clebsch - Gordan coefficients for the $SU_q(2)$ representations. With the help of (4.22) one can easily prove that the matrix elements of the powers of the operators $J_{\pm}$ are

$$\langle jm'|(J_+)^s|jm\rangle_q = \delta_{m',m+s}\sqrt{\frac{[j-m]![j+m+s]!}{[j+m]![j-m-s]!}}$$
$$\langle jm'|(J_-)^s|jm\rangle_q = \delta_{m',m-s}\sqrt{\frac{[j+m]![j-m+s]!}{[j-m]![j+m-s]!}} \tag{4.23}$$

[10]The presence of the operator J_0 in the denominator of (4.22) should not worry us because in any particular representation with basis vectors $|jm\rangle_q$ the operator J_0 must be replaced with m

4.3 Realizations of $SU_q(2)$ in terms of q-deformed boson operators

Biedenharn's representation of $SU_q(2)$. Biedenharn [52] gives a prescription for the expression of the $SU_q(2)$ generators and the basis vectors of the $SU_q(2)$ – representations in terms of q-deformed creation and annihilation operators. This is known as the *Biedenharn realization* of $SU_q(2)$.[11]

Let us first recall some facts connected with the representation of the "standard" Lie algebras in terms of "standard" creation and annihilation boson operators which satisfy the commutation relations

$$[b_k, b_p^\dagger] = \delta_{kp}$$

$$[b_k, b_p] = [b_k^\dagger, b_p^\dagger] = 0, \qquad i, j, = 1, 2, \ldots, n \tag{4.24}$$

Let us suppose that $\tilde{X}, \tilde{Y}$ and $\tilde{Z}$ are $(n \times n)$ – matrices which satisfy the commutation relation

$$[\tilde{X}, \tilde{Y}] = \tilde{Z} \tag{4.25}$$

and let us form operators which are bilinear combinations of the boson creation and annihilation operators

$$X = \sum_{k=1}^{p} b_p^\dagger \tilde{X}_{pk} b_k, \qquad Y = \sum_{k=1}^{p} b_p^\dagger \tilde{Y}_{pk} b_k, \qquad Z = \sum_{k=1}^{p} b_p^\dagger \tilde{Z}_{pk} b_k, \tag{4.26}$$

where $\tilde{X}_{pk}$ etc. are the matrix elements of the matrices $\tilde{X}, \tilde{Y}, \tilde{Z}$. Using the commutation relations (4.24) one can easily check that the operatores X, Y, Z satysfy the same commutation relation $[X, Y] = Z$ as the martices $\tilde{X}, \tilde{Y}, \tilde{Z}$.

The formulas (4.26) realize the mapping of the set of matrices $\tilde{X}$ into the set of bilinear combinations of the boson operators X, i.e. realize the mapping $\tilde{X} \longmapsto X$, where $X = \sum b_k^\dagger X_{kp} b_p$. This mapping is known as a

[11] Instead of "realization" the term "representation" is very often used. This, however, can lead to misunderstanding. To avoid this we shall use the term "*representation*" in the sense of Remark 1 of Sec. 4.2, i.e. as a mapping of the set of generators of the algebra onto the set of matrices. Any other mapping of the generators oto the set of other operators will be referred to as a "*realization*".

Jordan mapping. The Jordan mapping is a homomorphism, i.e. it preserves the commutation relations between the operators.

Let us now have the set of f matrices $\tilde{X}_\mu, \mu = 1, 2, \ldots f$ which satisfy the commutation relation

$$[\tilde{X}_\mu, \tilde{X}_\nu] = C^\lambda_{\mu\nu} \tilde{X}_\lambda \tag{4.27}$$

This set of matrices is said to form a Lie algebra $\mathcal{L}$, or, what is more precise, to form a matrix representation of this algebra. If one performs Jordan mapping $\tilde{X}_\mu \longmapsto X_\mu$ one will obtain the set of f bilinear combinations of the boson creation and annihilation operators

$$X_\mu = \sum_{k=1}^{n} b_p^\dagger (\tilde{X}_\mu)_{pk} b_k$$

which satisfies the same commutation relations (4.27) and in this sense forms the same algebra. The set of operators is said to form *the boson realization* or *boson representation* of the Lie algebra $\mathcal{L}$.

As an example we shall consider the boson representation of $SU(2)$. We shall introduce the notation

$$\tilde{L}_k = \frac{1}{2}\sigma_k, \quad k = 1, 2, 3,$$

where σ_k are the Pauli matrices

$$\sigma_1 = \begin{pmatrix} 0 & 1 \\ 1 & 0 \end{pmatrix}, \qquad \sigma_2 = \begin{pmatrix} 0 & -i \\ i & 0 \end{pmatrix}, \qquad \sigma_3 = \begin{pmatrix} 1 & 0 \\ 0 & -1 \end{pmatrix}.$$

The two dimensional matrices $\tilde{L}_k$ satisfy the commutation relations

$$[\tilde{L}_1, \tilde{L}_2] = i\tilde{L}_3, \qquad [\tilde{L}_2, \tilde{L}_3] = i\tilde{L}_1, \qquad [\tilde{L}_3, \tilde{L}_1] = i\tilde{L}_2.$$

If one introduces the new matrices

$$\tilde{L}_+ = \frac{1}{2}(\tilde{L}_1 + i\tilde{L}_2), \quad \tilde{L}_- = \frac{1}{2}(\tilde{L}_1 - i\tilde{L}_2) \quad \tilde{L}_0 = \tilde{L}_3$$

one can esily check that these matrices have the form

$$\tilde{L}_+ = \begin{pmatrix} 0 & 1 \\ 0 & 0 \end{pmatrix} \qquad \tilde{L}_- = \begin{pmatrix} 0 & 0 \\ 1 & 0 \end{pmatrix} \qquad \tilde{L}_0 = \begin{pmatrix} 1 & 0 \\ 0 & -1 \end{pmatrix}$$

and satisfy the commutation relations

$$[\tilde{L}_0, \tilde{L}_\pm] = \pm\tilde{L}_\pm, \qquad [\tilde{L}_+, \tilde{L}_-] = 2\tilde{L}_0$$

which, as is well known, are the commutation relations for the $SU(2)$ Lie algebra.

To obtain the boson realization of $SU(2)$ we need two boson creation (annihilation) operators $b_i^\dagger$ (b_i), $\quad i = 1, 2$. Using the prescription (4.26) we obtain the operators

$$L_+ = b_1^\dagger b_2 \qquad L_- = b_2^\dagger b_1 \tag{4.28a}$$

$$L_0 = \frac{1}{2}(b_1^\dagger b_1 - b_2^\dagger b_2) \quad . \tag{4.28b}$$

This realization of the generators of $SU(2)$ in terms of two boson creation and annihilation operators is known as a *Schwinger representation* of the $SU(2)$ algebra (the algebra of the angular momentum).

Biedenharn proposed the realization of the q-deformed $SU_q(2)$ algebra in terms of two independent q-deformed boson operators which satisfy the commuation relations

$$[N_k, a_j^\dagger] = \delta_{kj}, \qquad [N_k, a_j] = \delta_{kj} \tag{4.29a}$$

$$[a_k, a_j^\dagger]_q \equiv a_k a_j^\dagger - q a_j^\dagger a_k = \delta_{kj} q^{-N_j} \tag{4.29b}$$

(The other commutators vanish).

Obviously the commutation relations (4.29) are a generalization of (3.7) for the case of many operators. According to Biedenharn, the raising and lowering operators of $SU_q(2)$ have the same form as the raising and lowering operators of $SU(2)$, i.e. have the form

$$J_+ = a_1^\dagger a_2 \qquad J_- = a_2^\dagger a_1 \quad .$$

The operator L_0 given by (4.29b) is the half-difference of the number operators of the "standard" bosons. In the q-deformed case, however, the number of boson operators N_k *are not* $a_k^\dagger a_k$, $\quad k = 1, 2$. For this reason Biedenharn suggested that J_0 is constructed from the number operators of $SU_q(2)$

$$J_0 = \frac{1}{2}(N_1 - N_2) \quad .$$

One can immediatly check that the operators

$$J_+ = a_1^\dagger a_2 \qquad J_- = a_2^\dagger a_1$$

$$J_0 = \frac{1}{2}(N_1 - N_2) \tag{4.30}$$

satisfy the commutation relations (4.1) for the q-deformed $SU_q(2)$ algebra [12] and therefore qive a realization of this algebra in terms of q-deformed boson operators (Biedenharn representation)

Basis vectors of $SU_q(2)$ representations. The basic vectors of the representation $\mathcal{D}^j$ of $SU_q(2)$ may be obtained from the highest weight vector of the representation, which satisfies (4.13), i.e.

$$J_0|jj\rangle_q = j|jj\rangle_q \qquad J_+|jj\rangle_q = 0$$

Taking into account that $J_+ = a_1^\dagger a_2$, one can conclude from the second of the above equations that $|jj\rangle_q$ cannot contain $a_2^\dagger$ at all and must be of the form $|jj\rangle_q \sim (a_1^\dagger)^n|0\rangle_q$, where $|0\rangle_q$ is the q-deformed vacuum state $(a_k|0\rangle_q = 0, \quad k = 1,2)$. From (4.30b) and the first of the above equations one can find that $n = 2j$ and thus the normalazed highest weight vector is

$$|jj\rangle_q = \frac{(a_1^\dagger)^{2j}}{\sqrt{[2j]!}}|0\rangle_q \tag{4.31}$$

---

[12] As an example we shall calculate the commutator

$$\begin{aligned}[J_+, J_-] &= a_1^\dagger a_2 a_2^\dagger a_1 - a_2^\dagger a_1 a_1^\dagger a_2 \\ &= [N_1][N_2 + 1] - [N_1 + 1][N_2]\end{aligned}$$

where we have used (3.10). On the other hand for the q-numbers holds the relation

$$[a + 1][b] - [a][b + 1] = [a - b]$$

which can be easily checked using the definition of the q-numbers. Thus we have

$$[J_+, J_-] = [N_1 - N_2] = [2J_0].$$

Q.E.D.

Now to obtain the general vector $|jm\rangle_q$ one can use (4.19). We have

$$|jm\rangle_q = \frac{(a_1^\dagger)^{l+m}}{\sqrt{[l+m]!}} \frac{(a_2^\dagger)^{l-m}}{\sqrt{[l-m]!}} |0\rangle_q$$
$$= |j+m\rangle_q^1 \otimes |j-m\rangle_q^2 \qquad (4.32)$$

where

$$|j \pm m\rangle_q^k = \frac{(a_k^\dagger)^{j\pm m}}{\sqrt{[j \pm m]!}} |0\rangle_q.$$

and "$\otimes$" denotes the *tensor product* of $|n\rangle_q^1$ and $|n'\rangle_q^2$.[13] One can easily calculate the action of $J_\pm$ and J_0 on these vectors. For example

$$J_+|jm\rangle_q = a_1^\dagger |j+m\rangle_q^1 \otimes a_2 |j-m\rangle_q^2$$
$$= \sqrt{[j-m][j+m+1]} \frac{(a_1^\dagger)^{j+m+1}}{\sqrt{[j+m+1]!}} \frac{(a_2^\dagger)^{j-m-1}}{\sqrt{[j-m-1]!}} |0\rangle_q$$
$$= \sqrt{[j-m][j+m+1]} |jm+1\rangle_q.$$

We obtain

$$J_\pm |j,m\rangle_q = \sqrt{[j \mp m][j \pm m + 1]} |j, m \pm 1\rangle_q$$

$$J_0 |jm\rangle_q = m |jm\rangle_q$$

which is in agreement with (4.21). One can also calculate the eigenvalues of the Casimir operator $C_2^q(SU_q(2)) \equiv C_2^q$. Taking into account that the action of C_2^q on the vectors of a given representation gives one and the same result we can act with C_2^q on the highest weight vector (4.31) and obtain

$$C_2^q |jj\rangle_q = (J_- J_+ + [J_0][J_0+1])|jj\rangle_q = [j][j+1]|jj\rangle_q \quad . \qquad (4.33)$$

Thus the eigenvalues of C_2^q can be written in the form

[13] The states $|n\rangle_q^1$ and $|n'\rangle_q^2$ belong to two different Fock spaces and from a matematical point of view it is more correct to denote their product as tensor product (see footnote *1* of Sec. 4.4), in spite of the fact that in this case the "ordinary" and the tensor product coincide.

$$\langle C_2^q \rangle = [j][j+1] = \frac{sh(\tau j) sh\tau(j+1)}{sh\tau} \qquad \text{if } q = e^{\tau} \tag{4.34a}$$

and

$$\langle C_2^q \rangle = [j][j+1] = \frac{sin(\tau j) sin\tau(j+1)}{sin\tau} \qquad \text{if } q = e^{i\tau} \tag{4.34b}$$

Remark 3: $SU_q(2)$ *representations with modified operators.* The Biedenharn representation of $SU_q(2)$ can be realized also in terms of modified q-deformed boson operators introduced by (3.15).They satisfy the commutation relations

$$[\alpha_i^\dagger, \alpha_j] = \delta_{ij} q^{-2N_i}$$

$$[N_i, \alpha_j^\dagger] = \delta_{ij} \alpha_j^\dagger \qquad [N_i, \alpha_j] = -\delta_{ij} \alpha_j \tag{4.35}$$

where the use of q-commutator is avoided. In terms of these operators one can construct, by analogy with (4.30), the generators

$$J_+ = \alpha_1^\dagger \alpha_2 \qquad J_- = \alpha_2^\dagger \alpha_1 \qquad J_0 = \frac{1}{2}(N_1 - N_2) \tag{4.36}$$

It can be easilly checked that the commutator

$$[J_0, J_\pm] = \pm J_\pm$$

remains unchanged, but for the commutator $[J_+, J_-]$ we have

$$\begin{aligned} [J_+, J_-] &= [\alpha^{\dagger}{}_1 \alpha_2, \alpha_2^\dagger \alpha_1] \\ &= \alpha_1^\dagger [\alpha_2, \alpha_2^\dagger] \alpha_1 + \alpha_2^\dagger [\alpha_1^\dagger, \alpha_1] \alpha_2 \\ &= -\alpha_1^\dagger \alpha_1 q^{-2N_2} + \alpha_2^\dagger \alpha_2 q^{-2N_1} \end{aligned}$$

Using the relations (3.16) we obtain

$$\begin{aligned} [J_+, J_-] &= -[N_1] q^{-N_1+1-2N_2} + [N_2] q^{-N_2+1-2N_1} \\ &= q^{-(N_1+N_2+1)} ([N_2] q^{-N_1} - [N_1] q^{-N_2}) \\ &= q^{-(N_1+N_2+1)} [2J_0] \end{aligned}$$

Here we have used the identity

$$q^A[B] - q^B[A] = [B - A] \tag{4.37}$$

which can be proved taking into account the drfinition of the q-numbers. Thus instead of the standard commutation relation (4.1) we have

$$[J_+, J_-] = q^{-(N_1+N_2+1)}[2J_0]$$

This difference, however, is not essential. As a matter of fact one can construct, by analogy with (4.32), the basis

$$|jm\rangle_q = \frac{(\alpha_1^\dagger)^{j+m}}{\sqrt{[j+m]!}} \frac{(\alpha_2^\dagger)^{j-m}}{\sqrt{[j-m]!}} |jm\rangle_q \tag{4.38}$$

Acting with the commutator $[J_+, J_-]$ on this basis we obtain

$$[J_+, J_-]|jm\rangle_q = q^{-2j-1}[2m]|jm\rangle_q$$

This means that we can renormalize the operators $J_\pm$ with the factor $q^{j+1/2}$ introducing the operators $\tilde{J}_\pm = q^{j+1/2}J_\pm$, $\tilde{J}_0 = J_0$ so that in the new basis (4.38) the operators $\tilde{J}_m, (m = 0, \pm)$ will satisfy the same commutation relations as the operators J_m, given by (4.30), in the basis (4.32).

The q-deformed Heisneberg alqebra as a contracted form of $SU_q(2)$. As we have allready mentioned, the commutation relations for the q deformed Heisenberg – Weyl algebra (3.7) have an unusual form and we need some motivation to accept them. Fortunately the "standard" Heisenberg – Weyl algebra (which may be considered as an algebra of the harmonic oscillator) is closely related to the "standard" $SU(2)$ algebra (the algebra of angular momentum).

To be more exact, the Heisenberg – Weyl algebra $\mathcal{H}_4^q$ is a contracted form of the $SU(2)$ algebra (i.e. $\mathcal{H}_4^q$ can be obtained from $SU(2)$ through some standard operations). One can expect that the same relation between Heisenberg –Weyl and the $SU(2)$ algebra survives in the q-deformed case as well, and one can obtain $\mathcal{H}_2^q$ from $SU_q(2)$ by the same operations. If one believes that the q-deformed $SU_q(2)$ is a natural generalization of $SU(2)$ which

is needed to describe certain deviations from the euqlidity of the space or a certain deformability of the quantum system, then $\mathcal{H}_4^q$ obtained from $SU_q(2)$ may be considered as a natural generalization of $\mathcal{H}_4$ capable of describing the deviations of the euqlidity of the space or the deformability of the system. Here we shall show how one can obtain the q-deformed Heisenberg – Weyl algebra from the q-deformed $SU_q(2)$.

Let us first consder the connection between the standard $\mathcal{H}_4$ and the $SU(2)$ algebras and show that Heisenberg – Weyl algebra can be obtained if one considers certain limits of the representations of the $SU(2)$. We shall start with the well known relations

$$L_-L_+|lm\rangle = (l-m)(l+m+1)|lm\rangle$$

$$L_+L_-|lm\rangle = (l+m)(l-m+1)|lm\rangle$$

and shall write down the expressions

$$\frac{L_-}{\sqrt{2l}}\frac{L_+}{\sqrt{2l}}|lm\rangle = (l-m)\frac{(l+m+1)}{2l}|lm\rangle = n|lm\rangle \tag{4.39a}$$

and

$$\frac{L_+}{\sqrt{2l}}\frac{L_-}{\sqrt{2l}}|lm\rangle = \frac{(l+m)}{2l}(l-m+1)|lm\rangle = (n+1)|lm\rangle \tag{4.39b}$$

We shall consider the limit of these expressions when l and m tend to infinity but in such a way that their difference is a fixed number which can take the values 0, 1, 2, etc. This means that we have to take the limit of (4.39) in the case when

$$l \to \infty, \qquad m \to \infty, \qquad l-m=n, \qquad n=0,1,2\ldots \tag{4.40}$$

In order to obtain this limit we shall take into account that

$$\lim_{\substack{l\to\infty, m\to\infty \\ l-m=n}} \frac{(l+m+a)}{2l} = 1 \qquad a=0,\pm 1 \quad .$$

We can write down

$$\lim_{\substack{l\to\infty, m\to\infty \\ l-m=n}} \frac{L_-}{\sqrt{2l}}\frac{L_+}{\sqrt{2l}}|n\rangle = n \lim_{\substack{l\to\infty, m\to\infty \\ l-m=n}} |n\rangle \tag{4.41a}$$

and

$$\lim_{\substack{l\to\infty,m\to\infty\\ l-m=n}} \frac{L_+}{\sqrt{2l}}\frac{L_-}{\sqrt{2l}}|n\rangle = (n+1)\lim_{\substack{l\to\infty,m\to\infty\\ l-m=n}}|n\rangle \tag{4.41b}$$

where we have dented by $|n\rangle$ the states $|jm\rangle$ where $n = j - m, \quad j, m \to \infty$. Formally we can introduce the operators

$$b = \lim \frac{L_+}{\sqrt{2l}} \qquad b^\dagger = \lim \frac{L_-}{\sqrt{2l}} \tag{4.42}$$

and from (4.41) it follows that *in this basis* we have

$$b^\dagger b|n\rangle = n|n\rangle \qquad bb^\dagger|n\rangle = (n+1)|n\rangle \quad . \tag{4.43}$$

As a result we obtain

$$(bb^\dagger - b^\dagger b)|n\rangle = |n\rangle$$

for every $|n\rangle$. This, however, means that we can write down

$$[b, b^\dagger] = 1$$

which is the basic commutation relation for the Heisenberg Weyl algebra $\mathcal{H}_4$.

Thus in the limit (4.40) (i.e.when $j \to \infty, m \to \infty, j - m = n$) the $SU(2)$ commutation relations considered in the basis $|jm\rangle$ of the representation $\mathcal{D}^j$ coincide with the commutation relations of $\mathcal{H}_4$. Of course the new commutation relations obtained in such a way are valid *only in this particular basis.* However we can *postulate* that they are valid also in any other basis and these commuatation relations begin to live a life of their own. [14]

It turns out that the commutation relations of the q- deformed Heisenberg -Weyl algebra $\mathcal{H}_4^q$ can be obtained by an analogous prescription from the commutation relations of the q-deformed $SU_q(2)$. To show this we must

[14] It is often said that the commutation relations of $\mathcal{H}_4$ are obtained from the commutation relations of $SU(2)$ through contraction. This problem is a whole domain in the group representation theory [66] and we will not discuss it here in detail.

repeat the above considerations step by step. We shall start with the relations

$$J_-J_+|jm\rangle_q = [j-m][j+m+1]|jm\rangle_q$$

$$J_+J_-|jm\rangle_q = [j+m][j-m+1]|jm\rangle_q$$

and shall form the expressions

$$\frac{J_-}{\sqrt{[2j]}}\frac{J_+}{\sqrt{[2j]}}|jm\rangle_q = [j-m]\frac{[j+m+1]}{[2j]}|jm\rangle_q = [n]|jm\rangle_q \qquad (4.44a)$$

and

$$\frac{J_+}{\sqrt{[2j]}}\frac{J_-}{\sqrt{[2j]}}|jm\rangle_q = \frac{[j+m]}{[2j]}[j-m+1]|jm\rangle_q = [n+1]|jm\rangle_q \qquad (4.44b)$$

In order to take the limit of (4.44) in the case (4.40) let us consider the expression

$$\lim_{\substack{j\to\infty,m\to\infty\\ j-m=n}} \frac{[j+m+a]}{[2j]} \quad , \qquad a=0,1 \quad .$$

We must underline that this limit exists and equals to 1 *only when* q *is a real number.* In the case when $q = exp(i\tau)$, due to the fact that the q-number $[\alpha] \sim \sin(\tau\alpha)$, this limit does not exist. Even more complicated is the case when q is a root of unity but we shall not consider these cases here.

Provided that q is real and that $j-m=n$, we can write down

$$\lim_{\substack{j\to\infty,m\to\infty\\ j-m=n}} \frac{J_-}{\sqrt{[2j]}}\frac{J_+}{\sqrt{[2j]}}|n\rangle_q = [n]\lim_{\substack{j\to\infty,m\to\infty\\ j-m=n}}|n\rangle_q \qquad (4.45a)$$

and

$$\lim_{\substack{j\to\infty,m\to\infty\\ j-m=n}} \frac{J_+}{\sqrt{[2j]}}\frac{J_-}{\sqrt{[2j]}}|n\rangle_q = [n+1]\lim_{\substack{j\to\infty,m\to\infty\\ j-m=n}}|n\rangle_q \qquad (4.45b)$$

where $|jm\rangle_q, (n=j-m, \quad j,m\to\infty)$ is denoted by $|n\rangle_q$. Formally we can introduce, in analogy with (4.42), the operators

$$a = \lim\frac{J_+}{\sqrt{[2j]}} \qquad a^\dagger = \lim\frac{J_-}{\sqrt{[2j]}}$$

and write down

$$a^\dagger a|n\rangle_q = [n]|n\rangle_q = [N]|n\rangle_q$$
$$aa^\dagger|n\rangle_q = [n+1]|n\rangle_q = [N+1]|n\rangle_q \tag{4.46}$$

where N is an operatorr with property $N|n\rangle_q = n|n\rangle_q$. From (4.46) we can conclude that we can write down

$$a^\dagger a = [N], \qquad aa^\dagger = [N+1] \tag{4.47}$$

which of course is valid only in the particular basis under consideration.

We shall postulate that the relations (4.47) hold also in an arbitrary basis. Then from (4.47) we can obtain the commutation relations (3.7). For example we can multiply the first equation (4.47) by q and subtract it from the second equation. We obtain

$$aa^\dagger - qa^\dagger a = [N+1] - q[N] = q^{-N}$$

where we have used the identity

$$[N+1] - q[N] = q^{-N}$$

which can be easily checked using the definition of the q numbers.

We have shown that the commutation relations (3.7) of the q- deformed Heisenberg - Weyl algebra $\mathcal{H}_4^q$ can be obtained from the commutation relations of the q- deformed $SU_q(2)$ algebra considering the limit (4.40) of the matrix elements of the $SU_q(2)$ generators in the basis $|jm\rangle_q$. This limit exists only when q is a real number, but once this limit is obtained it can allow us to consider also the general case when the basis is an arbitrary one and when q is a pure phase or a root of unity. In this sense we can acccept that the "standard" and q - deformed boson operators are related in the same way as the standard $SU(2)$ algebra is related to the q deformed $SU_q(2)$ algebra.

§ 5. The Clebsch – Gordan Coefficients and Irreducible Tensor Operators for $SU_q(2)$

§ 5.1 Vector coupling of angular momenta in $SU_q(2)$

Addition of angular momenta in quantum mechanics. As is well known, the generators $L_m (m = 0, \pm)$ of the "standard" $SU(2)$ algebra can be interpreted as operators of angular momenta and the basis vectors $|lm\rangle$ (the eigenstates of $\mathbf{L}^2$ and L_0) can be considered as vectors of the states with angular momentum (l, m).

A typical problem of the quantum theory of the angular momentum is the addition of the angular momenta of two independent systems. Let us suppose that the system under consideration consists of two independent subsystems (*1*) and (*2*) described by the wave functions $\Psi_{l_1 m_1}(1) \equiv |l_1 m_1\rangle$ and $\Psi_{l_2 m_2}(2) \equiv |l_2 m_2\rangle$. We shall denote the operators of the angular momenta of these subsystems by $\mathbf{L}(1)$ and $\mathbf{L}(2)$. Then, by definition, the operators of the angular momenta $\mathbf{L}(12)$ for the composite system are given by

$$\begin{aligned} L_0(12) &= L_0(1) + L_0(2) \\ L_\pm(12) &= L_\pm(1) + L_\pm(2) \quad . \end{aligned} \tag{5.1a}$$

In vector notations we can write down

$$\mathbf{L}(12) = \mathbf{L}(1) + \mathbf{L}(2) \tag{5.1b}$$

and in this sense one can speak about the *vector addition* (or the *vector coupling*) of the angular momenta.

The operators themselves, however, are not measurable quantities. Measurable are their eigenvalues, expectation values, etc. Therefore we need a rule of "how to add" the quantum numbers $l_1 m_1$ and $l_2 m_2$ of the subsystems in order to obtain the quantum numbers of the angular momentum of the composite system.

The operators (5.1) satisfy the same commutation relations as the operators $L_m(\alpha)$, $(m = 0, \pm, \alpha = 1, 2)$ of the independent system, i.e.

$$[L_0(12), L_\pm] = \pm L_\pm$$
$$[L_+(12), L_-(12)] = 2L_0(12) \quad . \tag{5.2}$$

For this reason the common eigenvectors $|lm\rangle$ of the operators $\mathbf{L}^2(12)$ and $L_0(12)$ of the composite system have the same properties as the basis vectors $|l_i m_i\rangle$ $(i = 1, 2)$ of its independent parts and, in particular, the quantum numbers l and m can take the values $l = 0, 1/2, 1, 3/2, \ldots$ and $m = l, l - 1, \ldots - l$. However, due to the fact that the quantum numbers l_1 and l_2 are fixed, not all of these values of l are allowed. *The problem is to express* $|lm\rangle$ *in terms of* $|l_i m_i\rangle$ *and to find the values of* l *compatible with* l_1 *and* l_2.

As is well known, the basis vectors of the composite system can be expressed as

$$|l_1 l_2; lm\rangle = \sum_{m_1+m_2=m} C^{lm}_{l_1 m 1 l_2 m_2} |l_1 m_1\rangle |l_2 m_2\rangle \tag{5.3}$$

where $C^{lm}_{l_1 m 1 l_2 m_2}$ are the Clebsch - Gordan coefficients (the coefficients of vector coupling).[15] These coefficients vanish if the conditions

$$l_1 + l_2 \geq l \geq |l_1 - l_2| \tag{5.4a}$$

$$m_1 + m_2 = m \tag{5.4b}$$

are not satisfied. For this reason the values of (l, m) compatible with $l_1 m_1$ and $l_2 m_2$ are given by (5.4). These rules are also known as rules for addition (or rules for *vector coupling* of the angular momenta).

Remark: In the language of the representation theory one can say that $|l_1 m_1\rangle$ and $|l_2 m_2\rangle$ transform according to the unitary irreducible representations $\mathcal{D}^{l_1}$

[15]The letters l_1 and l_2 in the symbols $|l_1 l_2; lm\rangle$ indicate the origin of the state $|l_1 l_2; lm\rangle$ as a "sum" of the states $|l_1 m_1\rangle$ and $|l_2 m_2\rangle$. These symbols will be omitted if the origin of the state $|lm\rangle$ is clear from the context.

and $\mathcal{D}^{l_2}$ of $SU(2)$ and their product $|l_1 m_1\rangle|l_2 m_2\rangle$ transforms according to the tensor (or direct) product of these representations $\mathcal{D}^{l_1} \otimes \mathcal{D}^{l_2}$.[16]

However the tensor (or direct) product of the two representations $\mathcal{D}^{l_1}$ and $\mathcal{D}^{l_2}$ is not an irreducible one and it can be decomposed into a sum of irreducible representations $\mathcal{D}^{l}$, i.e.

$$\mathcal{D}^{l_1} \times \mathcal{D}^{l_2} = \sum_{l} \oplus \mathcal{D}^{l}$$

This decomposition is known as Clebsch - Gordan series for the representations and one can perform it using the Clebsch - Gordan coefficients.

The Clebsch – Gordan coefficients play also an important role in the calculation of the matrix elements of the tensor operators due to the Wigner – Eckart theorem according to which the matrix elements of the tensor operator T^l_m can be represented in the form

$$\langle l_2 m_2 | T^l_m | l_1 m_1 \rangle = \frac{1}{\sqrt{2j_2+1}} C^{j_2 m_2}_{j_1 m_1 l m} \langle l_1 || T^l || l_2 \rangle \tag{5.5}$$

where the reduced matrix element $\langle l_1 || T^l || l_2 \rangle$ does not depend on the projections m_1, m_2 and m.

As we shall see below, all these problems arise in the q- deformed case too. Many papers [72 -88] are devoted to the generalizatiton of the algebra of the angular momentum in the q -deformed case. Therfore here we shall consider the problems only to the extent needed for some simple applicatons.

[16]The meaning of the vector product of the representations can be understood as follows: Let us suppose that under a certain transformation of the coordinate system the vector $\mathbf{u}_j$ transforms by means of the matrix A_{ij}, i.e. $\mathbf{u}_j \longmapsto \mathbf{u}'_j = \sum A_{ji}\mathbf{u}_i$ and the vector $\mathbf{v}_p$ transforms by means of the matrix B_{pk}, i.e. $\mathbf{v}_p \longmapsto \mathbf{v}'_p = \sum B_{pk}\mathbf{v}_k$. Obviously their product $\mathbf{u}_j\mathbf{v}_p$ will transform according to the low $\mathbf{u}_i\mathbf{v}_p \longmapsto \mathbf{u}'_j v'_p = \sum A_{ji}B_{pk}\mathbf{u}_i\mathbf{v}_k$. However $A_{ji}B_{pk}$ is nothing else than the tensor product of the matrices A and B which is denoted by $A \otimes B$. We have $A_{ji}B_{pk} = (A \otimes B)_{jp,ik}$. Thus the product vector $\mathbf{u}_j\mathbf{v}_p$ transforms according to the tensor product $A \otimes B$ of the matrices A and B and is considered as tensor product $\mathbf{u}_j \otimes \mathbf{v}_p$ of the vectors $\mathbf{u}_j$ and $\mathbf{v}_p$.

Addition of the q-deformed angular momenta. Now we shall try to employ the above considerations in the case of the q-deformed $SU_q(2)$. As we have already seen, one can consider the generators of $SU_q(2)$ as operators of the q-deformed angular momenta and the basis vectors of its representation $|jm\rangle_q$, as vectors of the states with q-deformed angular momentum given by the quantum numbers j, m. The problem of the addition of two q-deformed angular momenta arises again when one considers the system which consists of two independent subsystems with q-deformed angular momenta $j_1 m_1$ and $j_2 m_2$. We shall denote the state vectors of the subsystems with $|j_i m_i\rangle_q$ and we are led into temptation to define, in analogy with (5.2), the operators of the q-angular momentum of the composite system as

$$\begin{aligned} J_0(12) &= J_0(1) + J_0(2) \\ J_\pm(12) &= J_\pm(1) + J_\pm(2) \quad . \end{aligned}$$

One can easily check however that the operators so defined do not satisfy the q-deformed commutation relation for the $SU_q(2)$ algebra. As a matter of fact we have

$$\begin{aligned} [J_0(12), J_\pm(12)] &= \pm J_\pm(12) \\ [J_+(12), J_-(12)] &= [2J_0(1)] + [2J_0(2)] \\ &\neq [2(J_0(1) + J_0(2))] \end{aligned}$$

which means that the operators $L_m(12)$ do not even close an algebra!

In order to revise and improve the above mentioned definition we must go back to the undeformed case and note that from the point of view of mathematics it is reasonable to represent the basis vectors of the composite system in the form of direct product

$$|j_1 m_1\rangle_q \otimes |j_2 m_2\rangle_q .$$

We shall also note that if the operator A acts in the space of the first particle (i.e if it affects only the vectors $|j_1 m_1\rangle_q$) and if the operator B acts in the space of the second particle we can write down

$$(A \otimes B)(|j_1 m_1\rangle_q \otimes |j_2 m_2\rangle_q) = A|j_1 m_1\rangle_q \otimes B|j_2 m_2\rangle_q$$

Taking this into account we can rewrite the "vector sum" definition (5.1) in the form

$$\mathbf{L}(12) = \mathbf{L}(1) \otimes 1_2 + 1_1 \otimes \mathbf{L}(2) \tag{5.6}$$

where we have denoted with 1_i the unit operator acting in the space $i = 1, 2$. Applying (5.6) on the vector $|l_1 m_1\rangle \otimes |l_2 m_2\rangle$ we obtain

$$\mathbf{L}(12)(|l_1 m_1\rangle \otimes |l_2 m_2\rangle = \mathbf{L}(1)|l_1 m_1\rangle \otimes |l_2 m_2\rangle + |l_1 m_1\rangle \otimes \mathbf{L}(2)|l_2 m_2\rangle$$

which coincides with the standard notions used in quantum mechanics.

It can be easily seen that if the operators $\mathbf{L}(i), i = 1, 2$ satisfy the standard commutation relations (5.2), the same is valid for the operators $\mathbf{L}(12)$. Now we can try to improve the definition (5.6) assuming that

$$\mathbf{J}(12) = \mathbf{J}(1) \otimes f(\mathbf{J}(2)) + g(\mathbf{J}(1)) \otimes \mathbf{J}(2)$$

where the functions f and g are chosen in such a way that if $\mathbf{J}(i), i = 1, 2$ satisfies the q-deformed commutation relation the same is valid for $\mathbf{J}(12)$.

These functions can be found after some tedious calculations as a result of which we obtain that the operators of the angular momenta J_m in the case of composite system must be replaced by operators[17] $\Delta(J_m) \equiv J_m(12)$, which can be written in the following way

$$\begin{aligned} J_0 &\longmapsto \Delta(J_0) = J_0 \otimes 1 + 1 \otimes J_0 \\ J_\pm &\longmapsto \Delta(J_\pm) = J_\pm \otimes q^{J_0} + q^{-J_0} \otimes J_\pm \end{aligned} \tag{5.7}$$

where the explicite form of the functions f and g is used. The relations (5.8) can also be written down in the form

$$\begin{aligned} J_0(12) &= J_0(1) + J_0(2) \\ J_\pm(12) &= J_\pm(1) q^{J_0(2)} + q^{-J_0(1)} J_\pm(2) \end{aligned} \tag{5.8}$$

[17]The notations used in (5.7) have an unusual form, but they are quite natural if one works in terms of Hopf algebra. Further we shall use the more familiar notation given by (5.8). See also footnote after the formulae (5.8).

which is more convenient from the point of view of the notations of the "standard" quantum mechanics.[18] It can be easily checked that operators (5.8) satisfy the commutation relarions

$$[J_0(12), J_\pm(12)] = \pm J_\pm(12)$$
$$[J_+(12), J_-(12)] = [2J_0(12)] \tag{5.9}$$

provided that $J_m(i), i = 1, 2$ satisfy the q-deformed commutation relation.

Now we have a set of operators (the operators of the "total" angular momentum of the composite system) which satisfy the q-deformed commutation relation. The action of these operators on the basis vectors $|j_1 m_1\rangle_q |j_2 m_2\rangle_q$ of the direct product of the irreducible representations is given by

$$J_0(12)|j_1 m_1\rangle_q |j_2 m_2\rangle_q = (m_1 + m_2)|j_1 m_1\rangle_q |j_2 m_2\rangle_q \tag{5.10a}$$

$$\begin{aligned} J_\pm(12)&|j_1 m_1\rangle_q |j_2 m_2\rangle_q \\ &= q^{m_2}\sqrt{[j_1 \mp m_1][j_1 \pm m_1 + 1]}|j_1 m_1 \pm 1\rangle_q |j_2 m_2\rangle_q \\ &+ q^{-m_1}\sqrt{[j_2 \mp m_2][j_2 \pm m_2 + 1]}|j_1 m_1\rangle_q |j_2 m_2 \pm 1\rangle_q \end{aligned} \tag{5.10b}$$

Using the formulae (4.7) and (5.8) one can introduce the resultant Casimir operator

$$\begin{aligned} C_2^q(12) &= J_-(12)J_+(12) + [J_0(12)][J_0(12) + 1] \\ &= J_-(1)J_+(2)q^{-J_0(1)+J_0(2)+1} + J_+(1)J_(2)q^{-J_0(1)+J_0(2)-1} \\ &+ (C_2^q(1) - [J_0(1][J_0(1) + 1]) + (C_2^q(2) - [J_0(2][J_0(2) + 1]) \\ &+ [J_0(12)][J_0(12) + 1] \quad . \end{aligned} \tag{5.11.}$$

[18]The "improvement" (5.8) of the "sum - definition" (5.1) may look as an artificial trick used only to close the "sum - algebra" at any costs. However this definition has a deep mathematical meaning and is a part of the mathematical structure of Hopf algebras. As a matter of fact, for Hopf algebras we can define an operation Δ, called "co-product", which assigns to every element $\mathbf{J}_i$ of the algebra a sum of direct products $\sum_j \mathbf{J}_j \otimes \mathbf{J}_j$ (i.e $\Delta(\mathbf{J}_i) \longmapsto \sum_j \mathbf{J}_j \otimes \mathbf{J}_j$) acting in the different subspaces of the direct product space. (See Appendix A).

The problem is to find the common eigenvectors of the operators $C_2^q(1)$, $C_2^q(2), C_2^q(12)$ and $J_0(12)$. We shall denote these common eigenvectors with $|j_1 j_2; jm\rangle_q$. They satisfy the equations

$$\begin{aligned} C_2^q(i)|j_1 j_2; jm\rangle_q &= [j_i][j_i+1]|j_1 j_2; jm\rangle_q \quad i=1,2 \\ C_2^q(12)|j_1 j_2; jm\rangle_q &= [j][j+1]|j_1 j_2; jm\rangle_q \\ J_0(12)|j_1 j_2; jm\rangle_q &= m|j_1 j_2; jm\rangle_q \\ m &= m_1 + m_2 \end{aligned} \tag{5.12}$$

Obviously the vectors $|j_1 j_2; jm\rangle_q$ can be represented as a linear combination of the basis vectors $|j_1 m_1\rangle_q |j_2 m_2\rangle_q$ of the direct product representation. We have

$$|j_1 j_2; jm\rangle_q = \sum_{m_1 m_2} \langle j_1 m_1 j_2 m_2 | jm\rangle_q |j_1 m_1\rangle_q |j_2 m_2\rangle_q \tag{5.13}$$

The coefficients $\langle j_1 m_1 j_2 m_2 | jm\rangle_q$ in the linear combination (5.13) are called the *Clebsch - Gordan coefficients* for the $SU_q(2)$ algebra and are denoted by

$${}^qC^{jm}_{j_1 m_1 j_2 m_2} = \langle j_1 m_1 j_2 m_2 | jm\rangle_q \tag{5.14}$$

In principle the Clebsch - Gordan coefficients can be found by solving the recursion relation which can be obtained by taking the scalar product of the expression

$$C_2^q(12)|j_1 j_2; jm\rangle_q = [j][j+1]|j_1 j_2; jm\rangle_q$$

with the vector $\langle j_1 m_1|\langle j_2 m_2|$. We should also take into account the explicit form of the Casimir operator (5.11), the properties of $J_\pm(i)$ operators, i.e

$$\langle j_i m_i | J_\pm(i) = \sqrt{[j_i \pm m_i][j_i \mp m_i + 1]}\langle j_i m_i \mp 1|$$

and the expansion (5.13). In such a way we obtain

$$\begin{aligned} & q^{-m_1+m_2+1}\sqrt{[j_1 - m_1][j_1 + m_1 + 1][j_2 + m_2][j_2 - m_2 + 1]}\times \\ & \qquad \langle j_1 m_1 + 1, j_2 m_2 - 1|jm\rangle_q + \\ & q^{-m_1+m_2-1}\sqrt{[j_1 + m_1][j_1 - m_1 + 1][j_2 - m_2][j_2 + m_2 + 1]}\times \\ & \qquad \langle j_1 m_1 - 1, j_2 m_2 + 1|jm\rangle_q + \\ & F(q, j_1, j_2, j, m_1, m_2, m)\langle j_1 m_1 j_2 m_2|jm\rangle_q = 0 \end{aligned} \tag{5.15a}$$

where

$$F(q,j_1,j_2,j,m_1,m_2,m) = q^{2m_2}([j_1][j_1+1]-[m_1][m_1+1])+ q^{-2m_1}([j_2][j_2+1]-[m_2][m_2+1])+ [m][m+1]-[j][j+1] \quad (5.15b)$$

This method of recursion relations was used to find the q-Clebsch – Gordan coefficients in ref [72]. Another method (the method of the projection operators) was suggested by Smirnov et al [81]. Without going into detail here we shall give the final results

$$ {}^qC^{jm}_{j_1m_1j_2m_2} = q^{-\frac{1}{2}(j_1+j_2-j)(j+j_1+j_2+1)+j_1m_2-j_2m_1}\times \sqrt{[2j+1]\frac{[j+m]![j_2-m_2]![j_1+j_2+j+1]![j_1-j_2+j]![j_1+j_2-j]!}{[j-m]![j_2+m_2]![j_1+m_1]![j_-m_1]![j-j_1+j_2]!}}\times \sum_z(-1)^{j_1+j_2-z}\frac{[2j_2-z]![j_1+j_2-m-z]!q^{z(j_1+m_1)}}{[z]![j_1+j_2-j-z]![j_2-m_2-z]![j_1+j_2+j+1+z]!} \quad (5.16)$$

Due to the fact that there are different methods for the derivation of the expressions for the Clebsch – Gordan coefficients for the quantum algebra $SU_q(2)$ there exist several different analytical expressions for these quantities (just as in the case of $SU(2)$) and there arises the problem of transforming one of these forms to another equivalent form. Here, however, this problem will not be cosidered.

Some basis properties of q-Clebsch –Gordan coefficients. Although the expression (5.16) for the Clebsch Gordan coefficients looks threateningly complicated these coefficients possess some simple properties which facilitate the treatment of the expressions in which these quantities take part. The derivation of these properties is based on the fact that, as it can be seen from eq. (5.13), the q-deformed Clebsch –Gordan coefficients can be considered as scalar products. Using (5.13) we can write down

$$ {}^qC^{jm}_{j_1m_1j_2m_2} \equiv \langle j_1m1j_2m_2|jm\rangle_q = ({}_q\langle j_1m_1|{}_q\langle j_2m_2|)\,|j_1j_2;jm\rangle_q \quad . \quad (5.17)$$

Utilizing the fact that the states $|jm\rangle_q$ form an orthogonal and complete system, one can easily derive the orthogonality conditions for the Clebsch – Gordan coefficients, which can be written in the form

$$\sum_{m_1 m_2} {}^qC^{jm}_{j_1 m_1 j_2 m_2} {}^qC^{j'm'}_{j_1 m_1 j_2 m_2} = \delta_{jj'}\delta_{mm'} \tag{5.18a}$$

and

$$\sum_{jm} {}^qC^{jm}_{j_1 m_1 j_2 m_2} {}^qC^{jm}_{j_1 m'_1 j_2 m'_2} = \delta_{m_1 m'_1}\delta_{m_2 m'_2} \quad . \tag{5.18b}$$

With the help of these relations one can, for example, reverse the eq. (5.13) writing down

$$|j_1 m_2\rangle_q |j_2 m_2\rangle_q = \sum_{jm} {}^qC^{jm}_{j_1 m_1 j_2 m_2} |j_1 j_2; jm\rangle_q \quad . \tag{5.19}$$

These relations are, as can be easily seen, completely analogical to the corresponding relations in the "standard" (undeformed) case.

The q-deformed Clebsch – Gordan coefficients possess also many symmetry properties which can be expressed in a very simple way if one introduces, by analogy with the standard case, the q-deformed $3-j$ symbols

$$\begin{pmatrix} j_1 & j_2 & j_3 \\ m_1 & m_2 & m_3 \end{pmatrix}_q = (-1)^{j_1 - j_2 - m_3} \frac{1}{\sqrt{[2j_3+1]}} q^{-\frac{1}{2}(m_1 - m_2)} {}^qC^{j_3 - m_3}_{j_1 m_1 j_2 m_2} \quad . \tag{5.20}$$

It can be shown that the $3-j$ symbols have the following symmetry properties

a) under the cyclical permutations of their columns the $3-j$ symbols are invariant, i.e.

$$\begin{pmatrix} j_1 & j_2 & j_3 \\ m_1 & m_2 & m_3 \end{pmatrix}_q = \begin{pmatrix} j_2 & j_3 & j_1 \\ m_2 & m_3 & m_1 \end{pmatrix}_q = \begin{pmatrix} j_3 & j_1 & j_2 \\ m_3 & m_1 & m_2 \end{pmatrix}_q \tag{5.21}$$

b) under the odd permutation of the columns the $3-j$ symbols obtain an additional phase factor $(-1)^{j_1+j_2+j_3}$, while q is replaced with q^{-1}, i.e

$$\begin{pmatrix} j_1 & j_2 & j_3 \\ m_1 & m_2 & m_3 \end{pmatrix}_q = (-1)^{j_1+j_2+j_3} \begin{pmatrix} j_2 & j_1 & j_2 \\ m_3 & m_1 & m_2 \end{pmatrix}_{q^{-1}}$$

$$= (-1)^{j_1+j_2+j_3} \begin{pmatrix} j_1 & j_3 & j_2 \\ m_1 & m_3 & m_2 \end{pmatrix}_{q^{-1}} = (-1)^{j_1+j_2+j_3} \begin{pmatrix} j_3 & j_2 & j_1 \\ m_3 & m_2 & m_1 \end{pmatrix}_{q^{-1}} \tag{5.22}$$

c) under the change of the signs of all the projections (i.e when $m_1 \longmapsto -m_i$), q is replaced with q^{-1} and the additional phase $(-1)^{j_1+j_2+j_3}$ appears, i.e

$$\begin{pmatrix} j_1 & j_2 & j_3 \\ m_1 & m_2 & m_3 \end{pmatrix}_q = (-1)^{j_1+j_2+j_3} \begin{pmatrix} j_1 & j_2 & j_3 \\ -m_1 & -m_2 & -m_3 \end{pmatrix}_{q^{-1}} \tag{5.23}$$

Remark: We see that there is a close analogy between the properties of the "standard" Clebsch - Gordan coefficients and the q-deformed ones, and one may jump to the conclusion that to obtain these coefficients it is sufficient to replace the ordinary numbers (x) in the standard formulae with the q-numbers $[x]$. This impression, however, is *completely wrong*. This is due to the fact that some algebraic relations which hold for the ordinary numbers (x) do not always hold when (x) is replaced with $[x]$. A trivial example is, that for the ordinary numbers we have $mk/k = m$, but for q-numbers $[mk]/[k] \neq [m]$! Or, for example, we can use the formula $[x]^2 - [y]^2 = [x+y][x-y]$ but $[x+1] + [x-1] \neq [2x]$.

There is however another much more important fact which must be always taken into account when one adds the q- deformed angular momenta. And it is the fact that *the result of the coupling of the angular momenta depends on their order*. For example we have

$$J_{\pm}(12) = J_{\pm}(1)q^{J_0(2)} + q^{-J_0(1)}J_{\pm}(2)$$

whereas

$$J_{\pm}(21) = J_{\pm}(2)q^{J_0(1)} + q^{-J_0(2)}J_{\pm}(1)$$

Therefore $J_{\pm}(12) \neq J_{\pm}(21)$ and the replacement $J_{\pm}(12) \longmapsto J_{\pm}(21)$ is possible only when q is replaced by q^{-1}. This asymmetry of the generators according to the permutation of indices (1) and (2) gives rise to one of the most important differences between the $SU(2)$ and $SU_q(2)$- algebras. As a result not all of the quantities which appear in the $SU(2)$ algebra have an analogue in $SU_q(2)$-algebra. For example there does not exist a simple q-analogue of $9j$ symbols [81].

The dependence of the sum of the angular momenta of their order may give rise to certain physical effects. However this an open field for future investigations.

Explicit expressions for some simple Clebsch – Gordan coefficients for $SU_q(2)$. In many cases, for particular values of $j_1 m_1 j_2 m_2 j m$, the expression (5.16) obtains a very simple form. For example for the special case $m = j$ we obtain

$$ {}^{q}C^{jj}_{j_1 m_1 j_2 m_2} = (-1)^{j_1 - m_1} q^{1/2(j_1+j_2-j)(j-j_1+j_2+1)-(j+1)(j_2-m_1)} \times $$

$$ \sqrt{\frac{[2j+1]![j_1+m_1]![j_2+m_2]![j_1+j_2-j]!}{[j_1-m_1]![j_2-m_2]![j_1-j_2+j]![j-j_1+j_2]![j+j_1+j_2+1]!}} \tag{5.24} $$

which in the limit $q = 1$ reduces to the standard formulae for the same case in $SU(2)$- algebra.

The coupling of two states to zero angular momenta is done by means of the Clebsch – Gordan coefficient

$$ \langle j_1 m_1 j_2 m_2 | 00 \rangle_q = \delta_{j_1 j_2} \delta_{m_1,-m_2} q^m \frac{(-1)^{j_1 - m_1}}{\sqrt{[2j_1+1]}} \tag{5.25a} $$

Using the symmetry properties of the Clebsch– Gordan coefficients we obtain the relations

$$ \langle 00 j m | j_1 m_1 \rangle_q = \langle j m 00 | j_1 m_1 \rangle_q = \delta_{j j_1} \delta_{m m_1} \tag{5.25b} $$

In the most of the cases relevant to practical calculations, one of the indices of the Clebsch - Gordan coefficients takes the values $j = 0, 1/2, 1$ or 2. The explicit expression for the Clebsch –Gordan coefficients of $SU_q(2)$-algebra for the case $j = 0$ is given by (5.22a) The expressions for these coeffisients for the cases $j = 1/2$ and $j = 1$ are given in tables I – II. In the general case one can use the formulae (5.16).

Table I

The coefficients ${}^qC^{jm}_{j_1 m_1 \frac{1}{2} m_2}$.

j	$m_2 = 1/2$	$m_2 = -1/2$
$j_1 + \frac{1}{2}$	$q^{\frac{1}{2}(j_1 - m + \frac{1}{2})}\sqrt{\frac{[j_1 + m + \frac{1}{2}]}{[2j_1 + 1]}}$	$q^{-\frac{1}{2}(j_1 + m + \frac{1}{2})}\sqrt{\frac{[j_1 - m + \frac{1}{2}]}{[2j_1 + 1]}}$
$j_1 - \frac{1}{2}$	$-q^{-\frac{1}{2}(j_1 + m + \frac{1}{2})}\sqrt{\frac{[j_1 - m + \frac{1}{2}]}{[2j_1 + 1]}}$	$q^{\frac{1}{2}(j_1 - m + \frac{1}{2})}\sqrt{\frac{[j_1 + m + \frac{1}{2}]}{[2j_1 + 1]}}$

Table II

The coefficients ${}^qC^{jm}_{j_1 m_1 1 m_2}$.

j	$m_2 = -1$	$m_2 = +1$
$j_1 + 1$	$q^{-(j_1 + m + 1)}\sqrt{\frac{[j_1 - m + 1][j_1 - m]}{[2j_1 + 2][2j_1 + 1]}}$	$q^{j_1 - m + 1}\sqrt{\frac{[j_1 + m + 1][j_1 + m]}{[2j_1 + 2][2j_1 + 1]}}$
j_1	$q^{-m}\sqrt{\frac{[2][j_1 + m + 1][j_1 - m]}{[2j_1 + 2][2j_1]}}$	$-q^{-m}\sqrt{\frac{[2][j_1 - m + 1][j_1 + m]}{[2j_1 + 2][2j_1]}}$
$j_1 - 1$	$q^{j_1 - m}\sqrt{\frac{[j_1 + m][j_1 + m + 1]}{[2j_1 + 1][2j_1]}}$	$q^{-(j_1 + m)}\sqrt{\frac{[j_1 - m][j_1 - m + 1]}{[2j_1][2j_1 + 1]}}$

j	$m_2 = 0$
$j_1 + 1$	$q^{-m}\sqrt{\frac{[2][j_1 + m + 1][j_1 - m + 1]}{[2j_1 + 2][2j_1 + 1]}}$
j_1	$q^{-m}\frac{q^{j_1 + 1}[j_1 + m] - q^{-j_1 - 1}[j_1 - m]}{\sqrt{[2j_1 + 2][2j_1]}}$
$j_1 - 1$	$-q^{-m}\sqrt{\frac{[2][j_1 - m][j_1 + m]}{[2j_1][2j_1 + 1]}}$

Table III

The coefficients ${}^qC^{jm}_{j_1m_12m_2}$.

j	$m_2 = 2$
j_1+2	$q^{2j_1-2m+4}\left(\frac{[j_1+m-1][j_1+m][j_1+m+1][j_1+m+2]}{[2j_1+1][2j_1+2][2j_1+3][2j_1+4]}\right)^{\frac{1}{2}}$
j_1+1	$-q^{j_1-2m+2}\left(\frac{[4][j_1+m-1][j_1+m][j_1+m+1][j_1-m+2]}{[2j_1][2j_1+1][2j_1+2][2j_1+4]}\right)^{\frac{1}{2}}$
j_1	$q^{-2m+1}\left(\frac{[3][4][j_1-m+1][j_1-m+2][j_1+m-1][j_1+m]}{[2][2j_1-1][2j_1][2j_1+2][2j_1+3]}\right)^{\frac{1}{2}}$
j_1-1	$-q^{-j_1-2m+1}\left(\frac{[4][j_1+m-1][j_1-m][j_1-m+1][j_1-m+2]}{[2j_1-2][2j_1][2j_1+1][2j_1+2]}\right)^{\frac{1}{2}}$
j_1-2	$q^{-2j_1-2m+2}\left(\frac{[j_1-m-1][j_1-m][j_1-m+1][j_1-m+2]}{[2j_1-2][2j_1-1][2j_1][2j_1+1]}\right)^{\frac{1}{2}}$
j	$m_2 = 1$
j_1+2	$q^{j_1-2m+2}\left(\frac{[4][j_1+m][j_1+m+1][j_1+m+2][j_1-m+2]}{[2j_1+1][2j_1+2][2j_1+3][2j_1+4]}\right)^{\frac{1}{2}}$
j_1+1	$-\left([3][j_1-m+1]-q^{2j_1+4}[j_1+m-1]\right)q^{-2m}\times\left(\frac{[j_1+m][j_1+m+1]}{[2j_1][2j_1+1][2j_1+2][2j_1+4]}\right)^{\frac{1}{2}}$
j_1	$\left([j_1-m]-q^{2j_1+3}[j_1+m-1]\right)q^{-j_1-2m+1}\times\left(\frac{[2][3][j_1+m][j_1-m+1]}{[2j_1-1][2j_1][2j_1+2][2j_1+3]}\right)^{\frac{1}{2}}$
j_1-1	$\left(q^{2j_1+2}[3][j_1+m-1]-[j_1-m-1]\right)q^{-2j_1-2m-1}\times\left(\frac{[j_1-m][j_1-m+1]}{[2j_1-2][2j_1][2j_1+1][2j_1+2]}\right)^{\frac{1}{2}}$
j_1-2	$-q^{-j_1-2m+1}\left(\frac{[4][j_1-m-1][j_1-m][j_1-m+1][j_1+m-1]}{[2j_1-2][2j_1-1][2j_1][2j_1+1]}\right)^{\frac{1}{2}}$

Table III. Continued

The coefficients ${}^{q}C^{jm}_{j_1 m_1 2 m_2}$.

j	$m_2 = 0$
$j_1 + 2$	$q^{-2m}\left(\dfrac{[3][4][j_1+m+1][j_1+m+2][j_1-m+1][j_1-m+2]}{[2][2j_1+1][2j_1+2][2j_1+3][2j_1+4]}\right)^{\frac{1}{2}}$
$j_1 + 1$	$q^{-j_1-2m-2}\left(q^{2j_1+4}[j_1+m]-[j_1-m]\right)\times \left(\dfrac{[2][3][j_1+m+1][j_1-m+1]}{[2j_1][2j_1+1][2j_1+2][2j_1+4]}\right)^{\frac{1}{2}}$
j_1	$q^{-2m}\Big(q^{2j_1+3}[j_1+m][j_1+m-1]- [2][2][j_1+m][j_1-m]+q^{-2j_1-3}[j_1-m][j_1-m-1]\Big)\times \Big([2j_1-1][2j_1][2j_1+2][2j_1+3]\Big)^{-\frac{1}{2}}$
$j_1 - 1$	$-q^{j_1-2m+1}\left([j_1+m-1]-q^{2j_1-2}[j_1-m-1]\right)\times \left(\dfrac{[2][3][j_1+m][j_1-m]}{[2j_1-2][2j_1][2j_1+1][2j_1+2]}\right)^{\frac{1}{2}}$
$j_1 - 2$	$q^{-2m}\left(\dfrac{[3][4][j_1+m-1][j_1+m][j_1-m][j_1-m-1]}{[2][2j_1-2][2j_1-1][2j_1][2j_1+1]}\right)^{\frac{1}{2}}$

Table III. Continued

The coefficients ${}^{q}C^{jm}_{j_1 m_1 2 m_2}$.

j	$m_2 = -1$
$j_1 + 2$	$q^{-j_1-2m-2}\left(\dfrac{[4][j_1+m+2][j_1-m][j_1-m+1][j_1-m+2]}{[2j_1+1][2j_1+2][2j_1+3][2j_1+4]}\right)^{\frac{1}{2}}$
$j_1 + 1$	$\left([3][j_1+m+1] - q^{-(2j_1+4)}[j_1-m-1]\right) q^{-2m} \times \left(\dfrac{[j_1-m][j_1-m+1]}{[2j_1][2j_1+1][2j_1+2][2j_1+4]}\right)^{\frac{1}{2}}$
j_1	$\left([j_1+m] - q^{-(2j_1+3)}[j_1-m-1]\right) q^{-j_1-2m+1} \times \left(\dfrac{[2][3][j_1-m][j_1+m+1]}{[2j_1-1][2j_1][2j_1+2][2j_1+3]}\right)^{\frac{1}{2}}$
$j_1 - 1$	$-\left(q^{-(2j_1+2)}[3][j_1-m-1] - [j_1+m-1]\right) q^{2j_1-2m+1} \times \left(\dfrac{[j_1+m][j_1+m+1]}{[2j_1-2][2j_1][2j_1+1][2j_1+2]}\right)^{\frac{1}{2}}$
$j_1 - 2$	$-q^{j_1-2m-1}\left(\dfrac{[4][j_1-m-1][j_1+m][j_1+m+1][j_1+m-1]}{[2j_1-2][2j_1-1][2j_1][2j_1+1]}\right)^{\frac{1}{2}}$
j	$m_2 = -2$
$j_1 + 2$	$q^{-2j_1-2m-4}\left(\dfrac{[j_1-m-1][j_1-m][j_1-m+1][j_1-m+2]}{[2j_1+1][2j_1+2][2j_1+3][2j_1+4]}\right)^{\frac{1}{2}}$
$j_1 + 1$	$q^{-j_1-2m-2}\left(\dfrac{[4][j_1-m-1][j_1-m][j_1-m+1][j_1+m+2]}{[2j_1][2j_1+1][2j_1+2][2j_1+4]}\right)^{\frac{1}{2}}$
j_1	$q^{-2m-1}\left(\dfrac{[3][4][j_1-m-1][j_1-m][j_1+m+1][j_1+m+2]}{[2][2j_1-1][2j_1][2j_1+2][2j_1+3]}\right)^{\frac{1}{2}}$
$j_1 - 1$	$q^{j_1-2m-1}\left(\dfrac{[4][j_1+m+2][j_1+m+1][j_1+m][j_1-m-1]}{[2j_1-2][2j_1][2j_1+1][2j_1+2]}\right)^{\frac{1}{2}}$
$j_1 - 2$	$q^{2j_1-2m-2}\left(\dfrac{[j_1+m-1][j_1+m][j_1+m+1][j_1+m+2]}{[2j_1-2][2j_1-1][2j_1][2j_1+1]}\right)^{\frac{1}{2}}$

§ 5.2 Irreducible tensor operators. Wigner – Eckart theorem

Irreducible tensor operators. In the "standard" $SU(2)$ - algebra an irreducible tensor operator T^l_m of rank l is an operator with $2l+1$ components $(m = l, l-1, \ldots, -l)$ which satisfy commutation relations

$$[L_0, T^l_m] = mT^l_m$$
$$[L_\pm, T^l_m] = \sqrt{(l \mp m)(l \pm m + 1)}T^l_{m\pm 1} \tag{5.26}$$

For this operator the Wigner - Eckart theorem holds, which states that if T^l_m is an irreducible tensor operator of rank l, and $|l_1 m_1\rangle$ and $|l_2 m_2\rangle$ are states vectors with angular momenta given by the quantum numbers $l_1 m_1$ and $l_2 m_2$ respectively, then

$$\langle l_2 m_2 | T^l_m | l_1 m_1 \rangle = \frac{1}{\sqrt{2j_2+1}} C^{j_2 m_2}_{j_1 m_1 l m} \langle l_1 || T^l || l_2 \rangle$$

where the reduced (double barred) matrix element $\langle l_2 m_2 || T^l_m || l_1 m_1 \rangle$ is independent of the z - components of angular momenta.

The commutation relationships (5.26) determine the transformation properties of T^l_m. For example one can easily check that the state

$$\Phi_{l_1 m_1 l_2 m_2} = T^{l_1}_{m_1} |l_2 m_2\rangle \tag{5.27}$$

transforms like direct product state $|l_2 m_2\rangle |l_1 m_1\rangle$. As a matter of fact acting with $L_m = L_m(1) + L_m(2)$ on (5.27) we obtain

$$L_0 \Phi_{l_1 m_1 l_2 m_2} = (m_1 + m_2)\Phi_{l_1 m_1 l_2 m_2}$$

$$L_\pm \Phi_{l_1 m_1 l_2 m_2} = \sqrt{(l_1 \mp m_1)(l_1 \pm m_1 + 1)}\Phi_{l_1 m_1 \pm 1 l_2 m_2}$$
$$+ \sqrt{(l_2 \mp m_2)(l_2 \pm m_2 + 1)}\Phi_{l_1 m_1 l_2 m_2 \pm 1} \tag{5.28}$$

The eq. (5.28) is a consequence of (5.26) and vice versa. It should be noted too that this equation is basically used in proving the theorem of Wigner – Eckart. These facts will play an important role in the generalization of the concept of the irreducible tensor operator for the q-deformed case.

Now we shall try to adapt the definition (5.26) for the $SU_q(2)$ algebra. For this purpose we have to introduce the condition that the state

$$\Phi^q_{j_1 m_1 j_2 m_2} = Q^{j_1}_{m_1}|j_2 m_2\rangle_q,$$

where Q^j_m is an irreducible $SU_q(2)$ tensor operator,[19] must transform as a tensor product of two $SU_q(2)$ - basis states, i.e. as $|j_1 m_1\rangle_q \otimes |j_2 m_2\rangle_q$. Using the definition (5.8), i.e.

$$\begin{aligned} J_0(12) &= J_0(1) + J_0(2) \\ J_\pm(12) &= J_\pm(1) q^{J_0(2)} + q^{-J_0(1)} J_\pm(2) \end{aligned}$$

we obtain

$$\begin{aligned} &J_0(12)|j_1 m_1\rangle_q |j_2 m_2\rangle_q = (m_1 + m_2)|j_1 m_1\rangle_q |j_2 m_2\rangle_q \\ &J_\pm(12)|j_1 m_1\rangle_q |j_2 m_2\rangle_q \\ &\qquad = q^{m_2}\sqrt{[j_1 \mp m_1][j_1 \pm m_1 + 1]}|j_1 m_1 \pm 1\rangle_q |j_2 m_2\rangle_q \\ &\qquad\quad + q^{-m_1}\sqrt{[j_2 \mp m_2][j_2 \pm m_2 + 1]}|j_1 m_1\rangle_q |j_2 m_2 \pm 1\rangle_q. \end{aligned}$$

One can easily check that these equations will hold for $\Phi^q_{j_1 m_1 j_2 m_2}$ if the relations

$$J_0(Q^{j_1}_{m_1}|j_2 m_2\rangle_q) = (m_1 + m_2) Q^{j_1}_{m_1}|j_2 m_2\rangle_q) \tag{5.29a}$$

$$\begin{aligned} J_\pm(Q^{j_1}_{m_1}|j_2 m_2\rangle_q) &= q^{m_1}\sqrt{(j_2 \mp m_2)(j_2 \pm m_2 + 1)} Q^{j_1}_{m_1}|j_2 m_2 \pm 1\rangle_q \\ &\quad + q^{m_2}\sqrt{(j_1 \mp m_1)(j_1 \pm m_1 + 1)} Q^{j_1}_{m_1 \pm 1}|j_2 m_2\rangle_q \end{aligned} \tag{5.29b}$$

are satisfied. Using this result we can find out that the irreducible tensor operator of $SU_q(2)$ must satisfy the following commutation relation

$$[J_0, Q^j_m] = m Q^j_m \tag{5.30a}$$

$$J_\pm Q^j_m = q^m Q^j_m J_\pm + \sqrt{(j \mp m)(j \pm m + 1)} Q^j_{m\pm 1} q^{J_0} \tag{5.30b}$$

[19] We shall denote the $SU_q(2)$ tensor operators with Q^j_m , and the ordinary $SU(2)$ tensor operators with T^l_m.

We shall consider (5.30) as a definition for the $SU_q(2)$ irreducible tensor operator in the same way as (5.26) is considered as a definition for the $SU(2)$ -irreducible tensor operators.

Now, using the fact that $\Phi^q_{j_1 m_1 j_2 m_2}$ transforms according to the direct product $\mathcal{D}^{j_1} \otimes \mathcal{D}^{j_2}$ of the irreducible $SU_q(2)$ - representations, we can prove the generalized Wigner – Eckart theorem. Making use of the Clebsh – Gordan coefficients we can expand $\Phi^q_{j_1 m_1 j_2 m_2}$ in terms of components $\Phi^q_{j_1 j_2; jm}$ which transform according to the irreducible $\mathcal{D}^j$ representation, i.e.

$$\Phi^q_{j_1 m_1 j_2 m_2} = \sum_{jm}^{q} C^{jm}_{j_1 m_1 j_2 m_2} \Phi^q_{j_1 j_2; jm} \quad .$$

Multiplying both sides of the above equation by ${}_q\langle j'm'|$ and using the orthonormality of the vectors ${}_q\langle j'm'|$ and $\Phi^q_{j_1 j_2; jm}$, we obtain

$${}_q\langle j'm'|\Phi^q_{j_1 m_1 j_2 m_2}\rangle = \delta_{jj'}\delta_{mm'}\phi_q(j_1 j_2; j')$$

where the function $\phi_q(j_1 j_2; j')$ does not depend on the projections of angular momenta. In this way we find that

$$\langle j'm'|Q^{j_1}_{m_1}|j_2 m_2\rangle_q = C^{j'm'}_{j_1 m_1 j_2 m_2}\phi_q(j_1 j_2; j') \tag{5.31}$$

This is a generalization of the Wigner – Ekart theorem which can be written in the standard form

$$\langle j_1 m_1|Q^j_m|j_2 m_2\rangle_q = (-1)^{2j}\frac{{}^qC^{j_1 m_1}_{j_2 m_2 jm}}{\sqrt{[2j_1+1]}}\langle j_1||Q^j||j_2\rangle_q \tag{5.32}$$

in analogy with (5.5)

An expression for the reduced matrix elements of the operators is easily found by the methods used in the "standard" quantum theory of the angular momentum.

It should be noted that, unlike the standard theory of angular momenta, the operator of angular momenta J_m does not form an irreducible tensor operator of rank 1. However from it one can construct the first- - rank irreducuble tensor $\mathcal{J}^1_m$ (see [72]), which satisfies the modified commutation

relations (5.30) in the following way

$$\mathcal{J}_{\pm} = \mp \frac{1}{\sqrt{[2]}} q^{-J_0} J_{\pm}$$
$$\mathcal{J}_0 = \frac{1}{[2]} \left(q^{-1}[2J_0] + (q - q^{-1}) J_+ J_- \right) \tag{5.33}$$

Obviosly in the limit $q \to 1$ the expression (5.33) goes into the standard expression of the quantum theory of angular momenta.

The reduced matrix elements of these operators can be easily found taking into account that

$$\mathcal{J}_0 |jj\rangle_q = \frac{[2j]}{[2]} |jj\rangle_q$$

and that

$${}^qC^{jj}_{jj10} = q\sqrt{\frac{[2j]}{[2j+2]}}$$

In this way, from (5.32) we obtain

$$\langle j_1 || \mathcal{J} || j \rangle_q = \delta_{j_1,j} \sqrt{[2j][2j+1][2j+2]} \tag{5.34}$$

By analogy for the identity operator we find

$$\langle j_1 || 1 || \rangle_q = \delta_{j_1,j} \sqrt{[2j+1]} \tag{5.35}$$

As in the case of the standard quantum theory of angular momenta, the use of the $SU_q(2)$ Clebsh – Gordan coefficiens and the Wigner – Eckart theorem considerably simplify the calculations with the q-deformed tensor operators.

6. Application of quantum algebras to the description of nuclear and molecular spectra

Here we shall consider some applications of quantum algebraic symmetries in nuclear and molecular physics. First we shall give an account of the description of rotational spectra of deformed nuclei in terms of $SU_q(2)$ and its relation to the Variable Moment of Inertia (VMI) model. We shall also consider the description of the superdeformed nuclear spectra by means of the same symmetry. These considerations can be applied immediately to the description of rotational spectra of diatomic molecules. This is due to the fact that these objects, in spite of their quite different structure, have certain common features and, in particular, they are deformable and their moments of inertia depend on the energy. The quantum groups turn out also to be quite successful for the description of vibrational spectra of diatomic molecules. The latter can be described in terms of the q-deformed anharmonic oscillator. An alternative description of the same spectra can be given also in the framework of $SU_q(1,1)$ - algebra.

6.1 $SU_q(2)$ description of rotational nuclear spectra and its relation to the Variable Moment of Inertia Model

Rotational spectra of nuclei. It has been suggested [13] that spectra of rotational nuclei can be fitted very accurately using a Hamiltonian proportional to the second order Casimir operator of the quantum algebra $SU_q(2)$. As a matter of fact, the Hamiltonian of the symmetric top, which describes, in first approximation, the rotational spectra of the nuclei and the molecules, can be written in the form

$$H = \frac{1}{2\mathcal{J}_1}\mathbf{J}^2 + \left(\frac{1}{2\mathcal{J}_3} - \frac{1}{2\mathcal{J}_1}\right) J_0^2 \tag{6.1}$$

Here $J_m, m = 1,2,3$ are the generators of $SU(2)$ - algebra, $\mathbf{J} = J_1^2 + J_2^2 + J_3^2$ is the Casimir operator of this algebra and $\mathcal{J}_i$ are the moments of inertia of

the rigid body. One can assume that the Hamiltonian of the corresponding asymmetric top described by the q - deformed algebra can be obtained from (6.1) by replacing J_m by the q - deformed $SU_q(2)$ generators. The second term in (6.1), however, is not of particular interest, because it does not influence the arrangements of the levels within the given band. For this reason we can assume that the Hamiltonian of the corresponding q-deformed asymmetric top can be written in the form

$$^qH = AC_2^q \tag{6.2}$$

where C_2^q is the Casimir operator of $SU_q(2)$- group and A is (scaling) constant.[20]

The eigenstates of this q-deformed rotator rotator described by the Hamiltonian (6.2) are $|jm\rangle_q$ and its energy spectrum is

$$E_j^q = A[j][j+1] = A\frac{\sinh(\tau j)\sinh(\tau(j+1))}{\sinh^2(\tau)} \tag{6.3}$$

in the case when $q = e^\tau, \tau$ real, and

$$E_j^q = A[j][j+1] = A\frac{\sin(|\tau|j)\sin(|\tau|(j+1))}{\sin^2(|\tau|)} \tag{6.4}$$

when the parameter of deformation q is of the form $q = e^{i|\tau|}$. These formulae differ from the usual energy formula $j(j+1)$ in the way they describe the increase in the intervals between the states. If τ (τ - real) is not very large, formulae (6.3) gives an "extended" spectrum in which the distances between the levels are bigger than in standard rotational bands. On the opposite, in the case of relatively small $|\tau|$ formula (6.4) gives a "squeezed" spectrum, i.e. a spectrum whose levels are closer than in the "standard" rotational bands. One can easily understand this behavior having in mind that with the growth

[20]We should underline that this description is purely *phenomenological* and *heuristic*. The reason for this conclusion is that *there is no evidence that the symmetry of space under rotations has any deviations whatsoever from the quantal rotation group* $SU2$. The success of quantum groups in describing the rotational nuclear and molecular spectra actually can be considered as a genuine research problem.

of j the moment of inertia $\mathcal{J}$ of the nucleus or the molecule also increases (stretching effect) and the interval between the levels becomes shorter.

A typical example of the "squeezing" of the q -deformed spectrum described by eq (6.4) is given in Table 6.1 where it is compared with the standard rotator (i.e with the $j(j+1)$ -low) and with experimental data for the nucleus ^{166}Er. It can be seen that the standard rotational formula $j(j+1)$ (which corresponds to the case $|\tau| = 0$) gives the results which differ very much from the experimental data in the high spin states. On the contrary, formula (6.4) gives the results which approximate very well the experimental data. It is therefore of great interest to understand the reasons of these results and their possible further consequences.

Table 6.1

Rotational states of ^{166}Er

j	$\|\tau\| = 0$	$\|\tau\| = 0,049$	exp
2	80,57	80,57	80,57
4	268,57	265,61	264,98
6	563,99	548,15	545,44
8	966.84	917,53	911,19
10	1477,12	1359,83	1349,50
12	2094,95	1858,35	1846,50
14	2819,95	2394,32	2839,30
16	3652.51	2947,50	2968,50

Here we shall examine the relation of the $SU_q(2)$ expression for energies of ground state rotational bands to the usual expansion in terms of powers of $j(j+1)$, as well as to the Variable Moment of Inertia (VMI) formula, which takes into account the stretching effects.

In [13] it has been found that good fits of rotational spectra of even–even rare earths and actinides are obtained with eq. (6.4). It is easy to check that eq. (6.3) fails in describing such spectra. In order to understand this difference, it is useful to make Taylor expansions of the quantities in the numerator of eq. (6.3) (eq. (6.4)) and collect together the terms containing

the same powers of $j(j+1)$ (all other terms cancel out), finally summing up the coefficients of each power. In the first case (eq.(6.3))the final result is

$$E_j = E_0 + \frac{1}{2I}\frac{1}{(\sqrt{\frac{\pi}{2\tau}}I_{1/2}(\tau))^2}(\sqrt{\frac{\pi}{2\tau}}I_{1/2}(\tau)j(j+1) + \tau\sqrt{\frac{\pi}{2\tau}}I_{3/2}(\tau)(j(j+1))^2$$

$$+\frac{2\tau^2}{3}\sqrt{\frac{\pi}{2\tau}}I_{5/2}(\tau)(j(j+1))^3 + \frac{\tau^3}{3}\sqrt{\frac{\pi}{2\tau}}I_{7/2}(\tau)(j(j+1))^4 + \ldots \qquad (6.5)$$

where $\sqrt{\frac{\pi}{2\tau}}I_{n+\frac{1}{2}}(\tau)$ are the modified spherical Bessel functions of the first kind [89]. In the second case (eq. (6.4)) following the same procedure one obtains

$$E_j = E_0 + \frac{1}{2I}\frac{1}{(j_0(|\tau|))^2}(j_0(|\tau|)j(j+1) - |\tau|j_1(|\tau|)(j(j+1))^2$$

$$+\frac{2}{3}|\tau|^2 j_2(|\tau|)(j(j+1))^3 - \frac{1}{3}|\tau|^3 j_3(|\tau|)(j(j+1))^4$$

$$+\frac{2}{15}|\tau|^4 j_4(|\tau|)(j(j+1))^5 - \ldots) \quad , \qquad (6.6)$$

where $j_n(\tau)$ are the spherical Bessel functions of the first kind [89].

Both results are of the form

$$E_j = E_0 + Aj(j+1) + B(j(j+1))^2 + C(j(j+1))^3 + D(j(j+1))^4 + \ldots, \quad (6.7)$$

which is the expansion in terms of powers of $j(j+1)$ used for fitting experimental rotational spectra [90]. Empirically it is known that the coefficients A, B, C, D, ... have alternating signs, starting with A positive. In addition, B is roughly three orders of magnitude smaller than A, C is about three orders of magnitude smaller than B, and D is also three orders of magnitude smaller than C [90].

It is interesting to check if the empirical characteristics of the coefficients A, B, C, D are present in the case of the expansions of eqs. (6.5), (6.6), especially for small values of τ or $|\tau|$. (Since we deal with rotational spectra, which are in first order approximation described by the usual algebra SU(2),

we expect τ (or $|\tau|$) to be relatively small, i.e. the deviation of $SU_q(2)$ from SU(2) to be small. This is in agreement with the findings of [13], where $|\tau|$ is found to be around 0.03.)

It can be easily seen that in (10) it is impossible to get alternating signs. For this reason we conclude that eq.(6.5) is inappropriate for describing nuclear rotational spectra.

In eq. (6.6), however, the situation is different and one can easily check that the condition of alternating signs is thus fulfilled. In order to check the order of magnitude of the coefficients for small values of $|\tau|$, it is useful to expand the spherical Bessel functions appearing in (6.6) and keep only the lowest order term in each expansion. The result is

$$E_j = E_0 + \frac{1}{2I}(j(j+1) - \frac{|\tau|^2}{3}(j(j+1))^2 + \frac{2|\tau|^4}{45}(j(j+1))^3$$
$$-\frac{|\tau|^6}{315}(j(j+1))^4 + \frac{2|\tau|^8}{14175}(j(j+1))^5 - \ldots). \qquad (6.8)$$

We see that each term contains a factor $|\tau|^2$ more than the previous one. For $|\tau|$ in the area of 0.03, $|\tau|^2$ is of the order of 10^{-3}, as it should. We conclude therefore that eq. (6.6) is suitable for fitting rotational spectra, since its coefficients have the same characteristics as the empirical coefficients of eq. (6.7). Examples of fits and parameter values are given in [14, 15]. In all cases the fits are of very good quality.

Variable Moment of Inertia Model. We now turn to the comparison of the expansion of eq. (6.6) to the Variable Moment of Inertia (VMI) [92] model. In this model the levels of the ground state band are given by

$$E_j = \frac{j(j+1)}{2\mathcal{J}(j)} + \frac{1}{2}C(\mathcal{J}(j) - \mathcal{J}_0)^2 \qquad (6.9)$$

where C and $\mathcal{J}_0$ are the two free parameters of the model, the latter being the ground state moment of inertia. The quantity $\mathcal{J}(j)$ plays the role of moment of inertia which is supposed to depend on the angular momenta (or, which is the same, on the energy) of the state. Therefore the first term in (6.9) gives the enery of the rotator whose moment of inertia depends on the energy due to the sretching of the body. The second term in (6.9) gives the

contribution to the energy due to the deviation of the moment of inertia of its equilibrium value.

The moment of inertia for each j is determined from the variational condition

$$\frac{\partial E_j}{\partial \mathcal{J}(j)}|_j = 0, \tag{6.10}$$

which is equivalent to the cubic equation

$$\mathcal{J}(j)^3 - \mathcal{J}(j)^2 \mathcal{J}_0 - \frac{j(j+1)}{2C} = 0. \tag{6.11}$$

This equation has only one real root, which can be written as

$$\mathcal{J}(j) = \sqrt[3]{\frac{j(j+1)}{4C} + \frac{\mathcal{J}_0^3}{27} + \sqrt{\frac{(j(j+1))^2}{16C^2} + \frac{\mathcal{J}_0^3 j(j+1)}{54C}}} + \sqrt[3]{\frac{j(j+1)}{4C} + \frac{\mathcal{J}_0^3}{27} - \sqrt{\frac{(j(j+1))^2}{16C^2} + \frac{\mathcal{J}_0^3 j(j+1)}{54C}}} + \frac{\mathcal{J}_0}{3}. \tag{6.12}$$

Expanding the roots in eq. (6.12) and keeping together terms containing the same powers of $j(j+1)$ one obtains

$$\mathcal{J}(j) = \mathcal{J}_0(1 + \frac{j(j+1)}{2C\mathcal{J}_0^3} - 2\frac{(j(j+1))^2}{(2C\mathcal{J}_0^3)^2} + 7\frac{(j(j+1))^3}{(2C\mathcal{J}_0^3)^3} - 30\frac{(j(j+1))^4}{(2C\mathcal{J}_0^3)^4} + \ldots). \tag{6.13}$$

Using (6.11) in (6.9) one has

$$E_j = \frac{C}{2}(\mathcal{J}(j) - \mathcal{J}_0)(3\mathcal{J}(j) - \mathcal{J}_0). \tag{(6.14)}$$

Using (6.13) in (6.14) one obtains the following expansion for the energy

$$E_j = \frac{1}{2\mathcal{J}_0}(j(j+1) - \frac{1}{2}\frac{(j(j+1))^2}{2C\mathcal{J}_0^3} + \frac{(j(j+1))^3}{(2C\mathcal{J}_0^3)^2} - 3\frac{(j(j+1))^4}{(2C\mathcal{J}_0^3)^3} + \ldots) \tag{6.15}$$

It is known [92] that C and $\mathcal{J}_0$ obtain positive values, while

$$\sigma = \frac{1}{2C\mathcal{J}_0^3}, \tag{6.16}$$

is the softness parameter, which for rotational nuclei is of the order of 10^{-3}. Thus the coefficients of the expansion of eq. (6.15) have the proper signs and orders of magnitude.

Comparing eqs (6.6) and (6.15) we see that both expansions have the same form. The moment of inertia parameter I of (6.6) corresponds to the ground state moment of inertia $\mathcal{J}_0$ of (6.15). The small parameter of the expansion is $|\tau|^2$ in the first case, while it is the softness parameter $1/(2C\mathcal{J}_0^3)$ in the second. However, the numerical coefficients in front of each power of $j(j+1)$ are not the same. In [14] a comparison is made between the parameters obtained from fitting the same spectra with eqs (6.6) and (6.15), the parameter values for the latter taken from [92]. The agreement between the theory and the experimental date is very good.

It is necessary for E_j to be an increasing function of j. In order to guarantee this in eq. (6.4) one must have

$$|\tau|(j+1) \leq \frac{\pi}{2}. \tag{6.17}$$

In the case of $|\tau| = 0.036$ (as in ^{232}U), one finds $j \leq 42$, this limiting value being larger than the highest observed j in ground state bands in the actinide region . Similarly, for $|\tau| = 0.046$ (as in ^{178}Hf [14]), one finds $j \leq 32$, this limiting value being again higher than the highest observed j in ground state bands in the rare earth region.

Here we have demonstrated that two different expansions of the second order Casimir operator of the quantum algebra $\mathrm{SU}_q(2)$ in terms of powers of $j(j+1)$ can be obtained, of which only one is suitable for the description of rotational ground state bands. This expansion is very similar to the one given by the Variable Moment of Inertia (VMI) model. The moment of inertia parameter, as well as the small parameter of the expansion, are very similar in both expansions. In this way we have shown that stretching effects (i.e. the increase of the moment of inertia with the energy) can be taken into account by allowing the algebra to deviate from the usual $SU(2)$ limit.

Superdeformed nuclear spectra. As we have seen the quantum algebra $SU_q(2)$ has been successfully used for fitting the ground state bands of deformed rare earth and actinide nuclei. The maximal spin of the states of these bands however is as a rule not very high. On the other hand, the experimental discovery of superdeformation [93] (for relevant reviews see [94, 95]) has stirred considerable activity in the study of high spin states. In this region one can observe the states with spins j=40 and higher. It is therefore of great interest to examine to what extent the data for superdeformed bands can be described by the quantum algebra $SU_q(2)$ and to point out the differences between such descriptions of rotational bands with normal and super deformations.

Eq. (6.4) has been used for fitting several superdeformed bands in the A=130 and A=150 regions, the results being reported in [15]. The recently discovered superdeformed bands in the A=190 region have also been fitted, as reported in [15]. In all cases the fits are of very good quality and include the highest spin state observed up to now in the nuclear rotational bands. In this connection the following comments can be made:

1) In the case of the bands with normal deformation the parameter $|\tau|$, which determines the spacing among the levels within a band, reaches values around 0.03. In addition, $|\tau|$ decreases with an increase in collectivity (increasing $R_4 = E_4/E_2$ ratio, for example).

2) In the case of superdeformed bands, $|\tau|$ obtains even smaller values, indicating that their symmetry is closer to the usual SU(2) symmetry. In particular, $|\tau|$ is about 0.01 in the A=130 and A=190 regions, which are assumed to correspond to axis ratios around 1.5:1 to 1.65:1 [93]. However it reaches even smaller values around 0.004 in the A=150 region, which contains the best examples of superdeformed bands found so far, corresponding to an axis ratio close to 2:1 [93].

Before concluding, it is appropriate to discuss in more detail the physical motivation for using the quantum algebra $SU_q(2)$ for the description of superdeformed bands. The following two comments can be made in this regards:

1) By defining, as usual,

$$J_+ = J_x + iJ_y, \qquad J_- = J_x - iJ_y, \qquad J_0 = J_z,$$

we can rewrite the $SU_q(2)$ commutation relations in the form

$$[J_x, J_y] = \frac{i}{2}[2J_z], \qquad [J_y, J_z] = iJ_x, \qquad [J_z, J_x] = iJ_y, \tag{6.18}$$

which is the q-generalization of the SO(3) commutation relations, which are obtained from eq. (6.18) in the limit $q \to 1$. We can see that while in the classical SO(3) case the three commutation relations have exactly the same form, in the quantum case the first commutation relation in eq. (24) differs (in the right hand side) from the other two, thus indicating that the $z-$ direction is not any more equivalent to the $x-$ and $y-$ directions. Therefore it is not surprising that the $SU_q(2)$ symmetry is more appropriate than the classical SU(2) symmetry for describing objects deformed in one of the 3 dimensions (like deformed and superdeformed nuclei).

2) One could argue that the better description of deformed and superdeformed spectra obtained in the $SU_q(2)$ case than in the SU(2) case is due to the extra parameter q (or, equivalently, τ) present in the first case. However, this is not an arbitrary additional parameter. As has been pointed out, the $SU_q(2)$ expansion given in eq. (11) has the same form as the expansion of the VMI formula in terms of $j(j+1)$ and the τ^2 parameter of $SU_q(2)$ corresponds [14] to the softness parameter σ of the VMI [92]. Therefore the parameter τ, which deforms the algebra, has a well-defined physical meaning.

The considerations of this section shows that the nuclear rotational bands with normal deformation and the superdeformed nuclear rotational bands as well, can be very accurately described in the framework of the quantum algebra $SU_q(2)$. Stretching effects are taken into account by allowing the algebra to deviate from the usual SU(2) limit. It has been demonstrated that this deviation is equivalent to an expansion in terms of powers of $j(j+1)$, summed up to all orders.

6.2. Description of rotational molecular spectra by the quantum algebra $SU_q(2)$

We have shown that the rotational bands in even–even nuclei can be described very accurately in terms of a Hamiltonian which is proportional to the second order Casimir operator of the quantum algebra $SU_q(2)$. In this section we shall try to find out if rotational spectra of diatomic molecules can be described in terms of the quantum algebra $SU_q(2)$.

It is known [96, 97] that rotational molecular spectra are described by an expansion of the form

$$E_v(j) = B_v j(j+1)+D_v(j(j+1))^2+H_v(j(j+1))^3+J_v(j(j+1))^4+\ldots, \quad (6.19)$$

where j is the angular momentum and v is the vibrational quantum number. More generally, rotation–vibration molecular spectra are described by the Dunham expansion [107] which has the form

$$E(v,j) = \sum_{ik} Y_{ik}(v+\frac{1}{2})^i(j(j+1))^k, \quad (6.20)$$

where Y_{ik} are numerical coefficients. The first few terms of the Dunham expansion can be obtained from the solution of the Schrödinger equation for the Morse potential [108]. By writing the Dunham expansion in the form

$$\begin{aligned} E(v,j) =& (Y_{00}+Y_{10}(v+\frac{1}{2})+Y_{20}(v+\frac{1}{2})^2+Y_{30}(v+\frac{1}{2})^3+\ldots)+ \\ &+j(j+1)(Y_{01}+Y_{11}(v+\frac{1}{2})+Y_{21}(v+\frac{1}{2})^2+Y_{31}(v+\frac{1}{2})^3+\ldots)+ \\ &(j(j+1))^2(Y_{02}+Y_{12}(v+\frac{1}{2})+Y_{22}(v+\frac{1}{2})^2+Y_{32}(v+\frac{1}{2})^3+\ldots)+ \\ &(j(j+1))^3(Y_{03}+Y_{13}(v+\frac{1}{2})+Y_{23}(v+\frac{1}{2})^2+Y_{33}(v+\frac{1}{2})^3+\ldots)+\ldots \end{aligned} \quad (6.21)$$

the relations between the coefficients B_v, D_v, H_v, ... and Y_{ik} become clear. Extensive tables of coefficients for several diatomic molecules can be found in [109].

For the quantum algebraic description of rotational molecular spectra we shall use the algebra $SU_q(2)$ and shall represent the Hamiltonian of rotational

motion as a Casimir operator of $SU_q(2)$, i.e we shall assume that it is of the form (6.2). As a result, we shall obtain expressions (6.3) and (6.4) for the energy. Expanding these expressions in series in powers of $j(j+1)$ we obtain eqs. (6.5) and (6.6). Both these expressions are of the form shown in eq. (6.19), which is used for fitting experimental rotational spectra both in molecules [96] and nuclei [90]. Empirically it is known that the coefficients B_v, D_v, H_v ... have alternating signs, starting with B_v positive [90, 96]. In addition, D_v is roughly 4–5 orders of magnitude smaller than B_v, and H_v is about 4–5 orders of magnitude smaller than D_v .

As in the case of rotational nuclear spectra, alternating signs are obtained only in eq. (6.6) (and not in eq. (6.5)). In eq. (6.8) we see that each term contains a factor $|\tau|^2$ more than the previous one. For $|\tau|$ in the area of 0.01, $|\tau|^2$ is of the order of 10^{-4}, as it should. We conclude therefore that eq. (6.6) (or eq. (6.4) is suitable for fitting rotational spectra, since its coefficients have the same characteristics as the empirical coefficients of eq. (6.19). Examples of fits are reported in [23], where the relevant coefficients in the Dunham expansion for the HF,HCl, HBr molecules are also calculated. In all cases the fits are of very good quality.

Since $|\tau|$ is small, it is clear from eq. (13) that $1/(2I)$ will be very close to $E_2(v)/6$. In addition, D_v/B_v should be approximately equal to $|\tau|^2/3$, i.e. $|\tau|$ should be close to $(3D_v/B_v)^{1/2}$. The values shown in [23] indicate that these approximate equalities hold very well. Even the small variation of the parameters between the $v=0$ and $v=1$ spectra of HCl are well reproduced.

It is known that the Y_{ik} coefficients of the Dunham expansion are proportional to powers of the quantity (B_e/ω_e), where B_e is the rotational constant in the equilibrium position and ω_e is the equilibrium vibrational constant [96]. A comparison of the expansion of eq. (13) to the expressions given in [107, 110, 111] shows that the role of the small parameter of the expansion played there by $(B_e/\omega_e)^2$ is played here by $|\tau|^2$. The situation resembles the case in nuclear physics, where, as we have seen in the previouse section, $|\tau|^2$ is connected with the softness parameter σ of the Variable Moment of Inertia (VMI) Model.

From what we have already seen, it is clear that the usual expansion of rotational spectra in terms of $j(j+1)$ (eq. (6.19) can be summed up by

using of the $SU_q(2)$ quantum algebra, as shown in eq. (6.4). As a matter of fact we can rewrite eq. (6.20) as follows

$$\begin{aligned} E(v,j) =& (Y_{00} + Y_{01}j(j+1) + Y_{02}(j(j+1))^2 + Y_{03}(j(j+1))^3 + \ldots) + \\ & (v+\frac{1}{2})(Y_{10} + Y_{11}j(j+1) + Y_{12}(j(j+1))^2 + Y_{13}(j(j+1))^3 + \ldots) + \\ & (v+\frac{1}{2})^2(Y_{20} + Y_{21}j(j+1) + Y_{22}(j(j+1))^2 + Y_{23}(j(j+1))^3 + \ldots) + \\ & (v+\frac{1}{2})^3(Y_{30} + Y_{31}j(j+1) + Y_{32}(j(j+1))^2 + Y_{33}(j(j+1))^3 + \ldots) + \\ & \ldots \end{aligned} \tag{6.22}$$

It can be pointed out that Y_{01}, Y_{02}, Y_{03}, Y_{04} have alternating signs (starting with Y_{01} positive) and magnitudes falling by about 4 orders of magnitude from one to the next. Thus the terms in the first couple of parentheses in the rhs of eq. (6.28) look like the expansion in eq. (6.19) and can be summed up as eq. (6.4). A similar situation occurs for Y_{11}, Y_{12}, Y_{13}, ..., having as a result the summation of the terms in the second line of eq. (6.22), as well as for Y_{21}, Y_{22}, ..., resulting in the summation of the terms in the third line of eq. (6.22). We conclude that eq. (6.22) can be written as

$$\begin{aligned} E(v,j) = (Y_{00} + Y_0 \frac{sin(\tau_0 j)sin(\tau_0(j+1))}{sin^2(\tau_0)}) + (Y_{10} + Y_1 \frac{sin(\tau_1 j)sin(\tau_1(j+1))}{sin^2(\tau_1)}) \\ + (Y_{20} + Y_2 \frac{sin(\tau_2 j)sin(\tau_2(j+1))}{sin^2(\tau_2)}) + \ldots \end{aligned} \tag{6.23}$$

which implies that the Dunham expansion (eq. (6.20) can be written in the form

$$E(v,j) = \sum_i (v+\frac{1}{2})^i (Y_{i0} + Y_i \frac{sin(\tau_i j)sin(\tau_i(j+1))}{sin^2(\tau_i)}), \tag{6.24}$$

where τ_i are real and positive, and the partial summation over powers of $j(j+1)$ has been carried out.

It is necessary for E_j to be an increasing function of j. In order to guarantee this in eq. (9) one must have

$$|\tau|(j+1) \leq \frac{\pi}{2}. \tag{6.25}$$

In the case of $|\tau| = 0.0174$ (as in HF [23]), one finds $j \leq 89$, while for $|\tau| = 0.0113$ (as in HBr [23]), one finds $j \leq 138$. These limiting values are higher than the highest j observed in these diatomic molecules.

5.3 Description of vibrational molecular spectra

Vibrational molecular spectra and the q-deformed anharmonic oscillator. In the previous section it has been demonstrated that in terms of the quantum algebra $SU_q(2)$ one can obtain a very accurate description of rotational molecular spectra. In this section we shall show that in the framework of quantum algebras one can also obtain an improved description of vibrational molecular spectra.

As has already been mentioned, the rotational–vibrational molecular spectra are usually described in terms of the Dunham expansion (eq. (6.21)). Ignoring angular momentum (i.e. ignoring the rotational bands built on each vibrational bandhead), the Dunham expansion takes the simplified form

$$E(v) = \sum_i Y_{i0}(v + \frac{1}{2})^i, \tag{6.26}$$

i.e. it has the form of an expansion in powers of $(v + \frac{1}{2})$.

The first terms of the Dunham expansion, as shown before, are obtained from the exact solution of the Schrödinger equation for the Morse potential [108]. However for the study of molecular rotation–vibration spectra [98–103] one can also apply algebraic techniques [98 – 103], in analogy to a similar approach used for nuclear spectra [104] (for recent surveys see [105, 106]). The basic features of this approach can be summarized as follows:

One assume that there exists a group $\mathcal{G}$, known as the *dynamical group* of the system, which contains, in one of its unitary irreducible representations (i.e. in one of its multiplets), all the states of the quantum system, or at least these states which are of interest for the problem under consideration. (For example we can assume that the dynamical group is chosen in such a way that all vibrational states of the molecule form a multiplet of this group). If the Hamiltonian H of the system was invariant according to the transformations belonging to the dynamical group, all the states of this multiplet would be degenerate (i.e they would have the same energy). However the Hamiltonian

H is invariant only according to the smaller group $\mathcal{G}_0 \subset \mathcal{G}$, known as the *symmetry group* of the Hamiltonian. In this way the Hamiltonian breaks down the primary symmetry according to $\mathcal{G}$ and the states of the multiplet obtain different energies. Due to this symmetry breaking the Hamiltonian generates the observed spectrum of the system. In the simplest version of this approach the Hamiltonian can be represented in the form

$$H = C_2(\mathcal{G}) + \alpha C_2(\mathcal{G}_0) \tag{6.27}$$

where $C_2(\mathcal{G})$ and $C_2(\mathcal{G}_0)$ are the Casimir operators of $\mathcal{G}$ and $\mathcal{G}_0$, recpectively, and α is a constant which has to be adjusted from the experimental data.[21]

The group $U(4)$ has been successfully used as a dynamical group in the algebraic model for spectra of diatomic molecules [102], which has also been extended to triatomic molecules [103]. In other algebraic approches, vibrational spectra of diatomic molecules have been described in terms of the anharmonic oscillator [112 – 116], using techniques similar to those used earlier in the algebraic approach to the Morse potential [116]. Here the dynamical group of the vibrational motion of the diatomic molecule is $U(2)$ and the group of symmetry is $O(2) \subset U(2)$.

Here we shall briefly summarize this approach, which we are going now to generalize for the q-deformed case. The generators of U(2) take the form [114]

$$J_+ = a_1^+ a_2, \quad J_- = a_2^+ a_1, \quad J_0 = \frac{1}{2}(a_1^+ a_1 - a_2^+ a_2), \tag{6.28 a}$$

$$N = a_1^+ a_1 + a_2^+ a_2 \equiv N_1 + N_2 \tag{6.28 b}$$

where a_1^+, a_1, a_2^+, a_2 satisfy standard boson commutation relations and $N_i = a_i^+ a_i$ are number of boson operators (of type i). The operators (6.28 a) are generators of SU(2) and satisfy the standard commutation relations

$$[J_0, J_\pm] = \pm J_\pm, \tag{6.29}$$

[21]The structure (6.27) of the Hamiltonian shows that it is constructed from the generators of $\mathcal{G}$ and therefore its eigenstates can be classified in the multiplets of this group. On the other hand the second term of (6.27) (and, as a result, the Hamiltonian itself) commute only with the generators of $\mathcal{G}_0$, which means that this term breaks down the symmetry according to $\mathcal{G}$.

$$[J_+, J_-] = 2J_0,$$

while the fourth generator N (total number of bosons operator) commutes with all the operators (6.28 a) and is at the same time the first order Casimir operator of $U(2)$. The $U(2)$- basis has the form

$$|v>= \frac{1}{\sqrt{(N-v)!v!}}(a_1^+)^v(a_2^+)^{N-v}|0>, \qquad (6.30))$$

with $v = N_1$ and $N - v = N_2$. In the above, N is the total number of bosons, N_1 (N_2) is the number of bosons with index 1 (index 2), and v is the vibrational quantum number.

We shall assume also that the symmetry group of the diatomic molecule is $SO(2)$. The second order Casimir operator of the O(2) subalgebra has the form

$$C_2(O(2)) = 4J_0^2 = (a_1^+a_1 - a_2^+a_2)^2 = (N_1 - N_2)^2, \qquad (6.31)$$

According to the prescription given above with eg (6.27), the Hamiltomian of the system, which generates the spectrum of the system, can be written in the form of a linear combination of the Casimir operators of $U(2)$ and $SO(2)$. Following [112, 115] we can write down

$$H = E_0 + A(C_1(U(2)))^2 - AC_2(O(2)) = 4(a_1^+a_1)(a_2^+a_2), \qquad (6.32)$$

where A is a free parameter (the overall scale). The eigenvalues of this Hamiltonian in the above basis (eq. (6.30)) are

$$E(N,v) = E_0 + A4v(N-v). \qquad (6.33)$$

This equation can be rewritten in the form

$$E(N,v) = -(2N+1) + 4(N+1)(v+\frac{1}{2}) - 4(v+\frac{1}{2})^2, \qquad (6.34)$$

which shows that eq. (6.34) contains the first two powers of $(v+\frac{1}{2})$ contained in the Dunham expansion of eq. (6.26), the ratio of the coefficient of the first power over the coefficient of the second power (i.e. Y_{10}/Y_{20}) being $-(N+1)$.

These considerations can be easily generalized in the q- deformed case. As we have seen in Sec. 4 in the case of $U_q(2)$, the generators take the form

$$J_+ = a_1^+a_2, \quad J_- = a_2^+a_1, \quad 2J_0 = N_1 - N_2,$$

where the operators a_i^+, a_i $(i = 1, 2)$ satisfy the q- deformed commutation relations and the generators of $SU_q(2)$ satisfy the commutation relations given in Sec. 4. The first order Casimir operator of $U_q(2)$ is

$$C_1(U_q(2)) = [N] = [N_1 + N_2]. \tag{6.35}$$

As in the classical case mentioned above, $U_q(2)$ is obtained by supplying $SU_q(2)$ with this additional operator $N = N_1 + N_2$.

By analogy with (6.30) the basis of the representation space of $U_q(2)$ takes the form

$$|v>= \frac{1}{\sqrt{[v]![N-v]!}}(a_1^+)^v(a_2^+)^{N-v}|0>, \tag{6.36}$$

where $v = N_1$, $N - v = N_2$. Again by analogy to the classical case (eq. (6.32)), the Hamiltonian takes the form

$$\begin{aligned} H &= E_0 + A(C_1(U_q(2)))^2 - AC_2(O_q(2)) \\ &= E_0 + A[N_1 + N_2][N_1 + N_2] - A[N_1 - N_2][N_1 - N_2]. \end{aligned} \tag{6.37}$$

Its eigenvalues in the basis of eq.(6.36), after a little of calculation, take the form

$$E(N, v) = E_0 + A[2v][2N - 2v]. \tag{6.38}$$

This result goes to eq. (6.33) in the limit $q \to 1$. In the case $q = e^\tau$ eq. (6.38) takes the form

$$E(N, v) = E_0 + A\frac{sinh(2v\tau)sinh((2N - 2v)\tau)}{sinh^2(\tau)}, \tag{6.39}$$

while in the case $q = e^{i\tau}$ one correspondingly has

$$E(N, v) = E_0 + A\frac{sin(2v\tau)sin((2N - 2v)\tau)}{sin^2(\tau)}. \tag{6.40}$$

It is instructive at this point to check how these two equations compare to the Dunham expansion of eq. (6.26). In each case one can take the Taylor expansions of the functions appearing in the numerator of the right hand side, collect together terms containing the same power of $(v + \frac{1}{2})$, and finally

sum up the coefficients of each power of $(v+\frac{1}{2})$. In the case of $q=e^{\tau}$ one obtains

$$\begin{aligned}E(N,v) =& E_0 + A\frac{\tau^2}{sinh^2(\tau)}[-\frac{sinh(\tau)sinh(\tau(2N+1))}{\tau^2}\\ &+(v+\frac{1}{2})2\frac{sinh(2\tau(N+1))}{\tau}-(v+\frac{1}{2})^2 4cosh(2\tau(N+1))\\ &+(v+\frac{1}{2})^3\frac{16}{3}\tau^2\frac{sinh(2\tau(N+1))}{\tau}-(v+\frac{1}{2})^4\frac{16}{3}\tau^2 cosh(2\tau(N+1))\\ &+(v+\frac{1}{2})^5\frac{64}{15}\tau^4\frac{sinh(2\tau(N+1))}{\tau}\\ &-(v+\frac{1}{2})^6\frac{128}{45}\tau^4 cosh(2\tau(N+1))+\ldots],\end{aligned} \tag{6.41}$$

while in the case of $q=e^{i\tau}$ one has

$$\begin{aligned}E(N,v) =& E_0 + A\frac{\tau^2}{sin^2(\tau)}[-\frac{sin(\tau)sin(\tau(2N+1))}{\tau^2}+(v+\frac{1}{2})2\frac{sin(2\tau(N+1))}{\tau}\\ &-(v+\frac{1}{2})^2 4cos(2\tau(N+1))+(v+\frac{1}{2})^3(-\frac{16}{3})\tau^2\frac{sin(2\tau(N+1))}{\tau}\\ &-(v+\frac{1}{2})^4(-\frac{16}{3})\tau^2 cos(2\tau(N+1))+(v+\frac{1}{2})^5\frac{64}{15}\tau^4\frac{sin(2\tau(N+1))}{\tau}\\ &-(v+\frac{1}{2})^6\frac{128}{45}\tau^4 cos(2\tau(N+1))+\ldots].\end{aligned} \tag{6.42}$$

We see that in both cases we obtain expressions resembling the Dunham expansion of eq. (6.26). In both cases in the limit $\tau\to 0$ one obtains the classical expression of eq. (6.34). For the ratio of the coefficient of the first power of $(v+\frac{1}{2})$ over the coefficient of the second power of $(v+\frac{1}{2})$ one has $-\tanh(2\tau(N+1))/(2\tau)$ in eq. (6.41), while one gets $-\tan(2\tau(N+1))/(2\tau)$ in eq. (6.42). In both cases in the limit $\tau\to 1$ one gets the classical value $-(N+1)$ [42]. However, it is clear that the extra parameter τ (or q), which is related to the deformation of the algebra, allows for this ratio to obtain values different from $-(N+1)$.

For a brief comparison to experimental data, we select the standard example of the $X^1\Sigma_g^+$ state of H_2 [117], which has been studied in the framework of the O(4) limit of the vibron model in [102]. (For a more sophisticated

fitting, in the framework of the vibron model including higher order terms, see [118].) The potential curve of the $X^1\Sigma_g^+$ state of H_2, reported in [25], has been obtained [61] through use of the Rydberg–Klein–Rees (RKR) method. For the $X^1\Sigma_g^+$ state of H_2 it is known that $v_{max} = 14$. Therefore, as in the case of [102], N can be either 28 or 29. We have selected the latter value, as in ref. [102]. (The former value also gives very similar results.) We have found [25] that an improved fit is obtained using eq. (6.42) (which corresponds to $q = e^{ir}$), while eq. (6.41) (which corresponds to $q = e^r$) does not improve the fit. The situation is the same as in the case of rotational spectra of diatomic molecules [25] or deformed nuclei [13 - 15]. In these cases it has also been found that only the choice $q = e^{ir}$ can give improved results. The results of the fit are given in [25], where a clear improvement can be seen.

In conclusion, we have shown that quantum algebras can be used for the description of vibrational spectra of diatomic molecules, using techniques similar to those used for the description of rotational spectra of diatomic molecules. While the Hamiltonian of the anharmonic oscillator, having the symmetry $U(2) \supset O(2)$, corresponds to the first two terms of the vibrational Dunham expansion, the Hamiltonian of the q-deformed anharmonic oscillator, having the generalized symmetry $U_q(2) \supset O_q(2)$, corresponds to all terms of the vibrational Dunham expansion, summed up in a closed form. It also corresponds to a partially summing up of the more general Dunham expansion. A similar partial summation of the Dunham series, concerning the rotational quantum number, has been obtained in [25] using a q-deformed rotor having $SU_q(2)$ symmetry. It is then plausible that one could fully sum up the Dunham series by considering a more general quantum algebra taking the vibrational quantum U(2) and the rotational quantum SU(2) (each of them having different value of q) as subalgebras.

The q-deformed $SU_q(1,1)$ and the description of vibrational molecular spectra. We have seen that an improved description of rotational spectra of diatomic molecules can be given by generalizing the classical SU(2) algebra into the quantum $SU_q(2)$ one. On the other hand it is well known that the Morse potential [108], which offers a widely accepted description of vibrational spectra of diatomic molecules , has been known to have the

symmetry SU(1,1). Vibrational spectra are then described by a Hamiltonian which is proportional to the second order Casimir operator of SU(1,1). It is therefore of interest to check the consequences and the physical content of generalizing SU(1,1) into the quantum algebra $SU_q(1,1)$.

In the classical case the $SO(2,1)$ - generators (or, what is the same, the $SU(1,1$ - generators) satisfy the commutation relations

$$[K_1, K_2] = -iK_3, \qquad [K_2, K_3] = iK_1, \qquad [K_3, K_1] = iK_2. \tag{6.43}$$

Defining

$$K_+ = K_1 + iK_2, \qquad K_- = K_1 - iK_2, \qquad K_3 = K_z, \tag{6.44}$$

one obtains the SU(1,1) commutation relations

$$[K_z, K_\pm] = \pm K_\pm, \qquad [K_+, K_-] = -2K_z. \tag{6.45}$$

The generators of SU(1,1) have the following well known boson representation

$$K_+ = a_1^+ a_2^+, \qquad K_- = a_1 a_2, \qquad K_z = \frac{1}{2}(a_1^+ a_1 + a_2^+ a_2 + 1), \tag{58}$$

where a_1^+, a_1, a_2^+, a_2 satisfy the standard boson commutation relations.

The second order Casimir operator of SO(2,1) is

$$C_2[SO(2,1)] = -(K_1^2 + K_2^2 - K_3^2). \tag{6.46}$$

If N is the number of excitation quanta given to the system (which is equal to the total number of bosons in the case of the boson representation) and v is the vibrational quantum number, the eigenvalues of the Casimir operator are given in

$$C_2[SO(2,1)]|N\omega >= \frac{1}{4}\omega(\omega + 2)|N\omega >, \tag{6.47}$$

where the quantum number ω is given by

$$v = \frac{1}{2}(N - \omega). \tag{6.48}$$

N is related to the maximum number of vibrational states by

$$N = 2v_{max} \quad or \quad N = 2v_{max} + 1. \tag{6.49}$$

Therefore the vibrational spectrum is given by

$$E(N,\omega) = E_0 - A < C_2[SO(2,1)] >= E_0 - \frac{A}{4}\omega(\omega+2), \tag{6.50}$$

where by $<>$ we denote the eigenvalue of the enclosed operator. Using (6.48) this can be rewritten as

$$E(N,v) = E_0 - A\frac{N^2-1}{4} + AN(v+\frac{1}{2}) - A(v+\frac{1}{2})^2. \tag{6.51}$$

We see that eq. (6.51) corresponds to the first two nonvanishing powers of $(v+\frac{1}{2})$ contained in the Dunham expansion. This can also be obtained by solving the corresponding Schrödinger equation for the Morse potential [108]. The same result is obtained in the O(4) limit of the vibron model [102] for diatomic molecules, which has been extended to triatomic molecules [103]. The ratio Y_{20}/Y_{10} (the anharmonicity constant [116]) is in the present case proportional to $1/N$, a result similar to the one obtained in the vibron model [102].

In the quantum case, the generators of $\mathrm{SU}_q(1,1)$ satisfy the commutation relations

$$[K_0, K_\pm] = \pm K_\pm, \qquad [K_+, K_-] = -[2K_0], \tag{6.52}$$

and the generators of $\mathrm{SU}_q(1,1)$ have the following boson representation

$$K_+ = a_1^+ a_2^+, \qquad K_- = a_1 a_2, \qquad K_0 = \frac{1}{2}(N_1 + N_2 + 1), \tag{6.53}$$

where the bosons a_i^+, a_i $(i = 1,2)$ satisfy the q-deformed commutation relations (3.7). The second order Casimir operator of $\mathrm{SU}_q(1,1)$ is

$$C_2[SU_q(1,1)] = [K_0][K_0 - 1] - K_+K_- = [K_0][K_0 + 1] - K_-K_+. \tag{6.54}$$

and its eigenvalues are

$$C_2[SU_q(1,1)]|\kappa\mu >= [\kappa][\kappa - 1]|\kappa\mu >, \tag{6.55}$$

where

$$\kappa = \frac{1 + |n_1 - n_2|}{2}, \quad \mu = \frac{1 + n_1 + n_2}{2}, \tag{6.66}$$

since the basis has the form, with $|\kappa\mu>=|n_1>|n_2>$, with [60]

$$|n_i>=\frac{1}{\sqrt{[n_i]!}}(a_i^+)^{n_i}|0>. \tag{6.67}$$

We see that the vibrational spectrum is given by

$$H=E_0-AC_2[SU_q(1,1)]. \tag{6.68}$$

Using the relation $|n_1-n_2|=\omega+1$ one obtains

$$E(N,\omega)=E_0-A\left[\frac{\omega}{2}\right]\left[\frac{\omega+2}{2}\right], \tag{6.69}$$

which in the limit $q\to 1$ goes to eq. (6.50). Using further eq. (6.48) one has

$$E(N,v)=E_0-A\left[v-\frac{N}{2}\right]\left[v+1-\frac{N}{2}\right], \tag{6.70}$$

which is the q-generalization of eq. (6.51).

It is interesting to check how eq. (6.70) is related to eq. (6.51) and to the Dunham expansion (eq. (6.26)). This can be done by taking the Taylor expansions of the hyperbolic (or trigonometric) functions in (6.70), collecting together terms containing the same power of $(v+\frac{1}{2})$, and finally summing up the coefficients of each power of $(v+\frac{1}{2})$. In the case of real q the final result is

$$\begin{aligned}E(N,v)=&E_0+\frac{A}{\sinh(\tau)^2}[-\frac{1}{2}(\cosh(\tau)-\cosh(\tau N))+\tau\sinh(\tau N)(v+\frac{1}{2})\\&-\tau^2\cosh(\tau N)(v+\frac{1}{2})^2+\frac{2}{3}\tau^3\sinh(\tau N)(v+\frac{1}{2})^3\\&-\frac{1}{3}\tau^4\cosh(\tau N)(v+\frac{1}{2})^4+\frac{2}{15}\tau^5\sinh(\tau N)(v+\frac{1}{2})^5\\&-\frac{2}{45}\tau^6\cosh(\tau N)(v+\frac{1}{2})^6+\ldots],\end{aligned} \tag{6.71}$$

while in the case of $q=e^{i\tau}$ the final result is

$$\begin{aligned}E(N,v)=&E_0+\frac{A}{\sin(\tau)^2}[-\frac{1}{2}(\cos(\tau)-\cos(\tau N))+\tau\sin(\tau N)(v+\frac{1}{2})\\&-\tau^2\cos(\tau N)(v+\frac{1}{2})^2+(-\frac{2}{3})\tau^3\sin(\tau N)(v+\frac{1}{2})^3\\&-(-\frac{1}{3})\tau^4\cos(\tau N)(v+\frac{1}{2})^4+\frac{2}{15}\tau^5\sin(\tau N)(v+\frac{1}{2})^5\\&-\frac{2}{45}\tau^6\cos(\tau N)(v+\frac{1}{2})^6+\ldots].\end{aligned} \tag{6.72}$$

The following remarks can now be made:

a) Both eq. (6.71) and eq. (6.72) reduce to eq. (6.51) in the limit $q \to 1$ ($\tau \to 0$).

b) While eq. (6.51) contains only the first two nonvanishing powers of $(v + \frac{1}{2})$, eqs (6.71) and (6.72) contain all possible powers. Thus eqs (6.71) and (6.72) correspond to the full Dunham expansion (eq. (6.26)). However, while the Y_{ik} coefficients in eq. (6.26) are not related to each other, their counterparts in eqs (6.71) (or eq. (6.72)) are interrelated, since they all depend on τ and N.

c) The anharmonicity constant (i.e. the ratio Y_{20}/Y_{10}), which in the classical case (eq. (6.51)) is fixed to $-1/N$, here is $-\tau/\sinh(\tau N)$ (in eq. (6.71)) or $-\tau/\sin(\tau N)$ (in eq. (6.72)). Therefore the anharmonicity constant is not fixed by N (or, equivalently through eq. (6.49), by v_{max}). This extra freedom is useful when one attempts to fit experimental data, as it will be demonstrated below.

For the briefest possible comparison to experimental data we consider the case of H_2 in its $X^1\Sigma_g^+$ state, which has been considered in the case of the anharmonic oscillator as well. We first fitted the data using the classical eq. (6.51). An attempt to use eq. (6.71) is doomed to failure, while eq. (6.72) gives a result much better than eq. (6.51), as can be seen in [26], where the results are reported. Thus the data indicate that q should be a phase, and not a real number.

This conclusion is the same as the one drawn from the comparison of the q-rotor (having the symmetry $SU_q(2)$) to the rotational spectra of deformed and superdeformed nuclei, as well as to the rotational spectra of diatomic molecules. It should also be pointed out that the parameter τ remains small in all cases.

The results of these considerations show that the quantum algebra $SU_q(1,1)$ can be used for the description of vibrational spectra of diatomic molecules, in the same way as the quantum algebra $SU_q(2)$ can be used for the description of rotational spectra of molecules and nuclei.

APPENDIX A

WHAT IS HOPF ALGEBRA ?

In this Appendix we shall try to give a more rigorous answer to the question "What is a Hopf algebra" from the point of view of mathematics. The aim of this Appendix is to make this answer as simple as possible for a reader who is not an expert in mathematics. Therefore we do not expect the reader to be acquainted with the mathematical concepts (more or less abstract) needed for this purpose, and they will be introduced in the appropriate places in this Appendix.

What is an algebra ?. The set of elements $a, b, c, \ldots \in \mathcal{A}$ are said to form an algebra if they have the following properties:

A.1. *The elements of* $\mathcal{A}$ *can be added.*
This means that for every $a, b \in \mathcal{A}$ there exists an element called their *sum*, which is denoted by $a + b$ and which is also an element of $\mathcal{A}$ (i.e. $a + b \in \mathcal{A}$). The sum of elements $a, b \in \mathcal{A}$ has the property $a + b = b + a$. It is assumed also that there exists an element 0, called zero element, such that $a + 0 = 0 + a = a$.

A.2. *The elements of* $\mathcal{A}$ *can be multiplied by real or complex numbers.*
This means that if $\alpha \in \mathcal{R}$ (or $\alpha \in \mathcal{C}$) and $a \in \mathcal{A}$, then there exists an element $\alpha a \in \mathcal{A}$. (Here $\mathcal{R}$ or $\mathcal{C}$ denotes the set of real or complex numbers).

A.3. *There exists an operation "$\circ$", called algebraic multiplication, such that for any two elements* $a, b \in \mathcal{A}$ *there exists an element* $a \circ b \in \mathcal{A}$ *called their product.*

This means that for every *ordered* pair (a, b), $a, b \in \mathcal{A}$ we put in correspondence a new element called their *algebraic product* denoted by $a \circ b$ such that $a \circ b \in \mathcal{A}$. We note that due to the fact that the pair (a, b) is ordered, in the general case $a \circ b \neq b \circ a$.

Remark: The set of elements which satisfies the conditions (**A.1 - A.2**)[22] is referred to as a *linear vector space.* In this sense we can say that *the algebra is a linear vector space, equipped with the operation called algebraic multiplication.*

Remark: The algebraic multiplication of the elements of $\mathcal{A}$ can be defined in different ways and, depending on the properties of the multiplication law, we distinguish different kinds of algebras. If, for example, the multiplication law is associative, i.e. if

$$a \circ (b \circ c) = (a \circ b) \circ c$$

we say that the algebra is associative. If in addition there exists a unit element I with the property $a \circ I = I \circ a = a$ (for every $a \in \mathcal{A}$) we speak about an *associative algebra with a unit element.*

An example for an associative algebra with a unit element is the set of all $n \times n$ nonsingular matrices where the algebraic multiplication of the matrices A and B is defined as an ordinary multiplication of two matrices, i.e. if $C = A \circ B$ then

$$C_{ij} = (A \circ B)_{ij} = \sum_k A_{ik} B_{kj} \quad ,$$

and the unit element I is the unit matrix

$$(I)_{ij} = \delta_{ij}$$

Another important example of an algebra is the set of all nonsingular matrices in which, in addition to the "ordinary" multiplication of the matrices, the algebraic multiplication "o" is defined as the commutator of the matrices, i.e.

$$A \circ B \equiv [A, B]$$

[22]Some additional axioms must be added to these conditions in order to fix the properties of the operations mentioned above. However for the sake of simplicity we shall not discuss these details.

Obviously when the algebraic multiplication is defined in the form of commutators the following properties are satisfied automatically:

$$[A,B] = -[B,A] \qquad \text{"anticommutativity"} \qquad (A.1)$$

$$[A,[B,C]] + [B,[C,A]] + [C,[A,B]] = 0 \qquad \text{"Jacobi identity"} \qquad (A.2)$$

The linear vector space with the algebraic multiplication law which satisfies eqs. (A.1) and (A.2) is called a *Lie algebra.* As is well known, the importance of Lie algebras is due to the fact that they arise in a natural way from the Lie groups which describe the different continuous symmetries in physical problems.

Let us turn now to an associative algebra with a unit element and let us discuss in more detail the algebraic multiplication defined in **A.3**. To form an ordered pair of elements (a,b), where a and b run over all elements of the algebra, means, as a matter of fact, to form the direct (or Kronecker) product of the algebra $\mathcal{A}$ with itself, which product is denoted by $\mathcal{A} \otimes \mathcal{A}$.

We can visualize this fact in the following way. Let us consider the associative algebra with a unit element (for example the algebra $\mathcal{A}$ of the matrices which is discussed in Remark 2). To form an "ordered pair" of two matrices A and B $(A, B \in \mathcal{A})$ simply means "to put these matrices one after the other" writing down $A_{ik}B_{sj}$. This is however nothing else but the Kronecker (or direct) product of these matrices, which is denoted by $A \otimes B$, or expressed by means of components

$$A_{ik}B_{sj} = (A \otimes B)_{is,kj}$$

The direct product $A \otimes B$ obviously belongs to the direct product of the algebra $\mathcal{A}$ by itself, i.e to $\mathcal{A} \otimes \mathcal{A}$. The algebraic multiplication m is an operation which reproduces, from this direct product of A and B, a new matrix $C_{ij} = \sum_k A_{ik}B_{kj} = \sum_k (A \otimes B)_{ik,kj}$ which belongs again to $\mathcal{A}$. In this sense *the multiplication (m) is a mapping of the direct product algebra* $\mathcal{A} \otimes \mathcal{A}$ *onto* $\mathcal{A}$, or symbolically

$$\text{"multiplication"} \qquad \mathrm{m}: \quad \mathcal{A} \otimes \mathcal{A} \overset{(m)}{\longmapsto} \mathcal{A} \qquad (A.3)$$

The existence of a unit element I allows to define another mapping, *the mapping of the set of complex numbers $\mathcal{C}$ onto the algebra $\mathcal{A}$*. Thus, for an arbitrary $\alpha \in \mathcal{C}$ we can form the element of the algebra $\alpha.I \in \mathcal{A}$. So we can consider the "unit" as a mapping

$$\text{"unit"} \qquad I: \qquad \mathcal{C} \overset{I}{\longmapsto} \mathcal{A} \tag{A.4}$$

These considerations seem to be too complicated and unnecessarily finical but they open the door for generalizations which lead to new types of algebras. Thus we can obtain a new kind of algebra "*if we can reverse the arrows*" in the expressions (A.3) and (A.4). Let us now consider this possibility in more detail.

Bialgebra. If we can inverse the arrows in (A.3) and (A.4) we obtain a new kind of algebra which is said to be a bialgebra. To inverse the arrow in (A.3) means that we can introduce a new operation Δ called *co-product* with the property:

$$\text{"co-product"} \qquad \Delta: \qquad \mathcal{A} \overset{\Delta}{\longmapsto} \mathcal{A} \otimes \mathcal{A}. \tag{A.5}$$

This means that to any element $a \in \mathcal{A}$ we can put in correspondence an ordered pair of elements $b, c \in \mathcal{A} \otimes \mathcal{A}$. This operation seems to be to some extent uncommon but, as a matter of fact, it is very simple and we apply it always when we add the angular momenta.

By way of illustration let us consider the system of two particles with coordinates 1 and 2 and with angular momenta $l_1 m_1$ and $l_2 m_2$ respectively. The wave functions of these particles are $\phi_{l_1 m_1}(1)$ and $\phi_{l_2 m_2}(2)$ and the total wave function of the two-particle system is

$$\Psi = \phi_{l_1 m_1}(1) \phi_{l_2 m_2}(2) \tag{A.6}$$

The operator of the total angular momentum of this system is written in the form

$$\mathbf{L} = \mathbf{L}(1) + \mathbf{L}(2) \tag{A.7}$$

where $\mathbf{L}(1)$ acts only on the coordinates of the first particle (i.e. on $\phi_{l_1 m_1}(1)$) and $\mathbf{L}(2)$ acts only on the coordinates of the second particle (i.e. on $\phi_{l_2 m_2}(2)$

). Taking this into account we write

$$\mathbf{L}\Psi = (\mathbf{L}(1)\phi_{l_1 m_1}(1))\phi_{l_2 m_2}(2) + \phi_{l_1 m_1}(1)\mathbf{L}(2)\phi_{l_2 m_2}(2). \qquad (A.8)$$

We should note however that the expressions (A.6 -A.8) are, strictly speaking, incorrect from a mathematical point of view. The configuration space of the two-particle system consists of two independent spaces 1 and 2 and can be considered as a direct product of the configuration spaces of the first and the second particles. For this reason instead of (A.6) we must write down

$$\Psi = (\phi_{l_1 m_1}(1) \otimes \phi_{l_2 m_2}(2)). \qquad (A.9)$$

Taking into account that for arbitrary operators A and B and for arbitrary states ϕ and ψ the following identity is valid

$$(A \otimes B)(\psi \otimes \phi) = (A\psi \otimes B\phi)$$

instead of (A.7) we must write

$$\mathbf{L} = \mathbf{L}(1) \otimes \mathbf{I} + \mathbf{I} \otimes \mathbf{L}(2). \qquad (A.10a)$$

Employing (A.10) on (A.9) we obtain

$$\mathbf{L}\Psi = (\mathbf{L}(1)\phi_{l_1 m_1}(1) \otimes \mathbf{I}\phi_{l_2 m_2}(2)) + (\mathbf{I}\phi_{l_1 m_1}(1) \otimes \mathbf{L}(2)\phi_{l_2 m_2}(2))$$

which is completely equivalent to (A.8).

Obviously one can consider (A.10a) as a co-product of the (abstract) operator of the angular momentum $\mathbf{L}$ since this equation puts in correspondence to $\mathbf{L}$ an ordered pair (as a matter of fact a sum of two ordered pairs $\mathbf{L}\otimes\mathbf{I}$ and $\mathbf{I}\otimes\mathbf{L}$) acting in the direct product space of the two-particle system. Thus we can write down

$$\Delta(\mathbf{L}) = \mathbf{L} \otimes \mathbf{I} + \mathbf{I} \otimes \mathbf{L}. \qquad (A.10b)$$

In such a way we can see that the co-product of the angular momentum operator arises every time when we add the angular momenta of two particles.

In the same way one can define an operation which "reverses the arrow" of the mapping (A.4). This operation (*co-unit*) allows to assign a complex number $\alpha \in \mathcal{C}$ to every element $a \in \mathcal{A}$. We write $\varepsilon(a) = \alpha \in \mathcal{C}$ for every $a \in \mathcal{A}$. Symbolically we have

$$\text{"co - unit"} \qquad \varepsilon : \qquad \mathcal{A} \overset{\varepsilon}{\longmapsto} \mathcal{C} \tag{A.11}$$

We have seen that the co-product is a very common and simple operation. We shall see later on that this is also the case with the co-unit operation.

Now we come to the following

DEFINITION. *A linear vector space $\mathcal{A}_c$ (i.e. the set of elements $a, b, c \ldots \in \mathcal{A}_c$) satisfying the conditions* **A.1** *and* **A.2** *is said to be* **co-algebra** $\mathcal{A}_c$ *if it is equipped with a co-product operation Δ (which maps $\mathcal{A}_c$ onto $\mathcal{A}_c \otimes \mathcal{A}_c$) and with the co-unit operation ε (which maps $\mathcal{A}_c$ onto $\mathcal{C}$).*

To define what is a bi-algebra we need also the concept of homomorphism. Let $\mathcal{A}$ and $\mathcal{A}'$ be two algebras and let φ be a mapping of $\mathcal{A}$ onto $\mathcal{A}'$. This means that an element $\varphi(a) \in \mathcal{A}'$ corresponds to any $a \in \mathcal{A}$. The mapping φ is said to be a *homomorphism* of $\mathcal{A}$ onto $\mathcal{A}'$ if it preserves all defined algebraic operations. For example if the relation $c = ab$ holds in $\mathcal{A}$ then the relation $\varphi(c) = \varphi(a)\varphi(b)$ must hold in $\mathcal{A}'$. Another example is the commutator of two elements. If in $\mathcal{A}$ we have

$$c = [a, b] \tag{A.12a}$$

then in $\mathcal{A}'$ we must have

$$\varphi(c) = [\varphi(a), \varphi(b)]. \tag{A.12b}$$

If the mapping is one-to-one φ, is said to be an *isomorphism.* If the relation $c = ab$ is mapped onto $\varphi(c) = \varphi(b)\varphi(a)$ (i.e. if φ interchanges the order of the elements a and b) the mapping φ is said to be an *anti-homomorphism.*

DEFINITION. *The associative algebra $\mathcal{A}$ with a unit element I equipped with a co-algebraic structure (i.e. with a co-product operation Δ mapping $\mathcal{A}$ onto*

$\mathcal{A} \otimes \mathcal{A}$ and with a co-unit operation ε mapping $\mathcal{A}$ onto $\mathcal{C}$) is said to be a **bi-algebra** *if Δ and ε are homomorphisms of $\mathcal{A}$ onto $\mathcal{A} \otimes \mathcal{A}$ and of $\mathcal{A}$ onto $\mathcal{C}$.*

The co-product and the co-unit operations must satisfy two additional axioms, namely

B.1. *Co-product axiom.*This axiom can be illustrated with the following diargam

$$\begin{array}{ccc} \mathcal{A} \otimes \mathcal{A} & \xrightarrow{\mathrm{id}\otimes\Delta} & \mathcal{A} \otimes \mathcal{A} \otimes \mathcal{A} \\ \uparrow{\scriptstyle \Delta} & & \uparrow{\scriptstyle \Delta\otimes\mathrm{id}} \\ \mathcal{A} & \xrightarrow[\Delta]{} & \mathcal{A} \otimes \mathcal{A} \end{array} \qquad (A.13)$$

Here id is the identity operation $id(a) = a$ or in general $id(\mathcal{A}) = \mathcal{A}$. The above diagram has the following meaning. We start with an algebra $\mathcal{A}$ (bottom left on the diagram) and going along the left up-arrow through the operation Δ we obtain $\mathcal{A} \otimes \mathcal{A}$ (top left on the diagram). Then we apply the operation $id \otimes \Delta$ to $\mathcal{A} \otimes \mathcal{A}$ (right arrow on the top of the diagram) and obtain $(id \otimes \Delta)(\mathcal{A} \otimes \mathcal{A}) = id(\mathcal{A}) \otimes \Delta(\mathcal{A}) \equiv \mathcal{A} \otimes \mathcal{A} \otimes \mathcal{A}$. However we can obtain the same result applying first Δ to $\mathcal{A}$ (right arrow at the bottom of the diagram) and then applying $\Delta \otimes id$ to $\mathcal{A} \otimes \mathcal{A}$ (right up-arrow) to obtain again $\mathcal{A} \otimes \mathcal{A} \otimes \mathcal{A}$. Thus the final result does not depend on the path on the diagram. The co-product axiom represented in the diagram (A.13) can be written down for any element $a \in \mathcal{A}$ in the form

$$(id \otimes \Delta)\Delta(a) = (\Delta \otimes id)\Delta(a). \qquad (A.14)$$

We should note that the proper understanding of this relation can be achieved if the operations which take part in (A.14) are read *from right to left.*

B.2. *Co-unit axiom.* This axiom can be represented with the following diagram

$$\begin{array}{ccc} \mathcal{A}\otimes\mathcal{A} & \xrightarrow{\varepsilon\otimes id} & \mathcal{A}\otimes\mathcal{C}=\mathcal{C}\otimes\mathcal{A}\equiv\mathcal{A} \\ \uparrow{\scriptstyle\Delta} & & \uparrow{\scriptstyle id\otimes\varepsilon} \\ \mathcal{A} & \xrightarrow[\Delta]{} & \mathcal{A}\otimes\mathcal{A} \end{array} \qquad (A.15)$$

The interpretation of this diagram is analogous to (A.13): starting from $\mathcal{A}$ (the left bottom of the diagram) independently on the path on the diagram applying $\varepsilon\otimes id$ or $id\otimes\varepsilon$ on the $\mathcal{A}\otimes\mathcal{A}$ we obtain $\mathcal{A}\otimes\mathcal{C}$ or $\mathcal{C}\otimes\mathcal{A}$ which is equivalent to $\mathcal{A}$. Thus for any elements $a\in\mathcal{A}$ we can write down

$$(\varepsilon\otimes id)\Delta(a)=(id\otimes\varepsilon)\Delta(a)=a. \qquad (A.16)$$

(Again we must read the operations in (A.16) from right to left.)

Hopf algebra. To obtain from a bi-algebra a Hopf algebra we need one more operation called *antipode*. The antipode S is an anti homomorphism from $\mathcal{A}$ to $\mathcal{A}$ (i.e. S maps $\mathcal{A}$ onto $\mathcal{A}$ in such a way that $S(ab)=S(b)S(a)$) and, as we shall see later on, that the antipode is an analogue of the inverse element. The properties of the antipode S are fixed with the following

B.3 *Antipode axiom.* This axiom can be expressed by means of the diagram given bellow

$$\begin{array}{ccccc} \mathcal{A}\otimes\mathcal{A} & \longrightarrow & \underset{id\otimes S}{\overset{S\otimes id}{\rightrightarrows}} & \longrightarrow & \mathcal{A}\otimes\mathcal{A} \\ \uparrow{\scriptstyle\Delta} & & & & \downarrow{\scriptstyle m} \\ \mathcal{A} & \xrightarrow[\varepsilon]{} & \mathcal{C} & \xrightarrow[I]{} & \mathcal{A} \end{array} \qquad (A.17)$$

The interpretation of this diagram is analogous to the interpretation of (A.13) and (A.15): applying the co-product Δ to $\mathcal{A}$ we obtain $\mathcal{A}\otimes\mathcal{A}$ (top left on the diagram). Then applying $S\otimes id$ or $id\otimes S$ to $\mathcal{A}\otimes\mathcal{A}$ we obtain again $\mathcal{A}\otimes\mathcal{A}$ (top right on the diagram). The next step is to apply the algebraic multiplication m to $\mathcal{A}\otimes\mathcal{A}$ to obtain $\mathcal{A}$ (bottom right on the diagram). However the same result can be obtained if we first apply the co-unit operation ε to $\mathcal{A}$ in order to obtain $\mathcal{C}$ and then using the unit element

we map $\mathcal{C}$ onto $\mathcal{A}$. The operation expressed on this diagram can be written down in the following form

$$m.(S \otimes id).\Delta(a) = m.(id \otimes S).\Delta(a) = \varepsilon(a).I \quad . \qquad (A.18)$$

(We recall that proper understanding of this relation can be achieved if one reads the operations in (A.18) from right to left.)

DEFINITION. *The bi-algebra $\mathcal{A}$ (i.e. the associative algebra with a unit element equipped with a co-product Δ which is a homomorphism from $\mathcal{A}$ to $\mathcal{A} \otimes \mathcal{A}$ and a co-unit ε which is homomorphism from $\mathcal{A}$ to $\mathcal{C}$) is said to be* **Hopf algebra** *if it is equipped with an anti-homomorphism S of $\mathcal{A}$ onto $\mathcal{A}$ which satisfies (A.17) an (A.18).*

Example of Hopf algebra. Let G be a continuous or finite group with elements g and let $f(g)$ be functions on G.[23] The set of functions on the group G form an associative algebra with a unit element if:

1. The sum of functions $f_1(g)$ and $f_2(g)$ is given by $(f_1 + f_2)(g) = f_1(g) + f_2(g)$, i.e by ordinary summation. We note that $f_1 + f_2$ is considered as a *new function* and its value at the point g is given by $f_1(g) + f_2(g)$.

2.The product of the functions $f_1(g)$ and $f_2(g)$ is given by $f_1(g)f_2(g)$ i.e. the multiplication law is

$$m : (f_1, f_2) = (f_1 f_2)(g) = f_1(g)f_2(g) \quad . \qquad (A.19)$$

Remark:This relation can be understood in the following way: The multiplication m is an operation which puts in correspondence to the pair of functions $f_1(g)$ and $f_2(g)$ a *new function* which is denoted by $(f_1 f_2)(g)$ and which equals to $f_1(g)f_2(g)$.

[23]We recall that the function on G is a mapping of G onto $\mathcal{C}$, i.e. the function on G is a "rule" which puts in correspondence a complex number $f(g)$ (the value of function) to every element $g \in G$ (an "argument" of the function). For example if G is a finite group with elements $g_1, g_2, \ldots, g_N$ a function on G is given by the set of (complex) numbers $f(g_1), f(g_2), \ldots, f(g_N)$; if G is continuous group then $f(g)$ is a continuous function of g .

3. The unit element is given by the function

$$I(g) = 1 \qquad \text{for every } g \in G\,. \tag{A.20}$$

We have $(If)(g) = (fI)(g) = f(g)$ for every $g \in G$.
Obviously the algebra of functions on the group so defined is *commutative*. It is at the same time an associative algebra with unit elements. Hereafter we shall denote this algebra as $Fun(G)$.

Remark: For the sake of simplicity we will use a specific realization of $Fun(G)$, namely, the algebra of the polynomials on G, which will be denoted by $Pol(G)$. The reason for this choice is, that it is almost evident that $Pol(G)$ has the property

$$Pol(G \otimes G) = Pol(G) \otimes Pol(G)$$

As a matter of fact the polynomials $p(g_1, g_2) \in Pol(G)$ are generated by

$$(g_1 \otimes g_2)^n = g_1^n \otimes q_2^n \in Pol(G) \otimes Pol(G)$$

(We recall that $(g_1 \otimes g_2)(g_1 \otimes g_2) = g_1^2 \otimes g_2^2$.)

Now we shall turn $Pol(G)$ into a Hopf algebra. For this purpose we shall introduce the co-product Δ, the co-unit ε and the antipode S which act on the elements p of $Pol(G)$ (i.e on the polynomial function on $g \in G$) by means of the relations

$$\Delta : p \longmapsto (\Delta p)(g_1, g_2) = p(g_1 g_2) \tag{A.22a}$$

$$\varepsilon : p \longmapsto (\varepsilon p)(g) = p(e) \tag{A.22b}$$

$$S : p \longmapsto (Sp)(g) = p(g^{-1}) \tag{A22.c}$$

Let us now discuss these definitions:

1.The relation (A.22a) means that the co-product Δ acts on p (we write $\Delta : p$) and as result we obtain the co-product $(\Delta p)(g_1, g_2)$.
(This is written in the form $\Delta \;:\; p \;\longmapsto\; (\Delta p)(g_1, g_2)$). Here (Δp) is a *new function* of two arguments g_1 and g_2 which satisfy the condition that its numerical value must equal to $p(g_1 g_2$ (i.e $(\Delta p)(g_1, g_2) = p(g_1 g_2)$). Obviously Δ acts on $p(g) \in Pol(G)$ and gives $(\Delta p)(g_1, g_2) \in Pol(G \otimes G)$. However $Pol(G \otimes G) = Pol(G) \otimes Pol(G)$, i.e Δ maps $Pol(G)$ onto $Pol(G) \otimes Pol(G)$ as it should be according to (A.5).

2. The co-unit ε acts on $p(g)$ and gives $(\varepsilon p)(g)$ (we write $\varepsilon : p \longmapsto (\varepsilon p)(g)$. However the function $(\varepsilon p)(g)$ by definition equals to $p(e)$, where e is the unit element of the group G. However $p(e)$ is a complex number and therefore ε maps $Pol(G)$ onto $\mathcal{C}$.

3. The antipode S acts on p and gives the function $(Sp)(g)$ (we write $S : p \longmapsto (Sp)(g)$) and this function is $p(g^{-1})$. Obviously both $p(g)$ and $p(g^{-1})$ belong to $Pol(G)$ and S maps $Pol(G)$ onto $Pol(G)$.

Let us note that the operations Δ, ε and S can be assumed as acting on the "arguments" of the functions. For example Δ replaces $g = g_1 g_2$ by (g_1, g_2); ε replaces g by e and S replaces g by g^{-1}.

Taking into account these considerations one can easily show that the operations (A.22) satisfy the axioms **B**.1−3 and therefore the algebra $Pol(G)$ is a Hopf algebra.

The properties of a Hopf algebra can be expressed in a very clear way in terms of the "coordinate functions" on the group which will be defined below. For the sake of simplicity we shall consider the group $SL(2, \mathcal{C})$, whose elements are

$$g = \begin{vmatrix} g_{11} & g_{12} \\ g_{21} & g_{22} \end{vmatrix}$$

We shall define the function $\tau_{ij}(g)$ on the group G with the following properties

$$\tau_{ij}(g) = \tau_{ij} \begin{pmatrix} g_{11} & g_{12} \\ g_{21} & g_{22} \end{pmatrix} = g_{ij} \qquad (i, j = 1, 2). \tag{A.23}$$

Since every element of $Pol(G)$ is polynomial of g_{ij}, $\quad i, j = 1, 2$, the element of $Pol(G)$ can be considered as polynomial of τ_{ij}.

Let us consider first the action of the co-product operation Δ on the coordinate functions $\tau_{ij}(g)$. Using the definiton (A.22a) we have

$$\Delta\tau_{11}(g, g') = \tau_{11}(g.g') = \tau_{11} \left(\begin{vmatrix} g_{11} & g_{12} \\ g_{21} & g_{22} \end{vmatrix} . \begin{vmatrix} g'_{11} & g'_{12} \\ g'_{21} & g'_{22} \end{vmatrix} \right)$$

Multiplying explicitly the matrices g and g', the right hand side of the above equation can be rewritten in the form

$$\begin{aligned} \tau_{11}(g.g') &= \tau_{11} \begin{pmatrix} g_{11}g'_{11} + g_{12}g'_{21} & g_{11}g'_{12} + g_{12}g'_{22} \\ g_{21}g'_{11} + g_{22}g'_{21} & g_{21}g'_{12} + g_{22}g'_{22} \end{pmatrix} \\ &= g_{11}g'_{11} + g_{12}g'_{21} \\ &= \tau_{11}(g)\tau_{11}(g') + \tau_{12}(g)\tau_{21}(g') \end{aligned}$$

where we have taken into account (A.23). We can note that the relation of the last row of the above equation can be rewritten in the form

$$(\tau_{11} \otimes \tau_{11} + \tau_{12} \otimes \tau_{21})(g, g')$$

Combining these equations for the coproduct of τ_{11} we can write down

$$\Delta(\tau_{11}) = \tau_{11} \otimes \tau_{11} + \tau_{12} \otimes \tau_{21}$$

In the same way one can obtain the more general expression for the co-product Δ acting on τ_{ij} :

$$\Delta(\tau_{ij}) = \sum_k \tau_{ik} \otimes \tau_{kj} \tag{A.24}$$

These considerations can be generalizied for the case when T is n-dimentional irreducible representation of the group G given by matrices $t_{ij}(g), i, j = 1 \ldots n$ which are polynomials on G. In this case the action of the co-product Δ, the co-unit ε and the antipode S can be found as follows:

Taking into account that

$$t_{ij}(g.g') = \sum_k t_{ik}(g) t_{kj}(g')$$

and making use of the formula (A.22a) we obtain

$$\Delta(t_{ij}) = \sum_k t_{ik} \otimes t_{kj} \tag{A.25a}$$

To find the action of the co-unit ε we take into account that $T(e) = I$, i.e $t_{ij}(e) = \delta_{ij}$. Using (A.22b) we obtain

$$\varepsilon(t_{ij}) = \delta_{ij} \tag{A.25b}$$

And to find the action of S, we have to employ that

$$T(g)T(g^{-1}) = T(g^{-1})T(g) = I$$

or, in terms of matrix elements

$$\sum_k t_{ik}(g) t_{kj}(g^{-1}) = \sum_k t_{ik}(g^{-1}) t_{kj}(g) = \delta_{ij}.$$

Making use of (A.22c) we obtain

$$\sum_k t_{ik} S(t_{kj}) = \sum_k S(t_{ik}) t_{kj} = \delta_{ij} \tag{A.25c}$$

These equations are widely used in the discussion of quantum algebras

Finaly, let us give the expressions of Δ, ε and S acting on the elements of $SU_q(2)$. We have

$$\begin{aligned} \Delta(J_\pm) &= J_\pm \otimes q^{J_0/2} + q^{-J_0/2} \otimes J_\pm \\ \Delta(J_0) &= J_0 \otimes 1 + 1 \otimes J_0 \end{aligned}$$

$$\begin{aligned} \varepsilon(J_\pm = 0 \qquad & \varepsilon(J_0) = 0 \\ S(J_0) = -J_0 \qquad & S(J_\pm) = -qJ_\pm \end{aligned} \tag{A.26}$$

This paper is partially supported by contract No F-10 with the Bulgarian Ministry of Science and Education. The author expresses his gratidude to Prof. Jean Maruani for his hospitality at "Universite Pierre et Marie Curie (Paris VI), Laboratoire de Chimie Physique".

References

[1]. E. Sklyanin, L. Takhtajan, L. Faddeev, *Quantum inverse scattering transform method*, TMF 40, Nr.2 (1979) 194 - 220 (in Russian)

[2]. L. Takhtajan, L. Faddeeev, *Quantum inverse transform method and XYZ Heisenberg model*, Usp. Mat. Nauk 34, Nr.5 (1979) 13 - 63 (in Russian)

[3]. L. Faddeev, *Integrable models in (1+1)-dimensional quantum field theory* (Lectures in Les Houches 1982), Elsevier Sc.Publ.B.V. 1984

[4]. P. Kulish, N. Reshetikhin, *Quantum linear problem for the Sine-Gordon equation and higher representations*, Zap.Nauch.Seminarov LOMI, 101 (1981) 101; ibid. J.Soviet Mat.Dokl. 23 (1983) 2435 (in Russian)

[5]. E. Sklyanin, *On certain algebraic structures connected with Yang-Baxter equation*, Funk.Analiz 16 Nr.4 (1982) 27 - 34 (in Russian), Funct. Anal. Appl. 16 (1982) 262

[6]. Kulish P.P. and Sklyanin E.K., *The study of the solution to the Yang-Baxter equation*, Lecture Notes in Physics, Vol.151 (Berlin - Springer) 1981 p.61

[7]. Reshetikhin N., L. Takhtajan, L. Faddeev, *Algebra and Analisis*, Vol.1, Nr.1, 1989, p.178

[8]. Woronzowich S.L., *Twisted $SU(2)$ group. An example of noncommutative differential calculus*, Publ. RIMS, Kyoto Univ. 1982 Vol.111 p.117 - 181

[9]. Woronzowich S.L., *Compact matrix pseudogroups*, Comm.Math.Phys. 1982 Vol.111 p.613 - 665 Hopf algebras

[10] V. Pasquier and H. Saleur, Nucl. Phys. B330 (1990) 523. Common structures between finite systems and conformal field theories through quantum groups. (Details on $U_q[SU(3)]$).

[11] S. Meljanac, M. Milekovic and S. Pallua, J. Phs. A 24 (1991) 581. Deformed SU(2) Heisenberg chain.

[12] P. P. Kulish and E. K. Sklyanin, J. Phys. A 24 (1991) L435. The general $U_q[sl(2)]$ invariant XXZ integrable quantum spin chain.

[13] P. P. Raychev, R. P. Roussev and Yu. F. Smirnov, J. Phys. G 16

(1990) L137. The quantum algebra $SU_q(2)$ and rotational spectra of deformed nuclei.

[14] D. Bonatsos, E. N. Argyres, S. B. Drenska, P. P. Raychev, R. P. Roussev and Yu. F. Smirnov, Phys. Lett. 251B (1990) 477. $SU_q(2)$ description of rotational spectra and its relation to the variable moment of inertia model.

[15] D. Bonatsos, S. B. Drenska, P. P. Raychev, R. P. Roussev and Yu. F. Smirnov, J. Phys. G17 (1991) L67. Description of superdeformed bands by the quantum algebra $SU_q(2)$.

[16] Yu. F. Smirnov and B. I. Zhilinsky, Sov. J. Nucl. Phys. 54 (1991) 10, Yad. Fiz. 54 (1991) 17. Phenomenological $SU_q(2)$ model description of nuclear and molecular rotational bands.

[17] D. Bonatsos, A. Faessler, P. P. Raychev, R. P. Roussev and Yu. F. Smirnov, J. Phys. A 25 (1992) 3275. B(E2) transition probabilities in the q-rotator model with $SU_q(2)$ symmetry.

[18] S. Iwao, Prog. Theor. Phys. 83 (1990) 363. Knot and conformal field theory approach in molecular and nuclear physics. (rotational spectra).

[19] S. Iwao, Prog. Theor. Phys. 83 (1990) 368. Spectroscopy in Witten's quantum universal enveloping algebra of SU(2) and strength of deformation of its representation space. (Magnetic moments).

[20] E. Celeghini, R. Giachetti, E. Sorace and M. Tarlini, Phys. Lett. 280B (1992) 180. Quantum groups of motion and rotational spectra of heavy nuclei.

[21] R. K. Gupta, J. Cseh, A. Ludu, W. Greiner and W. Scheid, J. Phys. G 18 (1992) L73. Dynamical symmetry breaking in SU(2) model and the quantum group $SU_q(2)$.

[22] J. Meng, C. S. Wu and J. Y. Zeng, Phys. Rev. C 44 (1991) 2545. Deviation of the $SU_q(2)$ prediction from observations in even-even deformed nuclei.

[23] D. Bonatsos, P. P. Raychev, R. P. Roussev and Yu. F. Smirnov, Chem.

Phys. Lett. 175 (1990) 300. Description of rotational molecular spectra by the quantum algebra $SU_q(2)$.

[24] J. G. Esteve, C. Tejel and B. E. Villarroya, J. Chem. Phys. 96 (1992) 5614. $SU_q(2)$ quantum group analysis of rotational spectra of diatomic molecules.

[25] D. Bonatsos, P. P. Raychev and A. Faessler, Chem. Phys. Lett. 178 (1991) 221. Quantum algebraic description of vibrational molecular spectra.

[26] D. Bonatsos, E. N. Argyres and P. P. Raychev, J. Phys. A24 (1991) L403. $SU_q(1,1)$ description of vibrational molecular spectra.

[27] D. Bonatsos and C. Daskaloyannis, Phys. Rev. A 46 (1992) 75. Generalized deformed oscillators for vibrational spectra of diatomic molecules.

[28] F. Pan, ICTP Trieste preprint (1992). Quantum deformation of $U(4) \supset SO(4) \supset SO(3)$ chain and the description of rotation-vibration spectra of diatomic molecules.

[29] Z. Chang, H. Y. Guo and H. Yan, Commun. Theor. Phys. 17 (1992) 183. Quantum groups and spectra of diatomic molecules.

[30] M. Kibler and T. Négadi, J. Phys. A 24 (1991) 5283. On the q-analogue of the hydrogen atom.

[31] J. Gora, J. Phys. A 25 (1992) L1281. Two models of a q-deformed hydrogen atom.

[32] M. Kibler and T. Négadi, Lyon preprint LYCEN 9121 (6/1991). On quantum groups and their potential use in mathematical chemistry.

[33] X. C. Song and L. Liao, J. Phys. A 25 (1992) 623. The quantum Schrödinger equation and the q-deformation of the hydrogen atom.

[34] T. Négadi and M. Kibler, J. Phys. A 25 (1992) L157. A q-deformed aufbau prinzip.

[35] D. Bonatsos, J. Phys. A 25 (1992) L101. Are q-bosons suitable for the description of correlated fermion pairs?

[36] D. Bonatsos and C. Daskaloyannis, Phys. Lett. 278B (1992) 1. Generalized deformed oscillator for the pairing interaction in a single-j shell.

[37] D. Bonatsos, A. Faessler, P. P. Raychev, R. P. Roussev and Yu. F. Smirnov, J. Phys. A 25 (1992) L267. An exactly soluble nuclear model with $SU_q(3) \supset SU_q(2) \supset SO_q(2)$ symmetry.

[38] D. P. Menezes, S. S. Avancini and C. Providência, U. São Paulo preprint IFUSP/P-964 (1/1992). Quantum algebraic description of the Moszkowski model.

[39] J. Cseh, Atomki preprint 6-1992-P (1992), appeared in J. Phys. A 25 (1992) L1225. Dynamic versus kinematic symmetry breaking in a two-dimensional model of collective motion.

[40] Feng Pan, ICTP Trieste preprint (11/1992). q-deformations in the Interacting Boson Model for Nuclei.

[41] S. Iwao, Progr. Theor. Phys. 86 (1991) 167. Magnetic moments of nuclei and g factors for baryons and quarks in SU_2 quantum universal enveloping algebra.

[42] V. G. Drinfel'd, Proceedings of the International Congress of Mathematicians, Berkeley, California, USA, 1986, ed. A. M. Gleason (American MAthematical Society, 1987) p. 798. Quantum groups.

[43] M. Jimbo, *Lett. Math. Phys.* 11 (1986) 247

[44] E. Abe, *Hopf Algebras* (Cambridge University Press, Cambridge, 1980)

[45] T. Tjin, Int. J. Mod. Phys. A 7 (1992) 6175. Introduction to quantized Lie groups and algebras.

[46] H. B. Doebner, J. D. Hennig and W. Lücke, Clausthal 1989, p. 29. Mathematical guide to quantum groups.

[47] *Quantum Groups (Clausthal 1989)*, ed. H. D. Doebner and J. D. Hennig (Springer, Berlin, 1990)

[48] L. A. Takhtajan, Clausthal 1989, p. 3. Introduction to quantum groups.

[49] L. C. Biedenharn, Moscow 1990, p. 147. An overview of quantum groups.

[50] L. C. Biedenharn, Wigner Symposium II, Goslar (7/1991). An overview and survey of some recent developments in quantum groups.

[51] Yu. I. Manin, in Proceedings of the International Congress of Mathematicians (Kyoto 1990) ed. I. Satake (Mathematical Society of Japan,

Tokyo, 1991) p. 3. On the mathematical work of Vladimir Drinfeld.; Commun. Math.Phys. 123 (1989) 163

[52] L. C. Biedenharn, J. Phys. A 22 (1989) L873. The quantum group $SU_q(2)$ and a q-analogue of the boson operators.

[53] A. J. Macfarlane, J. Phys. A 22 (1989) 4581. On q-analogues of the quantum harmonic oscillator and the quantum group $SU_q(2)$.

[54] Y. J. Ng, J. Phys. A23 (1990) 1023. Comment on the q-analogues of the harmonic oscillator.

[55] C. P. Sun and H. C. Fu, J. Phys. A 22 (1989) L983. The q-deformed boson realization of the quantum group SU(n) and its representations.

[56] A. Jannussis, U. Patras preprint (1/1990). Quantum group and the Lie-admissible Q-algebra.

[57] E. G. Floratos and T. N. Tomaras, Phys. Lett. 251B (1990) 163. A quantum mechanical analogue for the q-oscillator.

[58] Hong Yan, J. Phys. A 23 (1990) L1155. q-deformed oscillator algebra as a quantum group.

[59] X. C. Song, J. Phys. A 23 (1990) L821. The construction of the q-analogues of the harmonic oscillator operators from ordinary oscillator operators.

[60] A. Jannussis, G. Brodimas and R. Mignani, J. Phys. A 24 (1991) L775. Quantum groups and Lie-admissible time evolution.

[61] C. Zachos, *Paradigms of Quantum algebras*, Preprint ANL – HEP – 90 – 61, Aragonne National Laboratory

[62] C. Quesne, U. L. Bruxelles preprint PNT/1/92. Raising and lowering operators for $U_q(n)$.

[63] M. Chaichian, P. Kulish and J. Lukierski, Phys. Lett. 237B (1990) 401. q-deformed Jacobi identity, q-oscillators and q-deformed infinite dimensional algebras. (q-deformed osp(1/2), osp(2/2) and osp(2N/2).)

[64] G. E. Andrews, Regional Conference Series in Mathematics 66 (American Mathematical Society, Providence, RI, 1986). q-series: their development and applications in analysis, number theory, combinatorics, physics, and computer algebra.

[65] H. Exton, *q-Hypergeometric Functions and Applications* (Ellis Horwood, Chichester, 1983)

[66] R.Gilmore, Lie qroups, Lie algebras and Their applications

[67] Z. Chang, W. Chen, H. Y. Guo and H. Yan, J. Phys. A 24 (1991) 1427. $SU_{q,\hbar\to 0}(2)$ and $SU_{q,\hbar}(2)$, the classical and quantum q-deformations of the SU(2) algebra: II. When q is a root

[68] C. P. Sun and M. L. Ge, J. Phys. A 24 (1991) L969. The cyclic boson operators and new representations of the quantum algebra $sl_q(2)$ for q a root of unity.

[69] M. Couture, J. Phys. A 24 (1991) L103. On some quantum R matrices associated with representations of $U_q(sl(2,C))$ when q is a root of unity.

[70] C.P. Sun and M. L. Ge, J. Phys. A 24 (1991) 3265. The q-deformed boson realization of representations of quantum universal enveloping algebras for q a root of unity: (I) the case of $U_qSL(l)$. ($SL_q(2)$, $SL_q(3)$.)

[71] M. Rosso, Comm. Math. Phys. 117 (1988) 581

[72] Zhong-Qi Ma, Preprint IC/89/162, ICTP, Trieste (1989)

[73] L. C. Biedenharn, Clausthal 1989, p. 67. A q-boson realization of the quantum group $SU_q(2)$ and the theory of q-tensor operators.

[74] L. C. Biedenharn and M. Tarlini, Lett. Math. Phys. 20 (1990) 271. On q-tensor operators for quantum groups.

[75] C. Quesne, Brussels preprint PNT/10/92, to appear in Symmetries in Science VI (Bregenz 1992). q-bosons and irreducible tensors for q-algebras.

[76] M. Nomura and L. C. Biedenharn, J. Math. Phys. 33 (1992) 3636. On the q-symplectron realization of the quantum group $SU_q(2)$. (q-series).

[77] Feng Pan, J. Phys. A 24 (1991) L803. Irreducible tensor operators for the quantum algebra $SU_q(2)$.

[78] H. Ruegg, Clausthal 1989, p. 89. Polynomial basis for $SU_q(2)$ and Clebsch-Gordan coefficients.

[79] H. Ruegg, J. Math. Phys. 31 (1990) 1085. A simple derivation of the quantum Clebsch-Gordan coefficients for $SU_q(2)$.

[80] C. R. Lienert and P. H. Butler, J. Phys. A 25 (1992) 1223. Racah-Wigner algebra for q-deformed algebras. Clebsch-Gordan coefficients and irreducible tensor operators.

[81] Yu. F. Smirnov, V. N. Tolstoy and Yu. I. Kharitonov, Yad. Fiz. 53 (1991) 1746, Sov. J. Nucl. Phys. 53 (1991) 1068. Projection-operator method and the q-analog of the quantum theory of angular momentum. Racah coefficients, 3j and 6j symbols, and their symmetry properties.

[82] Yu. F. Smirnov, V. N. Tolstoy and Yu. I. Kharitonov, Sov. J. Nucl. Phys. 55 (1992) 1599. Tree technique and irreducible tensor operators for the $SU_q(2)$ quantum algebra. 9j symbols.

[83] I. I. Kachurik and A. U. Klimyk, Kiev preprint ITP-89-48E. On Clebsch-Gordan coefficients of quantum algebra $U_q(SU_2)$.

[84] V. A. Groza, I. I. Kachurik and A. U Klimyk, J. Math. Phys. 31 (1990) 2769. On Clebsch-Gordan coefficients and matrix elements of representations of the quantum algebra $U_q(SU_2)$.

[85] I. I. Kachurik and A. U. Klimyk, J. Phys. A 23 (1990) 2717. On Racah coefficients of the quantum algebra $U_q(SU_2)$.

[86] I. I. Kachurik and A. U. Klimyk, J. Phys. A 24 (1991) 4009. General recurrence relations for Clebsch-Gordan coefficients of the quantum algebra $U_q(SU_2)$.

[87] A. U. Klimyk, J. Phys. A 25 (1992) 2919. Wigner–Eckart theorem for the quantum group $U_q(n)$.

[88] T. Maekawa, J. Math. Phys. 32 (1991) 2598. On the Wigner and the Racah coefficients of $SU_q(2)$ and $SU_q(1,1)$.

[89] M. Abramowitz and I. A. Stegun, "*Handbook of Mathematical Functions*" (Dover, New York, 1972)

[90] F. X. Xu, C. S. Wu and J. Y. Zeng, Phys. Rev. C 40 (1989) 2337

[91] M. J. A. de Voigt, J. Dudek and Z. Szymański, Rev. Mod. Phys. 55 (1983) 949

[92] M. A. J. Mariscotti, G. Scharff–Goldhaber and B. Buck, Phys. Rev. 178 (1989) 1864

[93] P. J. Twin *et al.*, Phys. Rev. Lett. 57 (1986) 811

[94] P. E. Hodgson, Contemp. Phys. 28 (1987) 365

[95] P. J. Nolan and P. J. Twin, Ann. Rev. Nucl. Part. Sci. 38 (1988) 533

[96] G. Herzberg, *Molecular Spectra and Molecular Structure*, Vol. 1: *Spectra of Diatomic Molecules* (Van Nostrand, Toronto, 1950)

[97] G. M. Barrow, *Introduction to Molecular Spectroscopy* (McGraw–Hill, London, 1962)

[98] R. D. Levine and C. E. Wulfman, Chem. Phys. Lett. 60 (1979) 372

[99] C. E. Wulfman and R. D. Levine, Chem. Phys. Lett. 97 (1983) 361

[100] C. E. Wulfman and R. D. Levine, Chem. Phys. Lett. 104 (1984) 9

[101] F. Iachello, Chem. Phys. Lett. 78 (1981) 581

[102] F. Iachello and R. D. Levine, J. Chem. Phys. 77 (1982) 3046

[103] O. S. van Roosmalen, F. Iachello, R. D. Levine and A. E. L. Dieperink, J. Chem. Phys. 79 (1983) 2515

[104] A. Arima and F. Iachello, Ann. Phys. 99 (1976) 253; 111 (1978) 201; 123 (1979) 468

[105] F. Iachello and A. Arima, *The Interacting Boson Model* (Cambridge University Press, Cambridge, 1987)

[106] D. Bonatsos, *Interacting Boson Models of Nuclear Structure* (Clarendon, Oxford, 1988)

[107] J. L. Dunham, Phys. Rev. 41 (1932) 721

[108] P. M. Morse, Phys. Rev. 34 (1929) 57

[109] C. E. Miller, A. A. Finney and F. W. Inman, Atomic Data 5 (1973) 1

[110] H. W. Woolley, J. Chem. Phys. 37 (1962) 1307

[111] J. F. Ogilvie and R. H. Tipping, Int. Rev. Phys. Chem. 3 (1983) 3

[112] O. S. van Roosmalen, R. D. Levine and A. E. L. Dieperink, Chem. Phys. Lett. 101 (1983) 512

[113] O. S. van Roosmalen, I. Benjamin and R. D. Levine, J. Chem. Phys. 81 (1984) 5986

[114] I. Benjamin, Chem. Phys. Lett. 112 (1984) 403

[115] I. L. Cooper and R. D. Levine, J. Molec. Struct. 199 (1989) 201

[116] R. D. Levine, Chem. Phys. Lett. 95 (1983) 87

[117] S. Weissman, J. T. Vanderslice and R. Battino, J. Chem. Phys. 39 (1963) 2226

[118] S. K. Kim, I. L. Cooper and R. D. Levine, Chem. Phys. 106 (1986) 1

[119] L.Marinova, P.Raychev and J.Maruani - to be published in Molecular Physics

[120] L.C.Biedenharn -Private communication. See also "Quantum Groups: A Review" - to be published in the International Journal of Theoretical Physics

Index

C

D

E

F

G

H

I

J

K

L

M

N

O

P

Q

T

U

V

W

X

Y